UNIVERSIDADE DE LISBOA

FACULDADE DE CIÊNCIAS

New Potential Sodium-Glucose Co-Transporters Sugar-Based Inhibitors for the Treatment of Diabetes

Doutoramento em Química

Especialidade Quimica Orgânica

Ana Rita Xavier de Jesus

Tese orientada por:

Professora Doutora Amélia Pilar Rauter

Professor Doutor Timothy Dore

Professor Doutor Jian Liu

Documento especialmente elaborado para a obtenção do grau de doutor

2015

In collaboration with:

Professor Timothy Dore from New York University Abu Dhabi

Professor Jian Liu from Eshelman School of Pharmacy, University of North Carolina

Table of Contents

List of Figures

List of Schemes

List of Graphs

List of Tables

List of Acronyms

δ - chemical shift

ACN – Acetonitrile

AcOH – Acetic acid

aq – aqueous

ATP – Adenosine triphosphate

bp – Base pair

BSA – Bovine serum albumin

^{13}C-NMR – Carbon-13 Nuclear Magnetic Resonance

DAPA – Dapagliflozin

2-DG – 2-Deoxyglucose

2DG6P – 2-deoxyglucose-6-phospahte

DCM – Dichloromethane

DCE – Dichloroethane

DIPEA – *N,N*-Diisopropylethylamine

DM – Diabetes Mellitus

DMAP – 4-Dimethylaminopyridine

DMEM - Dulbecco's Modified Eagle Medium

DMF – *N,N*-dimethylformamide

DMSO – Dimethylsufoxide

EGFP – Enhanced green fluorescent protein

EOM group – Ethoxymethyl group

Equiv. – Equivalent

EtOAc – Ethyl acetate

FBS – Fetal bovine serum

FDA – Food and Drug Administration

G6P – Glucose 6-phosphate

G6PDH – Glucose 6-phosphate dehydrogenase

G418 – Geneticin

GFP – Green fluorescent protein

GLUT – Glucose facilitative transporter

GOI – Gene of interest

GTF – Glucosyl transferase

HEPES – 4-(2-hydroxyethyl)-1-piperazineethanesulfonic acid

IC_{50} – Half maximal inhibitory concentration

Kbp – Kilo base pair

KDa – Kilo Dalton

HEK293 cells – Human Embryonic Kidney 293 cells

KRPH – Kregs-Ringer-Phosphate-HEPES

HRMS – High Resolution Mass Spectrometry

HMQC – Heteronuclear Multiple-Quantum Correlation

HMBC – Heteronuclear Multiple Bond Correlation

LB – Luria Broth

m.p. – Melting point

MW – Micro-wave

$NADP^+$ – Nicotinamide adenine dinucleotide phosphate

NBDG – (2-(*N*-(7-Nitrobenz-2-oxa-1,3-diazol-4-yl)Amino)-2-Deoxyglucose)

NTA-agarose – Nitriloacetic acid- agarose

^{1}N NMR – Proton Nuclear Magnetic Resonance

PCR – Polymerase chain reaction

PDL – Poly-D-lysine

Phlo – Phlorizin

ppm – Parts per million

P. Ether – Petroleum Ether

rt – Room temperature

RT-PCR – Reverse transcription polymerase chain reaction

SDS-PAGE – sodium dodecyl sulfate - polyacrylamide gel electrophoresis

SGLT – Sodium-glucose co-transporter

SGLT1 – Sodium-glucose co-transporter 1

SGLT2 – Sodium-glucose co-transporter 2

TCA – Trichloroacetimidate

TDM1 – Type 1 Diabetes

TDM2 – Type 2 Diabetes

TEA – Triethanoloamine

TFA – Trifluoroacetate

TLC – Thin Layer Chromatography

TMU – Tetramethylurea

THF – Tetrahydrofuran

TMSOTf – Trimethylsilyl trifluoromethanesulfonate

U/mL – Units per millilitre

UT – Untransfected

n

Agradecimentos

Em primeiro lugar tenho de agradecer às duas pessoas que tornaram este meu sonho possível, os meus PAIS. Obrigado pela vossa ajuda e apoio desde o primeiro dia. Sem vocês hoje não estaria a defender este trabalho. Obrigado por me apoiarem nas minhas "aventuras" pelo mundo mas sobretudo por me orientarem da melhor forma ao longo da minha vida.

Obrigado ao meu irmão que esteve sempre presente nos momentos mais importantes da minha vida, sempre com as suas brincadeiras e boa-disposição e sempre com muito carinho. À minha cunhada claro que também foi muito importante com todo o seu apoio e carinho, obrigado a vocês.

Tanto ou mais importante tem sido o meu maridinho que desde o primeiro dia me apoia incondicionalmente em todas as decisões que tomo. Obrigado por não me deixares desistir nos momentos mais difíceis. Obrigado por teres tido paciência quando estive ausente. Obrigado por me tornares numa pessoa melhor ao longo destes anos.

Agradeço também aos meus sogros e cunhada que são os meus segundos pais/irmã especialmente quando a minha vida deu uma volta de 180º e fui viver para Abu Dhabi. Sem vocês teria sido sem dúvida mais difícil. Obrigado.

Obrigadinhooooooo aos meus amigos Otília, Vasco, Pirrolina e Coisinhas que sem vocês também nada disto seria possível. Obrigado por não me deixarem desistir das coisas quando estas se tornaram complicadas. Vocês aturaram dias a fio durante muitos anos as minhas loucuras mas também as minhas rabugices e parvoíces mas sempre com um sorriso na cara e boa disposição. Já tenho saudades de vos ter por perto e de me rir horas a fio. Mas, especialmente vou ter saudades das cantorias. Eu sei que vocês não vão. EHEH ☺

Obrigado aos colegas que já estive no CCG pelo companheirismo durante estes 8 anos no laboratório.

Aos meus colegas da UNC obrigado pela ajuda prestava durante os 4 meses que estive no vosso laboratório.

A todos os meus colegas da NYUAD (Mark, Cyril, Magnus, Shahienaz, Idrees, Louise, Adna, Sangram) mas, especialmente à Louise que me ensinou muitas das

coisas que sei sobre biologia molecular e cultura de células. Obrigado por me fazerem sentir como se estivesse em casa.

Aos meus amigos/colegas espalhados por Portugal e pelo Mundo (Betinha, Filipa, Milita, Vanessa, Justine, Stefan) obrigado por estarem sempre disponíveis para mim e fazerem parte da minha vida, sem duvida que é mais rica por vos ter. Obrigado a todos.

Obrigado ao Professor Jian Liu por me ter dado a oportunidade de estar no laboratório dele na UNC a aprender síntese enzimática. Foi sem dúvida muito interessante aprender novas coisas no gigante mundo que é a química.

Obrigado ao Professor Timothy Dore por me ter acolhido no seu laboratório na NYUAD durante 2 anos o que me permitiu descobrir uma nova área que gosto muito.

Por fim, obrigado à Professora Amélia Rauter por me ter aceite como sua doutoranda.

Acknowledgments

First, I have to thank the two persons who made this dream come true, my PARENTS. Thank you for all the support since day one. Without you I wouldn't be presenting this work. Thank you for supporting my "adventures" around the world. Thank you for making me who I am today.

I have to thank my brother who was always there for me, in all the important moments of my life with unconditional support. To my sister-in-law thank you for the support and care. Thank you both.

Also important is my husband that since day one has supported me unconditionally in all my decisions. Thank you for not letting me give up in the tougher moments. Thank you for your patience during my absences while I was abroad. And thank you for making me a better person over these years.

I thank to my in-laws as well as my other sister-in-law who are my second parents/sister specially when my life turned up side down and I went to Abu Dhabi. Without you all would have been more difficult. Thank you.

Thank yoouuuuuuuuuu my friends Otília, Vasco, Pirrolina and Coisinhas. Without you guys anything wouldn't have been possible. Thank you for the support and for not letting me down when things were complicated. You were always there for me even with my craziness and nonsense but always with a smile and happiness. I miss having you around and laughingfor hours with all of you. But, what I miss the most is the singing. That was so so funny even if you say it was not. EHEH ☺

Thank you to all my colleagues in CCG for the companionship over these 8 years in the lab.

To my colleagues at UNC thank you for the support and help while I was in the lab.

To my colleagues at NYUAD (Mark, Cyril, Magnus, Shahienaz, Idrees, Louise, Adna, Sangram), but specially Louise who helped me and taught me most of the things I know about cell biology. Thank you all for making me feel like home.

To my friends all over Portugal and throughout the world (Betinha, Filipa, Milita, Vanessa, Justine, Stefan) thank you for everything and making my life richer. Thank you all.

Professor Jian Liu, thank you for giving the opportunity to learn enzymatic synthesis. It was definitely exciting to learn new things on the giant world of chemistry.

Professor Timothy Dore, thank you for having me accepted me in your lab for almost 2 years and allowing me to discover this new field, which I like very much.

Finally, Professor Amélia Rauter, thank you for supervising my PhD.

Resumo

O objetivo deste trabalho consistiu na investigação da síntese de *C*-glucosil di-hidrochalconas como inibidoras das proteínas co-transportadoras de sódio e glucose 1 e 2 (SGLT). Estes novos compostos são análogos *C*-glucosilados da florizina, uma di-hidrochalcona *O*-glucosilada conhecida como inibidora não-seletiva das proteínas SGLT1 e SGLT2. Para tal, foi sintetizada uma pequena biblioteca de di-hidrochalconas com grupos diferentes substituintes (halogenetos, grupos alcoxi, e hidroxilo) em ambos os anéis aromáticos de forma a entender a importância dos mesmos em relação à bioactividade destes compostos. A via sintética englobou uma reação de condensação aldólica em meio básico a partir de 2′,4′,6′-tri-hidroxiacetofenona, 2′,4′-di-hidroxiacetofenona e 4′-fluoro-2′-di-hidroxiacetofenona e diversos aldeídos aromáticos, utilizando quer aquecimento convencional, quer promovido por radiação de micro-ondas. A desproteção das chalconas foi investigada, utilizando $FeCl_3 \cdot 6H_2O$, também pelo método convencional e assistido por micro-ondas. Com esta ultima metodologia, utilizando micro-ondas observou-se que os rendimentos não foram significativamente diferentes dos obtidos pelo método convencional, embora tenha sido possível diminuir os tempos de reação de 24 horas para 1 hora diminuindo de igual forma a formação de produtos secundários.

Uma hidrogenação *in situ* com o sistema Et_3SiH /Pd-C, aplicada pela primeira vez a chalconas, resultou na redução da ligação dupla das chalconas, originando as chamadas di-hidrochalconas em excelente rendimentos (90-99%). Curiosamente, partindo da chalcona com um grupo bromo na posição C-4′′ (anel B) não foi obtida a correspondente dihidrochalcona. Neste caso, ocorreu uma substituição do grupo bromo por um protão.

A *C*-glucosilação destas di-hidrochalconas foi posteriormente investigada e, após varias tentativas, foi possível obter os compostos β-D-*C*-glucosilados, com rendimentos na gama dos 35-50%, usando 2,3,4,6-tetra-*O*-benzil-α-D-glucopiranose como dador de glicosilo na presença de TMSOTf em quantidade catalítica. Quando a di-hidrochalcona com um grupo furanoílo no anel B foi usada na C-glucosilação, diversos compostos foram formados não tendo sido possível isolar o composto *C*-glucosilado pretendido. A

di-hidrochalcona *C*-glucosilada preparada a partir de 2′,4′,6′,4′′-tetra-hidroxi-di-hidrochalona não originou o produto desejado e, como tal, foi necessário utilizar uma via alternativa envolvendo a *C*-glucosilacao de 2′,4′,6′-tri-hidroxiacetofenona. O produto desta *C*-glucosilação, obtido com um rendimento de 57%, foi utilizado na reação de condensação aldólica de forma a obter a chalcona *C*-glucosilada em 63% de rendimento.

Utilizando outros dadores de glucosilo, 1-*O*-acetil-2,3,4,6-tetra-*O*-benzil-D-glucopiranose, 1,2,3,4,6-penta-*O*-acetil-D-glucopiranose, brometo de 2,3,4,6-tetra-*O*-acetil-α-D-glucopiranosilo ou tricloroacetimidato de 2,3,4,6-tetra-*O*-acetil-α-D-glucopiranosilo, não ocorreu qualquer reação de *C*-glucosilação, quer utilizando TMSOTf ou $Sc(OTf)_3$ como ativadores.

A remoção dos grupos protetores foi conseguida através de hidrogenação utilizando o sistema Et_3SiH/Pd-C, previamente mencionado, originando os compostos pretendidos, com um rendimento global de 25-40%.

Os sete compostos *C*-glucosilados foram, posteriormente, utilizados nos testes biológicos, bem como os correspondentes intermediários chalconas e di-hidrochalconas.

Relativamente aos estudos biológicos, o objetivo consistiu na determinação das propriedades inibidoras dos compostos acima mencionados relativamente às proteínas SGLT1 e SGLT2, duas isoformas das proteínas SGLT presentes nos rins e intestinos.

Foi necessário gerar duas linhas celulares estáveis que expressassem as proteínas SGLT1 e SGLT2, respetivamente. A linha de células escolhida para este estudo foi a HEK293 por terem uma capacidade de transfeção bastante elevada. O primeiro passo na geração dessas linhas celulares consistiu na otimização as condições de transfeção das células HEK293 tendo sido necessário preparar previamente os plasmídeos contendo os DNA's pretendidos (SGLT1 e SGLT2) através da transformação de células competentes da estirpe de *E. coli* DH5α. Foi utilizado o antibiótico ampicilina de forma a permitir apenas o crescimento de bactérias contendo os plasmídeos pretendidos. A extração do DNA plasmídeo foi efetuada por maxi-prep utilizando um kit comercial. A concentração do DNA foi determinada através um equipamento NanoDrop, o qual também fornece a razão A_{260}/A_{280} como uma medida da pureza do DNA (entre 1.8 e 1.9).

A pureza dos plasmídeos foi também avaliada realizando uma reação de restrição na qual são usados enzimas de restrição que cortam o DNA em zonas específicas e

após uma eletroforese em gel de agarose foram observados os produtos expectáveis através da análise do gel com uma lâmpada UV.

Relativamente à otimização do método de transfeção foi determinada a razão DNA/reagente necessária para obter uma máxima eficiência da mesma. Este processo foi efetuado com a proteína fluorescente EGFP (*Enhanced Green Fluorescent Protein*) recorrendo à microscopia confocal bem como à medição da fluorescência em cada condição utilizando um *multiplate reader*. Uma razão 2:1 DNA/reagente de transfeção originou a maior eficiência e, portanto foi a condição escolhida para os estudos seguintes.

Para gerar as linhas celulares estáveis é necessário, após a transfeção com o plasmídeo desejado, proceder a um tratamento com um antibiótico adequado de forma a matar todas as células não-transfectadas num período de 7 dias. Neste caso, os plasmídeos tinham na sua estrutura um gene que confere uma resistência ao antibiótico geneticina e, como tal, foi necessário determinar a concentração mínima (600-700 μg/mL) para matar todas as células não-transfectadas.

As células HEK293 foram, então, transfectadas com os plasmídeos SGLT1 e SGLT2 e após a adição do antibiótico foram gerados diversos clones que foram posteriormente criopreservados e caracterizados por diferentes técnicas. Foram utilizadas duas concentrações 600 e 700 μg/mL para gerar as linhas celulares de forma a obter clones com maior taxas de expressão destas proteínas.

Utilizando as técnicas Western Blot e RT-PCR foram identificados dois clones estáveis com elevada expressão das proteínas SGLT1 e SGLT2, 700B1 e 700A1, respetivamente. Estes dois clones estáveis foram então usados para os estudos de captação de glucose.

Em paralelo, foi estudada a toxicidade dos compostos sintetizados nas células HEK293. Foi utilizado o kit *Celltiter Blue* no qual um agente não-fluorescente, a resazurina, a qual após redução por células viáveis é transformada no composto fluorescence resofurina. Assim, a fluorescência produzida pela resofurina é proporcional ao número de células viáveis. As células não-viáveis perdem a capacidade metabólica e portanto não geram qualquer fluorescência. Este ensaio revelou que a uma concentração de 100 μM nenhum dos compostos mostrou mais de 50% de toxicidade

embora alguns tenham mostrado cerca de 30-50%. Contudo, as *C*-glucosil di-hidrochalconas bem como as chalconas e di-hidrochalconas revelaram mais de 90% de viabilidade celular.

Em seguida, o método de captação de glucose por células HEK293 e pelos clones estáveis foi otimizado usando quer o método 2-NBDG (análogo fluorescente da D-glucose) ou 2-DG (2-desoxiglucose) o qual envolve um ensaio enzimático. O método foi otimizado quer usando transfeção temporária quer usando linhas celulares estáveis.

Após otimização, as células foram incubadas apenas no tampão KRPH (*Krebs-Ringer-Phosphate-HEPES*). Após 24 h de incubação em DMEM (*Dulbeco's Modified Medium*) foram adicionados os compostos inibidores e/ou o composto 2-NBDG (100 μM) ou 2DG (1 mM).

No caso do ensaio com 2-NBDG, após 30 minutos de incubação as células foram lavadas e foi extraído todo o seu conteúdo através da adição de uma solução de lise. A fluorescência gerada por 2-NBDG que foi absorvido pelas células foi medida a 528 nm após excitação a 485 nm. Através de uma curva de calibração com diversas concentrações de 2-NBDG foi possível calcular a quantidade (ng/poço) absorvido pelas células durante o ensaio.

Da mesma forma, no ensaio com 2-DG, após incubação com os compostos e/ou 2-DG foi adicionada uma solução de lise básica. Após uma incubação a 80 ºC a solução foi neutralizada e tamponada; foi adicionada uma mistura *cocktail* contendo diaforase, G6PDH, NADP, resazurina e alguns sais e a mistura foi incubada a 37 ºC por algumas horas após as quais foi medida a fluorescência produzida pela redução da resazurina a 590 nm após excitação a 560 nm.

Apesar de ambos os métodos terem sido otimizados o método escolhido para o estudo das propriedade inibidores dos compostos sintetizados foi o segundo método (2DG), por gerar resultados mais fiáveis e reprodutíveis.

Numa primeira triagem todos os compostos foram adicionados às duas linhas celulares estáveis (700B1-SGLT1 e 700A1-SGLT2) a uma concentração final de 100 μM e todos os compostos inibiram a captação de glucose quer pela proteína SGLT1 quer pela SGLT2.

Os valores de IC_{50} foram calculados nas mesmas condições mas usando diversas concentrações entre 0.1 nM e 200 μM. O composto florizina foi usado como controlo positivo para ambas as proteínas e o composto dapagliflozina foi utilizado como controlo positivo para SGLT2 e negativo para SGLT1. De acordo com os resultados obtidos, todas as *C*-glucosil di-hidrochalconas inibiram a proteína SGLT2 seletivamente, com valores de IC_{50} inferiores ao do composto florizina (< 67.3 nM) mas superiores ao do composto dapagliflozina (> 0.9 nM). Relativamente às agliconas chalconas e di-hidrochalconas não-glucosiladas estas não são inibidoras seletivas da proteína SGLT2 e, aparentemente poderão ser também inibidores das proteínas GLUT pois inibiram também a absorção de 2-DG na ausência de sódio (substituindo NaCl por cloreto de colina). As proteínas SGLT1 e SGLT2 são chamadas sódio-dependentes, ou seja, necessitam da presença de iões de sódio para fazer o transporte das moléculas de glucose para dentro das células. Contrariamente, as proteínas GLUT transportam glucose quer na presença quer na ausência de sódio e portanto são chamadas sódio-independentes.

Em conclusão, foi possível demonstrar que a C-glucosilação é de facto uma característica estrutural determinante para a bioactividade requerida, pois os derivados C-glucosilados sintetizados foram selectivos para SGLT2 e mais potentes que a florizina, uma di-hidrochalcona O-glicosilada e os compostos não glucosilados inibiram apenas parcialmente SGLT1 e SGLT2 e não foram selectivos para nenhuma destas proteínas. Relativamente à toxicidade exibida por estes compostos nas células HEK293, foi comprovado que as chalconas, di-hidrochalconas e aglíconas dos derivados C-glucosilados que possuem três grupos hidroxilo no anel A não são tóxicas, enquanto que as chalconas e as di-hidrochalconas possuindo um ou dois grupos hidroxilo no anel A apresentaram uma toxicidade significativa. Os resultados obtidos nesta tese justificam a futura otimização estrutural dos derivados C-glucosilados, de forma a obter compostos líder e candidatos a fármacos antidiabéticos derivados desta família de compostos que provou não ser tóxica às concentrações testadas.

Palavras-chave: Diabetes, SGLT1, SGLT2, *C*-glucosil di-hidrochalconas, absorção de glucose

Abstract

A small library of *C*-glucosyl dihydrochalcones and their aglycones, chalcones and dihydrochalcones, were synthesized aiming at preparing new C-glucosyl analogues of phlorizin, a well-known non-selective sodium-glucose co-transporter inhibitor, bearing different substituents on the dihydrochalcone moiety. Chalcones were prepared by conventional aldol condensation methods and also by microwave-assisted synthesis. The yields using the latter were relatively similar to those obtained by conventional methods (70-95%) but it was possible to decrease the reaction time from 24 to 1 h. Dihydrochalcones were obtained in 90-99% by *in situ* hydrogenation using the system Et_3SiH/Pd-C, a method that was used for the first time in this family of compounds, that revealed very promising and simple to run.

C-Glucosylation of dihydrochalcones was investigated with the catalyst TMSOTf and using 2,3,4,6-tetra-*O*-benzyl-α-D-glucopyranose as glycosyl donor, instead of a donor with a more effective leaving group at the anomeric position, e.g. trichloroacetimidate, to decrease the number of reaction steps. The *C*-glucosylation proceeded smoothly with yields ranging from 40-47% and the following debenzylation by *in situ* hydrogenation (80-98% yield) afforded the *C*-glucosyl dihydrochalcones.

Cytoxicity of chalcones, dihydrochalcones and *C*-glucosyl dihydrochalcones was evaluated in HEK293 cells and no significant toxicity was found for those compounds bearing three hydroxyl groups in ring A. Conversely, chalcones and dihydrochalcones bearing one or two hydroxyl groups on ring B showed significant cytoxicity in the same cell line.

Two stable cell lines were generated, HEK293-SGLT1 and HEK293-SGLT2, and the two stable clones showing the highest expression by Western Blot and RT-PCR were used to evaluate the inhibitory properties of chalcones, dihydrochalcones, and *C*-glucosyl dihydrochalcones as well as to determine their IC_{50} values towards SGLT1 and SGLT2 proteins. Results showed that chalcones and dihydrochalcones are able to partially inhibit SGLT1 and SGLT2 without showing significant selectivity towards with SGLT1 or SGLT2. On the other hand, *C*-glucosyl dihydrochalcones inhibit both SGLT1 and SGLT2 at 100 μM but showed a > 500-fold SGLT2 selectivity. IC_{50} of these molecules were much better

than those of phlorizin, but slightly worse than the commercial drug dapagliflozin. Nevertheless, changing from the *O*-glucoside phlorizin to its *C*-glucosyl analog, it was possible to increase its inhibitory ability as well its selectivity.

Keywords: Diabetes, SGLT1, SGLT2, *C*-glucosyl dihydrochalcones, glucose uptake

Chapter 1. Diabetes, prevention and treatments

1.1 Diabetes mellitus

Diabetes mellitus (DM) is a group of metabolic diseases in which hyperglycemia results from deficiencies in secretion or action of insulin or both.[1] Frequent urination, increased thirst and increased hunger are among the most common symptoms of diabetes. If not treated, it can cause many and severe complications such as diabetes ketoacidosis[a] and nonketotic hyperosmolar coma[b]. Cardiovascular disease, strokes, kidneys failure, foot ulcers and damage in the eyes are the most serious long-term complications of the disease.[2,3]

Around the world, ca. 387 million people have diabetes and the International Diabetes Federation (IDF) had estimate that this number will rise to 592 million by 2035, with 80% of cases occurring in low-income and middle-income countries such as the Middle East and North Africa. In 2014, 4.9 million people died due to diabetes and around 179 million people had diabetes. More than 79 thousand children developed Type 1 Diabetes (TDM1) in 2013 and more than 21 million pregnancies were affected by diabetes.[4]

Diabetes can de divided into different types according to defect type[5] (Table 1.1). Type 1 diabetes (TDM1) is characterized by the deficiency of insulin production by the pancreas and it is also known as “insulin-dependent diabetes”. This type of diabetes is more common in young children/teenagers but its cause it is still unknown and the treatment includes daily insulin injections. Type 2 diabetes occurs mostly due to insulin resistance, e.g., when the cells are unable to respond adequately to normal levels of insulin, especially in the muscles, liver and fat tissue. The pancreas generally produces more insulin in cases of insulin resistance, but after some time a degeneration of the beta cells occurs and insulin is no longer sufficient and effective. It is most common in adults, especially if there is a history of overweight/obesity and not enough exercise. Oral medications are normally used in this type of the disease. Another type of diabetes is

[a] Results from a shortage of insulin. The body burns fatty acids and produces acidic ketones which cause most of the
[b] High blood sugars cause severe dehydration, increases in osmolality and a high risk of complications, coma, and death

gestational diabetes, which occurs in pregnant women without a history of diabetes and generally resolves by itself after the birth.[1]

There are two others types of DM, though not so common. Prediabetes is characterized by high glucose levels, higher than the normal but not high enough to be considered as TDM2 (many type 2 diabetic people spend many years in this state before developing TDM2) and latent autoimmune diabetes of adults (LADA), is a type 1 DM that is developed while adult. Most of patients are misdiagnosed as type 2 diabetic.[4]

Table 1.1. Some major differences between TDM1 and TDM2

Feature	Type 1 Diabetes	Type 2 Diabetes
Onset	Sudden	Gradual
Age at onset	Childhood	Adulthood
Body type	Thin or normal	Overweight
Ketoacidosis	Common	Absent
Endogenous insulin	Low or absent	Normal, decreased or increased
Prevalence	~ 10%	~ 90%

The human body obtains glucose by intestinal absorption of this monosaccharide resulting from food digestion, breakdown of glycogen[c] and gluconeogenesis[d]. The hormone that regulates these three processes is insulin, which balances glucose levels. It is released by beta cells (β-cells), found in the islets of Langerhans in the pancreas, as a consequence of high glucose levels, especially after meals. If the glucose levels are low, a decrease in insulin occurs and glucagon acts by breaking down glycogen into glucose.[6] Consequently, diabetic ketoacidosis (DKA) will occur and, in response, the body starts to burn fatty acids, producing acidic ketone bodies (Figure 1.1) causing nauseas, dehydration, gasping breathing, confusion and coma. Treatment typically requires intravenous fluids to restore dehydration and insulin to suppress the production of these ketones. DKA was first described in 1886 and, until insulin's discovery in the 1920s, it was almost fatal in every cases. Nowadays mortality related to DKA is less than 1% if treated on time and adequately[6] but can be a serious life-threatening complication TDM1 patients.

[c] Storage form of glucose in the liver
[d] Generation of glucose from non-carbohydrate substrates

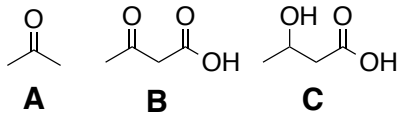

Figure 1.1 Examples of acidic ketone bodies. **A.** acetone; **B.** acetoacetic acid; **C.** beta-hydroxybutyric acid

Similarly, kidneys also play an important role, which consists in the reabsorption of glucose to maintain the blood glucose levels. Under normal conditions almost of the filtered glucose is reabsorbed and returned to the bloodstream in the proximal tubule. Sodium co-transporters (SGLTs) in concert with facilitative glucose transporters (GLUTs) are responsible for this process. However, if glucose concentration is too high the kidneys will reach a threshold of reabsorption and glucose is excreted in urine (glycosuria). This process will increase the osmotic pressure of the urine and promote the inhibition of water reabsorption by the kidneys leading to an increase of urine production (polyuria) and consequently dehydration and thirst (three of the most common symptoms in early stage of diabetes).[6]

1.2 Prevention

There are no known preventive measures for TDM1. This type of diabetes is partly inherited and can be triggered by one or more environmental factors such as a viral infection or diet. On the other hand, TDM2 can be prevented in most cases by healthy habits and a normal body weight[7]. Nevertheless, recent studies have combined genetic data from a large number of people and scientists have identified many gene variants that increase susceptibility to TDM2. These genes appear to affect insulin production rather than insulin resistance. An example is the variant of TCF7L2 gene (transcription factor 7-like 2)[e], which increases susceptibility to TDM2. For people who inherit two copies of the variant, the risk of TDM2 is about 80% higher that for those who do not carry this gene variant.[8]

[e] TCF7L2 is a transcription factor influencing the transcription of several genes thereby exerting a large variety of functions within the cell

1.3 Treatments

Type 1 diabetic patients are typically administrated a combination of regular and NPH[f] insulin as well as synthetic analogues. Conversely, TDM2 is treated with oral medications. Currently, there are several drugs available in the market, divided into 4 major classes: insulin sensitizers, insulin secretagogues, alpha glucosidase inhibitors and sodium-glucose co-transporters inhibitors. The first three classes will be discussed briefly and the latter will be discussed in more detail in Chapter 2.

1.3.1 Insulin sensitizers

1.3.1.1 Biguanides

The most used drug in this family is metformin (Scheme 1.1, C), which acts mostly at the liver by reducing glucose output and by augmenting glucose uptake in the peripheral tissues, especially muscles. Its safety profile, benefic cardiovascular and metabolic effects, and capacity to be associated with other antidiabetic agent make it the first-line drug when it comes to choosing a lowering agent to treat TDM2.[9]

The production of this drug is a very simple process. It was described for the first time in 1922 and involves the reaction of dimethylamine hydrochloride (**A**) and 2-cyanoguanidine (**B**).[10]

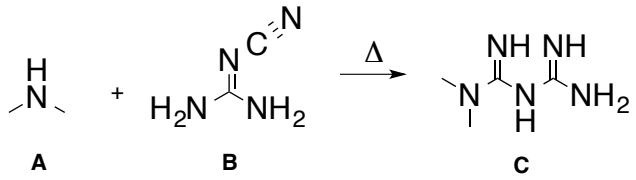

Scheme 1.1.Synthesis of metformin (**C**)

1.3.1.2 Thiazolidinediones

The thiazolidinediones (TZDs) or 'glitazones' (Figure 1.2) are a class of oral antidiabetic drugs that improve metabolic control in patients with type 2 diabetes through the improvement of insulin sensitivity. TZDs exert their antidiabetic effects through a mechanism that involves activation of the gamma isoform of the peroxisome proliferator-activated receptor (PPARγ)[g]. TZD-induced activation of PPAR gamma alters the

[f] Neutral Protamine Hagedorn insulin - long acting insulin given to help control the blood sugar level.
[9] Regulates fatty acid storage and glucose metabolism

transcription of several genes involved in glucose and lipid metabolism and energy balance, including those that code for lipoprotein lipase, fatty acid transporter protein, adipocyte fatty acid binding protein, fatty acyl-CoA synthase, malic enzyme, glucokinase and the GLUT4 glucose transporter. TZDs reduce insulin resistance in adipose tissue, muscle and the liver.[11] Generally, the insulin-sensitising effects occur in the skeletal muscle but TZDs seem to act in the free fatty acid supply from the adipocytes. Although there are still many unknowns about the mechanism of action of TZDs in type 2 diabetes, it is clear that these agents have the potential to benefit the full 'insulin resistance syndrome' associated with the disease.[12]

The most prescribed drugs in this class are rosiglitazone, pioglitazone, englitazone and troglitazone (Figure 1.2A-D),[13] specially when insulin resistance is present. There is evidence in animal models and in human studies that TZD treatment may preserve beta cell function, i.e. preserve the cells responsible for the production of insulin, which is the most beneficial effect of these drugs.[14] However, the most common side effects are the weight gain, fluid retention and oedema.[11]

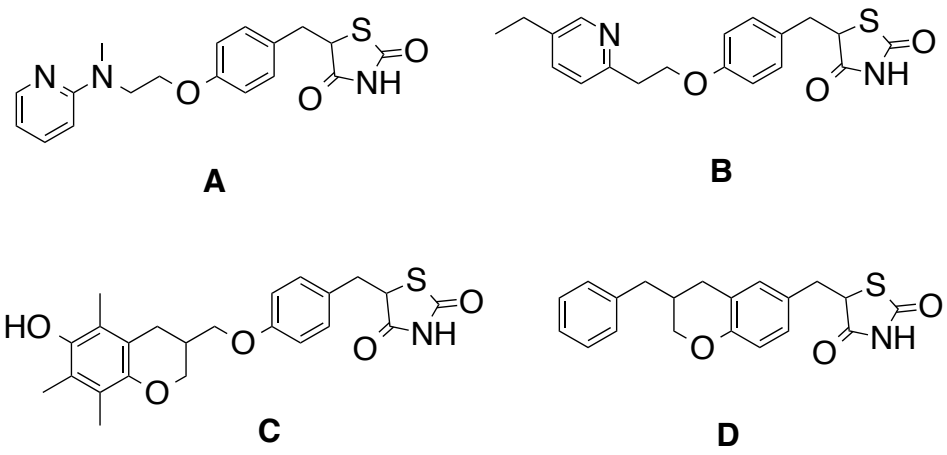

Figure 1.2 Structure of **A.** rosiglitazone, **B.** pioglitazone, **C**. englitazone, and **D.** troglitazone

1.3.2 Secretagoges

1.3.2.1 Sulfonylureas

This class of drugs binds to ATP-sensitive K^+ (K_{ATP}) channel on the cell membrane of pancreatic β-cells inhibiting a hyperpolarizing efflux of K^+, which causes electric potential over the membrane. This process of depolarization opens the Ca^{2+} channels

leading to an increase in intracellular Ca^{2+} promoting the fusion of insulin granule[h] with the cell membrane causing the secretion of proinsulin[15], which is the precursor of the insulin and C-peptide. After its synthesis, proinsulin is packaged into secretory granules, where it is processed to C-peptide and insulin by prohormone convertases (PC1/3 and PC2) and carboxypeptidase E. Only 1 to 3% of proinsulin is secreted intact.

In contrast to metformin, sulfonylureas (Figure 1.3) have several side effects especially hypoglycemia and weight gain. The first may occur if the dose is too high or if the patient is fasting and the second results from the increase in insulin levels.[15] There are three generations of these drugs. The first includes tolbutamide; the second one includes glipizide, glicazide and glibenclamide; and the third includes glimepiride (Figure 1.3A-E).

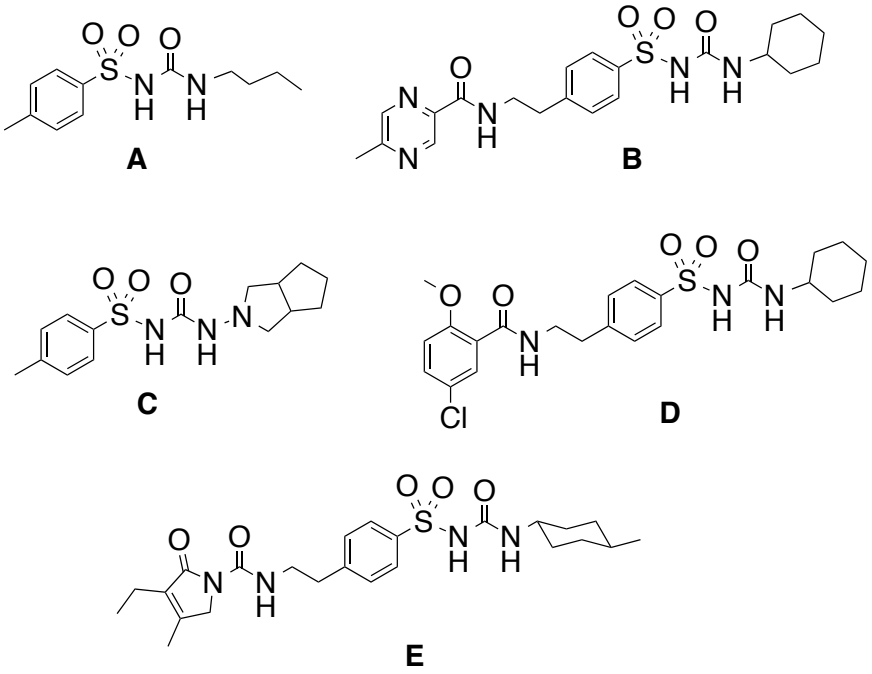

Figure 1.3 Structure of **A.** tolbutamide, **B.** glipizide, **C.** glicazide, **D.** glibenclamide, and **E.** glimepiride

1.3.2.2 Glinides

This family of drugs (Figure 1.4) represents a group of insulin-secreting agents characterized by their rapid onset and short duration of action. Their action is based on the closure of the ATP-dependent K^+ channel, in a manner similar to sulphonylureas.

[h] Secretory vesicle within the β-cell

According to several studies this class of drugs appears to be particularly useful in early stages of TDM2 and can be combined with metformin.[16] The three major drugs in this class are repaglinide, nateglinide, and mitiglinide (Figure 1.4A-C). The side effects include weight gain and hypoglycemia. The potential for hypoglycemia is lower than for those on sulfonylureas, but it is still a serious potential side effect.[16]

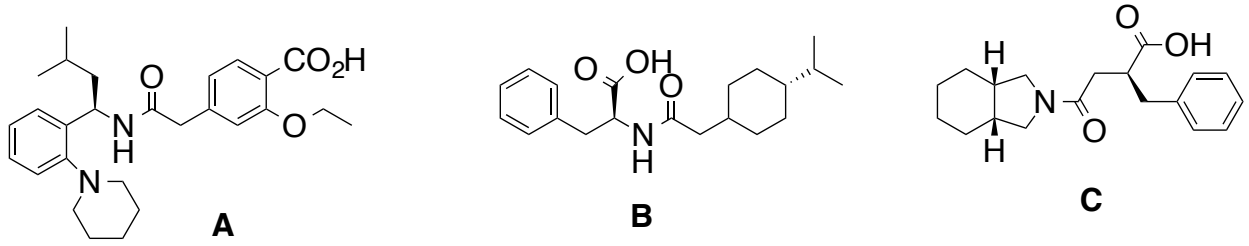

Figure 1.4 Structure of **A.** repaglinide, **B.** nateglinide, and **C**. mitiglinide

1.3.2.3 Glucagon-like peptide-1 agonist

Another important therapeutic approach was developed which targeted the incretin[i] system.[17,18] Some studies suggested that the incretin effect is severely reduced or lost in TDM2 patients. Augmentation of GLP-1 by the treatment with these drugs leads to an improvement of β-cell health in a glucose-dependent manner (post-prandial hyperglycemia) and suppression of glucagon (fasting hyperglycemia). The approved drugs are exenatide, liraglutide, lixisenatide and albiglutide. One advantage of these drugs is that the incidence of hypoglycemia is relatively low (except when combined with sulfonylureas), because their mechanism of action is glucose-dependent.[19] These drugs are normally prescribed for patients who have not been able to control their condition with tablet medication. However, its administration can result in side effects such as diarrhea, nausea, vomiting, increased sweating, and loss of appetite.

1.3.2.4 Dipeptidyl peptidase-4 (DPP4) inhibitors

The enzyme responsible for the degradation of incretin in the human body is the dipeptidyl peptidase-4. The inhibition of this enzyme originates an increase of incretin physiological activity, including the stimulation of insulin secretion and the inhibition of gastric emptying. The mechanism of action of these inhibitors is similar to the GLP-1 agonists.[20] Examples of drugs in this family are sitagliptin and vildagliptin (Figure 1.5A-B),

[i] Group of metabolic hormones that stimulate an increase of insulin released from pancreatic beta cells

among others. Adverse effects include nasopharyngitis, headache, nauseas, heart failure, hypersensibility and skin reactions.[20]

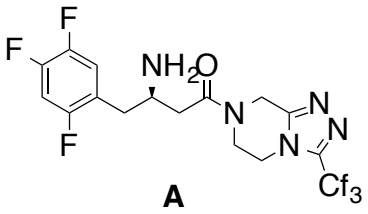

A

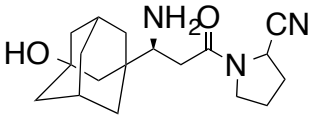

B

Figure 1.5 Structures of **A.** sitagliptin and **B.** vildagliptin

1.3.3 Alpha-glucosidase inhibitors

Alpha-glucosidase is an enzyme that hydrolyses terminal non-reducing 1-4 linked alpha-glucose residues, releasing single units of alpha-glucose. The inhibition of this enzyme is one of the most common methods used in diabetes therapy. Using alpha-glucosidases inhibitors, it is possible to delay the absorption of carbohydrates from the small intestine leading to a lowering effect on postprandial blood glucose and insulin levels.[21] These drugs have two major side effects: flatulence and diarrhea. These inhibitors prevent the degradation of complex oligosaccharides in glucose and, therefore the carbohydrates will remain in the intestines. Subsequently, bacteria in the gut degrade these molecules generating gases (e.g. oxygen, nitrogen, carbon dioxide, hydrogen, and methane). Nevertheless, starting the treatment with a small dose and increasing it is one way of avoiding these side effects. The three commercially available drugs from this family are acarbose, miglitol, and voglibose (Figure 1.6A-C).[21] Although the mechanism of action of acarbose and miglitol are similar, there are some differences between them. Stemming from the fact that acarbose is an oligosaccharide, whereas miglitol resembles a monosaccharide.[22,23]

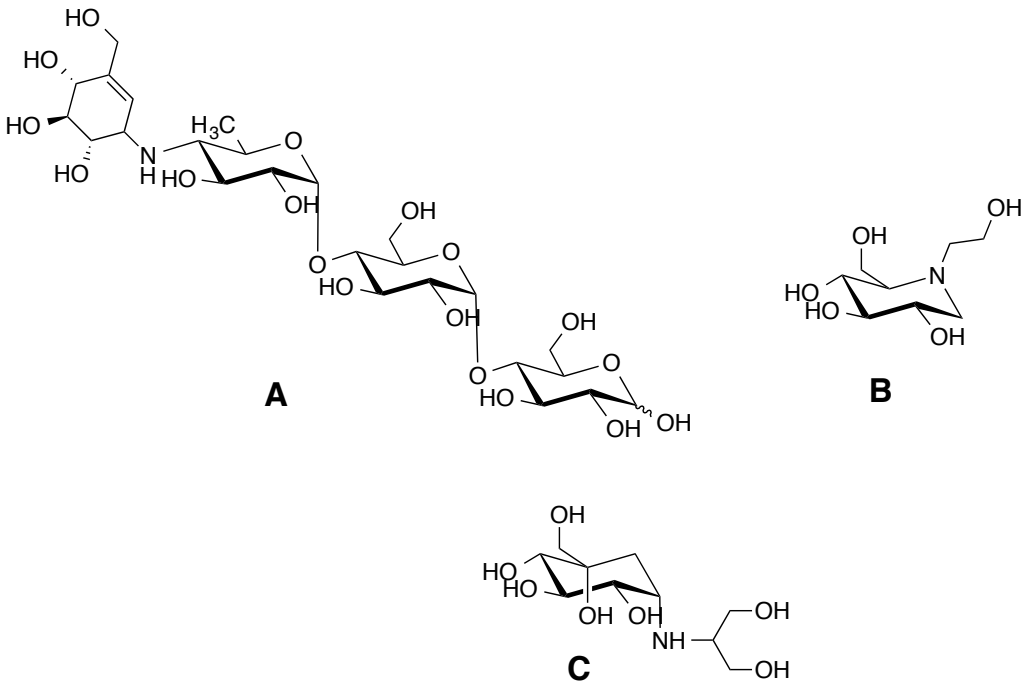

Figure 1.6 Structures of **A.** acarbose, **B.** miglitol, and **C.** voglibose

1.3.4 Sodium-glucose co-transporters inhibitors

As previously mentioned SGLTs are partly responsible for the reabsorption of glucose in the kidneys and intestines. However, when diabetes is developed, the kidneys reach a threshold of reabsorption and glucose is excreted in urine. Researchers found that inhibiting these SGLTs would be possible to decrease glucose blood levels and some SGLT inhibitors were developed. In this work new potential SGLT inhibitors were synthesized and were evaluated *in vitro*. Therefore, the characteristics, structure, physiology, properties, and the development of SGLTs inhibitors will be further discussed in Chapter 2.

In summary, diabetes is a metabolic disease characterized by high levels of glucose in the bloodstream. There are more than two types of diabetes but the most common are TDM1 and TDM2. Type 1 diabetic patients require daily injections of insulin, while type 2 diabetic patients need the administration of oral hypoglycemic agents. Taken together, the main strategy for treating TDM2 is to lower the levels of glucose in the circulation, which can be accomplished by either increasing the sensitivity of the insulin, increasing

its segregation, reducing the formation of glucose molecules by inhibiting the activity of the enzyme alpha glucosidase, or inhibiting the glucose reabsorption by the kidneys, which will be discussed in detail in the next chapter.

Chapter 2. Sodium-glucose co-transporter Inhibitors

2.1 Sodium-glucose co-transporters

2.1.1 General Characteristics of SGLTs

One of the characteristics of diabetes is the high levels of blood glucose; therefore, the control of plasma glucose level is of utmost importance in the treatment of this disease. The idea of inhibiting the glucose absorption in the intestine resulted in the development of inhibitors such as the alpha-glucosidase inhibitors (Chapter 1). However, more recently the inhibition of glucose reabsorption by the kidneys has gained more interest.[24-27]

The kidney plays a crucial role in controlling the body's energy. Glucose is filtered from the blood in the glomerulus and is reabsorbed by the kidneys. The average concentration of plasma glucose is ~5.5 mmol/L in normoglycemic[j] humans, the glomerular filtration rate (GFR) is 125 mL/min in adults. Approximately 180 g of glucose are filtered on a daily basis, with >99% being reabsorbed in the tubules, primarily in the proximal tubules[28-30] by a protein family called sodium-glucose co-transporters (SGLTs).

In diabetic patients, hyperglycemia can lead to hyperfiltration where the increased luminal glucose exceeds the maximal reabsorption rate, resulting in glucosuria[k]. This can lead to increased plasma glucose levels; therefore inhibition of renal reabsorption is a possible approach to resolving this problem.[31]

Glucose transportation is mostly mediated by two types of transporters namely sodium-glucose co-transporters (SGLTs, discovered by Robert Crane in 1960,[32,33] (Figure 2.1) and facilitative glucose transporters (GLUTs).

[j] Non-diabetic people
[k] Excretion of glucose through urine.

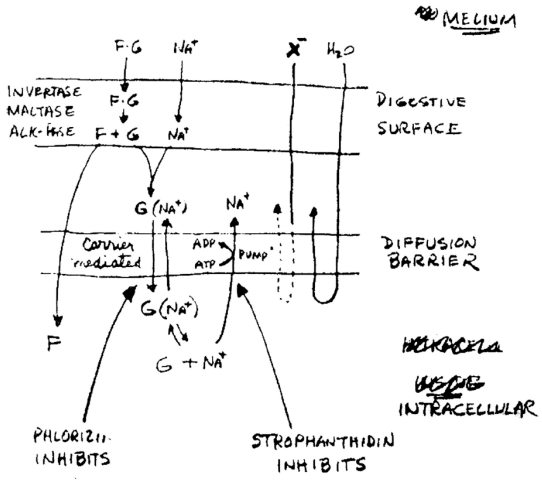

Figure 2.1 The co-transport model drawn by Crane on August 24, 1960 in Prague[33]

2.1.2 Human SLC5 Family

SGLTs are members of the solute carrier family[I] 5A (SLC5A) and there are six SGLT isoforms (Table 2.1)[31,34] but the two most well known are SGLT1 and SGLT2, both of them mainly involved in diabetes. These proteins are symporters, i.e. they are integral membrane proteins that are involved in movement of two or more different molecules or ions across a phospholipid membrane such as the plasma membrane in the same direction. SLGT3, however, is not a transporter but a sensor.[35,36] Other proteins from the SLC5 family were later discovered, the renal Na^+/myo-inositol (SMIT1),[37] the thyroid Na^+/iodine (NIS)[38] and the Na^+/multivitamin (SMVT).[32]

All members of the SLC5 family code for 60-80 kDa proteins, containing 596-681 residues. The organization of all 6 SGLT genes is quite similar with 15 exons, although their length can span from 8 to 72 Kbp (Figure 2.2).

[I] Group of membrane transport proteins

Table 2.1. Sodium-glucose co-transporters' isoforms

Gene	Protein	Substrate	Localization
SLC5A1	SGLT1	Glucose and galactose	Small intestine, heart, trachea and kidney
SLC5A2	SGLT2	Glucose	Kidney
SLC5A3	SGLT3	Glucose sensor	Small intestine, uterus, lungs, thyroid and testicles
SLC5A4	SGLT4	Mannose, glucose, fructose and 1,5-anhydroglucitol	Small intestine, kidney, lung, liver
SLC5A5	SGLT5	Fructose, mannose	Kidney
SLC5A6	SGLT6	*Myo*-inositol, xylose and *chiro*-inositol	Spinal cord, kidney, brain and small intestine

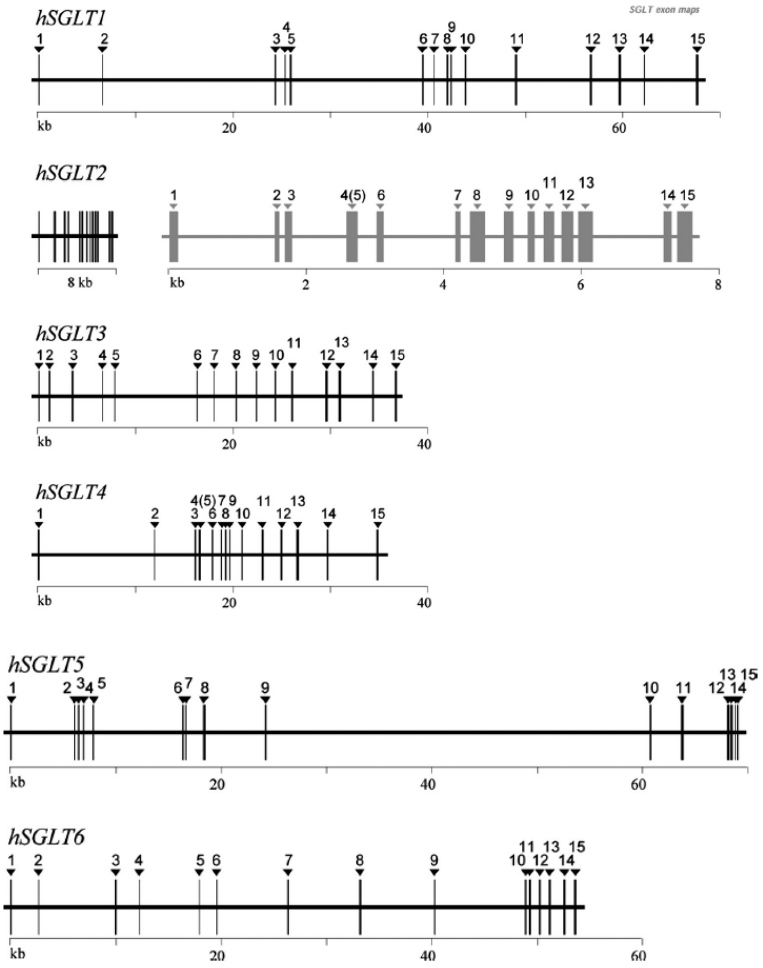

Figure 2.2 Organization of human SGLT1-6 genes.

Western blot has been used to map SGLT expression in human cells and tissues. Interestingly, membrane proteins run faster on SDS-PAGE gels than what would be based on their molecular weight. The bands are broad, presumably due to incomplete denaturing of membrane proteins by SDS. The molecular weight of these proteins can vary from 69 to 79 kDa depending on the different degree of glycosylation. SGLT1 was identified in mouse intestinal brush border membrane by Western blot using two different antibodies (Figure 2.3).[33]

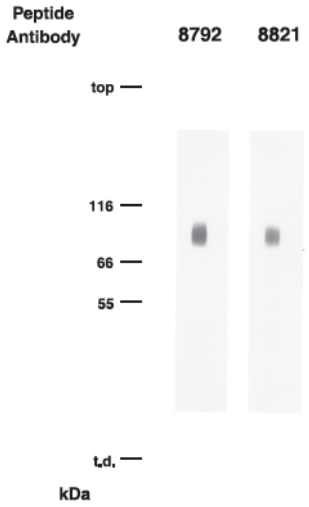

Figure 2.3 Western blot of mouse intestinal brush border membranes[29].

Relative to human SGLT1, there is 50-70-% identity and 67-84% similarity in the sequences for the remaining SGLTs (2-6). The main divergence in the sequence occurs at the extracellular NH_2-terminal domain and the COOH-terminal third of the proteins.[32]

Regarding the secondary structure of these proteins the amino acid sequence of hSGLT1 superimposed on a 14-transmembrane helix model as represented in Figure 2.4.[33] The crystal structure of human SGLTs is unknown but one from the grape vine, *vitis vinifera* is known (Figure 2.5).

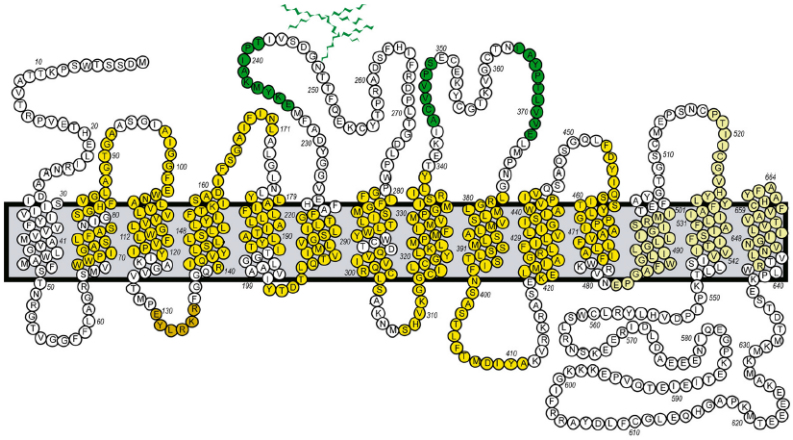

Figure 2.4 Secondary structure model of SGLT1 (Highlighted are the locations of the helical domains based on the vSGLT structure)[26]

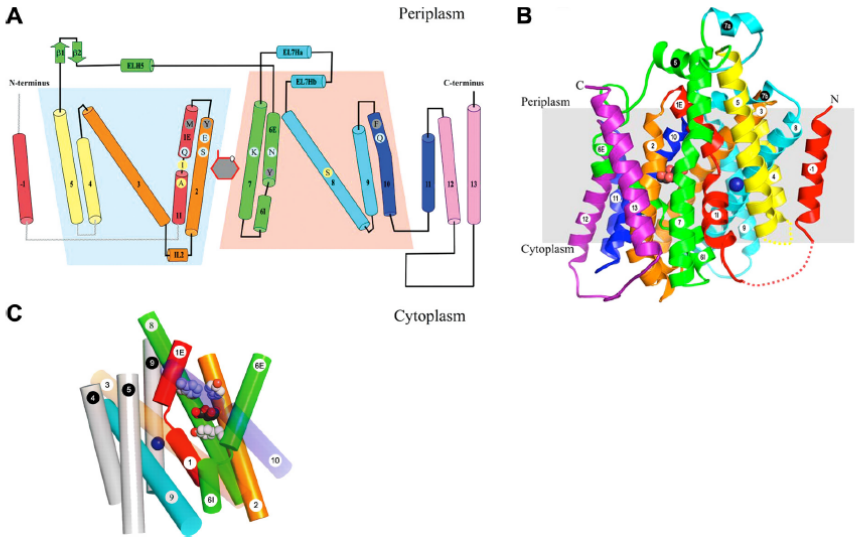

Figure 2.5 Struture of vSGLT. A: topology model; B: side view of the 3D structure viewed from the membrane plane. The sugar binding site is located on the black and red spheres; C: ligand biding sites in vSGLT. Overview of the galactose and sodium binding sites[33]

2.1.3 Mechanism of SGLTs

Glucose is a polar molecule; therefore, to cross lipid-rich cell membranes, it requires a membrane-associated carrier protein's active transport (SGLTs). These proteins transport a glucose molecule against a concentration gradient into cells by coupling the "uphill" transport of sugar across the cell membrane with the "downhill" transport of sodium. SGLT1 is able to transport two molecules of glucose with one sodium ion, while SGLT2 transports only one glucose molecule with one sodium ion.[39] The ability of these

proteins to accumulate sugar is highly dependent on the stoichiometry of the Na^+ and sugar fluxes.

The stoichiometry of SGLT1 was determined in 1998 by Wright *et al* [40] by measuring the currents and radioactive tracer fluxes into single oocytes expressing rabbit SGLT1. In Figure 2.6A is represented the measurement of the current in the absence of the sugar (α-D-methylglucopyranoside, αMDG) and radioactive tracer (2 min baseline) and after the addition of both for 10 minutes. The integrated sugar-induced currents (charge expressed in moles) are plotted against the ^{22}Na uptakes is shown in Figure 2.6B, with a slope of 1.0 ± 1.0 s^{-1}. This means that the sugar-induced current is exclusively a Na^+ current. The same experiment was performed measuring the currents upon the uptake of different concentrations of αMDG (Figure 2.6C) over 10 minutes. The slope for this was 1.6 ± 0.3 s^{-1}; therefore the αMDG to Na^+ ratio is 1:1.9. However, for SGLT2 the αMDG to Na^+ ratio is 1:1, using the same methodology.

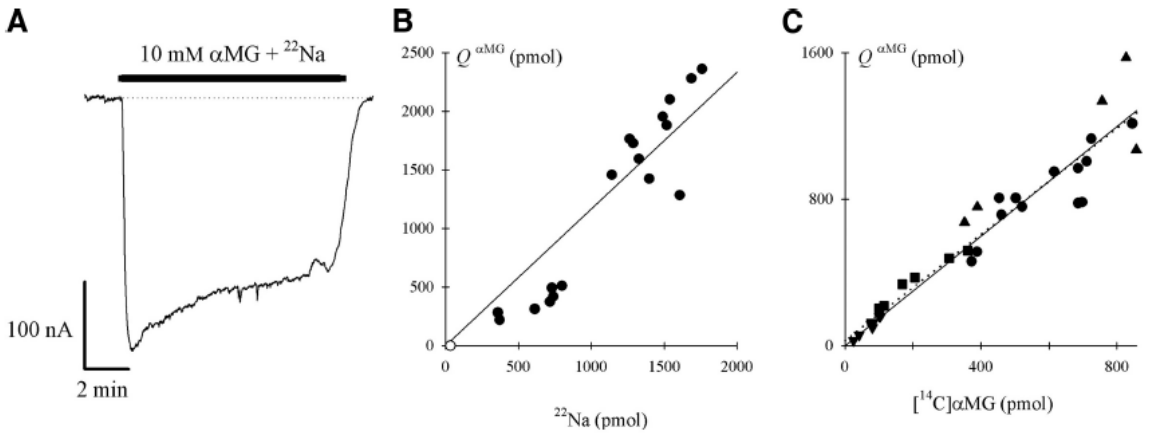

Figure 2.6 Determination of the stoichiometry of SGLT1. **A**. Measurement of the current changes by the addition of sugar and radioactive tracer; **B.** Measurement of the integrated sugar-induced currents against the ^{22}Na uptake; **C**. Measurement of the integrated sugar-induced currents against the αMDG uptake[40]

The mechanism of transport of glucose is based on the model described by Schultz in 1985, from the cell illustrated in Figure 2.7. The states 1-3 face outward and 4-6 faces inward. At first (state 1), the unloaded negatively charged carrier has low affinity for external sugar before sodium binds. After sodium and sugar binding, the carrier changes its conformational form to present sodium and sugar binding sites to the cytoplasm where

they are released. A further conformational change (state 6) is required to reexpose the binding sites to the external surface of the membrane.[33]

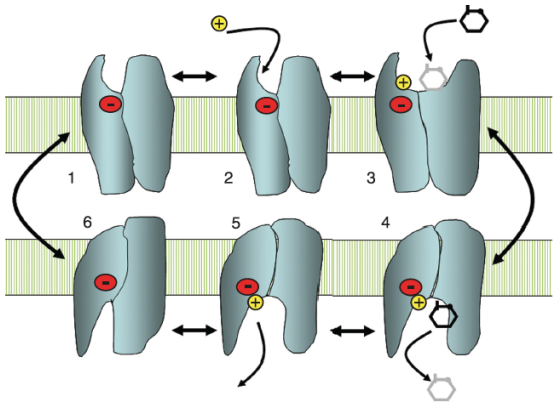

Figure 2.7 Mechanical model for Na^+-coupled sugar transport.[33]

2.1.4 Role of SGLT1 and SGLT2 in the kidneys

The two isoforms that transport glucose and are located in the kidney are SGLT1 and SGLT2. The inhibition of these proteins leads to a decrease in glucose reabsorption. This fact has gained interest in the scientific community and efforts to develop SGLTs inhibitors have been made.

SGLT2 and SGLT1 are expressed in the luminal membrane of the early and late proximal tubule (Figure 2.8a/b), respectively. SGLT2 is responsible for ~97% of the reabsorption of glucose while SGLT1 is only responsible for ~3% in normoglycemia. However, SGLT2 inhibition induces glucosuria only after the glucose reabsorption capacity of SGLT1 is fully saturated.[30,41] Hyperglycemia increases the expression of SGLT2 possibly because the increase of angiotensin II (AngII), hepatocyte nuclear factor HNF-1α, and/or tubular growth. Increased SGLT2 expression enhances glucose and Na^+ reabsorption in the proximal tubule, and glucose enters the blood stream through basolateral GLUT2 (Figure 2.8c).[30]

Mutations on the gene encoding SGLT1 lead to malabsorption of glucose and galactose, whose intestinal absorption is mediated by this protein. On the other hand, mutations on the gene encoding SGLT2 results in persistent renal glycosuria but can also originate some adverse effects such as genitourinary, including frequent urination, discomfort with urination, and vaginal or penile mycotic infections.[42]

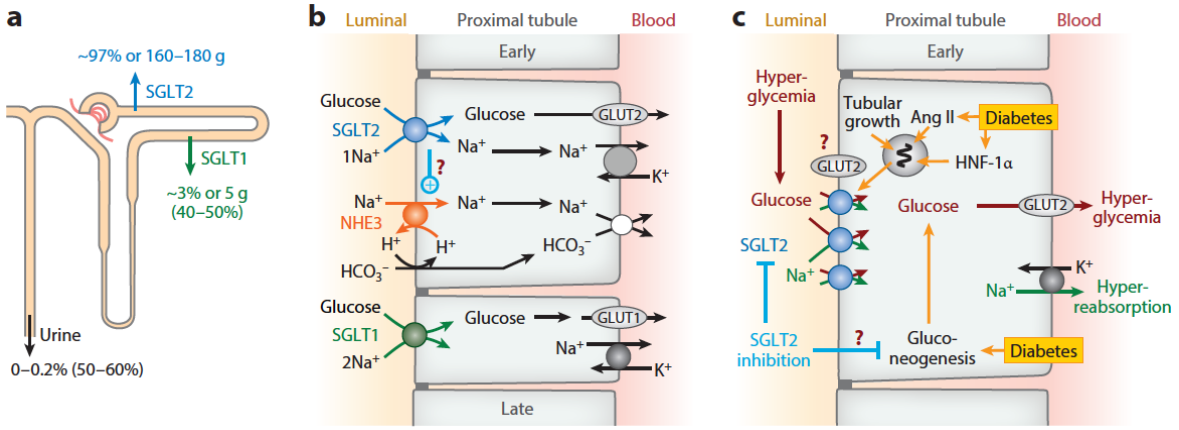

Figure 2.8 Reabsorption of glucose in proximal tubules by SGLT1 and SGLT2. **a/b**. Expression of SGLT1/SGLT2. **c**. Increase of renal membrane expression of SGLT2 with hyperglycemia[30]

2.2 Sodium-glucose co-transporters inhibitors

2.2.1 Phlorizin and SGLTs

Phlorizin, a dihydrochalcone glucoside (Figure 2.9), was first isolated from the bark of the apple tree in 1835 by French chemists. The Merck index of 1887 lists phlorizin as a "Glycosid aus der Wurzelrinde des Apfelbaumes" ("glycoside from the bark of apple trees"). Later editions of the Merck Index noted that phlorizin in doses greater than 1.0 g produces glucosuria, encouraging scientists to investigate this compound and its properties. After some studies in animals, researchers confirmed that phlorizin was able to lower blood glucose levels by glucosuria.[43]

In the 1950s, it was found that phlorizin at concentrations ranging from 0.1 mM to 1 µM was able to block the transport of glucose in both kidney and intestine[39]. Later, it was discovered that phlorizin originates serious adverse effects in the gastrointestinal tract like diarrhea and dehydration (due to malabsorption of galactose) because it inhibits both hSGLT1 and hSGLT2 (K_i = 200-300 nM and K_i = 10-39 nM, respectively). SGLT1 also transports galactose; thus, inhibiting this protein causes an inhibition of both glucose and galactose absorption. For this reason, phlorizin was not suitable for clinical trials. Nevertheless, these studies were very useful in the development of new potential candidates, especially SGLT2 inhibitors.

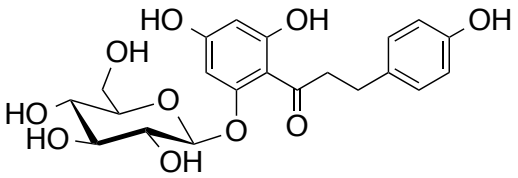

Figure 2.9 Phlorizin

As showed in Figure 2.2 SGLT1 and SGLT2 are 59% identical[m] (sharing the same 15 exons, although SGLT2 is only 8 Kbp compared with 50 Kbp of SGLT1). How, then, is it possible to produce a selective SGLT2 inhibitor?

2.2.2 Development of SGLT inhibitors

As mentioned before, phlorizin is a nonselective SGLT inhibitor with poor oral bioavailability but with a high affinity towards SGLT2 (~ 400 nM). Over the years many pharmaceutical companies have exploited this problem by modifying the phlorizin structure to enhance selectivity. One example is T-1095A (Figure 2.10B), which is absorbed as a methyl carbonate (Figure 2.10A) and then is metabolized into its active form. This drug is absorbed without interacting significantly with the intestinal SGLT1 and the active form had a fourfold increase in SGLT2/SGLT1.[33,44] However it did not proceed to clinical trials due to its poor bioavailability.

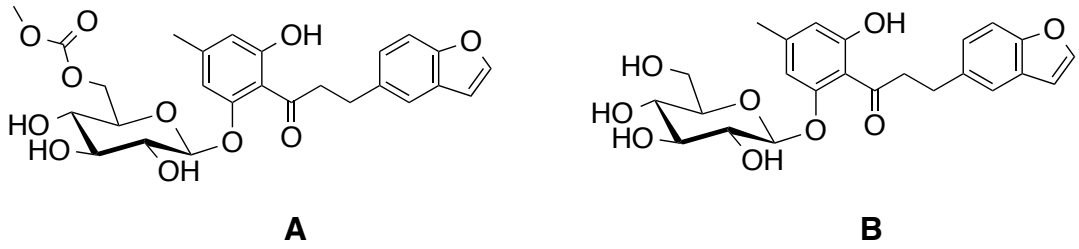

A **B**

Figure 2.10 Structure of **A.**T-1095 and **B.** T-1095A

This compound, however, encouraged the search for new molecular entities with higher potency, selectivity, and oral bioavailability by adding various substituents to the aglycone. The major change consisted on the replacement of *O*-glucosides by their

[m] Sequence identity is the amount of characters which match exactly between two different sequences

C-glucosyl analogs, which have higher resistance to endogenous enzymes, leading to an increased half-life and duration of action.

In 2012 Powell *et al*[45], from Lexicon Pharmaceuticals, reported a randomized, placebo-controlled trial using a compound, LX4211, with a dual SGLT1/SGLT2 inhibitory activity. SGLT1 is also expressed on L cells and K cells[n], particularly in the small intestine. These cells secrete the incretin glucagon-like peptide 1 (GLP-1) and glucose-dependent insulinotropic peptide (GIP)[o], respectively, in response to ingested glucose. The incretins act on pancreatic β cells to increase insulin release in a glucose-dependent manner.[30,46] Some studies on *SGLT1*$^{-/-}$ mice with phlorizin suggested that SGLT1 in the proximal small intestine serves as the intestinal glucose sensor for the acute (within 5 minutes) glucose-induced incretin secretion.[30,45,47] Studies also provided evidence that the inhibition of SGLT1 (in mice and healthy humans) and consequent increase of glucose into the more distal gut and colon induced a sustained increase of circulating GLP-1 for up to 6 hours.[45,47,48] The most remarkable fact on these studies using dual SGLT1/SGLT2 inhibitors was that there was no evidence of increased gastrointestinal side effects, which were expected to result from to SGLT1 inhibition.[45] LX4211 is currently at Phase 2 of clinical trials and this achievement is a great breakthrough since so far researchers have looked only for SGLT2-selective inhibitors.

For the last couple of years several glycosides with different aglycones were developed as SGLT inhibitors. Some of them are illustrated in Figure 2.11.

[n] L cells and K cells are enteroendocrine cells, specialized endocrine of the gastrointestinal tract and pancreas, that produce gastrointestinal or peptides

o Also called gastrointestinal inhibitory peptide or gastric inhibitory peptide and was found to decrease the secretion of stomach to protect the small from acid damage, reduce the rate at which food is transferred through the stomach, and inhibit the GI motility and secretion of acid

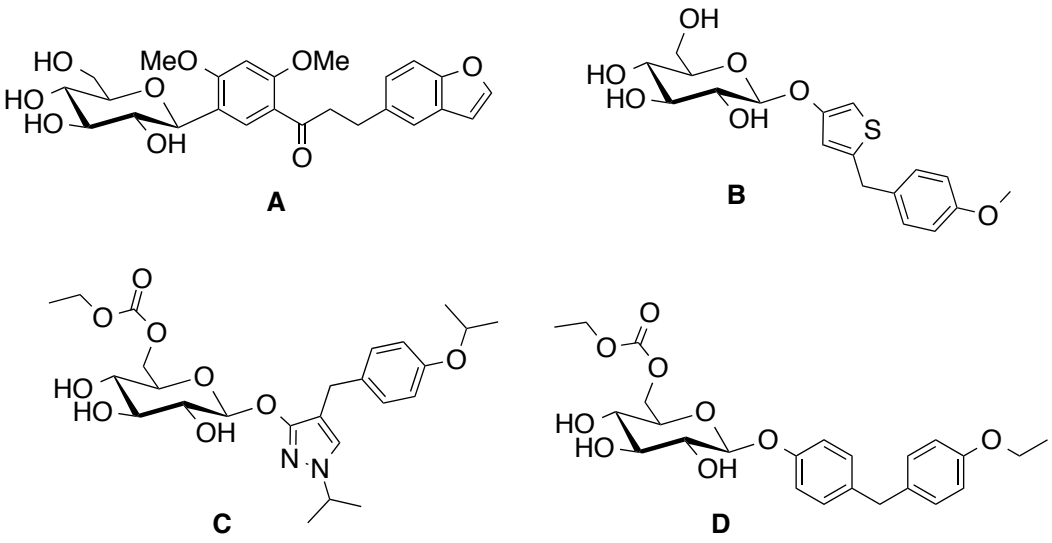

Figure 2.11 Some new SGLT inhibitors of synthetic origin

Table 2.2 - Sodium glucose co-transporters in advanced development or already approved[49]

Molecule	Approval/development status
Canagliflozin (A)	40 countries including EU, USA, China, Russia
Dapagliflozin (B)	40 countries including EU, USA, Japan,
Empagliflozin (C)	Phase 3
Ipragliflozin (D)	Japan
Luseogliflozin (E)	Under review for approval in Japan
Tofogliflozin (F)	Phase 3

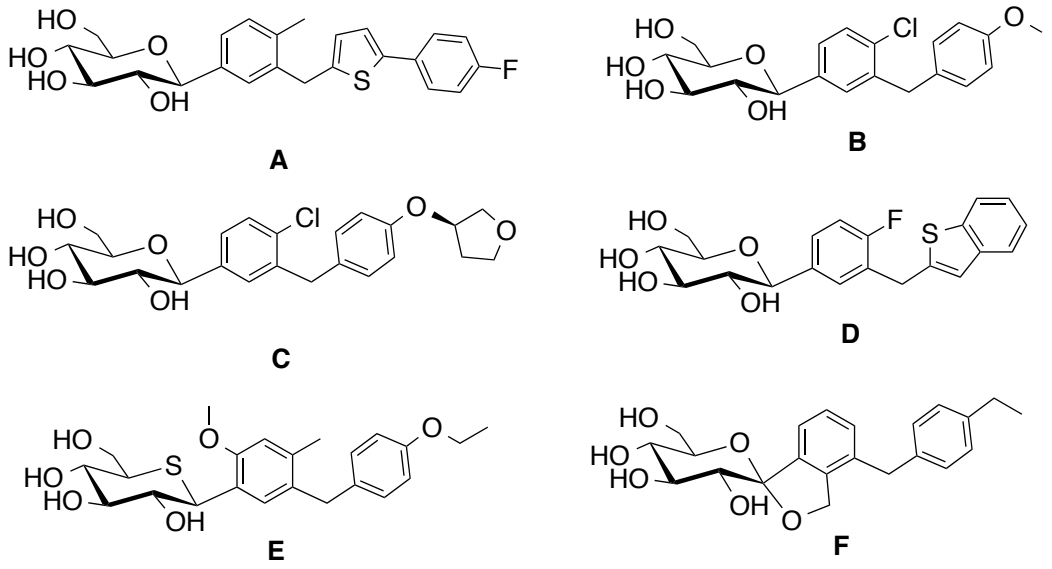

Figure 2.12 Structures of sodium-glucose co-transporters in advanced development or already approved

After some years of research, FDA approved a few drugs and some of them are already in the market while other compounds are in phase 3 of clinical trials (Table 2.2 Figure 2.12).

Canagliflozin and dapagliflozin were the first SGLT inhibitors to be approved. Their safety and efficacy has received the attention in the past year. According to these studies these two drugs are considered safe although long-term safety remains unknown. Both drugs present communal adverse effects such as urinary tract infections, renal-related adverse events, and adverse events related to volume depletion, documented hypoglycaemia episodes, female genital mycotic infections, and nasopharyngitis.[50,51] New drugs with fewer adverse effects are still needed.

There are no records that the *C*-glucosyl derivative of phlorizin acts either as SGLT1 or SGLT2 or as dual inhibitor. Hence, the purpose of this work was to develop a variety of new *C*-glucosyl dihydrochalcones and evaluate their inhibitory properties. The synthesis of these types of compounds will be discussed in Chapter 3.

2.2.3 Protective effects of SGLT inhibitors on the kidneys and cardiovascular system

The primary consequence of diabetes is the chronic kidney disease (CKD), and the combination of CKD and hyperglycemia increases the risk of cardiovascular diseases. Diabetic kidney growth and its contribution to senescence have been linked to diabetic nephropathy. Knockdown of SGLT2 in STZ/diabetic mice lowered blood glucose levels but did not limit the rise in kidney weight or markers of kidney growth, inflammation, and injury after 4.5 months, indicating that SGLT2-mediated glucose reabsorption itself is not critical for these changes.[52] The SGLT2 inhibitor empagliflozin however induced a stronger blood glucose-lowering effect in mice. It did not prevent kidney growth but it strongly attenuated it and reduced molecular markers of renal growth and inflammation when compared to hyperglycemia.[47] Another inhibitor, luseogliflozin, was able to reduce the degree of glomerular injury, renal fibrosis, and tubular necrosis.[53] These results suggested that SGLT2 inhibition induces a reduction of all these factors, despite a high glucose load on the early proximal tubule.

2.2.4 Screening Methods

The activity of SGLTs has been evaluated using different methodologies; including transport assays with radioactively labeled sugars in brush border membrane vesicles and transiently or stably transfected cells.[54-58] Voltage-clamp techniques have yielded interesting and important details regarding the mechanisms underlying the binding and translocation reactions of the transporter[59] as described in section 2.1.3.

Methods using radioactive labeled substances are expensive due to the amount of the radioactive compound and also require a certain expertise handling these materials. Therefore, methods using fluorescent probes (section 2.2.4.1) or using an enzymatic reaction (section 2.2.4.2) were developed to avoid the problems with waste disposal and safety from radioactive methods.

2.2.4.1 Fluorescent probes for direct glucose uptake measurement

Prior to the development of fluorescent-tagged glucose bioprobes, radioisotopically tagged sugars were used for the measurement of glucose uptake by cells. The most common radiolabeled tracers include [^{14}C] 2-deoxy-D-glucose, [^{18}F] fluoro-2-deoxy-D-glucose (FDG), and [^{14}C] or [^{3}H] 3-methyl-D-glucose. FDG is still used as non-invasive tool for monitoring glucose uptake and FDG-PET is routinely used for brain mapping or cancer diagnosis.[60]

6-(*N*-(7-Nitrobenz-2-oxa-1,3-diazol-4-yl)amino)-2-D-deoxyglucose (6-NBDG) (Figure 2.13A) was developed in 1985 and was the first fluorescent glucose derivative developed to probe the behavior of glucose transport systems.[61,62] During the development of this fluorescent probe, fluorophore 7-nitrobenz-2-oxa-1,3-diazol-4-yl (NBD) was selected because of its relative strong fluorescence and the C-6 position of 2-deoxyglucose was preferred because it can not be phosphorylated.[62] A study in red blood cells showed that 6-NBDG can enter the cells, but its uptake is inhibited by D-glucose. This indicated that 6-NBDG entered the cell through glucose transporters (GLUTs).[62] This was further validated by showing that the entrance was also inhibited by cytochalasin B, a mycotoxin and high affinity GLUT inhibitor that disrupts actin polymerization.[63] However, 6-NBDG enters the cell with a much lower rate (V_{max}) than glucose.[60] After compound

commercialization by two companies, research involving this probe was quite scarce (only four reports were published over nine years).

In 1996, a group from Tokyo (Japan) was interested in monitoring bacteria viability and metabolic events. The probe 6-NBDG could not be use due to the substituent NBD in position 6 that would inhibit the phosphorylation pathway. Therefore, the NBD group in position C-2 would be a much better choice for their studies and would allow phosphorylation by hexokinase and subsequent degradation to non-fluorescent metabolites. 2-NBDG (Figure 2.13B) was found to accumulate in live cells but not in dead cells and, similarly to 6-NBDG, its uptake was inhibited by D-glucose but not by L-glucose.[60]

A follow-up study regarding the intracellular fate of 2-NBDG revealed that this compound is phosphorylated after uptake, producing a fluorescent derivative, 2-NBDG-6-phosphate, by hexokinase, which is converted back into 2-NBDG by glucose 6-phosphatase and finally degraded into non-fluorescent products by the glycolytic pathway.[64,65] In the same year 2-NBDG was validated as an indicator of cell viability.[66]

In the last few years a large number of publications report the use of 2-NBDG to validate novel anti-diabetic compounds with similar effects as the hormone insulin, *i.e.*, the promotion of glucose uptake in insulin-sensitive cells, such as adipocytes and skeletal muscle cells.[67-72] In cancer research, 2-NBDG has been playing a significant role on targeting cell metabolism to develop cancer drugs and monitoring glucose uptake in cancer cells (the Warburg effect[p]).[73-75] Potential clinical applications for 2-NBDG have also been developed as a tracer for cisplatin treatment in ovarian cancer.[76]

In 2010, another research group successfully synthesized and tested 1-NBDG as a glucose probe. When used well-known inhibitors were used they obtained similar results to those so far published.[77] Nevertheless, some issues concerning the use of NBDG glucose probes still remain. One example is the kinetic behavior of these tracers, *e.g.* NBDG permeates the cell 50-100 times slower than glucose, which means that the NBDG uptake can be easily inhibited by glucose.[78] Hence, to quantify the cellular glucose

[p] The Warburg effect is the observation that most cancer cells predominantly produce energy by a high rate of glycolysis followed by lactic acid fermentation in the cytosol, rather than by a comparatively low rate of glycolysis followed by oxidation of pyruvate in mitochondria as in most normal cells

uptake in specific cases other methodologies, such the indirect method using the enzymatic assay, must be used.

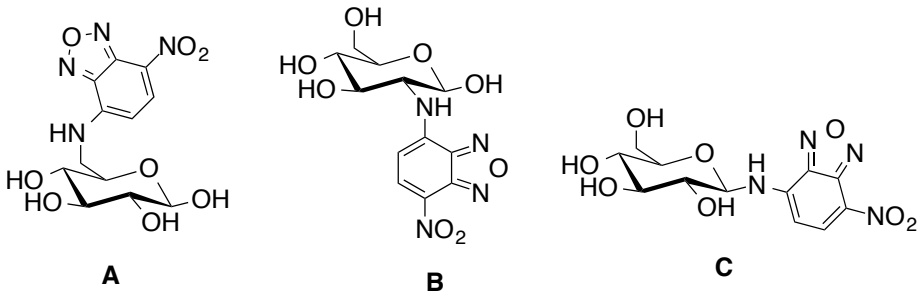

Figure 2.13 Structures of **A**. 6-NBDG, **B**. 2-NBDG, **C**. 1-NBDG

2.2.4.2 Enzymatic assay for glucose uptake measurement

2-Deoxyglucose (2DG) and glucose are similarly transported into the cells and are phosphorylated by hexokinases. However, 2-deoxyglucose 6-phosphate (2DG6P) cannot be either converted to an analogue like fructose 6-phosphate, or rapidly metabolized like glucose. Therefore, after 2DG passes through the cell membrane it is completely phosphorylated and accumulated inside the cell providing a measurement of glucose consumption.[79]

In 1987 Lowry *et al*[79] reported sensitive enzymatic methods for the measurement of 2DG and 2DG6P as well as glucose and glucose 6-phosphate (G6P) in the same tissue sample. These methods are based on the fact that both G6P and 2DG6P can be oxidized by G6P dehydrogenase (G6PDH). The NADH or NADPH produced indicated the relative amount of sugar. Higher levels of G6P and 2DG6P can be measured using of NADPH, which absorbance can be read at 390 nm or fluorescence at 470 nm. However, the weak fluorescence of NADPH and the interference from other autofluorescent biological molecules does not allow the direct measurement of lower levels of NADPH (detection limit ~ 3 μM).[79-81]

Methods to increase the sensitivity of the enzyme immunoassays have been developed (e.g. amplification detection systems) and are based on the addition of an enzyme that produces a catalytic activator for a secondary system, which amplifies the detectable change. An example is the diaphorase-rezasurin system (Scheme 2.1).[82-85] This system has been successfully applied in cell quantification of glucose, G6P, 2DG,

and 2DG6P. In these assays NADPH reduces the weakly fluorescent dye resazurin to the highly fluorescent resofurin in the presence of diaphorase. As the emission peak of resofurin is around 570 nm the autofluorescence from biological samples is negligible.[81] The reaction mixture includes ATP, $NADP^+$, hexokinase, G6PDH, diaphorase and rezasurin. However, to measure 2DG6P alone, ATP and hexokinase can be left out and the amount of resofurin should be equal to the amount of 2DG6P, which is also proportional to the amount of 2DG that was phosphorylated upon entry on the cell.[85] Other recycling systems can be used in this assay such as the glutathione-DTNB[q] system,[86] with the same principle.

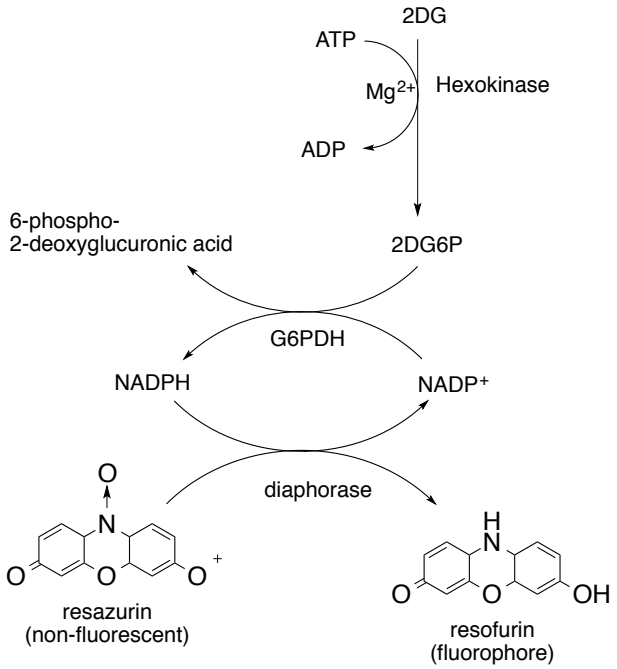

Scheme 2.1. Principle of the assay for measuring 2DG and/or 2DG6P.

In summary, glucose is transported by SGLT1 and SGLT2 in the kidneys and intestines. SGLT1 inhibition can lead to severe side effects in the gastrointestinal tract; but the inhibition of SGLT2 can provide benefits for diabetic patients, lowering their plasma glucose levels by glucose excretion through the urine. Phlorizin was the first SGLT inhibitor and it helped, throughout the years, the development of new selective SGLT2 inhibitors. The assessment of new SGLT2 inhibitors can be accomplished by a

[q] 5,5′-dithiobis(2-nitrobenzoic acid)

variety of methods including radioactive analogs, fluorescent probes, and using an enzymatic assay to quantify indirectly the amount of glucose taken up by the cells.

Despite the fact that some compounds have already been approved by FDA and are already being commercialized some studies regarding they long-term safety are required to fully understand the outcomes in patients with normal or impaired kidney function and to clarify the potential benefit and relevance of compounds with additional SGLT1 inhibition.

Chapter 3. Synthesis of *C*-glucosyl dihydrochalcones

3.1 Synthesis of chalcones and dihydrochalcones

Chalcones and dihydrochalcones are a class of polyphenols constituted by two aromatic rings as illustrated in Figure 3.1, linked by the a C3 chain containing an α,β-unsaturated carbonyl functionality (chalcones), as shown in structure-type **A**, while dihydrochalcones (structure-type **B**) the three carbon atom chain linking both aromatic rings does not embody a double bond.

In the literature, synthesis and biological activities of chalcones are very well documented. Some examples of chalcones biological properties are antimalarial,[87,88] anticancer,[89-92] antibacterial,[93] anti-obesity,[94] antidiabetic,[95] and antioxidant.[94] They have also been reported as PET probes for *in vivo* imaging of β-amyloid plaques in Alzheimer's disease.[96]

The most common method to synthesize chalcones is based on aldol condensation under basic conditions which mechanism is shown In Scheme 3.1. Other renowned techniques for chalcone preparation include the Suzuki reaction,[97] the Heck reaction,[98] the Wittig reaction,[99] or organometallic-catalyzed reactions.[100] These techniques employ several catalysts and reagents, some expensive, toxic or explosive, such as $SOCl_2$,[101] lithium nitrate,[102] zeolites,[103] zinc oxide,[104] or silica-supported materials.[105] The main disadvantage of these methodologies is the fact that they require the preparation of starting compounds prior to the aldol condensation itself. Two examples are the pre-preparation of the corresponding boronic acid for the Suzuki reaction or the ylide for the Wittig reaction. Most boronic acids are unstable in air atmosphere and need to be used right after their preparation or to be prepared *in situ*.

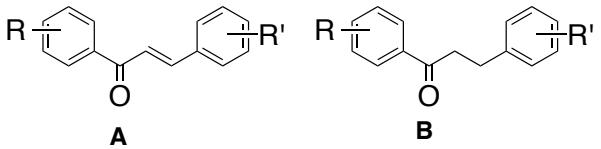

Figure 3.1 General structure of **A.** chalcones and **B.** dihydrochalcones.

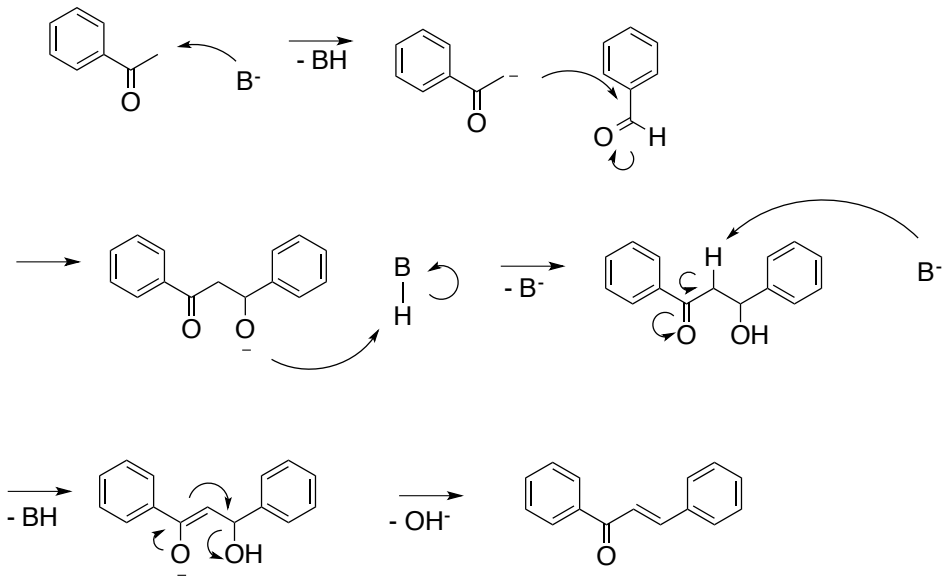

Scheme 3.1 Mechanism of a basic aldol condensation for the synthesis of chalcones

In nature, di-hydrochalcones are often glycosylated. The most well-known di-hydrochalcone glycosides are narigenin dihydrochalcone (Figure 3.2A), neohesperidin dihydrochalcones (Figure 3.2B), and phlorizin (Figure 3.2C). However, a natural non-glycosylated dihydrochalcone, found in apple trees and other tree barks[39] is phloretin (Figure 3.2D). A natural *C*-glucosyl dihydrochalcone, found in rooibos, is nothofagin (Figure 3.2E).[106]

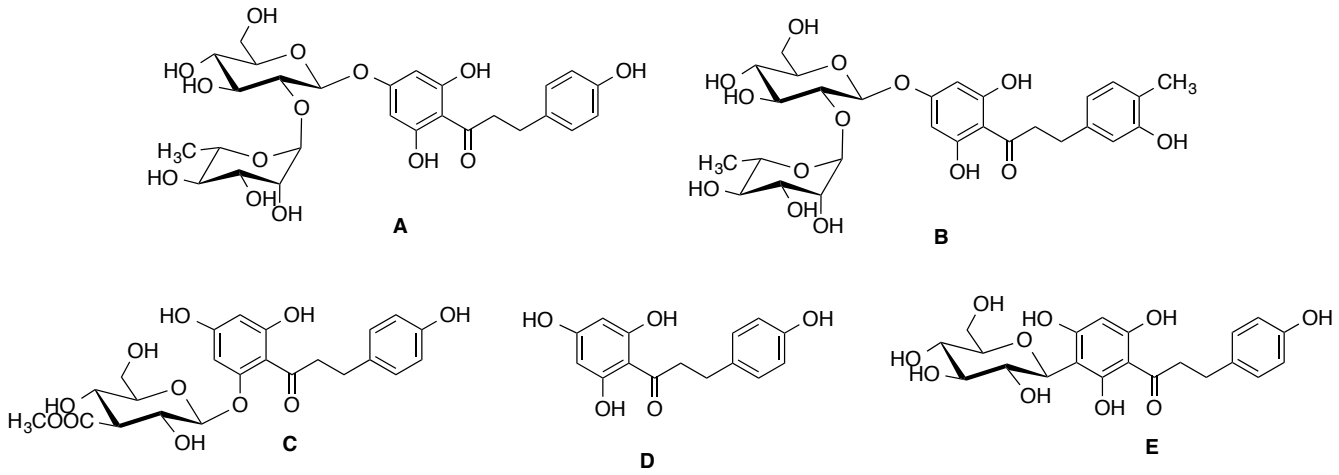

Figure 3.2 Structures of **A**. Narigenin dihydrochalcones, **B**. Neohesperidin dihydrochalcones, **C**. Phlorizin, **D**. Phloretin and **E**. Nothofagin

In 1968, Riter *et al*[107] reported the synthesis of glycosylated dihydrochalcones starting from a glycosylated acetophenone and an aldehyde, forming the glycosylated chalcone prior the hydrogenation to afford the glycosylated dihydrochalcones.

The synthesis of non-glycosylated dihydrochalcones can be achieved by reduction of the double bond of chalcones using the common catalytic hydrogenation methods (H_2, Pd-C) or directly via palladium-catalyzed coupling of aryl halides and 1-arylprop-2-en-1-ols.[108] In 2008, selective reduction of the double bond using zinc systems was published.[109,110] However the latter method cannot be use if susceptible groups (e.g. esters, some ethers, amides, etc.) are present.

To avoid handling of explosive H_2 it was developed a system based on Pd-C and triethylsilane (Et_3SiH) that produces H_2 *in situ,* achieving efficient reduction of multiple bonds, azides, imines, and nitro groups, as well as deprotecting benzyl and allyl groups under mild, neutral conditions.[111]

3.2 Synthesis of *C*-glucosyl compounds

C-Glucosyl compounds possess a furanosyl or pyranosyl group linked to an aglycone (aliphatic or aromatic) through a C-C bond, as illustrated in Figure 3.3. The synthesis of these molecules is particularly challenging, especially when glycosylation takes place in aromatic rings.

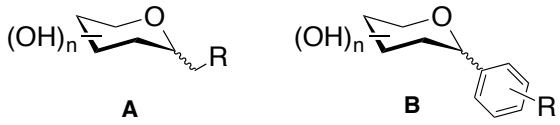

Figure 3.3 Model structures of **A.** aliphatic *C*-glycosyl compounds and **B.** aromatic *C*-glycosyl compounds

For several years researchers searched for an easy way to synthesize *C*-glycosyl compounds. Although Wittig-like reactions[112] (Scheme 3.2A), Mitsunobu transformations[113,114] (Scheme 3.2B), reactions catalyzed by palladium[115,116] (Scheme 3.2C) or promoted by samarium[114,117] (Scheme 3.2D), and free radical reactions[118] (Scheme 3.2E), have been applied for *C*-glycosylation, the most common methods involve a glycosyl donor as starting material which activation yields the electrophile species that reacts with the carbon nucleophile to form a C-C bond.

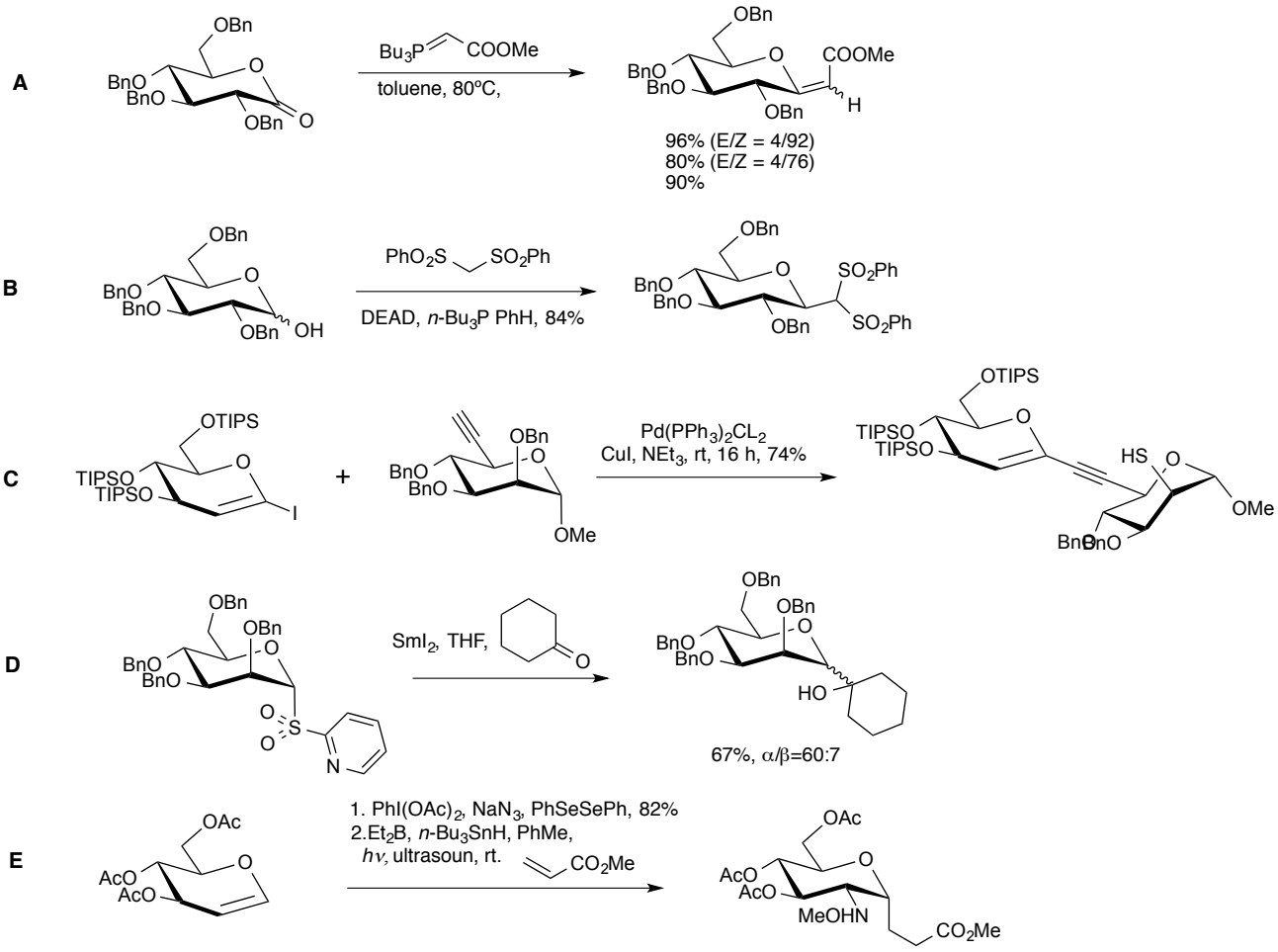

Scheme 3.2 *C*-glycosylation by **A.** Wittig-like reaction, **B.** Mitsunobu reaction, **C.** palladium-catalyzed reaction, **D**. samarium-catalyzed reaction, **E.** radical reaction.

The glycosyl donors commonly used are divided into four groups: good leaving groups (after appropriate activation) (Scheme 3.3A) (e.g fluoride, trichloroacetimidate, phosphate), glycals (Scheme 3.3B), 2,3-anhydrosugars (Scheme 3.3C), and sugar lactones (Scheme 3.3D). These glycosyl donors can react with organocuprates (Scheme 3.4A), Grignard species (Scheme 3.4B), or other activated compounds (e.g phenols, Scheme 3.4C) to yield the *C*-glycosyl derivatives.

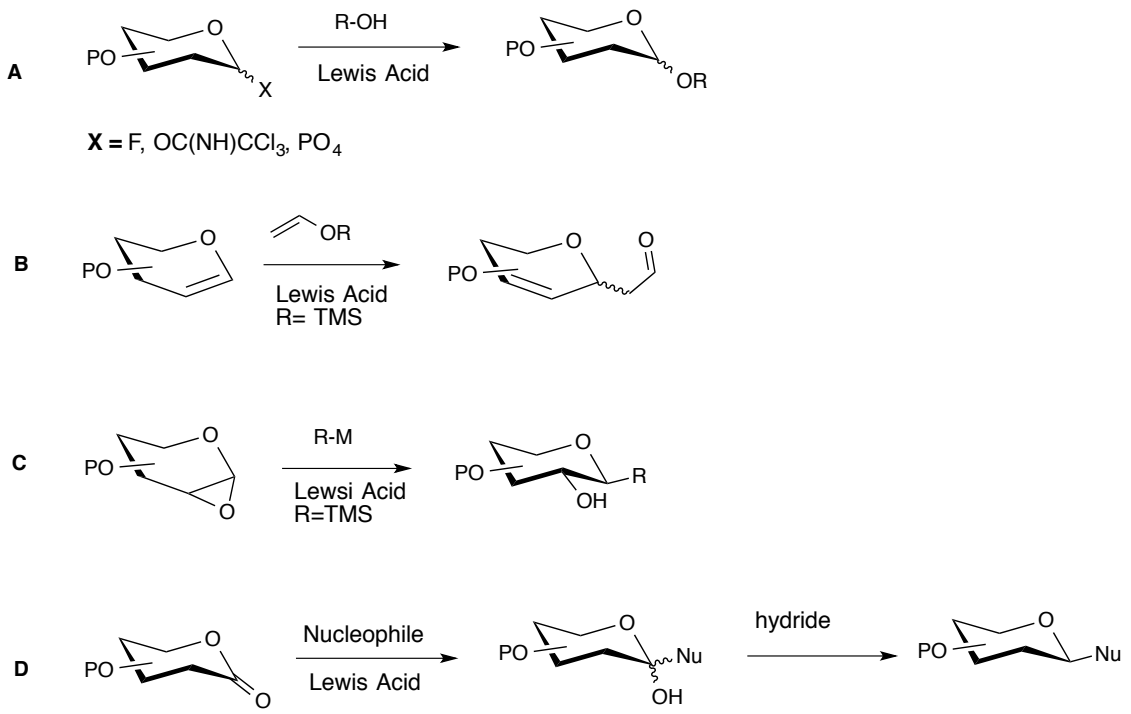

Scheme 3.3 *C*-glycosylation using **A.** good leaving groups (after activation); **B.** glycals; **C.** anhydrosugars; **D.** lactones.

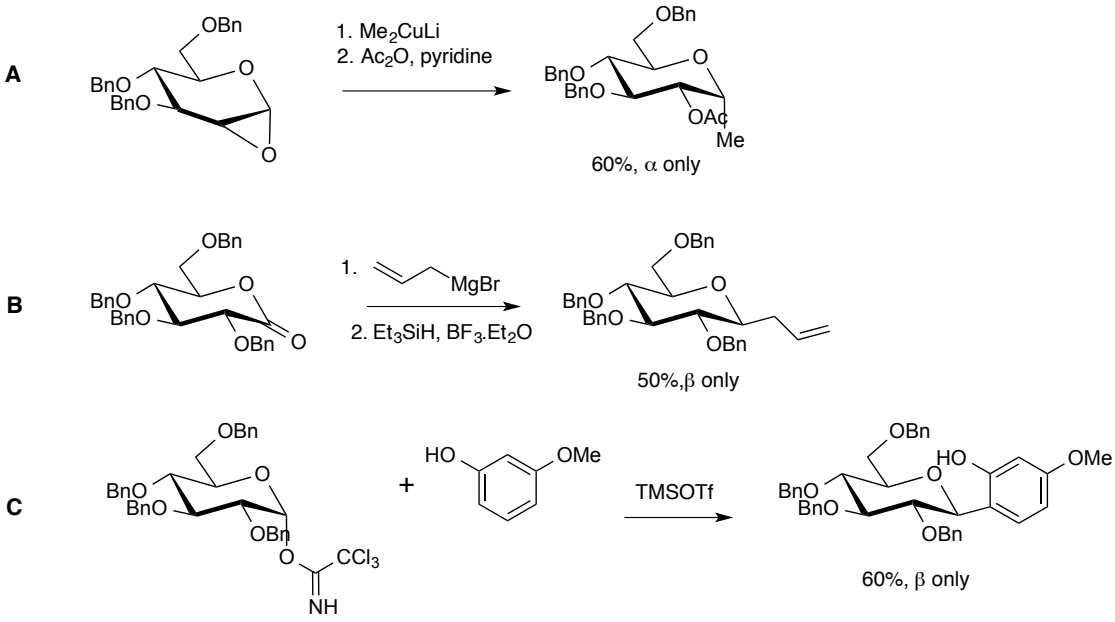

Scheme 3.4 *C*-glycosylation using different glycosyl donors and **A.** organocuprate reagent, **B.** Grignard reagent, and **C.** phenols

The stereoselectivity of *C*-glycosylations is mostly determined by the stereochemistry of the substituent in position C-2 of the glycosyl donor and usually 1,2-*trans* products are obtained. For example, with a glucosyl donor formation of the β-anomer is preferred, but if a D-mannosyl donor is used, the major product has

α-anomeric configuration. However, when the glycosyl acceptor is an aromatic compound, the electron density of the aromatic ring, the protecting groups of the glycosyl donor, and the reaction conditions strongly determine reaction selectivity for either *O*- or *C*-glycosylation.[114] Oyama *et al*[119] demonstrated, by treating glycosyl fluoride either with boron trifluoride etherate ($BF_3{\cdot}Et_2O$) (Scheme 3.5A) or the combination of $BF_3{\cdot}Et_2O$ and 2,6-di-*tert*-butyl-4-methyl pyridine (DTBMP) (Scheme 3.5B), that the former catalyst promoted *C*-glycosylation, whilst the latter promoted the *O*-glycosylation.

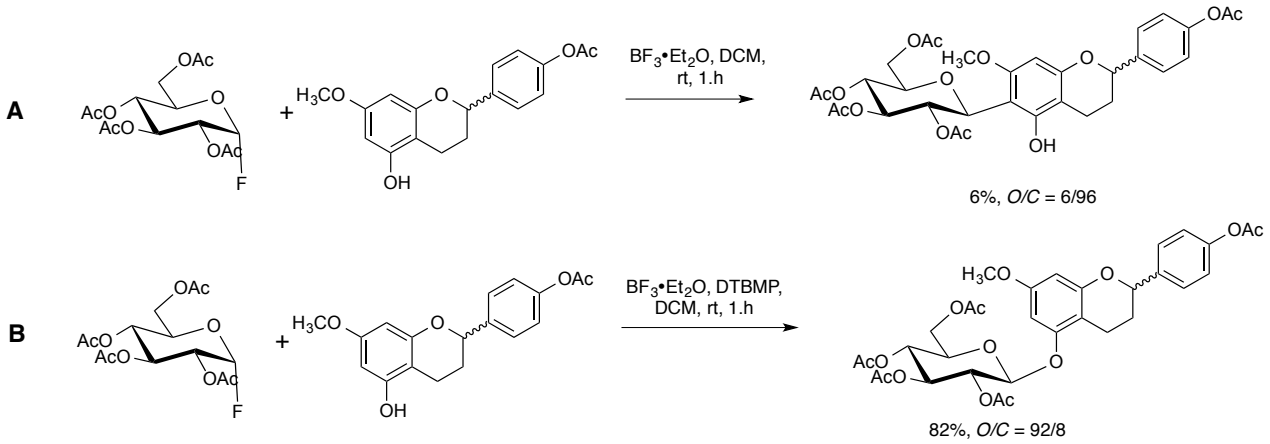

Scheme 3.5 *O- vs C*-glucosylation using **A.** $BF_3{\cdot}Et_2O$, and **B.** the combination of $BF_3{\cdot}Et_2O$ and DTBMP

The mostly described methodology to afford *C*-glycosylation of aromatic compounds is based on the Fries-type reaction (Scheme 3.6). This one-pot reaction involves a glycosyl donor, an activator and a glycosyl acceptor. It proceeds through an initial glycoside that is rapidly formed at low temperature. Upon warming, an *in situ O→C* rearrangement occurs to give regioselectively an ortho-hydroxy *C*-glycosyl aromatic compound. [120]

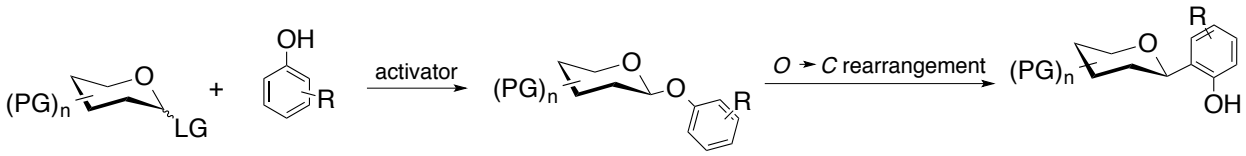

Scheme 3.6 Fries-type rearrangement for the synthesis of *C*-glycosyl compounds

The activators reported in literature for this type of reaction include: boron trifluoride etherate ($BF_3{\cdot}Et_2O$)[120-122] (Scheme 3.7A), tin chloride ($SnCl_4$)[120,123,124] (Scheme 3.7B), biscyclopentadienyl hafnium dichloride/silver perchlorate (Cp_2HfCl_2-$AgClO_4$)[124,125] (Scheme 3.7C), trimethylsilyl trifluoromethane-sulfonate (TMSOTf)[126-128]

(Scheme 3.7D), scandium(III) trifluoromethanesulfonate ($Sc(OTf)_3$)[129] (Scheme 3.7E), protic acid in ionic liquids[130] (Scheme 3.7F), and montmorillonite K-10[131] (Scheme 3.7G). All of these activators have been reported to succeed in the synthesis of simple and small phenols.[120]

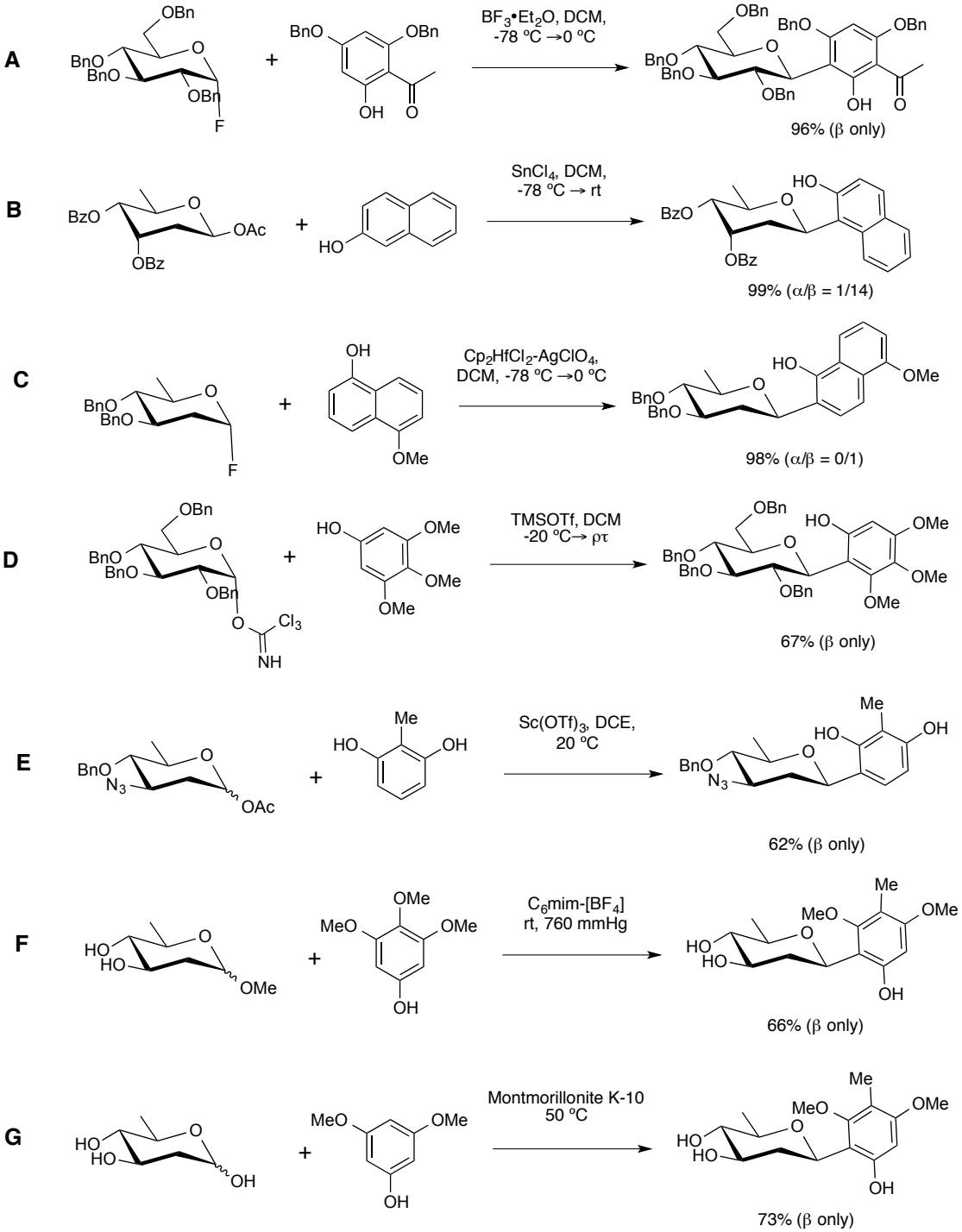

Scheme 3.7 *C*-glucosylation using **A.** $BF_3{\cdot}Et_2O$, **B.** $SnCl_4$, **C.** Cp_2HfCl_2-$AgClO_4$, **D.** TMSOTf, **E.** $Sc(OTf)_3$, **F.** Ionic Liquids, and **G.** Montmorillonite K-10

More recently, the coupling between unprotected sugars and unprotected narigenin (a flavananone) was reported using rare-earth metal triflates (e.g $Sc(OTf)_3$, $Y(OTf)_3$, $Pr(OTf)_3$, etc) [132] (Scheme 3.8), however, there are no reports of direct *C*-glucosylation of unprotected dihydrochalcones.

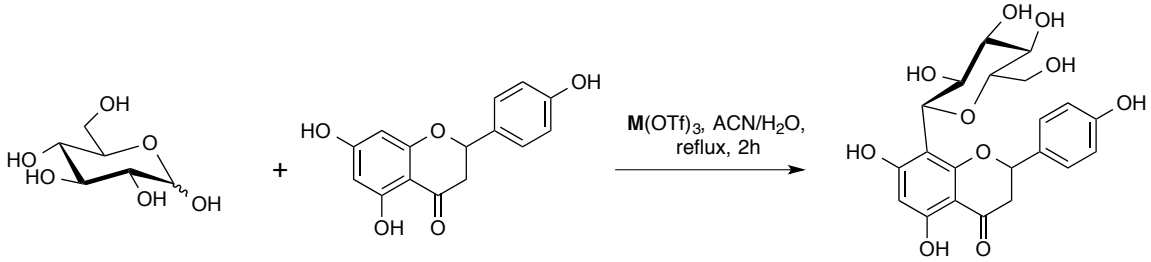

M=Sc, 18.9%
M=Y, 18.0%
M=Pr, 41.2%
M=Yb, 2.2%
M=Gd, 21.4%

Scheme 3.8 *C*-glucosylation of narigenin using different rare-earth metal triflates

Hence, this project' goals comprise the development of an easy to carry out and good yielding pathway for the synthesis of *C*-glucosyl dihydrochalcones and evaluate the prepared compounds *in vitro* as SGLT inhibitors (Scheme 3.9).

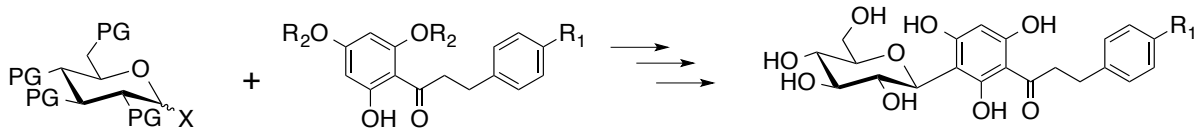

PG= protecting group
R_1 and R_2= Substituents
X= Leaving group

Scheme 3.9 General Strategy for the synthesis of *C*-glucosyl di-hydrochalcones

3.3 Chemo-enzymatic synthesis of glucosyl compounds

The main problem for the pharmacological application of most of the biologically active compounds is their solubility in water; but the introduction of a higher number of sugar units with or without substituents such as phosphate or sulfates can, very often, solve the problem. However, in general, the synthesis of complex carbohydrate and related structures can be a difficult task, especially from a practical point of view. Chemo-enzymatic synthesis, however, can be very advantageous resolving most of the issues,

because it employs both chemical and enzymatic synthesis to obtain the desired molecules.

In literature it is possible to find several reports regarding the chemo-enzymatic synthesis of glycans,[133] glycoproteins,[134] heparin derivatives,[135] and other natural products.[136] Many oligosaccharides can be synthesized on multi-gram or kilogram scales using glycosyltransferases (GTFs),[137] which are enzymes that catalyse the transfer of a saccharide from a sugar nucleotide (sugar-UDP[r]) to a glycposyl acceptor (e.g ROH) (Scheme 3.10). The biosynthesis of oligosaccharides, catalyzed by GTFs resembles the corresponding chemical procedure, whereas a glycosyl donor is activated in the first step, followed by the transfer of the activated sugar to an appropriate acceptor sugar. Leloir GTFs[s] primarily utilize one of eight different nucleotide mono- or diphosphates (UDP-Glc, UDP-GlcNAc[t], UDP-Gal[u], UDP-GalNAc[v], GDP-Man[w], GDPFuc[x], UDP-GlcA[y], and CMP-NeuAc[z]) as monosaccharide donors to build the new glycosidic bond.

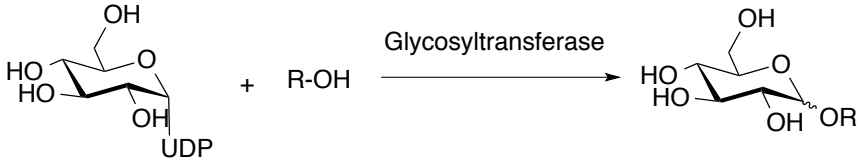

Scheme 3.10 Glycosylation using a glycosyltransferase

Glycosyltransferases are specific for the type of linkage (α or β), and the linkage position of the glycoside bond formed [e.g. $\alpha(1\rightarrow3)$ or $\beta(1\rightarrow4)$]. They were initially considered to be specific for a single glycosyl donor and acceptor, however subsequent observations have refuted the theory of absolute enzymatic specificity by describing the transfer of analogues of some nucleoside mono- or diphosphate sugar donors. This class of enzymes can tolerate modifications to the acceptor sugar, if the acceptor meets

[r] Uridine diphosphate
[s] Glycosyltransferases that use UDP sugars as glycosyl donors. Non-Leloir glycosyltransferases use non-nucleotide donors such as sugar phosphates
[t] Uridine diphosphate *N*-acetylglucosamine
[u] Uridine diphosphate galactose
[v] Uridine diphosphate *N*-acetylgalactosamine
[w] Guanosine diphosphate mannose
[x] Guanosine diphosphate fucose
[y] Uridine diphosphate glucosuronic acid
[z] *N*-acylneuraminate cytidylyltransferase

specific structural requirements (e.g. appropriate stereochemistry and availability of the reactive hydroxyl group involved in the glycosidic bond).[138,139]

According to the Carbohydrate-Active enZymes Datable (CAZY) there are ca. 97 families of GTFs. Among them only few C-GTF are known, and the most well characterized C-GT is the C-GT *Urd*GT2 (from *streptomyces fradiae*) with its crystal structure already determined. This enzyme catalyse the *C*-glucosylation between TDP-D-olivose and different polyhydroxylated anthraquinones. Other C-GTs, which crystal structure is still unknown, are *IroB* (from *E. coli*) that catalyse C-glycosylation between UDP-D-glucose and the tricatecholic sidophore enterobactin, and *Os*_C-GT (from rice, *Oryza sativa*) that catalyse the glycosyl transfer from UDP-D-glucose to 2,5,7-tri-hydroxy-substituted flavanones and dihydrochalcones acceptors (e.g. phloretin, Figure 2.9). One common fact between all these enzymes is the fact that the *C*-glucosylation occurs at positions *ortho* or *para* to phenolic hydroxyls, suggesting that the mechanism underneath this reaction is a Fries-type rearrangement (Scheme 3.6).

The enzymatic synthesis of di- and trisaccharides was investigated, and the chemical *O*- and *C*-glycosylation of dihydrochalcones using these oligosaccharides would provide new and original structures as potential SGLT2 inhibitors.

Chapter 4. Results and Discussion: Chemical & Enzymatic Synthesis

One of the goals of this Ph.D. project was to synthesize *C*-glucosyl dihydrochalcones. In Scheme 4.1 are shown the two main envisioned approaches that were investigated in this Ph. D. project, as well as the synthesis of required glucosyl donors and acceptors.

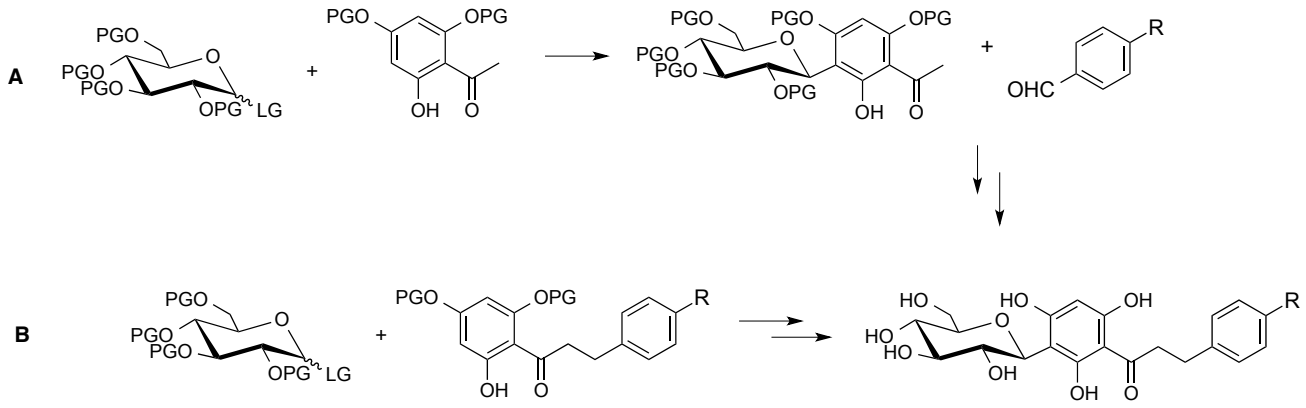

Scheme 4.1 Approaches investigated in this work for the synthesis of *C*-glucosyl dihydrochalcones

4.1 Synthesis of glucosyl donors

As mentioned in chapter 3 (section 3.2) sugars bearing a good leaving in the anomeric position can be used as glycosyl donors in electrophilic *C*-glycosylations. Therefore, the synthesis of a variety of glycosyl donors with different leaving groups was investigated.

4.1.1 Synthesis of 1-O-acetyl-2,3,4,6-tetra-O-benzyl-α-D-glucopyranose and 2,3,4,6-tetra-O-benzyl-α-D-glucopyranose

The synthesis of 1-*O*-acetyl-2,3,4,6-tetra-*O*-benzyl-α-D-glucopyranose (**4**) (Scheme 4.2) was successfully accomplished in 63% overall yield over a three step procedure, comprising benzylation of α-methyl-D-glucopyranoside (**1**), followed by acid catalysed anomeric demethylation of **2** to afford compound **3**, in which an acetyl group was introduced at the anomeric position.

Another approach for the synthesis of glycosyl donor **4** was investigated starting from D-glucose, as illustrated in Scheme 4.3.

The first step consisted on the protection of the anomeric position with an isopropyl group. Without further purification of the residue obtained, it was used directly for the benzylation reaction to obtain compound **6**. Hydrolysis of isopropyl group and acetylation afforded compound **4** in 60% overall yield, which is slightly lower than that achieved by the other pathway. However, the synthesis of compound **4** is accomplished in less time and with less purification steps.

Both compounds **3** and **4** were tried as glucosyl donors in the *C*-glucosylation reaction as it will be discussed in section 4.4.

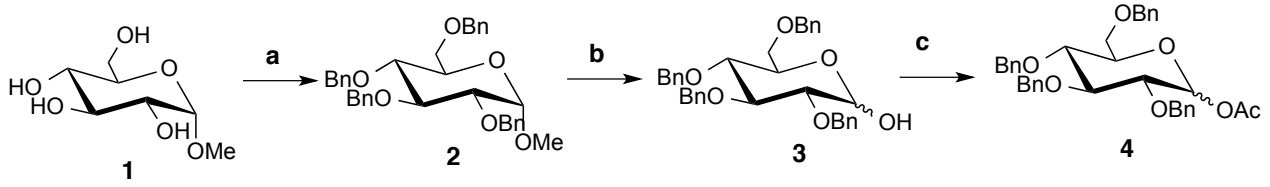

Scheme 4.2 Synthesis of glycosyl donor 1-*O*-acetyl-2,3,4,6-tetra-*O*-benzyl-α-D-glucopyranose.

Reaction conditions: **a.** BnBr (4.4 equiv.), NaH (4.4 equiv.), DMF, 0 ºC then rt, 24h, 82%; **b.** 2N H_2SO_4, AcOH, reflux, 24h, 81%; **c.** Ac_2O (1.2 equiv.), pyridine, DMAP (cat.), rt, 30 min, 96%.

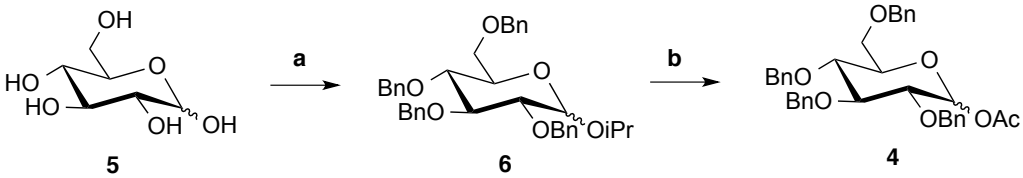

Scheme 4.3 Alternative synthesis of glycosyl donor 1-*O*-acetyl-2,3,4,6-tetra-*O*-benzyl-α-D-glucopyranose

Reaction conditions: **a.** 1. iPrOH, Dowex H^+ exchange resin, reflux, 5 h, 2. BnBr, NaH, DMF, rt, 15 h, 79%; **b.** 1. 2N H_2SO_4, AcOH, reflux, 24 h, 2. Ac_2O, pyridine, DMAP, rt, 30 min, 76%.

4.1.2 Synthesis of 2,3,4,6-tetra-O-trimethylsilyl-D-gluconolactone

C-glycosyl compounds can also be synthesized using lactones as glycosyl donors; therefore, gluconolactone (**7**) required protection of hydroxy groups prior to the *C*-glucosylation step. Benzyl groups are one of the most stable protecting groups because they are easily introduced and endure numerous reaction conditions. However, the usual conditions for the introduction of benzyl groups (strong base with benzyl

halogenides and acid conditions with benzyl trichloroacetimidate) are unsuited when a lactone is the starting material and, therefore trimethylsilyl (TMS) groups were used as an alternative (Scheme 4.4). TMS groups were introduced in weakly basic conditions using pyridine as solvent and catalyst; and 2,3,4,6-tetra-*O*-trimethylsilyl-D-gluconolactone (**8**) was obtained in 96% yield.

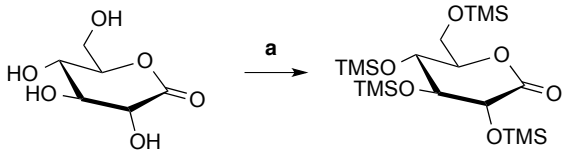

7 8

Scheme 4.4 Synthesis of lactone 2,3,4,6-tetra-*O*-trimethylsilyl-D-gluconolactone (**8**)
Reaction conditions: **a.** TMSCl, pyridine, DCM, -15 ºC then rt, 1 h, 96%

4.1.3 Synthesis of 2,3,4,6-tetra-O-acetyl-α-D-glucopyranosyl bromide and 2,3,4,6-tetra-O-acetyl-α-D-glucopyranosyl trichloroacetimidate

The synthesis of 2,3,4,6-tetra-*O*-acetyl-α-D-glucopyranosyl trichloroacetimidate (**11**) and 2,3,4,6-tetra-*O*-acetyl-α-D-glucopyranosyl bromide (**12**) followed a straightforward pathway in which D-glucose (**5**) was peracetylated affording compound **9**; which was either used directly to form the glycosyl bromide (**13**) or, after selective anomeric deacetylation to give **10**, used to obtain the glycosyl tricholoroacetimidate (Scheme 4.5). Due to its reactivity, compound **12** was not purified prior to the *C*-glycosylation reaction.

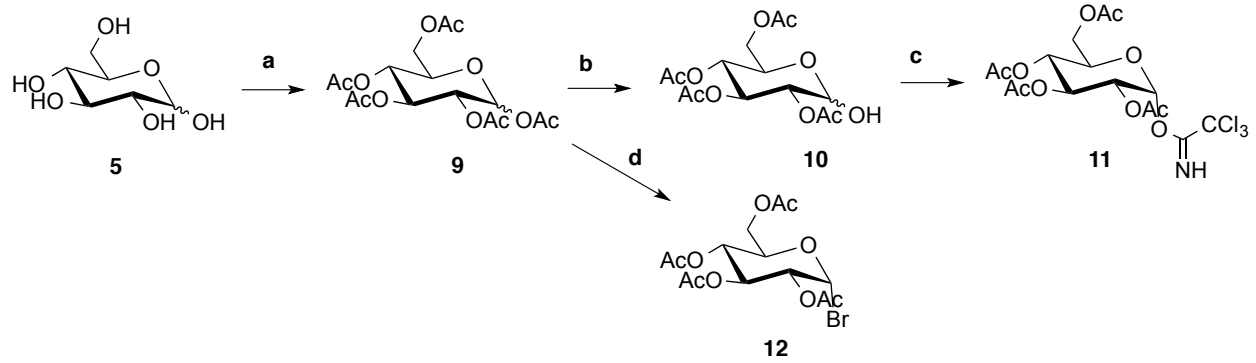

5 9 10 11 12

Scheme 4.5 ynthesis of glycosyl trichloroacetimidate and glycosyl bromide
Reaction conditions: **a.** Ac_2O, pyridine, DMAP, rt, 30 min, > 99%; **b.** $BnNH_2$, THF, 24 h, rt, 98%; **c.** $ClCCl_3CN$, DCM, K_2CO_3, rt, 24 h, 80%; **d.** AcBr, MeOH, AcOH (without purification)[aa]

[aa] Kindly prepared and provided by Patricia Serra

4.3 Synthesis of glucosyl acceptors

4.3.1 Synthesis of 2′,4′-di-O-benzyl-6′-hydroxyacetophenone

According to Scheme 4.1, strategy A, a protected acetophenone is required to be used as glycosyl acceptor in the first step. Therefore, 2′,4′-di-*O*-benzyl-6′-hydroxyacetophenone (**14**) was synthesized starting from 2′,4′,6′-trihydroxyacetophenone (**13**), which was dibenzylated with benzyl bromide under basic conditions (Scheme 4.6). However, in the purification step a second product was detected with a similar polarity to compound **14**, making the isolation of the desired product very challenging. Nevertheless, after careful separation and purification, it was possible to confirm by NMR the structure of this second product as that of compound **15**. A singlet at δ 3.96 ppm, integrating two protons and five extra protons on the aromatic region (at δ 7.53-7.11 ppm) indicated the presence of a benzyl group (Figure 4.1). A benzyloxy group was ruled out on the basis of the methylene chemical shift (at δ 3.96 ppm). The benzylic protons would be expected to appear at δ 5.27 ppm. In 2D spectra (HMBC) it was possible to observe a correlation between the signal at δ 3.96 ppm and C4′ and C6′ carbons (Figure 4.2) suggesting that the benzyl substituent was located at position C5′. The signals of carbons C4′ (at δ 163.7 ppm) and C6′ (at δ 162.7 ppm) were identified by their correlation with the signal of OH-2′ (at δ 14.24 ppm) in the HMBC spectrum. This type of alkylation of acetophenones has aalready been reported by Jain *et al*[140] using a potassium carbonate in the presence of benzyl chloride.

Compounds **14** and **15** were isolated in 40% and 30% yield, respectively.

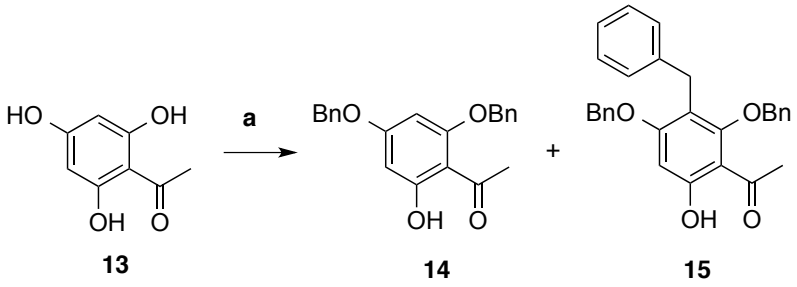

13 **14** **15**

Scheme 4.6 Synthesis of 2′,4′-di-*O*-benzyl-6′-hydroxyacetophenone.
Reaction conditions: **a.** BnBr, K_2CO_3, DMF, 0 ºC to rt, 1 h, **14**. 40%, **15**. 30%.

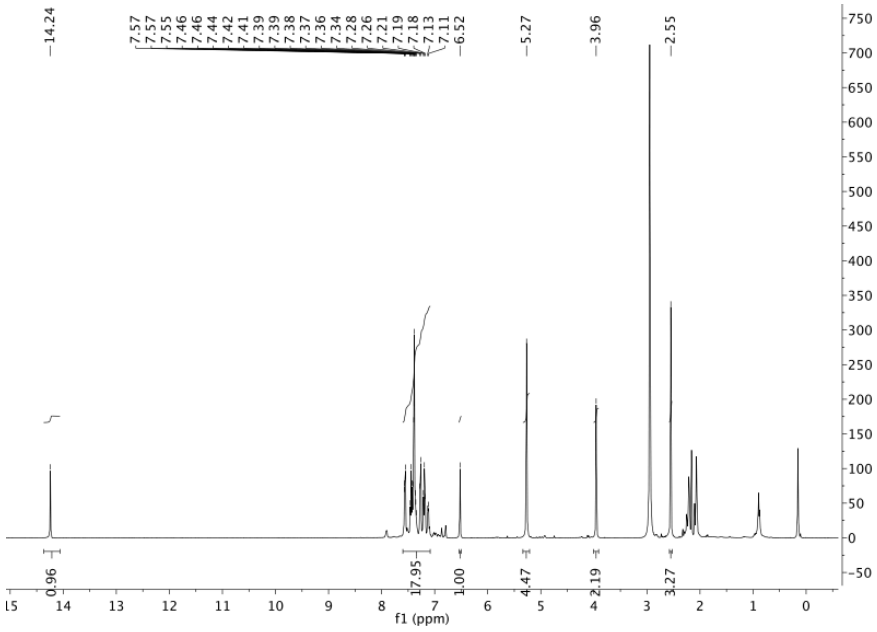

Figure 4.1 ^{1}H-NMR of compound **15** in $CDCl_3$

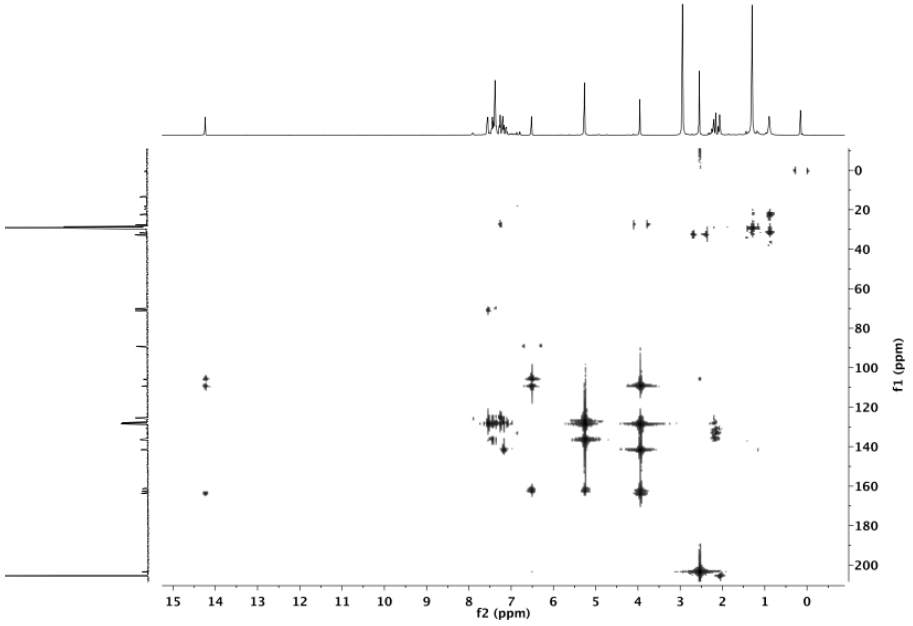

Figure 4.2 HMBC spectrum of compound **15** in $CDCl_3$

4.3.1 Synthesis of chalcones

To investigate the feasibility of strategy B described earlier on Scheme 4.1 a partly benzylated dihydrochalcone was prepared (Scheme 4.7). The first step on its synthesis consisted on the aldol condensation of compound **14** with the benzaldehyde derivative **16** under basic conditions, and the corresponding chalcone **17** was isolated in 73% yield. Catalytic hydrogenation (step b) and selective dibenzylation (step c) of **18** lead to the

formation of the desired benzylated dihydrochalcone (**19**) in 46% overall yield. Nevertheless, *C*-glucosylation of compound **18** was also investigated.

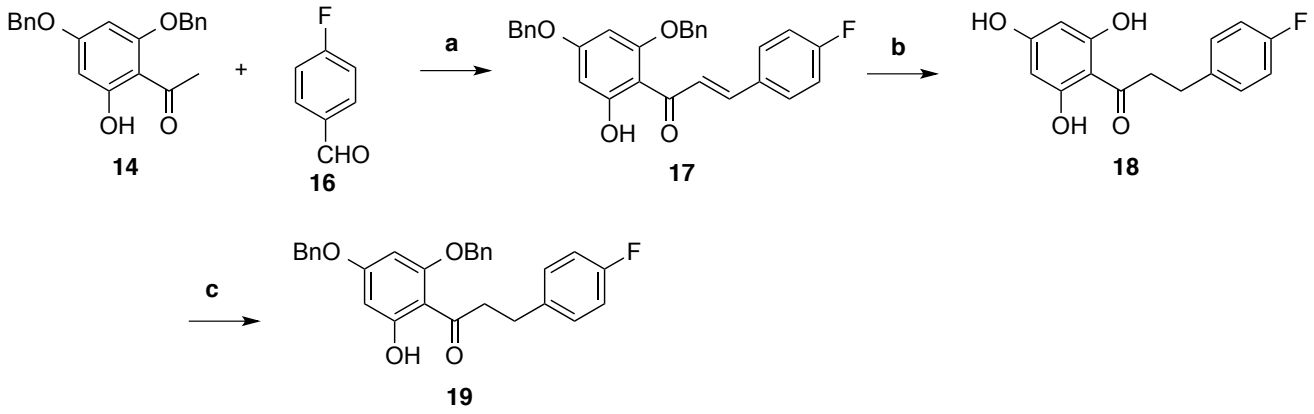

Scheme 4.7. Synthesis of benzylated dihydrochalcone.
Reaction conditions**: a.** 50% (w/v) NaOH, 1,4-Dioxane, rt, 24 h, 73%; **c.** Pd/C, Et_3SiH, EtOAc, MeOH, 5 h, rt, 90%; **d.** BnBr, K_2CO_3, DMF, 0 ºC then rt, 2 h, 70%.

With the optimized procedure in hand, a library of chalcones and dihydrochalcones was synthesized. Chalcones, as mentioned in Chapter 3, are also important biological molecules and in this study were investigated as potential SGLT inhibitors. To obtain the unprotected chalcones derivatives benzyl groups cannot be used as protecting groups. Hence, ethoxymethyl ($CH_3CH_2OCH_2$) (EOM) groups were used instead because like benzyl groups they are easily introduced under mild conditions but unlike benzyl groups they can be cleaved in mild acidic conditions without reducing the double bond. After protection of 2′,4′,6′-trihydroxyacetophenone (**13**), chalcones (**21a-21i**, Scheme 4.8) were obtained in very good yields (85-95%) by aldol condensation of compound **13** with a variety of aromatic aldehydes (**16a-16i**). Aldehydes **16e-16g** were prepared in the laboratory prior their used in the aldol condensation reaction; their preparation included the reaction of 4′-hydroxybenzaldehyde with the corresponding alkyl halide under basic conditions (e.g. KOH or K_2CO_3) (Scheme 4.9).

Deprotection of these chalcones was investigated. In literature there are no reports regarding the removal of EOM group, but the analogue methoxymethyl group is generally removed with HCl[141] or other strong acids[142]. However, when the hydrolysis of EOM groups was performed in the presence of HCl the corresponding isoflavanone was obtained as the major product. Using a weak acid, such as $FeCl_3{\cdot}6H_2O$ (Scheme 4.8), the

removal of EOM groups was achieved with no further problems and unprotected chalcones (**22a-22i**) were obtained in moderate to very good yields (67-96%).

Microwave-assisted synthesis has been extensively exploited over the last couple of years. Conventional heating usually involves a furnace or an oil bath, which heats the walls of the container by convection or conduction and the samples take a longer time to achieve the desired temperature. On the other hand, with microwave heating it is possible to heat the target compounds without heating the entire container, which saves energy and time. Another advantage of this technology is the fact that it is possible to run reactions at a temperature higher than the boiling point of the solvent in use. This generally leads to cleaner/faster reactions with less secondary products.

To evaluate the reliability of this technology synthesis of chalcones and chalcone deprotection were carried out in a microwave oven and in a conventional heating plate (Table 4.1).

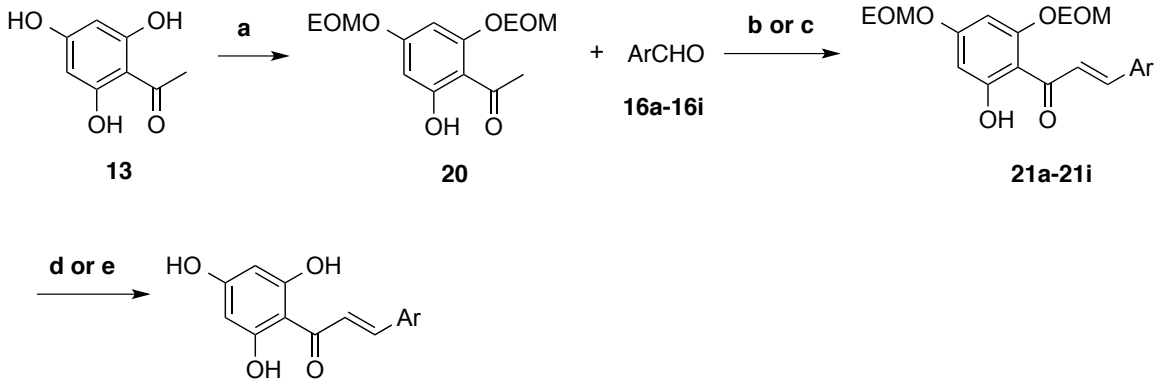

13 **20** **21a-21i** **22a-22i**

Scheme 4.8 Synthesis of 2′,4′,6′-trihydroxychalcones.
NOTE: EOM= $CH_3CH_2OCH_2$; Reaction conditions: **a.** $ClCH_2OCH_2CH_3$, DCM, DIPEA, 0 ºC then rt, 2 h, 74%; **b.** 50% aq. NaOH (w/v), 1,4-Dioxane, rt, 24 h; **c.** 50% aq. NaOH (w/v), 1,4-Dioxane, 120 ºC, 250W, 1 h; **d.** $FeCl_3 \cdot 6H_2O$, MeOH, reflux, 2-3 h; **e.** $FeCl_3 \cdot 6H_2O$, MeOH, 80ºC, 250W, 7-10 min.

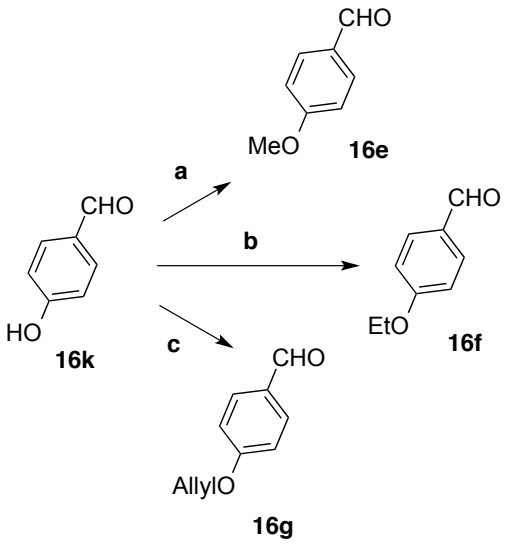

Scheme 4.9 Synthesis of aromatic aldehydes
Conditions used: **a.** MeI, Acetone, K_2CO_3, reflux, 6h, 98.5% ; **b.** EtBr, EtOH, KOH, reflux, 6 h, 98.6%; **c.** AllylBr, EtOH, KOH, reflux, 7 h, 98.6%

In order to study the importance of substituents on both chalcone rings two other chalcone families were prepared, starting from different acetophenones. On both the hydroxy group on position C-6′ was removed; and the hydroxy group on position C-4′ was either maintained or replaced by a fluorine atom. Then, aldol condensation of both 2′,4′-dihydroxyacetophenone (**23**, Scheme 4.10) or 4′-fluoro-2′-hydroxyacetophenone (**27**, Scheme 4.11) with different aromatic aldehydes afforded the chalcone scaffolds in good yields (67-98%). In the case of acetophenone **27** it did not require any protection prior the reaction while acetophenone **23** was protected with an EOM group as previously described. Removal of EOM group was accomplished as before, in the presence of $FeCl_3 \cdot 6H_2O$ and the desired 2′,4′-dihydroxychalcones were obtained in good yields.

Interestingly, when aldol condensation was carried out with acetophenones **23** or **27** in 1,4-dioxane, a precipitate was formed, that dissolved when ethanol was added to the reaction mixture. Consequently, reactions with these two acetophenones were carried out in ethanol to guarantee full homogeneity of the reaction mixture. This precipitate resulted probably from the extra hydroxy group in the acetophenone, that ionized in the presence of the base.

In Table 4.1 is summarized the results obtained for the synthesis of these three families of chalcones using either the conventional method or using the microwave equipment.

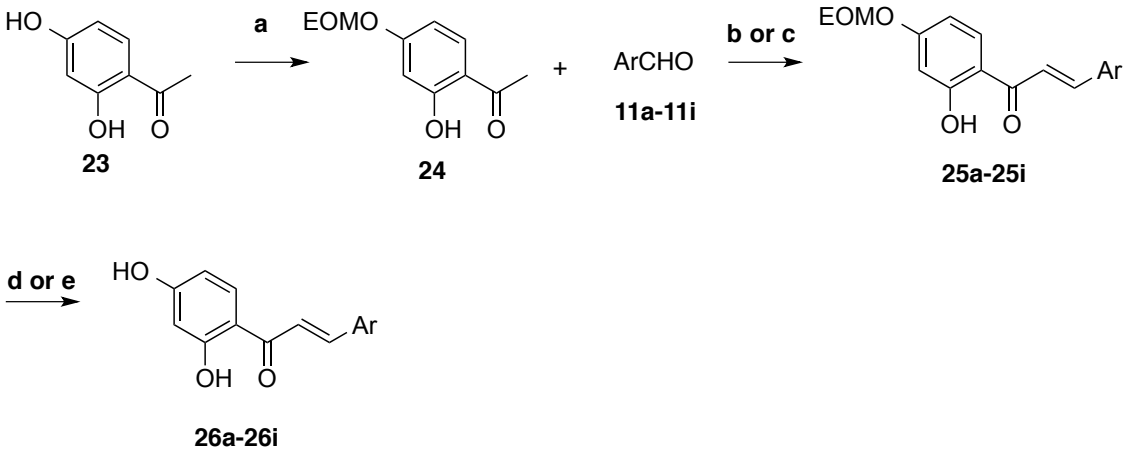

Scheme 4.10 Synthesis of 2′,4′-dihydroxychalcones
Reaction conditions: **a.** $ClCH_2OCH_2CH_3$, DCM, DIPEA, 0 ºC then rt, 1 h, 93.8%; **b.** 50% aq. NaOH (w/v), EtOH, rt, 24 h; **c.** 50% aq. NaOH (w/v), EtOH, 120 ºC, 250 W, 1 h; **d.** $FeCl_3{\cdot}6H_2O$, MeOH, reflux, 2-3 h; **e.** $FeCl_3{\cdot}6H_2O$, MeOH, 80 ºC, 250 W, 7-10 min

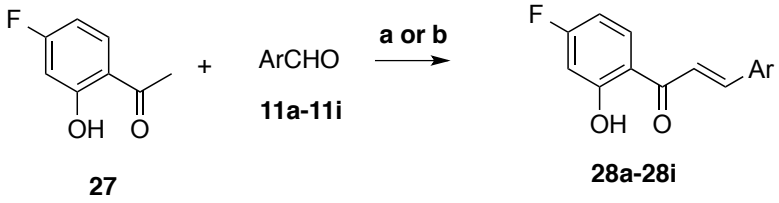

Scheme 4.11 Synthesis of 4′-fluoro-2′-hydroxychalcones
Reaction conditions: **a.** 50% aq. NaOH (w/v), EtOH, rt, 24 h; **b.** 50% aq. NaOH (w/v), EtOH, 120 ºC, 250 W, 1 h

Table 4.1. Synthesis of 2′,4′,6′-trihydroxychalcones, 2′,4′-dihydroxychalcones and 4′-fluoro-2′-hydroxychalcones using conventional and microwave methodologies

Aldehyde	Compound	Ar group		Yield (%)	
			R	Conventional	Microwave
16a	**21a**	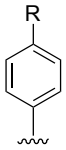	F	91.6	97.8
16b	**21b**		Br	91.0	96.6
16c	**21c**		H	95.2	96.0
16d	**21d**		Me	91.6	96.0
16e	**21e**		OMe	87.0	90.8
16f	**21f**		OEt	86.3	92.3

Table 4.1 Synthesis of 2′,4′,6′-trihydroxychalcones, 2′,4′-dihydroxychalcones and 4′-fluoro-2′-hydroxychalcones using conventional and microwave methodologies (*cont.*)

Aldehyde	Compound	Ar group	R	Yield (%)	
				Conventional	Microwave
16g	**21g**		OAllyl	98.7	98.9
16h	**21h**		OBn	87.7	92.3
16i	**21i**	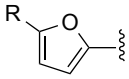	Me	67.1	98.8
16a	**22a**		F	87.7	97.1
16b	**22b**		Br	96.0	94.6
16c	**22c**		H	79.9	82.0
16d	**22d**	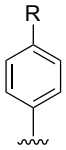	Me	80.7	73.0
16e	**22e**		OMe	79.6	83.4
16f	**22f**		OEt	88.5	89.8
16g	**22g**		OAllyl	82.4	88.8
16h	**22h**		OBn	86.8	85.9
16i	**22i**	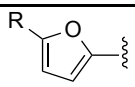	Me	67.1	92.8
16a	**25a**		F	91.2	86.3
16b	**25b**	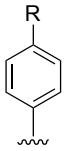	Br	85.0	86.0
16d	**25d**		Me	89.2	92.8
16h	**25h**		OBn	92.3	93.8
16i	**25i**	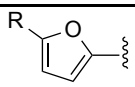	Me	68.9	74.6
16a	**26a**		F	84.6	94.5
16b	**26b**	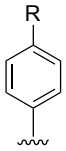	Br	93.7	98.2
16d	**26d**		Me	96.8	97.2
16h	**26h**		OBn	96.7	97.8
16i	**26i**	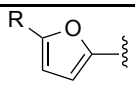	Me	90.9	97.6
16a	**28a**		F	72.6	87.5
16b	**28b**	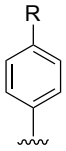	Br	87.3	93.4
16d	**28d**		Me	83.0	95.1
16h	**28h**		OBn	89.9	90.5
16i	**28i**	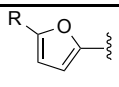	Me	84.6	89.9

According to these results, when the synthesis was performed in the microwave oven the yields did not change substantially but the reaction time was drastically decreased; from 24 hours to 1 hour in the aldol condensation step; and from 2-3 hours to 7-10 minutes in the case of the deprotection of chalcones. The only disadvantage of this new technology was the limit on the amount of reactants/volume that the vessel could tolerate (max. 10 mL). In this case, the maximum of starting acetophenone/chalcone that was possible to use was 1 g. In traditional reaction vessel it was possible to scale up using 5 g of starting material, without significant losses of materials/products. However, microwave assisted synthesis has proven to be extremely efficient for the preparation of these chalcone families.

4.3.2 Synthesis of dihydrochalcones

In situ generation of molecular hydrogen by addition of triethylsilane to palladium-charcoal catalyst was then applied for the first time to chalcones, resulting in a rapid and efficient reduction of chalcone olefinic bond to afford the corresponding dihydrochalcones (Scheme 4.12). The reaction was carried out at room temperature for 10 min and the yields were very good (93.0-98.8%, Table 4.2). Reaction completion could be detected by discoloration of the yellow-reddish colour of the chalcone solution.

All the reactions afforded the desired compound in high yield, except compounds **22b, 26b**, **28b, 28i** and **26i** were used as starting material. In the case of compounds **22b**, **26b** and **28b**, reduction of the bromoaryl moiety occurred and **18c**, **29c** and **30c**, respectively, were formed (Table 4.3). Some authors have already reported this exchange by other hydrosilane derivatives[143]. NMR confirmed the assigned structure resulted from the hydrogenation of compound **22b** (Figure 4.3), in particular by the signal at $\delta \sim 7.20$ ppm integrating 5 protons corresponding to the phenyl group. HRMS also confirmed this exchange and the mass of resulted product was the same as of compound **18c** (Figure 4.4); the calculated mass for $C_{15}H_{14}NaO_4$ of compound **18c** s 281.07843 m/z and the mass found was 281.07847 m/z.

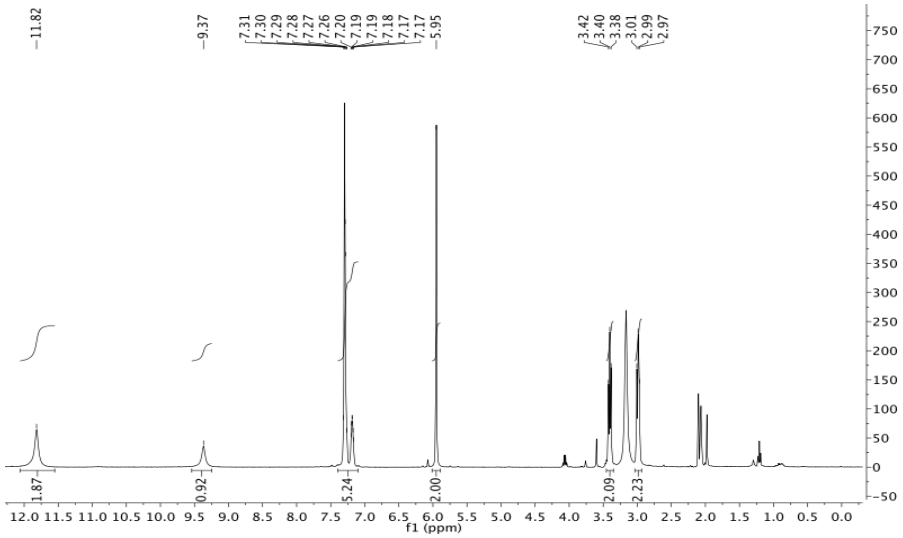

Figure 4.3 ^{1}H-NMR spectrum of **18c** resulted from **22b** hydrogenation

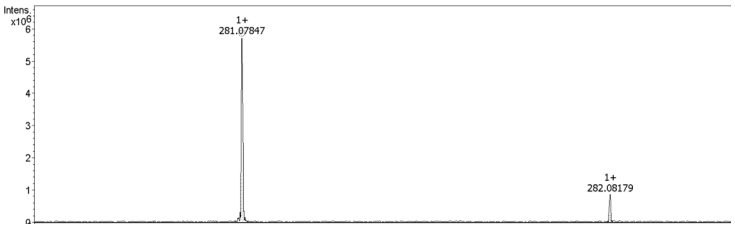

Figure 4.4 HRMS spectrum of **18c** resulted from **22b** hydrogenation

Hydrogenation of compound **28i** gave two products, **30i** and **30j**, whose structures (see Table 4.2) were confirmed by NMR spectroscopy. While NMR spectrum of compound **30i** presented the signals characteristic of the desired dihydrochalcone, the NMR signals of compound **30j** confirm that it is a dihydrochalcone bearing a tetrahydrofuranyl group, resulting from reduction of both double bonds of the furanyl group.

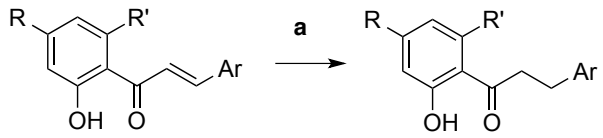

22a-22i R=R'=OH
26a-26i R=OH, R'=H
28a-28i R=F, R'=H

18a-18i R=R'=OH
29a-29i R=OH, R'=H
30a-30j R=F, R'=H

Scheme 4.12 Synthesis of 2′,4′,6′-trihydroxydihydrochalcones, 2′,4′-dihydroxydihdrochalcones and 4′-fluoro-2′-hydroxydihydrochalcones
Reaction conditions: **a.** Et_3SiH, Pd-C, MeOH, EtOAc, rt, 10 min

Table 4.2. Synthesis of 2′,4′,6′-trihydroxydihydrochalcones, 2′,4′-dihydroxydihdrochalcones and 4′-fluoro-2′-hydroxy-dihydrochalcones

Compound	Ar group	R	Yield (%)
18a	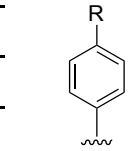	F	97.9
18c		H	94.4
18d		Me	98.8
18e		OMe	96.9
18f		OEt	96.1
18g		OPr	93.8
18h		OH	97.4
18i	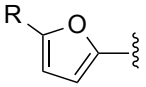	Me	98.9
29a	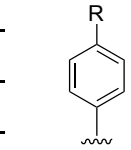	F	99.7
29c		H	98.7
29d		Me	99.1
29h		OH	99.0
29i	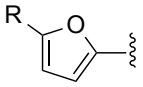	Me	98.2
30a	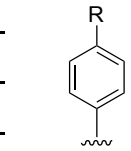	F	99.3
30c		H	99.0
30d		Me	99.0
30h		OH	99.4
30i	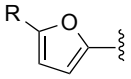	Me	58.4
30j	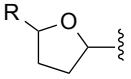	Me	40.8

4.4 Synthesis of *C*-glucosyl dihydrochalcones

As shown in Scheme 4.1 different approaches were investigated to synthesize *C*-glucosyl dihydrochalcones by a methodology easy to carry out, high yielding and comprising only a few reaction steps. Two strategies were envisioned, namely pathway A depicted on scheme 4.1 (strategy 1) based on C-glycosylation with an acetyl protected

anomeric position, using as glycosyl donor a lactone (strategy 2) or by investigation of O→C rearrangement (strategy 3).

Strategy 1:

The first strategy (pathway A on Scheme 4.1) consisted on the *C*-glucosylation of 2′,4′-di-*O*-benzyl-6′-hydroxyacetophenone (**13**) using 1-*O*-acetyl-2,3,4,6-tetra-*O*-benzyl-D-glucopyranose (**4**) as glycosyl donor in the presence of a catalytic amount of $Sc(OTf)_3$ (Scheme 4.13). The chalcone derivative (**32**) prepared by an aldol condensation, from compound **31** with aldehyde **16a** under basic conditions, was deprotected with Et_3SiH/Pd-C, affording the desired *C*-glucosyl dihydrochalcone (**33**) in 28% overall yield.

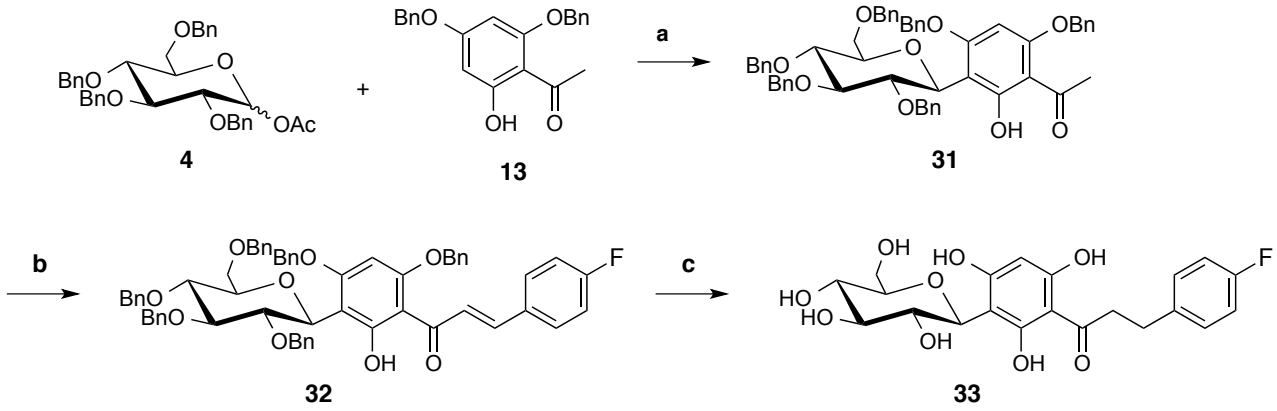

Scheme 4.13 *C*-glycosylation of 2′,4′-di-*O*-benzyl-6′-hydroxyacetophenone

Reaction conditions: **a.** $Sc(OTf_3)$ (0.5 equiv.), DCE, Drierite, -30 ºC then rt, 5 h, 49%; **b. 16a**, 50% (w/v) NaOH, 1,4-Dioxane, reflux, 24 h, 60%; **c.** Pd-C, Et_3SiH, EtOAc, MeOH, 5 h, rt, 96%.

The strategy showed in Scheme 4.13 was developed in our group, in a different project, to prepared the intermediate for the synthesis of *C*-glucosyl isoflavones.[144] In the current project the goal was to develop an original pathway for the synthesis of this type of compounds; therefore other methodologies were investigated.

Strategy 2:

As mentioned in Chapter 3, *C*-glucosyl compounds can also be synthesized using lactones as glycosyl donors. Hence, using 5′-bromo-2′-hydroxyacetophenone (**34**) as glycosyl acceptor and treating lactone **8** with *n*-BuLi, it was expected to obtain the

intermediate hemiacetal, which after reduction by Et_3SiH and $BF_3{\cdot}Et_2O$ would afford the ether **35** (Scheme 4.14). However, experimentally there was no formation of the desired product.

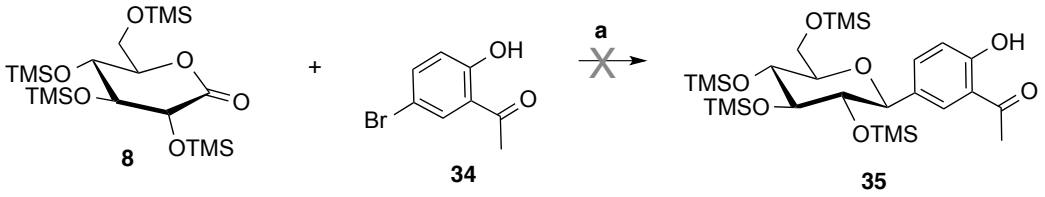

Scheme 4.14 *C*-glucosylation using lactone as glycosyl donor.

Reaction conditions: **a.**1. *n*-BuLi, THF/Toluene, -78 ºC, 40 min, 2. Et_3SiH, $BF_3{\cdot}Et_2O$, MeCN/DCM, -25 ºC, 24 h.

Strategy 3:

Alternatively, and based on the fact that the mechanism of *C*-glucosylation by a Fries-type rearrangement involves the formation of a glycoside prior to the O→C rearrangement, *C*-glucosylation starting from a glucoside was considered. Glucosides can be synthesized by a variety of methods, two of them using either glycosyl trichloroacetimidates (**11**) or glycosyl bromides (**12**) as glycosyl donors.

Small glycosyl acceptors (**13**, **14** or **34)** were used to prepare the glucosides (Scheme 4.15); however, despite the efforts, no products were detected from the reaction between glycosyl donors **11** or **12** with these glycosyl acceptors, using three different reaction conditions. The only compound detected, using both glycosyl donors, was compound **10** resulted from the hydrolysis of the glycosyl trichloroacetimidate or the glycosyl bromide, respectively.

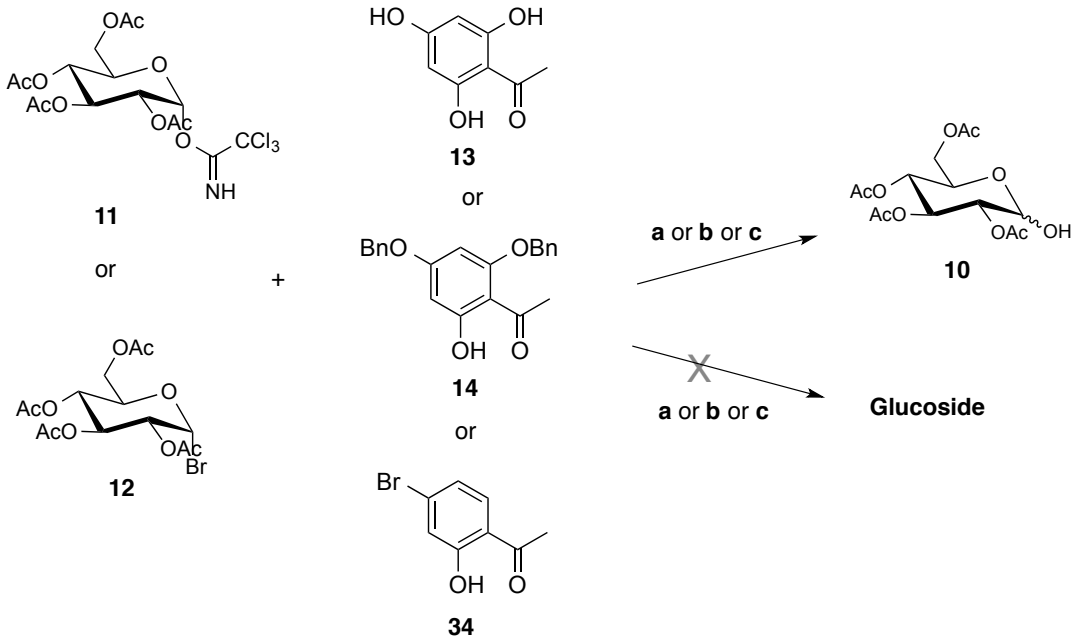

Scheme 4.15 Glycosylation using glycosyl donors **11** or **12** with glycosyl acceptors **13**, **14** and **34**, activated by $BF_3{\cdot}Et_2O$, $Sc(OTf)_3$ or AgOTf, depending on the glycosyl donor used

Reaction conditions: **a. 11**, **13** or **14** or **34**, $BF_3{\cdot}Et_2O$, DCM, 24 h, rt then 50 ºC, 90%; **b. 11**, **13** or **15** or **34**, $Sc(OTf)_3$, DCE, 24 h, -30 ºC then rt, **10.**92%; **c. 12**, **13** or **14**, AgOTf, DCM, TMU, -20 ºC then rt, **10.** 85%.

Strategy 4:

According to strategy 1, *C*-glucosylation should occur without significant problems when using compound **4** as glycosyl donor and a benzylated dihydrochalcone as glycosyl acceptor in the presence of catalytic amount of $Sc(OTf)_3$. To confirm that dihydrochalcone **19** was used as glycosyl acceptor (Scheme 4.16); but no products were detected from this reaction. Replacing $Sc(OTf)_3$ by TMSOTf, and glycosyl donor **4** by **3**, no product were obtained up to 48 h.

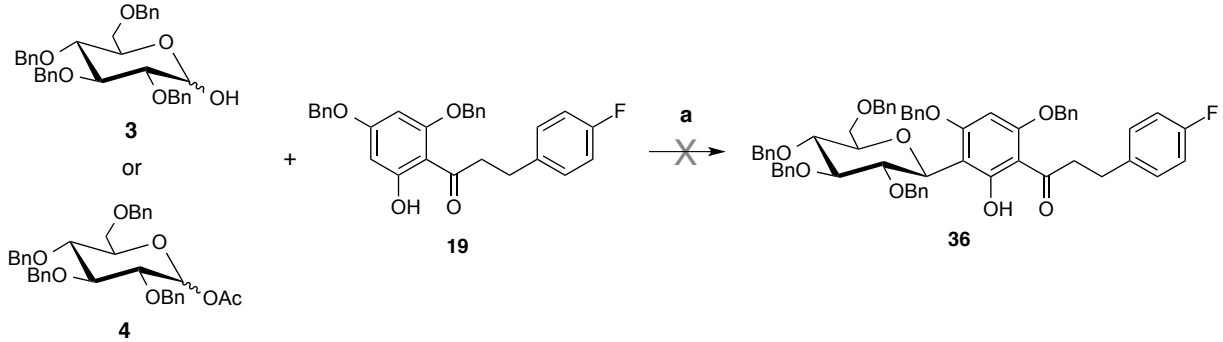

Scheme 4.16 *C*-glycosylation of a benzylated dihydrochalcone.

Reaction conditions: **a.** $Sc(OTf)_3$ or TMSOTf, DCE, drierite, -30 ºC then rt, 48h.

Alternatively, dihydrochalcone **19** was replaced by dihydrochalcone **18a** and the reaction was carried out in the conditions above described, with both activators ($Sc(OTf)_3$ and TMSOTf) and both glycosyl donors (**3** and **4**). Only when compound **3** was used as glycosyl donor and TMSOTf (0.25 equiv.) as activator the expected product was obtained, and in 12% yield (Scheme 4.16). Increasing the amount of catalyst up to 0.5 equiv. the yield increased to 43%, whereas the increase up to 0.75 equiv. led to the formation of secondary products. After deprotection by catalytic hydrogenation, the corresponding *C*-glucosyl dihydrochalcone was obtained in 36% overall yield. The overall yield resulted from this innovative pathway was significantly higher that with the one described in strategy 1, which was 28%. The *C*-glucosylation of dihydrochalcones **18a-18g** was then carried out using the conditions described above (Scheme 4.17) and *C*-glucosyl dihydrochalcones were successfully prepared in moderate to good yields (39-52%).

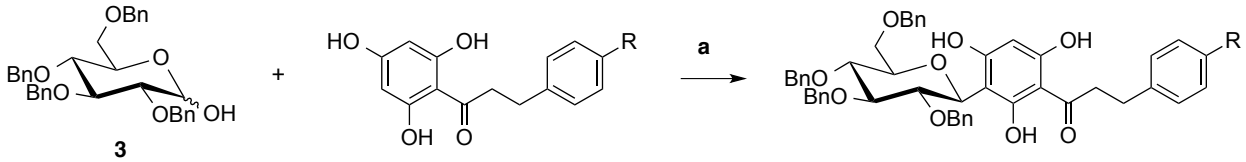

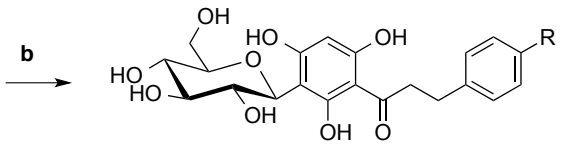

Scheme 4.17 Synthesis of *C*-glucosyldihydrochalcones.
Reaction conditions: **a.** TMSOTf, DCM, ACN, drierite, 0 ºC then rt, 2-5 h; **b.** Et_3SiH, MeOH, EtOAc, rt, 5 h

When dihydrochalcone **18i** was used in the *C*-glucosylation step several products were detected on the TLC plate and it was not possible to isolate the desired compound.

The C-glucosylation of dihydrochalcone **18h** did not afford any product, possibly due to the presence of the hydroxyl group in position 4′′ on the aglycone. Hence *C*-glucosyl dihydrochalcone **33h** was synthesized using the methodology described in strategy 1 with a slightly modification, in which 2′,4′,6′-trihydroxyacetophenone (**13**) was *C*-glucosylated without protection, generating compound **38** in 56.4% yield (Scheme 4.18). The aldol condensation step did not occur with 4′-hydroxybenzaldehyde (**16i**) neither with 4′-benzyloxybenzaldehyde (**16h**) due to the acidity of the hydroxyl groups from the acetophenone moiety. In alternative, compound **38** was selectively dibenzylated affording compound **32** in 73.8% yield, which was used in the aldol condensation. Protected *C*-glucosyl chalcone, obtained in 62.5% yield, was deprotected yielding the desired compound **33h**. The overall yield of this pathway was 36%, slightly higher than the one described in strategy 1 for the synthesis of an analogue, with the same number of steps. This methodology revealed to be more suitable than strategy 1 because it avoids the formation of the secondary product (compound **15**) that occurred when dibenzylation of 2′,4′,6′-trihydroxyacetophenone (**13**) was carried out prior to *C*-glycosylation (Scheme 4.6).

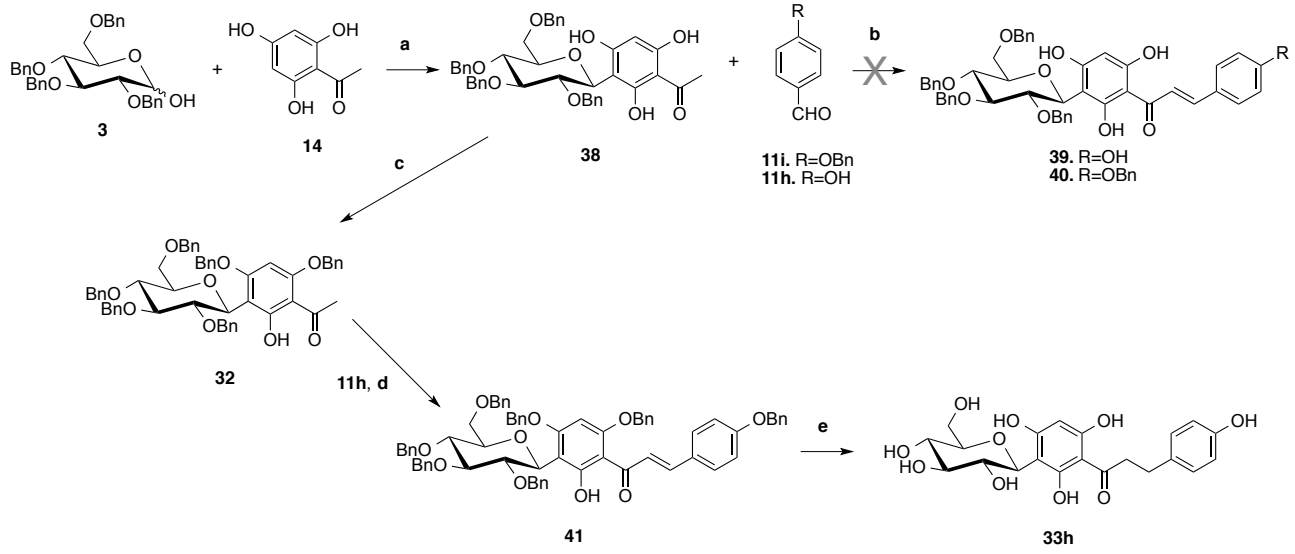

Scheme 4.18 Synthesis of compound **33h**

Reaction conditions: **a.** TMSOTf, DCM, ACN, drierite, 0 ºC then rt, 2-5 h, 56.4%; **b.** 50% aq NaOH (w/v), 1,4-Dioxane, reflux, 24h; **c.** BnBr, K_2CO_3, DMF, rt, 1-2 h, 73.8%; **d.** 50% aq NaOH (w/v), 1,4-Dioxane, reflux, 24h, 62.5%; **e.** Et_3SiH, Pd-C, MeOH, EtOAc, rt, 5 h, 87.4%

Reaction with dihydrochalcones **29a-29i** and **30a-30j** (Scheme 4.19) applying the same conditions described above for the *C*-glycosylation reaction, no products were formed, possibly due to a lower reactivity of these molecules when compared to 2′,4′,6′-trihydroxydihydrochalcones.

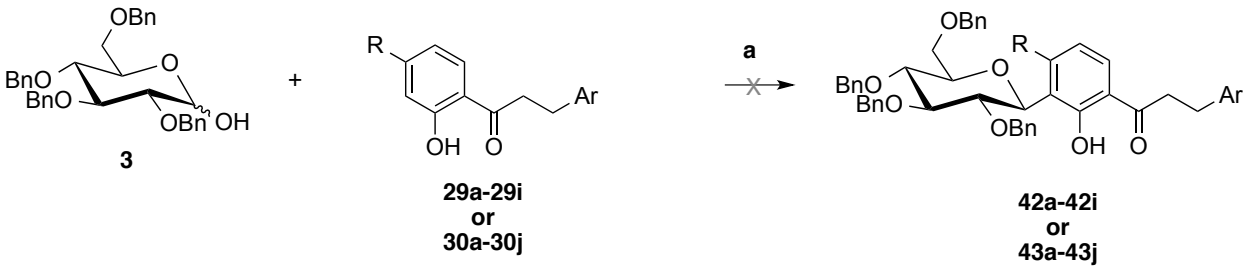

Scheme 4.19 *C*-glucosylation of 2′,4′-dihydroxydihydrochalcones and 4′-fluoro-2′-hydroxydihydrochalcones
Reaction conditions: TMSOTf, ACN, DCM, drierite, 0 ºC then rt, 24h

4.5 Enzymatic Synthesis of trisaccharides

As mentioned in Chapter 4 oligosaccharides can induce solubility in compounds with low solubility in water. Therefore, the synthesis of two trisaccharides was investigated.

The synthesis of one of the trisaccharides started from the monomer *p*-nitrophenol glucuronic acid (GlcApnp, **44**), which was converted into the disaccharide α-D-GlcNAc-(1→4)-β-D-GlcApnp (**45**) *via N*-acetyl-D-glucosaminyl transferase (KfiA) using UDP-GlcNAc (**46**, Figure 4.5) as glucosyl donor, in 70.7% yield (Scheme 4.20). Next, using UDP-GlcA (**47**, Figure 4.5) in the presence of *Pasteurella multocida* heparosan synthase (pmHS2), compound **45** was converted into the trisaccharide β-D-GlcA-(1→4)-α-D-GlCNAc-(1→4)-β-D-GlcApnp (**46**) in 89.9% yield. The overall yield for the synthesis of **46** was 63.0%, over two steps. Alternatively, synthesis accomplished solely by chemical methods would require several steps including protection/deprotection steps. The avoidance of these extra steps is a major advantage of the enzymatic synthesis.

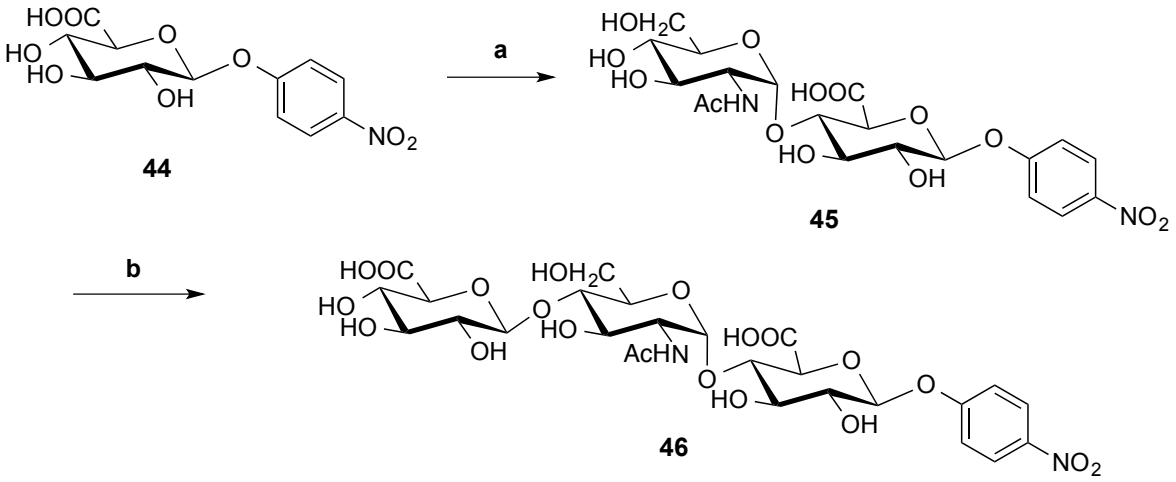

Scheme 4.20 Enzymatic synthesis of trisaccharide β-D-GlcA-(1→4)-α-D-GlCNAc-(1→4)-β-D-GlcApnp
Reaction conditions: **a.** UDP-GlcNAc, KfiA, Tris (pH 7.2), $MgCl_2$, 70.7%; **b.** UDP-GlcA, pmHS2, Tris (pH 7.2), $MgCl_2$, 89.9%

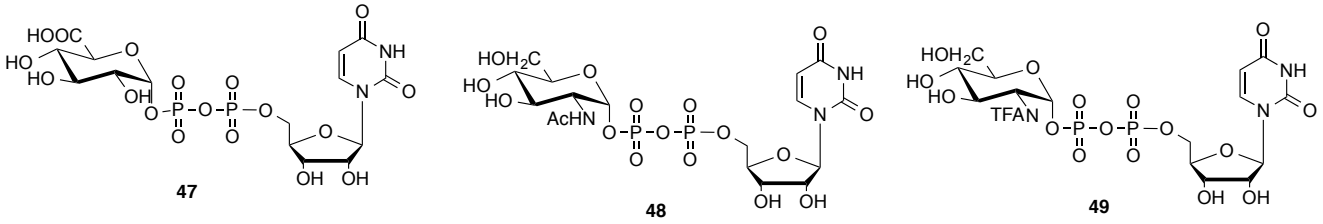

Figure 4.5 Struture of compounds **48.** UDP-GlcNAc, **49.** UDP-GlcA, and **50.**UDP-GlcNTFA

The second trisaccharide contained GlcNTFA units instead of GlcNAc. The conditions were the same as in the previous case and disaccharide **50** was obtained in 89.7% yield using UDP-GlcNTFA as glycosyl donor in the presence of KfiA, followed by the synthesis of the trisaccharide **51** in 88.2% yield using UDP-GlcA as glycosyl donor in the presence pmHS2. The overall yield of this synthesis was 79.1% over two steps.

The enzyme KfiA could be applied in this pathway because it recognizes both GlcNAc and GlcNTFA units; but pmHS2 only recognizes glucoronic acid units.

All compounds were purified by HPLC and the structures were confirmed either by NMR or ESI-MS. Unfortunately, it was not possible to test the *C*-glycosylation reaction of dihydrochalcones with disaccharides or trisaccharides as glycosyl donors, not available when research on dihydrochalcone *C*-glycosylation was carried out.

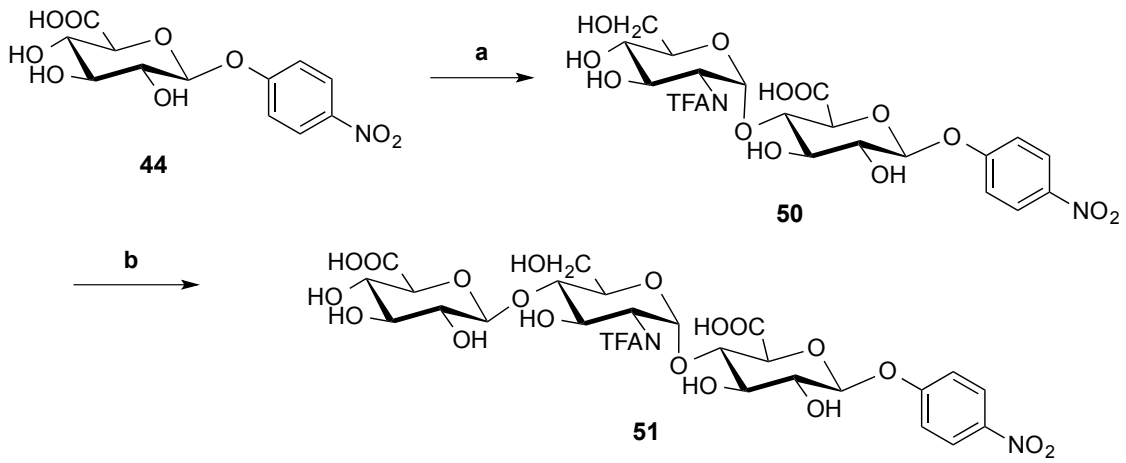

Scheme 4.21 Enzymatic synthesis of trisaccharide β-D-GlcA-(1→4)-α-D-GlcNTFA-(1→4)-β-D-GlcApnp
Reaction conditions: **a.** UDP-GlcNTFA, KfiA, Tris (pH 7.2), $MgCl_2$, 88.2%; **b.** UDP-GlcA, pmHS2, Tris (pH 7.2), $MgCl_2$, 89.7%

In parallel, pmHS2 enzyme was expressed in bacterial cells and purified. BL21 cells were grown overnight in Luria Broth (LB) containing 50 μg/mL of ampicillin and then, one portion was expanded to a bigger volume, in same growth media, which was incubated for a couple of hours until an optimal density[bb] at 600 nm was reached (4-6 hours).

The temperature was decreased and isopropyl β-D-1-thiogalactopyranoside, which is effective inducer of protein expression, was added to the medium. The incubation proceeded until an optimum induction yield was reached (ca. 18 hours). The expressed enzyme was harvested and purified using an NTA-agarose column yielding 0.17 μg/μL of pure enzyme.

To test the activity of this enzyme a 100 μL reaction to synthesize disaccharide **45** was carried out. An aliquot of the reaction mixture was used for HPLC to ensure that > 95% of UPD-GlcNAc was consumed. To confirm the purity of the enzyme a SDS-PAGE electrophoresis was conducted and analysing the gel it was possible to conclude that the enzyme was considerably pure (Figure 4.6).

[bb] The optimal density at 600 nm estimates the concentration of bacterial or other cells in the liquid phase

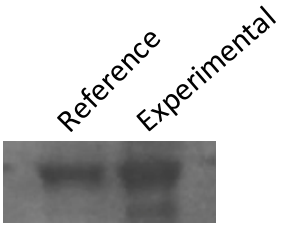

Figure 4.6 SDS-PAGE Electrophoresis Gel of pmHS2

In summary, in chapter 4 the successful generation of a small library of chalcones and dihydrochalcones bearing different substituents on both aromatic rings is described. Microwave assisted synthesis proved to be an excellent methodology for the synthesis of chalcones, with the ability of decreasing substantially reaction time providing the same high yields. The combination of Et_3SiH and Pd-C is an alternative to the use of H_2, and is an innovative method for the synthesis of dihydrochalcones. However, it cannot be applied if substituents or functionalities, that will be also reduced, should be kept in the target chalcone, such as bromides or double bonds.

Moreover, an original and innovative methodology for the synthesis of *C*-glucosyl dihydrochalcones was developed based on a direct *C*-glycosylation of dihydrochalcones in moderate overall yields, few steps and less secondary products.

An enzymatic approach was successful for the synthesis of two disaccharides and two trisaccharides, that can be later transformed into glycosyl donors for glycosylation reactions to induce solubility in compounds with low solubility in water. An enzyme was expressed in bacterial cells and purified; SDS-PAGE was used to confirm its purity.

With all the *C*-glucosyl dihydrochalcones in hand, biological studies were investigated and carried out. This will be discussed in detail in Chapter 5.

Chapter 5. Results and Discussion: *In vitro* studies

5.1 Generation of stable cell lines

Evaluation of SGLT inhibition using chemical compounds is, in general, accomplished by a glucose uptake assay in live cells. There are two different methods currently described in the literature. One uses either the fluorescent analogue of glucose 2-NBDG whereas the other uses 2-DG. Both are described in more detail in Chapter 2. The advantage of using these two sugars as probes of glucose uptake when compared with glucose is the fact that they accumulate inside the cells, whereas glucose is further metabolized. Ideally, the biological studies should be carried out using a stable cell line, i.e., a cell line that has been transfected with foreign DNA that has been "stably" incorporated into the cell's genome.

Briefly, the generation of a stable cell line requires two main steps: a transient[cc] transfection with the gene of interest; and the addition of a specific antibiotic, after a certain period of time, to kill all the non-transfected cells (all the growing cells will have the gene integrated). Some preparation/optimization steps are require to obtain a stable clone with high expression of the gene of interest, such as the preparation of the plasmid(s), the optimization of the transfection process, the determination of the effective concentration of antibiotic to be added to the cells, among others. These will be discussed within this chapter.

5.1.1 Preparation of the plasmids hSGLT1 and hSGLT2

DH5α cells were transformed with pCMV6-Neo vectors containing human SGLT1 and SGLT2 complementary DNAs (cDNAs) and plated on LB agar plates containing ampicillin (Figure 5.1). The pCMV6-Neo vectors contain a gene conferring ampicillin resistance to bacterial cells; therefore, it was possible to grow only cells containing these plasmids. A negative control was used, in which no vector was added and no cell growth was observed.

[cc] Temporary

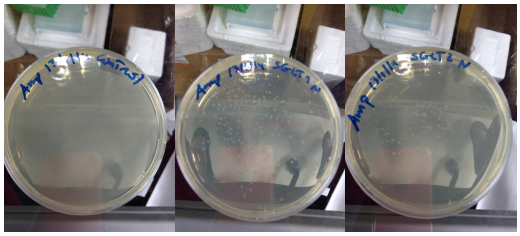

A **B** **C**

Figure 5.1 Agar plates of transformed DH5α cells after 24 h of incubation: **A.** Control; **B.** SGLT1; **C.** SGLT2

After an overnight incubation two colonies were picked and grown overnight in media that contained the same antibiotic at the same concentration. The media was removed by centrifugation and the bacteria were recovered in a pellet form that was later purified using a Maxiprep kit® from Sigma.

The purity and concentration of each plasmid was confirmed using a NanoDrop spectrometer. The purity of DNA using a spectrometer is given by the ratio of the absorbance at 260 and 280 nm, which should fall in the range of 1.8–1.9. In this case plasmids had a ratio A_{260}/A_{280} of 1.87 and 1.89, respectively. SGLT1 and SGLT2 concentrations were 5.8 μg/μL and 5.0 μg/μL, respectively.

A digest restriction was performed to verify the integrity of the two plasmids. Herein, the restriction enzymes used were BamHI, KpnI, SacI and SacII. The products were separated in an agarose gel electrophoresis and the resulted bands were visualized using a fluorescent UV light (Figure 5.2). A standard DNA ladder was used to be able to identify the molecular weight of each fragment. The two lanes on the left side of the gel are the wild type plasmids without digestion, in their circular form; on the right side are the bands of the fragments after digestion. If one enzyme cuts only in one site of the sequence the resulted band has the same molecular weight as the wild type plasmid, but if the enzyme cuts in two or more sites two or more fragments are obtained. To predict the number of sites where each enzyme is able to cut restriction maps were generated using the Vector NTI® software (Figure 5.3). Therefore, e.g. enzyme SacI cuts SGLT2 DNA only in one place and the predicted molecular weight is the same as the wild type (~8Kbp); but SacII cuts SGLT2 DNA in two places originating two fragments, one with a very low molecular weight (~900bp, which is not detected in the gel) and other with a slightly lower molecular weight than the wild type (~7Kbp). The same analogy can be applied for the other enzymes. Both plasmids seemed to be intact because the fragments

resulted from the digest restriction are in concordance with the expected from the restriction map.

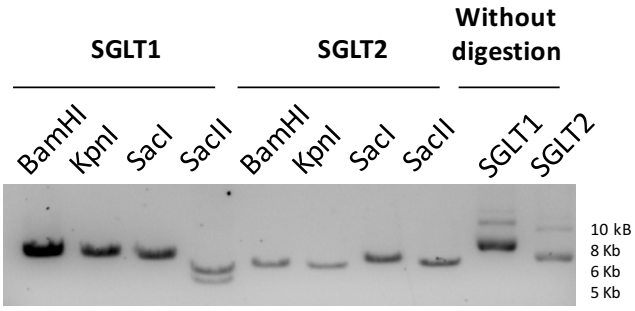

Figure 5.2 Gel Electrophoresis of the products from the digest restriction of SGLT1 and SGLT2 plasmids

Figure 5.3 Restriction maps for SGLT1 and SGLT2 plasmids
NOTE: In parenthesis is the exact location of the cut size of each enzyme.

To further confirm the integrity and correct sequence of the plasmids prior the stable cell line generation, they were sequenced (Bioneer). Using the Clustal W2 software, theoretical and experimental sequences were superimposed (Figure 5.4) and it was found that they were completely aligned, for both plasmids, meaning that the amplified plasmids have the right sequence. A partial alignment sequence for SGLT1 and SGLT2 is shown in Figure 5.4. (For the full sequences see Supplemental Section) NOTE: The symbol star (*) under each nucleotide unit means that the nucleotide was found.

Based on the results obtained from Bioneer along with the results from the digest restriction it was possible to confirm that the plasmids had the right sequence and they could be used for the stable cell line generation.

Figure 5.4 Partial alignment sequence of **A.** SGLT1 and **B.** SGLT2 plasmids

5.1.2 Transfection Optimization

To generate a stable cell line is necessary to introduce the gene of interest (GOI) into the cells through a process called transfection. One of the most common methods to transfect cells is by 'Cationic Lipid Transfection' whereas a cationic lipid-based reagent spontaneously form condensed nucleic acid-cationic lipid complexes via electrostatic interactions between the negatively charged nucleic acid and the positively charged head group of the synthesis lipid. Despite the fact that the exact mechanism remains unknown it is believed that the cells take up these complexes through endocytosis and then released into the cytoplasm followed by the translocation to the nucleus where it will be expressed. The advantage of this method relies on the fact that a broad range of cell lines can be transfected with high efficiency, it can be applied to high-throughput screens and it can deliver all sizes of DNA as well as RNA and proteins. However, the efficiency of cationic lipid-mediated transfection depends on the cell type and culture conditions, requiring the optimization of transfection conditions for each cell type and transfection reagent.

HEK293 cells were chosen for this project due to their quick and easy reproduction and maintenance, a high amenability to transfection using a wide variety of methods/reagents, and a high efficiency of transfection and protein production.

The optimization of HEK293 cell line transfection was required and Lipofectamine LTX® to transfect this cell line with EGFP, which is a fluorescent protein that belongs to the GFP (Green Fluorescent Protein) family. Among other purposes, this protein is greatly used for the optimization of transfection conditions since transfected cells can be seen by fluorescence microscopy or the fluorescence can be measured using a microplate reader.

The first step in this optimization process consisted in the determination of the optimal cell number to use in a 96-well plate. HEK293 cells were plated with different 1.0×10^4, 2.0×10^4, 3.0×10^4 and 1.0×10^4 cells/well, in duplicate. After 24 hours of incubation cells were observed under the microscope and the cell number was that provided 80-90% confluence. For example, 50% confluence means that roughly half of the surface is covered and there is still space for cells to grow; 100% confluence means the surface is completely covered by the cells, and no more space is left for the cells to grow as a monolayer. Thus, 2.0×10^4 cells/well was the cell number chosen for the transfection. HEK293 cells were plated and transfected using eight different conditions (Table 5.1). These conditions were chosen based the specifications from the manufacturer; whereas the amount of DNA must be lower than 2.5 μg and the volume of Lipofectamine should be between 1 and 2.5 μL. Nevertheless, DNA and Lipofectamine amounts should never be higher enough to cause toxicity to the cells neither should be lower enough to cause a low transfection yield.

As it is possible to observe on Graph 5.1 the condition 7 (ratio 1:2, DNA/Lipofectamine) was the one that afforded the highest fluorescence intensity. Conditions 1, 7 and 8 were chosen for analysis by fluorescence confocal microscopy (Figure 5.5) and it was confirmed that condition 8 is indeed the best condition to use in transfection of HEK293 cells due to the higher number of fluorescent cells, which means a higher number of transfected cells with EGFP protein.

Table 5.1 Conditions for Transfection Optimization

Condition	Characteristics
1	2.5 μL lipo + 1.25 μg DNA
2	2.0 μL lipo + 1.25 μg DNA
3	1.5 μL lipo + 1.25 μg DNA
4	1.0 μL lipo + 1.25 μg DNA
5	1.0 μL lipo + 0.5 μg DNA
6	0.8 μL lipo + 0.4 μg DNA
7	0.6 μL lipo + 0.3 μg DNA
8	0.4 μL lipo + 0.2 μg DNA

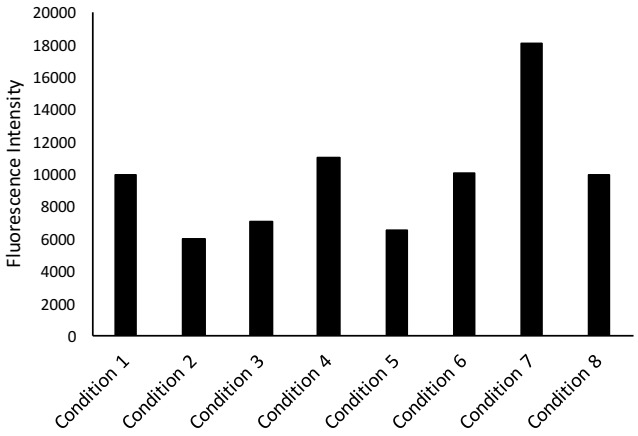

Graph 5.1 Fluorescence results using different conditions in transfection

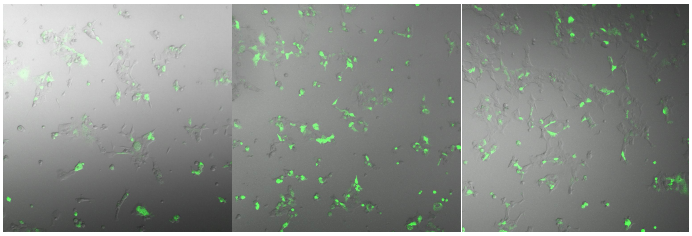

Figure 5.5 Confocal fluorescence microscopy on transfected cells

5.1.3 Generation of SGLT1 and SGLT2 stable cell lines

To generate a stable cell line it is necessary to transfect the cells with the GOI and treat them with a specific antibiotic for a period of time, necessary to kill all of the non-transfected cells and guarantee that the growing cells will have incorporated the gene.

In this case, SGLT1/SGLT2 plasmids are hosted in a pCMV6-Neo vector, which means that they have a Neo (neomycin) resistance gene, i.e. if the cells are treated with neomycin or similar antibiotic all of the non-transfected cells dye after a certain period of time, normally 7 days. Neomycin or kanamycin can be used to select prokaryotes but geneticin (G418) is generally needed for selection in eukaryotes.

The antibiotic concentration requires optimization, using a killing curve to guarantee that all of the non-transfected were killed after 7 days of treatment. According to the literature[145] the optimal concentration of G418 as a selection antibiotic should fall in the range of 400-800 μg/mL; therefore, HEK293 cells were plated in a 96-well plate and after 24 h of incubation, G418 was added to each well so that the final concentration ranged from 0-1000 μg/mL, in 100 μg/mL increments. The media was replaced every two days adding fresh antibiotic for up to 7 days of treatment. Results can be classified as low, optimal or high dose. Low dose is the concentration where there is a minimal visual toxicity apparent even after 7 days of selection. Optimal dose is the lowest concentration at which all cells are dead after 7 days of selection. High dose is the concentration where a visual toxicity (cells start to become rounded and start to detached from the well) is evident and all cells are dead after 2-3 days. The low dose was 100-500 μg/mL, optimal dose was 600 μg/mL, and the high dose was > 800 μg/mL. Therefore, 600-700 μg/mL was the concentration of G418 chosen to select the SGLT1/SGLT2-HEK293 transfected cells.

After selecting the optimal concentration of G418, HEK293 cells were transfected to generate the stable cell lines in two different conditions.

First, HEK293 were plated on two 24-well plates and incubated for 24 h, after which cells were transfected with SGLT1 and SGLT2, respectively, with TrueFect with a ratio of DNA/TrueFect 1:2. NOTE: TrueFect was used instead of Lipofectamine because it was the reagent available at the moment of the generation of the stable cell lines. Nevertheless, the conditions optimized for Lipofectamine were tested with TrueFect and

the same results were obtained. On the next day media was changed and the cells were incubated for another 24 h after which G418 was added to each well. The media was replaced every two days and fresh G418 was added for up to 7 days. After this period the concentration of G418 was reduced to 300 μg/mL and cells were allowed to grow until confluent enough for cryopreservation. Cells treated with TrueFect alone were used as control and after the 7 days of treatment all cells were dead. Clones resulted from this condition were named 600-Row-Column-Plasmid, e.g., 600B1SGLT1.

Second, HEK293 cells were plated on three 60 mm dishes and 24 h later cells were transfected with both plasmids, respectively, and Truefect alone was used for the control as previously described. On the next day cells were trypsinized and plated onto a 24-well plate and incubated for another 24 h after which G418 was added to a concentration of 700 μg/mL. The same procedure was followed until the cells were confluent for cryopreservation. Clones resulted from this condition were named 700-Row-Column-Plasmid, e.g., 700B1SGLT1.

Several clones of HEK293-SGLT1 and HEK293-SGLT2 were cryopreserved and some clones were characterized by Western Blot and RT-PCR. The stable clones used in the glucose uptake assay, to determine the inhibitory properties of the target compounds, were also evaluated by 2-NBDG assay using fluorescence confocal microscopy.

5.2 Western Blot

The Western Blot is a widely used analytical technique to detect specific proteins in a sample using antibodies. The native proteins are separated by SDS-PAGE and then are transferred to a membrane, generally nitrocellulose or PVDF (Polyvinylidene fluoride) membrane. This membrane is later incubated with a primary antibody, which bind to the immobilized target protein. A second solution is then added, containing a secondary antibody that binds specifically to the first one (Figure 5.6). This secondary antibody can possess a fluorescent dye or a radioactive label that enables the visualization of protein-antibody complexes. This technique is sensitive to the amount of the target protein present in the sample, and therefore it can be used to monitor how well a stable cell line overexpresses the GOI.

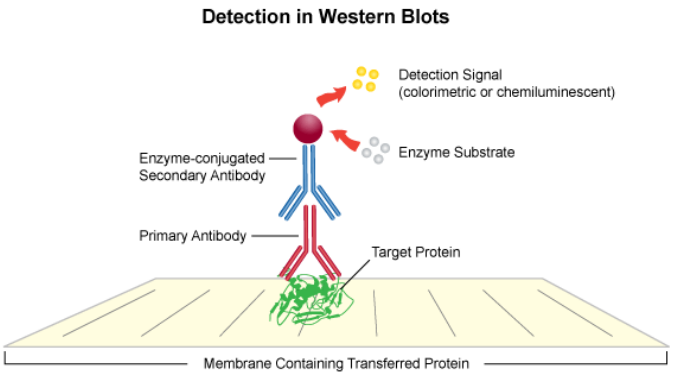

Figure 5.6 Illustration of detection of a protein by Western Blot

Stable clones were plated on 60 mm dishes and after 24h of incubation cells were lysed and protein content was quantified by the Bradford protein assay. For each clone, an aliquot of 50 μg of protein was used in the SDS-PAGE. Proteins were then transferred to a nitrocellulose membrane, which was blocked with a solution of TBST (tris-buffered saline) containing non-fat milk and Tween-20 (a detergent) to avoid non-specific binding. NOTE: Before the incubation with antibodies it is necessary to block the remaining binding surface otherwise the antibodies or other detection reagents will bind to any remaining sites that initially served to immobilize the proteins of interest.

The primary antibody (1:200 for SGLT1-AB and 1:500 for SGLT2-AB) in TBS-T and 5% of BSA was added to the membrane and then incubated for 75 min at room temperature. After that period the membrane was washed three times with TBS-T and then incubated with the secondary antibody (1:2000 for SGLT1 and 1:4000 for SGLT2) for 45 minutes. ECL reagent (Enhanced ChemiLuminescence) was added to each membrane and incubated for a short period (3-5 minutes). The membranes were imaged on a film and protein blots were visualized (Graph 5.2) and the blots were quantified using Fiji software (Graph 5.9). According to the results all the clones overexpress SGLT1protein, but clone 700B1 seemed to be the one with the higher expression, as showed in Graph 5.2. Regarding the SGLT2 expression, clone 700A1 revealed the highest expression although clones 700A3 and 700A4 are also overexpressing the protein.

Since the process of growing the stable clones is a time-consuming process some clones were evaluated using this technique while others were directly used in the glucose uptake assay, which will be discussed later in detail.

Figure 5.7 Western Blot for some SGLT1 and SGLT2 stable clones

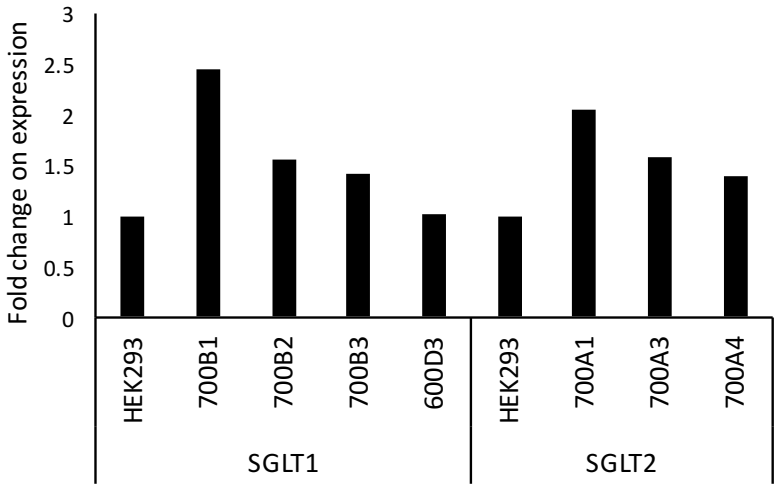

Graph 5.2 Quantification of SGLT1 and SGLT2 expression by Western Blot

Analyzing the results it was established that clones 700B1SGLT1 and 700A1SGLT2 were those overexpressing the proteins in higher proportion and, therefore used for the glucose uptake assay (discussed later). During the generation of these clones some conclusions were taken: cells must be trypsinized and diluted after 24 h post-transfection to avoid overgrowth (high confluence), the addition of the selection antibiotic must be added only 48 h post-transfection to guarantee a maximum of transient expression of the GOI and increase the number of transfected cells, and the addition of the antibiotic must be continued after the days of treatment otherwise the plasmid might be expelled from the cells since it is foreign DNA.

5.4 RT-PCR

Reverse transcription polymerase chain reaction (RT-PCR) is a technique commonly used in molecular biology to detect gene expression through the synthesis of complementary DNA (cDNA) transcripts from RNA, which is subsequently amplified using traditional PCR (Figure 5.8). After the addition of a fluorescent dye to the reaction mixture, an agarose gel electrophorese is carried out and the products are visualized using fluorescence UV light.

Figure 5.8 Schematic illustration of cDNA synthesis and RT-PCR

The presence of hSGLT1 and hSGLT2 genes in the two clones (700B1SGLT1 and 700A1SGLT2) was confirmed by RT-PCR, which revealed strong PCR products (bright bands) in both cell lines, as it is possible to visualize in Figure 5.9 and Graph 5.3. Moreover, the two products observed on the gel were in agreement with the expected size 328 bp and 321 bp for SGLT1 and SGLT2, respectively. No expression of either protein was observed on wild type HEK293 cells. Transiently transfected cells served as positive controls, and it was possible to observe the expected increase in expression of both proteins in stable cell lines.

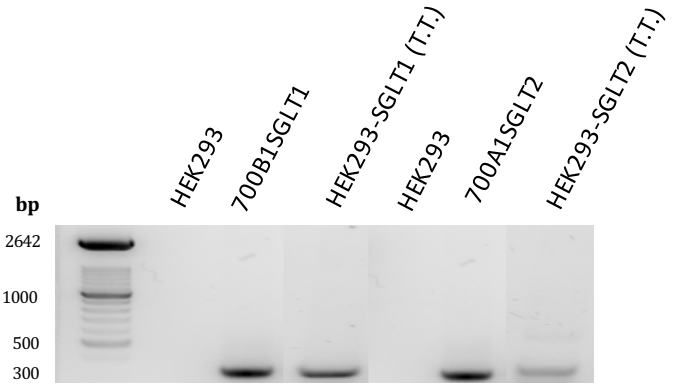

Figure 5.9 RT-PCR products using the two stable clones 700B1SGLT1 and 700A1SGLT2

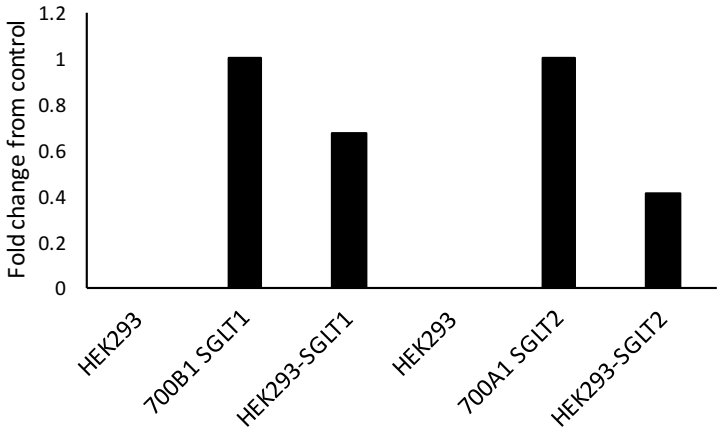

Graph 5.3 Quantification of the mRNA

5.5 Cytotoxicity assays

Cytotoxicity assays are widely used in *in vitro* toxicology studies and used by researchers to screen for cytotoxicity in compound libraries. Compounds that have cytotoxic effects often compromise cell membrane integrity. There are several methods to evaluate the cytoxicity in live cells. Some dyes, such as trypan blue or propidium iodide, freely cross the membrane of dead cells or non-healthy cells, when the membranes have been compromised, and stain intracellular components. This method is commonly used in cell culture.

Membrane integrity can also be assessed by monitoring the passage of substances that are normally retained inside the cells, such as lactate dehydrogenase. One of the most common methods to evaluate cytoxicity is the MTT assay (Scheme 5.1A), in which 3-(4,5-dimethyl-2-thiazolyl)-2,5-diphenyl-2H-tetrazolium bromide (MTT) is added to the cells, and the viable ones reduce the reagent generating the corresponding formazan product, which is colored. Its absorbance can be read and it is proportional to the number of live cells. A similar method has also been developed using the non-fluorescent dye resazurin, which after reduction by live cells generates the fluorescent resofurina (Scheme 5.1B). Similarly, fluorescence output is proportional to the number of live cells. Nonviable cells rapidly lose metabolic capacity and thus do not generate a fluorescent signal. In this study the method used was the CellTiter-Blue® Cell Viability Assay, which is based on the latter method mentioned above.

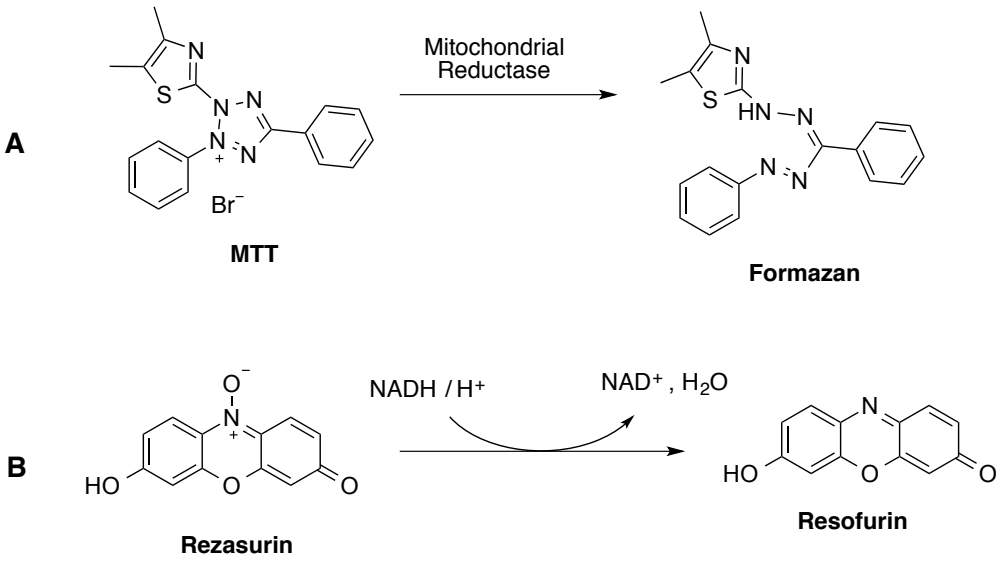

Scheme 5.1 A. Reaction of MTT assay, **B.** Reaction of CellTiter-Blue® assay

All the compounds synthesized were tested toward their toxicity in the cell line used in this study prior the glucose uptake assay. Compounds at a concentration of 100 μM were added to the cells, in triplicate, and incubated for 20-24 h. After this period CellTiter-Blue® was added to each well and incubated for 4 h. Fluorescence was measured at λ_{em} = 590 nm after excitation at λ_{exc} = 530 nm. DMSO treated cells were used as the positive control and the cell viability (%) was calculated by comparison with the untreated cells.

Compounds **18a-18h**, **22a-22h** and **33a-33h** revealed no significant cytoxicity towards HEK293 cells (Graph 5.4). On the other hand, compounds **26a-26h**, **28a-28h**, **29a-29h** and **30a-30a** showed significant cytoxicity, although none of them showed more then 50% of cell toxicity.

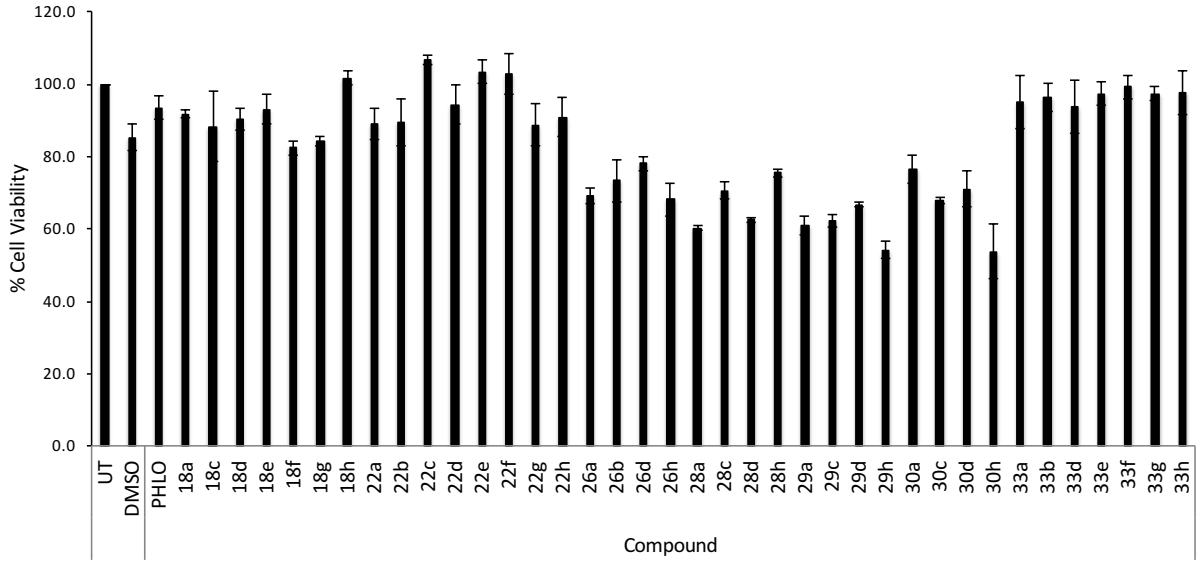

Graph 5.4 Cell viability assay

5.6 Glucose uptake assay

The ability of a compound to inhibit SGLTs has been measured using several methods, including transport assays with radiolabelled sugars, voltage-clamps experiments, and more recently using fluorescent sugars and enzymatic methods, which are less expensive and easier to perform.

5.6.1 2-NBDG uptake assay

The 2-NBDG method (Chapter 2.2.4.1) seemed to be the easiest method to use for this study and its feasibility was investigated in transiently transfected cells, while the stable cell lines was being established. HEK293 and HEK293 SGLT1-transiently transfected cells were plated in a 96-well plate and incubated overnight in DMEM without FBS (Fetal Bovine Serum). NOTE: The serum-starvation is to ensure that all the cells are in the same stage of growth and to avoid the action of insulin present on FBS. On the next day the media was removed, cells were carefully washed with Krebs-Ringer-Phosphate-HEPES buffer and incubated for 40 min. After this period, 2-NBDG at 100 and 200 μM was added to the wells followed by incubation for 60 min after which the media was removed, cells were washed three times with KRPH buffer and lysed. Fluorescence of lysate was measured at λ_{em} = 528 nm and λ_{exc}=485 nm. The same experiment was performed using COS-7 cells, to compare the ability of both cell lines to uptake

2-NBDG (Graph 5.5). In both assays the 96-well plates were pre-coated with poly-D-lysine to avoid the detachment of the cells. Moreover, two different lysis buffers were tested, specifically 0.1 N NaOH, 0.1 N HCl and 0.5% SDS, and 40 mM, 20 mM Tris (pH 7.4) and 1% sodium deoxycholate. The former abolished fluorescence whereas the latter did not.

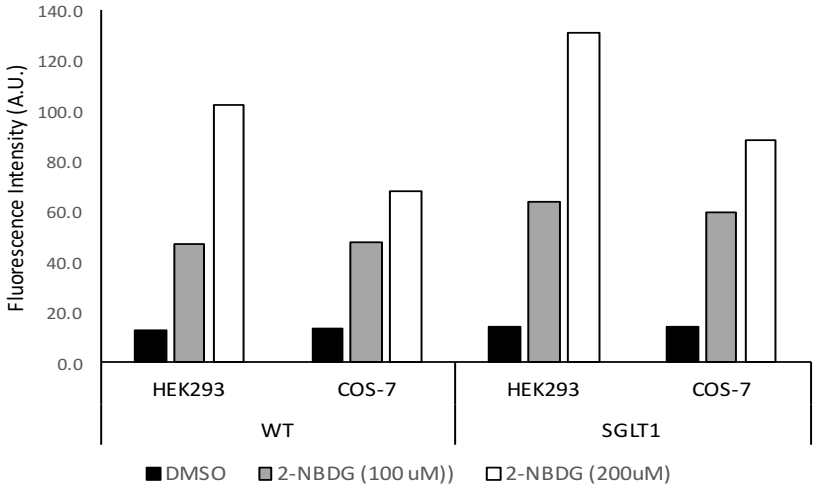

Graph 5.5 2-NBDG uptake on HEK293 and COS-7 wild type cells *vs* SGLT1-transfected HEK293 and COS-7 cells.

In Graph 5.5 it is possible to observe that there was a slight increase on the uptake of 2-NBDG in SGLT1-transfected cells on both cell lines, when it was given 100 μM of 2-NBDG. However, when the concentration was increased to 200 μM their fluorescence increased almost 2-fold, when compared to the 100 μM values. Nevertheless, HEK293 cells, transfected and non-transfected, seemed to uptake 2-NBDG to a higher degree than COS-7 cells. Later, the same assay was run with non-transfected HEK293 cells in the presence of phlorizin (Figure 2.9) and almost no inhibition was observed. Another feature observed always in this assay was that there was no consistency among the three wells and no reproducibility between assays. For this reason, the other assay (2-deoxyglucose uptake) was investigated to obtain more consistent results.

5.6.2 2DG uptake assay

In this assay, HEK293 were cultured on a 96-well plate and incubated overnight. On the next day media was removed and cells were washed with KRPH buffer and incubated

for 40 minutes prior the addition of 2-DG at a concentration of 1 mM. Cells were incubated for 1 h 30, then washed three times and lysed with a 0.1 N NaOH solution. Lysates were incubated at 80-85 ºC for 40 minutes, and then neutralized with 0.1 N HCl solution and buffered with TEA buffer (triethanolamine, pH 8.2). To an aliquot of each lysate was added a solution containing 50 mM TEA pH 8.2, 50 mM KCl, 0.5 mM $MgCl_2$, 0.02% BSA, 670 μM ATP, 0.12 μM NADP, 5.5. U/mL hexokinase, 16 U/mL G6PDH, 1 U/mL diaphorase and 25 μM resazurin, later incubated at 37 ºC for 1 h 30. Fluorescence was measured in a microplate reader at λ_{em} = 590 nm and λ_{exc} = 560 nm (Graph 5.6). However, after some repetitions using exactly the same conditions it was found that the results were not reproducible. The 2-DG that enters the cell is phosphorylated by endogenous hexokinase but, if the cells are not properly washed and all the extracellular 2-DG removed, the hexokinase present in the cocktail mixture will be able to phosphorylate the remaining 2-DG leading to misread values.

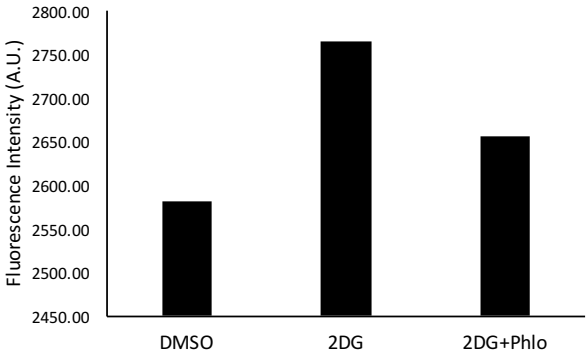

Graph 5.6 2DG uptake in HEK293 wild type cells

Hexokinase can be left out and fluorescence values represent the amount of 2DG6P, which is the amount of 2DG that entered into the cell and phosphorylated by endogenous hexokinase. Therefore, not using hexokinase in the enzymatic cocktail completely removes the error from the extracellular 2-DG since the cells do not require the washing step, leading to more reproducible results. To verify and confirm this hypothesis a standard curve of serial dilutions of 2DG6P was performed using a cocktail mixture containing 50 mMTEA (pH 8.1), 50 mM KCl, 0.02% BSA, 1 mM NADP, 0.5 U/mL

G6PDH, 0.1 U/mL diaphorase, 10 μM resazurin. Similarly, an aliquot of 2DG6P solutions at different concentration were placed into a 96-well plate and this cocktail mixture was added. Fluorescence was measured after overnight incubation to guarantee that the reading corresponded to the end-point of the enzymatic reaction (Graph 5.7). It was observed that more than 4 h of incubation gives the most accurate results. NOTE: the cocktail mixture was prepared on the day of the assay from stock solutions of the several components. This experiment was repeated more than once and showed that the assay is reliable and can be used to evaluate the 2DG uptake into the cells.

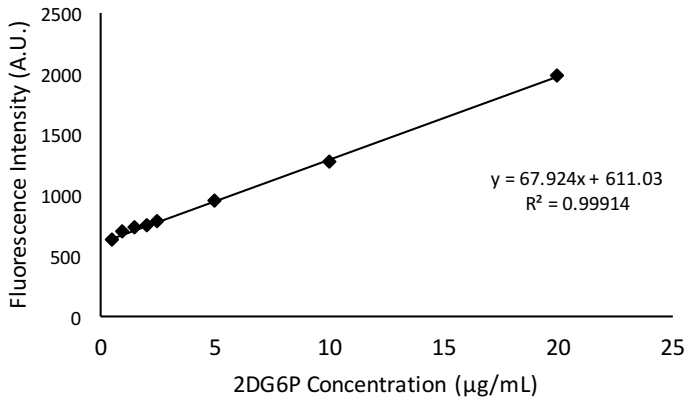

Graph 5.7 2DG6P standard curve

To use transiently transfected cells for the evaluation of the compounds, HEK293 and HEK293T cells were transfected with SGLT1 and SGLT2 plasmids using two different transfection reagents, TrueFect and X-TremeGene. The enzymatic assay was carried out and it was observed that HEK293T after transfection can uptake more 2-DG than HEK293 cells (Graph 5.8). Moreover, X-TremeGene reagent seemed to have a better transfection efficiency and it seemed to be less toxic to the cells than TrueFect as a high percentage of cell death was observed before running the assay when the later was used to transfect cells.

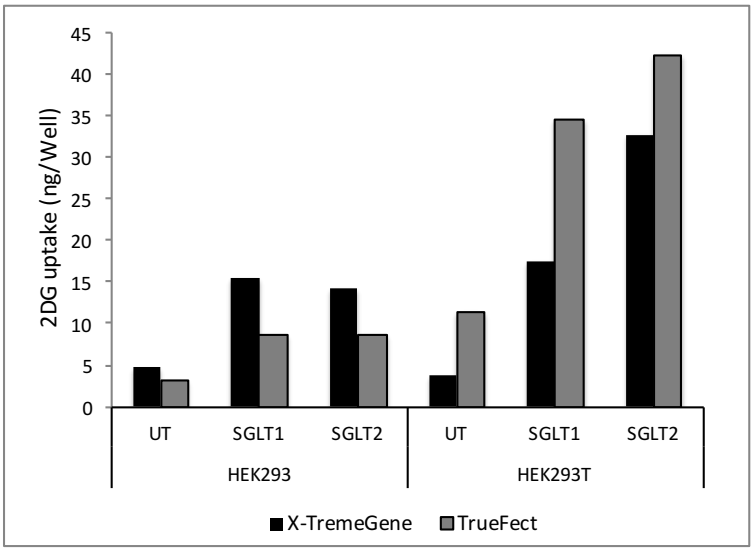

Graph 5.8 2DG uptake on HEK293 *vs* HEK293T cells and TrueFect *vs* X-TremeGene

Western Blotting on HEK293 and HEK293T using these two transfection reagents also confirmed the fact that HEK293T is a better cell line to work with if the assay is ran with transiently transfected cells (Figure 5.10, Graph 5.9). Unfortunately, HEK293T cannot be used to generate a stable cell line since they possess a neomycin resistance gene; therefore, in the presence of G418 the cells will not die.

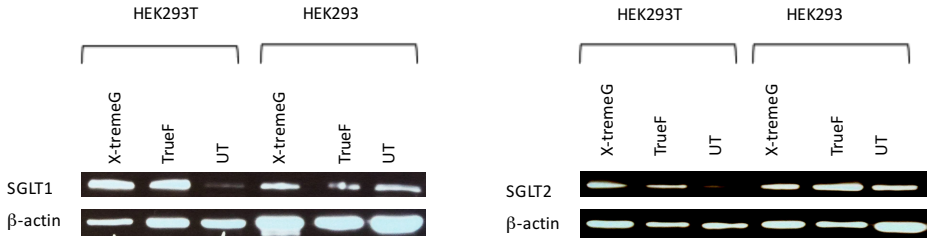

Figure 5.10 Western Blot of HEK293 and HEK293T cells using different transfection reagents

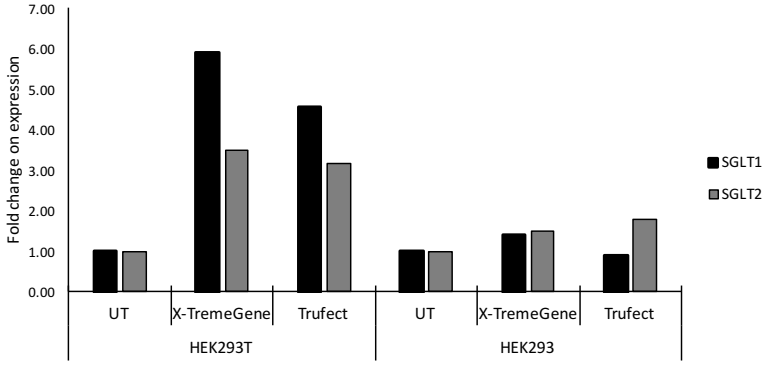

Graph 5.9 SGLT1 and SGLT2 expression quantification by Western Blot

HEK293T cells were chosen to proceed on the optimization of the enzymatic method to evaluate the inhibition properties of the target compounds. Therefore, HEK293T cells were plated on 35 mm dishes and incubated overnight. Two dishes were transfected with SGLT1 and SGLT2, respectively and the third was used as a control and only transfection reagent was added (no DNA). The media was replaced by DMEM without FBS prior the addition of DNA mixtures and the dishes were incubated overnight. On the next day, media was replaced by KRPH buffer after a brief washing step, and the cells were incubated for 1 h. After this period phlorizin was added to the wells at a final concentration of 100 μM along with 2-DG (0.5 mM or 1 mM) in different conditions as showed in Table 5.2.

Table 5.2 Different conditions used during optimization of 2DG uptake assay

Condition	Method	Remarks
1	1 μL Phlo (100 μM) + 10 μL 2-DG (10 mM)	Added together, same time
2	1 μL Phlo (100 μM) + 5 μL 2-DG (10 mM)	Added together, same time
3	1 μL Phlo (100 μM) then 10 μL 2-DG (10 mM)	10 min apart
4	1 μL Phlo (100 μM) then 5 μL 2-DG (10 mM)	10 min apart
5	10 μL Phlo (1mM) + 10 μL 2-DG (10 mM)	Added together, same time
6	10 μL Phlo (1mM) + 5 μL 2-DG (10 mM)	Added together, same time
7	10 μL Phlo (1mM) then 10 μL (10 mM)	10 min apart
8	10 μL Phlo (1mM) then 5 μL (10 mM)	10 min apart

After the addition of 2-DG the plates were incubated for 1 h and the enzymatic assay was performed as described previously. Fluorescence (Graph 5.10) was measured and it was observed that, when phlorizin is added from the stock solution of 10 mM (1 μL) there is very low inhibition (40-60%), whereas when phlorizin is added from a buffer diluted solution (from 1 mM, 10 μL) the inhibition percentage is much higher, which means that some insolubility might be the responsible for such low values of inhibition. Therefore, phlorizin and all the others compounds were pre-diluted before their addition to the cells to avoid solubility issues.

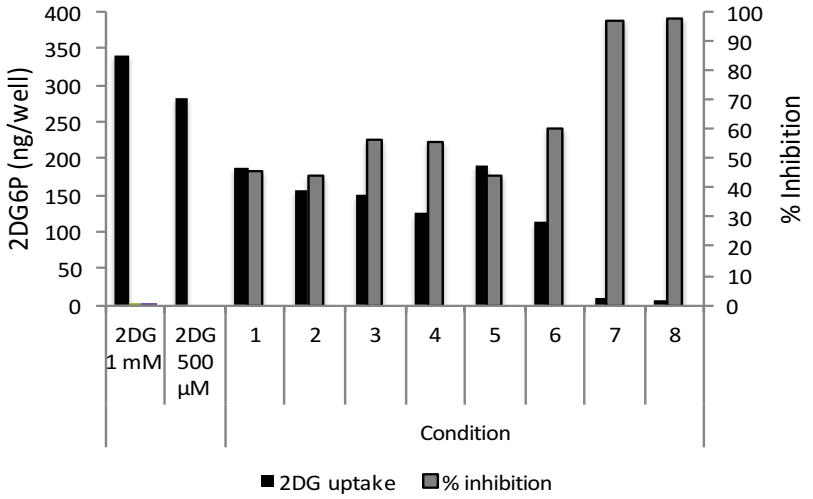

Graph 5.10 2DG uptake assay using different conditions

Once the conditions for the assay were optimized, some stable clones were confluent enough for cryopreservation, some were used for Western Blot (as showed before), and some were also used in this assay to evaluate their ability to uptake 2DG more efficiently than the wild type cell line. The stable clones were plated on 96-well plate and, using condition 7 (Table 5.2), assayed as described previously (Graph 5.11). The assay confirmed the data from the Western Blot, RT-PCR and microscopy that the clones 700B1SGLT1 and 700A1SGLT2 were the ones with higher expression of the proteins and consequently higher uptake of 2DG.

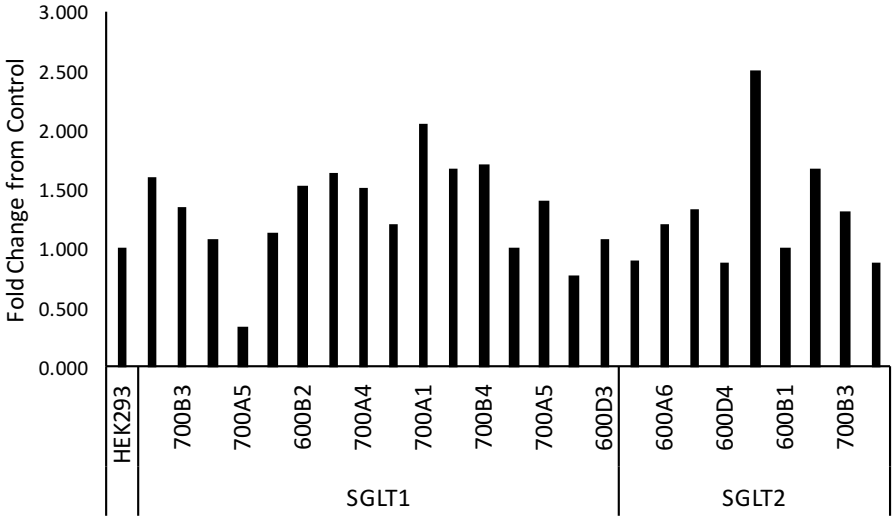

Graph 5.11 2DG uptake using the stable clones of SGLT1 and SGLT2

With the two stable cell lines in hand all the compounds were screened at a concentration of 100 μM (Graph 5.12) and at this concentration all the compounds completely inhibited the 2-DG uptake in both cell lines.

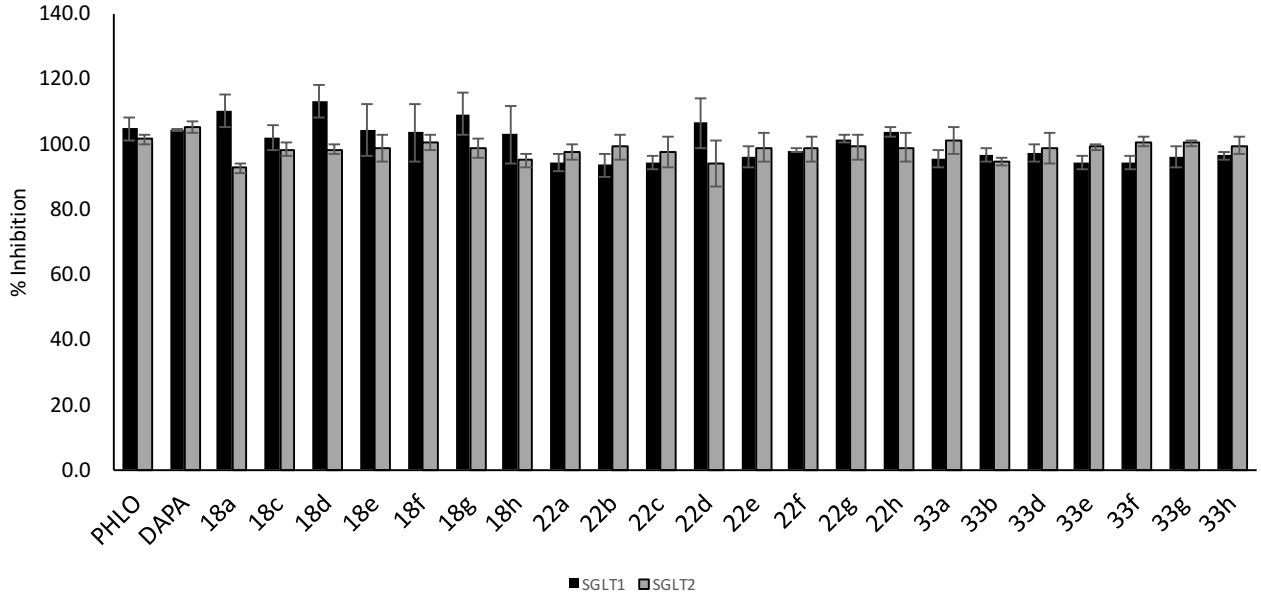

Graph 5.12 2DG uptake inhibition at 100μM

IC_{50} values were determined using the enzymatic assay. Both cell lines were plated in 96-well plates and incubated in low-glucose DMEM without FBS. On the next day cells were treated as described previously and compounds **18a-18h**, **22a-22h**, **33a-33h**, phlorizin (Phlo, Figure 5.11A) and dagliflozin (DAPA, Figure 5.11B) were added at different concentrations, ranging from 0.1 nM up to 200 μM. Phlorizin (a non-selective SGLT1/SGLT2 inhibitor) and dapagliflozin (a FDA approved selective SGLT2 inhibitor) were used as controls.

Adequate diluted stock solutions in KRPH buffer were prepared on the day of the assay, to guarantee maximum solubility.

The inhibition curves (Figure 5.12 and Table 5.3) were obtained using Prism6 software and are given by the mean of three independent assays.

From the results obtained, it was possible to observe that all the aglycones **18a-18h** and **22a-22h** have similar IC_{50} values and do not have significant selectivity towards either SGLT1 or SGLT2. On the other hand all the *C*-glycosyl dihydrochalcones (**33a-33h**) are SGLT2 selective inhibitors with a much higher selectivity for SGLT2 than

phlorizin. However, none of these compounds as potent and SGLT2 selective than the commercial drug Dapagliflozin (DAPA) neither a similar IC_{50}.

Among all the compounds, **33h** was to be the best lead. The IC_{50} of this compound toward SGLT1 (19.0 μM) is 10-fold higher than the IC_{50} of DAPA (1.8 μM) and 20-fold higher than the than the IC_{50} of phlorizin (~ 0.5 μM), which means that its SGLT1 inhibition is significantly lower than both DAPA and phlorizin.

Regarding the inhibition of SGLT2 protein, the IC_{50} of DAPA and phlorizin is 0.8 and 67.3 nM, respectively, whereas the IC_{50} of compound **33h** is 11.9 nM; therefore, compound **33h** is 10 times less active than DAPA but 7 times more active than phlorizin.

Comparing the selectivity toward SGLT2 protein, compound **33h** is highly selective, although selectivity of DAPA is 1.4 times higher. Nevertheless, changing from an *O*-glucoside (phlorizin) to the corresponding *C*-glucosyl derivative (**33h**) it was possible to increase its selectivity and decrease the SGLT1 inhibition.

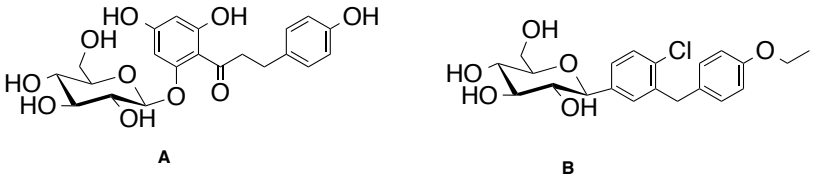

Figure 5.11 Structures of **A.** Phlorizin and **B.** Dapagliflozin

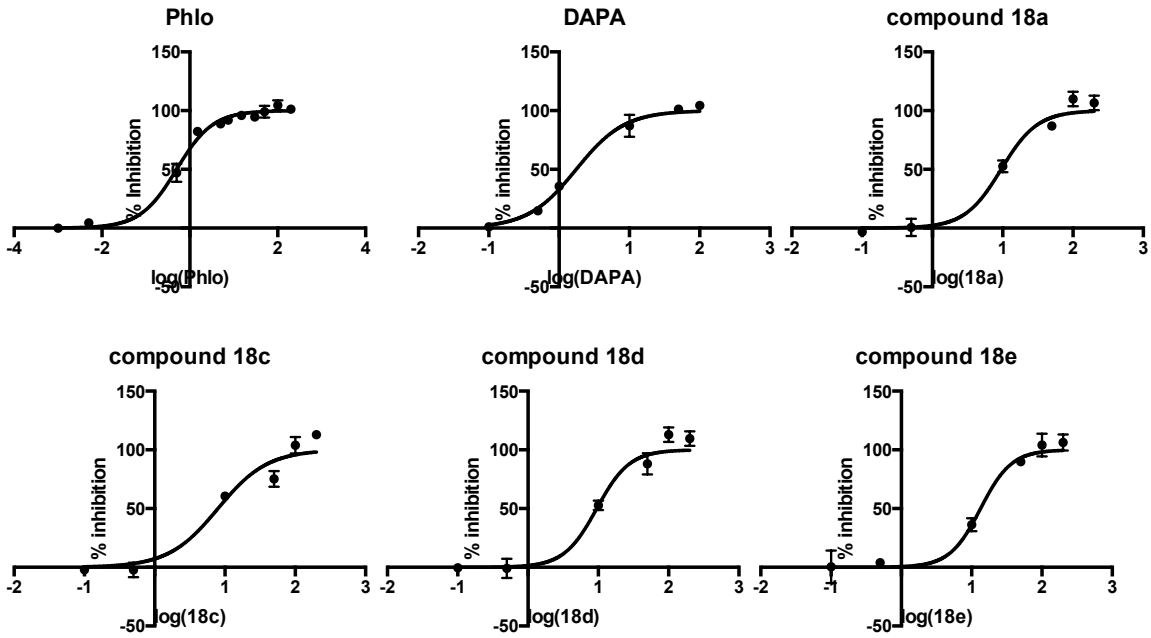

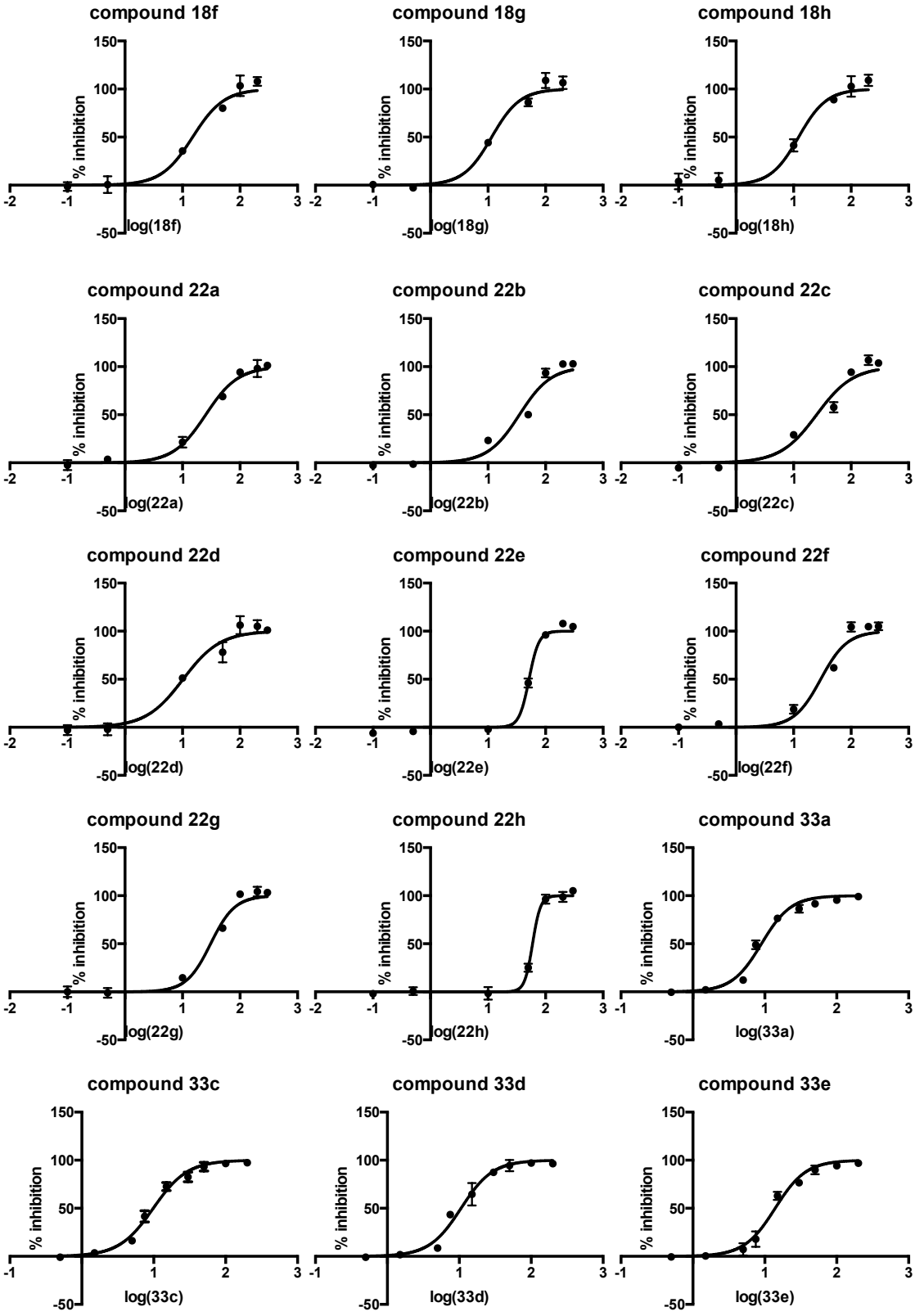
compound 18f
% inhibition
log(18f)
compound 18g
% inhibition
log(18g)
compound 18h
% inhibition
log(18h)
compound 22a
% inhibition
log(22a)
compound 22b
% inhibition
log(22b)
compound 22c
% inhibition
log(22c)
compound 22d
% inhibition
log(22d)
compound 22e
% inhibition
log(22e)
compound 22f
% inhibition
log(22f)
compound 22g
% inhibition
log(22g)
compound 22h
% inhibition
log(22h)
compound 33a
% inhibition
log(33a)
compound 33c
% inhibition
log(33c)
compound 33d
% inhibition
log(33d)
compound 33e
% inhibition
log(33e)

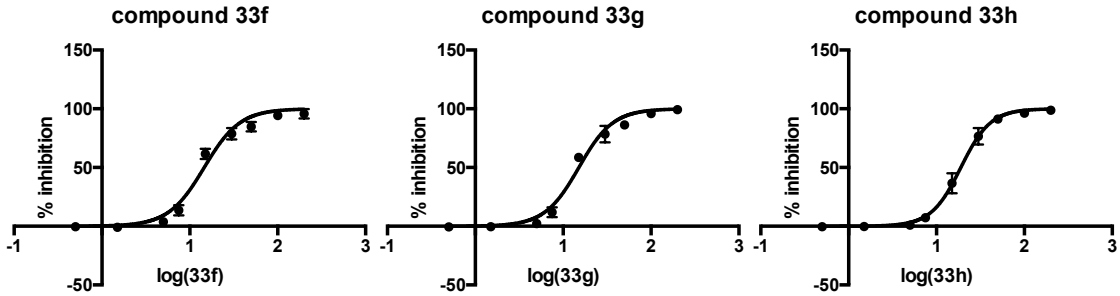

Figure 5.12 Inhibition curves of compounds **Phlo**, **DAPA**, **18a-18h**, **22a-22h**, and **33a-33h** for SGLT1 protein

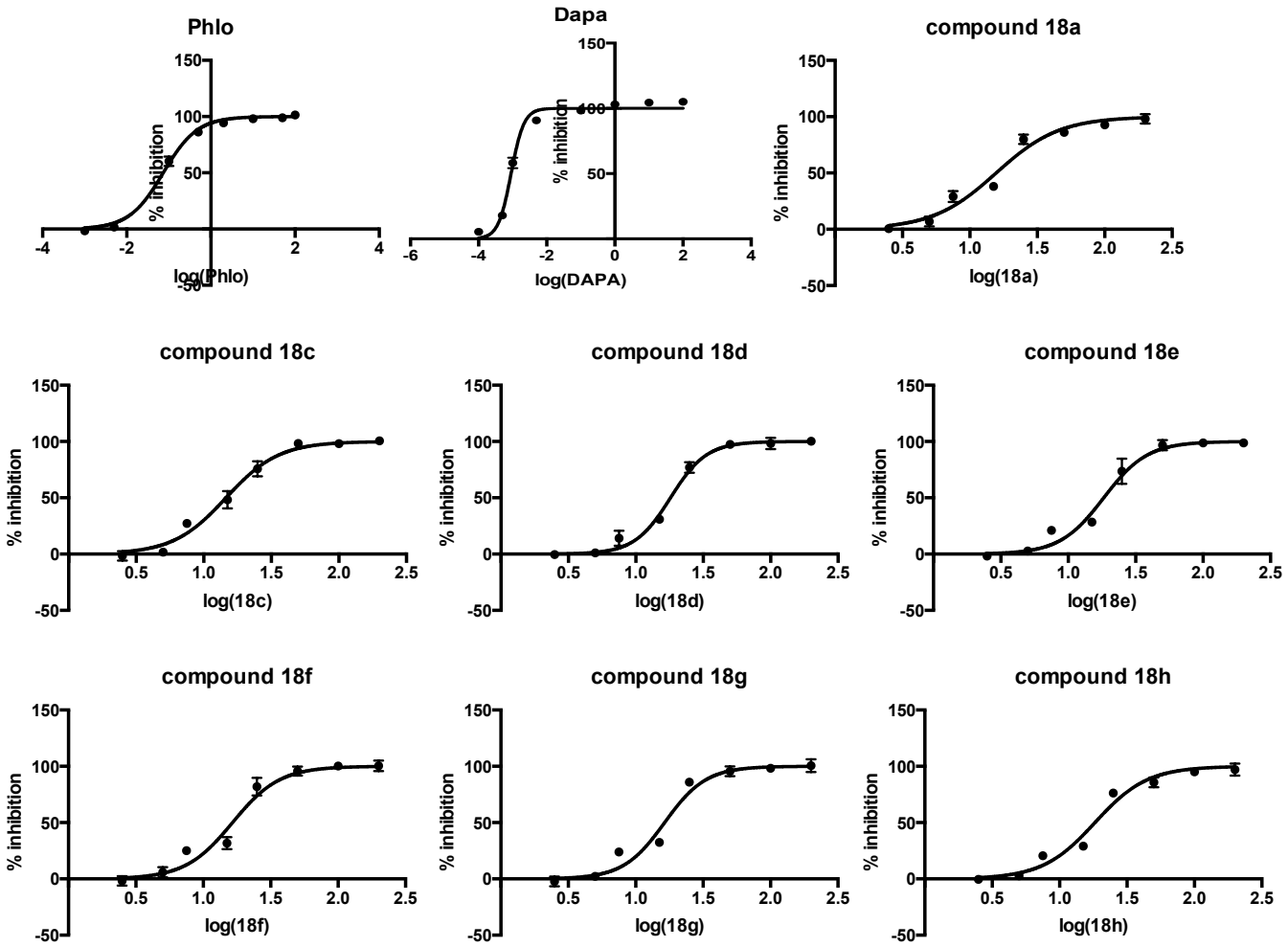

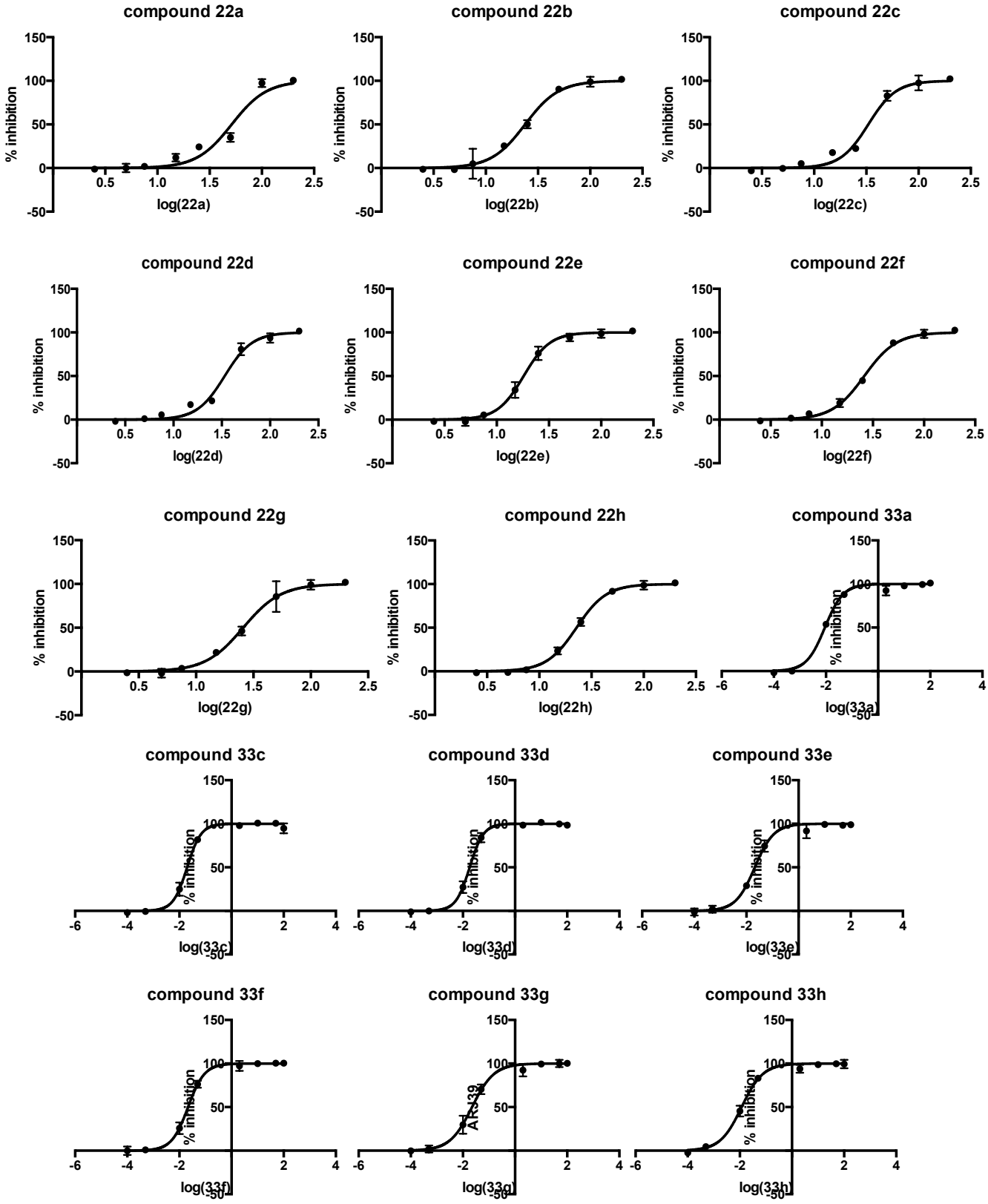

Figure 5.13 Inhibition curves of compounds **Phlo**, **DAPA**, **18a-18h**, **22a-22h**, and **33a-33h** for SGLT2 protein

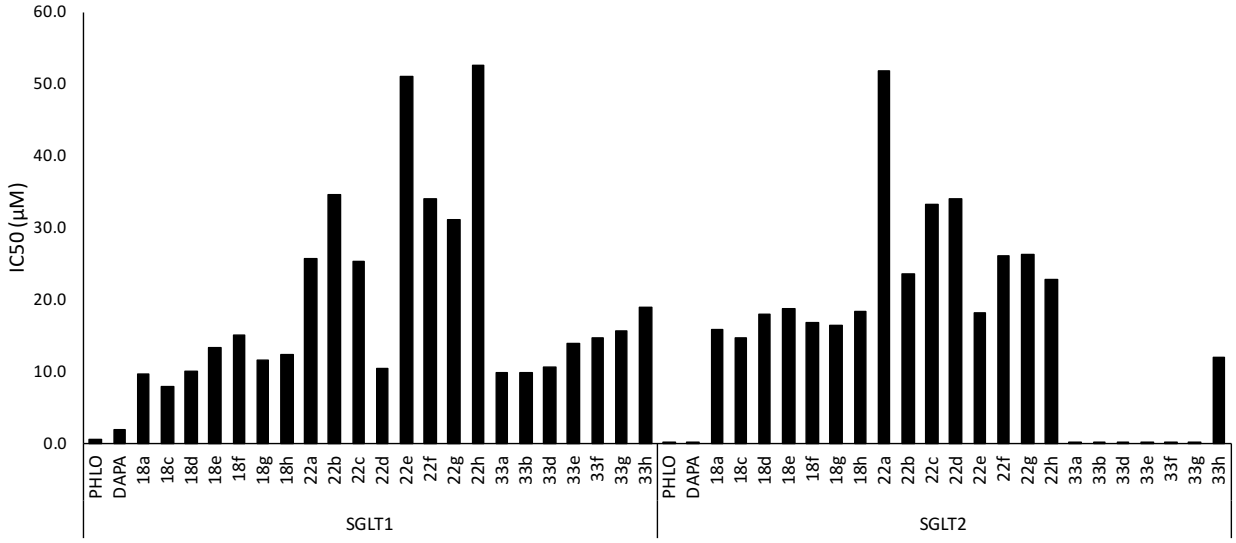

Graph 5.13 IC_{50} values for SGLT1 and SGLT2

Table 5.3 *In vitro* screening data for SGLT inhibitory activity and selectivity

Compound	SGLT1 IC_{50} (μM)[a]	SGLT2 IC_{50} (μM)[a]	Selectivity
Phlorizin	0.499 ± 0.12	0.0673 ± 5.1	7.4
Dapagliflozin	1.8 ± 0.33	0.008 ± 0.29	2250
18a	9.6 ± 0.87	15.8 ± 1.1	-
18c	7.9 ± 1.0	14.7 ± 0.63	-
18d	9.9 ± 0.78	18.0 ± 0.95	-
18e	13.3 ± 0.65	18.7 ± 1.4	-
18f	15.1 ± 0.61	16.7 ± 1.7	-
18g	11.6 ± 0.60	16.4 ± 1.0	-
18h	12.4 ± 1.4	18.3 ± 0.59	-
22a	25.6 ± 1.73	51.7 ± 1.9	-
22b	34.6 ± 0.98	23.5 ± 1.2	-
22c	25.4 ± 1.98	33.3 ± 0.99	-
22d	10.4 ± 0.70	34.1 ± 1.7	-
22e	50.9 ± 1.37	18.2 ± 0.24	-
22f	33.9 ± 1.0	26.0 ± 1.4	-
22g	31.0 ± 1.30	26.2 ± 2.4	-
22h	52.6 ± 0.39	22.7 ± 0.73	-

Table 5.3 In vitro screening data for SGLT inhibitory activity and selectivity (cont.)

Compound	SGLT1 IC_{50} (μM)[a]	SGLT2 IC_{50} (μM)[a]	Selectivity
33a	9.7 ± 0.89	0.0091 ± 0.00057	1065
33c	9.9 ± 0.43	0.0198 ± 0.0024	500
33d	10.6 ± 0.89	0.0182 ± 0.0020	582
33e	13.8 ± 0.57	0.0213 ± 0.0031	648
33f	14.6 ± 0.10	0.0217 ± 0.0044	673
33g	15.6 ± 0.92	0.0227 ± 0.0039	661
33h	19.0 ± 1.3	0.0119 ± 0.0026	1596

[a] IC_{50} is ± standard deviation

Interestingly, when the 2-DG uptake assay was performed in choline buffer (NaCl substituted by choline chloride) (Graph 5.14) the *C*-glucosyl dihydrochalcones did not inhibit the uptake, but on the other hand all the aglycones (chalcones and dihydrochalcones) inhibited both SGLT1 and SGLT2. Cytochalasin B was used as a GLUT positive control. This could mean that these compounds can inhibit both SGLT proteins and GLUT proteins, because GLUTs are sodium-independent proteins, i.e., they do not require the presence of sodium ions to transport glucose; but SGLTs are sodium-dependent proteins, i.e., they do required sodium to do the co-transport. Therefore, if the compounds are able to inhibit in presence or absence of sodium they might act as inhibitors of both family of proteins. Nevertheless, further studies would be required to fully understand their action.

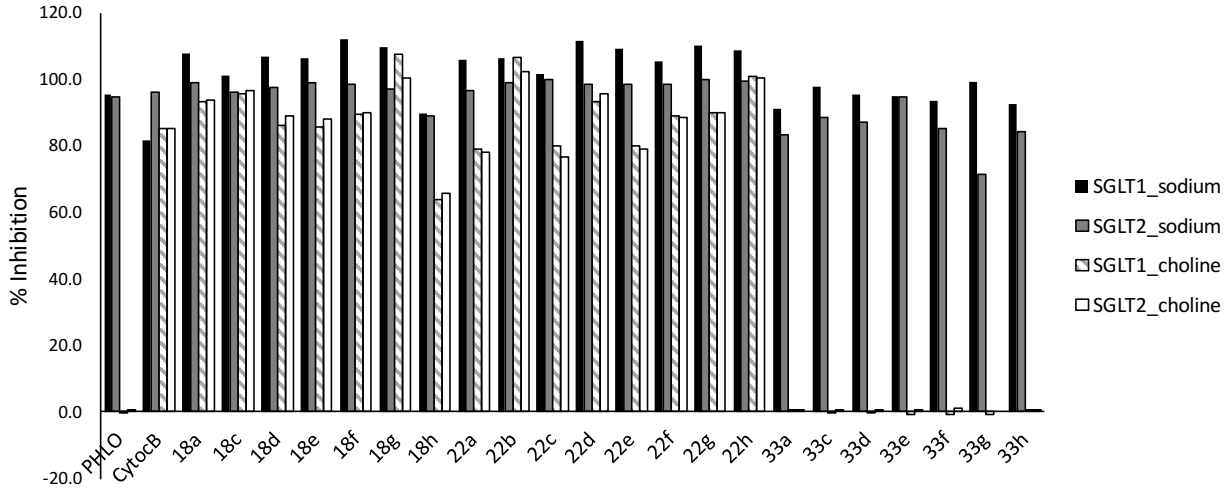

Graph 5.14 Sodium *vs* choline buffer 2-DG uptake

The clones selected for the glucose uptake assay were also elected for Fluorescence Confocal Microscopy (Figure 5.14) using the fluorescent analog of D-glucose, 2-NBDG, to evaluate if the two stable clones were able to uptake more 2-NBDG than the wild type HEK293 cells.

Cells were cultured in a glass bottom 4-well dish, previously coated with poly-D-lysine (PDL) and incubated overnight. Media was then removed and cells were washed and incubated with KRPH for 1 h after which 2-NBDG (600 μM) was added to the wells containing the two stable clones and HEK293 wild type cells. The other well containing HEK293 cells were treated with DMSO alone and served as the negative control. After 30 minutes of incubation at 37 ºC the media was removed and cells were washed carefully three times with KRPH buffer to ensure that all the extracellular 2-NBDG was removed. Cells were maintained in KRPH buffer for fluorescence confocal microscopy. As expected the two clones were able take up much more 2-NBDG than the wild type HEK293 cells.

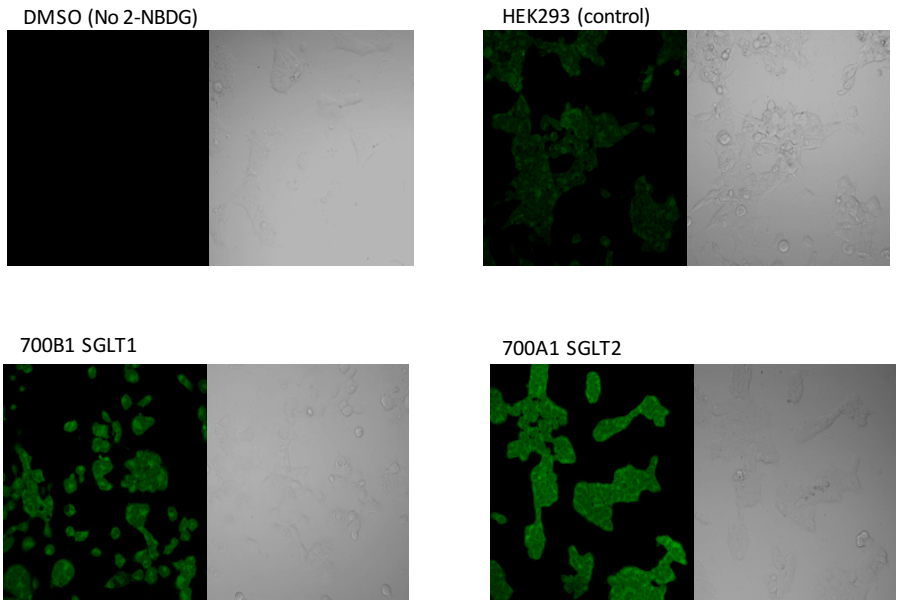

Figure 5.14 Fluorescence Confocal Microscopy on stable clones using 2-NBDG uptake assay

In summary, all the *C*-glucosyl dihydrochalcones showed a significant selectivity for SGLT2, but more interesting the change from a glucoside the corresponding *C*-glucosyl derivative resulted in a completely different behavior. Nevertheless, further structural

optimization of these *C*-glucosyl dihydrochalcones is required to increase their selectivity/potency as SGLT2 inhibitors.

Chapter 6. Conclusions

In this work, an innovative and original pathway for the synthesis of *C*-glucosyl dihydrochalcones was developed. The synthesis included the preparation of the glucosyl acceptors dihydrochalcones, which were prepared by the formation of the intermediate chalcone, through an aldol condensation, followed by a catalytic hydrogenation. Three different families of chalcones were prepared, but only one proved to be suitable for the *C*-glucosylation reaction.

The toxicity of *C*-glucosyl dihydrochalcones as well as their aglycones, chalcones and dihydrochalcones, was evaluated in HEK293 cells. None of the *C*-glucosyl dihydrochalcones showed cytotoxicity, but some of the aglycones showed cytotoxicity between 30-50%.

Two HEK293 stable cell lines were generated, overexpressing SGLT1 and SGLT2 proteins, respectively. After the characterization and evaluation of the expression levels of each protein, the best clone from each cell line was used in the glucose uptake assays.

The glucose uptake assay was assessed directly using a fluorescent analogue of D-glucose, 2-NDBG; but also using an indirect method based on an enzymatic reaction in which a non-fluorescent compound is transformed into a fluorescent derivative. The latter proved to be the most reliable assay and provided the more consistent results.

Using the enzymatic assay, all the compounds were screened in both stable cell lines at the same concentration, and the IC_{50} of each compound towards either SGLT1 or SGLT2 were determined. All the *C*-glucosyl dihydrochalcones proved to be selective SGLT2 inhibitors whereas, all the aglycones showed no selectivity. The best compound, the *C*-glucosyl derivative of phlorizin, has a significantly higher selectivity for SGLT2 than phlorizin, and showed a drastic increase in the inhibition of SGLT2 and a tremendous decrease in the inhibition of SGLT1.

In summary, the goals of this project were successfully accomplished, but further studies and structural optimization are required to improve the selectivity and potency of *C*-glucosyl dihydrochalcones as SGLT2 inhibitors.

Chapter 7. Experimental

Materials and Methods – CHEMISTRY

Solvents and reagents were bought from Fluka, Merck, Sigma, Alfa Aeser or Acros Organics. Solutions were concentrated below 50 ºC in vacuum on Büchi rotary evaporators. Qualitative TLC was performed on pre-coated silica gel G-50 UV_{254} plates (Macherey-Nagel); compounds were detected by UV light (254 nm) and spraying with a 10% methanolic solution of sulfuric acid or with a 5% ethanolic solution of iron chloride hexahydrate ($FeCl_3 \cdot 6H_2O$) followed by heating. Column chromatography was carried out on silica gel (40-60 μm) from Acros Organics. Microwave-assisted synthesis was carried out with a CEM Discover system. NMR spectra were recorded on Bruker spectrometer Advance 400 (400.13 MHz for ^{1}H-NMR and 100.62 MHz for ^{13}C-NMR). Chemical shifts are given in ppm relative to tetramethylsilane. Assignments were made, when needed, with the help of COSY, HMQC, and HMBC experiments. HRMS spectra were acquired in an Apex Ultra FTICR Mass Spectrometer equipped with an Apollo II Dual ESI/MALDI ion source, from Bruker Daltonics, and a 7T actively shielded magnet from Magnex Scientific. The samples were introduced by direct infusion into the ESI source with a flow rate of 720 μL/h. Mass spectra were acquired in the positive ion mode with an acquisition size of 512k in the mass range of 195 to 1200 and 20 scans were accumulated for each sample. The nebulizer gas flow rate was set to 2.0 L/min, the dry gas flow rate was set to 4.0 L/min at a temperature of 200 ºC. The capillary voltage was set to 4100 V and the spray shield voltage was set to 3700 V. The ions were accumulated in the collision cell during 0.5 s with a time of flight of 1.8 ms prior to their transfer to the ICR cell. Samples (1 mg) were diluted in 1 mL of methanol or dichloromethane and further diluted in 1 mL of methanol. FTICR was externally calibrated with Luteinizing Hormone-Releasing Hormones fragments (1 μL in 600 μL of methanol and 400 μL of water miliq). All the data were processed by Compass Data Analysis version 4.1. Melting points were determined with a Stuart SMP 30 apparatus.

7.1 Synthesis of starting materials

7.1.1 Glycosyl donors

Methyl 2,3,4,6-tetra-*O*-benzyl-α-D-glucopyranoside (**2**)

To a 1M solution of NaH in DMF at 0 ºC (4.4 equiv.) was added dropwise a 1.3 M solution in DMF of α-methyl D-glucopyranoside (**1**, 5.14 mmol). The reaction mixture was stirred for 30 minutes at 0 ºC and then temperature was allowed to increase to room temperature. BnBr (4.4 equiv.) was added dropwise and the stirring continued for more 24 h. MeOH was added until no effervescence and DMF removed under vacuum. The residue was dissolved in DCM, washed with water and brine. The organic layer was dried over $MgSO_4$ and concentrated. The resulting syrup was purified on a silica gel column (15:1 P. Ether/EtOAc) to give compound **2** (87%) as colourless oil. R_f 0.68 (3:1 P. Ether/ETOAc); **^{1}H NMR ($CDCl_3$), δ (ppm)** 1 7.54-7.31 (m, 20H, Ar<u>H</u>); 5.17, 5.00 (each d, 2H, *J*=11.53 Hz, -OC<u>H</u>$_2$Ph); 5.02, 4.67 (each d, 2H, *J*=11.10 Hz, -OC<u>H</u>$_2$Ph); 4.91, 4.80 (each d, 2H, *J*=11.87 Hz, -OC<u>H</u>$_2$Ph); 4.83 (*d*, 1H, $J_{1,2}$ =3.85 Hz, H-1); 4.73, 4.60 (each d, 2H, *J*=12.54 Hz, -OC<u>H</u>$_2$Ph); 4.21 (*t*, 1H, $J_{3,4}$=9.25 Hz, H-3); 3.94 (ddd, 1H, $J_{5,6a}$ =1.73 Hz, $J_{5,6b}$ =3.23 Hz, H-5); 3.90-3.78 (m, 3H, H-4, H-6a, H-6b); 3.75 (dd, 1H, $J_{2,3}$ =9.67 Hz, H-2); 3.52 (*s*, 3H, -OC<u>H</u>$_3$-1); **^{13}C NMR ($CDCl_3$) δ (ppm)** 1139.9, 138.4, 138.4, 138.1 (<u>C</u>$_q$-Ph), 128.7, 128.6, 128.6, 128.3, 128.2, 128.1, 128.1, 127.8, 127.9 (<u>C</u>H, ArH), 98.4 (C-1), 82.3 (C-3), 80.0 (C-2), 77.8 (C-4), 75.9, 75.2, 73.7, 73.8 (-O<u>C</u>H$_2$Ph), 70.2 (C-5), 68.6 (C-6), 55.4 (-O<u>C</u>H$_3$-1)

2,3,4,6-tetra-*O*-benzyl-1-isopropyl-α-D-glucopyranose (**6**)

D-glucose (**5**) (5.55 mmol) was dissolved in isopropyl alcohol (62.5 mL) and kept at reflux temperature. Then, Dowex H^+ exchange resin (2g) was added to the reaction vessel (previously washed with methanol). After 5 h the resin was filtered off and the solvent removed under vacuum. This residue was then dissolved in DMF (62.5 mL) and NaH (12.0 equiv.) added at 0 ºC. BnBr (10 equiv.) was added at 0 ºC and then the temperature was allowed to reach 25 ºC and the reaction continued for 15 h. Methanol was added until no effervescence was observed and the solvents removed by vacuum. The residue was purified by column chromatography yielding the desired product in oil

form in 79.0%. R_f = 0.71 (Hexane/EtOAc 6:1); **^{1}H NMR ($CDCl_3$) δ (ppm)** 7.44-7.20 (m, 20H, ArH); 5.05-4.49 (m, 10H, -OC<u>H</u>2Ph, H-1, H-2); 4.16 (q, 1H, *J*=6.61 Hz, *J*=14.43 Hz, -OC<u>H</u>$(CH_3)_2$); 3.83-3.43 (m, 5H, H-3, H-4, H-5, H-6a, H-6b); 1.30 (t, 6H, -OCH(C<u>H</u>$_3)_2$); **^{13}C NMR ($CDCl_3$) δ (ppm)** 138.6, 138.4, 138.2, 138.1 (<u>C</u>$_q$-Ph); 128.5, 128.4, 128.3, 128.2, 127.9, 127.8, 127.7, 127.5 (-<u>C</u>H, Ar); 102.6 (C-1); 84.8 (C-3); 82.3 (C-2); 77.9 (C-4); 75.8 (C-5); 74.9, 73.5, 73.4 (-O<u>C</u>H_2Ph); 68.9 (C-6); 60.4 (-O<u>C</u>H$(CH_3)_2$); 21.1 (-OCH(<u>C</u>$H_3)_2$)

2,3,4,6-tetra-*O*-benzyl-D-glucopyranose (**3**)

To a solution of **2** or **6** (9.0 mmol) in AcOH (79.5 mL) was added a solution of 2N H_2SO_4 (39.5 mL) and the reaction mixture stirred at 90-95 ºC for 24 h. Cold water (300 mL) was added and the stirring continuing for 30 minutes. A white powder was recrystallized from hot hexane, filtered off and washed with iced cold hexane and dried in vacuum affording compound **3** in 81% yield. mp. 135.8 – 137.4 ^{o}C; R_f = 0.54 (Et.P/EtOAc 3:1); **^{1}H NMR ($CDCl_3$) δ (ppm)** 7.37-7.15 (m, 60H, Ar<u>H</u>); 5.25 (t, 2H, $J_{1\alpha,2}$=3.52 Hz, H-1α); 4.99-4.50 (m, 25H, H-1β, -OC<u>H</u>$_2$Phα, -OC<u>H</u>$_2$Phβ); 4.07 (ddd, 2H, $J_{5\alpha,6a\alpha}$ =1.87 Hz, $J_{5\alpha,6b\alpha}$ =3.35 Hz, $J_{4\alpha,5\alpha}$=10.01 Hz, H-5α), 4.02 (t, 2H, $J_{2,3\beta}$ = 9.31 Hz, H-3β); 4.01 (0.58H, $J_{2,3\alpha}$ = 9.31 Hz, H-3α), 3.75-3.41 (m, 10H, H-2α, H-4β, H-4α, H-5β, H-6a, H-6b); **^{13}C NMR ($CDCl_3$) δ (ppm)** 138.7; 138.2; 137.9; 137.8 (<u>C</u>$_q$-Phα); 137.8; 137.9; 138.5; 138.4 (<u>C</u>$_q$-Phβ); 128.5; 128.4; 128.4; 128.2; 128.1; 128.0; 127.9; 127.9; 127.8; 127.7; 127.7 (-<u>C</u>H, Ar α and β); 97.5 (C-1β); 91.3 (C-1α); 84.6 (C-3α); 83.1 (C-2β); 81.8 (C-3α); 79.97 (C-2α); 77.8 (C-4α); 74.7 (C-4β); 75.8; 75.1; 75.0; 73.5; 73.3 (-O<u>C</u>H_2Phα); 75.7; 75.1, 74.8; 74.5 (-O<u>C</u>H_2Phβ); 70.25 (C-5α, C-5β); 68.9 (C-6β); 68.6 (C-6α).

1-*O*-acetyl-2,3,4,6-tetra-*O*-benzyl-D-glucopyranose (**4**)

To a solution of **3** (1.0 g, 1.72 mmol) in pyridine (10 mL) acetic anhydride (1.5 equiv.) and DMAP (5% mol) were added. The reaction proceeded for 30 minutes and after completion confirmed by TLC pyridine was co-evaporated with toluene and compound **4** was purified by column chromatography (7:1 Hexane/ EtOAc) in the form of oil in 96 % yield. R_f = 0.50 (Et.P/EtOAc 4:1); **^{1}H NMR ($CDCl_3$) δ (ppm)** 7.40-7.19 (m, 80H, Ar<u>H</u>α, Ar<u>H</u>β); 6.44 (d, 3H, $J_{1\alpha,2\alpha}$ =4.27 Hz, H-1α); 5.69 (d, 1H, $J_{1\beta,2\beta}$ = 7.83 Hz, H-1β); 5.05-4.53 (m, 32H, -OC<u>H</u>$_2$Phα, -OC<u>H</u>$_2$Phβ); 4.03 (t, 3H, $J_{2\alpha,3\alpha}$ =8.81 Hz, H-3α); 3.97-

3.63 (m, 3H, H-5α); 3.85-3.63 (m, 18H, H-2α, H-4α, H-6aα, H-6bα, H-2β, H-3β, H-4β, H-5β, H-6aβ, H-6bβ); 2.20 (s, 9H, -COOC$\underline{H}_3$α); 2.12 (s, 3H, -COOC$\underline{H}_3$β); **^{13}C NMR ($CDCl_3$) δ (ppm)** 169.5 (-$\underline{C}$OOCH_3α); 169.4 (-$\underline{C}$OOCH_3β); 138.7, 138.1, 137.8, 137.6 (C_q-Phα); 138.4, 138.1, 138.0, 137.9 (C_q-Phβ); 128.6, 128.5, 128.4, 128.2, 128.0, 127.9, 127.8, 127.7 (-$\underline{C}H_2$Phα, -$\underline{C}H_2$Phβ); 94.1 (C-1β); 90.1 (C-1α); 84.9 (C-3β); 81.7 (C-3α); 81.1 (C-2β); 78.9 (C-2α); 77.2 (C-4β); 76.9 (C-4α); 75.8 (-O$\underline{C}H_2$Phβ); 75.7 (-O$\underline{C}H_2$Phα); 75.5 (-O$\underline{C}H_2$Phβ); 75.4 (-O$\underline{C}H_2$Phα); 75.1, 75.0 (-O$\underline{C}H_2$Phβ); 73.6 (-O$\underline{C}H_2$Phα); 73.5 (C-5β); 73.3 (-O$\underline{C}H_2$Phα); 72.9 (C-5α); 68.1 (C-6α); 68.0 (C-6β); 21.2 (-COO$\underline{C}H_3$α); 21.1 (-COO$\underline{C}H_3$β)

1,2,3,4,6-tetra-*O*-acetyl-D-glucopyranose (**9**)

To a DMF (50 mL) solution of D-glucose (**5**) (5.0 g, 28.7 mmol) was added Ac_2O (26.5 mL) and DMAP (100 mg). Upon completion after 75 min the solvent was removed under vacuum. Compound **9** was purified by column chromatography (EtOAc /cyclohexane 1:2) and obtained in quantitative yield. Colorless oil, R_f = 0.50 (EtOAc/Cyclohexane 1:2); **^{1}H NMR ($CDCl_3$) δ (ppm)** 6.34 (d, 1H, $J_{1\alpha,2\alpha}$ =3.65 Hz, H-1α); 5.72 (d, 1H, $J_{1\beta,2\beta}$ =8.32 Hz, H-1β); 5.48 (t, 1H, $J_{3\alpha,4\alpha}$ =9.88 Hz, H-3α); 5.26 (t, 1H, $J_{3\beta,4\beta}$ =9.41 Hz, H-3β); 5.17-5.12 (m, 4H, H-2α, H-2β, H-4α, H-4β); 4.29, 4.26 (each d, 2H, H-6aα, H-6bα); 4.14-4.08 (m, 3H, H-5α, H-6aβ, H-6bβ); 3.84 (ddd, 1H, *J* =2.17 Hz, *J* =12.34 Hz, H-5β); 2.19, 2.10, 2.05, 2.03, 2.02 (s, 15H, -COOC$\underline{H}_3$); **^{13}C NMR ($CDCl_3$) δ (ppm)** 170.7, 170.1, 169.4, 168.6 (-$\underline{C}$OOCH_3); 91.4 (C-1β); 88.8 (C-1α); 72.9 (C-5β); 72.8 (C-3β); 69.7 (C-5α); 69.6 (C-3α); 69.0 (C-2α, C-2β); 68.0 (C-4α, C-4β); 61.2 (C-6α, C-6β); 20.5 (-COO$\underline{C}H_3$)

2,3,4,6-tetra-*O*-acetyl-D-glucopyranose (**10**)

Compound **9** (2.0 g, 5.1 mmol) was dissolved in THF (15 mL) and $BnNH_2$ was added (2.0 equiv.). The reaction was carried out at room temperature for 24 h. After the completion of the reaction THF was evaporated and compound **10** was purified by column chromatography (EtOAc /cyclohexane 1:2) and obtained in 98% yield. Colorless oil, R_f = 0.40 (EtOAc/Cyclohexane 1:2); **^{1}H NMR ($CDCl_3$) δ (ppm)** 5.5 (t, 1H, $J_{3\beta,4\beta}$ =9.74 Hz, H-3β); 5.26 (t, 1H, $J_{3\alpha,4\alpha}$ =9.56 Hz, H-3α); 5.47 (d, 1H, $J_{1\alpha,2\alpha}$ =3.20 Hz, H-1α); 5.09 (t,

2H, H-4α, H-4β); 4.93-4.88 (m, 2H, H-2α, H-2β); 4.75 (d, 1H, $J_{1\beta,2\beta}$ =7.99 Hz, H-1β); 4.23-4.20 (m, 3H, H-5α, H-6aα, H-6bα); 4.17-4.11 (m, 2H, H-6aβ, H-6bβ); 3.76 (ddd, 1H, *J* =2.17 Hz, *J* =12.34 Hz, H-5β); 2.10, 2.09, 2.04, 2.02 (s, 12H, -COOC<u>H</u>$_3$); **^{13}C NMR (CDCl$_3$) δ (ppm)** 95.4 (C-1β); 90.0 (C-1α); 71.7 (C-5β); 70.9 (C-3β); 71.0 (C-2α, C-2β); 69.8 (C-3α); 68.3 (C-4α, C-4β); 67.2 (C-5α); 61.6 (C-6α, C-6β)

2,3,4,6-tetra-*O*-acetyl-α-D-glucopyranyl trichloroacetimidate (**11**)

To a solution of compound **10** (3.5 g, 7.9 mmol) in DCM (10.6 mL) was added $CNCCl_3$ (2.0 equiv.) and K_2CO_3 (2.0 equiv.). After 24 h at room temperature the reaction mixture was filtered off through celite and the organic filtrate was concentrated. Compound **11** was purified by column chromatography (EtOAc/CycloHexane 1:2) and obtained in 80%. Colorless oil, R_f = 0.590 (EtOAc/CycloHexane 1:2); **^{1}H NMR (CDCl$_3$) δ (ppm)** 8.71 (s, 1H, -OCN<u>H</u>CCl$_3$); 6.58 (d, 1H, $J_{1,2}$ =3.70 Hz, H-1); 5.58 (t, 1H, $J_{2,3}$ = $J_{3,4}$ =9.59 Hz, H-3); 5.20 (t, 1H, H-4); 5.15 (dd, 1H, H-2); 4.31, 4.28 (each d, 1H, H-6a); 4.23 (ddd, 1H, *J* = 1.70 Hz, *J* = 4.04 Hz, *J* =10.04 Hz, H-5); 4.16, 4.13 (each d, 1H, H-6b); 2.10, 2.07, 2.05, 2.04 (-COOC<u>H</u>$_3$); **^{13}C NMR (CDCl$_3$) δ (ppm)** 69.8 (C-1); 67.9 (C-4); 69.0 (C-2); 69.8 (C-5); 61.7 (C-6); 20.5 (-COO<u>C</u>H$_3$)

7.1.2 Protected acetophenones

Synthesis of 2′,4′-bis(benzyloxy)-6′-hydroxyacetophenone (14)

2′,4′,6′-trihydroxyacetophenone (**13**, 5.95 mmol) was dissolved in DMF (10 mL) and K_2CO_3 (2.2 equiv.) was added at 0 ºC. After 15 minutes BnBr (2.2 equiv.) was added to the reaction and kept at 0 ºC for an extra 20 minutes. The ice bath was removed and the reaction proceeded at room temperature for 1 h. The reaction was neutralized after completion and extracted with DCM. The organic layers were combined, washed with brine and dried over $MgSO_4$. The desired product (**15**) was purified by column chromatography (30:1 Hexane/ EtOAc) and obtained in 52% yield. The secondary product (**9**) was isolated in 41% yield.

<u>2′,4′-bis(benzyloxy)-6′-hydroxyacetophenone, **14**:</u> R_f = 0.35 (8:1 P. Ether/EtOAc); m.p. 103.5-104.0 ºC; **^{1}H NMR (CDCl$_3$) δ (ppm)** 14.17 (s, 1H, OH-2′); 7.47-7.40 (m, 20H,

ArH); 6.22 (d, 1H, $J_{5,7}$ =2.32 Hz, H-5′); 6.15 (d, 1H,H-3′); 5.09 (s, -OCH_2Ph); 5.08 (s, -OCH_2Ph); 2.61 (s, 3H, -COOCH_3); **^{13}C NMR ($CDCl_3$) δ (ppm)** 203.2 (-COOCH_3); 167.6 (C-4′, C-6′); 162.1 (C-2′); 135.9, 135.7 (C_q-Ph); 128.8, 128.7, 128.5, 128.4, 128.1, 127.7 (CH, Ph); 106.3 (C-1′); 94.8 (C-5′); 92.4 (C-3′); 71.2 (-OCH_2Ph); 70.3 (-OCH_2Ph); 33.4 (-COOCH_3).

2′,4′-bis(benzyloxy)-3′-benzyl-6′-hydroxyacetophenone, **15**: R_f = 0.33 (8:1 P. Ether/EtOAc); m.p. 103.3-104.6 ºC; **^{1}H NMR (acetone-d^6) δ (ppm)** 14.24 (s, 1H, OH-2′); 7.57-7.11 (m, 15H, ArH); 6.52 (s, 1H, H-3′); 5.27 (s, 4H, -OCH_2Ph); 3.96 (s, 2H, -CH_2Ph-5′); 2.55 (s, 3H, -COCH_3); **^{13}C NMR (acetone-d^6) δ (ppm)** 203.4 (-COCH_3); 163.7 (C-4′); 162.7 (C-6′); 161.4 (C-2′); 141.6 (C_q, -CH_2Ph); 136.7, 136.3 (C_q, -OCH_2Ph); 128.6, 128.5, 128.4, 128.3, 127.9 127.8, 127.5 (CH, -CH_2Ph, -OCH_2Ph); 109.4 (C-5′); 105.8 (C-1′); 89.3 (C-3′); 71.0, 70.0 (-OCH_2Ph); 32.8 (-COCH_3); 27.7 (-CH_2Ph).

1-(2,4-bis(ethoxymethoxy)-6-hydroxyphenyl)ethan-1-one (20)

To a solution of 2′,4′,6′-trihydroxyacetophenone (**13**) (29.7 mmol) in DCM (50.3 mL) was added *N,N*-diisopropylethylamine (2.2 equiv.) at 0 ºC and stirred for 15 minutes. Ethoxymethyl ether chloride (2.2 equiv.) was added and the reaction continued for 15 minutes at 0 ºC and then allowed to reach room temperature. The reaction was controlled by TLC and after 2h the mixture was poured into water and extracted with dichloromethane. The organic layers were combined, washed with brine, dried over $MgSO_4$ and concentrated in vacuum. The product, as oil at room temperature, was purified by column chromatography (30:1 hexane/ EtOAc) and obtained in 75.8% yield. R_f (6:1 Hexane/EtOAcEtOAc)=0.51; **^{1}H NMR ($CDCl_3$), δ (ppm)** 13.73 (s, 1H, OH-4); 6.25 (d, 1H, $J_{5,7}$=2.21 Hz, H-7); 6.22 (d, 1H, H-5); 5.27 (s, 2H, H-1′′); 5.19 (s, 2H, H-1′); 3.74 (d, 2H, $J_{2'',3a''}$= 7.13 Hz, $J_{2'',3b''}$= 14.20 Hz, H-2′′); 3.71 (q, 2H, $J_{2',3a'}$= 7.19 Hz, $J_{2',3b'}$=14.19 Hz, H-2'); 2.64 (s, 3H, H-1); 1.22 (t, 3H, H-3′′); 1.19 (t, 3H, H-3′); **^{13}C NMR ($CDCl_3$), δ (ppm)** 203.2 (C-2); 166.7 (C-4); 163.6 (C-6); 160.5 (C-8); 106.7 (C-3); 96.9 (C-5); 94.0 (C-7); 93.2 (C-1′′); 92.7 (C-1′); 65.0 (C-2′′); 64.7 (C-2′); 33.0 (C-1); 15.0 (C-3′, C-3′′); HRMS calcd for $C_{14}H_{20}NaO_6$ 307.11521 (MNa^+) found 307.11544

1-(2-(ethoxymethoxy)-6-hydroxyphenyl)ethan-1-one (24)

To a solution of 2′,4′-dihydroxyacetophenone (**23**) (65.7 mmol) in DCM (55.0 mL) was added *N,N*-diisopropylethylamine (2.2 equiv.) at 0 ºC and stirred for 15 minutes. Ethoxymethyl ether chloride (2.2 equiv.) was added and the reaction continued for 15 minutes at 0 ºC and then at room temperature. The reaction was controlled by TLC, and after 2 h the mixture was poured into water and extracted with dichloromethane. The organic layers were combined, washed with brine, dried over $MgSO_4$ and concentrated in vacuum. The product, as oil at room temperature, was purified by column chromatography (60:1 hexane/ EtOAc) and obtained in 93.8% yield. R_f (6:1 Hexane/ EtOAc)=0.60; **^{1}H NMR ($CDCl_3$), δ (ppm)** 12.63 (s, 1H, OH-4); 7.62 (d, 1H, $J_{7,8}$=8.87 Hz, H-8); 6.59 (d, 1H, $J_{3,5}$=1.66 Hz, H-5); 6.55 (dd, 1H, H-7); 5.25 (s, 2H, H-1'); 3.72 (q, 2H, $J_{2',3a'}$=7.11 Hz, $J_{2',3b'}$=14.19 Hz, H-2′); 2.56 (s, 3H, H-1); 1.22 (t, 3H, H-3′); **^{13}C NMR ($CDCl_3$), δ (ppm)** 202.7 (C-2); 164.8 (C-4); 163.8 (C-6); 132.4 (C-8); 114.6 (C-3); 108.2 (C-7); 103,7 (C-5); 92.7 (C-1′); 64.8 (C-2′); 26.3 (C-1); 15.1 (C-3′); HRMS calcd for $C_{11}H_{15}O_4$ 211.09649 (MH^+) found 211.09656

7.1.3 Aromatic Aldehydes

4-methoxybenzaldehyde (16e)

4-hydroxybenzaldehyde (5g, 40.9 mmol) was dissolved in acetone (94.4 mL) and K_2CO_3 (1.1 equiv.) was added. The mixture stirred for 30 minutes at reflux and then MeI (1.3 equiv.) was added and the mixture was kept stirring overnight at reflux. After completion of the reaction (confirmed by TLC) the salt was filtered off, acetone was removed, the flask was washed with DCM and starting material was filtered off. Solvent was evaporated and 4-methoxybenzaldehyde was obtained as a liquid without further purification in 98.5% yield. R_f (6:1 Hexane/ EtOAc)=0.39; **^{1}H NMR ($CDCl_3$), δ (ppm)** 9.89 (s, 1H, H-1); 7.84 (d, 2H, $J_{3,4}$ =$J_{6,7}$ =8.79 Hz, H-3, H-7); 7.01 (d, 2H, H-4, H-6); 3.89 (s, 3H, -OC<u>H</u>$_3$); **^{13}C NMR ($CDCl_3$), δ (ppm)** 190.8 (<u>C</u>-1); 164.6 (C-5) 131.9 (C-3, C-7); 129.9 (C-2); 114.3 (C-4, C-6); 55.6 (-O<u>C</u>H$_3$).

4-ethoxybenzaldehyde (16f)

4-hydroxybenzaldehyde (5g, 40.9 mmol) was dissolved in acetone (94.4 mL) and K_2CO_3 (1.1 equiv.) was added. The mixture stirred for 30 minutes at reflux and then ethyl bromide (1.3 equiv.) was added and the mixture was kept stirring overnight at reflux. After completion of the reaction (confirmed by TLC) the salt was filtered off, acetone was removed, the flask was washed with DCM and starting material was filtered off. Solvent was evaporated and 4-ethoxybenzaldehyde was obtained as a liquid without further purification in 98.6% yield. R_f (6:1 Hexane/ EtOAc)=0.34; **^{1}H NMR ($CDCl_3$), δ (ppm)** 9.90 (s, 1H, H-1); 7.86 (d, 2H, $J_{3,4}$ =$J_{6,7}$ =8.90 Hz, H-3, H-7); 7.06 (d, 2H, H-4, H-6); 4.13 (q, 2H, *J*=6.28 Hz, *J*=14.12 Hz, -OC<u>H</u>$_2$CH$_3$); 1.40 (t, 3H, -OCH$_2$C<u>H</u>$_3$); **^{13}C NMR ($CDCl_3$), δ (ppm)** 190.8 (<u>C-1</u>); 164.0 (C-5); 131.9 (C-3, C-7); 129.7 (C-2); 114.7 (C-4, C-6); 63.9 (-O<u>C</u>H$_2$CH$_3$); 14.6 (-OCH$_2$<u>C</u>H$_3$)

4-allyloxybenzaldehyde (16g)

4-hydroxybenzaldehyde (5g, 40.9 mmol) was dissolved in ethanol (94.4 mL) and KOH (1.5 equiv.) was added. The mixture was kept at reflux for 30 minutes and then allyl bromide (1.5 equiv.) was added. The reaction stirred for 7 h until reaction completion and the salt was filtered off, ethanol removed, the flask washed with DCM and starting material filtered off. Solvent was evaporated and pure 4-allyloxybenzaldehyde was obtained as a liquid without further purification in 98.6% yield. R_f (6:1 Hexane/ EtOAc)=0.60; **^{1}H NMR ($CDCl_3$), δ (ppm)** 9.87 (s, 1H, H-1); 7.83 (d, 2H, $J_{3,4}$ =$J_{6,7}$ =7.52 Hz, H-3, H-7); 7.02 (d, 2H, H-4, H-6); 6.09-6.02 (m, 1H, -OCH$_2$C<u>H</u>CH$_2$); 5.45, 5.32 (each d, 2H, *J*=17.47 Hz, *J*=9.78 Hz, -OCH$_2$CHC<u>H</u>$_2$); 4.62 (dd, 2H, *J*=1.67 Hz, *J*=5.03 Hz, -OC<u>H</u>$_2$CHCH$_2$); **^{13}C NMR ($CDCl_3$), δ (ppm)** 190.9 (C-1); 163.6 (C-5); 132.3 (-OCH$_2$<u>C</u>HCH$_2$); 132.0 (C-3, C-7); 129.9 (C-2); 118.3 (-OCH$_2$CH<u>C</u>H$_2$); 115.0 (C-4, C-6); 68.9 (-O<u>C</u>H$_2$CHCH$_2$).

7.2 Synthesis of Chalcones

7.2.1 General conventional procedure for the synthesis of 2′,4′-bis(ethoxymethoxy)-6′-hydroxychalcones

To solution of 1-(2,4-bis(ethoxymethoxy)-6-hydroxyphenyl)ethan-1-one (**20**) (200 mg, 0.703 mmol) and an aryl aldehyde (**16a-16i**, 2.0 equiv.) in 1,4-dioxane (4.1 mL) was added at room temperature sodium hydroxide aqueous solution 50% (w/v) (4.1 mL). The reaction stirred for 24 h at room temperature. The solution was neutralized using 10% HCl aqueous solution and extracted with DCM. The organic layers were combined, washed with brine, dried over $MgSO_4$ and concentrated in vacuum. The chalcones derivatives were purified by column chromatography (30:1 hexane/ EtOAc).

7.2.2 General microwave assisted procedure for the synthesis of 2′,4′-bis(ethoxy-methoxy)-6′-hydroxychalcones

To solution of 1-(2,4-bis(ethoxymethoxy)-6-hydroxyphenyl)ethan-1-one (**24**) (200 mg, 0.703 mmol) and the aryl aldehyde (**16a-16i**, 2.0 equiv.) in 1,4-dioxane (2.1 mL) was added at room temperature sodium hydroxide aqueous solution 50% (w/v) (2.1 mL). The reaction proceeded in a microwave oven at 150 W and 40 ºC for 2-3 h. The solution was neutralized using 10% HCl aqueous solution and extracted with DCM. The organic layers were combined, washed with brine, dried over $MgSO_4$ and concentrated in vacuum. The chalcones derivatives were purified by column chromatography (30:1 hexane/ EtOAc).

(*E*)-1-[2,4-bis(ethoxymethoxy)-6-hydroxyphenyl]-3-(4-fluorophenyl)prop-2-en-1-one (21a): Yield 94.7%; orange solid; m.p.=58.5-59.0 ºC; R_f (6:1 Hexane/EtOAc)=0.54; **^{1}H NMR ($CDCl_3$), δ (ppm)** 13.86 (s, 1H, OH-2′); 7.87 (d, 1H, $J_{2,3}$ =16.01 Hz, H-2); 7.73 (d, 1H, H-3); 7.58 (dd, 2H, $J_{2'',3''} = J_{5'',6''}$=8.46 Hz, $J_{2'',F} = J_{3'',F} = J_{6'',F} = J_{5'',F}$=5.80 Hz, H-2′′, H-6′′); 7.10 (t, 2H, H-3′′, H-5′′); 6.32 (d, 1H, $J_{3',5'}$ =2,17 Hz, H-3′); 6.25 (d, 1H, H-5′); 5.33 (s, 2H, H-1′′′′); 5.24 (s, 2H, H-1′′′); 3.79-3.70 (m, 4H, H-2′′′, H-2′′′′); 1.24 (t, 6H, $J_{3''',2'''} = J_{3'''',2''''}$=7.02 Hz, H-3′′′, H-3′′′′); **^{13}C NMR ($CDCl_3$), δ (ppm)** 192.7 (C-1); 167.4 (C-2′); 163.8 (C-4′,); 163.7 (d, J = 251.3 Hz, C-4′′); 159.9 (C-6′); 141.1 (C-3); 131.7 (d, J = 3.3 Hz, C-1′′); 130.1 (d, J = 8.5 Hz C-2′′, C-6′′); 127.2 (C-2); 116.1 (d, J = 21.2 Hz, C-3′′, C-5′′); 107.3 (C-1′); 97.4 (C-3′); 94.8

(C-5′); 93.9 (C-1′′′′); 92.8 (C-1′′′); 65.3 (C-2′′′′); 64.8 (C-2′′′); 15.0 (C-3′′′, C-3′′′′); HRMS calcd for $C_{21}H_{23}FNaO_6$ 413.13709 (MNa^+) found 413.13773

(*E*)-3-(4-bromophenyl)-1-[2,4-bis(ethoxymethoxy)-6-hydroxyphenyl]prop-2-en-1-one (21b): Yield 91.0%; orange solid; m.p.=80.9-81.6 ºC; R_f (6:1 Hexane/EtAOc)=0.58;**^{1}H NMR ($CDCl_3$), δ (ppm)** 13.83 (s, 1H, OH-2′); 7.94 (d, 1H, $J_{2,3}$=16.29 Hz, H-2); 7.71 (d, 1H, H-3); 7.56 (d, 2H, $J_{2'',3''}$ = $J_{5'',6''}$ =8.15 Hz, H-3′′, H-5′′); 7.48 (d, 2H, H-2′′, H-6′′); 6.34 (d, 1H, $J_{3',5'}$ =2.32 Hz, H-3′); 6.26 (d, 1H, H-5′); 5.35 (s, 2H, H-1′′′′); 5.25 (s, 2H, H-1′′′); 3.78 (q, 2H, $J_{2'''',3a''''}$=7.08 Hz, $J_{2'''',3b''''}$ =14.18 Hz, H-2′′′′); 3.75 (q, 2H, $J_{2''',3a'''}$ =7.08 Hz, $J_{2''',3b'''}$ =14.08 Hz, H-2′′′); 1.26 (t, 6H, H-3′′′, H-3′′′′); **^{13}C NMR ($CDCl_3$), δ (ppm)** 192.6 (C-1); 167.4 (C-2′); 163.9 (C-4′); 159.9 (C-6′); 140.9 (C-3); 134.4 (C-1′′); 132.2 (C-3′′, C-5′′); 129.7 (C-2′′, C-6′′); 128.1 (C-2); 124.3 (C-4′′); 107.3 (C-1′); 97.4 (C-3′); 94.8 (C-5′); 93.9 (C-1′′′′); 92.8 (C-1′′′); 65.4 (C-2′′′′); 64.9 (C-2′′′); 15.1 (C-′′′, -3′′′′); HRMS calcd for $C_{21}H_{23}BrNaO_6$ 473.05702 (MNa^+) found 473.05807

(*E*)-1-[2,4-bis(ethoxymethoxy)-6-hydroxyphenyl]-3-(phenyl)prop-2-en-1-one (21c): Yield 95.2%; orange solid; m.p.=52.7-53.1 ºC; R_f (10:1 Heptane/EtOAc)=0.24; **^{1}H NMR ($CDCl_3$), δ (ppm)** 13.91 (s, 1H, OH-2′); 7.96 (d, 1H, $J_{2,3}$=15.23 Hz, H-2); 7.81 (d, 1H, H-3); 7.63 (dd, 2H, $J_{2'',3''}$= $J_{5'',6''}$= $J_{3'',4''}$= $J_{4'',5''}$=7.45 Hz, $J_{2'',4''}$= $J_{4'',6''}$=2.02 Hz, Hz, H-3′′, H-5′′); 7.43-7.42 (m, 3H, H-2′′, H-4′′, H-6′′); 6.35 (d, 1H, $J_{3',5'}$=2.0 Hz, H-3′); 6.28 (d, 1H, H-5′); 5.36 (s, 2H, H-1′′′′); 5.26 (s, 2H, H-1′′′); 3.82-3.72 (m, 4H, H-2′′′, H-2′′′′); 1.28-1.24 (m, 6H, H-3′′′, H-3′′′′); **^{13}C NMR ($CDCl_3$), δ (ppm)** 192.9 (C-1); 167.4 (C-2′); 163.7 (C-4′); 160.0 (C-6′); 142.4 (C-3); 135.5 (C-1′′); 130.2 (C-4′′); 128.9 (C-2′′, C-6′′); 128.3 (C-3′′, C-5′′); 127.5 (C-2); 107.4 (C-1′); 97.4 (C-3′); 94.8 (C-5′); 93.9 (C-1′′′′); 92.8 (C-1′′′); 65.3 (C-2′′′′); 64.8 (C-2′′′); 15.1 (C-3′′′, C-3′′′′); HRMS calcd for $C_{21}H_{24}NaO_6$ 395.14651 (MNa^+) found 395.14672

(*E*)-1-[2,4-bis(ethoxymethoxy)-6-hydroxyphenyl]-3-(4-methylphenyl)prop-2-en-1-one (21d): Yield 91.6%; orange solid; m.p.=55.9-56.7 ºC; R_f (6:1 Hexane/EtOAc)=0.41; **^{1}H NMR ($CDCl_3$), δ (ppm)** 13.93 (s, 1H, OH-2′); 7.89 (d, 1H,

$J_{2,3}$=15.81 Hz, H-2); 7.77 (d, 1H, H-3); 7.50 (d, 2H, $J_{2'',3''}$= $J_{5'',6''}$=7.94 Hz, H-2″, H-6″); 7.21 (d, 2H, H-3″, H-5″); 6.32 (d, 1H, $J_{3',5'}$=1.70 Hz, H-3′); 6.25 (d, 1H, H-5′); 5.33 (s, 2H, H-1‴′); 5.24 (s, 2H, H-1‴); 3.80-3.70 (m, 4H, H-2‴, H-2‴′); 2.39 (s, 3H, C$\underline{H}_3$-4″); 1.26-1.22 (m, 6H, H-3‴, H-3‴′); **^{13}C NMR ($CDCl_3$), δ (ppm)** 192.9 (C-1); 167.4 (C-2′); 163.6 (C-4′); 159.9 (C-6′); 142.6 (C-3); 140.7 (C-4″); 132.7 (C-1″); 129.7 (C-3″, C-5″); 128.4 (C-2″, C-6″); 126.4 (C-2); 107.4 (C-1′); 97.4 (C-3′); 94.7 (C-5′); 93.9 (C-1‴′); 92.8 (C-1‴); 65.3 (C-2‴′); 64.8 (C-2‴); 15.1 (C-3‴, C-3‴′); 21.5 ($\underline{C}H_3$-4″); HRMS calcd for $C_{22}H_{26}NaO_6$ 409.16216 (MNa^+) found 409.16287

(*E*)-1-[2,4-bis(ethoxymethoxy)-6-hydroxyphenyl]-3-(4-methoxyphenyl)prop-2-en-1-one (21e): Yield 87%; orange solid; m.p.=62.7-62.9 ºC; R_f (10:1 Hexane/EtOAc)= 0.28; **^{1}H NMR ($CDCl_3$), δ (ppm)** 14. 02 (s, 1H, OH-2′); 7.86 (d, 1H, $J_{2,3}$=15.30 Hz, H-2); 7.79 (d, 1H, H-3); 7.57 (d, 2H, $J_{2'',3''}$= $J_{5'',6''}$=8.52 Hz, H-2″, H-6″); 6.94 (d, 2H, H-3″, H-5″); 6.34 (d, 1H, $J_{3',5'}$=1.37 Hz, H-3′); 6.27 (d, 1H, H-5′); 5.35 (s, 2H, H-1‴′); 5.25 (s, 2H, H-1‴); 3,87 (s, 3H, -OC$\underline{H}_3$-4″); 3.80-3.74 (m, 4H, H-2‴, H-2‴′); 1.28-1.24 (m, 6H, H-3‴, H-3‴′); **^{13}C NMR ($CDCl_3$), δ (ppm)** 192.2 (C-1); 167.3 (C-2′); 163.5 (C-4′); 161.4 (C-4″); 159.9 (C-6′); 142.5 (C-3); 130.2 (C-2″, C-6″); 128.2 (C-1″); 124.9 (C-2); 114.4 (C-3″, C-5″); 107.4 (C-1′); 97.4 (C-3′); 94.8 (C-5′); 93.9 (C-1‴′); 92.8 (C-1‴); 65.3 (C-2‴′); 64.8 (C-2‴); 55.4 (-O$\underline{C}H_3$-4″); 15.1 (C-3‴, C-3‴′); HRMS calcd for $C_{22}H_{26}NaO_6$ 425.15707 (MNa^+) found 425.15769

(*E*)-1-[2,4-bis(ethoxymethoxy)-6-hydroxyphenyl]-3-(4-ethoxyphenyl)prop-2-en-1-one (21f): Yield 86.3%; orange solid; m.p.=72.9-73.3 ºC; R_f (10:1 Hexane/EtOAc)= 0.29; **^{1}H NMR ($CDCl_3$), δ (ppm)** 14.01 (s, 1H, OH-2′); 7.86 (d, 1H, $J_{2,3}$=15.68 Hz, H-2); 7.80 (d, 1H, H-3); 7.57 (d, 2H, $J_{2'',3''}$= $J_{5'',6''}$=8.33 Hz, H-2″, H-6″); 6.93 (d, 2H, H-3″, H-5″); 6.34 (d, 1H, $J_{3',5'}$=2.26 Hz, H-3′); 6.27 (d, 1H, H-5′); 5.35 (s, 2H, H-1‴′); 5.26 (s, 2H, H-1‴); 4.13-4.07 (m, 2H, -OC$\underline{H}_2$CH$_3$-4″); 3.82-3.72 (m, 4H, H-2‴, H-2‴′); 1.46 (t, 3H, J=6.71 Hz, -OCH$_2$C$\underline{H}_3$-4″); 1.28-1.24 (m, 6H, H-3‴, H-3‴′); **^{13}C NMR ($CDCl_3$), δ (ppm)** 192.9 (C-1); 167.3 (C-2′); 163.5 (C-4′); 160.8 (C-4″); 142.7 (C-3); 130.1 (C-6′, C-2″, C-6″); 129.9 (C-1″); 124.9 (C-2); 114.9 (C-3″, C-5″); 107.5 (C-1′); 97.4 (C-3′); 94.8 (C-5′);

93.9 (C-1′′′′); 92.8 (C-1′′′); 65.7 (C-2′′′′); 65.3 (-O<u>C</u>H$_2$CH$_3$-4′′); 64.8 (C-2′′′); 15.1 (C-3′′′, C-3′′′′); 14.8 (-OCH$_2$<u>C</u>H$_3$-4′′); HRMS calcd for $C_{23}H_{28}NaO_7$ 439.17272 (MNa^+) found 439.17331

(*E*)-1-[2,4-bis(ethoxymethoxy)-6-hydroxyphenyl]-3-(4-allyloxyphenyl)prop-2-en-1-one (21g): Yield 98.7%; dark orange solid; m.p.=79.4-79.9 ºC; R_f (10:1 Hexane/ EtOAc)= 0.39; **^{1}H NMR ($CDCl_3$), δ (ppm)** 14.01 (s, 1H, OH-2′); 7.86 (d, 1H, $J_{2,3}$=15.06 Hz, H-2); 7.79 (d, 1H, H-3); 7.57 (d, 2H, $J_{2'',3''}$= $J_{5'',6''}$=8.51 Hz, H-2′′, H-6′′); 6.96 (d, 2H, H-3′′, H-5′′); 6.34 (d, 1H, $J_{3',5'}$ =1.34 Hz, H-3′); 6.27 (d, 1H, H-5′); 6.13-6.03 (m, 1H, -O-CH$_2$C<u>H</u>CH$_2$-4′′); 5.45, 5.34 (each d, 2H, *J*=17.41 Hz, *J*=9.96 Hz, -O-CH$_2$CHC<u>H</u>$_2$-4′′); 5.35 (s, 2H, H-1′′′′); 5.26 (s, 2H, H-1′′′); 4.61 (d, 2H, *J*=4.23 Hz, -O-C<u>H</u>$_2$CHCH$_2$-4′′); 3.78-3.74 (m, 4H, H-2′′′, H-2′′′′); 1.28-1.23 (m, 6H, H-3′′′, H-3′′′′); **^{13}C NMR ($CDCl_3$), δ (ppm)** 192.8 (C-1); 167.3 (C-2′); 163.5 (C-4′); 160.4 (C-4′′); 142.5 (C-3); 133.8 (-OCH$_2$<u>C</u>HCH$_2$-4′′); 130.1 (C-6′); 130.1 (C-6′, C-2′′, C-6′′); 128.3 (C-1′′); 125.1 (C-2); 118.1 (-OCH$_2$CH<u>C</u>H$_2$-4′′); 115.1 (C-3′′, C-5′′); 107.4 (C-1′); 97.4 (C-3′); 94.8 (C-5′); 93.9 (C-1′′′′); 92.8 (C-1′′′); 68.8 (-O<u>C</u>H$_2$CHCH$_2$-4′′); 65.3 (C-2′′′′); 64.8 (C-2′′′); 15.1 (C-3′′′, C-3′′′′); HRMS calcd for $C_{24}H_{28}NaO_6$ 451.17272 (MNa^+) found 451.17347

(*E*)-3-(4-(benzyloxy)phenyl)-1-(2,4-bis(ethoxymethoxy)-6-hydroxyphenyl)prop-2-en-1-one (21h): Yield 87.7%; reddish solid; m.p.=97.7-98.3 ºC; R_f (6:1 Hexane/ EtOAc)=0.64; **^{1}H NMR ($CDCl_3$), δ (ppm)** 13.99 (s, 1H, OH-2′); 7.87 (d, 1H, $J_{2,3}$=15.87 Hz, H-2); 7.80 (d, 1H, H-3); 7.58 (d, 2H, $J_{2'',3''}$ = $J_{5'',6''}$=6.51 Hz, H-2′′, H-6′′); 7.47-7.37 (m, 5H, C<u>H</u>, Ph); 7.03 (d, 2H, H-3′′, H-5′′); 6.35 (d, 1H, $J_{3',5'}$ =2.10 Hz, H-3′); 6.28 (d, 1H, H-5′); 5.35 (s, 2H, H-1′′′′); 5.26 (s, 2H, H-1′′′); 5.14 (s, 2H, C<u>H</u>$_2$Ph); 3.80 (q, 2H, $J_{2'''',3a''''}$=7.08 Hz, $J_{2'''',3b''''}$= 14.32 Hz, H-2′′′′); 3.75 (q, 2H, $J_{2''',3a'''}$ =7.24 Hz, $J_{2''',3b'''}$ =14.16 Hz, H-2′′′); 1.26 (t, 6H, H-3′′′, H-3′′′′); **^{13}C NMR ($CDCl_3$), δ (ppm)** 192.9 (C-1); 167.3 (C-2′); 163.5 (C-4′); 160.6 (C-4′′); 159.9 (C-6′); 142.5 (C-3); 136.5 (<u>C</u>$_q$, Ph); 130.1 (C-2′′, C-6′′); 128.7, 128.2, 127.5 (<u>C</u>H, Ph); 128.5 (C-1′′); 115.3 (C-3′′, C-5′′); 125.2 (C-2); 107.4 (C-1′); 97.5 (C-3′); 94.8 (C-5′); 93.9 (C-1′′′′); 92.8 (C-1′′′); 70.1 (<u>C</u>H$_2$Ph); 65.3 (C-2′′′′); 64.8 (C-2′′′); 15.1 (C-3′′′, C-3′′′′); HRMS calcd for $C_{28}H_{30}NaO_7$ 501.18837 (MNa^+) found 501.18976

(*E*)-1-[(2,4-bis(ethoxymethoxy)-6-hydroxyphenyl]-3-(5-methylfuran-2-yl)prop-2-en-1-one (21i): Yield 67.1%; reddish solid; m.p.=88.6-89.2 ºC; R_f (10:1 Hexane/ EtOAc)= 0.29; **^{1}H NMR ($CDCl_3$), δ (ppm)** 14.03 (s, 1H, OH-2′); 7.75 (d, 1H, $J_{2,3}$=16.16 Hz, H-2); 7.54 (d, 1H, H-3); 6.59 (d, 1H, $J_{2'',3''}$ =2.91 Hz, H-2′′); 6.30 (d, 1H, $J_{3',5'}$ =2.58 Hz , H-5′); 6.24 (d, 1H, H-3′); 6.12 (d, 1H, H-3′′); 5.34 (s, 2H, H-1′′′′); 5.23 (s, 2H, H-1′′′); 3.84 (q, 2H, $J_{2'''',3a''''}$ =7.25 Hz, $J_{2'''',3b''''}$=14.23 Hz H-2′′′′); 3.72 (q, 2H, $J_{2''',3a'''}$ =7.11 Hz, $J_{2''',3b'''}$ =14.10 Hz H-2′′′); 1.30-1.22 (m, 6H, H-3′′′, H-3′′′′); 2.37 (s, 3H, C$\underline{H}_3$-4′′); **^{13}C NMR ($CDCl_3$), δ (ppm)** 192.2 (C-1); 167.3 (C-2′); 163.4 (C-4′); 159.8 (C-6′); 155.5 (C-4′′); 150.9 (C-1′′); 129.3 (C-2); 123.1 (C-3); 117.7 (C-2′′); 109.3 (C-3′′); 107.4 (C-1′); 97.3 (C-3′); 94.5 (C-5′); 93.5 (C-1′′′′); 92.8 (C-1′′′); 65.2 (C-2′′′′); 64.8 (C-2′′′); 15.1 (C-3′′′, C-3′′′′), 14.0 (C$\underline{H}_3$-4′′); HRMS calcd for $C_{20}H_{24}NaO_7$ 399.14142 (MNa^+) found 399.14203

7.2.3 General conventional procedure for the synthesis of 2-ethoxymethoxy-6-hydroxy-chalcones

To solution of 1-(2-ethoxymethoxy-6-hydroxyphenyl)ethan-1-one (**24**) (200 mg, 0.951 mmol) and an aryl aldehyde (**16a-16i**, 2.0 equiv.) in ethanol (7.4 mL) was added at room temperature sodium hydroxide aqueous solution 50% (w/v) (7.4 mL). The reaction stirred for 24h at room temperature. The solution was neutralized using 10% aq. HCl and extracted with DCM. The organic layers were combined, washed with brine, dried over $MgSO_4$ and concentrated in vacuum. The chalcones derivatives were purified by column chromatography (30:1 hexane/ EtOAc).

7.2.4 General microwave procedure for the synthesis of 2-ethoxymethoxy-6-hydroxy-chalcones

To solution of 1-2-ethoxymethoxy-4,6-dihydroxyphenyl)ethan-1-one (2′,4′-dihydroxyacetophenone) (**24**) (200 mg, 0.951 mmol) and an aryl aldehyde (**16a-16i**, 2.0 equiv.) in ethanol (7.4 mL) was added at room temperature sodium hydroxide aqueous solution 50% (w/v) (7.4 mL). The reaction proceeded in a microwave oven at 150 W and 40 ºC for 1 h. The solution was neutralized using 10% HCl aqueous solution and extracted with DCM. The organic layers were combined, washed with brine, dried over

$MgSO_4$ and concentrated in vacuum. The chalcones derivatives were purified by column chromatography (30:1 hexane/ EtOAc).

(*E*)-1-(4-ethoxymethoxy-2-hydroxyphenyl)-3-(4-fluorophenyl)prop-2-en-1-one (24a): Yield 91.2%; orange solid; m.p.=96.3-96.8 ºC; R_f (8:1 Hexane/ EtOAc)= 0.44; **^{1}H NMR ($CDCl_3$) δ (ppm)** 13.27 (s, 1H, OH-2′); 7.88 (d, 1H, $J_{2,3}$=15.43 Hz, H-3); 7.86 (d, 1H, $J_{5',6'}$ =8.82 Hz, H-6′); 7.67 (dd, 2H, $J_{2'',F}$ =$J_{6'',F}$=5.40 Hz, $J_{2'',3''}$ =$J_{6'',5''}$=8.72 Hz, H-2′′, H-6′′); 7.53 (d, 1H, H-2); 7.15 (t, 2H, H-3", H-5′′); 6.68 (d, 1H, $J_{3',5'}$ =2.32 Hz, H-3′); 6.62 (dd, 1H, H-5′); 5.30 (s, 2H, H-1′′′); 3.76 (q, 2H, $J_{2''',3a'''}$ =7.13 Hz, $J_{2''',3b'''}$ =14.11 Hz, H-2′′′); 1.28 (t, 3H, H-3′′′); **^{13}C NMR ($CDCl_3$) δ (ppm)** 191.8 (C-1); 166.3 (C-2′); 163.9 (C-4′); 163.9 (d, *J* = 252.5 Hz C-4′′); 143.2 (C-3); 131.0 (d, *J* = 3.4 Hz, C-1′′); 131.3 (C-6′); 130.5 (d, *J* = 8.4 Hz , C-2′′, C-6′′); 120.0 (C-2); 116.2 (d, *J* =21.7 Hz , C-3′′, C-5′′); 114.8 (C-1′); 108.3 (C-5′); 103.9 (C-3′); 92.8 (C-1′′′); 64.9 (C-2′′′); 15.1 (C-3′′′); HRMS calcd for $C_{18}H_{17}FNaO_4$ 339.10031 (MNa^+) found 339.10069

(*E*)-3-(4-bromophenyl)-1-(4-ethoxymethoxy-2-hydroxyphenyl)prop-2-en-1-one (24b): Yield 85.0%; orange solid; m.p=78.7-79.2 ºC; R_f (8:1 Hexane/ EtOAc)=0.36; **^{1}H NMR (acetone-d^6) δ (ppm)** 13.35 (s, 1H, OH-2′); 8.23 (d, 1H, $J_{5',6'}$ =8.57 HZ, H-6′); 8.03 (d, 1H, $J_{2,3}$=15.21 Hz, H-2); 7.86 (d, 2H, H-3); 7.84 (dd, 2H, $J_{2'',3''}$ =$J_{6'',5''}$ =8.97 Hz, H-2′′, H-6′′); 7.66 (d, 2H, H-3′′, H-5′′); 6.64 (dd, 1H, $J_{3',5'}$=2.39 Hz, H-5′); 6.61 (d, 1H, H-3′); 5.36 (s, 2H, H-1′′′); 3.74 (q, 2H, $J_{2''',3a'''}$ =7.07 Hz, $J_{2''',3b'''}$ =14.08 Hz, H-2′′′); 1.20 (t, 3H, H-3′′′); **^{13}C NMR (acetone-d^6) δ (ppm)** 192.1 (C-1); 166.3 (C-2′); 164.2 (C-4′); 142.9 (C-3); 134.2 (C-1′′); 132.2 (C-6′); 132.1 (C-2′′, C-6′′); 130.6 (C-3′′, C-5′′); 124.3 (C-4′′); 121.6 (C-2); 114.6 (C-1'); 108.3 (C-5'); 103.3 (C-3'); 92.8 (C-1'"); 64.4 (C-2'"); 14.6 (C-3'"); HRMS calcd for $C_{18}H_{17}BrNaO_4$ 399.02024 (MNa^+) found 399.02084

(*E*)-1-(4-ethoxymethoxy-2-hydroxyphenyl)-3-(4-methylphenyl)prop-2-en-1-one (24d): Yield 89.2%; orange solid; m.p.= 91.7-92.1 ºC; R_f (8:1 Hexane/ EtOAc)= 0.24; **^{1}H NMR ($CDCl_3$) δ (ppm)**13.34 (s, 1H, OH-2′); 7.88 (d, 1H, $J_{2,3}$=15.04 Hz, H-3); 7.84 (d, 1H, $J_{5',6'}$ =8.11, H-6′); 7.55 (d, 2H, $J_{2'',3''}$ =$J_{5'',6''}$ =7.73 Hz, H-2′′, H-6′′); 7.54 (d, 1H, H-2); 7.23 (d, 2H, H-3′′, H-5′′); 6.65 (d, 1H, $J_{3',5'}$ =1.52 Hz, H-3′); 6.59 (dd, 1H, H-5′); 5.27 (s, 2H, H-

1′′′); 3.73 (q, 2H, $J_{2''',3a'''}$=7.03 Hz, $J_{2''',3b'''}$ =14.05 Hz, H-2′′′); 2.40 (s, 3H, C$\underline{H}_3$-4′′); 1.23 (t, 3H, H-3′′′); **^{13}C NMR ($CDCl_3$) δ (ppm)** 192.1 (C-1); 166.2 (C-2′); 163.8 (C-4′); 144.7 (C-3); 141.3 (C-4′′); 132.0 (C-1′′); 131.3 (C-6′); 129.8 (C-3′′, C-5′′); 128.6 (C-2′′, C-6′′); 119.3 (C-2); 114.9 (C-1′); 108.2 (C-5′); 103.9 (C-3′); 92.8 (C-1′′′); 64.8 (C-2′′′); 21.6 (C$\underline{H}_3$-4′′); 15.1 (C-3′′′); HRMS calcd for $C_{19}H_{20}NaO_4$ 335.12538 (MNa^+) found 335.12582

(*E*)-3-(4-(benzyloxy)phenyl)-1-(4-ethoxymethoxy-2-hydroxyphenyl)prop-2-en-1-one (24h): Yield 92.3%; orange solid; m.p.=101.5-102.0 ºC; R_f (8:1 Hexane/ EtOAc)= 0.56; **^{1}H NMR ($CDCl_3$) δ (ppm)** 13.40 (s, 1H, OH-2′); 7.86 (d, 1H, $J_{2,3}$=14.14 Hz, H-3); 7.83 (d, 1H, $J_{6',5'}$ =8.45 Hz, H-6′); 7.61 (d, 2H, $J_{2'',3''}$ = $J_{2'',3''}$ =8.45 Hz, H-2′′, H-6′′); 7.48-7.32 (m, 6H, H-2, Ar$\underline{H}$); 7.02 (d, 2H, H-3′′, H-5′′); 6.65 (d, 1H, $J_{3',5'}$ =2.26 Hz, H-3′); 6.58 (dd, 1H, H-5′); 5.27 (s, 2H, H-1′′′); 5.12 (s, 2H, -OC$\underline{H}_2$-); 3.73 (q, 2H, $J_{2''',3a'''}$=7.20 Hz, $J_{2''',3b'''}$=14.36Hz, H-2′′′); 1.23 (t, 3H, H-3′′′); **^{13}C NMR ($CDCl_3$) δ (ppm)** 192.0 (C-1); 166.1 (C-2′); 163.7 (C-4′); 160.9 (C-4′′); 144.3 (C-3); 136.4 (C$\underline{q}$, Ph); 131.2 (C-6′); 130.4 (C-2′′, C-6′′); 128.7, 128.2, 127.5 (C$\underline{H}$, Ph); 127.7 (C-1′′); 117.9 (C-2); 115.3 (C-3′′, C-5′′); 114.9 (C-1′); 108.2 (C-5′); 103.9 (C-3′); 92.8 (C-1′′′); 70.1 (-OC$\underline{H}_2$-); 64.8 (C-2′′′); 15.1 (C-3′′′); HRMS calcd for $C_{25}H_{24}NaO_5$ 427.15159 (MNa^+) found 427.15250

(*E*)-1-(4-ethoxymethoxy-2-hydroxyphenyl)-3-(5-methylfuran-2-yl)prop-2-en-1-one (24i): Yield 68.9%; reddish solid; m.p.=127.4-127.7 ºC; R_f (8:1 Hexane/ EtOAc)= 0.52; **^{1}H NMR (acetone-d^6) δ (ppm)** 13.52 (s, 1H, OH-2′); 8.06 (d, 1H, $J_{5',6'}$=8.95, H-6′); 7.66 (d, 1H, $J_{2,3}$=15.14 Hz, H-2); 7.53 (d, 1H, H-3); 6.94 (d, 1H, $J_{2'',3''}$ =3.60 Hz, H-2′′); 6.65 (d, 1H, $J_{3',5'}$ =2.20 Hz, H-5′); 6.59 (dd, 1H, H-3′); 6.31 (d, 1H, H-3′′); 5.36 (s, 2H, H-1′′′); 3.75 (q, 2H, $J_{2''',3'''}$ = 7.10 Hz, $J_{2''',3b'''}$ =14.20 Hz, H-2′′′); 2.42 (s, 3H, C$\underline{H}_3$-4′′); 1.20 (t, 3H, H-3′′′); **^{13}C NMR (acetone-d^6) δ (ppm)** 191.7 (C-1); 166.1 (C-2′); 163.9 (C-4′); 156.7 (C-4′′); 150.4 (C-1′′); 131.7 (C-6′); 130.6 (C-2); 119.0 (C-2′′); 115.8 (C-3); 114.6 (C-1′); 109.7 (C-3′′); 108.3 (C-5′); 103.3 (C-3′); 92.7 (C-1′′′); 64.4 (C-2′′′); 14.5 (C-3′′′); 13.0 (C$\underline{H}_3$-4′′); HRMS calcd for $C_{17}H_{18}NaO_5$ 325.10464 (MNa^+) found 325.10494

7.2.5 General conventional procedure for the synthesis of 4′-fluoro-2- hydroxy-chalcones

To solution of 1-(4-fluoro-2-hydroxyphenyl)ethan-1-one (**27**) (200 mg, 1.30 mmol) and an aryl aldehyde (**16a-16i**, 2.0 equiv.) in ethanol (2.5 mL) was added at room temperature sodium hydroxide aqueous solution 50% (w/v) (2.5 mL). The reaction stirred for 24h at room temperature. The solution was neutralized using 10% HCl aqueous solution and extracted with DCM. The organic layers were combined, washed with brine, dried over $MgSO_4$ and concentrated in vacuum. The chalcones derivatives were purified by column chromatography (40:1 hexane/ EtOAc).

7.2.6 General microwave assisted procedure for the synthesis of 4′-fluoro-2-hydroxy-chalcones

To solution of 1-(4-fluoro-2-hydroxyphenyl)ethan-1-one (**27**) (200 mg, 1.300 mmol) and an aryl aldehyde (**16a-16i**, 2.0 equiv.) in ethanol (2.5 mL) was added at room temperature sodium hydroxide aqueous solution 50% (w/v) (2.5 mL). The reaction proceeded in a microwave oven at 150 W and 40 ºC for 1.5 h. The solution was neutralized using 10% HCl aqueous solution and extracted with DCM. The organic layers were combined, washed with brine, dried over $MgSO_4$ and concentrated in vacuum. The chalcones derivatives were purified by column chromatography (30:1 hexane/ EtOAc).

(*E*)-1-(4-fluoro-2-hydroxyphenyl)-3-(4-fluorophenyl)prop-2-en-1-one (28a): Yield 72.6%; orange solid; m.p.=90.9-91.4 ºC; R_f (10:1 Hexane/ EtOAc)= 0.63; **^{1}H NMR (acetone-d^6) δ (ppm)** 13.33 (s, 1H, OH-2′); 8.42 (dd, 1H, $J_{6',F}$ =6.82, $J_{5',6'}$ =8.93, H-6′); 8.04-7.93 (m, 4H, H-2, H-3, H-2′′, H-6′′); 7.27 (t, 2H, $J_{2'',3''}$=$J_{5'',6''}$=8.66 Hz, H-3′′, H-5′′); 6.80-6.74 (m, 2H, H-3′, H-5′); **^{13}C NMR (acetone-d^6) δ (ppm)** 192.9 (C-1); 166.2 (C-4′); 166.2 (d, *J* = 7.8 Hz, C-2′); 167.2 (d, *J* = 254.1 Hz, C-4′′); 144.3 (C-3); 133.4 (d, *J* = 12.4 Hz, C-6′); 131.4 (d, *J* = 8.4 Hz, C-1′′, C-2′′, C-6′′); 120.4 (C-2); 117.2 (C-1′); 115.9 (d, *J* = 21.8 Hz, C-3′′, C-5′); 106.9 (d, *J* = 21.8 Hz, C-5′); 104.3 (d, *J* = 24.4 Hz, C-3′); HRMS calcd for $C_{15}H_{11}F_2O_2$ 261.07216 (MNa^+) found 261.07361

(*E*)-3-(4-bromophenyl)-1-(4-fluoro-2-hydroxyphenyl)prop-2-en-1-one (28b): Yield 87.3%; yellow solid; m.p.=89.4-89.9 ºC; R_f (10:1 Hexane/ EtOAc)= 0.59; **^{1}H NMR (acetone-d^6) δ (ppm)** 13.29 (s, 1H, OH-2′); 8.43 (dd, 1H, $J_{6',F}$ =7.04, $J_{5',6'}$ =8.71, H-6′); 8.11 (d, 1H, $J_{2,3}$=15.68 Hz, H-2); 7.93 (d, 1H, H-3); 7.88 (d, 2H, $J_{2'',3''}$ =$J_{5'',6''}$=8.28 Hz, H-2′′, H-6′′); 7.69 (d, 2H, H-3′′, H-5′′); 6.83-6.75 (m, 2H, H-3′, H-5′); **^{13}C NMR (acetone-d^6) δ (ppm)** 193.9 (C-1); 169.6 (C-4′); 167.1 (d, J = 13.9 Hz, C-2′); 144.9 (C-3); 125.6 (C-4′′); 134.4 (d, J = 11.9Hz, C-6′); 134.8 (C-1′′); 133.0 (C-3′′, C-5′′); 131.7 (C-2′′, C-6′′); 122.2 (C-2); 118.1 (C-1′); 107.8 (d, J = 23.6 Hz, C-5′); 105.2 (d, J = 23.5 Hz, C-3′); HRMS calcd for $C_{15}H_{11}BrFO_2$ 320.99210 (MNa^+) found 320.99422

(*E*)-1-(4-fluoro-2-hydroxyphenyl)-3-(4-methylphenyl)prop-2-en-1-one (28d): Yield 83.0%; red solid; m.p.=87.9-88.3 ºC; R_f (10:1 Hexane/ EtOAc)= 0.54; **^{1}H NMR (acetone-d^6) δ (ppm)** 13.43 (s, 1H, OH-2′); 8.42 (dd, 1H, $J_{6',F}$ =6.50, $J_{5',6'}$ =8.83, H-6′); 8.02 (d, 1H, $J_{2,3}$=15.38 Hz, H-2); 7.95 (d, 1H, H-3); 7.81 (d, 2H, $J_{2'',3''}$ =$J_{5'',6''}$ =8.73 Hz, H-2′′, H-6′′); 7.32 (d, 2H, H-3′′, H-5′′); 6.82-6.74 (m, 2H, H-3′, H-5′); 2.40 (s, 1H, C$\underline{H}_3$-4′′); **^{13}C NMR (acetone-d^6) δ (ppm)** 193.0 (C-1); 169.5 (C-4′); 167.1 (C-2′); 146.6 (C-3); 142.6 (C-4′′); 134.2 (d, J = 11.7 Hz, C-6′); 132.9 (C-1′′); 130.6 (C-3′′, C-5′′); 130.1 (C-2′′, C-6′′); 120.2 (C-2); 118.2 (C-1′); 107.7 (d, J = 23.7 Hz, C-5′); 105.2 (d, J = 23.9 Hz, C-3′); 21.5 ($\underline{C}H_3$-4′′); HRMS calcd for $C_{16}H_{14}FO_2$ 257.09723 (MNa^+) found 257.09759

(*E*)-3-(4-(benzyloxy)phenyl)-1-(4-fluoro-2-hydroxyphenyl)prop-2-en-1-one (28h): Yield 89.9%; reddish solid; m.p.=95.4-95.7.0 ºC; R_f (10:1 Hexane/ EtOAc)= 0.60; **^{1}H NMR (acetone-d^6) δ (ppm)** 13.50 (s, 1H, OH-2′); 8.40 (dd, 1H, $J_{6',F}$ =6.60, $J_{5',6'}$ =8.97, H-6′); 7.96 (d, 1H, $J_{2,3}$=15.32 Hz, H-2); 7.90 (d, 1H, H-3); 7.88 (d, 2H, $J_{2'',3''}$ = $J_{5'',6''}$ =8.66 Hz, H-2′′, H-6′′); 7.53-7.35 (m, 5H, C$\underline{H}$, Ph); 7.15 (t, 2H, H-3′′, H-5′′); 6.81-6.72 (m, 2H, H-3′, H-5′); 5.24 (s, 2H, C$\underline{H}_2$Ph); **^{13}C NMR (acetone-d^6) δ (ppm)** 192.9 (C-1); 168.5 (C-4′); 165.6 (C-2′); 161.5 (C-4′′); 145.6 (C-3); 136.9 ($\underline{C}_q$, Ph); 133.2 (d, J = 11.6 Hz, C-6′); 131.1 (C-2′′, C-6′′); 128.5 ($\underline{C}$H, Ph); 127.9 ($\underline{C}$H, Ph); 127.6 ($\underline{C}$H, Ph); 127.5 (C-1′′); 117.9 (C-2); 117.3 (C-1′); 115.4 (C-3′′, C-5′′); 106.7 (d, J = 22.4 Hz, C-5′); 104.2 (d, J = 23.8 Hz, C-3′); 69.8 ($\underline{C}H_2$Ph); HRMS calcd for $C_{15}H_{11}BrFO_2$ 320.99210 (MNa^+) found 320.99422

(*E*)-1-(4-fluoro-2-hydroxyphenyl)-3-(5-methylfuran-2-yl)prop-2-en-1-one (28i): Yield 84.6%; reddish oil; R_f (10:1 Hexane/ EtOAc)=0.63; **^{1}H NMR (acetone-d^6) δ (ppm)** 13.33 (s, 1H, OH-2′); 8.10 (dd, 1H, $J_{6',F}$ =7.12, $J_{5',6'}$ =8.57, H-6′); 7.56 (d, 1H, $J_{2,3}$=14.84 Hz, H-2); 7.42 (d, 1H, H-3); 6.87 (d, 1H, $J_{2'',3''}$=2.70 Hz, H-2′′); 6.59 (dd, $J_{3',5'}$=1.89 Hz, $J_{3',F}$ =10.75 Hz, H-3′); 6.68-6.63 (m, 1H, H-5′); 6.19 (d, 1H, $J_{3',5'}$=2.52 Hz, $J_{3',F}$ =10.68 Hz, H-3′′); 2.28 (s, 3H, C$\underline{H}_3$-4′′); **^{13}C NMR (acetone-d^6) δ (ppm)** 192.4 (C-1); 167.5 (C-4′); 166.0 (C-2′); 157.2 (C-4′′); 150.3 (C-1′′); 132.9 (d, J = 11.9 Hz, C-6′); 131.5 (C-2); 119.9 (C-2′′); 117.2 (C-1′); 115.3 (C-3); 109.9 (C-3′′); 106.8 (d, J = 22.9 Hz, C-5′); 104.3 (d, J = 23.4 Hz, C-3′); 13.1 ($\underline{C}H_3$-4′); HRMS calcd for $C_{14}H_{12}FO_3$ 247.07650 (MH^+) found 247.07688

7.3 Chalcones Deprotection

7.3.1 General conventional procedure for the synthesis of 2′,4′,6′-trihydroxychalcones and 2′,4′-dihydroxychalcones

The protected chalcones (**21a-21i** and **28a-28i**) (0.5 mmol) were dissolved in methanol (6.4 mL) and $FeCl_3 \cdot 6H_2O$ (2.5 equiv.) was added and the deprotection proceeded for 2h-3h at reflux. The residues were concentrated and purified by column chromatography (3:1 hexane/ EtOAc) affording the desired products.

7.3.2 General microwave assisted procedure for the synthesis of 2′,4′,6′-trihydroxy-chalcones and 2′,4′-dihydroxychalcones

The protected chalcones (**21a-21i** and **28a-28i**) (0.5 mmol) were dissolved in methanol (6.4 mL) and $FeCl_3 \cdot 6H_2O$ (2.5 equiv.) was added and the deprotection proceeded in a microwave oven at 150 W at 80 ºC for 10 minutes. The residues were concentrated and purified by column chromatography (3:1 hexane/ EtOAc) yielding the desired chalcones.

(*E*)-3-(4-fluorophenyl)-1-(2,4,6-trihydroxyphenyl)prop-2-en-1-one (22a): Yield 87.7%; yellow solid; m.p.=178.2-179.3 ºC; R_f (2:1 Hexane/ EtOAc)=0.36; **^{1}H NMR (acetone-d^6), δ (ppm)** 12.01 (s, 2H, OH-2′, OH-6′); 9.39 (s, 1H, OH-4′); 8.21 (d, 1H, $J_{2,3}$

=14.54 Hz, H-2); 7.80-7.76 (m, 3H, H-3, H-2′′, H-6′′); 7.23 (t, 2H, $J_{2'',3''} = J_{5'',6''}$ =8.73 Hz, H-3′′, H-5′′); 6.0 (s, 2H, H-3′, H-5′); **^{13}C NMR (acetone-d^6), δ (ppm)** 192.2 (C-1); 164.9 (C-4′); 164.8 (C-2′, C-6′); 162.4 (C-4′′); 140.5 (C-3); 132.2 (d, *J* = 3.2 Hz, C-1′′); 130.4 (d, *J* = 7.9 Hz, C-2′′, C-6′′); 127.5 (C-2); 115.9 (d, *J* = 21.6 Hz, C-3′′, C-5′′); 104.8 (C-1′); 95.2 (C-3′, C-5′); HRMS calcd for $C_{15}H_{12}FO_4$ 275.07141 (MH^+) found 275.07163

(*E*)-3-(4-bromophenyl)-1-(2,4,6-trihydroxyphenyl)prop-2-en-1-one (22b): Yield 96.0%; yellow solid; m.p.=187.4-188.3 ºC; R_f (4:1 Hexane/EtOAc)=0.52; **^{1}H NMR (acetone-d^6), δ (ppm)** 11.99 (s, 2H, OH-2′, OH-6′); 9.39 (s, 1H, OH-4′); 8.27 (d, 1H, $J_{2,3}$=15.66 Hz, H-2); 7.73 (d, 1H, H-3); 7.66 (d, 2H, $J_{2'',3''}$=$J_{5'',6''}$=8.73 Hz, H-3′′, H-5′′); 7.63 (d, 2H, H-2′′, H-6′′); 6.0 (s, 2H, H-3′, H-5′); **^{13}C NMR (acetone-d^6), δ (ppm)** 192.1 (C-1); 164.9 (C-4′); 164.8 (C-4′, C-6′); 140.2 (C-3); 134.9 (C-1′′); 132.1 (C-3′′, C-5′′); 129.9 (C-2′′, C-6′′); 128.5 (C-2); 123.6 (C-4′′); 104.8 (C-1′); 95.2 (C-3′, C-5′); HRMS calcd for $C_{15}H_{12}BrO_4$ 334.99135 (MH^+) found 334.99157

(*E*)-3-(phenyl)-1-(2,4,6-trihydroxyphenyl)prop-2-en-1-one (22c): Yield 79.9%; yellow solid; m.p.=172.7-172.9 ºC; R_f (4:1 Hexane/EtOAc)= 0.26; **^{1}H NMR (acetone-d^6), δ (ppm)** 8.27 (d, 1H, $J_{2,3}$ =15.72 Hz, H-2); 7.79 (d, 1H, H-3); 7.70 (d, 2H, $J_{2'',3''}$ =$J_{5'',6''}$ =6.90 Hz, H-2′′, H-6′′); 7.48-7.42 (m, 3H, H-3′′, H-4′′, H-5′′); 6.00 (s, 2H, H-3′, H-5′); **^{13}C NMR (acetone-d^6), δ (ppm)** 192.3 (C-1); 164.7 (C-2′, C-4′, C-6′); 142.0 (C-3); 135.7 (C-1′′); 130.0 (C-4′′); 128.9 (C-3′′, C-5′′); 128.3 (C-2′′, C-6′′); 127.7(C-2); 104.7 (C-1′); 95.1 (C-3′, C-5′); HRMS calcd for $C_{15}H_{13}O_4$ 257.08084 (MH^+) found 257.08106

(*E*)-3-(4-methylphenyl)-1-(2,4,6-trihydroxyphenyl)prop-2-en-1-one (22d): Yield 80.7%; yellow solid; m.p.=157.0-157.9 ºC; R_f (4:1 Hexane/EtOAc)=0.30; **^{1}H NMR (acetone-d^6), δ (ppm)** 12.07 (s, 2H, OH-2′, OH-6′); 9.42 (s, 1H, OH-4′); 8.23 (d, 1H, $J_{2,3}$=16.20 Hz, H-2); 7.78 (d, 1H, H-3); 7.60 (d, 2H, $J_{2'',3''}$ =$J_{5'',6''}$=7.90 Hz, H-2′′, H-6′′); 7.28 (d, 2H, H-3′′, H-5′′); 5.99 (s, 2H, H-3′, H-5′); 2.38 (s, 3H, C$\underline{H}_3$-4′′); **^{13}C NMR (acetone-d^6), δ (ppm)** 192.3 (C-1); 164.8 (C-2′, C-4′, C-6′); 141.9 (C-3); 140.4 (C-4′′); 132.9 (C-1′′); 129.6 (C-3′′, C-5′′); 128.3 (C-2′′, C-6′′); 126.6(C-2); 104.8 (C-1′); 95.2 (C-3′, C-5′); 20.5 (C$\underline{H}_3$-4′′); HRMS calcd for $C_{16}H_{14}NaO_4$ 293.07843 (MNa^+) found 293.07846

(*E*)-3-(4-methyloxyphenyl)-1-(2,4,6-trihydroxyphenyl)prop-2-en-1-one (22e): Yield 79.6%; yellow solid; m.p.=186.8-186.9 ºC; R_f (2:1 Toluene/EtOAc)= 0.20; **^{1}H NMR (acetone-d^6), δ (ppm)** 8.17 (d, 1H, $J_{2,3}$ =15.83 Hz, H-2); 7.74 (d, 1H, H-3); 7.66 (d, 2H, $J_{2'',3''}$ =$J_{5'',6''}$ =8.68 Hz, H-2″, H-6″); 7.02 (d, 2H, H-3″, H-5″); 5.98 (s, 2H, H-3′, H-5′); 3.87 (s, 3H, -OC<u>H</u>$_3$-4″); **^{13}C NMR (acetone-d^6), δ (ppm)** 192.3 (C-1); 164.6 (C-4′); 164.5 (C-2′, C-6′); 161.6 (C-4″); 141.9 (C-3); 130.3 (C-2″, C-6″); 128.1 (C-1″); 125.2 (C-2); 114.4 (C-3″, C-5″); 104.7 (C-1′); 95.0 (C-3′, C-5′); 54.9 (-O<u>C</u>H$_3$-4″); HRMS calcd for $C_{16}H_{14}NaO_5$ 309.07334 (MNa^+) found 309.07333

(*E*)-3-(4-ethyloxyphenyl)-1-(2,4,6-trihydroxyphenyl)prop-2-en-1-one (22f): Yield 88.5%; yellow solid; m.p.=182.3-182.6 ºC; R_f (2:1 Toluene/ EtOAc)= 0.32; **^{1}H NMR (acetone-d^6), δ (ppm)** 12.09 (s, 2H, OH-2′, OH-6′); 9.43 (s, 1H, OH-4′); 8.16 (d, 1H, $J_{2,3}$=15.69 Hz, H-2); 7.78 (d, 1H, H-3); 7.75 (d, 2H, $J_{2'',3''}$ =$J_{5'',6''}$=8.73 Hz, H-2″, H-6″); 7.00 (d, 2H, H-3″, H-5″); 5.98 (s, 2H, H-3′, H-5′); 4.12 (q, 2H, *J*=7.13 Hz, *J*=13.97 Hz, -OC<u>H</u>$_2$CH$_3$-4″); 1.98-1.96 (m, 3H, -OCH$_2$C<u>H</u>$_3$-4″)**; ^{13}C NMR (acetone-d^6), δ (ppm)** 192.3 (C-1); 164.8 (C-2′, C-6′); 164.5 (C-4′); 160.9 (C-4″); 142.1 (C-3); 130.1 (C-2″, C-6″); 128.1 (C-1″); 124.9 (C-2); 114.8 (C-3″, C-5″); 104.8 (C-1′); 95.1 (C-3′, C-5′); 63.4 (-O<u>C</u>H$_2$CH$_3$-4″); 14.1 (OCH$_2$<u>C</u>H$_3$-4″); HRMS calcd for $C_{17}H_{16}NaO_5$ 323.08899 (MNa^+) found 323.08910

(*E*)-3-(4-allyloxyphenyl)-1-(2,4,6-trihydroxyphenyl)prop-2-en-1-one (22g): Yield 82.4%; yellow solid; m.p.=175.1-175.4 ºC; R_f (2:1 Toluene/ EtOAc)= 0.55; **^{1}H NMR (acetone-d^6), δ (ppm)** 12.06 (s, 2H, OH-2′, OH-6′); 9.30 (s, 1H, OH-4′); 8.16 (d, 1H, $J_{2,3}$=14.82 Hz, H-2); 7.79 (d, 1H, H-3); 7.66 (d, 2H, $J_{2'',3''}$ =$J_{5'',6''}$=8.40 Hz, H-2″, H-6″); 7.04 (d, 2H, H-3″, H-5″); 6.15-6.05 (m, 1H, -OCH$_2$C<u>H</u>CH$_2$-4″); 5.99 (s, 2H, H-3′, H-5′); 5.45, 5.28 (each d, 2H, *J*=17.51 Hz, *J*=10.74 Hz, OCH$_2$CHC<u>H</u>$_2$-4″); 4.66 (d, 2H, *J*=5.27 Hz, -OCH$_2$CHC<u>H</u>$_2$-4″); **^{13}C NMR (acetone-d^6), δ (ppm)** 192.3 (C-1); 164.8 (C-2′, C-6′); 164.5 (C-4′); 160.5 (C-4″); 141.9 (C-3); 133.4 (-OCH$_2$<u>C</u>HCH$_2$-4″); 130.0 (C-2″, C-6″); 128.3 (C-1″); 125.2 (C-2); 118.8 (-OCH$_2$CH<u>C</u>H$_2$-4″); 115.1 (C-3″, C-5″); 104.8 (C-1′);

95.1 (C-3′, C-5′); 68.5 (-O<u>C</u>H_2CHCH_2-4′′); HRMS calcd for $C_{18}H_{16}NaO_5$ 335.08899 (MNa^+) found 335.08908

(*E*)-3-(4-(benzyloxy)phenyl)-1-(2,4,6-trihydroxyphenyl)prop-2-en-1-one (22h): Yield 86.8%; yellow solid; m.p.=163.0-164.7 ºC; R_f (6:1 Hexane/ EtOAc)=0.30; **^{1}H NMR (acetone-d^6), δ (ppm)** 8.16 (d, 1H, $J_{2,3}$=15.25 Hz, H-2); 7.78 (d, 1H, H-3); 7.66 (d, 2H, $J_{2'',3''}$ =$J_{5'',6''}$ =8.46 Hz, H-2′′, H-6′′); 7.50 (d, 2H, *J*=8.03 Hz, Ar<u>H</u>); 7.41 (t, 2H, *J*=7.88 Hz, Ar<u>H</u>); 7.35 (d, 1H, Ar<u>H</u>); 7.10(d, 2H, H-5′′, H-6′′); 5.98 (s, 2H, H-3', H-5′); 5.20 (s, 2H, C<u>H</u>$_2$Ph); **^{13}C NMR (acetone-d^6), δ (ppm)** 192.3 (C-1); 164.8 (C-4′); 168.6 (C-2′, C-6′); 160.7 (C-4′′); 141.9 (C-3); 137.1 (C-1′′, <u>C</u>$_q$, Ph); 130.1 (C-2′′, C-6′′); 128.5, 127.9, 127.6 (<u>C</u>H-Ph); 125.2 (C-2); 115.3 (C-3′′, C-5′′); 104.8 (C-1′); 95.2 (C-3′, C-5′); 69.7 (-O<u>C</u>H_2Ph); HRMS calcd for $C_{22}H_{18}NaO_5$ 385.10464 (MNa^+) found 385.10470

(*E*)-3-(5-methylfuran-2-yl)-1-(2,4,6-trihydroxyphenyl)prop-2-en-1-one (22i): Yield 93.5%; dark orange solid; m.p.=118.2-118.9 ºC; R_f (6:1 Hexane/ EtOAc)=0.50; **^{1}H NMR (acetone-d^6), δ (ppm)** 12.06 (s, 2H, OH-2′, OH-6′); 9.30 (s, 1H, OH-4′); 8.04 (d, 1H, $J_{2,3}$=15.99 Hz, H-3); 7.56 (d, 1H, H-2); 6.78 (d, 1H, $J_{2'',3''}$=2.96 Hz, H-2′′); 6.25 (d, 1H, H-3′′); 5.97 (s, 2H, H-3′, H-5′); 2.30 (s, 3H, C<u>H</u>$_3$-4′′); **^{13}C NMR (acetone-d^6), δ (ppm)** 191.8 (C-1); 164.8 (C-2′, C-6′); 164.5 (C-4′); 155.7 (C-4′′); 150.9 (C-1′′); 128.8 (C-2); 123.0 (C-3); 117.7 (C-2′′); 109.3 (C-3′′); 104.7 (C-1′); 95.1 (C-3′, C-5′); 12.9 (<u>C</u>H$_3$-4′′**);** HRMS calcd for $C_{14}H_{12}NaO_5$ 283.05769 (MNa^+) found 283.05777

(*E*)-1-(2,4-dihydroxyphenyl)-3-(4-fluorophenyl)prop-2-en-1-one (26a): Yield 84.6%; yellow solid; m.p.=129.1-129.8 ºC; R_f (3:1 Hexane/EtOAc)= 0.30; **^{1}H NMR (acetone-d^6) δ (ppm)** 13.49 (s, 1H, OH-2′); 9.52 (s, 1H, OH-4′); 8.17 (d, 1H, $J_{5',6'}$=8.93, H-6′); 7.98-7.93 (m, 3H, H-2, H-2′′, H-6′′); 7.87 (d, 1H, $J_{2,3}$=15.53 Hz, H-3); 7.26 (t, 2H, $J_{2'',3''}$ =$J_{5'',6''}$ =J=$_{5'',F}$ =$J_{6'',F}$ =8.84 Hz, H-3′′, H-5′′); 6.50 (dd, 1H, $J_{3',5'}$ =1.44 Hz, H-5′); 6.40 (dd, 1H, H-3′); **^{13}C NMR (acetone-d^6) δ (ppm)** 191.8 (C-1); 166.8 (C-2′); 165.0 (C-4′); 164.0 (d, *J* = 248.7 Hz, C-4′′); 142.6 (C-3); 132.7 (C-6′); 131.6 (d, *J* = 2.9 Hz, C-1′′); 131.1 (d, *J* = 8.8 Hz, C-2′′, C-6′′); 120.7 (C-2); 115.9 (d, *J* = 22.1 Hz, C-3′′, C-5′′); 113.6

(C-1′); 108.0 (C-5′); 102.9 (C-3′); HRMS calcd for $C_{15}H_{12}FO_3$ 259.07650 (MH^+) found 259.07678

(*E*)-3-(4-bromophenyl)-1-(2,4-dihydroxyphenyl)prop-2-en-1-one (26b): Yield 93.7%; yellow solid; m.p.=134.6-135.0 ºC; R_f (3:1 Hexane/ EtOAc)= 0.45; **^{1}H NMR (acetone-d^6) δ (ppm)** 13.42 (s, 1H, OH-2′); 9.64 (s, 1H, OH-4′); 8.17 (d, 1H, $J_{5',6'}$ =8.86, H-6′); 8.02 (d, 1H, $J_{2,3}$=15.28 Hz, H-2); 7.86-7.83 (m, 3H, H-3, H-2′′, H-6′′); 7.67 (d, 2H, $J_{2'',3''}$ =$J_{5'',6''}$ =8.39 Hz, H-3′′, H-5′′); 6.50 (dd, 1H, $J_{3',5'}$ =1.92 Hz, H-5′); 6.40 (d, 1H, H-3′); **^{13}C NMR (acetone-d^6) δ (ppm)** 191.7 (C-1); 166.8 (C-2′); 165.1 (C-4′); 142.4 (C-3); 134.3 (C-1′′); 132.7 (C-6′); 132.1 (C-3′′, C-5′′); 130.5 (C-2′′, C-6′′); 124.2 (C-4′′); 121.7 (C-2); 113.6 (C-1′); 108.1 (C-5′); 102.9 (C-3′); HRMS calcd for $C_{15}H_{12}BrO_3$ 318.99643 (MH^+) found 318.99680

(*E*)-1-(2,4-dihydroxyphenyl)-3-(4-methylphenyl)prop-2-en-1-one (26c): Yield 96.8%; yellow solid; m.p.=132.1-133.4 ºC; R_f (3:1 Hexane/ EtOAc)= 0.12; **^{1}H NMR (acetone-d^6) δ (ppm)** 13.55 (s, 1H, OH-2′); 9.56 (s, 1H, OH-4′); 8.18 (d, 1H, $J_{5',6'}$ =7.19, H-6′); 7.93 (d, 1H, $J_{2,3}$=15.53 Hz, H-2); 7.86 (d, 1H, H-3); 7.77 (d, 2H, $J_{2'',3''}$ =$J_{5'',6''}$ =7.86 Hz, H-2′′, H-6′′); 7.31 (d, 2H, H-3′′, H-5′′); 6.50 (dd, 1H, $J_{3',5'}$ =1.97 Hz, H-5′); 6.39 (dd, 1H, H-3′); 2.40 (s, 1H, C$\underline{H}_3$-4′′); **^{13}C NMR (acetone-d^6) δ (ppm)** 191.9 (C-1); 166.8 (C-2′); 164.9 (C-4′); 144.0 (C-3); 141.1 (C-4′′); 132.6 (C-6′); 132.3 (C-1′′); 119.7 (C-2); 129.6 (C-3′′, C-5′′);128.9 (C-2′′, C-6′′); 113.6 (C-1′); 107.9 (C-5′); 102.8 (C-3′); 20.6 ($\underline{C}H_3$-4′′); HRMS calcd for $C_{16}H_{14}NaO_3$ 277.08352 (MNa^+) found 277.08370

(*E*)-3-(4-(benzyloxy)phenyl)-1-(2,4-dihydroxyphenyl)prop-2-en-1-one (26h): Yield 96.7%; yellow solid; m.p.=127.5-128.1 ºC; R_f (3:1 Hexane/ EtOAc)= 0.21; **^{1}H NMR (acetone-d^6) δ (ppm)** 13.62 (s, 1H, OH-2′); 9.68 (s, 1H, OH-4′); 8.15 (d, 1H, $J_{5',6'}$ =8.88, H-6′); 7.89-7.80 (m, 4H, H-2, H-3, H-2′′, H-6′′); 7.52-7.36 (m, 5H, Ar$\underline{H}$, Ph); 7.12 (d, 2H, $J_{2'',3''}$ =$J_{5'',6''}$ =8.71 Hz, H-3′′, H-5′′); 6.49 (dd, 1H, $J_{3',5'}$=2.19 Hz, H-5′); 6.40 (d, 1H, H-3′); 5.22 (s, 2H, -OC$\underline{H}_2$Ph); **^{13}C NMR (acetone-d^6) δ (ppm)** 191.9 (C-1); 166.7 (C-2′); 164.8 (C-4′); 161.1 (C-4′′); 143.9 (C-3); 137.0 ($\underline{C}_q$, Ph); 132.5 (C-6′); 130.7 (C-2′′, C-6′′); 128.8

(CH, Ph); 128.2 (CH, Ph); 127.9 (CH, Ph); 127.8 (C-1′′); 118.4 (C-2); 115.3 (C-3′′, C-5′′); 113.6 (C-1′); 107.8 (C-5′); 102.9 (C-3′); 69.7 (-OCH$_2$Ph); HRMS calcd for $C_{22}H_{18}NaO_4$ 369.10973 (MNa^+) found 369.10992

(*E*)-1-(2,4-dihydroxyphenyl)-3-(5-methylfuran-2-yl)prop-2-en-1-one (26i): Yield 90.9%; yellow solid; m.p.=125.6-125.9 ºC; R_f (3:1 Hexane/ EtOAc)= 0.35; **^{1}H NMR (acetone-d^6) δ (ppm)** 13.43 (s, 1H, OH-2′); 9.41 (s, 1H, OH-4′); 7.85 (d, 1H, $J_{5',6'}$ =8.65, H-6′); 7.48 (d, 1H, $J_{2,3}$=14.92 Hz, H-2); 7.37 (d, 1H, H-3); 6.78 (d, $J_{2'',3''}$ =2.84 Hz, H-2′′); 6.36 (dd, 1H, $J_{3',5'}$ =1.98 Hz, H-5′); 6.23 (d, 1H, H-3′); 6.16 (d, 1H, H-3′′); 2.27 (s, 3H, CH$_3$-4′′); **^{13}C NMR (acetone-d^6) δ (ppm)** 191.3 (C-1); 166.6 (C-2′); 164.8 (C-4′); 156.4 (C-4′); 150.4 (C-1′′); 132.2 (C-6′); 130.2 (C-2); 118.7 (C-2′′); 115.9 (C-3); 113.5 (C-1′); 109.6 (C-3′′); 108.0 (C-5′); 102.9 (C-3′); 13.0 (CH$_3$-4′′); HRMS calcd for $C_{14}H_{13}O_4$ 245.08084 (MH^+) found 245.08115

7.4 Synthesis of dihydrochalcones

7.4.1 General procedure for the synthesis of dihydrochalcones

To a solution of chalcone (**22a-22i**, **26a-26i** and **28a-28i**, 2.0 mmol) in EtOAc (5 mL) and MeOH was added (2-3 mL) Pd/C (10% mmol) in N_2 atmosphere. Et_3SiH (10 equiv.) was added dropwise while effervescence was observed (meaning that hydrogen was being formed *in situ*). After all the Et_3SiH was added the reaction was kept at room temperature for another 10 minutes until change in the color (orange/yellow to colourless). TLC was used to confirm the completion of the reaction. Catalyst was filtered off through celite, 2/3 of volume of solvent was removed under vacuum and extraction with ACN/Hex was used to remove most of the Et_3SiH from the mixture. The final product was purified by column chromatography (10:1 or 7:1 hexane/ EtOAc).

3-(4-fluorophenyl)-1-(2,4,6-trihydroxyphenyl)propan-1-one (18a): Yield 97.9 %; white solid; m.p.=199.9-200.5 ºC; R_f (3:1 Hexane/ EtOAc)= 0.35; **^{1}H NMR (acetone-d^6), δ (ppm)** 11.76 (s, 2H, OH-2′, OH-6′); 9.31 (s, 1H, OH-4′); 7.31 (dd, 2H, $J_{2'',F}$ =$J_{6'',F}$ =6.60 Hz, $J_{2'',3''}$=$J_{5'',6''}$ =8.39 Hz, H-2′, H-6′); 7.03 (t, 2H, H-3′, H-5′); 5.94 (s, 2H, H-3′, H-5′); 3.38 (t, 2H, $J_{2,3}$=7.54 Hz, H-2); 2.97 (t, 2H, H-3); **^{13}C NMR (acetone-d^6), δ (ppm)** 204.1 (C-1);

164.5 (C-4′); 164.4 (C-2′, C-6′); 165.9 (d, J = 261.8 Hz, C-4′′); 138.0 (C-1′′); 130.1 (d, J = 7.8 Hz, C-2′′, C-6′′); 114.8 (d, J = 20.8 Hz, C-3′′, C-5′′); 104.2 (C-1′); 94.9 (C-3′, C-5′); 45.5 (C-2); 30.3 (C-3)**;** HRMS calcd for $C_{15}H_{13}FNaO_4$ 299.06901 (MNa^+) found 299.06902

3-(phenyl)-1-(2,4,6-trihydroxyphenyl)propan-1-one (18c): Yield 94.4%; white solid; m.p.=133.0-133.4 ºC; R_f (2:1 Hexane/ EtOAc)= 0.28; **^{1}H NMR (acetone-d^6), δ (ppm)** 11.82 (s, 2H, OH-2′, OH-6′); 9.37 (s, 1H, OH-4′); 7.31-7.17 (m, 5H, H-2′′, H-3′′, H-4′′, H-5′′, H-6′′); 5.95 (s, 2H, H-3′, H-5′); 3.40 (t, 2H, $J_{2,3}$=7.86 Hz, H-2); 2.99 (t, 2H, H-3); **^{13}C NMR (acetone-d^6), δ (ppm)** 204.3 (C-1); 164.5 (C-4′); 164.4 (C-2′, C-6′); 142.0 (C-1′′); 128.4 (C-3′′, C-5′′); 128.3 (C-2′′, C-6′′); 125.7 (C-4′′); 104.2 (C-1′); 94.9 (C-3′, C-5′); 45.5 (C-2); 30.5 (C-3); HRMS calcd for $C_{15}H_{14}NaO_4$ 281.07843 (MNa^+) found 281.07847

3-(4-methylphenyl)-1-(2,4,6-trihydroxyphenyl)propan-1-one (18d): Yield 98.8%; white solid; m.p.=198.7-199.4 ºC; R_f (3:1 Hexane/ EtOAc)= 0.17; **^{1}H NMR (acetone-d^6), δ (ppm)** 11.83 (s, 2H, OH-2′, OH-6′); 9.38 (s, 1H, OH-4′); 7.17 (d, 2H, $J_{2'',3''} = J_{5'',6''}$ =7.40 Hz, H-2′′, H-6′′); 7.09 (d, 2H, H-3′′, H-5′′); 5.94 (s, 2H, H-3′, H-5′); 3.37 (t, 2H, $J_{2,3}$=7.29 Hz, H-2); 2.94 (t, 2H, H-3); 2.28 (s, 3H, C$\underline{H}_3$-4′′); **^{13}C NMR (acetone-d^6), δ (ppm)** 204.4 (C-1); 164.6 (C-4′); 164.5 (C-2′, C-6′); 138.9 (C-1′′); 134.9 (C-4′′); 128.9 (C-3′′, C-5′′); 128.3 (C-2′′, C-6′′); 104.2 (C-1′); 94.9 (C-3′, C-5′); 45.7 (C-2); 30.1 (C-3); 20.1 ($\underline{C}H_3$-4′′); HRMS calcd for $C_{16}H_{16}NaO_4$ 295.09408 (MNa^+) found 295.09410

3-(4-methoxyphenyl)-1-(2,4,6-trihydroxyphenyl)propan-1-one (18e): Yield 96.9%; white solid; m.p.=200.8-201.4 ºC; R_f (2:1 Toluene/ EtOAc)= 0.29; **^{1}H NMR (acetone-d^6), δ (ppm)** 11.74 (s, 2H, OH-2′, OH-6′); 9.27 (s, 1H, OH-4′); 7.20 (d, 2H, $J_{2'',3''} = J_{5'',6''}$ =7.81 Hz, H-2′′, H-6′′); 6.86 (d, 2H, H-3′′, H-5′′); 5.95 (s, 2H, H-3′, H-5′); 3.77 (s, 3H, -OC$\underline{H}_3$-4′′); 3.37 (t, 2H, $J_{2,3}$=8.07 Hz, H-2); 2.93 (t, 2H, H-3); **^{13}C NMR (acetone-d^6), δ (ppm)** 204.5 (C-1); 164.5 (C-4′); 164.3 (C-2′, C-6′); 158.0 (C-4′′); 133.8 (C-1′′); 129.3 (C-2′′, C-6′′); 113.7 (C-3′′, C-5′′); 104.2 (C-1′); 94.9 (C-3′, C-5′); 54.5 (-O$\underline{C}H_3$-4′′); 45.8 (C-2); 29.6 (C-3); HRMS calcd for $C_{16}H_{16}NaO_5$ 311.08899 (MNa^+) found 311.08905

3-(4-ethoxyphenyl)-1-(2,4,6-trihydroxyphenyl)propan-1-one (18f): Yield 96.1%; white solid; m.p.=187.9-188.2 ºC; R_f (2:1 Toluene/ EtOAc)= 0.25; **^{1}H NMR (acetone-d^6), δ (ppm)** 11.96 (s, 2H, OH-2′, OH-6′); 9.65 (s, 1H, OH-4′); 7.18 (d, 2H, $J_{2'',3''} = J_{5'',6''}$ =8.39 Hz, H-2′′, H-6′′); 6.83 (d, 2H, H-3′′, H-5′′); 5.93 (s, 2H, H-3′, H-5′); 4.00 (q, 2H, *J*=6.74 Hz, *J*=14.96 Hz, -OC$\underline{H}_2$CH$_3$-4′′); 3.34 (t, 2H, $J_{2,3}$=8.07 Hz, H-2); 2.91 (t, 2H, H-3); 1.35 (t, 3H, -OCH$_2$C$\underline{H}_3$-4′′); **^{13}C NMR (acetone-d^6), δ (ppm)** 204.5 (C-1); 164.6 (C-4′); 164.5 (C-2′, C-6′); 157.3 (C-4′′); 133.7 (C-1′′); 129.3 (C-2′′, C-6′′); 114.2 (C-3′′, C-5′′); 104.2 (C-1′); 94.9 (C-3′, C-5′); 62.9 (-O$\underline{C}$H$_2$CH$_3$-4′′); 45.9 (C-2); 29.7 (C-3); 14.3 (-OCH$_2\underline{C}$H$_3$-4′′); HRMS calcd for $C_{17}H_{18}NaO_5$ 325.10464 (MNa^+) found 325.10470

3-(4-propyloxyphenyl)-1-(2,4,6-trihydroxyphenyl)propan-1-one (18g): Yield 93.8%; white solid; m.p.=187.9-188.2 ºC; R_f (2:1 Toluene/ EtOAc)= 0.24; **^{1}H NMR (acetone-d^6), δ (ppm)** 11.77 (s, 2H, OH-2′, OH-6′); 9.27 (s, 1H, OH-4′); 7.19 (d, 2H, $J_{2'',3''} = J_{5'',6''}$ =8.39 Hz, H-2′′, H-6′′); 6.84 (d, 2H, H-3′′, H-5′′); 5.95 (s, 2H, H-3′, H-5′); 3.90 (t, 2H, *J*=8.60 Hz, -OC$\underline{H}_2$CH$_2$CH$_3$-4′′); 3.36 (t, 2H, $J_{2,3}$=8.07 Hz, H-2); 2.92 (t, 2H, H-3); 1.76 (sextet, 2H, *J*=13.35 Hz, *J*=6.34 Hz, -OCH$_2$C$\underline{H}_2$CH$_3$-4′′); 1.07 (t, 3H, OCH$_2$CH$_2$C$\underline{H}_3$-4′′); **^{13}C NMR (acetone-d^6), δ (ppm)** 205.5 (C-1); 164.5 (C-4′); 164.4 (C-2′, C-6′); 157.5 (C-4′′); 133.7 (C-1′′); 129.3 (C-2′′, C-6′′); 114.2 (C-3′′, C-5′′); 104.2 (C-1′); 94.9 (C-3′, C-5′); 69.0 (-O$\underline{C}$H$_2$CH$_2$CH$_3$-4′′); 45.9 (C-2); 29.6 (C-3); 22.4 (-OCH$_2\underline{C}$H$_2$CH$_3$-4′′); 9.9 (-OCH$_2$CH$_2\underline{C}$H$_3$-4′′); HRMS calcd for $C_{18}H_{20}NaO_5$ 339.12029 (MNa^+) found 339.12041

3-(4-hydroxyphenyl)-1-(2,4,6-trihydroxyphenyl)propan-1-one (18h): Yield 97.4%; white solid; m.p.=200.9-201.2 ºC; R_f (3:1 Hexane/ EtOAc)= 0.45; **^{1}H NMR (acetone-d^6), δ (ppm)** 11.76 (s, 2H, OH-2′, OH-6′); 9.26 (s, 1H, OH-4′); 8.10 (s, 1H, OH-4′′); 7.11 (d, 2H, $J_{2'',3''} = J_{5'',6''}$=7.63 Hz, H-2′, H-6′); 6.76 (d, 2H, H-3′, H-5′); 5.95 (s, 2H, H-3′, H-5′); 3.35 (t, 2H, $J_{2,3}$=8.05 Hz, H-2); 2.89 (t, 2H, H-3); **^{13}C NMR (acetone-d^6), δ (ppm)** 204.6 (C-1); 164.5 (C-4′); 164.4 (C-2′, C-6′); 155.5 (C-4′′); 132.6 (C-1′′); 129.3 (C-2′′, C-6′′); 115.1 (C-3′′, C-5′′); 104.2 (C-1′); 94.9 (C-3′, C-5′); 45.9 (C-2); 29.7 (C-3)**;** HRMS calcd for $C_{15}H_{14}NaO_5$ 297.07334 (MNa^+) found 297.07341

3-(5-methylfuran-2-yl)-1-(2,4,6-trihydroxyphenyl)propan-1-one (18i): Yield 98.4%; white solid; m.p.=182.7-183.3 ºC; R_f (3:1 Hexane/ EtOAc)=0.40; **^{1}H NMR (acetone-d^6), δ (ppm)** 11.73 (s, 2H, OH-2′, OH-6′); 9.28 (s, 1H, OH-4′); 5.96 (s, 2H, H-3′, H-5′), 5.91 (d, 1H, $J_{2'',3''}$ =2.41Hz, H-2′′), 5.87 (d, 1H, H-3′′); 3.42 (t, 2H, $J_{2,3}$=7.94 Hz, H-2); 2.94 (t, 2H, H-3); 2.21 (s, 3H, C$\underline{H}_3$-4′′); **^{13}C NMR (acetone-d^6), δ (ppm)** 203.7 (C-1); 164.5 (C-4′); 164.4 (C-2′, C-6′); 153.6 (C-1′′); 149.9 (C-4′′); 105.9 (C-2′); 105.5 (C-3′′); 94.9 (C-3′, C-5′); 42.0 (C-2); 31.9 (C-3); 12.6 ($\underline{C}H_3$-4′′)**;** HRMS calcd for $C_{14}H_{14}NaO_5$ 285.07334 (MNa^+) found 285.07345

1-(2,4-dihydroxyphenyl)-3-(4-fluorophenyl)propan-1-one (29a): Yield 99.7%; white solid; m.p.=187.6-187.9 ºC; R_f (3:1 Hexane/ EtOAc)= 0.29; **^{1}H NMR (acetone-d^6), δ (ppm)** 12.61 (s, 2H, OH-2′); 9.52 (s, 1H, OH-4′); 7.68 (d, 1H, $J_{5',6'}$ =8.78 Hz, H-6′); 7.20 (d, 2H, $J_{2'',3''}$ = $J_{5'',6''}$=7.99 Hz, H-2′′, H-6′′); 6.90 (d, 2H, H-3′′, H-5′′); 6.28 (dd, 1H, $J_{3',5'}$=2.48 Hz, H-5′); 6.19 (d, 1H, H-3′); 3.18 (t, 2H, $J_{2,3}$=7.37 Hz, H-2); 2.88 (t, 2H, H-3); **^{13}C NMR (acetone-d^6), δ (ppm)** 203.7 (C-1); 165.3 (C-2′); 164.7 (C-4′); 161.4 (d, J = 24.4 Hz, C-4′′); 137.3 (d, J = 3.3 Hz, C-1′′); 132.7 (C-6′); 130.2 (d, J = 8.1 Hz, C-2′′, C-6′′); 114.8 (d, J = 21.0 Hz, C-3′′, C-5′′); 112.9 (C-1′); 107.9 (C-5′); 102.7 (C-3′); 39.0 (C-2); 29.1 (C-3); HRMS calcd for $C_{15}H_{14}FO_3$ 261.09215 (MH^+) found 261.09245

1-(2,4-dihydroxyphenyl)propan-1-one)-3-phenyl-propan-1-one (29c): Yield 98.7%; white solid; m.p.=190.9-191.4 ºC; R_f (3:1 Hexane/ EtOAc)=0.50; **^{1}H NMR (acetone-d^6), δ (ppm)** 12.80 (s, 2H, OH-2′); 9.47 (s, 1H, OH-4′); 7.87 (d, 1H, $J_{5',6'}$=9.90 Hz, H-6′); 7.33-7.28 (m, 4H, H-2′′, H-3′′, H-5′′, H-6′′); 7.20 (t, 1H, $J_{4'',5''}$ =$J_{5'',6''}$ =7.56 Hz, H-4′′); 6.44 (dd, 1H, $J_{3',5'}$ =2.42 Hz, H-5′); 6.34 (d, 1H, H-3′); 3.34 (t, 2H, $J_{2,3}$=7.23 Hz, H-2); 3.03 (t, 2H, H-3); **^{13}C NMR (acetone-d^6), δ (ppm)** 203.9 (C-1); 165.4 (C-2′); 164.6 (C-4′); 141.3 (C-1′′); 132.7 (C-6′); 128.4 (C-2′′, C-6′′); 128.3 (C-3′′, C-5′′); 125.0 (C-4′′); 112.9 (C-1′); 107.9 (C-5′); 102.7 (C-3′); 39.0 (C-2); 30.0 (C-3); HRMS calcd for $C_{15}H_{14}NaO_3$ 265.08532 (MNa^+) found 265.08366

1-(2,4-dihydroxyphenyl)-3-(4-methylphenyl)propan-1-one (29d): Yield 99.1%; white solid; m.p.=190.0-190.7 ºC; R_f (3:1 Hexane/ EtOAc)= 0.25; **^{1}H NMR (acetone-d^6), δ**

(ppm) 12.80 (s, 2H, OH-2′); 9.62 (s, 1H, OH-4′); 7.84 (d, 1H, $J_{5',6'}$=8.78 Hz, H-6′); 7.19 (d, 2H, $J_{2'',3''} = J_{5'',6''}$ =7.90 Hz, H-2′′, H-6′′); 7.10 (d, 2H, H-3′′, H-5′′); 6.43 (dd, 1H, $J_{3',5'}$ =2.34 Hz, H-5′); 6.33 (d, 1H, H-3′); 3.30 (t, 2H, $J_{2,3}$=7.41 Hz, H-2); 2.99 (t, 2H, H-3); 2.89 (s, 3H, -CH_3-4′′); **^{13}C NMR (acetone-d^6), δ (ppm)** 204.8 (C-1); 165.3 (C-2′, C-4′); 138.2 (C-4′′); 135.7 (C-1′′); 128.9 (C-2′′, C-6′′); 128.3 (C-3′′, C-5′′); 132.7 (C-6′); 112.9 (C-1′); 107.9 (C-5′); 102.7 (C-3′); 39.2 (C-2); 29.5 (C-3); 20.1 (-CH_3-4′′); HRMS calcd for $C_{16}H_{16}NaO_3$ 279.09917 (MNa^+) found 279.09922

1-(2,4-dihydroxyphenyl)-3-(4-hydroxyphenyl)propan-1-one (29h): Yield 99.0%; white solid; m.p.=205.9-206.4 ºC; R_f (3:1 Hexane/ EtOAc)= 0.25; **^{1}H NMR (acetone-d^6), δ (ppm)**12.84 (s, 1H, OH-2′); 8.64 (brs, 1H, OH-4′); 7.81 (d, 1H, $J_{5',6'}$ =9.13, H-6′); 7.12 (d, 2H, $J_{2'',3''}$ =$J_{5'',6''}$ =8.91 Hz, H-2′′, H-6′′); 6.78 (d, 2H, H-3′′, H-5′′); 6.44 (dd, 1H, $J_{3',5'}$ =2.40 Hz H-5′); 6.35 (d, 1H, H-3′); 3.24 (t, 2H, $J_{2,3}$=7.86 Hz, H-2); 2.93 (t, 2H, H-3); **^{13}C NMR (acetone-d^6), δ (ppm)** 204.2 (C-1); 165.4 (C-2′); 164.6 (C-4′); 155.6 (C-4′′); 132.7 (C-6′); 131.9 (C-1′′); 129.4 (C-2′′, C-6′′); 115.2 (C-3′′, C-5′′); 113.0 (C-1′); 107.9 (C-5′); 102.7 (C-3′); 39.5 (C-2); 29.4 (C-3); HRMS calcd for $C_{15}H_{14}NaO_4$ 281.07843 (MNa^+) found 281.07850

1-(2,4-dihydroxyphenyl)-3-(5-methylfuran-2-yl)propan-1-one (29i): Yield 98.2%; white solid; m.p.=198.3-198.5 ºC; R_f (3:1 Hexane/ EtOAc)= 0.40; **^{1}H NMR (acetone-d^6), δ (ppm)** 12.73 (s, 1H, OH-2′); 9.57 (s, 1H, OH-4′); 7.84 (d, 1H, $J_{5',6'}$ =8.84, H-6′); 5.97 (d, 1H, $J_{2'',3''}$ =2.25 Hz, H-2′′); 5.86 (d, 1H, H-3′′); 6.46 (dd, 1H, $J_{3',5'}$ =1.86 Hz H-5′); 6.35 (d, 1H, H-3′); 3.31 (t, 2H, $J_{2,3}$=7.56 Hz, H-2); 2.98 (t, 2H, H-3); 2.21 (s, 3H, C$\underline{H}_3$-4′′); **^{13}C NMR (acetone-d^6), δ (ppm)** 203.9 (C-1); 165.3 (C-2′); 164.7 (C-4′); 152.8 (C-1′′); 150.2 (C-4′′); 132.7 (C-6′); 112.9 (C-1′); 107.9 (C-2′′); 106.0 (C-3′′); 105.9 (C-5′); 102.7 (C-3′); 35.7 (C-2); 22.4 (C-3); 12.6 ($\underline{C}H_3$-4′′); HRMS calcd for $C_{14}H_{14}NaO_4$ 269.07843 (MNa^+) found 269.07860

1-(4-fluoro-2-hydroxyphenyl)-3-(4-fluorophenyl)propan-1-one (30a): Yield 99.3%; white solid; m.p.=212.7-213.3 ºC; R_f (3:1 Hexane/ EtOAc)=0.62; **^{1}H NMR (acetone-d^6), δ (ppm)** 12.51 (s, 1H, OH-2); 7.95 (dd, 1H, $J_{6',F}$ =6.87, $J_{5',6'}$ =8.70, H-6′);

7.21 (dd, 2H, $J_{2'',3''}$ =$J_{5'',6''}$ =8.20 Hz, $J_{2'',F}$ =$J_{6'',F}$ =5.93 Hz, H-2′′, H-6′′); 6.91 (t, 2H, $J_{3'',F}$ =$J_{5'',F}$ =8.68 Hz, H-3′′, H-5′′); 6.61-6.53 (m, 2H, H-3′, H-5′); 3.31 (t, 2H, $J_{2,3}$=7.83 Hz, H-2); 2.91 (t, 2H, H-3); **^{13}C NMR (acetone-d^6), δ (ppm)** 205.1 (C-1); 167.1 (d, *J* = 251.4 Hz, C-4′); 164.8 (d, *J* = 14.4 Hz, C-2′); 137.0 (d, *J* = 3.2 Hz, C-1′′); 161.4 (d, *J* = 246.4 Hz, C-4′′); 133.5 (d, *J* = 11.5 Hz, C-6′); 114.9 (d, *J* = 2.3 Hz, C-3′′, C-5′′); 130.2 (d, *J* = 7.9 Hz, C-2′′, C-6′′); 116.7 (d, *J* = 2.3 Hz, C-1′); 106.8 (d, *J* = 22.4 Hz, C-5′); 104.2 (d, *J* = 22.5 Hz, C-3′); 39.7 (C-2); 28.6 (C-3); HRMS calcd for $C_{15}H_{13}F_2O_2$ 263.08781 (MH^+) found 263.08951

1-(4-fluoro-2-hydroxyphenyl)-3-(phenyl)propan-1-one (30c): Yield 99.4% ; liquid solid; R_f (3:1 Hexane/ EtOAc)= 0.62; **^{1}H NMR (acetone-d^6), δ (ppm)** 12.71 (s, 1H, OH-2′); 8.11 (dd, 1H, $J_{6',F}$ =6.78, $J_{5',6'}$ =9.31, H-6′); 7.34-7.28 (m 4H, H-2′′, H-3′′, H-5′′, H-6′′); 7.21 (t, 1H, $J_{3'',4''}$ =$J_{4'',5''}$ =7.02, H-4′′); 6.77-6.69 (m, 2H, H-3′, H-5′); 3.46 (t, 2H, $J_{2,3}$=7.94 Hz, H-2); 3.06 (t, 2H, H-3); **^{13}C NMR (acetone-d^6), δ (ppm)** 205.1 (C-1); 167.1 (d, *J* = 259.2 Hz, C-4′); 164.8 (d, *J* = 12.6 Hz, C-2′); 141.0 (C-1′′); 133.3 (*J* = 13.3 Hz, C-6′); 128.5 (C-3′′, C-5′′); 128.4 (C-2′′, C-6′′); 126.1 (C-4′′); 116.7 (C-1′); 106.9 (d, *J* = 23.6 Hz, C-5′); 104.3 (d, *J* = 24.6 Hz, C-3′); 39.8 (C-2); 29.2 (C-3); 20.2 ($\underline{C}H_3$-4′′); HRMS calcd for $C_{15}H_{14}FO_2$ 245.09723 (MH^+) found 245.0986

1-(4-fluoro-2-hydroxyphenyl)-3-(4-methylphenyl)propan-1-one (30d): Yield 99.0%; white solid; m.p.=210.9-211.4 ºC; R_f (3:1 Hexane/ EtOAc)=0.53; **^{1}H NMR (acetone-d^6), δ (ppm)** 12.72 (s, 1H, OH-2′); 8.04 (dd, 1H, $J_{6',F}$ =6.85, $J_{5',6'}$ =8.62, H-6′); 7.19 (d, 2H, $J_{2'',3''}$=$J_{5'',6''}$ =7.75 Hz, H-2′′, H-6′′); 7.10 (d, 2H, H-3′′, H-5′′); 6.74-6.67 (m, 2H, H-3′, H-5′); 3.37 (t, 2H, $J_{2,3}$=7.55 Hz, H-2); 3.00 (t, 2H, H-3); 2.29 (s, 3H, C$\underline{H}_3$-4′′); **^{13}C NMR (acetone-d^6), δ (ppm)** 205.2 (C-1); 167.1 (d, *J* = 256.3 Hz, C-4′); 164.8 (d, *J* = 17.5 Hz, C-2′); 137.9 (C-1′′); 135.3 (C-4′′); 133.6 (d, *J* = 11.5 Hz, C-6’); 129.0 (C-3′′, C-5′′); 128.3 (C-2′′, C-6′′); 116.7 (C-1′); 106.9 (d, *J* = 22.6 Hz, C-5′); 104.2 (d, *J* = 23.7 Hz, C-3′); 39.8 (C-2); 29.2 (C-3); 20.2 ($\underline{C}H_3$-4′′); HRMS calcd for $C_{16}H_{15}FNaO_2$ 281.09483 (MNa^+) found 281.09501

1-(4-fluoro-2-hydroxyphenyl)-3-(4-hydroxyphenyl)propan-1-one (30h): Yield 98.2%; white solid; m.p.=209.6-209.9 ºC; R_f (3:1 Hexane/ EtOAc)= 0.65; **^{1}H NMR (acetone-d^6), δ (ppm)** 12.73 (s, 1H, OH-2′); 8.16 (s, 1H, OH-4′′); 8.10 (dd, 1H, $J_{6',F}$ =6.64, $J_{5',6'}$ =8.74, H-6′); 7.13 (d, 2H, $J_{2'',3''}$ =$J_{5'',6''}$ =7.93 Hz, H-2′′, H-6′′); 6.77 (d, 2H, H-3′′, H-5′′); 6.76-6.68 (m, 2H, H-3', H-5'); 3.38 (t, 2H, $J_{2,3}$=7.49 Hz, H-2); 2.96 (t, 2H, H-3); **^{13}C NMR (acetone-d^6), δ (ppm)** 205.5 (C-1); 167.1 (d, *J* = 253.8 Hz, C-4′); 164.8 (d, *J* = 13.9 Hz, C-2′); 155.7 (C-4′′); 133.5 (d, *J* = 11.9 Hz, C-6′); 131.5 (C-1′′); 115.2 (C-3′′, C-5′′); 129.3 (C-2′′, C-6′′); 116.7 (C-1′); 106.8 (d, *J* = 22.3 Hz, C-5′); 104.1 (d, *J* = 23.6 Hz, C-3′); 40.1 (C-2); 26.6 (C-3); HRMS calcd for $C_{15}H_{13}FNaO_3$ 283.07409 (MNa^+) found 283.07579

1-(4-fluoro-2-hydroxyphenyl)-3-(5-methylfuran-2-yl)propan-1-one (30i): Yield 58.4%; liquid; R_f (3:1 Hexane/ EtOAc)=0.80; **^{1}H NMR (acetone-d^6), δ (ppm)** 12.63 (s, 1H, OH-2′); 8.10 (dd, 1H, $J_{6',F}$ =6.31, $J_{5',6'}$ =8.32, H-6′); 6.78-6.69 (m, 2H, H-3′, H-5′); 5.99 (s, 1H, H-2′′); 5.89 (s, 1H, H-3′′); 3.44 (t, 2H, $J_{2,3}$=7.24 Hz, H-2); 3.01 (t, 2H, H-3); 2.22 (s, 3H, C$\underline{H}_3$-4′′); **^{13}C NMR (acetone-d^6), δ (ppm)** 204.7 (C-1); 167.1 (d, *J* = 252.2 Hz, C-4′); 164.8 (d, *J* = 13.6 Hz, C-2′); 152.6 (C-4′′); 150.2 (C-1′′); 133.4 (d, *J* = 11.4 Hz, C-6′); 116.7 (C-1′); 106.9 (d, *J* = 22.6 Hz, C-5′); 106.0 (C-3′′); 105.9 (C-2′′); 104.2 (d, *J* = 23.8 Hz, C-3′); 36.4 (C-2); 22.1 (C-3); 12.5 ($\underline{C}H_3$-4′′); HRMS calcd for $C_{14}H_{14}FO_3$ 249.09215 (MH^+) found 249.09372

1-(4-fluoro-2-hydroxyphenyl)-3-(5-methyltetrahydrofuran-2-yl)propan-1-one (30j): Yield 40.8%; liquid; R_f (3:1 Hexane/ EtOAc)=0.69; **^{1}H NMR (acetone-d^6), δ (ppm)** 12.74 (s, 1H, OH-2′); 8.10 (dd, 1H, $J_{6',F}$ =6.69, $J_{5',6'}$ =8.94, H-6′); 6.78-6.68 (m, 2H, H-3′, H-5′); 3.93-3.85 (m, 2H, H-1′′, H-4′′); 3.21-3.16 (m, 2H, H-2); 2.08-1.83 (m, 4H, H-3,H-2a′′, H-3a′′); 1.63-1.56 (m, 1H, H-2b′′); 1.48-1.42 (m, 1H, H-3b′′); 1.17 (d, 3H, $J_{4'',5''}$=5.86 Hz, C$\underline{H}_3$-′4′); **^{13}C NMR (acetone-d^6), δ (ppm)** 206.2 (C-1); 167.0 (d, 253.6 Hz, C-4′); 164.8 (d, *J* = 14.7 Hz, C-2′); 133.4 (d, *J* = 11.6 Hz, C-6′); 116.7 (C-1′); 106.8 (d, *J* = 22.2 Hz, C-5′); 104.1 (d, *J* = 23.5 Hz, C-3′); 77.9 (C-1′′); 75.0 (C-4′′); 34.8 (C-2); 32.7 (C-3′′);

30.9 (C-2′′); 30.5 (C-3); 26.6 (CH_3-4′′); HRMS calcd for $C_{14}H_{17}FNaO_3$ 275.10539 (MNa^+) found 275.10557

7.5 *C*-glucosylation

7.5.1 General Procedure for the synthesis of protected C-glucosyl dihydrochalcones

A solution of dihydrochalcone (**18a-18i**, 2 equiv.) in ACN (2 mL) was added to a solution of 2,3,4,6-tetra-*O*-benzyl-D-glucopyranose (3, 1.23 mmol) in DCM (10 mL) at room temperature. Drierite (200mg) was added and the reaction vessel was maintained under N_2. The mixture was cooled to -30 ºC and TMSOTf (0.5 equiv.) was added dropwise. After 20-30 minutes the reaction was allowed to reach room temperature. The total consumption of the glycosyl donor was confirmed by TLC (1:1 Hexane/Acetone) and after 2h-5h (depending on substrate) the reaction was quenched with NaCl sat. solution. Drierite was filtered off under celite and the residue was extracted with DCM, washed with brine and dried over anhydrous $MgSO_4$. The benzylated *C*-glucosyldihydrochalcones were purified as oil by column chromatography (7:1 Hexane/Acetone).

3-(4-fluorophenyl)-1-[3-(2,3,4,6-tetra-*O*-benzyl-β-D-glucopyranosyl)-2,4,6-trihydroxyphenyl]propan-1-one (37a): Yield 42.9%; R_f (3:1 Hexane/ EtOAc)=0.58; **^{1}H NMR ($CDCl_3$) δ (ppm)** 14.30 (s, 2H, OH-2′, OH-6′); 9.72 (s, 1H, OH-4′); 7.37-6.95 (m, 24H, ArH, H-2′′, H-3′′, H-5′′, H-6′′); 6.01 (s, 1H, H-5′); 4.98 (s, 2H, -OCH_2Ph); 4.88-4.86 (m, 3H, -OCH_2Ph, H-1′′′); 4.73, 4.29 (each d, 2H, *J* =10.65 Hz, -OCH_2Ph); 4.57, 4.48 (each d, 2H, *J* =9.18 Hz, -OCH_2Ph); 4.57, 4.48 (each d, 2H, *J* =9.18 Hz, -OCH_2Ph); 3.90-3.60 (m, 6H, H-2′′′, H-3′′′, H-4′′′, H-5′′′, H-6a′′′, H-6b′′′); 3.28-4.24 (m, 2H, H-2); 2.95 (t, 2H, $J_{2,3}$=7.21 Hz, H-3); **^{13}C NMR ($CDCl_3$) δ (ppm)** 135.9 (C-1′′); 138.2, 137.7, 137.4, 137.3 (C_q-Ph); 129.9 (C-2′′, C-6′′); 128.7, 128.6, 128.5, 128.3, 128.0, 127.8, 127.6 (CH-Ph); 115.2 (C-3′′, C-5′′); 105.6 (C-3′); 103.4 (C-1′); 99.9 (C-5′); 86.2 (C-2′′′); 78.7 (C-3′′′); 77.2 (C-4′′′); 76.3 (C-5′′′); 75.7 (-OCH_2Ph); 75.3 (C-1′′′); 75.0, 74.6, 73.4 (-OCH_2Ph); 67.5 (C-6′′′); 42.9 (C-2); 29.6 (C-3); HRMS calcd for $C_{49}H_{47}FNaO_9$ 821.30963 (MNa^+) found 821.30943

3-phenyl-1-[3-(2,3,4,6-tetra-*O*-benzyl-β-D-glucopyranosyl)-2,4,6-trihydroxy-phenyl]-propan-1-one (37c): Yield 41.8%; R_f (3:1 Hexane/Acetone)=0.19; **^{1}H NMR ($CDCl_3$) δ (ppm)** 7.35-6.98 (m, 25H, ArH, H-2″, H-3″, H-3″, H-4″, H-5″, H-6″); 5.96 (s, 1H, H-5′); 4.95 (s, 2H, -OCH_2Ph); 4.85 (d, 1H, $J_{1‴,2‴}$ =8.67 Hz, H-1‴); 4.83, 4.51 (each d, 2H, *J*=11.03 Hz, -OCH_2Ph); 4.69, 4.27 (each d, 2H, *J*=9.97 Hz, -OCH_2Ph); 4.55, 4.46 (each d, 2H, *J*=11.27 Hz, -OCH_2Ph); 3.86-3.58 (m, 6H, H-2‴, H-3‴, H-4‴, H-5‴, H-6a‴, H-6b‴); 3.30-3.26 (m, 2H, H-2); 2.97 (t, 2H, $J_{2,3}$=8.94 Hz, H-3); **^{13}C NMR ($CDCl_3$) δ (ppm)** 205.0 (C-1);141.8 (C-1″); 138.2, 137.7, 137.3, 136.2 (C_q-Ph); 128.7, 128.5, 128.4, 128.3, 128.0, 127.9, 127.8, 127.6 (CH-Ph, C-2″, C-3″, C-5″, C-6″); 125.9 (C-4″); 106.0 (C-3′); 102.8 (C-1′); 99.9 (C-5′); 86.2 (C-2‴); 78.7 (C-3‴); 77.2 (C-4‴); 76.3 (C-5‴); 75.7 (-OCH_2Ph); 75.3 (C-1‴); 75.2, 75.0, 73.4 (-OCH_2Ph); 67.5 (C-6‴); 45.9 (C-2); 30.5 (C-3); HRMS calcd for $C_{49}H_{48}NaO_9$ 803.31905 (MNa^+) found 803.32129

3-(4-methylphenyl)-1-[3-(2,3,4,6-tetra-O-benzyl-β-D-glucopyranosyl)-2,4,6-tri-hydroxy-phenyl]propan-1-one (37d): Yield 52.1%; R_f (3:1 Hexane/ EtOAc)=0.60; **^{1}H NMR ($CDCl_3$) δ (ppm)** 14.03 (s, 2H, OH-2′, OH-6′); 9.87 (s, 1H, OH-4′); 7.34-6.97 (m, 24H, ArH, H-2″, H-3″, H-5″, H-6″); 5.89 (s, 1H, H-5′); 4.95 (dd, 2H, *J*=9.99 Hz, *J*=17.18 Hz, -OCH_2Ph); 4.87 (d, 1H, $J_{1‴,2‴}$ =9.98 Hz, H-1‴); 4.83 (d, 1H, *J*=8.53 Hz, part A system AB of -OCH_2Ph); 4.62, 4.21 (each d, 2H, *J*=10.55 Hz, -OCH_2Ph); 4.57-4.47 (m, 3H, part B system AB of -OCH_2Ph, -OCH_2Ph); 3.80-3.59 (m, 6H, H-2‴, H-3‴, H-4‴, H-5‴, H-6a‴, H-6b‴); 3.27 (t, 2H, $J_{2,3}$=7.36 Hz, H-2); 2.97 (t, 2H, H-3); 2.92 (s, 3H, -OCH_3-4″); **^{13}C NMR ($CDCl_3$) δ (ppm)** 205.2 (C-1); 138.8 (C-1″); 138.3, 137.8, 137.1, 136.4 (C_q-Ph); 135.4 (C-4″); 129.1, 128.7, 128.6, 128.5, 128.4, 128.2, 128.1, 128.0, 127.8, 127.7 (CH-Ph, C-2″, C-3″, C-5″, C-6″); 105.7 (C-3′); 102.5 (C-1′); 97.5 (C-5′); 86.2 (C-2‴); 81.7 (C-3‴); 78.3 (C-4‴); 77.3 (C-5‴); 76.1 (C-1‴); 75.7, 75.3, 74.9, 73.5 (-OCH_2Ph); 67.9 (C-6‴); 46.1 (C-2); 30.1 (C-3); HRMS calcd for $C_{50}H_{50}NaO_9$ 817.33478 (MNa^+) found 817.33552

3-(4-methyloxyphenyl)-1-[3-(2,3,4,6-tetra-*O*-benzyl-β-D-glucopyranosyl)-2,4,6-tri-hydroxyphenyl]propan-1-one (37e): Yield 39.3%; R_f (1:1 Hexane/Acetone)=0.19; **^{1}H**

NMR ($CDCl_3$) δ (ppm) 14.43 (s, 2H, OH-2′, OH-6′); 7.33-7.12 (m, 20H, ArH); 6.98 (d, 2H, $J_{2'',3''}$ =$J_{5'',6''}$ =7.83 Hz, H-2′′, H-6′′); 6.82 (d, 2H, H-3′′, H-5′′); 5.89 (s, 1H, H-5′); 4.96-4.81 (m, 2H, -OCH_2Ph, H-1′′′); 4.59, 4.20 (each d, 2H, *J* =8.89 Hz, -OCH_2Ph); 4.55-4.46 (m, 3H, -OCH_2Ph); 3.80-3.59 (m, 6H, H-2′′′, H-3′′′, H-4′′′, H-5′′′, H-6a′′′, H-6b′′′); 3.27 (t, 2H, $J_{2,3}$ =7.32 Hz, H-2); 2.93 (t, 2H, H-3); **^{13}C NMR ($CDCl_3$) δ (ppm)** 205.2 (C-1); 138.4, 137.7, 137.1, 136.6 (C_q-Ph); 133.9 (C-1′′); 129.5 (C-2′′, C-6′′); 128.7, 128.6, 128.5, 128.1, 128.0, 127.7 (CH-Ph); 113.8 (C-3′′, C-5′′); 105.6 (C-3′); 102.5 (C-1′); 97.3 (C-5′); 86.2 (C-2′′′); 81.1 (C-3′′′); 78.8 (C-4′′′); 77.4 (C-5′′′); 76.0 (C-1′′′); 75.8, 75.3, 74.8, 73.5 (-OCH$_2$Ph); 68.0 (C-6′′′); 55.3 (-OCH$_3$-4′′); 46.2 (C-2); 31.9 (C-3); HRMS calcd for $C_{50}H_{50}NaO_{10}$ 833.32962 (MNa^+) found 833.33521

3-(4-ethyloxyphenyl)-1-[3-(2,3,4,6-tetra-*O*-benzyl-β-D-glucopyranosyl)-2,4,6-trihydroxy-phenyl]propan-1-one (37f): Yield 46.7%; R_f (1:1 Hexane/Acetone)=0.16; **^{1}H NMR ($CDCl_3$) δ (ppm)** 7.32-7.11 (m, 20H, ArH); 6.98 (d, 2H, $J_{2'',3''}$ =$J_{5'',6''}$ =7.58 Hz, H-2′′, H-6′′); 6.81 (d, 2H, H-3′′, H-5′′); 5.92 (s, 1H, H-5′); 4.97-4.82 (m, 4H, -OCH_2Ph, part A-OCH_2Ph, H-1′′′); 4.63, 4.22 (each d, 2H, *J* =10.33 Hz, -OCH_2Ph); 4.56-4.55 (m, 3H, -OCH_2Ph, part B-OCH_2Ph); 4.00 (q, 2H, *J*=7.37 Hz, *J*=13.13 Hz, -OCH_2CH$_3$-4′′); 3.81-3.59 (m, 6H, H-2′′′, H-3′′′, H-4′′′, H-5′′′, H-6a′′′, H-6b′′′); 3.28-3.24 (m, 2H, H-2); 2.91 (t, 2H, $J_{2,3}$ =7.63 Hz, H-3); 1.40 (t, 3H, -OCH$_2$CH$_3$-4′′); **^{13}C NMR ($CDCl_3$) δ (ppm)** 205.2 (C-1); 157.1 (C-4′′); 138.3, 137.7, 137.2, 136.4 (C_q-Ph); 133.8 (C-1′′); 129.4 (C-2′′, C-6′′); 128.7, 128.5, 128.4, 128.1, 128.0, 127.8, 127.6 (CH-Ph); 114.4 (C-3′′, C-5′′); 105.7 (C-3′); 102.6 (C-1′); 97.5 (C-5′); 86.2 (C-2′′′); 81.9 (C-3′′′); 78.7 (C-4′′′); 77.2 (C-5′′′); 76.1 (C-1′′′); 67.8 (C-6′′′); 75.7, 75.3, 74.9, 73.4 (-OCH$_2$Ph); 63.4 (-OCH$_2$CH$_3$-4′′); 46.2 (C-2); 29.7 (C-3); 14.9 (-OCH$_2$CH$_3$-4′′); HRMS calcd for $C_{51}H_{52}NaO_{10}$ 847.34527 (MNa^+) found 847.34662

3-(4-propyloxyphenyl)-1-[3-(2,3,4,6-tetra-*O*-benzyl-β-D-glucopyranosyl)-2,4,6-tri-hydroxyphenyl]propan-1-one (37g): Yield 45.9%; R_f (1:1 Hexane/Acetone)=0.18; **^{1}H NMR ($CDCl_3$) δ (ppm)** 7.34-7.12 (m, 20H, ArH); 6.98 (d, 2H, $J_{2'',3''}$ =$J_{5'',6''}$ =6.80 Hz, H-2′′, H-6′′); 6.82 (d, 2H, H-3′′, H-5′′); 5.93 (s, 1H, H-5′); 4.97-4.91 (m, 1H, -OCH_2Ph); 4.88 (d, 1H, $J_{1''',2'''}$ =9.57 Hz, H-1′′′); 4.83 (d, 1H, *J*=10.52 Hz, part A -OCH_2Ph); 4.65, 4.24 (each d, 2H, *J* =10.33 Hz, -OCH_2Ph); 4.56-4.45 (m, 3H, -OCH_2Ph, part B-OCH_2Ph); 3.89 (t, 2H,

J=6.88 Hz, -OC<u>H</u>$_2$CH$_2$CH$_3$-4′′); 3.82-3.60 (m, 6H, H-2′′′, H-3′′′, H-4′′′, H-5′′′, H-6a′′′, H-6b′′′); 3.30-3.18 (m, 2H, H-2); 2.91 (t, 2H, $J_{2,3}$ =7.12 Hz, H-3); 1.79 (q, 2H, *J*=14.06 Hz, *J*=20.43 Hz, -OCH$_2$C<u>H</u>$_2$CH$_3$-4′′); 1.03 (t, 3H, -OCH$_2$CH$_2$C<u>H</u>$_3$-4′′); **^{13}C NMR ($CDCl_3$) δ (ppm)** 205.2 (C-1); 157.3 (C-4′′); 138.3, 137.7, 137.3, 136.7 (C_q-Ph); 133.7 (C-1′′); 129.4 (C-2′′, C-6′′); 128.7, 128.5, 128.4, 128.2, 128.1, 128.0, 127.9, 127.8, 127.6 (<u>C</u>H-Ph); 114.4 (C-3′′, C-5′′); 105.8 (C-3′); 102.7 (C-1′); 97.7 (C-5′); 86.2 (C-2′′′); 81.7 (C-3′′′); 78.7 (C-4′′′); 77.2 (C-5′′′); 76.2 (C-1′′′); 69.5 (C-6′′′); 75.7, 75.3, 74.9, 73.4 (-O<u>C</u>H$_2$Ph); 67.7 (-O<u>C</u>H$_2$CH$_2$CH$_3$-4′′); 46.2 (C-2); 29.7 (C-3); 22.7 (-OCH$_2$<u>C</u>H$_2$CH$_3$-4′′); 10.6 (-OCH$_2$CH$_2$<u>C</u>H$_3$-4′′); HRMS calcd for $C_{52}H_{54}NaO_{10}$ 861.36092 (MNa^+) found 861.36124

7.5.2 Synthesis of compound 37h

7.5.2.1 C-glucosylation

<u>Method A:</u> A solution of 2′,4′,6′-trihydroxyacetophenone (**13**, 2 equiv.) in ACN (5 mL) was added to a solution of 2,3,4,6-tetra-*O*-benzyl-D-glucopyranose (**3**, 1.49 mmol) in DCM/CAN (1:1) (13.5 mL) at room temperature. Drierite (300mg) was added and the reaction vessel was maintained under N_2. The mixture was cooled to -30 ºC and TMSOTf (0.5 equiv.) was added dropwise. After 20-30 minutes the reaction was allowed to reach room temperature. The total consumption of the glycosyl donor was confirmed by TLC (1:1 Hexane/Acetone) and after 5h the reaction was quenched with NaCl sat. solution. Drierite was filtered off under celite and the residue was extracted with DCM, washed with brine and dried over anhydrous $MgSO_4$. Compound **39** was purified by column chromatography (7:1 Hexane/Acetone) and obtained as colourless oil in 56.4% yield. R_f = 0.23 (3:1 Hexane/ EtOAc); **^{1}H NMR ($CDCl_3$) δ (ppm)** 7.34-6.98 (m, 20H; Ar<u>H</u>), 5.89 (s, 1H; H-3′), 4.88 (d, 1H, $J_{1'',2''}$ =9.71 Hz, H-1′′); 4.97-4.48 (m, 8H; -C<u>H</u>$_2$Ph), 3.81-3.60 (m, 6H; H-2′′, H-3′′, H-4′′, H-5′′, H-6a′′, H-6b′′), 2.56 (s, 3H; H-2); **^{13}C NMR ($CDCl_3$) δ (ppm)** 203.9 (C-1); 164.0 (C-4′); 161.9 (C-2′); 161.4 (C-6′); 138.3, 137.7, 137.0, 136.6 (C_q-Ph); 128.6, 128.5, 128.3, 128.1, 127.7, 127.6 (<u>C</u>H, Ph); 105.7 (C-3′); 102.4(C-1′); 97.1 (C-5′); 86.2 (C-2′′); 81.7 (C-3′′); 78.7 (C-4′′); 77.4 (C-5′′); 75.7 (C-1′′); 75.9, 75.2, 74.8, 74.5 (-O<u>C</u>H$_2$Ph); 68.1 (C-6′′); 32.9 (C-2); HRMS calcd for $C_{42}H_{42}NaO_{19}$ 713.27210 (MNa^+) found 713.27335.

Compound **39** (1.67 mmol) was dissolved in DMF (23 mL) and K_2CO_3 (2.2 equiv.) was added at 0 ºC. After 10 minutes BnBr (2.2. equiv.) was added to the reaction and 10 minutes later the ice bath was removed and the reaction was allowed to reach room temperature. The reaction proceeded for 1 hour at room temperature and then was neutralized with 2M HCl. The residue was extracted with DCM, washed with brine and dried over anhydrous $MgSO_4$. Compound **31** was purified by column chromatography (7:1 Hexane/ EtOAc) and obtained as oil in 73.8% yield. R_f = 0.30 (5:1 Hexane/ EtOAc).

Method B: Compounds **4** (2.20 mmol) and **14** (2.0 equiv.) were dissolved in DCE (10 mL) in the presence of drierite (ca. 100 mg). The solution was stirred at -30 ºC and $Sc(OTf)_3$ (0.25 equiv.) was added. The stirring continued for 30 min at -30 ºC and then at room temperature for 5 h. The reaction was quenched with water and filtered through celite, extracted with DCM and concentrated. Compound **31** was purified by CC (10:1 P. Ether/EtOAc) and obtained in 49 % yield. R_f =0.33 (4:1 Et.P./EtOAc); **^{1}H NMR ($CDCl_3$) δ (ppm)** 14.11 (s, 1H; OH-2′), 7.43-6.89 (m, 30H; ArH), 6.36 (s, 1H, H-3′), 4.96-4.45 (m, 13H; -OCH_2Ph, H-1′′), 3.74-3.37 (m, 6H; H-2′′, H-3′′, H-4′′, H-5′′, H-6a′′, H-6b′′); 2.52 (s, 3H; H-2); **^{13}C NMR ($CDCl_3$) δ (ppm)** 203.1 (C-1); 164.7 (C-2′); 163.5 (C-4′); 160.7 (C-6′); 138.7, 138.6, 138.2, 138.1, 137.9, 137.4, 137.5, 136.4, 135.8; (C_q-Ph); 128.5, 128.5, 128.4, 128.3, 128.2, 128.1, 128.0, 128.0, 127.9, 127.8, 127.7, 127.6, 127.6, 127.6, 127.3, 126.2 (CH. Ph); 111.5 (C-5); 105.9 (C-1′); 90.0 (C-5′); 82.1 (C-3′′); 78.8 (C-5′′); 77.6 (C-4′′); 77.4, 77.1, 76.7, 75.7, 75.7, 75.7, 75.3, 75.3, 75.0, 73.5, 73.4, 73.2 (-OCH_2Ph); 72.8 (C-2′′); 70.0 (C-1′′); 68.4 (C-6′′); 33.5 (C-2); HRMS calcd for $C_{56}H_{54}NaO_9$ 893.36600 (MNa^+) found 893.36942. **NOTE:** All signals are duplicated due to the presence of rotamers

7.5.2.2 Synthesis of the C-glucosyl chalcone

Compound **31** (1.14 mmol) and 4-benzyloxybenzaldehyde (**16h**, 2.0 equiv.) were dissolved in 1,4-Dioxane (11.3 mL) and 50% (w/v) aq. NaOH. The mixture was kept under reflux for 24 h and then neutralized with 2M HCl. The orange residue was extracted with DCM, washed with brine and dried over $MgSO_4$. The pure compound **41** was obtained as orange oil in 62.5% yield after purification by column chromatography (7:1 Hexane/ EtOAc). R_f=0.24 (3:1 Hexane/ EtOAc); **^{1}H NMR ($CDCl_3$) δ (ppm)** 15.02 (s, 1H,

OH-2′); 7.75-6.75 (m, 41H, ArH, H-2′′, H-3′′, H-4′′, H-6′′, H-2, H-3); 6.06 (s, 1H, H-5′); 5.12-4.24 (m, 16H, -OCH$_2$Ph, H-1′′′, H-2′′′, H-3′′′); 3.84-3.60 (m, 5H, H-4′′′, H-5′′′, H-6a′′′, H-6b′′′); **^{13}C NMR (CDCl$_3$) δ (ppm)** 192.9 (C-1); 166.9, 166.1 (C-2′)*; 164.2, 163.4 (C-4′); 162.1, 161.9 (C-6′); 142.9, 142.6 (C-2); 139.1, 138.9, 138.6, 138.5, 138.4, 138.3, 136.6, 136.4, 136.3, 135.5, 135.3 (C$_q$-Ph, C-1′′); 130.2, 130.1 (C-2′′, C-6′′); 115.0, 114.9 (C-3′′, C-5′′); 129.0-126.9 (CH-Ph); 125.6, 125.4 (C-2); 107.5, 107.1 (C-3′); 106.7, 106.1 (C-1′); 89.2, 89.0 (C-5′); 87.9 (C-5′′′); 79.4 (C-3′′′); 78.4 (C-4′′′); 75.6, 75.5, 75.2, 74.4, 74.3, 73.5, 73.3, 72.9, 72.5, 71.4, 71.3, 70.7, 70.2, 70.1 (-OCH$_2$Ph, C-1′′′, C-2′′′); 69.4 (C-6′′′); HRMS calcd for $C_{70}H_{64}NaO_{10}$ 1087.43917 ($MHNa^+$) found 1088.44461. **NOTE:** All signals are duplicated due to the presence of rotamers.

7.5.3 General procedure for the synthesis of C-glucosyl dihydrochalcones

Compounds **37a-37h** and **41** (0.5 mmol) were dissolved in EtOAc (1 mL) methanol (2 mL). The catalyst Pd/C or $Pd(OH)_2$ (5% mol) was added was the reaction vessel was kept under N_2. Et_3SiH (10 equiv.) was added drop wise while effervescence was observed (meaning that hydrogen was being formed *in situ*). After all the Et_3SiH was added the reaction was kept at room temperature for another 10 minutes until change in the colour (orange/yellow to colourless). TLC was used to confirm the completion of the reaction. Catalyst was filtered off through celite, 2/3 of volume of solvent was removed under vacuum and extraction with ACN/Hex was used to remove most of the Et_3SiH from the mixture. The final product was purified by column chromatography (EtOAc only).

3-(4-fluorophenyl)-1-[3-β-D-glucopyranosyl)-2,4,6-trihydroxyphenyl]propan-1-one (33a): Yield 84.0%; m.p= 80.2-80.7 ºC; R_f (7:1 DCM/MeOH)=0.36; **^{1}H NMR (acetone-d^6) δ (ppm)** 7.33 (dd, 2H, $J_{2'',3''} = J_{5'',6''}$ =8.37 Hz, $J_{2'',F} = J_{6'',F'}$=5.16 HZ, H-2′′, H-6′′); 7.05 (t, 2H, $J_{5'',F} = J_{3'',F}$ =8.73 Hz, H-3′′, H-5′′); 5.95 (s, 1H, H-5′); 4.94 (d, 1H, $J_{1''',2'''}$ =9.59 Hz, H-1′′′); 3.91-3.83 (m, 2H, H-6a′′′, H-6b′′′); 3.67 (t, 2H, $J_{2''',3'''}$=9.02 Hz, H-2′′′, H-3′′′); 3.58 (t, 1H, $J_{3''',4'''}$=9.17 Hz, H-4′′′); 3.50 (ddd, 1H, $J_{4''',5'''}$=9.55 Hz, $J_{5''',6a'''}$=6.05 Hz, $J_{5''',6b'''}$=2.98 Hz, H-5′′′); 3.39 (t, 2H, $J_{2,3}$=7.27 Hz, H-2); 2.98 (t, 2H, H-3); **^{13}C NMR (acetone-d^6) δ (ppm)** 204.5 (C-1′); 163.0 (C-4′); 162.4 (C-2′, C-6′); 160.0 (C-4′′); 137.8 (d, J = 39.6 Hz, C-1′′); 130.2 (d, J = 7.2 Hz, C-2′′, C-6′′); 114.8 (d, J = 21.1 Hz, C-3′′, C-

5″); 104.5 (C-3′); 103.4 (C-1′); 95.6 (C-5′); 81.1 (C-5‴); 78.3 (C-4‴); 75.4 (C-1‴); 73.3 (C-3‴); 69.6 (C-2‴); 60.9 (C-6‴); 45.9 (C-2); 29.7 (C-3); HRMS calcd for $C_{21}H_{23}FNaO_9$ 461.12183 (MNa^+) found 461.12238

3-phenyl-1-[3-β-D-glucopyranosyl)-2,4,6-trihydroxyphenyl]propan-1-one (33c): Yield 82.0%; m.p= 80.0-80.1 ºC; R_f (7:1 DCM/MeOH)=0.40; **^{1}H NMR (acetone-d^6) δ (ppm)** 12.20 (s, 1H, OH-6′); 11.50 (s, 1H, OH-2′); 9.10 (s, 1H, OH-4′); 7.30-7.26 (m, 4H, H-2″, H-3″, H-5″, H-6″); 7.21-7.17 (m, 1H, H-4″); 5.95 (s, 1H, H-5′); 4.94 (d, 1H, $J_{1‴,2‴}$ =9.72 Hz, H-1‴); 3.91-3.81 (m, 2H, H-6a‴, H-6b‴); 3.70-3.62 (m, 2H, H-2‴, H-3‴); 3.58-3.46 (m, 2H, H-4‴, H-5‴); 3.40 (t, 2H, $J_{2,3}$=7.71 Hz, H-2); 2.99 (t, 2H, H-3); **^{13}C NMR (acetone-d^6) δ (ppm)** 205.5 (C-1); 163.0 (C-2′, C-4′, C-6′); 141.9 (C-1″); 128.5 (C-2″, C-6″); 128.3 (C-3″, C-5″); 125.8 (C-4″); 104.5 (C-3′); 103.8 (C-1′); 95.6 (C-5′); 81.1 (C-5‴); 78.7 (C-4‴); 75.4 (C-1‴); 73.3 (C-3‴); 69.9 (C-2‴); 60.7 (C-6‴); 45.8 (C-2); 30.4 (C-3); HRMS calcd for $C_{21}H_{24}NaO_9$ 443.13125 (MNa^+) found 443.13169

3-(4-methylphenyl)-1-[3-β-D-glucopyranosyl)-2,4,6-trihydroxyphenyl]propan-1-one (33d): Yield 82.0%; m.p= 117.0-117.5 ºC; R_f (7:1 DCM/MeOH)=0.38; **^{1}H NMR (acetone-d^6) δ (ppm)** 7.19 (d, 2H, $J_{2″,3″}$= $J_{5″,6″}$=7.16 Hz, H-2″, H-6″); 7.11 (d, 2H, H-3″, H-5″); 5.96 (s, 1H, H-5′); 4.95 (d, 1H, $J_{1‴,2‴}$ =9.13 Hz, H-1‴); 3.91-3.84 (m, 6H, H-6a‴, H-6b‴); 3.67 (t, 2H, $J_{2‴,3‴}$= 9.08 Hz, H-2‴, H-3‴); 3.58 (t, 1H, $J_{3‴,4″}$= 9.00 Hz, H-4‴); 3.50 (ddd, 1H, $J_{4‴,5″}$=9.46 Hz, $J_{5‴,6a″}$= 6.57 Hz, $J_{5‴,6a″}$=2.94 Hz H-5‴); 3.38 (t, 2H, $J_{2,3}$=6.95 Hz, H-2); 2.95 (t, 2H, H-3); 2.30 (s, 3H, -C$\underline{H}_3$-4″); **^{13}C NMR (acetone-d^6) δ (ppm)** 204.8 (C-1); 163.2 (C-2′, C-6′); 163.0 (C-4′); 138.9 (C-1″); 134.9 (C-4″); 128.9 (C-2″, C-6″); 128.2 (C-3″, C-5″); 104.5 (C-3′); 103.4 (C-1′); 95.6 (C-5′); 81.1 (C-5‴); 78.4 (C-4‴); 75.4 (C-1‴); 73.4 (C-3‴); 69.6 (C-2‴); 60.7 (C-6‴); 45.9 (C-2); 30.0 (C-3); 20.5 (-$\underline{C}$H$_3$-4″); HRMS calcd for $C_{22}H_{26}NaO_9$ 457.14690 (MNa^+) found 457.14758

3-(4-methoxyphenyl)-1-[3-β-D-glucopyranosyl)-2,4,6-trihydroxyphenyl]-propan-1-one (12e): Yield 84.0%; m.p= 90.4-90.7 ºC; R_f (7:1 DCM/MeOH)=0.31; **^{1}H NMR (acetone-d^6) δ (ppm)** 12.29 (s, 2H, OH-2′, OH-6′); 11.57 (s, 1H, OH-4′); 9.17 (s, 1H, OH-4″); 7.21 (d, 2H, $J_{2″,3″}$= $J_{5″,6″}$=7.68 Hz, H-2″, H-6″); 6.85 (d, 2H, H-3″, H-5″); 5.94

(s, 1H, H-5′); 4.94 (d, 1H, $J_{1''',2'''}$ =9.71 Hz, H-1′′′); 3.91-3.87 (m, 6H, H-6a′′′, H-6b′′′); 3.77 (s, 3H, -OC<u>H</u>$_3$-4′′); 3.66 (t, 2H, $J_{2''',3'''}$= 8.99 Hz, H-2′′′, H-3′′′); 3.56 (t, 1H, $J_{3''',4'''}$=8.72 Hz, H-4′′′); 3.50 (ddd, 1H, $J_{4''',5'''}$=9.85 Hz, $J_{5''',6a'''}$=6.74 Hz, $J_{5''',6b'''}$=3.28 Hz, H-5′′′); 3.36 (t, 2H, $J_{2,3}$=7.60 Hz, H-2); 2.92 (t, 2H, H-3); **^{13}C NMR (acetone-d^6) δ (ppm)** 205.3 (C-1); 162.9 (C-2′, C-4′, C-6′); 158.0 (C-4′′); 133.8 (C-1′′); 129.4 (C-2′′, C-6′′); 113.7 (C-3′′, C-5′′); 104.5 (C-3′); 104.5 (C-1′); 95.6 (C-5′); 81.1 (C-5′′′); 78.4 (C-4′′′); 75.4 (C-1′′′); 73.4 (C-3′′′); 69.6 (C-2′′′); 60.6 (C-6′′′); 54.5 (-O<u>C</u>H$_3$-4′′); 46.2 (C-2); 29.5 (C-3); HRMS calcd for $C_{22}H_{26}NaO_{10}$ 473.14182 (MNa^+) found 473.14245

3-(4-ethoxyphenyl)-1-[3-β-D-glucopyranosyl)-2,4,6-trihydroxyphenyl]propan-1-one (33f): Yield 89.0%; m.p= 91.4-92.0 ºC; R_f (EtOAc)=0.10; **^{1}H NMR (acetone-d^6) δ (ppm)** 12.36 (s, 1H, OH-6′); 11.45 (s, 1H, OH-2′); 9.11 (s, 1H, OH-4′); 7.17 (d, 2H, $J_{2'',3''}$= $J_{5'',6''}$ =8.21 Hz, H-2′′, H-6′′); 6.82 (d, 2H, H-3′′, H-5′′); 5.94 (s, 1H, H-5′); 4.93 (d, 1H, $J_{1''',2'''}$ =9.67 Hz, H-1′′′); 3.99 (q, 2H, J=7.22 Hz, J=13.32 Hz, -OC<u>H</u>$_2$CH$_3$-4′′); 3.89-3.86 (m, 6H, H-6a′′′, H-6b′′′); 3.72-3.47 (m, 4H, H-2′′′, H-3′′′, H-4′′′, H-5′′′); 3.33 (t, 2H, $J_{2,3}$=9.44 Hz, H-2); 2.89 (t, 2H, H-3); 1.34 (t, 3H, -OCH$_2$C<u>H</u>$_3$-4′′); **^{13}C NMR (acetone-d^6) δ (ppm)** 204.9 (C-1); 163.1 (C-2′, C-6′); 163.0 (C-4′′); 157.3 (C-4′′); 133.7 (C-1′′); 129.4 (C-2′′, C-6′′); 114.3 (C-3′′, C-5′′); 104.5 (C-3′); 103.1 (C-1′); 95.6 (C-5′); 81.1 (C-5′′′); 78.4 (C-4′′′); 75.3 (C-1′′′); 73.3 (C-3′′′); 69.7 (C-2′′′); 62.9 (-O<u>C</u>H$_2$CH$_3$-4′′); 60.8 (C-6′′′); 46.1 (C-2); 29.6 (C-3); 14.3 (-OCH$_2$<u>C</u>H$_3$-4′′); HRMS calcd for $C_{23}H_{28}NaO_{10}$ 487.15747 (MNa^+) found 487.15789

3-(4-propyloxyphenyl)-1-[3-β-D-glucopyranosyl)-2,4,6-trihydroxyphenyl]-propan-1-one (33g): Yield 90.6%; m.p= 80.0-80.2 ºC; R_f (EtOAc)=0.10; **^{1}H NMR (acetone-d^6) *δ* (ppm)** 7.11 (d, 2H, $J_{2'',3''}$= $J_{5'',6''}$ =7.55 Hz, H-2′′, H-6′′); 6.85 (d, 2H, H-3′′, H-5′′); 5.95 (s, 1H, H-5′); 4.94 (d, 1H, $J_{1''',2'''}$ =8.78 Hz, H-1′′′); 3.94-3.90 (m, 2H, -OC<u>H</u>$_2$CH$_2$CH$_3$-4′′); 3.89-3.83 (m, 6H, H-6a′′′, H-6b′′′); 3.66 (t, 2H, $J_{2''',3'''}$ =$J_{3''',4'''}$=9.34 Hz, H-2′′′, H-3′′′); 3.58-3.49 (m, 2H, H-4′′′, H-5′′′); 3.36 (t, 2H, $J_{2,3}$=7.56 Hz, H-2); 2.92 (t, 2H, H-3); 1.81-1.73 (m, 2H, -OCH$_2$C<u>H</u>$_2$CH$_3$-4′′); 1.02 (t, 3H, -OCH$_2$CH$_2$C<u>H</u>$_3$-4′′); **^{13}C NMR (acetone-d^6) δ (ppm)** 204.8 (C-1); 162.9 (C-2′, C-4′, C-6′); 157.5 (C-4′′); 133.7 (C-1′′);

129.3 (C-2′′, C-6′′); 114.3 (C-3′′, C-5′′); 104.5 (C-3′); 103.4 (C-1′); 95.6 (C-5′); 81.1 (C-5′′′); 78.5 (C-4′′′); 75.4 (C-1′′′); 73.3 (C-3′′′); 69.6 (C-2′′′); 69.1 (-$\underline{C}H_2CH_2CH_3$-4′′); 60.6 (C-6′′′); 40.2 (C-2); 29.7 (C-3); 22.4 (-$CH_2\underline{C}H_2CH_3$-4′′); 9.9 (-$CH_2CH_2\underline{C}H_3$-4′′); HRMS calcd for $C_{24}H_{30}NaO_{10}$ 501.17312 (MNa^+) found 501.17373

3-(4-hydroxyphenyl)-1-[3-β-D-glucopyranosyl)-2,4,6-trihydroxyphenyl]-propan-1-one (33h): Yield 78.8%; m.p= 133.3-133.4 ºC; R_f (7:1 DCM/MeOH)=0.26; **^{1}H NMR (acetone-d^6) δ (ppm)** 7.11 (d, 2H, $J_{2'',3''} = J_{5'',6''}$ =8.04 Hz, H-2′′, H-6′′); 6.75 (d, 2H, H-3′′, H-5′′); 5.96 (s, 1H, H-5′); 4.94 (d, 1H, $J_{1''',2'''}$ =9.58 Hz, H-1′′′); 3.90-3.83 (m, 2H, H-6a′′′, H-6b′′′); 3.30-3.64 (m, 2H, H-2′′′, H-3′′′); 3.56 (t, 1H, $J_{3''',4'''}$= 8.86 Hz, H-4′′′); 3.50 (ddd, 1H, $J_{4''',5'''}$= 9.63Hz, $J_{5''',6a'''}$= 6.59 Hz, $J_{5''',6b'''}$= 3.12 Hz, H-5′′′); 3.34 (t, 2H, $J_{2,3}$=7.27 Hz, H-2); 2.88 (t, 2H, H-3); **^{13}C NMR (acetone-d^6) δ (ppm)** 204.9 (C-1′); 163.1 (C-2′, C-4′); 162.9 (C-6′); 155.5 (C-4′′); 132.5 (C-1′′); 129.4 (C-2′′, C-6′′); 115.1 (C-3′′, C-5′′); 104.5 (C-3′); 103.4 (C-1′); 81.1 (C-5′′′); 78.5 (C-4′′′); 75.4 (C-1′′′); 73.3 (C-3′′′); 69.6 (C-2′′′); 60.6 (C-6′′′); 46.3 (C-2); 29.7 (C-3); HRMS calcd for $C_{21}H_{24}NaO_{10}$ 459.12617 (MNa^+) found 459.12664

Materials and Methods – ENZYMATIC SYNTHESIS

p-Nitrophenol glucuronic acid, UDP-GlcA, Luria Broth, and other generic chemicals (Trizma, $MgCl_2$, NaCl, imidazole, etc) were purchased from Sigma. Polyamine-based HPLC column was used to purify the saccharides. UDP-GlcNAc and UDP-GlcNTFA were prepared and gently supplied by the co-workers from the lab.

7.6 Synthesis of disaccharides

Disaccharide α-D-GlCNAc-(1→4)-β-D-GlcApnp (45)

The monomer *p*-nitrophenol glucuronic acid (GlcApnp, **44**) (10 mg, 31.7 μmol) was incubated with UDP-GlcNAc (**48**, 1.2 equiv.) and KfiA (0.2 μg/μL) in buffer (12.7 mL) containing 25 mM Tris-HCl (pH 7.2) and 10 mM $MgCl_2$. The reaction was incubated at room temperature overnight. An aliquot of the reaction mixture was analyzed by a polyamine-based (PAMN-HPLC) column to ensure that >95% of UDP-GlcNHAc was

converted to UDP. After purification, compound **45** was dried and obtained in 70.7% yield.

Disaccharide α-D-GlCNTFA-(1→4)-β-D-GlcApnp (50)

The monomer *p*-nitrophenol glucuronic acid (GlcApnp, **44**) (10 mg, 31.7 μmol) was incubated with UDP-GlcNTFA (**48**, 1.2 equiv.) and KfiA (0.2 μg/μL) in buffer (12.6 mL) containing 25 mM Tris-HCl (pH 7.2) and 10 mM $MgCl_2$. The reaction was incubated at room temperature overnight. An aliquot of the reaction mixture was analysed by a polyamine-based (PAMN-HPLC) column to ensure that >95% of UDP-GlcNAc was converted to UDP. The desired saccharide **50** was obtained in 89.7% yield.

7.7 Synthesis of trisaccharides

Trisaccharide β-D-GlcA-(1→4)-α-D-GlCNAc-(1→4)-β-D-GlcApnp (46)

The disaccharide (**45**) (11.6 mg, 22.4 μmol) was incubated with UDP-GlcA (**47**, 1.2 equiv.) and pmHS2 (0.2 μg/μL) in buffer (8.9 mL) containing 25 mM Tris-HCl (pH 7.2) and 10 mM $MgCl_2$. The reaction was incubated at room temperature overnight. An aliquot of the reaction mixture was analysed by a polyamine-based (PAMN-HPLC) column to ensure that >95% of UDP-GlcNHAc was converted to UDP. After purification the product was dried and obtained in 89.9% yield.

Trisaccharide (β-D-GlcA-(1→4)-α-D-GlCNTFA-(1→4)-β-D-GlcApnp) (51)

The disaccharide **50** (13.6 mg, 22.4 μmol) was incubated with UDP-GlcA (**47**, 1.2 equiv.) and pmHS2 (0.2 μg/μL) in buffer (11.4 mL) containing 25 mM Tris-HCl (pH 7.2) and 10 mM $MgCl_2$. The reaction was incubated at room temperature overnight. An aliquot of the reaction mixture was analysed by a polyamine-based (PAMN-HPLC) column to ensure that >95% of UDP-GlcNHAc was converted to UDP. After purification the product (88.2 % yield) was confirmed by electrospray ionization (ESI) mass spectrometry.

7.7.1 General methodology for the purification of oligosaccharides

Upon the complete consumption of UDP-GlcA (**47**), UDP-GlcNHAc (**48**) or UDP-NTFA (**49**) 30% trifluoroacetic acid (TFA) solution was added until pH 2.0. The

mixture was centrifuged for 15-20 minutes and then purified by a C_{18} column under reverse phase HPLC (RP-HPLC) conditions. The column was eluted with a linear gradient from 90% solution A (0.1% TFA in water) to 50% solution A for 40 min at a flow rate of 0.5 mL/min, then followed by an additional wash for 20 min with 100% solution B (0.1% TFA in acetonitrile) at a flow rate of 0.5 mL/min.

7.8 pmHS2 expression and purification

BL21 cells (carrying pmHS2) were grown in Luria Broth (LB) containing 50μg/mL carbenicillin overnight at 37 ºC. A small portion (1 mL) of the overnight culture was diluted into 1 L of the same growth media and the incubated at 37 ºC for 4-5 hours at 300 rpm until optimal density at 600 nm (OD_{600}) reached 0.6-0.8. The temperature was decreased to 22 ºC and the culture was maintained at that temperature for at least 30 minutes. Isopropyl β-D-1-thiogalactopyranoside was added to the media to the final concentration of 0.2 mM and the shaking was maintained at 22 ºC overnight (ca. 18 hours).

Bacteria were harvested by spinning the bacterial culture at 6000 g for 15 minutes. The bacteria pellet were resuspended in 25 mL of buffer containing 25 mM Tris (pH 7.5), 500 mM NaCl, and 10 mM imidazole (Buffer A). The suspension was sonicated for 3×30 seconds with 8-9 output power and 50% cycle and kept in ice during the process. The lyase was spinned 10,000g for 30 minutes. The supernatant was kept and filtered through a 0.45 μm filter. The lysate was loaded into a 10 mL NTA-agarose column, which was equilibrated with Buffer A and eluted with a linear gradient of Buffer B (containing 25 mM Tris pH 7.5, 500 mM NaCl, and 250 mM imidazole).

7.8.1 Testing the activity of pmHS2

The activity of the expressed enzyme was tested in a 100 μL reaction. The primer GlcApnp (0.25 μg) was incubated with UDP-GlcNHAc (1.2 equiv.) and pmHS2 (0.1 μg/μL) in 100 μL buffer containing 25 mM Tris (pH 7.2), 10 mM $MgCl_2$. The reaction was incubated at room temperature overnight. An aliquot of the reaction mixture was analysed by a polyamine-based (PAMN-HPLC) column to ensure that >95% of UDP-GlcNHAc was converted to UDP.

7.8.2 Testing the purity of pmHS2 by SDS-PAGE

The sample of the expressed enzyme (10 μL) was mixed with loading buffer (10 μL, containing 50 μL of 2-mercaptoethanol and 950 μL of Laemmli sample buffer) and then heated at 100 ºC for 1 minute in a waterbath. The solution was spinned down at 13,000 rpm for 2 minutes and placed in ice to decrease the internal temperature. The samples (including the protein marker) were applied in the gel and ran at 106 V. After this the gel was washed with deionized water. The gel was immersed on SDS dye and kept in the dancer for 40 minutes. The gel was washed with 10% acetic acid and placed in the dancer for several minutes and replacing the acetic acid until the excess blue color disappear.

Materials and Methods – Cell Biology

2-deoxy-D-glucose, 2-deoxy-D-glucose 6-phosphate sodium salt, hexokinase (from *Saccharomyces cerevisae*), glucose-6-phosphate dehydrogenase (G6PDH, from *Leuconostoc mesenteroides*), resazurin sodium salt, triethanolamine (TEA) buffer, HEPES, β-nicotinamide adenine dinucleotide phosphate (β-$NADP^+$), adenosine 5′-triphosphate disodium salt (ATP), phlorizin, cytochalasin B, diaphorase (from *Clostridium kluyveri* type II-L), bovine serum albumin (BSA), potassium chloride, sodium deoxycholate, choline chloride, fetal bovine serum (FBS), Dulbeco's modified Eagle's medium (DMEM), geneticin (G418®) and phosphate buffered saline were purchased from Sigma. 2-(*N*-(7-Nitrobenz-2-oxa-1,3-diazol-4-yl)amino)-2-deoxyglucose (2-NBDG), 6-(*N*-(7-Nitrobenz-2-oxa-1,3-diazol-4-yl)amino)-2-deoxyglucose (6-NBDG) and Dapagliflozin were purchased from Cayman Chemical.

7.9 Cell Culture

Human Embryonic kidney cells (HEK293) were obtained from the American Type Culture Collection (ATCC). COS-7 cells were obtained from another group from NYUAD and HEK293T cells were obtained from Georgia University (USA). All cell lines were grown in DMEM supplemented with 10% FBS and maintained at 37 ºC in a 5% CO_2 atmosphere.

7.10 Cell Viability Assay

HEK293 cells were plated in a 96-well plate at a density of 2.0×10^4 cells/well 24 hours prior the assay. Each compound (**18a-18h**, **22a-22h**, **26a-26h**, **28a-28h**, **29a-29h**, **30a-30h**, **33a-33h**) was added at a concentration of 100 μM to three wells and incubated for 20-24 h at 37 ºC in a 5% CO_2 atmosphere.

Cell titter Blue® (20 μL) was added to each well and incubated at 37 ºC for 4 h. Fluorescence was measure in a microplate reader (λ_{exc}=560 nm, λ_{em}=590 nm). Cell viability (%) was calculated in comparison with non-treated cells. Cells treated with DMSO were used as a positive control.

7.11 Preparation of pCMV6-Neo containing hSGLT1 and hSGLT2

DH5α cells were transformed with vectors containing human SGLT1 and SGLT2 complementary DNAs (cDNAs) (pCMV6-Neo, Origene) and plated on Luria-Bertani (LB) agar plates overnight at 37 ºC. After 24 h of incubation two colonies were picked and grown further in LB broth at 37 ºC overnight. pCMV6-Neo vectors containing SGLT1 and SGLT2 cDNA, respectively, were purified using A PureLink HiPure Plasmid Filter Maxiprep kit (Sigma). Purity and concentration of each plasmid was confirmed by NanoDrop spectrometer before use.

7.12 Determination of geneticin concentration – Killing Curve

HEK293 cells were plated in a 96-well plate at a density of 2.0×10^4 cells/well 24 hours prior the addition of geneticin (G418). Geneticin was added to each well (in duplicate) at concentrations ranging from 0-1000 μg/mL. The media was replaced every two days and fresh antibiotic was added and the treatment was carried out for 7 days. The working concentration of G418 was determined as the lowest concentration that killed all the cells in the period of the treatment.

7.13 Transient transfection

Both hSGLT1 and hSGLT2 constructs were subjected to restriction enzyme digestion analysis prior transfection. Moreover, both SGLT1 and SGLT2 insert clones were fully sequenced (Bioneer, South Korea) and their nucleotide sequences confirmed.

Cells were plated on an appropriate plate at a proper density according to each experiment. Each construct was transfected into the cells using TrueFect. In addition, cells treated with transfection reagent alone were used as vehicle control.

7.14 Stable cell lines

HEK293 cells were seeded on 35 mm dish at a density of 4.0×10^5 cells/dish and incubated at 37 ºC overnight. Each dish was transfected with hSGLT1, hSGLT2 plasmids using Truefect. A third dish using only Truefect was used as control. Cells were trypsinized 24 h post-transfection and plated on 24-well plate at a density of 0.8×10^5 cells/well. G418 was added to each well (700 μg/mL) 48 h post-transfection. The medium was replaced every 2 days and adding fresh antibiotic for 7 days. After this period, the concentration of G418 was reduced to 300 μg/mL and the clones were allowed to grow for several weeks until confluent enough for cryopreservation.

7.15 RNA isolation and reverse transcription PCR

Stable clones were plated on 35 mm dishes at 4.0×10^5 cells/dish and incubated at 37 ºC overnight. Total RNA of each clone was isolated using the High Pure RNA isolation kit (Roche 11828665001). Reverse transcriptase reactions were performed using SuperScript® VILO™ cDNA Synthesis Kit (Invitrogen) for first-strand cDNA synthesis. Polymerase chain reaction (PCR) was performed using Taq DNA polymerase (Invitrogen). The primers used were designed using Primer-3 Software.

The primers for SGLT1 were 5′-TCCACTCATTTTGGCATTCA-3′ (forward) and 5′-AAACCAACCCTGCTGACATC-3′ (reverse). The primers for SGLT2 were 5′-AGAGCCTGACCCACATCAAG-3′ (forward) and 5′-GCGTGTAGATGTCCATGGTG-3′ (reverse). The RT-PCR was carried out in a thermal cycler using the following conditions: 94 ºC for 2 min, 30 cycles of 94 ºC for 30 seconds, 60 ºC for 30 seconds, 72 ºC for 1

minute, then 72 ºC for 5 minutes, hold at 4 ºC. Agarose gel electrophoreseis was used to separate PCR-amplified products whose were visualized under UV light.

7.16 Western Blot

Cells were plated on 60 mm dishes at 6.0×10^5 cells/dish and incubated at 37 ºC overnight. Cells were lysed and 50 μg of each lysate was separated by sodium dodecyl sulphate polyacrylamide gel (SDS-PAGE). After electrophoresis, protein was transferred to nitrocellulose membranes (Z613630 Whatman from Sigma) and then blocked with 10% milk in TBST (20 mM Tris [pH 7.6], 140 mM NaCl and 0.1% Tween 20) for 75 minutes. The membranes were washed with TBST and subsequently incubated with primary antibody SGLT1 (1:200, H-85 Santa Cruz Biotechnology) and SGLT2 (1:500, H-45 Santa Cruz Biotechnology) in 5% BSA for 75 minutes at room temperature. Beta-actin was used as a loading control and the membrane was incubated with the corresponding primary antibody (1:1000, #4967, Cell Signaling). After washing the membranes with TBST, all the membranes were incubated with anti-rabbit horseradish peroxidase-conjugated secondary antibody (1:2000 for SGLT1/β-Actin and 1:4000 for SGLT2) for 1 r at room temperature. Signal was detected by chemiluminescence using ECL detection system (Milipore WBLUR0100).

7.17 Fluorescence microscopic analysis – 2-NBDG uptake assay

HEK293, HEK293-SGLT1 and HEK293-SGLT2 cells were grown until 80% confluent. Medium was removed and cells washed with Krebs-Ringer-Phosphate-HEPES (KRPH) buffer (140 mM NaCl, 20 mM HEPES [pH 7.4], 1mM $MgSO_4$, 1 mM $CaCl_2$, 4.7 mM KCl, 5 mM KH_2PO_4). KRPH buffer (500 μL) was added to each well and incubated at 37 ºC for 1 h. 2-NBDG (600 μM) was added to each well and the cells were incubated at 37 ºC for 30 minutes. Cells were washed with choline buffer (140 mM choline chloride, 20 mM HEPES [pH 7.4], 1mM $MgSO_4$, 1 mM $CaCl_2$, 4.7 mM KCl, 5 mM KH_2PO_4) three times and cells were examined with Olympus inverted confocal microscope, with a 30X objective. As a control, the above experiment was repeated in the absence of 2-NBDG and cells were treated with DMSO as vehicle.

7.18 2-Deoxyglucose uptake assay

HEK293 and SGLT1/SGLT2-transfected cells were plated at 2.0×10^4 cells/well in a 96-well plate. After 24 h of incubation the culture media was removed and cells were rinsed once with KRPH buffer and incubated in the same buffer for 1 h at 37 ºC. 2-Deoxyglucose (1 mM) was added to each well and the cells were incubated at 37 ºC for 1 hour after which, cells were lysed with 50 μL of 0.1 M NaOH and then incubated at 80-85 ºC for 40 minutes. After this period, lysate was neutralized with 50 μL of 0.1 M HCl and 50 μL of TEA buffer was added. In a 96-well plate, 100 μL of lysate was dispensed into each well and incubated at 37 ºC for 15-20 h after the addition of an enzymatic cocktail solution consisting of 50 mM TEA (pH 8.2), 50 mM KCl, 0.02 % BSA, 1 mM NADP, 0.5 U/mL G6PDH, 0.1 U/mL diaphorase, 10 μM resazurin. Fluorescence was measured at 590 nm using a Multiplate reader (Biotek) after excitation at 560 nm. The fluorescence of resofurin, the reduced form of resazurin, is a measure of the amount of 2DG inside the cells.

7.19 Determination of IC_{50}

To determine the IC_{50} values of compounds **18a-18h**, **22a-22h** and **33a-33h** HEK293 and SGLT1/SGLT2-transfected cells were plated at 2.0×10^4 cells/well in a 96-well plate. After 24 h of incubation the culture media was removed and cells were rinsed once with KRPH buffer and incubated in the same buffer for 1 h at 37 ºC. Each compound (0.1 nM to 200 μM was added to the buffer and incubated for 10 minutes. 2-Deoxyglucose (1 mM) was added to each well and the cells were incubated at 37 ºC for 1 hour. Cells were lysed with 50 μL of 0.1 M NaOH and then incubated at 80-85 ºC for 40 minutes. After this period, lysate was neutralized with 50 μL of 0.1 M HCl and 50 μL of TEA buffer was added. The enzymatic assay to determine the ammout of 2DG was performed as mention above.

References

(1) American Diabetes, A. Diagnosis and classification of diabetes mellitus. *Diabetes Care* **2004**, *27 Suppl 1*, S5-S10.

(2) Kitabchi, A. E.; Umpierrez, G. E.; Miles, J. M.; Fisher, J. N. Hyperglycemic crises in adult patients with diabetes. *Diabetes Care* **2009**, *32*, 1335-1343.

(3) Landin-Olsson, M. Latent Autoimmune Diabetes in Adults. *Annals NY Ac Sci* **2002**, *958*, 112-116.

(4) Shi, Y.; Hu, F. B. The global implications of diabetes and cancer. *Lancet* **2014**, *383*, 1947-1948.

(5) Buse, J. B.; Polonsky, K. S.; Burant, C. F.: Type 2 Diabetes Mellitus. In *Williams Textbook of Endocrinology*; Elsevier, 2012; pp 1427.

(6) Ozougwu, J. C.; Obimba, K. C.; Belonwu, C. D.; Unakalamba, C. B. The pathogenesis and pathophysiology of type 1 and type 2 diabetes mellitus. *J Phys Pathol* **2013**, *4*, 46-57.

(7) http://www.who.int/mediacentre/factsheets/fs312/en/.

(8) Grant, R. W.; Moore, A. F.; Florez, J. C. Genetic Architecture of Type 2 Diabetes: Recent Progress and Clinical Implications. *Diabetes Care* **2009**, *32*, 1107-1114.

(9) Rojas, L. B.; Gomes, M. B. Metformin: an old but still the best treatment for type 2 diabetes. *Diabetol Metab Syndr* **2013**, *5*, 6.

(10) Werner, E. A.; Bell, J. CCXIV.-The preparation of methylguanidine, and of [small beta][small beta]-dimethylguanidine by the interaction of dicyanodiamide, and methylammonium and dimethylammonium chlorides respectively. *J Chem Soc Trans* **1922**, *121*, 1790-1794.

(11) Diamant, M.; Heine, R. J. Thiazolidinediones in type 2 diabetes mellitus: current clinical evidence. *Drugs* **2003**, *63*, 1373-1405.

(12) Hauner, H. The mode of action of thiazolidinediones. *Diabetes Metab Res Rev* **2002**, *18 Suppl 2*, S10-15.

(13) Saltiel, A. R.; Olefsky, J. M. Thiazolidinediones in the Treatment of Insulin Resistance and Type II Diabetes. *Diabetes* **1996**, *45*, 1661-1669.

(14) Stafford, J. M.; Elasy, T. Treatment update: thiazolidinediones in combination with metformin for the treatment of type 2 diabetes. *Vascular Health and Risk Management* **2007**, *3*, 503-510.

(15) MacDonald, P. E.; El-Kholy, W.; Riedel, M. J.; Salapatek, A. M.; Light, P. E.; Wheeler, M. B. The multiple actions of GLP-1 on the process of glucose-stimulated insulin secretion. *Diabetes* **2002**, *51 Suppl 3*, S434-442.

(16) Blickle, J. F. Meglitinide analogues: a review of clinical data focused on recent trials. *Diabetes Metab* **2006**, *32*, 113-120.

(17) Holst, J. J.; Vilsboll, T.; Deacon, C. F. The incretin system and its role in type 2 diabetes mellitus. *Mol Cell Endocrinol* **2009**, *297*, 127-136.

(18) Dicker, D. DPP-4 Inhibitors: Impact on glycemic control and cardiovascular risk factors. *Diabetes Care* **2011**, *34*, S276-S278.

(19) Dupre, J.; Behme, M. T.; Hramiak, I. M.; McFarlane, P.; Williamson, M. P.; Zabel, P.; McDonald, T. J. Glucagon-Like Peptide I Reduces Postprandial Glycemic Excursions in IDDM. *Diabetes* **1995**, *44*, 626-630.

(20) McIntosh, C. H. S.; Demuth, H.-U.; Pospisilik, J. A.; Pederson, R. Dipeptidyl peptidase IV inhibitors: how do they work as new antidiabetic agents? *Regul Peptides* **2005**, *128*, 159-165.

(21) van de Laar, F. A.; Lucassen, P. L.; Akkermans, R. P.; van de Lisdonk, E. H.; Rutten, G. E.; van Weel, C. Alpha-glucosidase inhibitors for patients with type 2 diabetes: results from a Cochrane systematic review and meta-analysis. *Diabetes Care* **2005**, *28*, 154-163.

(22) Ahr, H. J.; Boberg, M.; Krause, H. P.; Maul, W.; Muller, F. O.; Ploschke, H. J.; Weber, H.; Wunsche, C. Pharmacokinetics of acarbose. Part I: Absorption, concentration in plasma, metabolism and excretion after single administration of [14C]acarbose to rats, dogs and man. *Arzneimittel-Forschung* **1989**, *39*, 1254-1260.

(23) Ahr, H. J.; Boberg, M.; Brendel, E.; Krause, H. P.; Steinke, W. Pharmacokinetics of miglitol. Absorption, distribution, metabolism, and excretion following administration to rats, dogs, and man. *Arzneimittel-Forschung* **1997**, *47*, 734-745.

(24) SGLT Inhibitors as New Therapeutic Tools in the Treatment of Diabetes. In *Handbook of Experimental Pharmacology, Diabetes - Perspectives in Drug Therapy*; H., R. K., Castaneda, F., Eds.; Springer, 2011; Vol. 203; pp 105-126.

(25) Ceriello, A. PROactive Study: (r)evolution in the therapy of diabetes? *Diabetic Med* **2005**, *22*, 1463-1464.

(26) Asano, N. Glycosidase inhibitors: update and perspectives on practical use. *Glycobiology* **2003**, *13*, 93r-104r.

(27) Borges de Melo, E.; da Silveira Gomes, A.; Carvalho, I. α- and β-Glucosidase inhibitors: chemical structure and biological activity. *Tetrahedron* **2006**, *62*, 10277-10302.

(28) Bishop, J. H.; Green, R.; Thomas, S. Free-flow reabsorption of glucose, sodium, osmoles and water in rat proximal convoluted tubule. *J Physiol* **1979**, *288*, 331-351.

(29) Rajesh, R.; Naren, P.; Vidyasagar, S.; Unnikrishnan; Pandey, S.; Varghese, M.; Gang, S. Sodium Glucose Co transporter 2 (SGLT2) Inhibitors: A New Sword for the Treatment of Type 2 Diabetes Mellitus. *Int J Pharm Sci Res* **2010**, *1*, 139-147.

(30) Vallon, V. The mechanisms and therapeutic potential of SGLT2 inhibitors in diabetes mellitus. *Annu Rev Med* **2015**, *66*, 255-270.

(31) Su, S.-L. Sodium-Glucose Transporters. *Formos J Endocrin Metab* **2009**, *1*, 1-5.

(32) Wright, E. M.; Turk, E. The sodium/glucose cotransport family SLC5. *Pflugers Arch* **2004**, *447*, 510-518.

(33) Wright, E. M.; Loo, D. D.; Hirayama, B. A. Biology of human sodium glucose transporters. *Physiol Rev* **2011**, *91*, 733-794.

(34) Jabbour, S. A.; Goldstein, B. J. Sodium glucose co-transporter 2 inhibitors: blocking renal tubular reabsorption of glucose to improve glycaemic control in patients with diabetes. *Int J Clin Prat* **2008**, *62*, 1279-1284.

(35) Bianchi, L.; Diez-Sampedro, A. A single amino acid change converts the sugar sensor SGLT3 into a sugar transporter. *PloS one* **2010**, *5*, e10241.

(36) Díez-Sampedro, A.; Hirayama, B. A.; Osswald, C.; Gorboulev, V.; Baumgarten, K.; Volk, C.; Wright, E. M.; Koepsell, H. A glucose sensor hiding in a family of transporters. *Prod Nat Acad Sci* **2003**, *100*, 11753-11758.

(37) Kwon, H. M.; Yamauchi, A.; Uchida, S.; Preston, A. S.; Garcia-Perez, A.; Burg, M. B.; Handler, J. S. Cloning of the cDNa for a Na+/myo-inositol cotransporter, a hypertonicity stress protein. *J Biol Chem* **1992**, *267*, 6297-6301.

(38) Dai, G.; Levy, O.; Carrasco, N. Cloning and characterization of the thyroid iodide transporter. *Nature* **1996**, *379*, 458-460.

(39) Ehrenkranz, J. R.; Lewis, N. G.; Kahn, C. R.; Roth, J. Phlorizin: a review. *Diabetes Metab Res Rev* **2005**, *21*, 31-38.

(40) Mackenzie, B.; Loo, D. D.; Wright, E. M. Relationships between Na+/glucose cotransporter (SGLT1) currents and fluxes. *J Membr Biol* **1998**, *162*, 101-106.

(41) Rieg, T.; Masuda, T.; Gerasimova, M.; Mayoux, E.; Platt, K.; Powell, D. R.; Thomson, S. C.; Koepsell, H.; Vallon, V. Increase in SGLT1-mediated transport explains renal glucose reabsorption during genetic and pharmacological SGLT2 inhibition in euglycemia. *Am J Physiol Renal Physiol* **2014**, *306*, F188-193.

(42) Santer, R.; Calado, J. Familial renal glucosuria and SGLT2: from a mendelian trait to a therapeutic target. *Clin J Am Soc Nephrol* **2010**, *5*, 133-141.

(43) Rossetti, L.; Smith, D.; Shulman, G. I.; Papachristou, D.; DeFronzo, R. A. Correction of hyperglycemia with phlorizin normalizes tissue sensitivity to insulin in diabetic rats. *J Clin Invest* **1987**, *79*, 1510-1515.

(44) Kalra, S. Sodium Glucose Co-Transporter-2 (SGLT2) Inhibitors: A Review of Their Basic and Clinical Pharmacology. *Diabetes Ther* **2014**, *5*, 355-366.

(45) Zambrowicz, B.; Freiman, J.; Brown, P. M.; Frazier, K. S.; Turnage, A.; Bronner, J.; Ruff, D.; Shadoan, M.; Banks, P.; Mseeh, F.; Rawlins, D. B.; Goodwin, N. C.; Mabon, R.; Harrison, B. A.; Wilson, A.; Sands, A.; Powell, D. R. LX4211, a Dual SGLT1/SGLT2 Inhibitor, Improved Glycemic Control in Patients With Type 2 Diabetes in a Randomized, Placebo-Controlled Trial. *Clin Pharmacol Ther* **2012**, *92*, 158-169.

(46) Drucker, D. J. Incretin Action in the Pancreas: Potential Promise, Possible Perils, and Pathological Pitfalls. *Diabetes* **2013**, *62*, 3316-3323.

(47) Powell, D. R.; Smith, M.; Greer, J.; Harris, A.; Zhao, S.; DaCosta, C.; Mseeh, F.; Shadoan, M. K.; Sands, A.; Zambrowicz, B.; Ding, Z. M. LX4211 increases serum glucagon-like peptide 1 and peptide YY levels by reducing sodium/glucose cotransporter 1 (SGLT1)-mediated absorption of intestinal glucose. *J Pharmacol Exp Ther* **2013**, *345*, 250-259.

(48) Shibazaki, T.; Tomae, M.; Ishikawa-Takemura, Y.; Fushimi, N.; Itoh, F.; Yamada, M.; Isaji, M. KGA-2727, a novel selective inhibitor of a high-affinity sodium glucose cotransporter (SGLT1), exhibits antidiabetic efficacy in rodent models. *J Pharmacol Exp Ther* **2012**, *342*, 288-296.

(49) Chao, E. C. SGLT-2 Inhibitors: A New Mechanism for Glycemic Control. *Clinical Diabetes* **2014**, *32*, 4-11.

(50) Oku, A.; Ueta, K.; Arakawa, K.; Ishihara, T.; Nawano, M.; Kuronuma, Y.; Matsumoto, M.; Saito, A.; Tsujihara, K.; Anai, M.; Asano, T.; Kanai, Y.; Endou, H. T-1095, an inhibitor of renal Na+-glucose cotransporters, may provide a novel approach to treating diabetes. *Diabetes* **1999**, *48*, 1794-1800.

(51) Anderson, S. L. Dapagliflozin efficacy and safety: a perspective review. *Ther Adv Drug Safety* **2014**, *5*, 242-254.

(52) Vallon, V.; Rose, M.; Gerasimova, M.; Satriano, J.; Platt, K. A.; Koepsell, H.; Cunard, R.; Sharma, K.; Thomson, S. C.; Rieg, T. Knockout of Na-glucose transporter

SGLT2 attenuates hyperglycemia and glomerular hyperfiltration but not kidney growth or injury in diabetes mellitus. *Am J Physiol Renal Physiol* **2013**, *304*, F156-167.

(53) Kojima, N.; Williams, J. M.; Takahashi, T.; Miyata, N.; Roman, R. J. Effects of a New SGLT2 Inhibitor, Luseogliflozin, on Diabetic Nephropathy in T2DN Rats. *J Pharm Exp Ther* **2013**, *345*, 464-472.

(54) Kinne, R. H.; Castaneda, F.: SGLT Inhibitors as New Therapeutic Tools in the Treatment of Diabetes. In *Diabetes - Perspectives in Drug Therapy*; Schwanstecher, M., Ed.; Handbook of Experimental Pharmacology; Springer Berlin Heidelberg, 2011; Vol. 203; pp 105-126.

(55) Pajor, A. M.; Randolph, K. M.; Kerner, S. A.; Smith, C. D. Inhibitor binding in the human renal low- and high-affinity Na+/glucose cotransporters. *J Pharmacol Exp Ther* **2008**, *324*, 985-991.

(56) Lin, J.-T.; Kormanec, J.; Wehner, F.; Wielert-Badt, S.; Kinne, R. K. H. High-level expression of Na+/d-glucose cotransporter (SGLT1) in a stably transfected Chinese hamster ovary cell line. *Biochimica et Biophysica Acta (BBA) - Biomembranes* **1998**, *1373*, 309-320.

(57) Castaneda, F.; Kinne, R. K. A 96-well automated method to study inhibitors of human sodium-dependent D-glucose transport. *Mol Cell Biochem* **2005**, *280*, 91-98.

(58) Katsuno, K.; Fujimori, Y.; Takemura, Y.; Hiratochi, M.; Itoh, F.; Komatsu, Y.; Fujikura, H.; Isaji, M. Sergliflozin, a novel selective inhibitor of low-affinity sodium glucose cotransporter (SGLT2), validates the critical role of SGLT2 in renal glucose reabsorption and modulates plasma glucose level. *J Pharmacol Exp Ther* **2007**, *320*, 323-330.

(59) Wright, E. M.; Hirayama, B. A.; Loo, D. F. Active sugar transport in health and disease. *J Intern Med* **2007**, *261*, 32-43.

(60) Kim, W. H.; Lee, J.; Jung, D. W.; Williams, D. R. Visualizing sweetness: increasingly diverse applications for fluorescent-tagged glucose bioprobes and their recent structural modifications. *Sensors (Basel)* **2012**, *12*, 5005-5027.

(61) Speizer, L.; Haugland, R.; Kutchai, H. Asymmetric transport of a fluorescent glucose analogue by human erythrocytes. *Biochim Biophys Acta* **1985**, *815*, 75-84.

(62) Speizer, L.; Haugland, R.; Kutchai, H. Asymmetric transport of a fluorescent glucose analogue by human erythrocytes. *Biochimica et Biophysica Acta (BBA) - Biomembranes* **1985**, *815*, 75-84.

(63) Devés, R.; Krupka, R. M. Cytochalasin B and the kinetics of inhibition of biological transport. A case of asymmetric binding to the glucose carrier. *Biochimica et Biophysica Acta (BBA) - Biomembranes* **1978**, *510*, 339-348.

(64) Yoshioka, K.; Saito, M.; Oh, K. B.; Nemoto, Y.; Matsuoka, H.; Natsume, M.; Abe, H. Intracellular fate of 2-NBDG, a fluorescent probe for glucose uptake activity, in Escherichia coli cells. *Biosci Biotechnol Biochem* **1996**, *60*, 1899-1901.

(65) Louzao, M. C.; Espina, B.; Vieytes, M. R.; Vega, F. V.; Rubiolo, J. A.; Baba, O.; Terashima, T.; Botana, L. M. "Fluorescent glycogen" formation with sensibility for in vivo and in vitro detection. *Glycoconj J* **2008**, *25*, 503-510.

(66) Yoshioka, K.; Oh, K. B.; Saito, M.; Nemoto, Y.; Matsuoka, H. Evaluation of 2-[N-(7-nitrobenz-2-oxa-1,3-diazol-4-yl)amino]-2-deoxy-d-glucose, a new fluorescent derivative of glucose, for viability assessment of yeast Candida albicans. *Appl Microbiol Biotechnol* **1996**, *46*, 400-404.

(67) Zhang, W. Y.; Lee, J. J.; Kim, I. S.; Kim, Y.; Myung, C. S. Stimulation of glucose uptake and improvement of insulin resistance by aromadendrin. *Pharmacology* **2011**, *88*, 266-274.

(68) Wang, L.; Xu, M. L.; Rasmussen, S. K.; Wang, M.-H. Vomifoliol 9-O-α-arabinofuranosyl (1→6)-β-d-glucopyranoside from the leaves of Diospyros Kaki stimulates the glucose uptake in HepG2 and 3T3-L1 cells. *Carbohydr Res* **2011**, *346*, 1212-1216.

(69) Huan, Y.; Li, L.; Liu, Q.; Liu, S.; Shen, Z. A cell-based fluorescent glucose transporter assay for SGLT2 inhibitor discovery. *Acta Pharm Sinica C* **2013**, *3*, 97-101.

(70) Zou, C.; Wang, Y.; Shen, Z. 2-NBDG as a fluorescent indicator for direct glucose uptake measurement. *J Biochem Biophys Methods* **2005**, *64*, 207-215.

(71) Blodgett, A. B.; Kothinti, R. K.; Kamyshko, I.; Petering, D. H.; Kumar, S.; Tabatabai, N. M. A fluorescence method for measurement of glucose transport in kidney cells. *Diabetes technology & therapeutics* **2011**, *13*, 743-751.

(72) Jung, D. W.; Ha, H. H.; Zheng, X.; Chang, Y. T.; Williams, D. R. Novel use of fluorescent glucose analogues to identify a new class of triazine-based insulin mimetics possessing useful secondary effects. *Mol Biosyst* **2011**, *7*, 346-358.

(73) Ponisovskiy, M. R. Warburg effect mechanism as the target for theoretical substantiation of a new potential cancer treatment. *Crit Rev Eukaryot Gene Expr* **2011**, *21*, 13-28.

(74) Israel, M.; Schwartz, L. The metabolic advantage of tumor cells. *Mol Cancer* **2011**, *10*, 70.

(75) O'Neil, R. G.; Wu, L.; Mullani, N. Uptake of a fluorescent deoxyglucose analog (2-NBDG) in tumor cells. *Mol Imaging Biol* **2005**, *7*, 388-392.

(76) Egawa-Takata, T.; Endo, H.; Fujita, M.; Ueda, Y.; Miyatake, T.; Okuyama, H.; Yoshino, K.; Kamiura, S.; Enomoto, T.; Kimura, T.; Inoue, M. Early reduction of glucose uptake after cisplatin treatment is a marker of cisplatin sensitivity in ovarian cancer. *Cancer Sci* **2010**, *101*, 2171-2178.

(77) Chang, H. C.; Yang, S. F.; Huang, C. C.; Lin, T. S.; Liang, P. H.; Lin, C. J.; Hsu, L. C. Development of a novel non-radioactive cell-based method for the screening of SGLT1 and SGLT2 inhibitors using 1-NBDG. *Mol Biosyst* **2013**, *9*, 2010-2020.

(78) Barros, L. F.; Bittner, C. X.; Loaiza, A.; Ruminot, I.; Larenas, V.; Moldenhauer, H.; Oyarzun, C.; Alvarez, M. Kinetic validation of 6-NBDG as a probe for the glucose transporter GLUT1 in astrocytes. *J Neurochem* **2009**, *109 Suppl 1*, 94-100.

(79) Chi, M. M. Y.; Pusateri, M. E.; Carter, J. G.; Norris, B. J.; McDougal Jr, D. B.; Lowry, O. H. Enzymatic assays for 2-deoxyglucose and 2-deoxyglucose 6-phosphate. *Anal Biochem* **1987**, *161*, 508-513.

(80) Sasson, S.; Oron, R.; Cerasi, E. Enzymatic Assay of 2-Deoxyglucose 6-Phosphate for Assessing Hexose Uptake Rates in Cultured Cells. *Anal Biochem* **1993**, *215*, 309-311.

(81) Zhu, A.; Romero, R.; Petty, H. R. An enzymatic fluorimetric assay for glucose-6-phosphate: application in an in vitro Warburg-like effect. *Anal Biochem* **2009**, *388*, 97-101.

(82) Self, C. H. Enzyme amplification--a general method applied to provide an immunoassisted assay for placental alkaline phosphatase. *J Immunol Methods* **1985**, *76*, 389-393.

(83) Johannsson, A.; Ellis, D. H.; Bates, D. L.; Plumb, A. M.; Stanley, C. J. Enzyme amplification for immunoassays: Detection limit of one hundredth of an attomole. *J Immunol Methods* **1986**, *87*, 7-11.

(84) Stanley, C. J.; Ellis, D. H.; Bates, D. L.; Johannsson, A. Enzyme-amplified immunoassays. *J Pharm Biomed Anal* **1987**, *5*, 811-820.

(85) Yamamoto, N.; Sato, T.; Kawasaki, K.; Murosaki, S.; Yamamoto, Y. A nonradioisotope, enzymatic assay for 2-deoxyglucose uptake in L6 skeletal muscle cells cultured in a 96-well microplate. *Anal Biochem* **2006**, *351*, 139-145.

(86) Saito, K.; Lee, S.; Shiuchi, T.; Toda, C.; Kamijo, M.; Inagaki-Ohara, K.; Okamoto, S.; Minokoshi, Y. An enzymatic photometric assay for 2-deoxyglucose uptake in insulin-responsive tissues and 3T3-L1 adipocytes. *Anal Biochem* **2011**, *412*, 9-17.

(87) Smit, F. J.; N'Da, D. D. Synthesis, in vitro antimalarial activity and cytotoxicity of novel 4-aminoquinolinyl-chalcone amides. *Bioorg Med Chem* **2014**, *22*, 1128-1138.

(88) Insuasty, B.; Ramírez, J.; Becerra, D.; Echeverry, C.; Quiroga, J.; Abonia, R.; Robledo, S. M.; Vélez, I. D.; Upegui, Y.; Muñoz, J. A.; Ospina, V.; Nogueras, M.; Cobo, J. An efficient synthesis of new caffeine-based chalcones, pyrazolines and pyrazolo[3,4-b][1,4]diazepines as potential antimalarial, antitrypanosomal and antileishmanial agents. *Eur J Med Chem* **2015**, *93*, 401-413.

(89) Kamal, A.; Srinivasulu, V.; Nayak, V. L.; Sathish, M.; Shankaraiah, N.; Bagul, C.; Reddy, N. V.; Rangaraj, N.; Nagesh, N. Design and synthesis of C3-pyrazole/chalcone-linked beta-carboline hybrids: antitopoisomerase I, DNA-interactive, and apoptosis-inducing anticancer agents. *ChemMedChem* **2014**, *9*, 2084-2098.

(90) Kumar, D.; Raj, K. K.; Malhotra, S. V.; Rawat, D. S. Synthesis and anticancer activity evaluation of resveratrol-chalcone conjugates. *MedChemComm* **2014**, *5*, 528-535.

(91) Kim, S. Y.; Lee, I. S.; Moon, A. 2-Hydroxychalcone and xanthohumol inhibit invasion of triple negative breast cancer cells. *Chem Biol Interact* **2013**, *203*, 565-572.

(92) Katsori, A. M.; Hadjipavlou-Litina, D. Chalcones in cancer: understanding their role in terms of QSAR. *Curr Med Chem* **2009**, *16*, 1062-1081.

(93) Khan, S. A.; Asiri, A. M. Green synthesis, characterization and biological evaluation of novel chalcones as anti bacterial agents. *Arab J Chem*.

(94) El Sayed Aly, M. R.; Abd El Razek Fodah, H. H.; Saleh, S. Y. Antiobesity, antioxidant and cytotoxicity activities of newly synthesized chalcone derivatives and their metal complexes. *Eur J Med Chem* **2014**, *76*, 517-530.

(95) Enoki, T.; Ohnogi, H.; Nagamine, K.; Kudo, Y.; Sugiyama, K.; Tanabe, M.; Kobayashi, E.; Sagawa, H.; Kato, I. Antidiabetic activities of chalcones isolated from a Japanese Herb, Angelica keiskei. *J Agric Food Chem* **2007**, *55*, 6013-6017.

(96) Ono, M.; Watanabe, R.; Kawashima, H.; Cheng, Y.; Kimura, H.; Watanabe, H.; Haratake, M.; Saji, H.; Nakayama, M. Fluoro-pegylated chalcones as positron emission tomography probes for in vivo imaging of beta-amyloid plaques in Alzheimer's disease. *J Med Chem* **2009**, *52*, 6394-6401.

(97) Eddarir, S.; Cotelle, N.; Bakkour, Y.; Rolando, C. An efficient synthesis of chalcones based on the Suzuki reaction. *Tetrahedron Lett* **2003**, *44*, 5359-5363.

(98) Guo, T.; Jiang, Q.; Yu, L.; Yu, Z. Synthesis of chalcones via domino dehydrochlorination/Pd(OAc)2-catalyzed Heck reaction. *Chinese J Catal* **2015**, *36*, 78-85.

(99) Xu, C.; Chen, G.; Huang, X. CHALCONES BY THE WITTIG REACTION OF A STABLE YLIDE WITH ALDEHYDES UNDER MICROWAVE IRRADIATION. *Org Prep Proc Int* **1995**, *27*, 559-561.

(100) Yu, S.; Li, X. Mild Synthesis of Chalcones via Rhodium(III)-Catalyzed C–C Coupling of Arenes and Cyclopropenones. *Org Lett* **2014**, *16*, 1220-1223.

(101) Petrov, O.; Ivanova, Y.; Gerova, M. SOCl2/EtOH: Catalytic system for synthesis of chalcones. *Catal Comm* **2008**, *9*, 315-316.

(102) Sebti, S. d.; Solhy, A.; Smahi, A.; Kossir, A.; Oumimoun, H. Dramatic activity enhancement of natural phosphate catalyst by lithium nitrate. An efficient synthesis of chalcones. *Catal Comm* **2002**, *3*, 335-339.

(103) Climent, M. J.; Garcia, H.; Primo, J.; Corma, A. Zeolites as catalysts in organic reactions. Claisen-Schmidt condensation of acetophenone with benzaldehyde. *Catal Lett* **1990**, *4*, 85-91.

(104) Saravanamurugan, S.; Palanichamy, M.; Arabindoo, B.; Murugesan, V. Solvent free synthesis of chalcone and flavanone over zinc oxide supported metal oxide catalysts. *Catal Comm* **2005**, *6*, 399-403.

(105) Siddiqui, Z. N. A convenient synthesis of coumarinyl chalcones using HClO4–SiO2: A green approach. *Arab J Chem*.

(106) Ku, S. K.; Kwak, S.; Kim, Y.; Bae, J. S. Aspalathin and Nothofagin from Rooibos (Aspalathus linearis) inhibits high glucose-induced inflammation in vitro and in vivo. *Inflammation* **2015**, *38*, 445-455.

(107) Krbechek, L.; Inglett, G. E.; Holik, M.; Dowling, B.; Wagner, R.; Riter, R. Dihydrochalcones. Synthesis of potential sweetening agents. *J Agric Food Chem* **1968**, *16*, 108-112.

(108) Briot, A.; Baehr, C.; Brouillard, R.; Wagner, A.; Mioskowski, C. Concise Synthesis of Dihydrochalcones via Palladium-Catalyzed Coupling of Aryl Halides and 1-Aryl-2-propen-1-ols. *J Org Chem* **2004**, *69*, 1374-1377.

(109) Li, J.-P.; Zhang, Y.-X.; Ji, Y. Selective 1,4-Reduction of Chalcones with Zn/NH4Cl/C2H5OH/H2O. *J Chinese Soc* **2008**, *55*, 390-393.

(110) Liang, Z.; Weige, Z.; Xin, W.; Kai, B.; Guodong, L.; Jinshun, L. Ultrasound Assisted Selective Reduction of Chalcones to Dihydrochalcones by Zn/HOAc. *Lett Org Chem* **2008**, *5*, 370-373.

(111) Mandal, P. K.; McMurray, J. S. Pd–C-Induced Catalytic Transfer Hydrogenation with Triethylsilane. *J Org Chem* **2007**, *72*, 6599-6601.

(112) Nishikawa, T.; Adachi, M.; Isobe, M.: *C -Glycosylation*; Springer, 2008. pp. 756-811.

(113) Pasetto, P.; Walczak, M. C. A Mitsunobu route to C-glycosides. *Tetrahedron* **2009**, *65*, 8468-8477.

(114) C-Glycosides. In *Synthesis and Characterization of Glycosides*; Springer US, 2007; pp 247-271.

(115) Wellington, K. W.; Benner, S. A. A review: synthesis of aryl C-glycosides via the heck coupling reaction. *Nucleosides, nucleotides & nucleic acids* **2006**, *25*, 1309-1333.

(116) Koester, D. C.; Leibeling, M.; Neufeld, R.; Werz, D. B. A Pd-Catalyzed Approach to (1→6)-Linked C-Glycosides. *Org Lett* **2010**, *12*, 3934-3937.

(117) *Science of Synthesis: Houben-Weyl Methods of Molecular Transformations*; Thieme, 2008; Vol. 37. pp. 770.

(118) SanMartin, R.; Tavassoli, B.; Walsh, K. E.; Walter, D. S.; Gallagher, T. Radical-mediated synthesis of alpha-C-glycosides based on N-acyl galactosamine. *Org Lett* **2000**, *2*, 4051-4054.

(119) Oyama, K.-i.; Kondo, T. Total Synthesis of Flavocommelin, a Component of the Blue Supramolecular Pigment from Commelina communis, on the Basis of Direct 6-C-Glycosylation of Flavan. *J Org Chem* **2004**, *69*, 5240-5246.

(120) Santos, R. G.; Jesus, A. R.; Caio, J. M.; Rauter, A. P. Fries-type Reactions for the C-Glycosylation of Phenols. *Curr Org Chem* **2011**, *15*, 128-148.

(121) Sato, S.; Hiroe, K.; Kumazawa, T.; Jun-ichi, O. Total synthesis of two isoflavone C-glycosides: genistein and orobol 8-C-β-d-glucopyranosides. *Carbohydr Res* **2006**, *341*, 1091-1095.

(122) Chen, Q.; Zhong, Y.; O'Doherty, G. A. Convergent De Novo Synthesis of Vineomycinone B2 Methyl Ester. *Chemical communications (Cambridge, England)* **2013**, *49*, 10.1039/c1033cc44050h.

(123) Matsumoto, T.; Hosoya, T.; Suzuki, K. Improvement in O→C-glycoside rearrangement approach to C-aryl glycosides: Use of 1-O-acetyl sugar as stable but efficient glycosyl donor. *Tetrahedron Lett* **1990**, *31*, 4629-4632.

(124) Matsumoto, T.; Katsuki, M.; Suzuki, K. New approach to C-aryl glycosides starting from phenol and glycosyl fluoride. Lewis acid-catalyzed rearrangement of O-glycoside to C-glycoside. *Tetrahedron Lett* **1988**, *29*, 6935-6938.

(125) Matsumoto, T.; Katsuki, M.; Jona, H.; Suzuki, K. Synthetic study toward vineomycins. Synthesis of c-aryl glycoside sector via Cp2HfCl2瑴AgClO4-promoted tactics. *Tetrahedron Lett* **1989**, *30*, 6185-6188.

(126) Mahling, J.; Schmidt, R. C-Glycosides from O-Glycosyltrichloroacetimidates and Phenol Derivatives with Trimethyl Trifluoromethanesulfonate (TMSOTf) as the Catalyst. *Synthesis-Stuttgart* **1993**, *3*, 325-328.

(127) El Telbani, E.; El Desoky, S.; Hammad, M. A.; Abdel Rahman, A. R. H.; Schmidt, R. R. C-Glycosides of Visnagin Analogues. *Euro J Org Chem* **1998**, *1998*, 2317-2322.

(128) Palmacci, E. R.; Seeberger, P. H. Synthesis of C-Aryl and C-Alkyl Glycosides Using Glycosyl Phosphates. *Org Lett* **2001**, *3*, 1547-1550.

(129) Ben, A.; Yamauchi, T.; Matsumoto, T.; Suzuki, K. Sc(OTf)3 as efficient catalyst for aryl C-glycoside synthesis. *Synlett* **2004**, 225-230.

(130) Yamada, C.; Sasaki, K.; Matsumura, S.; Toshima, K. Aryl C-glycosylation using an ionic liquid containing a protic acid. *Tetrahedron Lett* **2007**, *48*, 4223-4227.

(131) Toshima, K.; Ushiki, Y.; Matsuo, G.; Matsumura, S. Environmentally benign aryl C-glycosidations of unprotected sugars using montmorillonite K-10 as a solid acid. *Tetrahedron Lett* **1997**, *38*, 7375-7378.

(132) Santos, R. G.; Xavier, N. M.; Bordado, J. C.; Rauter, A. P. Efficient and First Regio- and Stereoselective Direct C-Glycosylation of a Flavanone Catalysed by Pr(OTf)3 Under Conventional Heating or Ultrasound Irradiation. *Euro J Org Chem* **2013**, *2013*, 1441-1447.

(133) Wang, Z.; Chinoy, Z. S.; Ambre, S. G.; Peng, W.; McBride, R.; de Vries, R. P.; Glushka, J.; Paulson, J. C.; Boons, G.-J. A General Strategy for the Chemoenzymatic Synthesis of Asymmetrically Branched N-Glycans. *Science* **2013**, *341*, 379-383.

(134) Zhao, G.; Liu, Y.; Wu, Z.; Zhu, H.; Yu, Z.; Fang, J.; Wang, P. G. Chemoenzymatic synthesis of glycoproteins. *Glycoscience: Biol Med* **2014**, *43*, 1-8.

(135) Jesus, A. R.; Rauter, A. P.; Liu, J.: Recent Advances in enzymatic synthesis of heparin. In *Carbohydrate Chemistry: Chemical and Biological Applications*; RSC 2013; Vol. 39; pp 38-57.

(136) Wever, W. J.; Bogart, J. W.; Baccile, J. A.; Chan, A. N.; Schroeder, F. C.; Bowers, A. A. Chemoenzymatic Synthesis of Thiazolyl Peptide Natural Products Featuring an Enzyme-Catalyzed Formal [4 + 2] Cycloaddition. *J Am Chem Soc* **2015**, *137*, 3494-3497.

(137) Wong, C.-H. Enzymatic and chemo-enzymatic synthesis of carbohydrates. *Pure Appl Chem* **1995**, *67*, 1609-1616.

(138) Hanson, S.; Best, M.; Bryan, M. C.; Wong, C.-H. Chemoenzymatic synthesis of oligosaccharides and glycoproteins. *Trends Biochem Sci* **2004**, *29*, 656-663.

(139) Khaled, A.; Piotrowska, O.; Dominiak, K.; Augé, C. Exploring specificity of glycosyltransferases: synthesis of new sugar nucleotide related molecules as putative donor substrates. *Carbohydr Res* **2008**, *343*, 167-178.

(140) Jain, A. C.; Nayyar, N. K.; Arya, P. *Indian J. Chem.* **1986**, *25B*, 259-263 .

(141) Sato, S.; Hiroe, K.; Kumazawa, T.; Jun-ichi, O. Total synthesis of two isoflavone C-glycosides: genistein and orobol 8-C-beta-D-glucopyranosides. *Carbohydr Res* **2006**, *341*, 1091-1095.

(142) White, J. D.; Hrnciar, P.; Stappenbeck, F. Asymmetric Total Synthesis of (+)-Codeine via Intramolecular Carbenoid Insertion. *J Org Chem* **1999**, *64*, 7871-7884.

(143) Whitmore, F. C.; Pietrusza, E. W.; Sommer, L. H. Hydrogen-Halogen Exchange Reactions of Triethylsilane. A New Rearrangement of Neopentyl Chloride1. *J Am Chem Soc* **1947**, *69*, 2108-2110.

(144) Jesus, A. R.; Dias, C.; Matos, A. M.; de Almeida, R. F.; Viana, A. S.; Marcelo, F.; Ribeiro, R. T.; Macedo, M. P.; Airoldi, C.; Nicotra, F.; Martins, A.; Cabrita, E. J.; Jimenez-Barbero, J.; Rauter, A. P. Exploiting the therapeutic potential of 8-beta-d-glucopyranosylgenistein: synthesis, antidiabetic activity, and molecular interaction with islet amyloid polypeptide and amyloid beta-peptide (1-42). *J Med Chem* **2014**, *57*, 9463-9472.

(145) Ning, B.-T.; Tang, Y.-M. Establishment of the cell line, HeLa-CD14, transfected with the human CD14 gene. *Oncol Lett* **2012**, *3*, 871-874.

Supplementary Section

1. NMR & MS Data

1.1 Glucosyl donors

Methyl 2,3,4,6-tetra-*O*-benzyl-α-D-glucopyranoside (2)

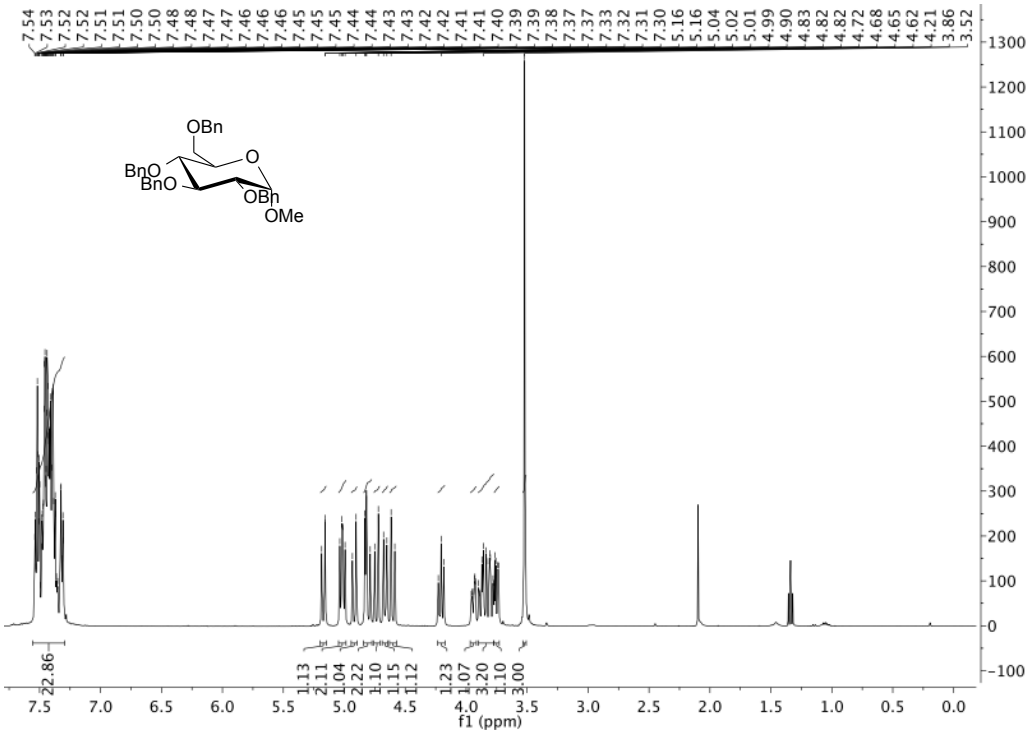

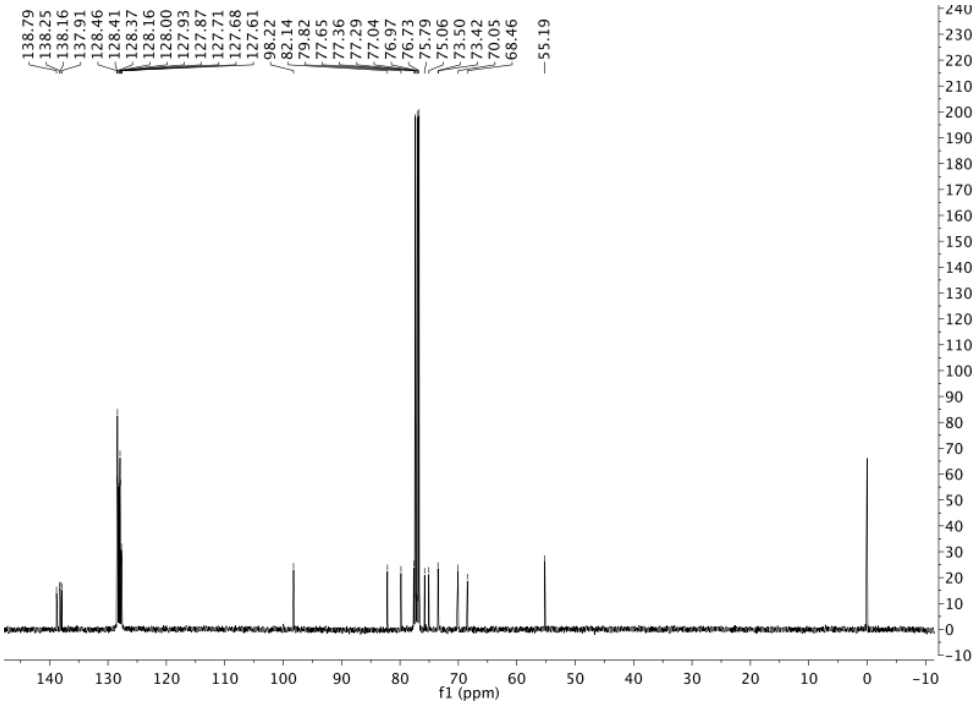

2,3,4,6-tetra-*O*-benzyl-1-isopropyl-α-D-glucopyranose (6)

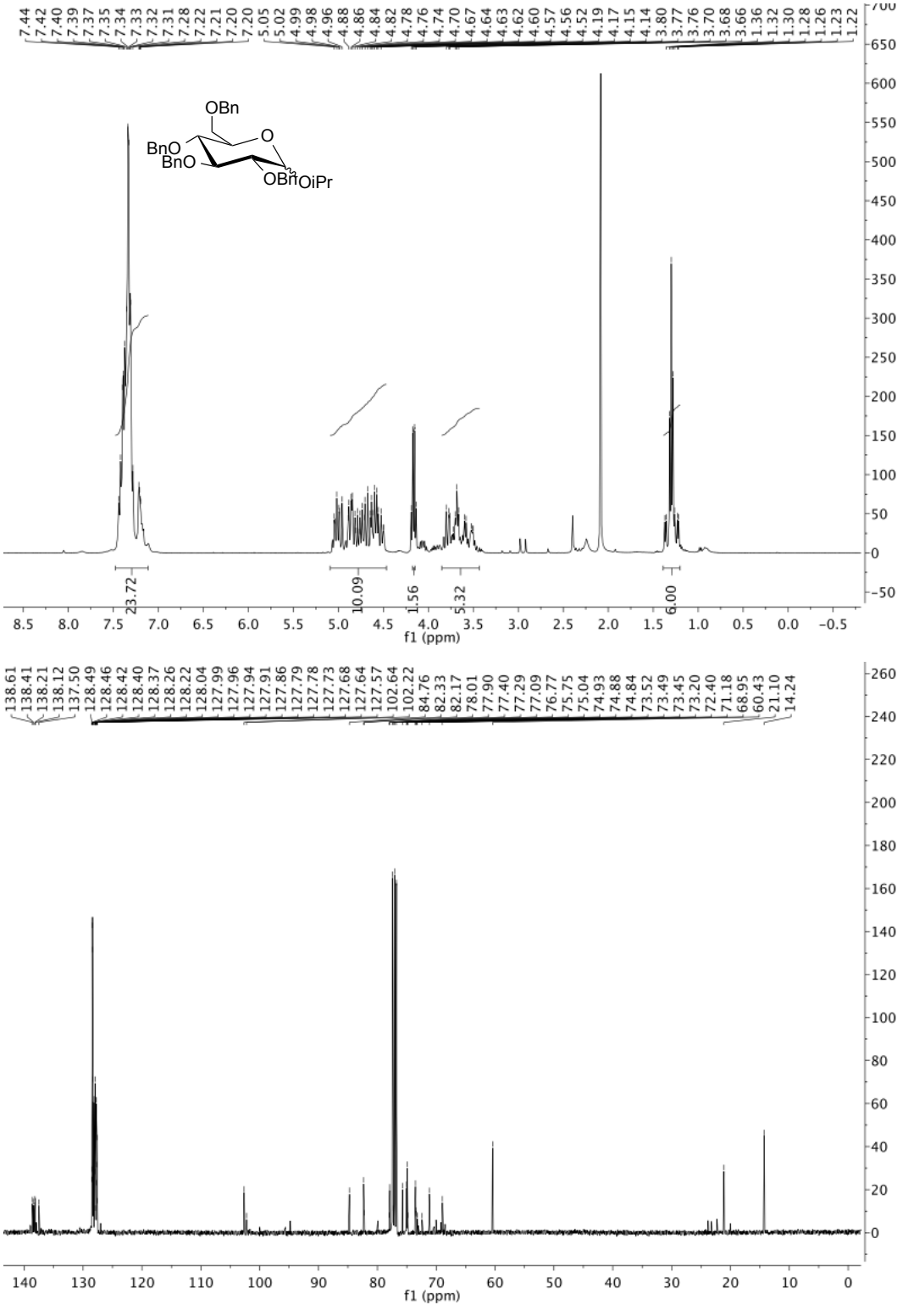

2,3,4,6-tetra-*O*-benzyl-α-D-glucopyranose (**3**)

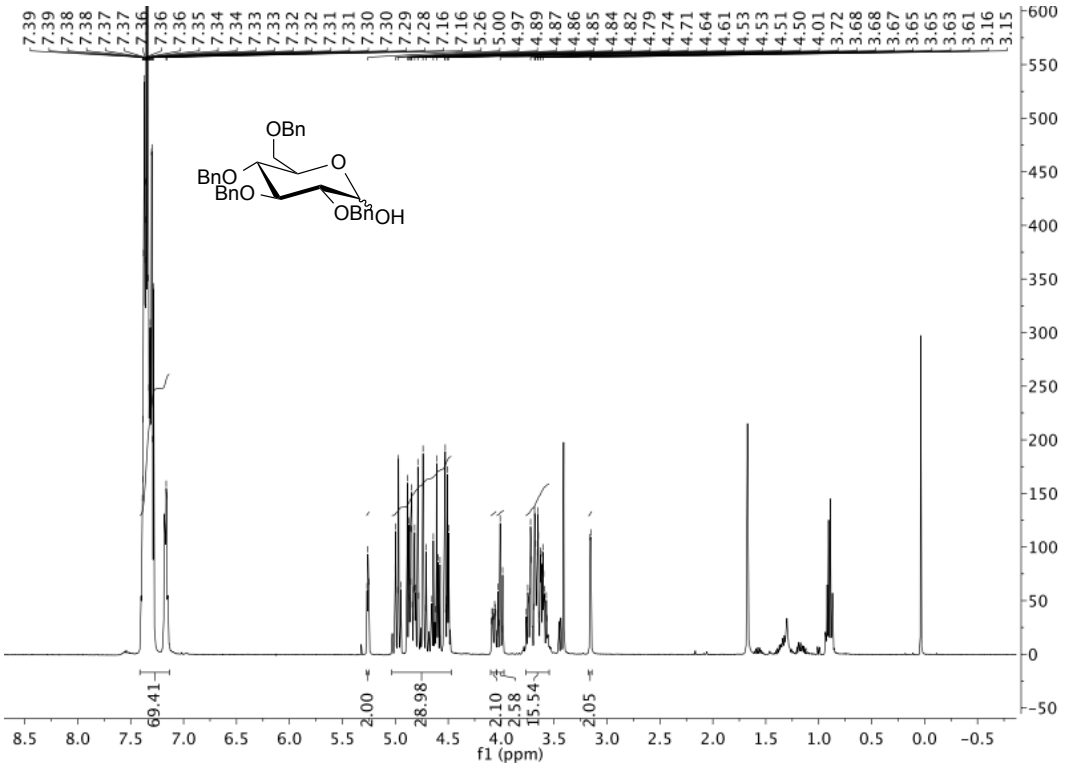

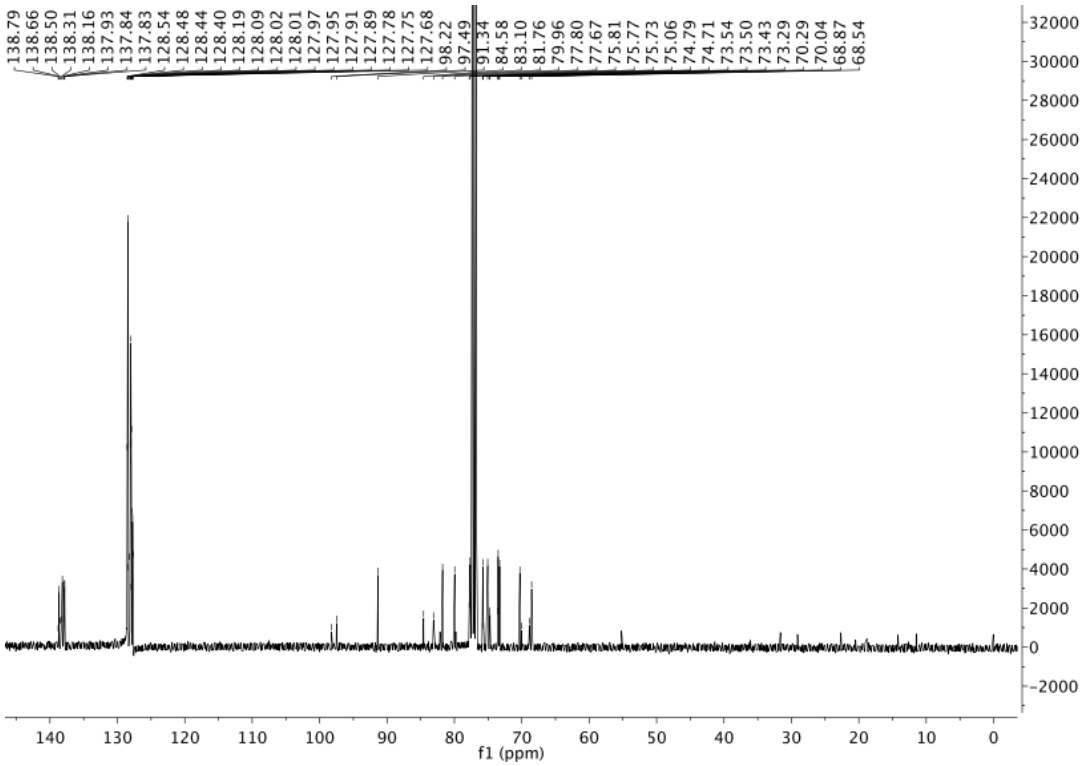

2,3,4,6-tetra-*O*-benzyl-α-D-glucopyranose (4)

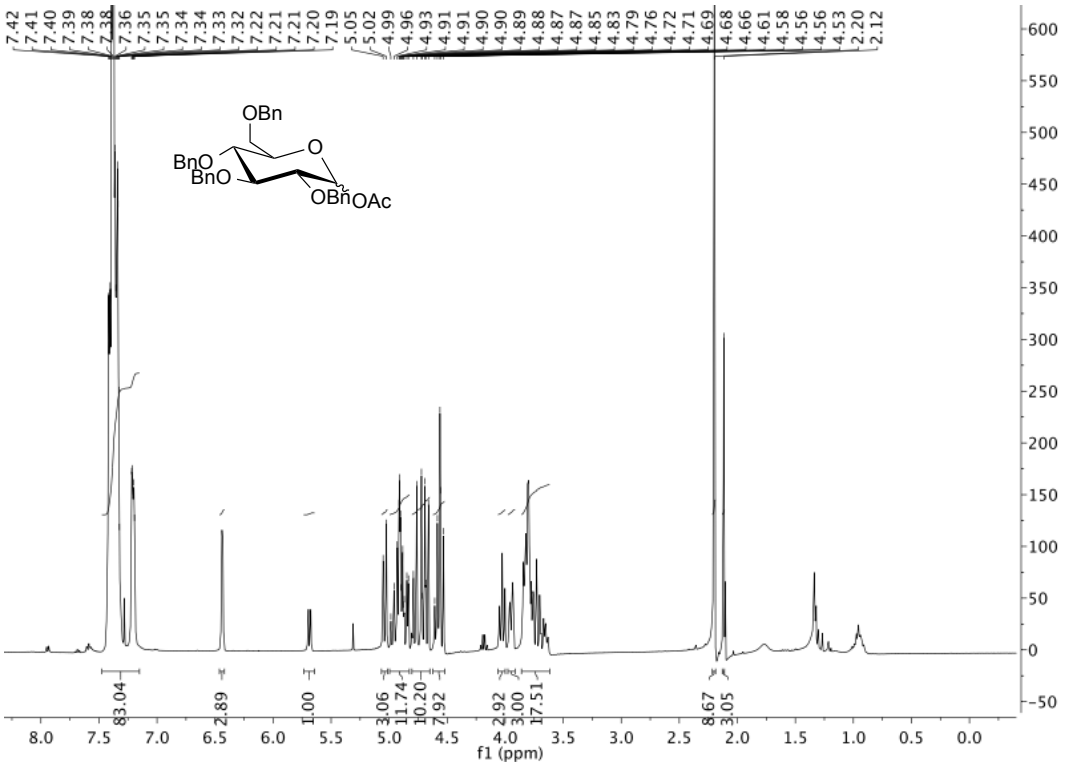

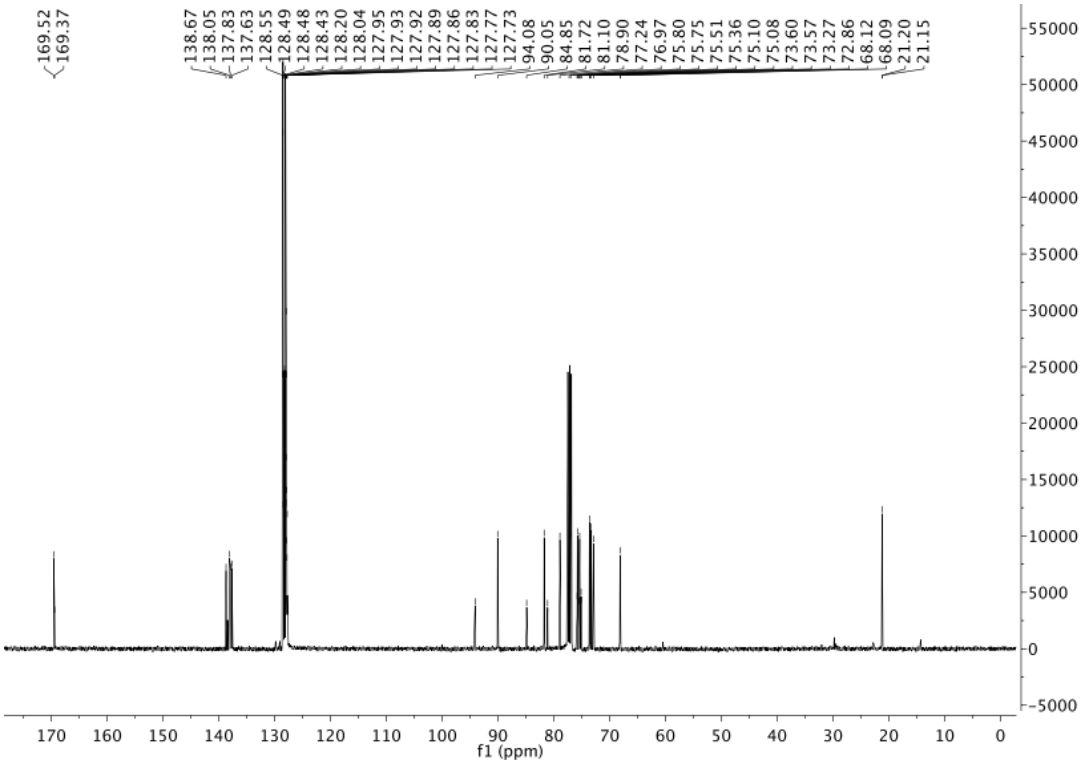

1,2,3,4,6-penta-*O*-acetyl-α-D-glucopyranose (9)

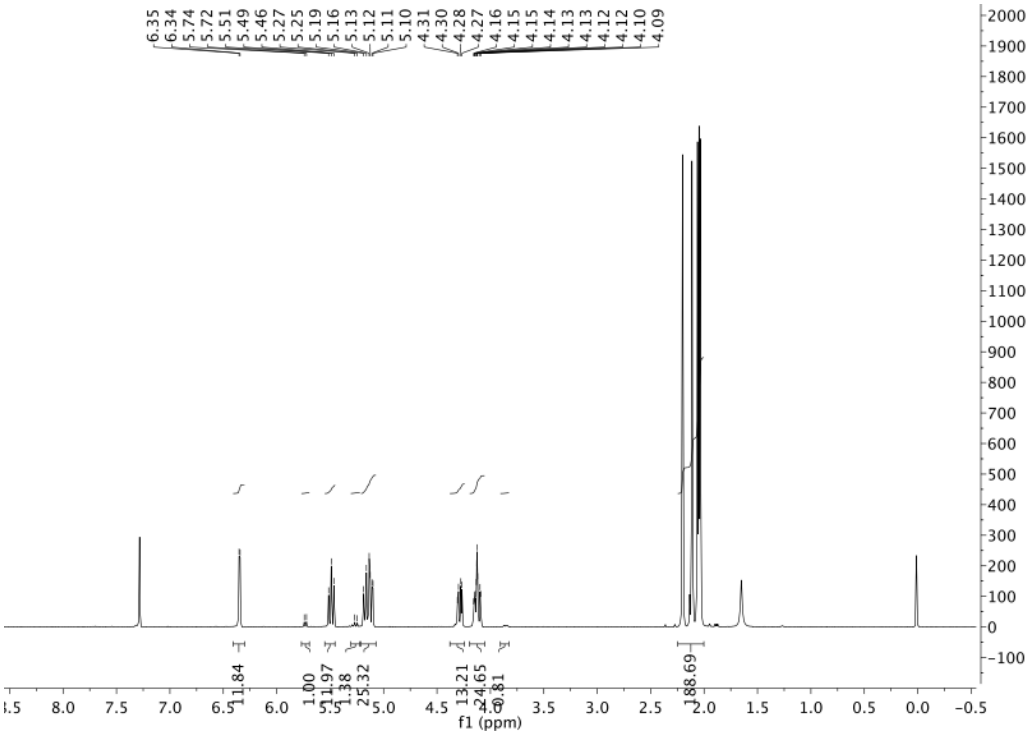

2,3,4,6-tetra-*O*-acetyl-α-D-glucopyranose (10)

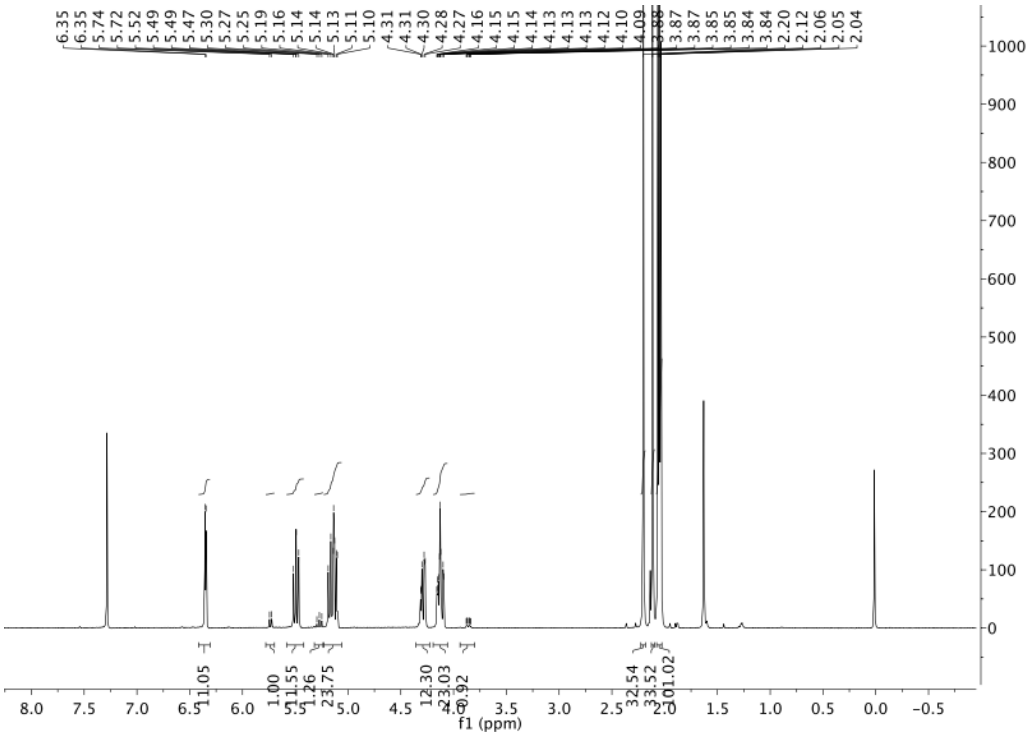

2,3,4,6-tetra-*O*-acetyl-α-D-glucopyranosyl trichloriacetimidate (11)

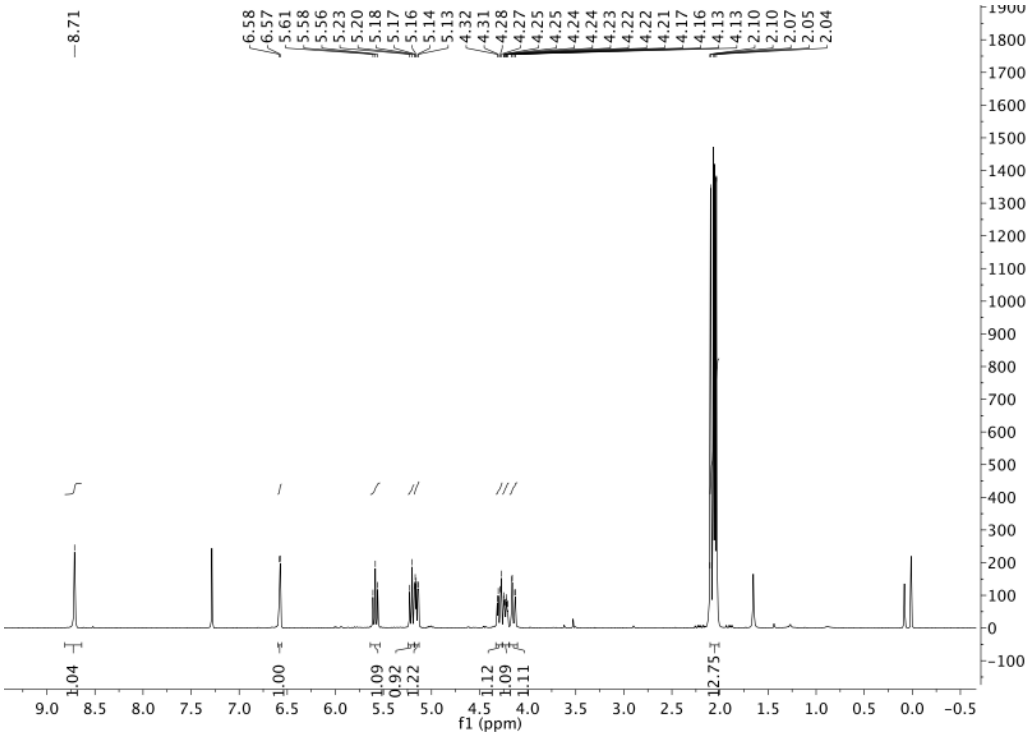

1.2 Protected acetophenones

2′,4′-bis(benzyloxy)-6′-hydroxyacetophenone (14)

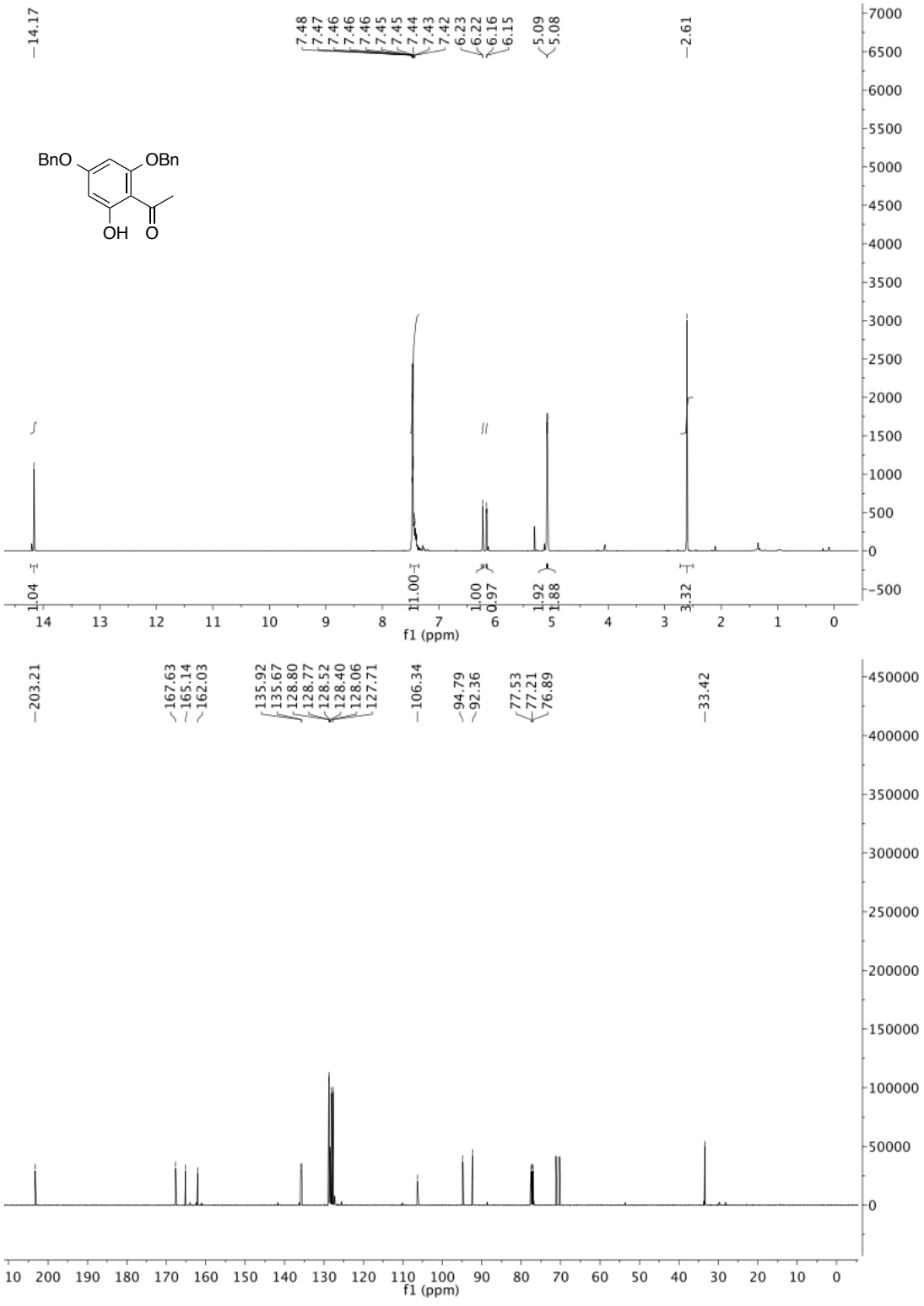

2′,4′-bis(benzyloxy)-3′-benzyl-6′-hydroxyacetophenone (15)

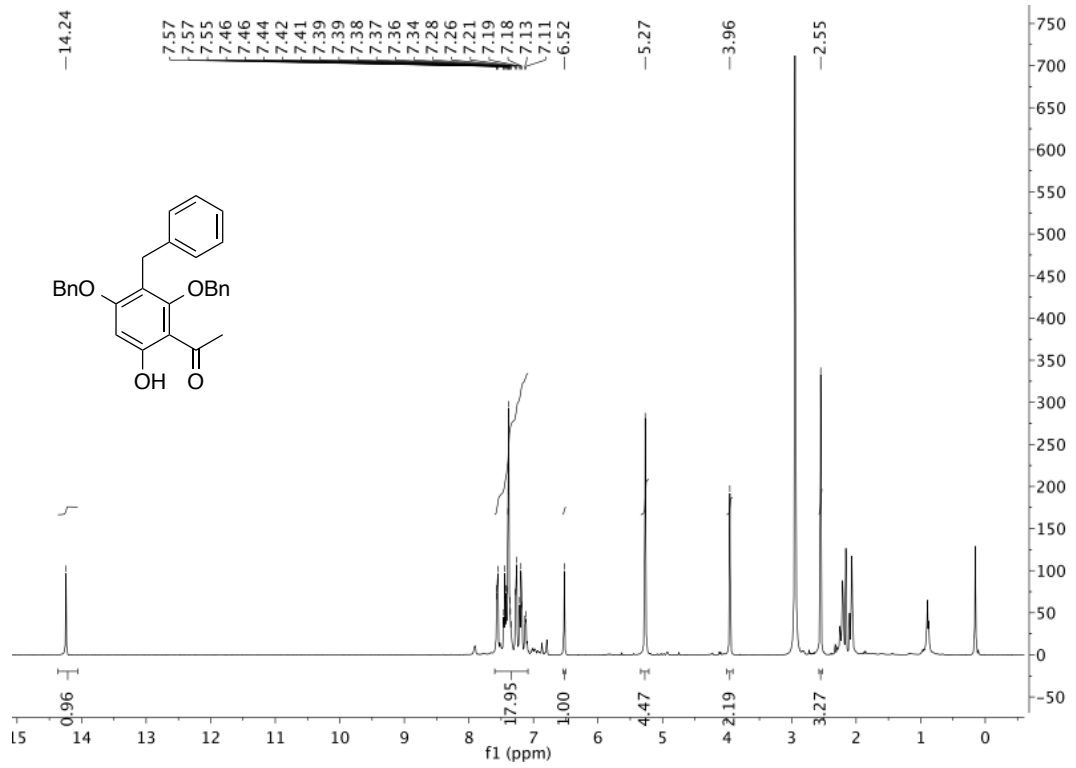

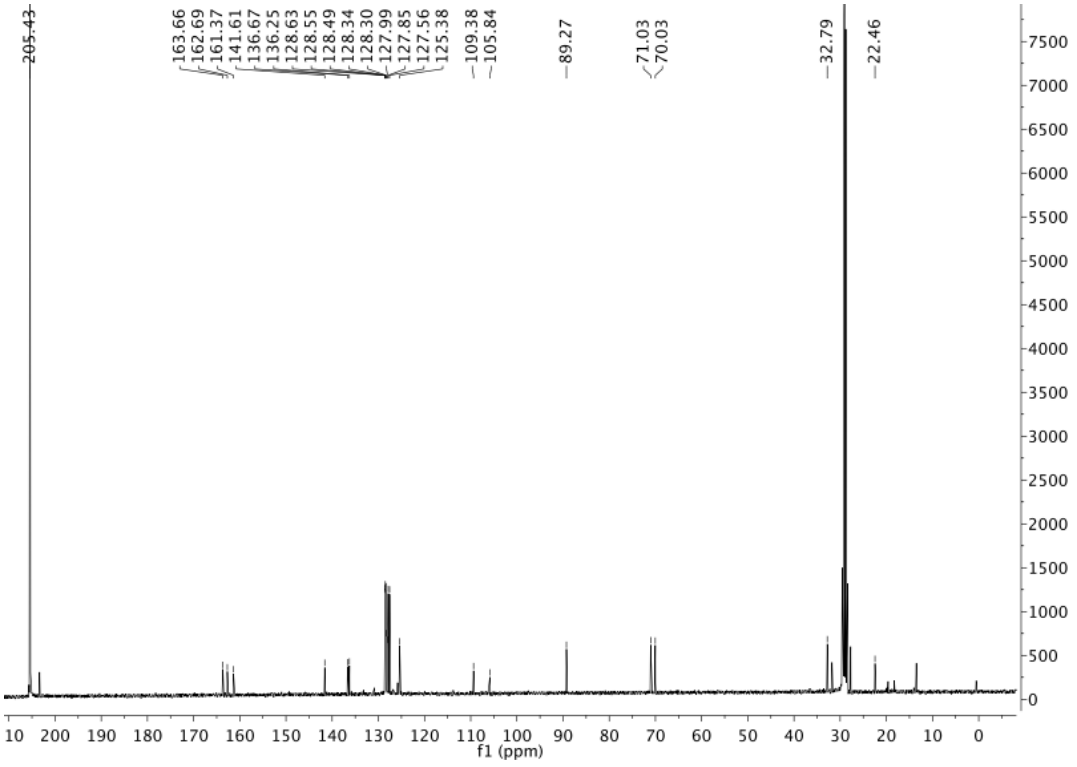

1-(2,4-bis(ethoxymethoxy)-6-hydroxyphenyl)ethan-1-one (20)

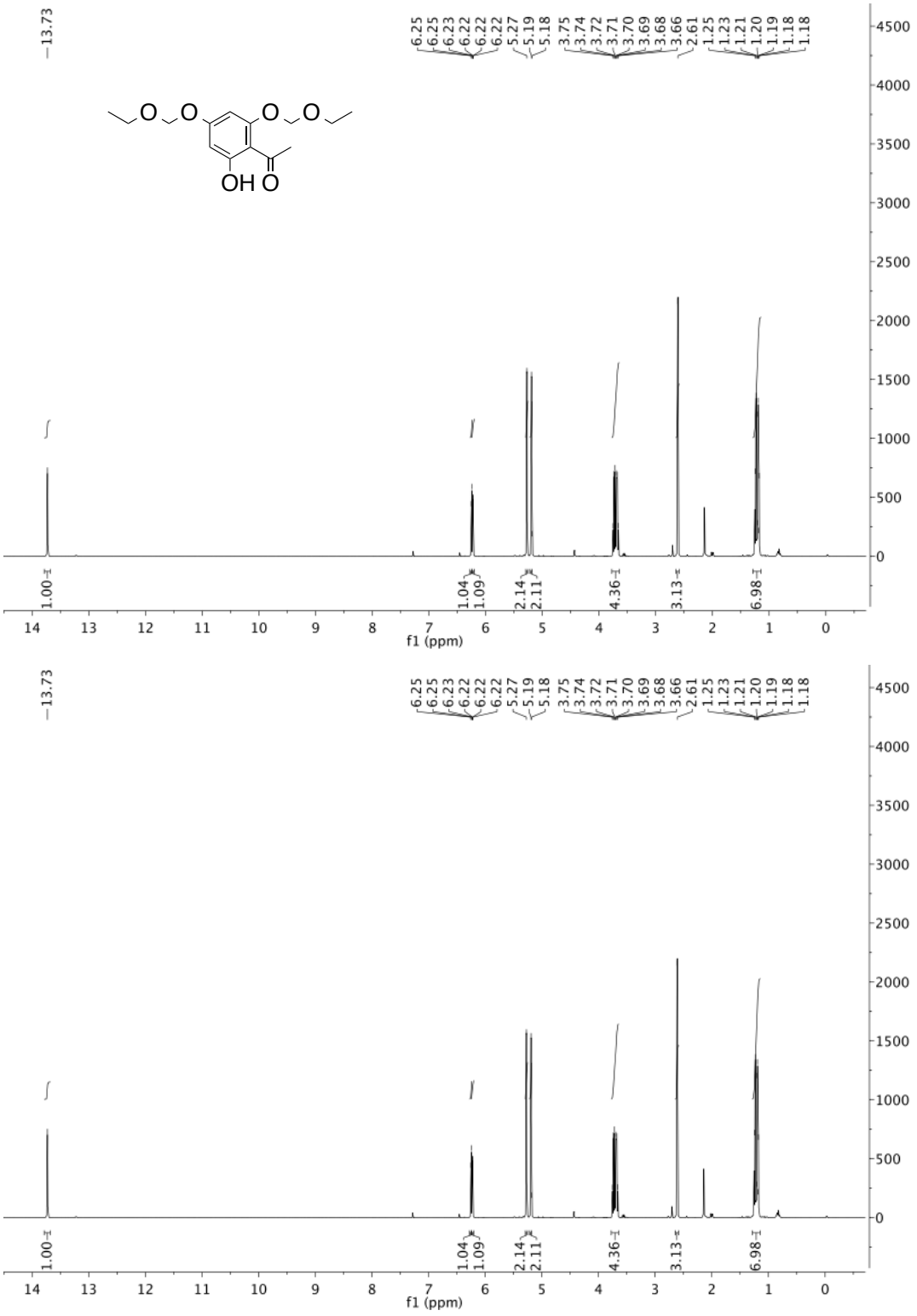

1-(2-(ethoxymethoxy)-6-hydroxyphenyl)ethan-1-one (24)

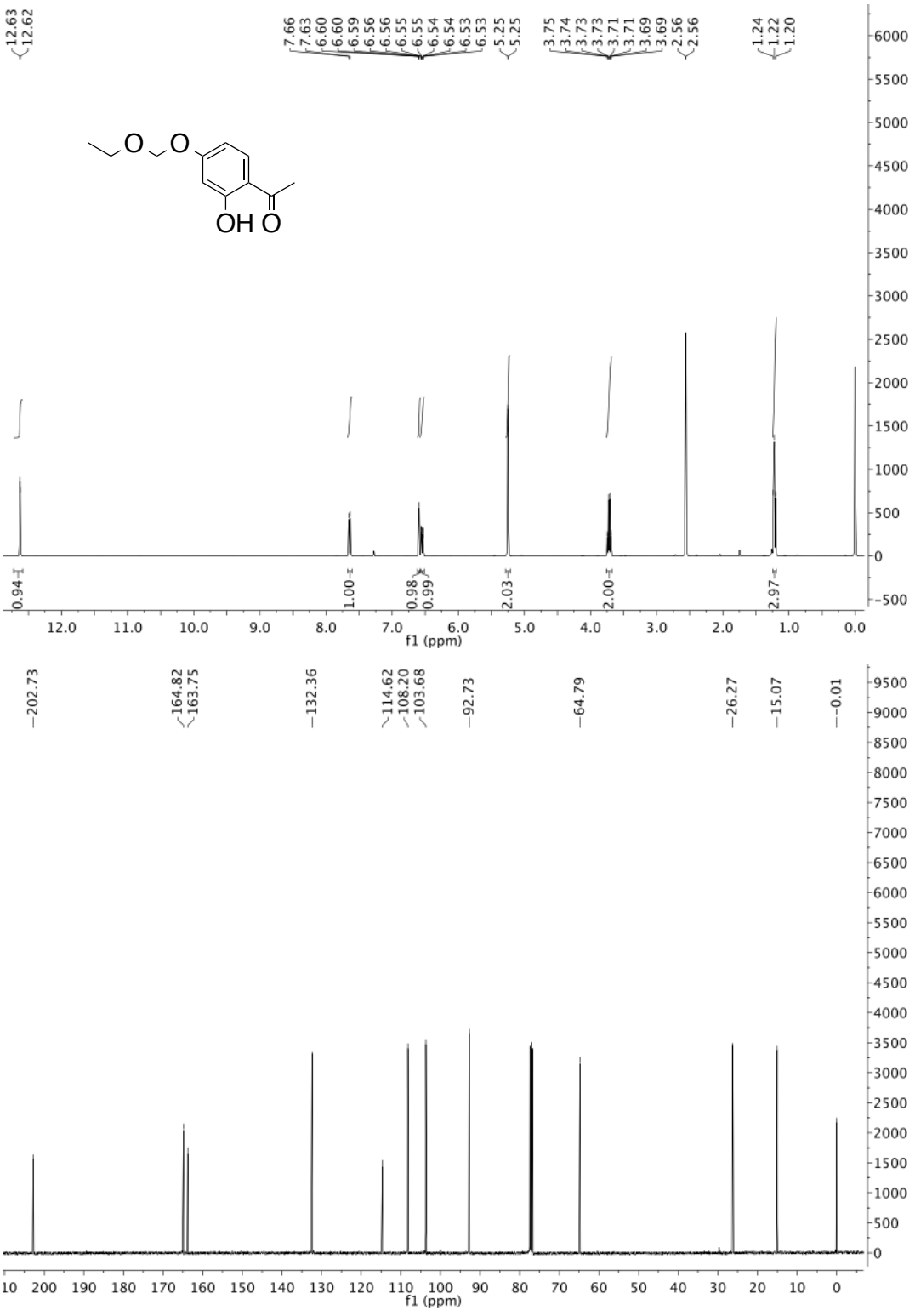

1.3 Aromatic Aldehydes

4-methoxybenzaldehyde (16e)

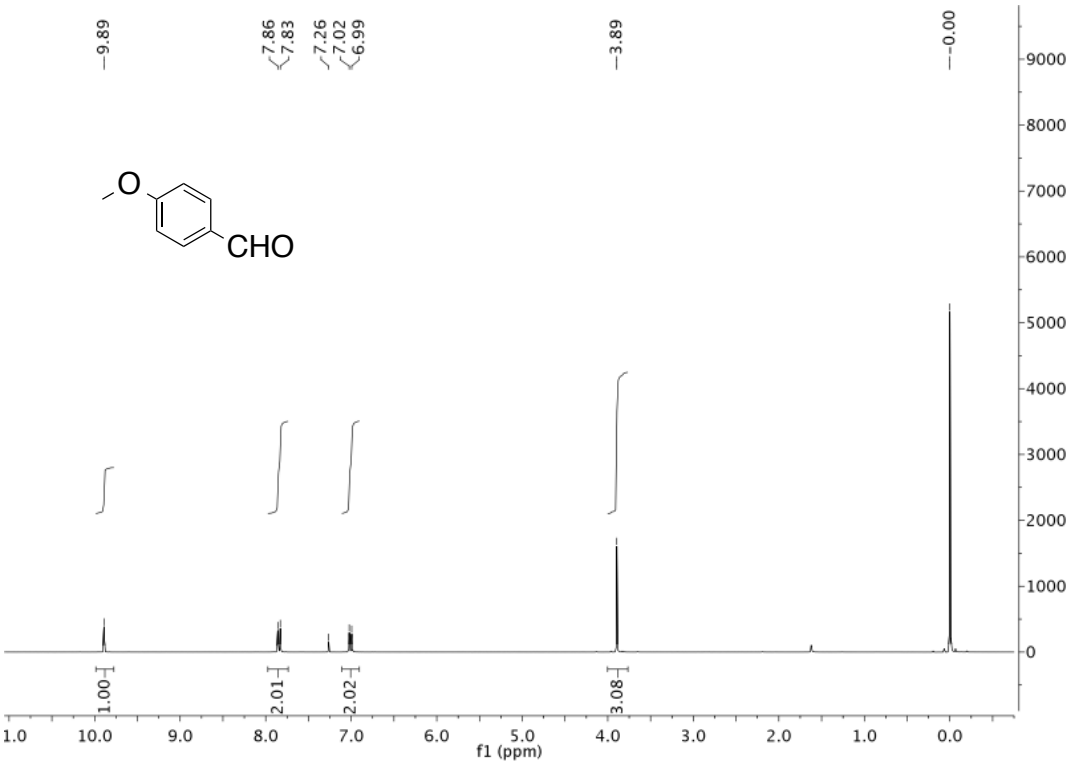

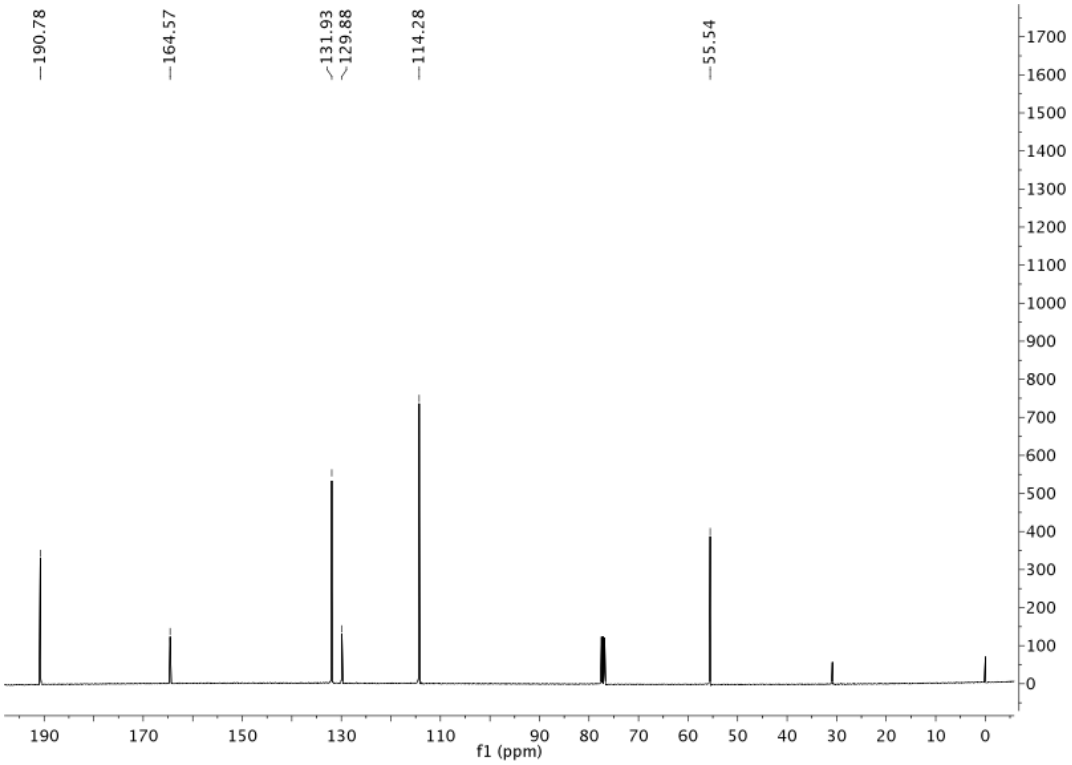

4-ethoxybenzaldehyde (16f)

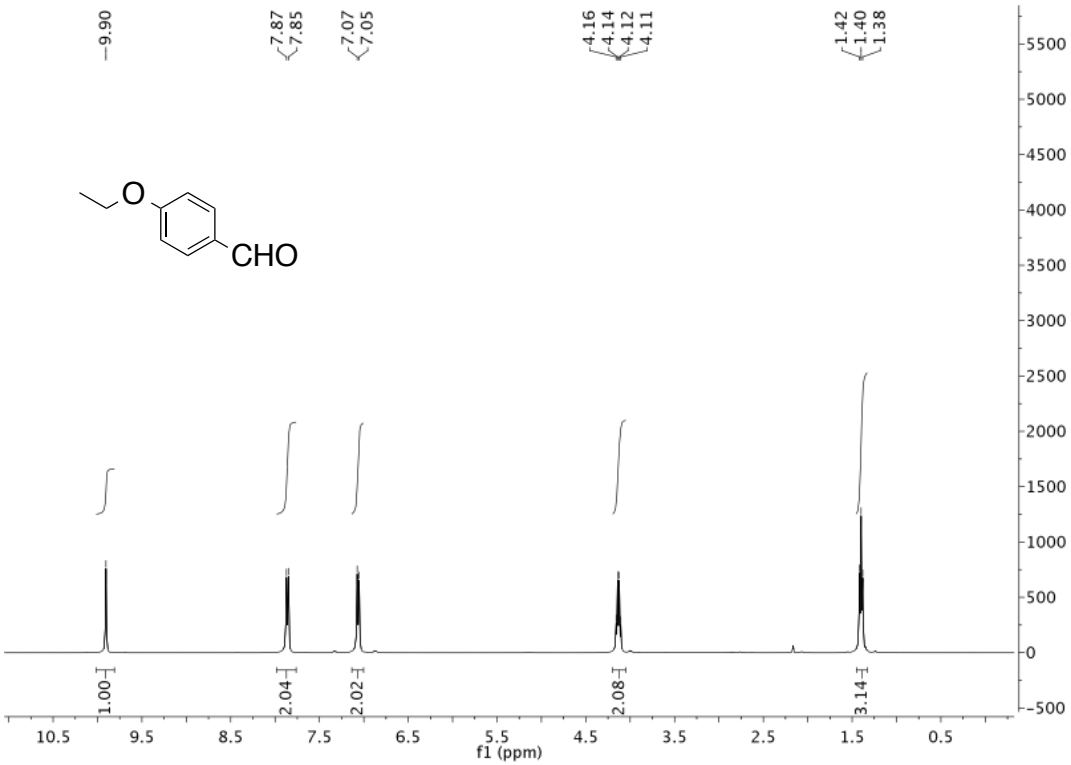

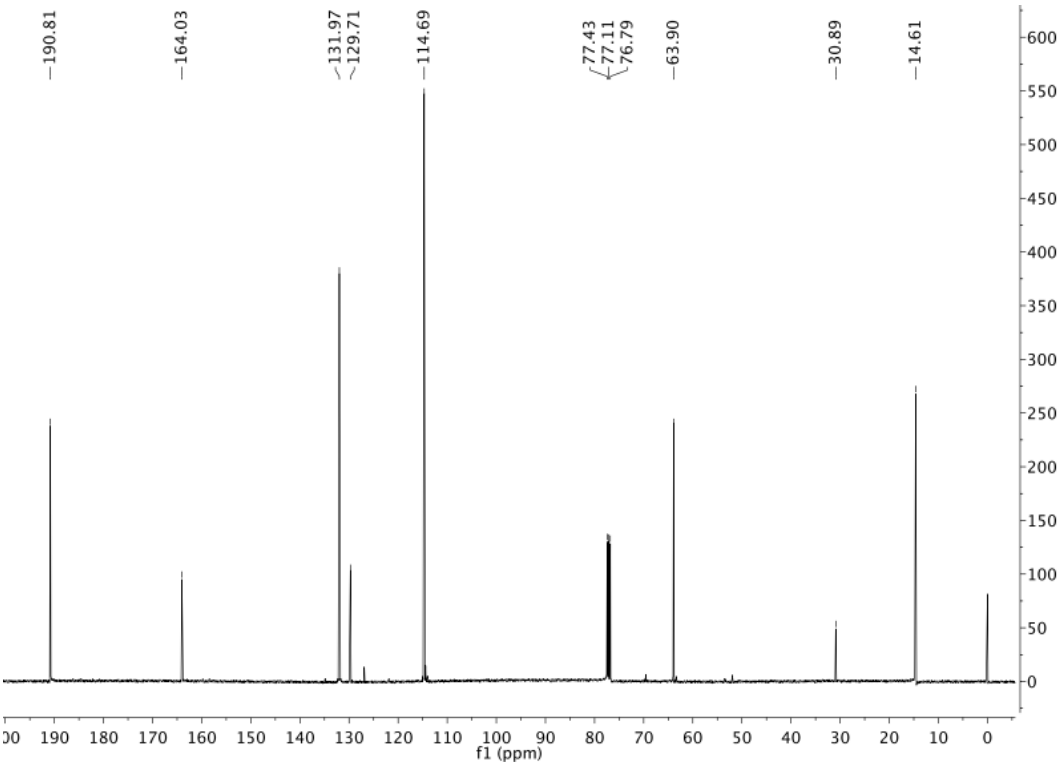

4-allyloxybenzaldehyde (16g)

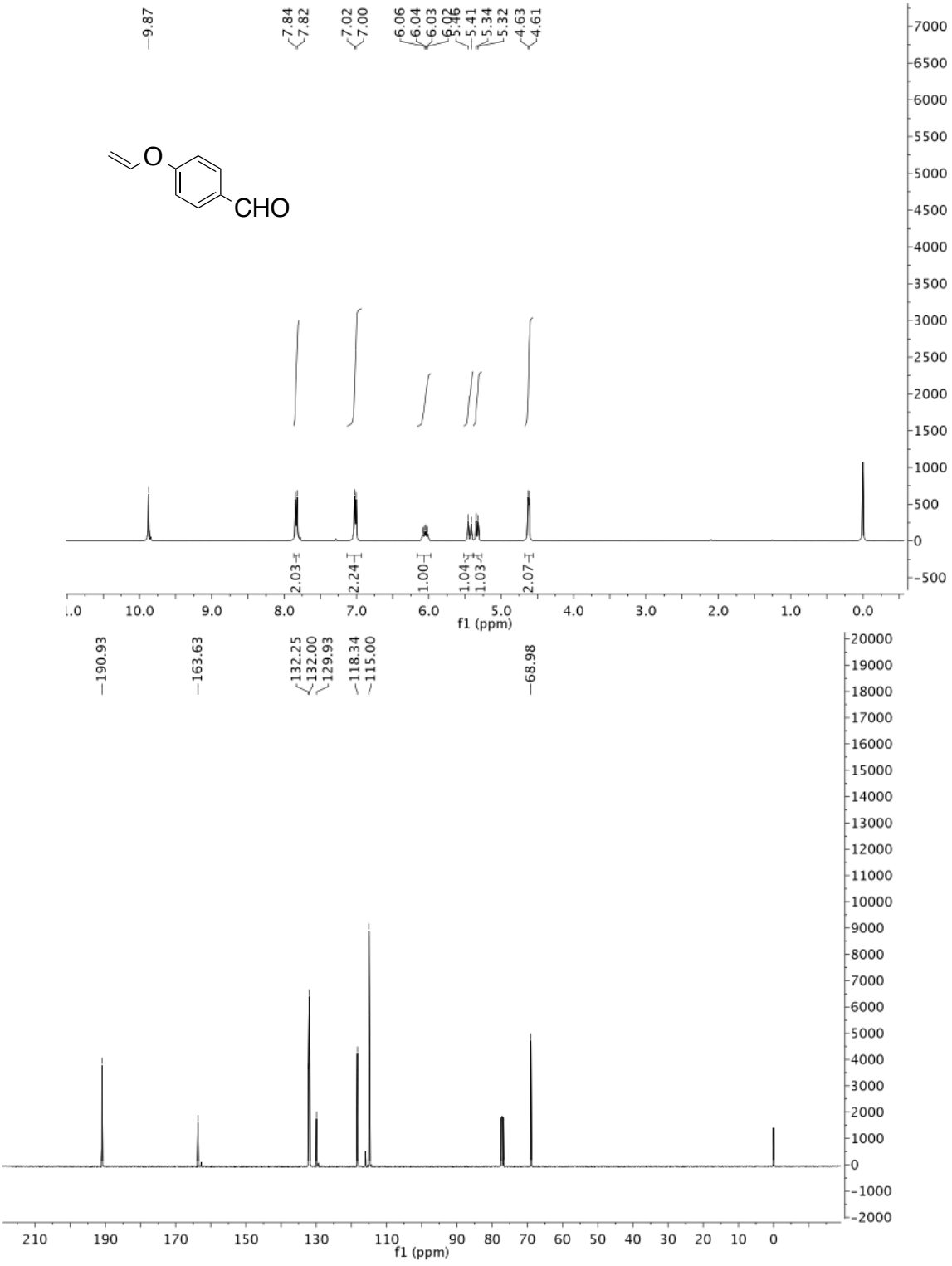

1.4 Protected chalcones

(*E*)-1-[2,4-bis(ethoxymethoxy)-6-hydroxyphenyl]-3-(4-fluorophenyl)prop-2-en-1-one (21a)

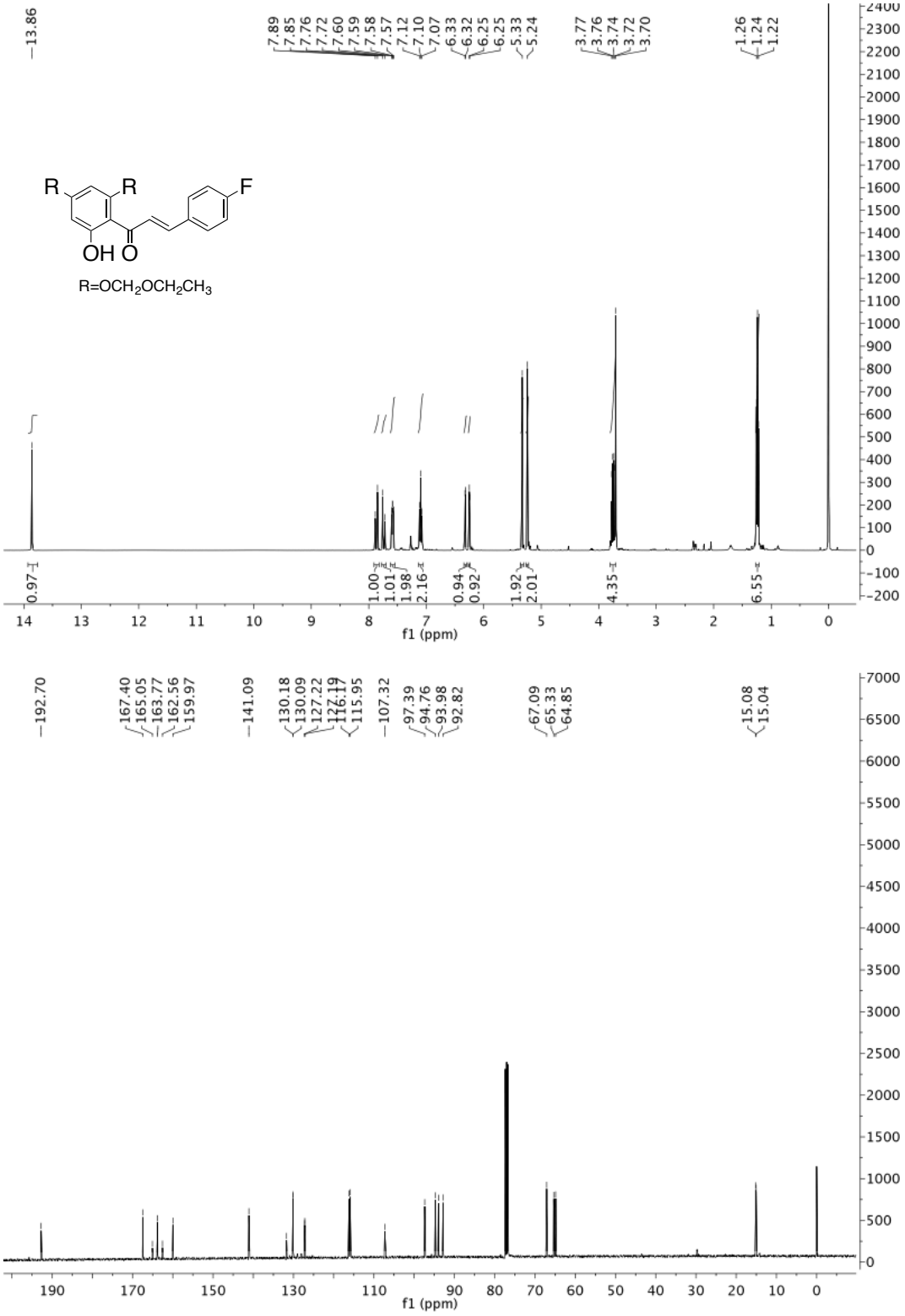

***(E)*-3-(4-bromophenyl)-1-[2,4-bis(ethoxymethoxy)-6-hydroxyphenyl]prop-2-en-1-one (21b)**

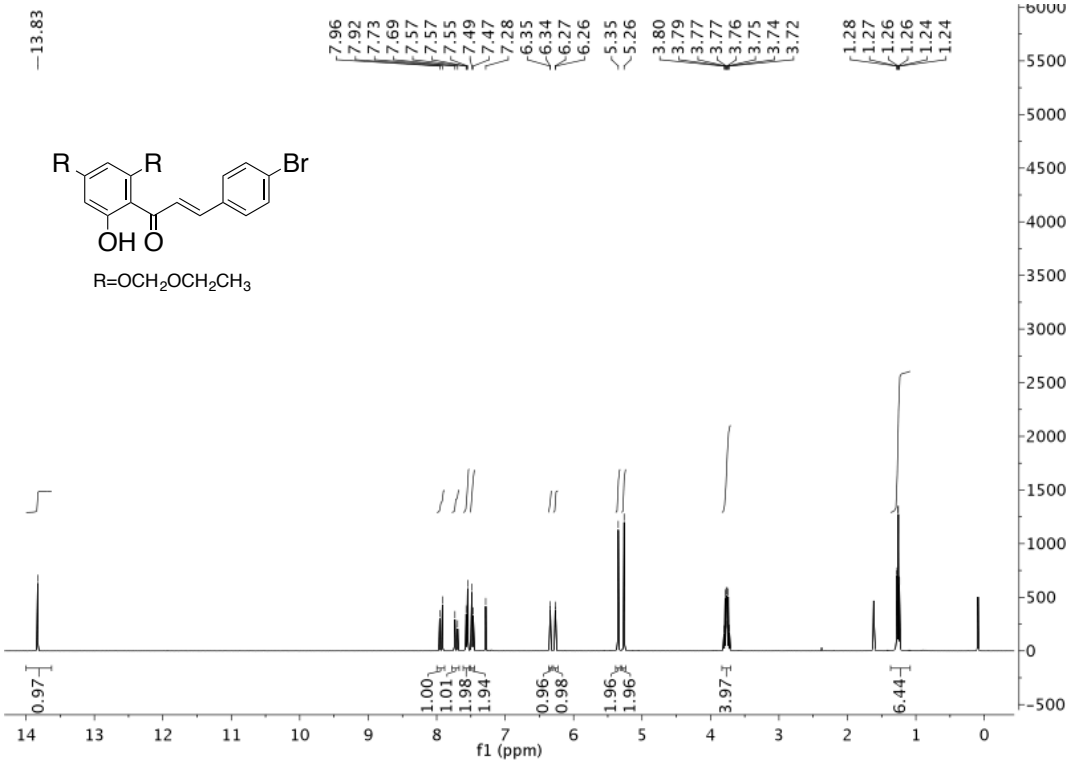

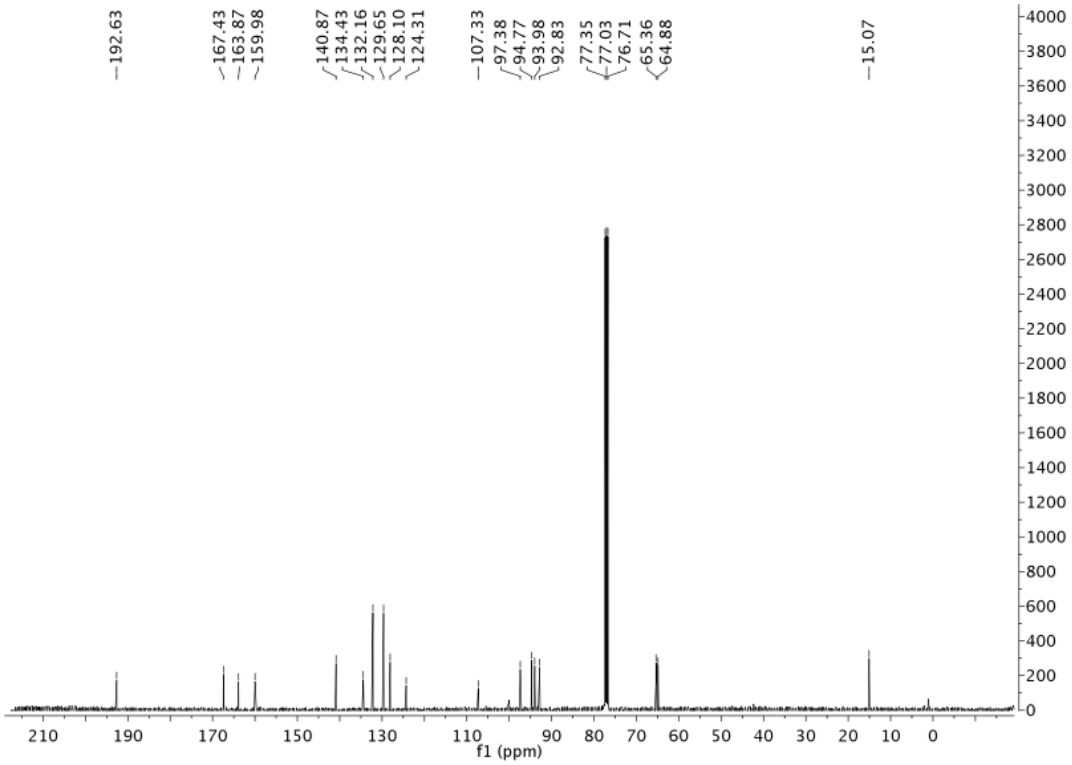

***(E)*-1-[2,4-bis(ethoxymethoxy)-6-hydroxyphenyl]-3-(phenyl)prop-2-en-1-one (21c)**

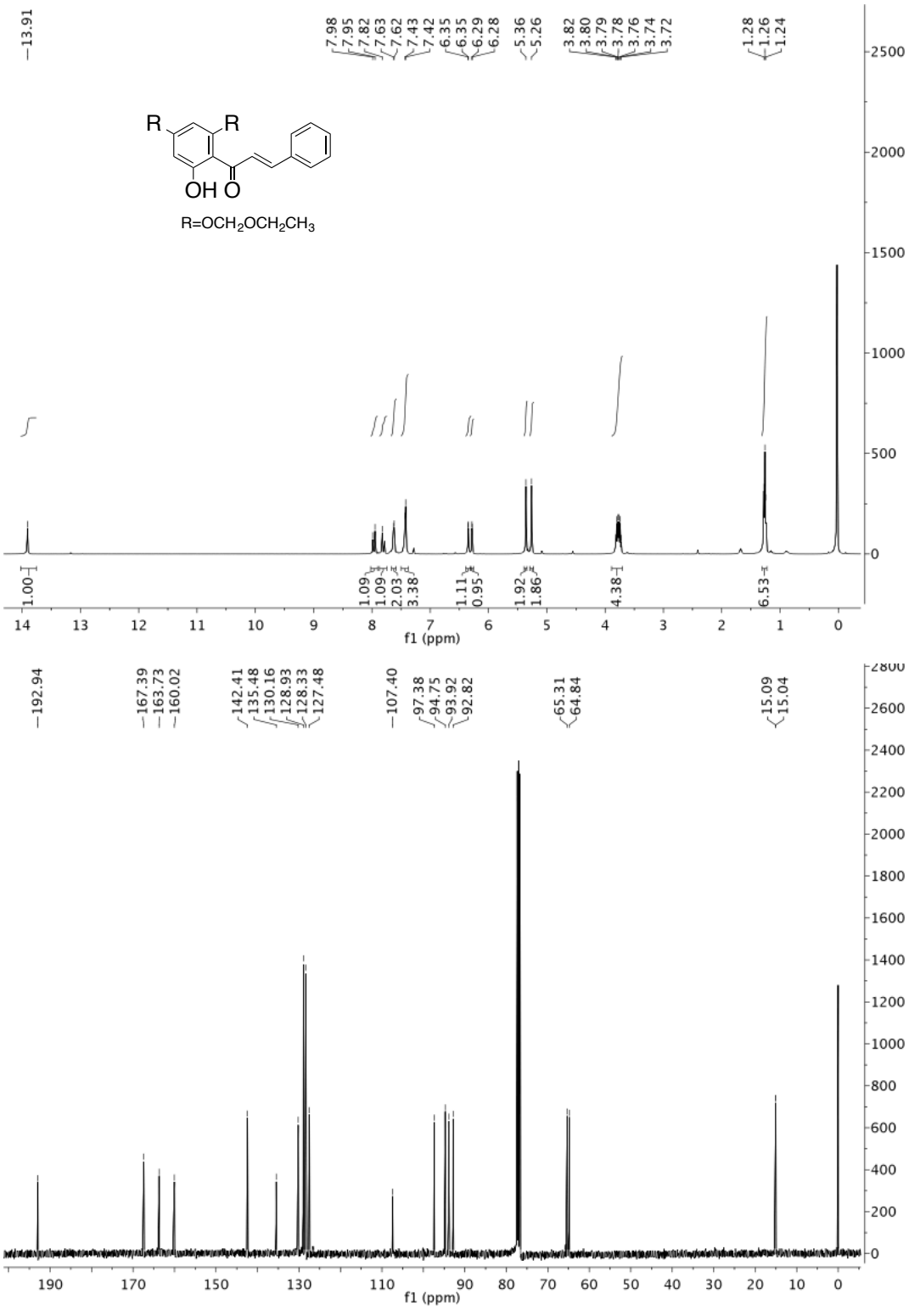

***(E)*-1-[2,4-bis(ethoxymethoxy)-6-hydroxyphenyl]-3-(4-methylphenyl)prop-2-en-1-one (21d)**

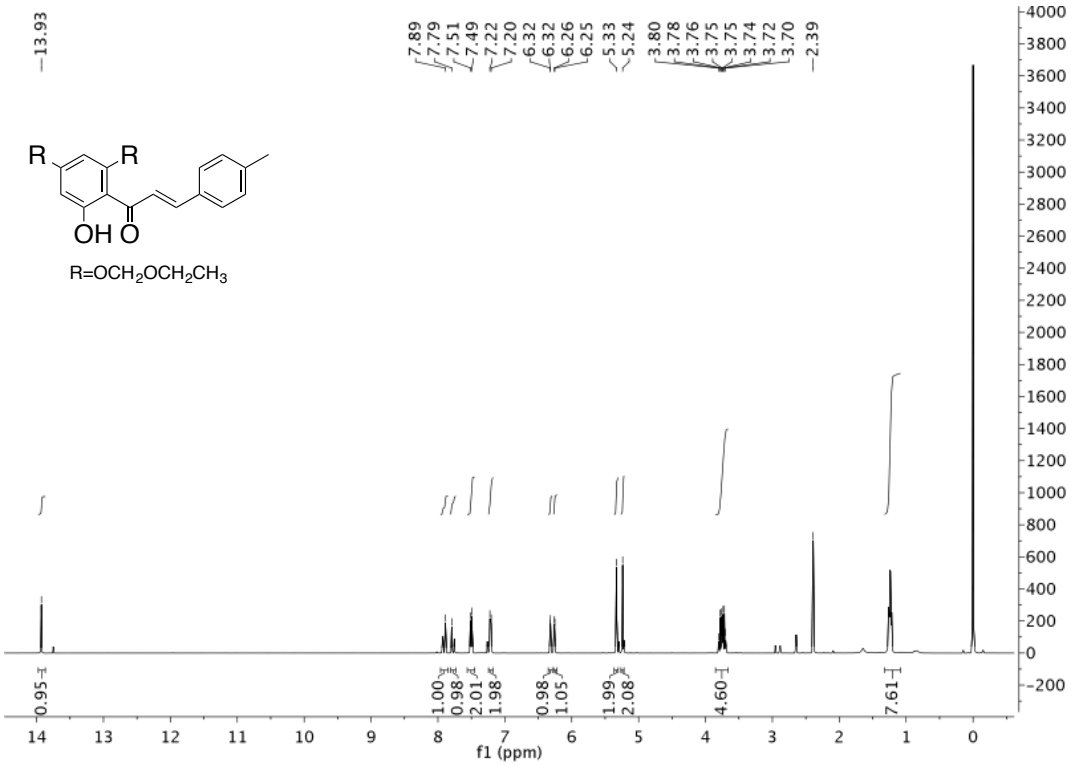

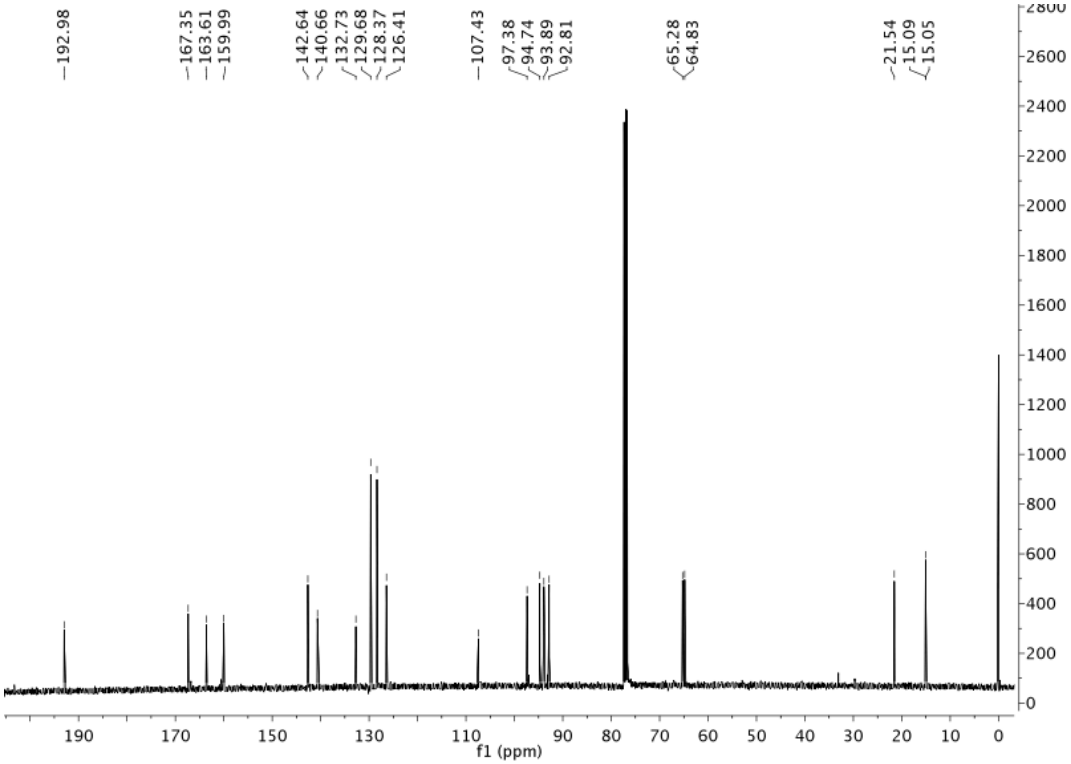

***(E)*-1-[2,4-bis(ethoxymethoxy)-6-hydroxyphenyl]-3-(4-methoxyphenyl)prop-2-en-1-one (21e)**

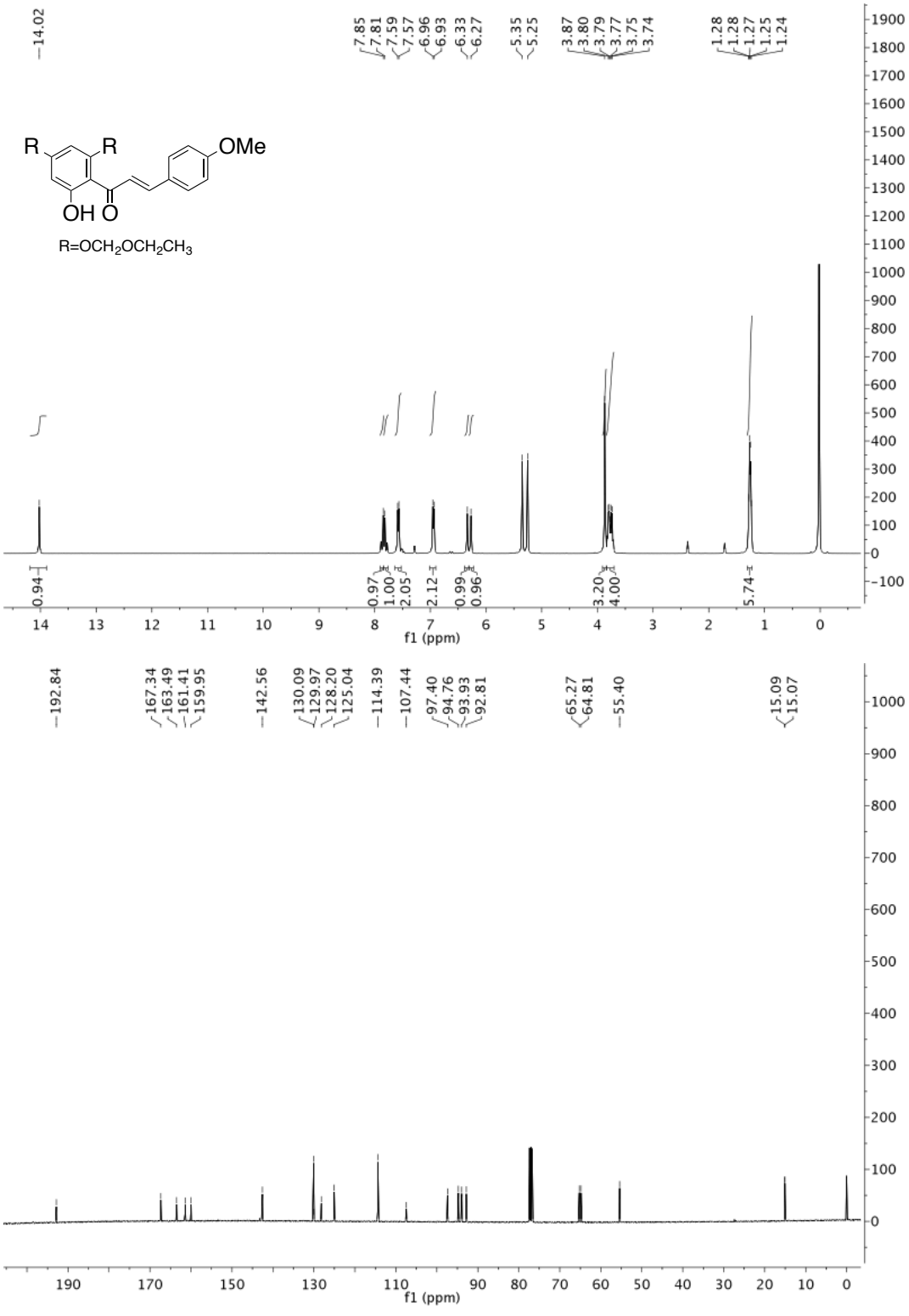

***(E)*-1-[2,4-bis(ethoxymethoxy)-6-hydroxyphenyl]-3-(4-ethoxyphenyl)prop-2-en-1-one (21f)**

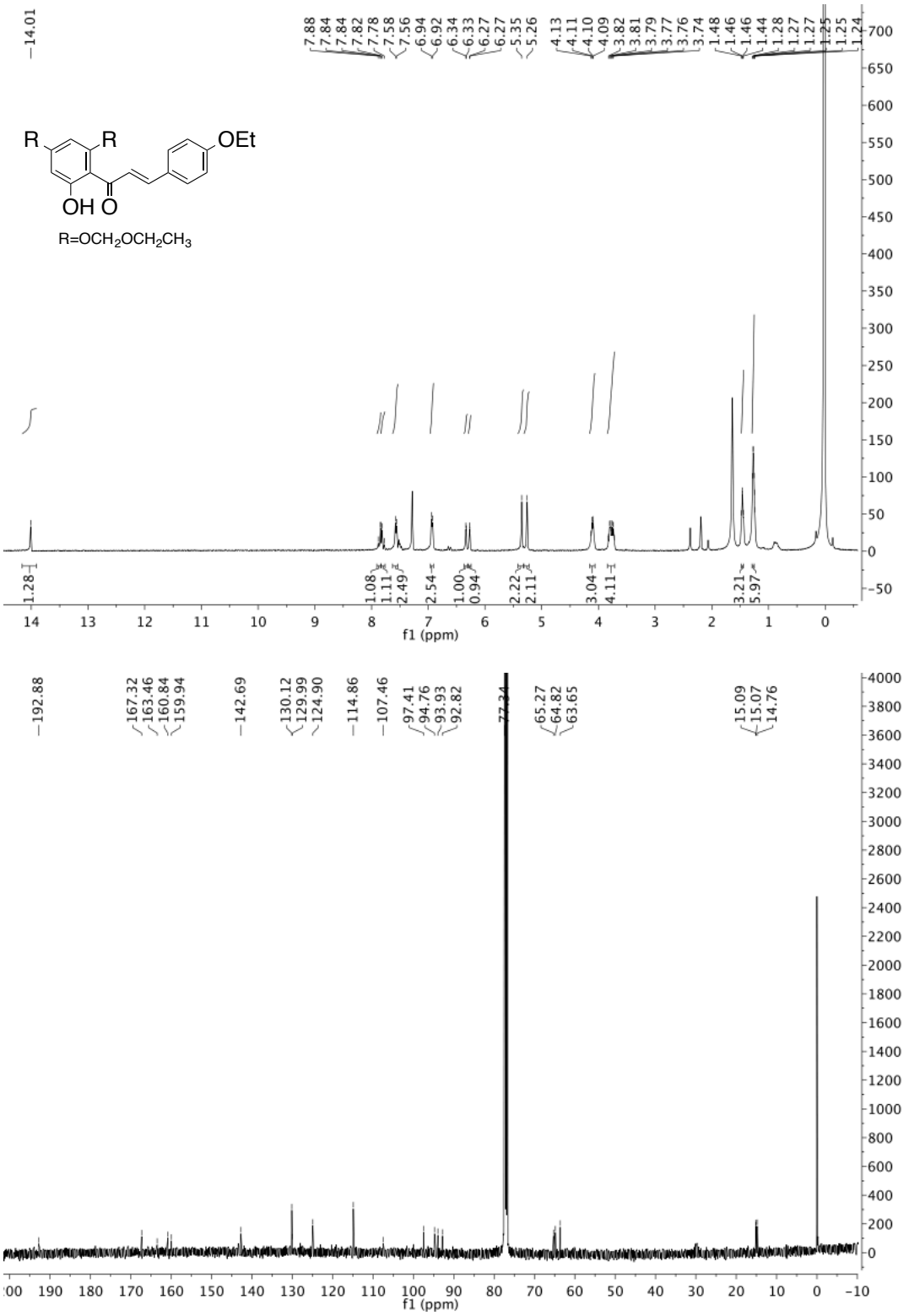

***(E)*-1-[2,4-bis(ethoxymethoxy)-6-hydroxyphenyl]-3-(4-allyloxyphenyl)prop-2-en-1-one (21g)**

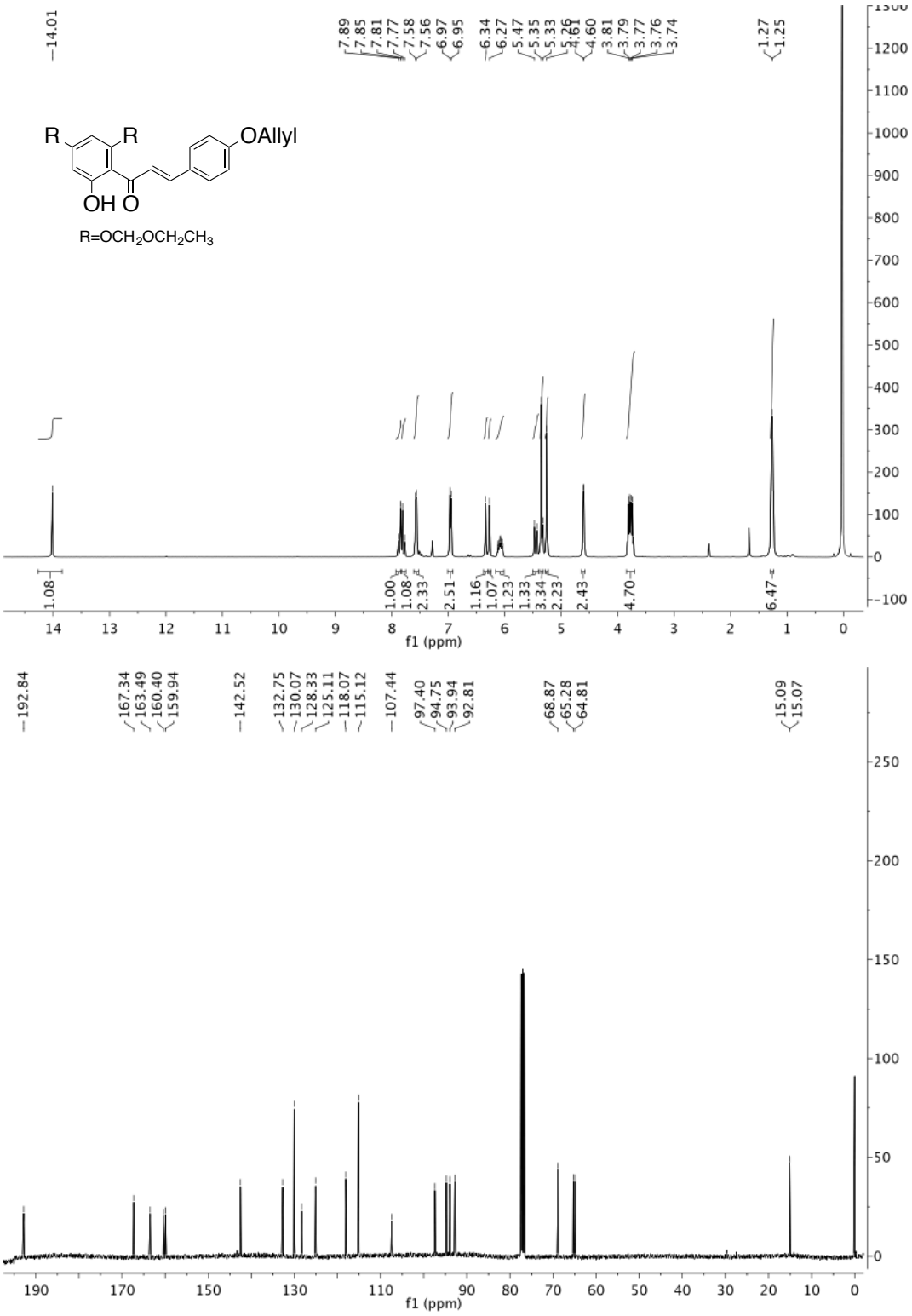

***(E)*-3-(4-(benzyloxy)phenyl)-1-(2,4-bis(ethoxymethoxy)-6-hydroxyphenyl)prop-2-en-1-one (21h)**

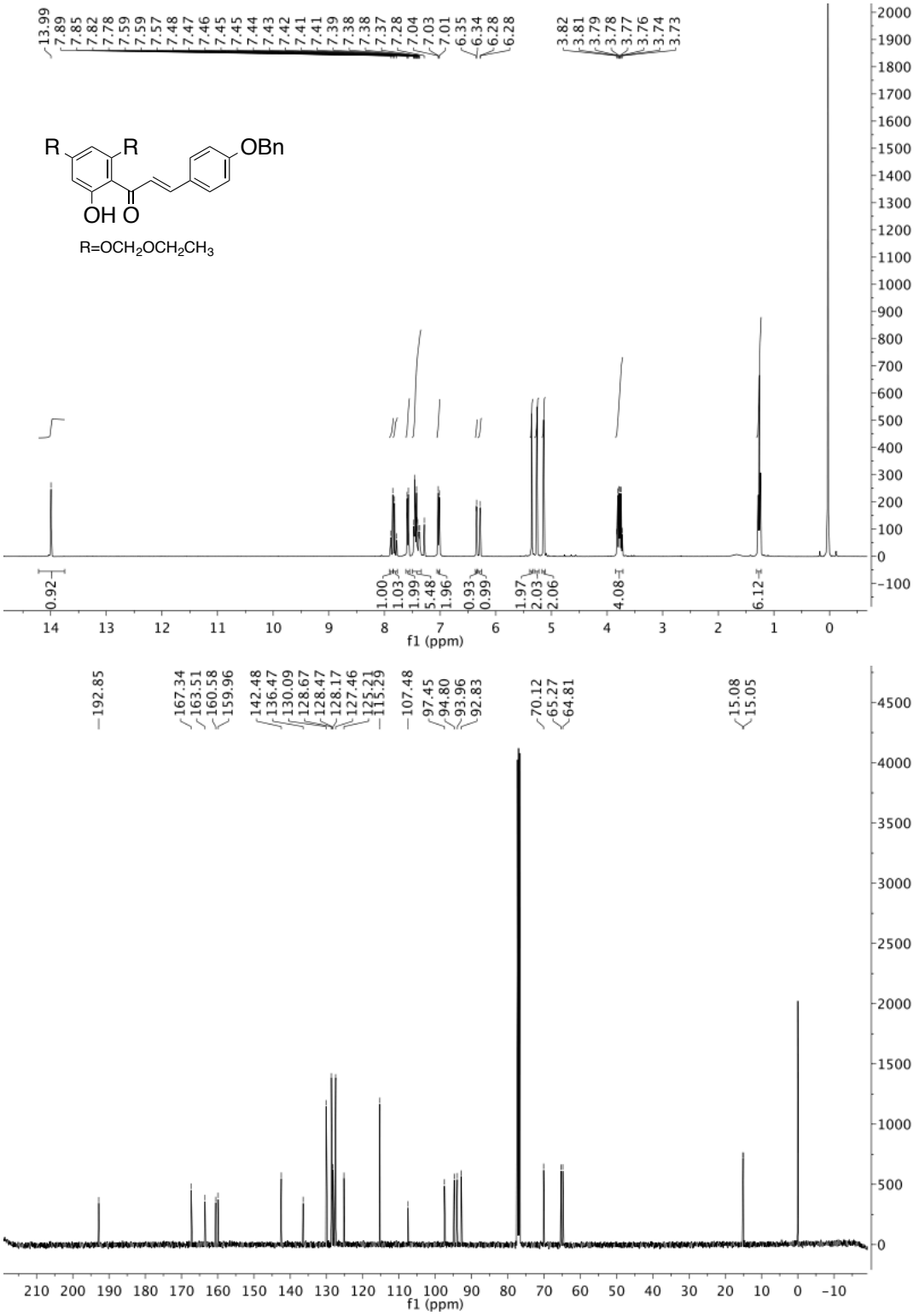

***(E)*-1-[(2,4-bis(ethoxymethoxy)-6-hydroxyphenyl]-3-(5-methylfuran-2-yl)prop-2-en-1-one (21i)**

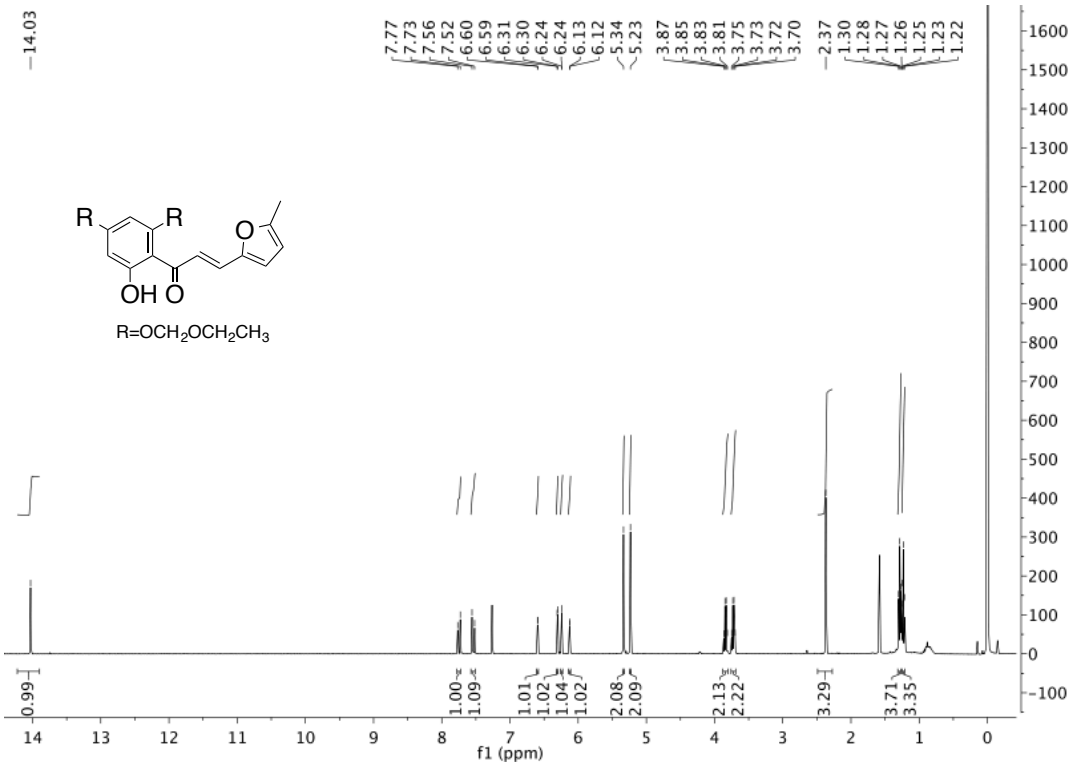

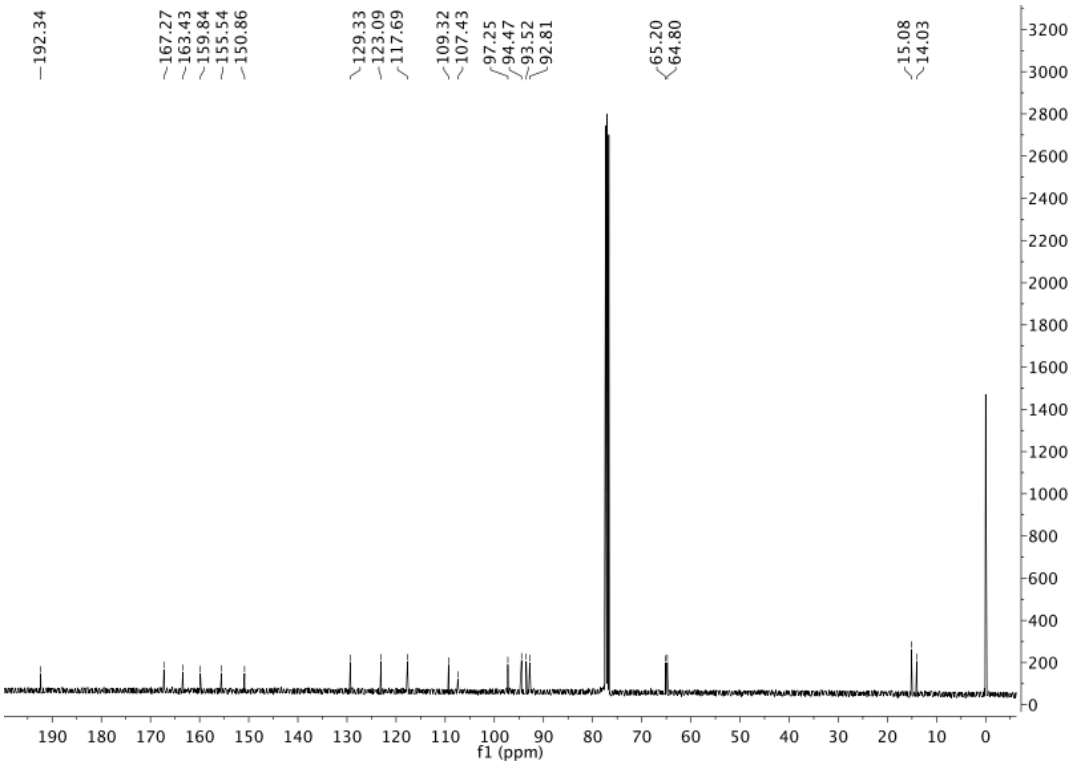

(E)-1-(4-ethoxymethoxy-2-hydroxyphenyl)-3-(4-fluorophenyl)prop-2-en-1-one (25a)

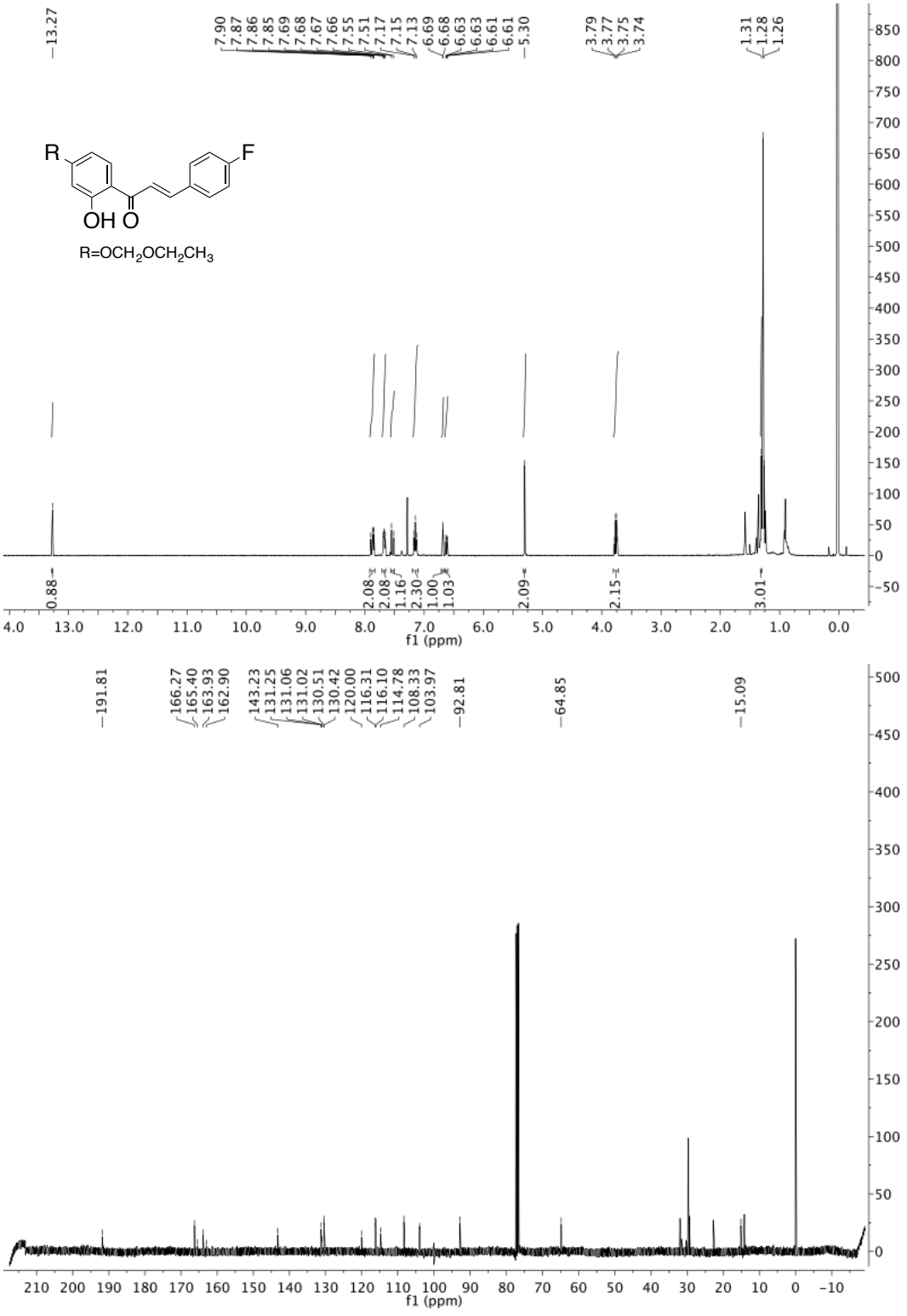

(E)-3-(4-bromophenyl)-1-(4-ethoxymethoxy-2-hydroxyphenyl)prop-2-en-1-one (25b)

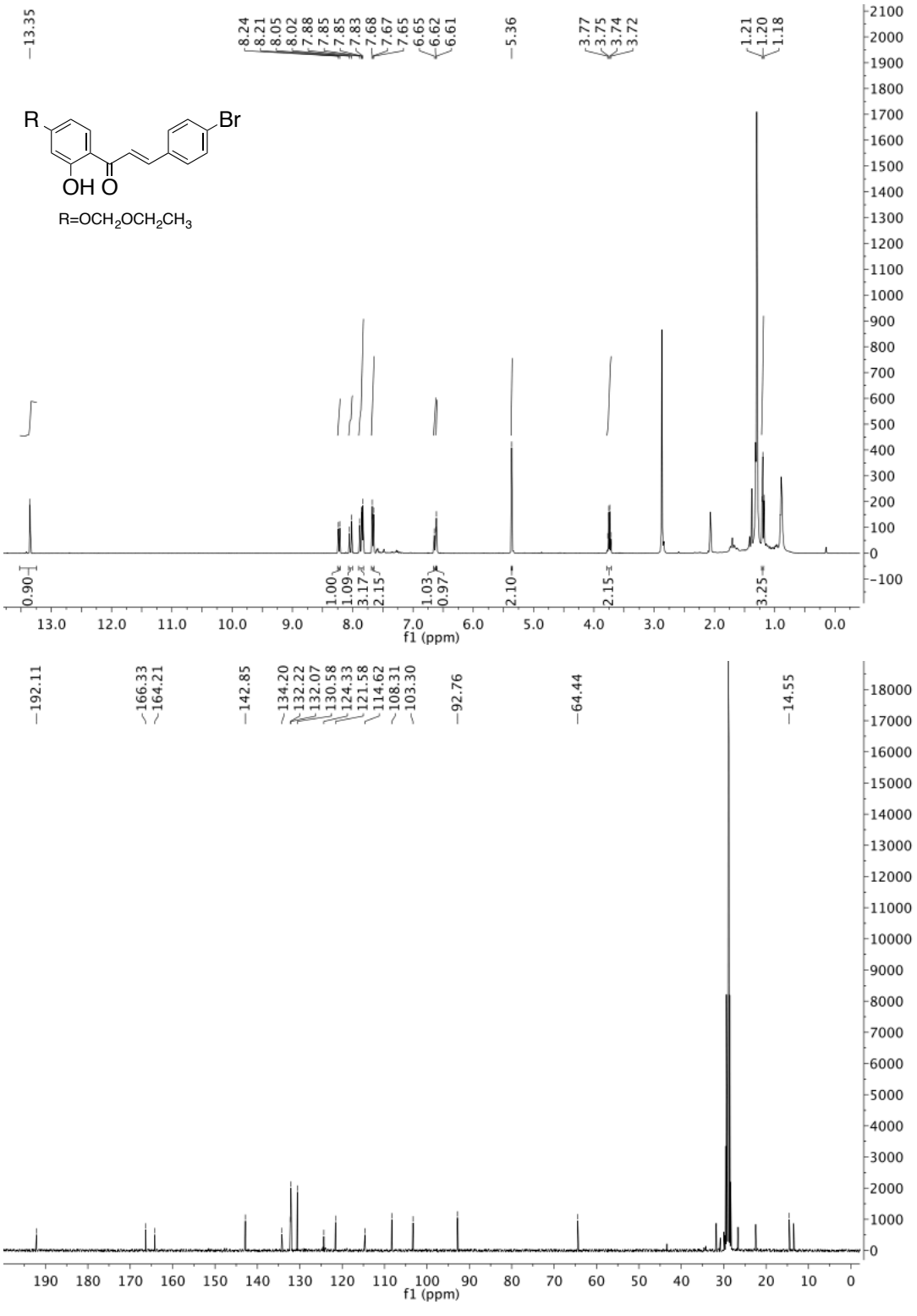

***(E)*-1-(4-ethoxymethoxy-2-hydroxyphenyl)-3-(4-methylphenyl)prop-2-en-1-one (25c)**

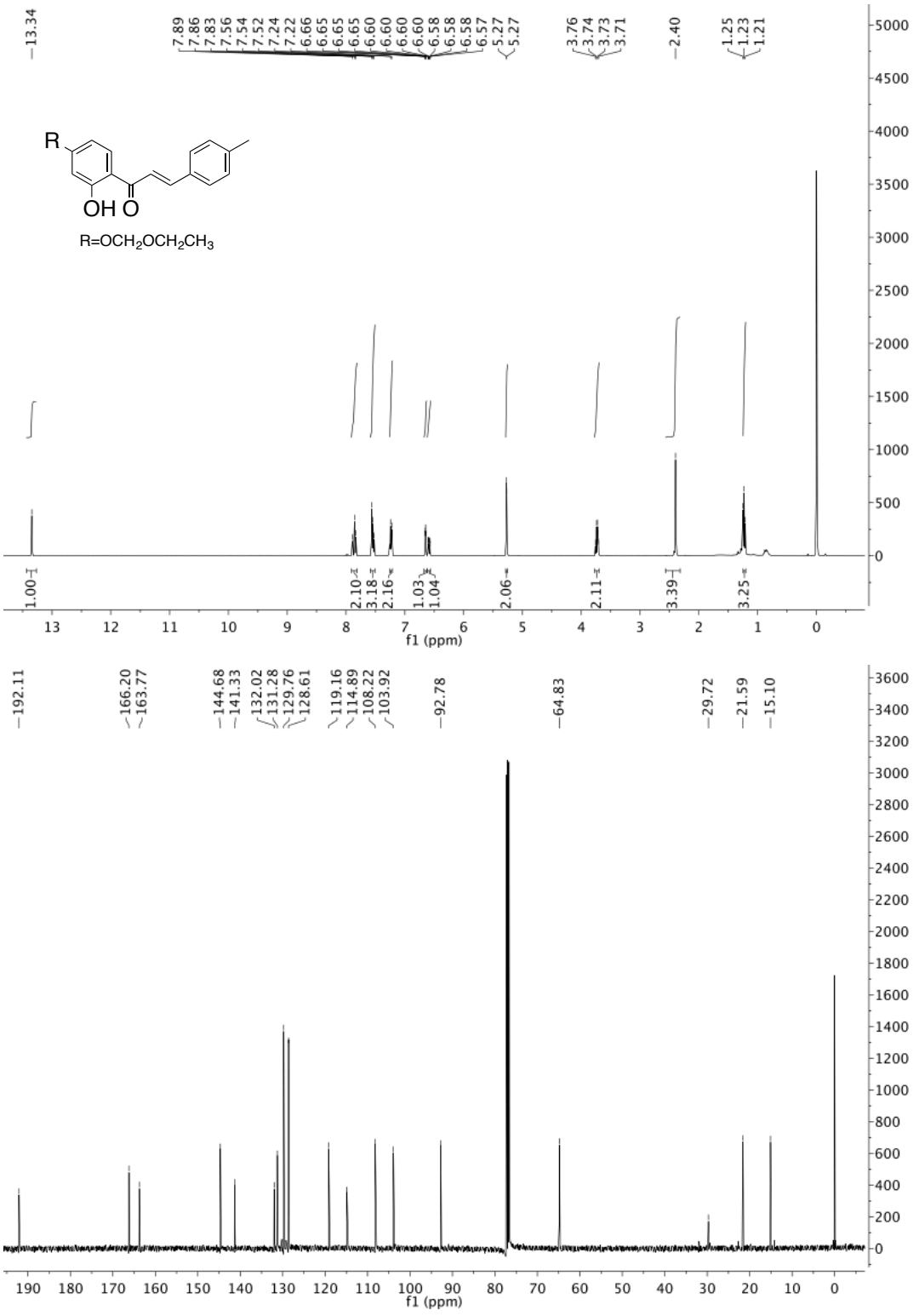

***(E)*-3-(4-(benzyloxy)phenyl)-1-(4-ethoxymethoxy-2-hydroxyphenyl)prop-2-en-1-one (25h)**

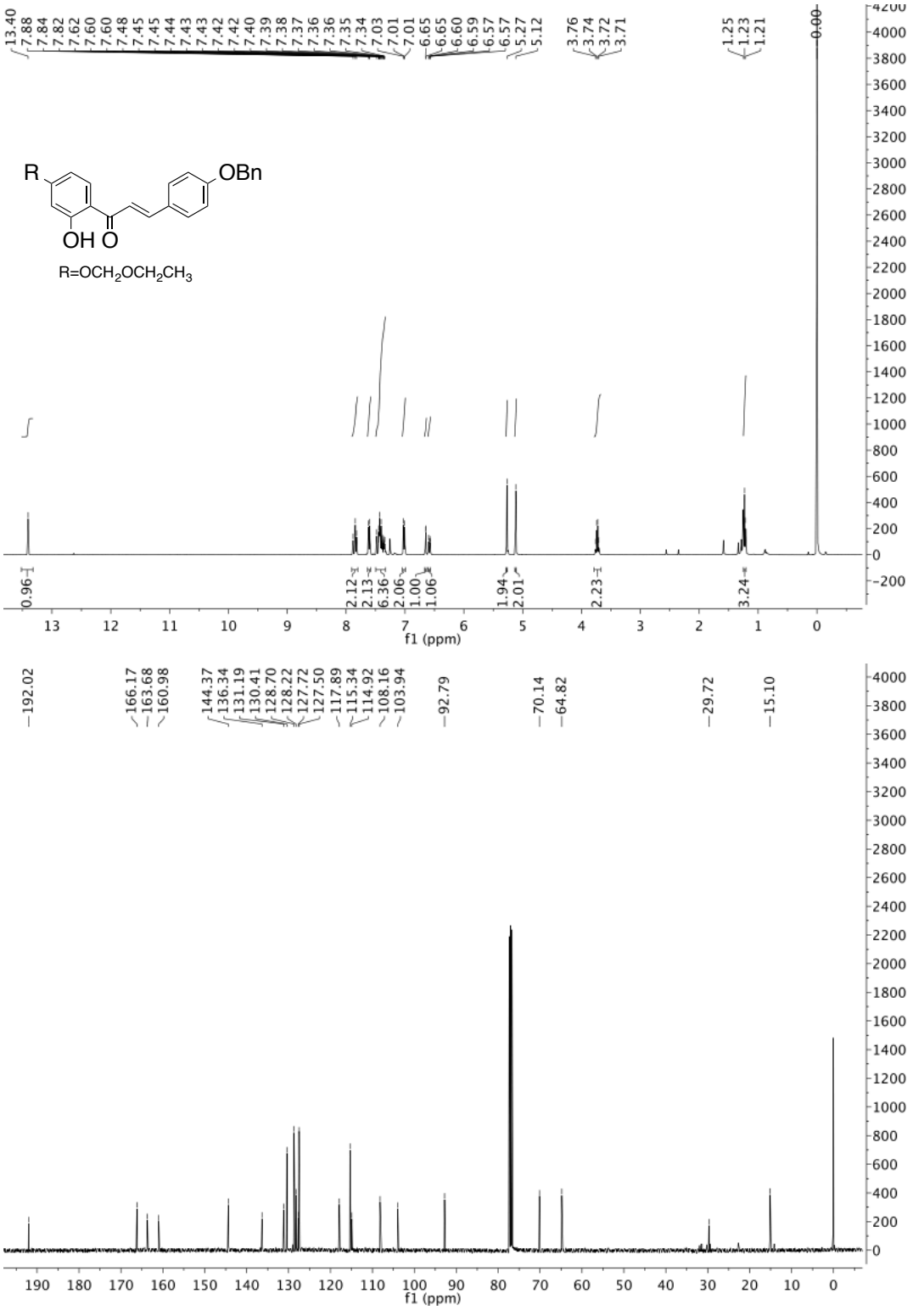

***(E)*-1-(4-ethoxymethoxy-2-hydroxyphenyl)-3-(5-methylfuran-2-yl)prop-2-en-1-one (25i)**

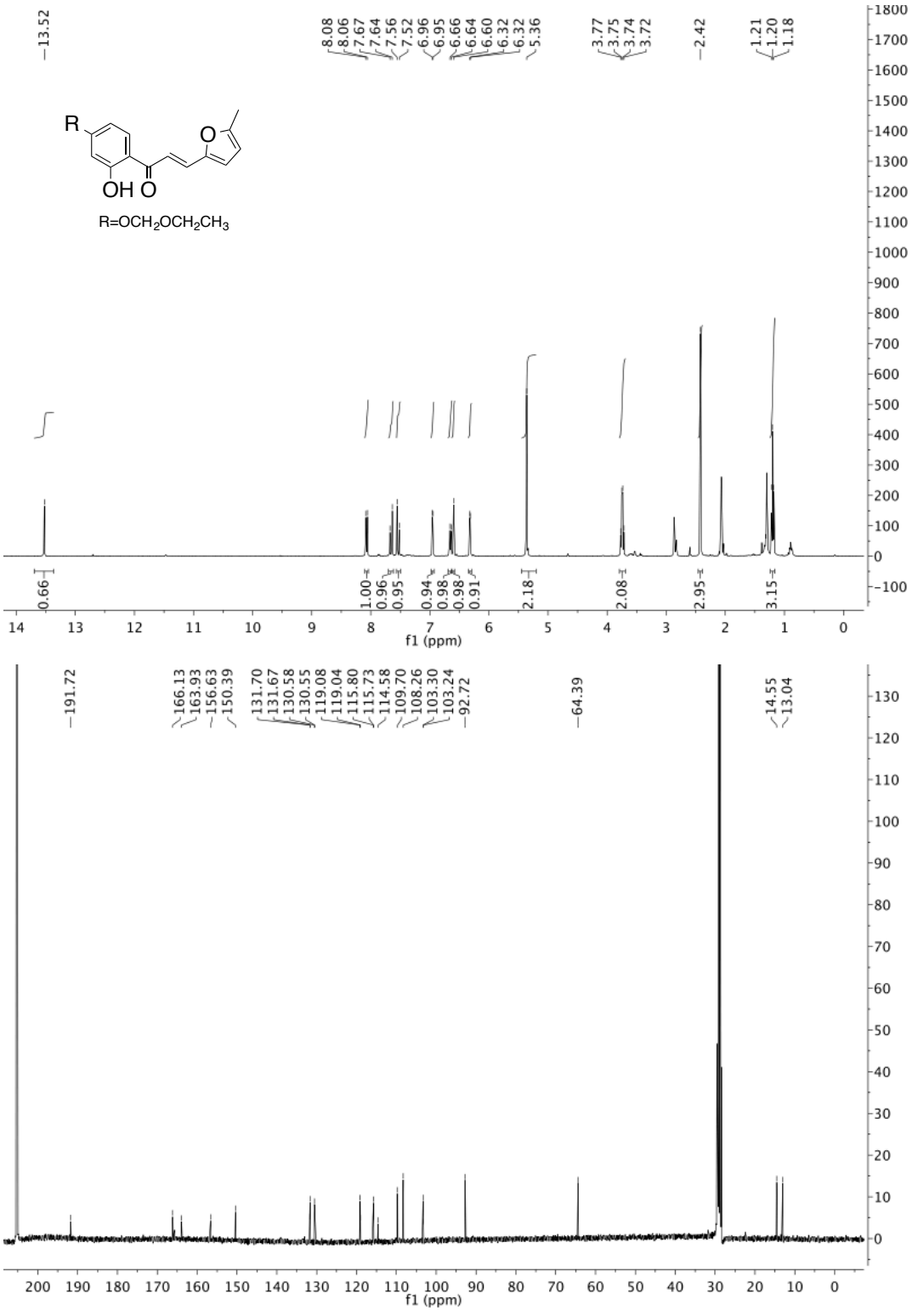

***(E)*-1-(4-fluoro-2-hydroxyphenyl)-3-(4-fluorophenyl)prop-2-en-1-one (28a)**

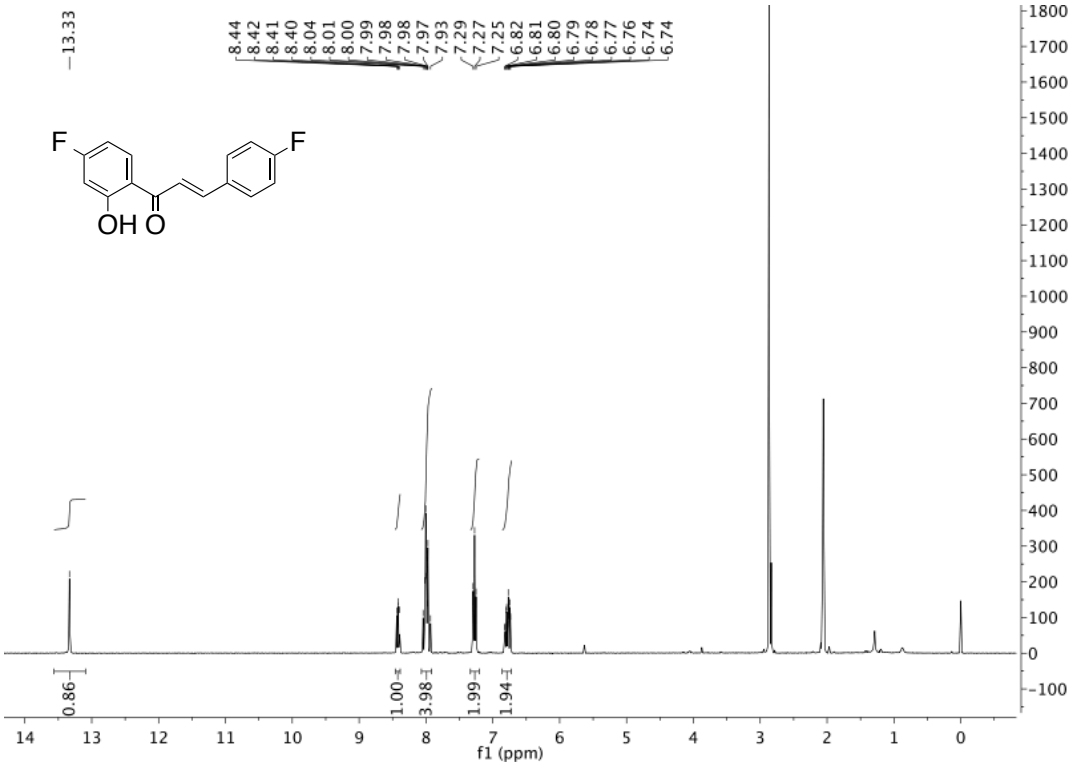

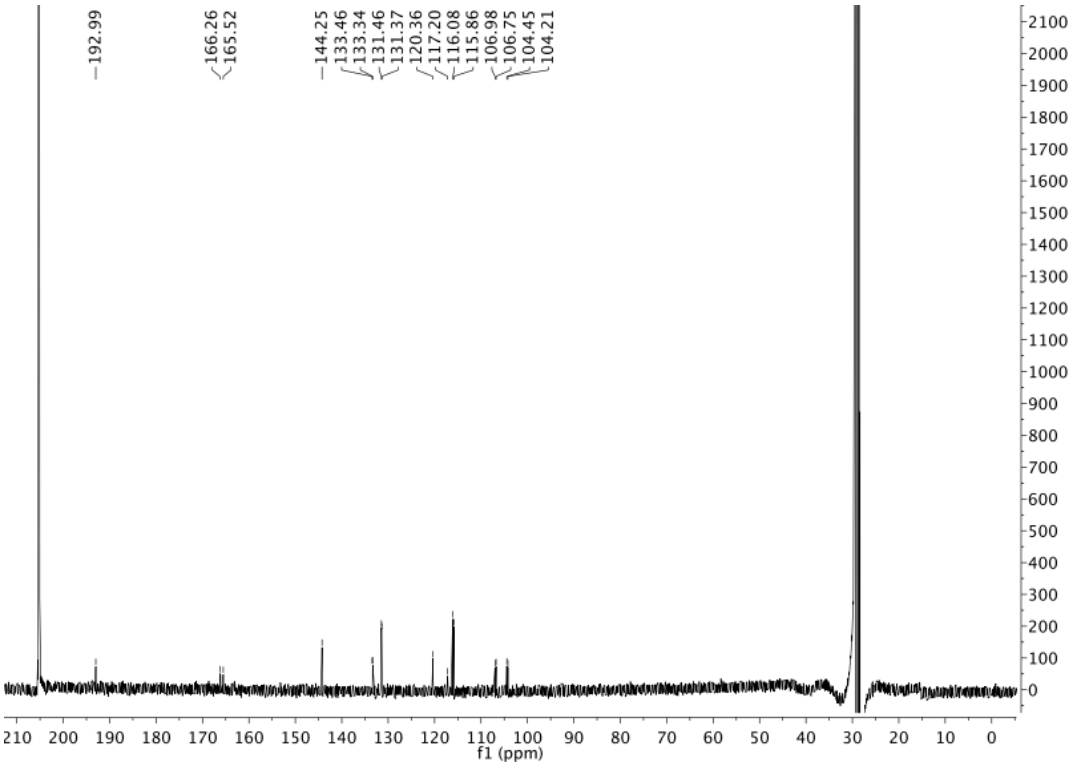

***(E)*-3-(4-bromophenyl)-1-(4-fluoro-2-hydroxyphenyl)prop-2-en-1-one (28b)**

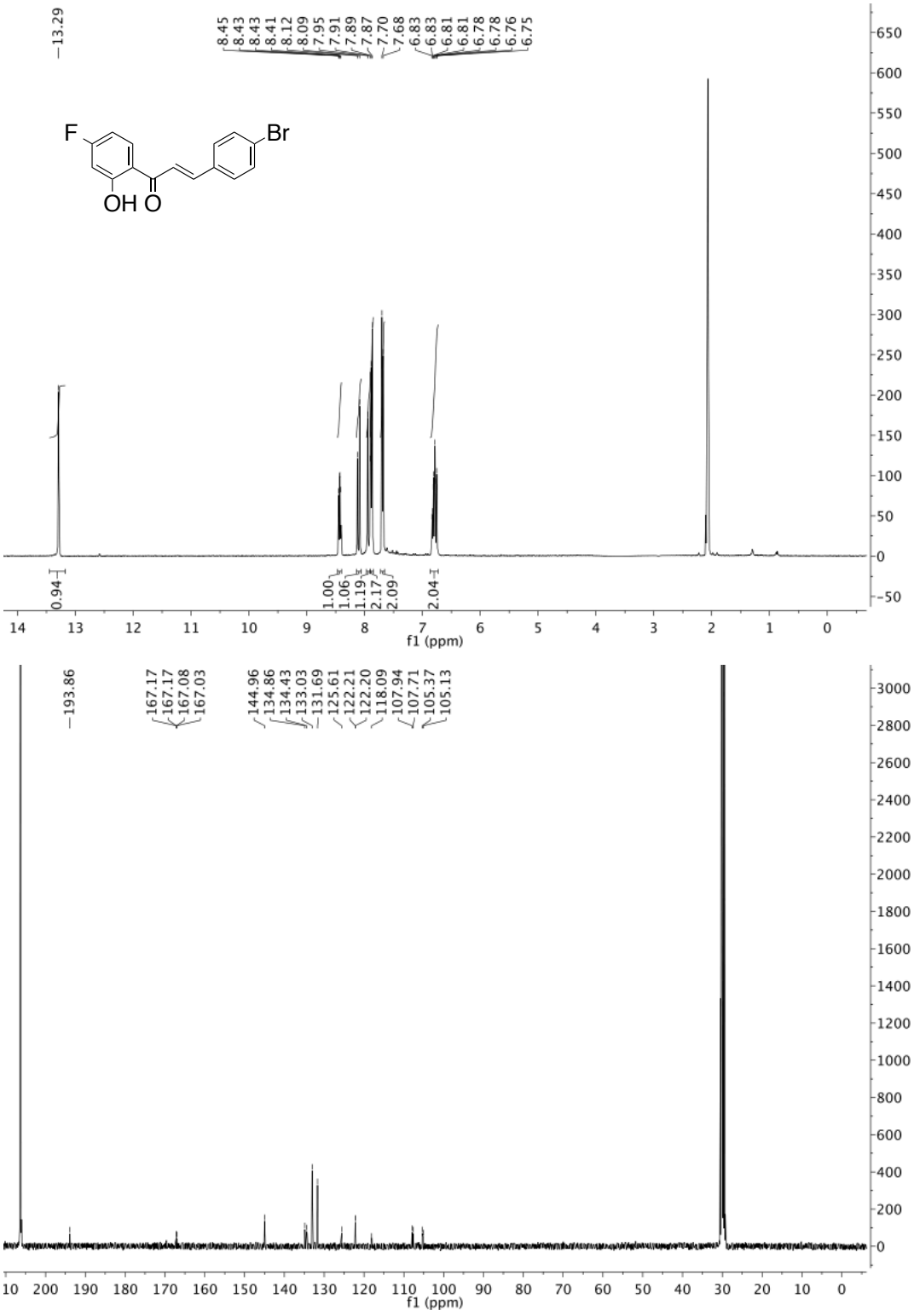

***(E)*-1-(4-fluoro-2-hydroxyphenyl)-3-(4-methylphenyl)prop-2-en-1-one (28c)**

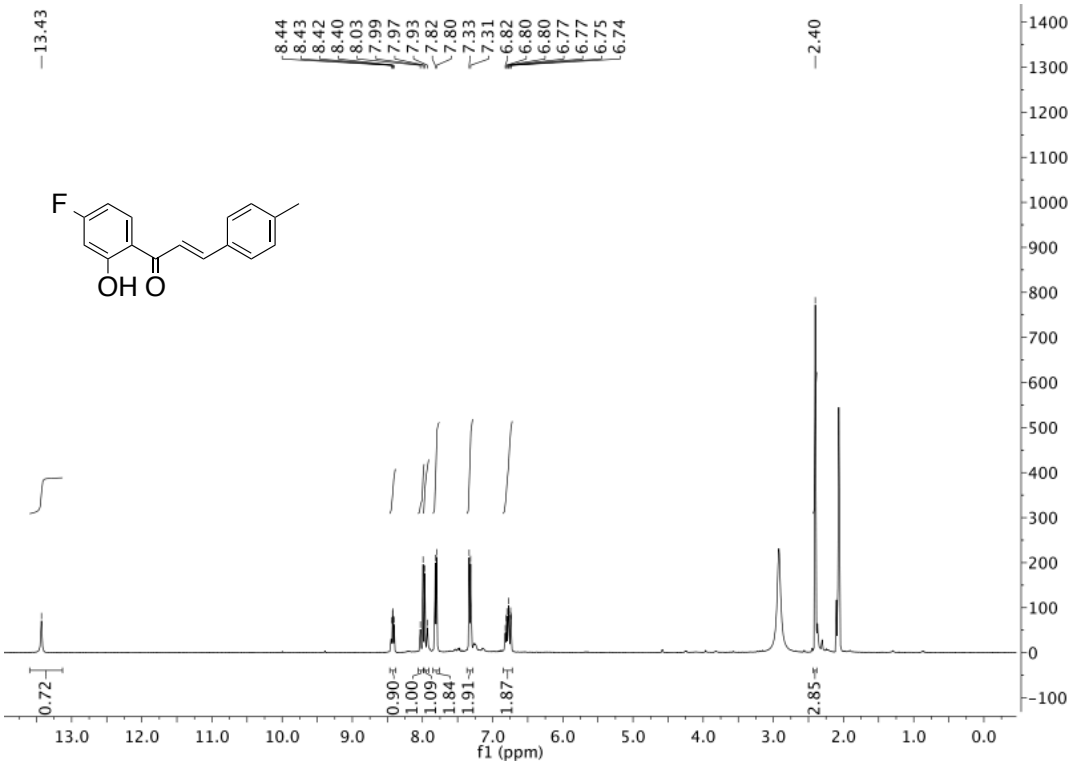

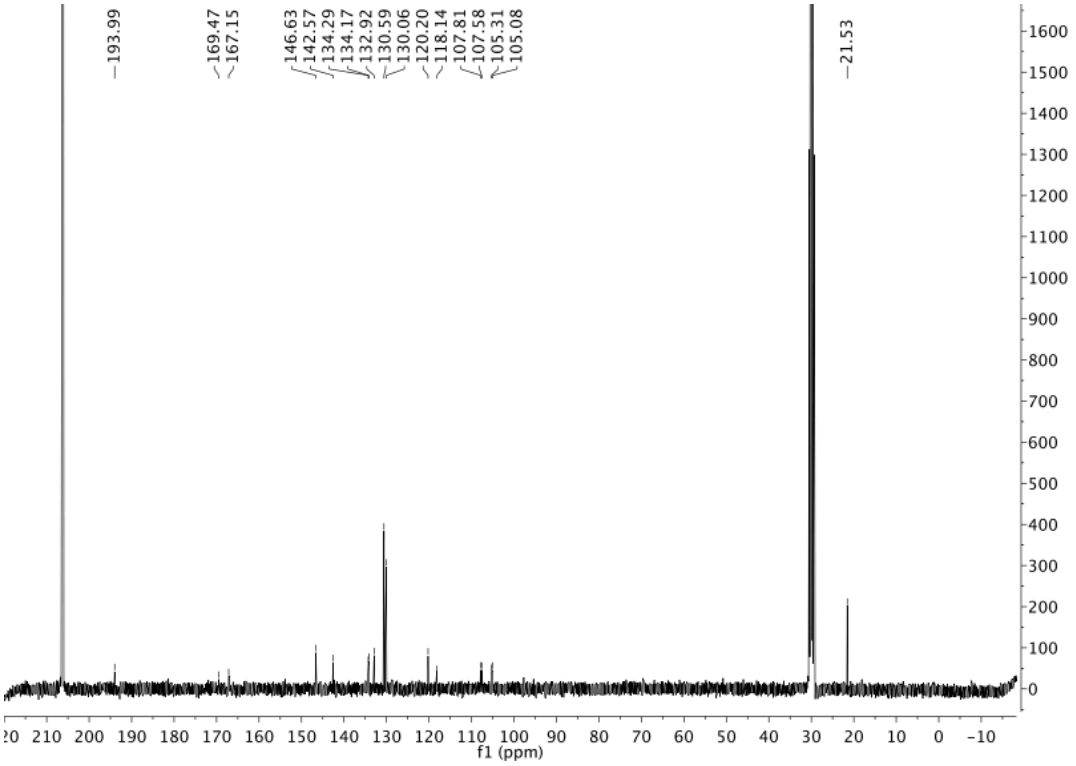

_(E)_-3-(4-(benzyloxy)phenyl)-1-(4-fluoro-2-hydroxyphenyl)prop-2-en-1-one (28h)

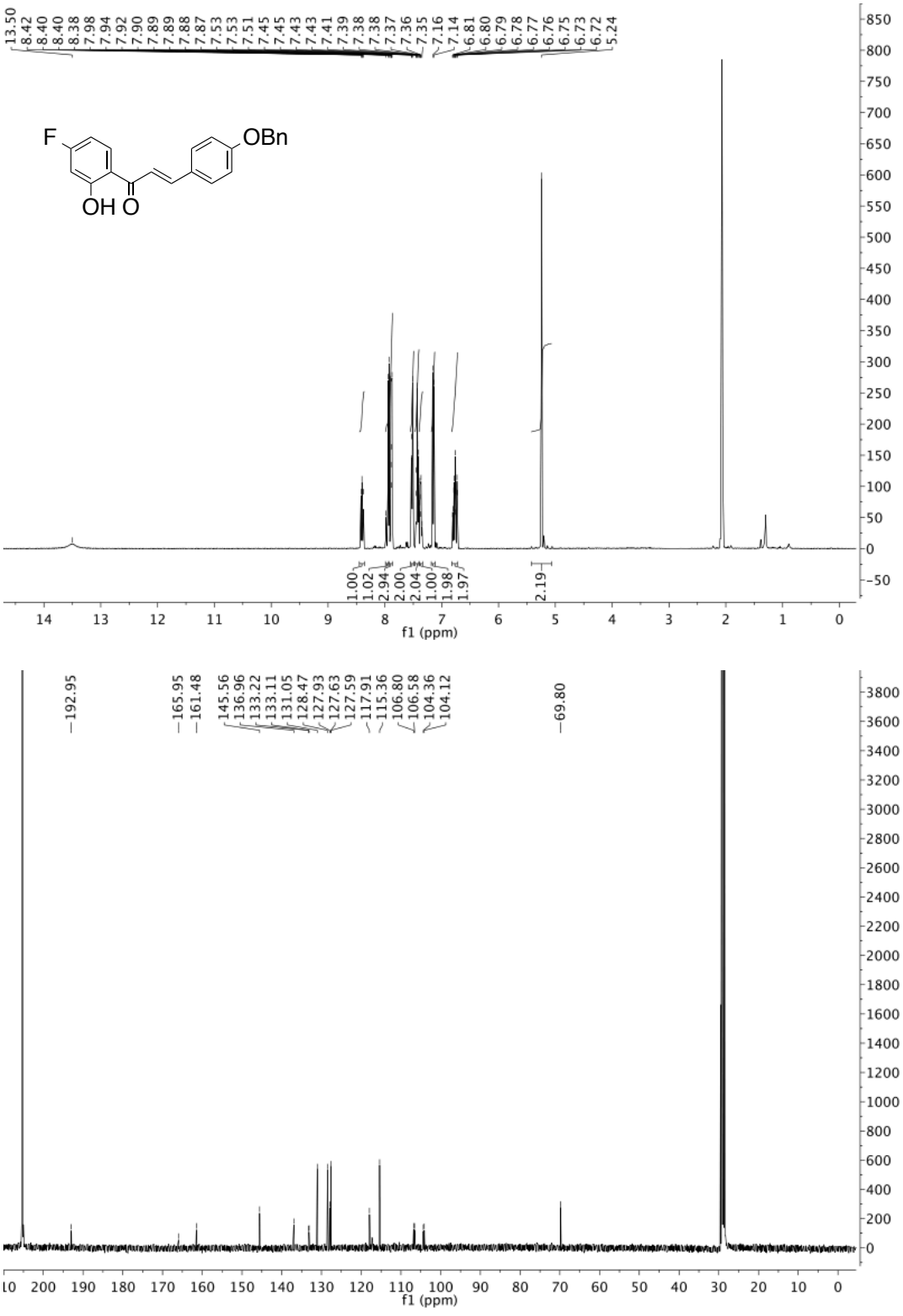

***(E)*-1-(4-fluoro-2-hydroxyphenyl)-3-(5-methylfuran-2-yl)prop-2-en-1-one (28i)**

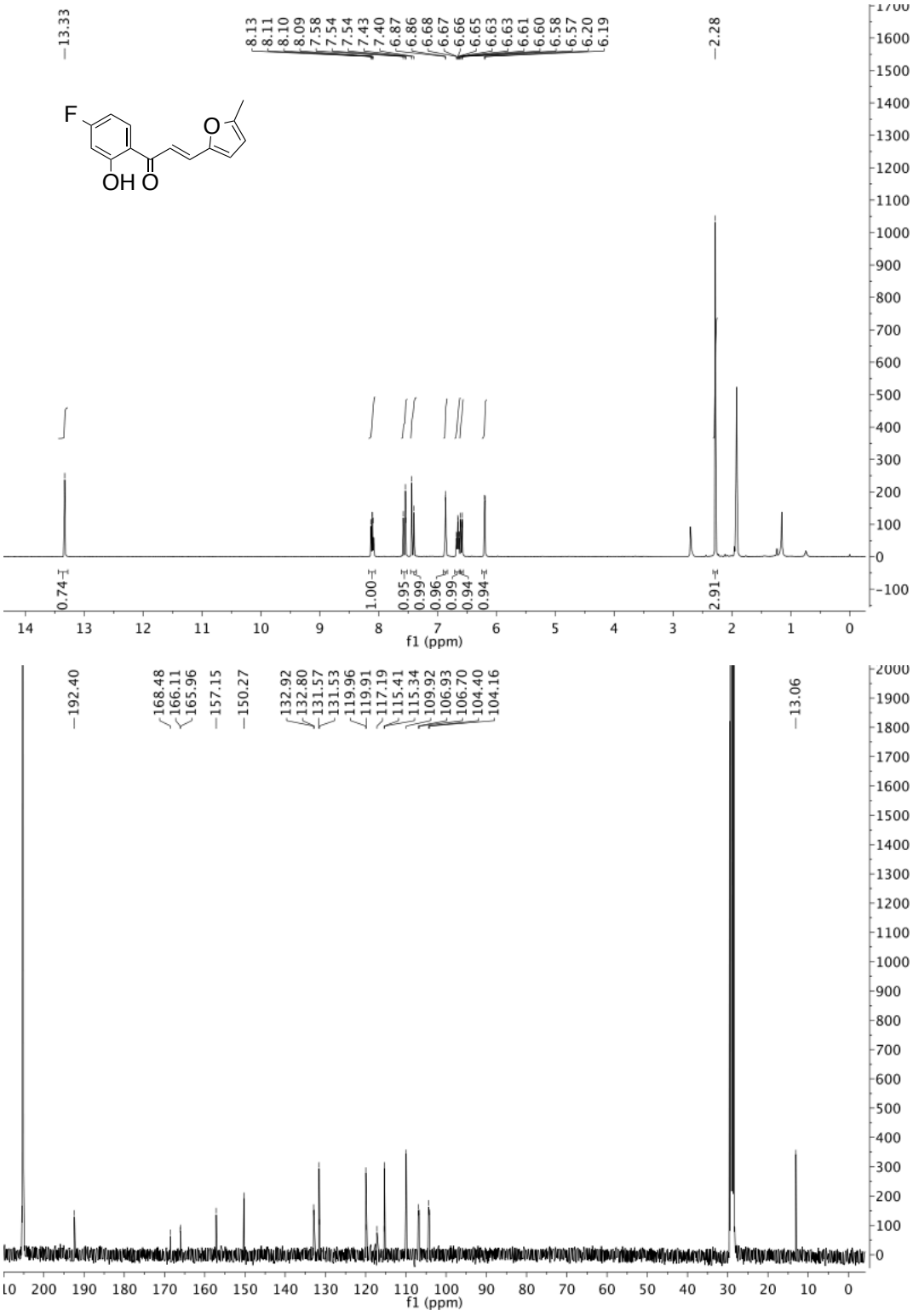

1.5 Chalcones Deprotection

(E)-3-(4-fluorophenyl)-1-(2,4,6-trihydroxyphenyl)prop-2-en-1-one (22a)

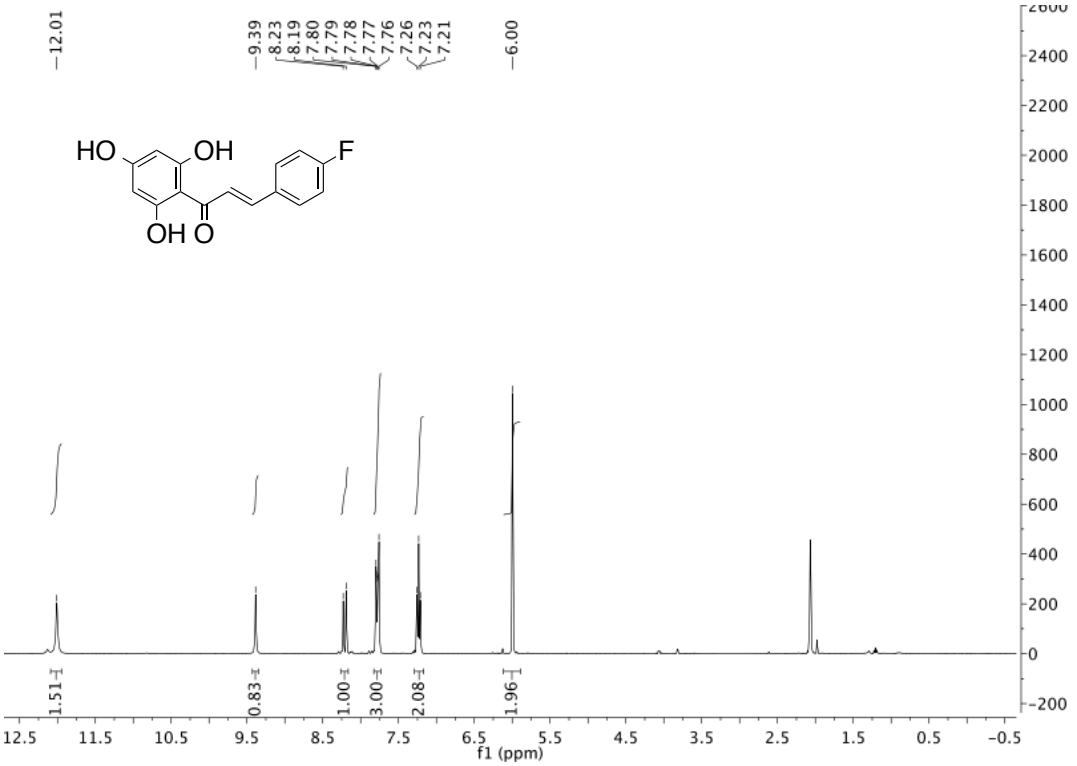

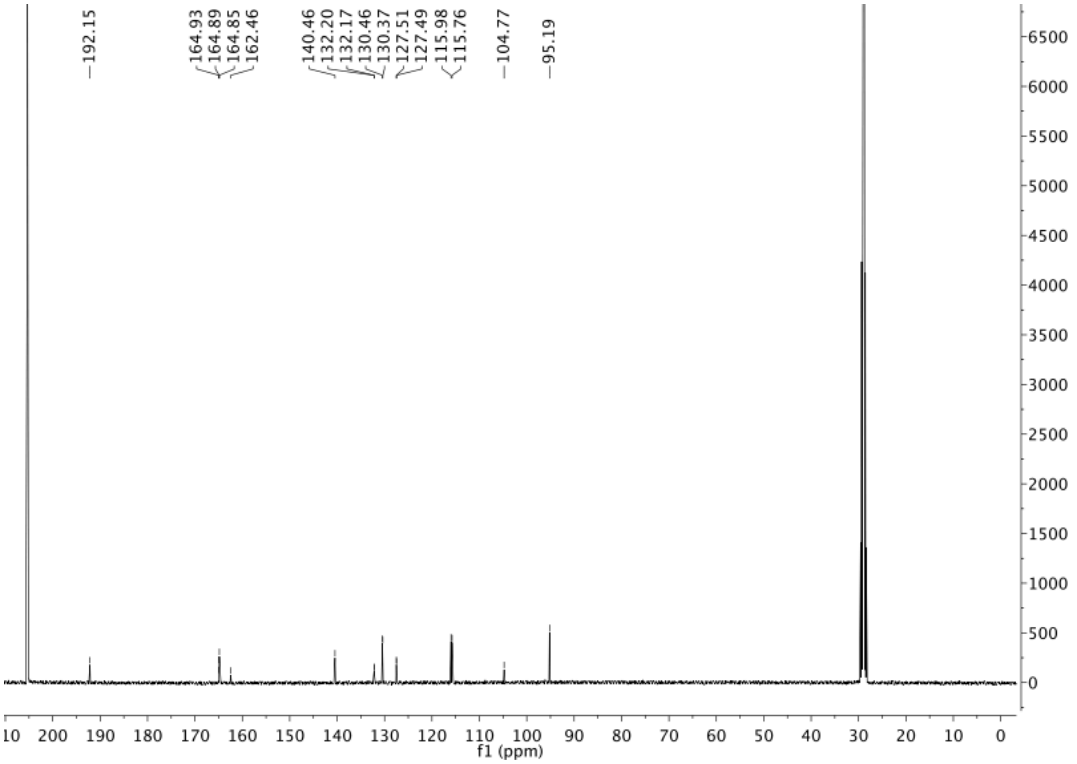

***(E)*-3-(4-bromophenyl)-1-(2,4,6-trihydroxyphenyl)prop-2-en-1-one (22b)**

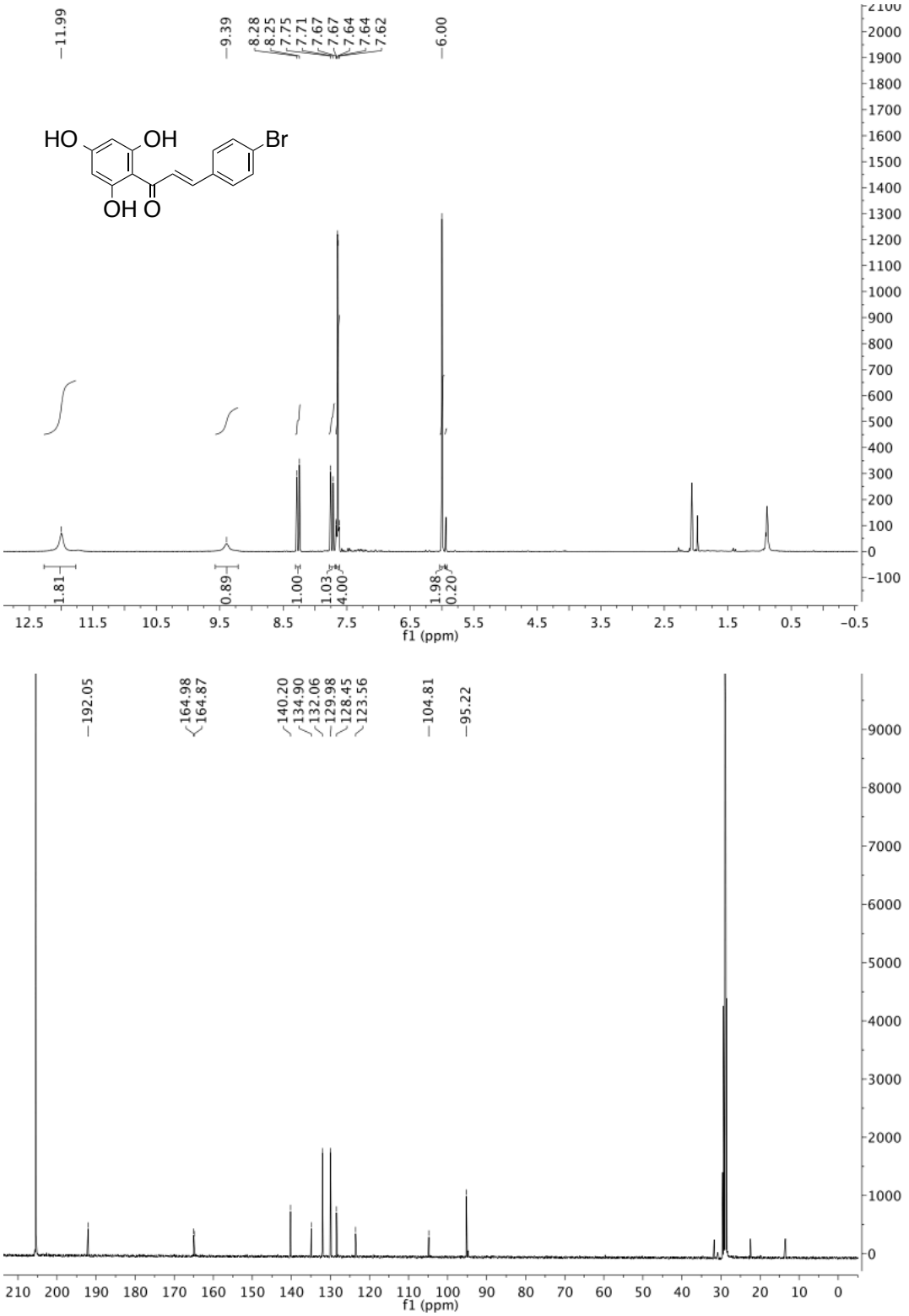

***(E)*-3-(phenyl)-1-(2,4,6-trihydroxyphenyl)prop-2-en-1-one (22c)**

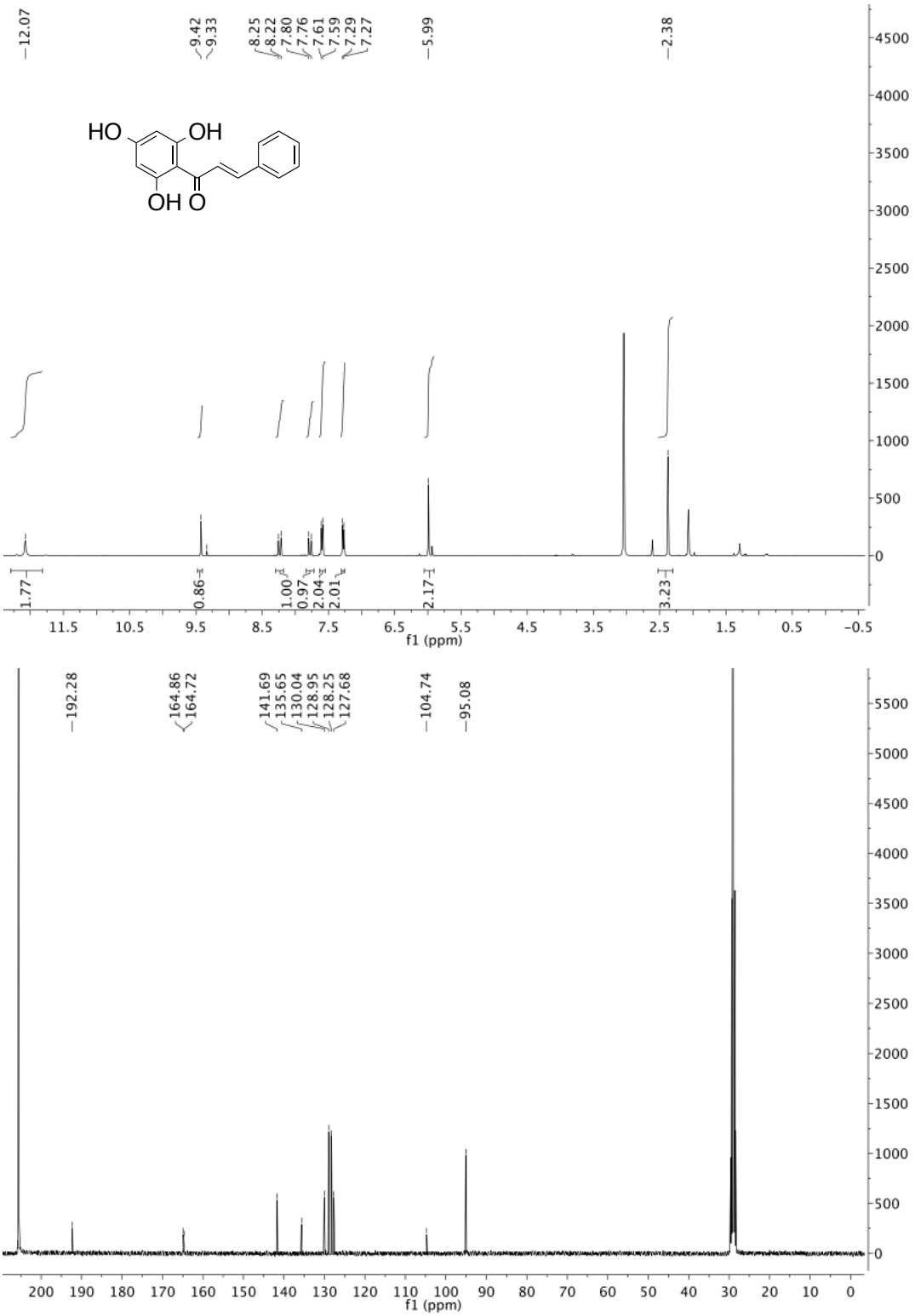

(*E*)-3-(4-methylphenyl)-1-(2,4,6-trihydroxyphenyl)prop-2-en-1-one (22d)

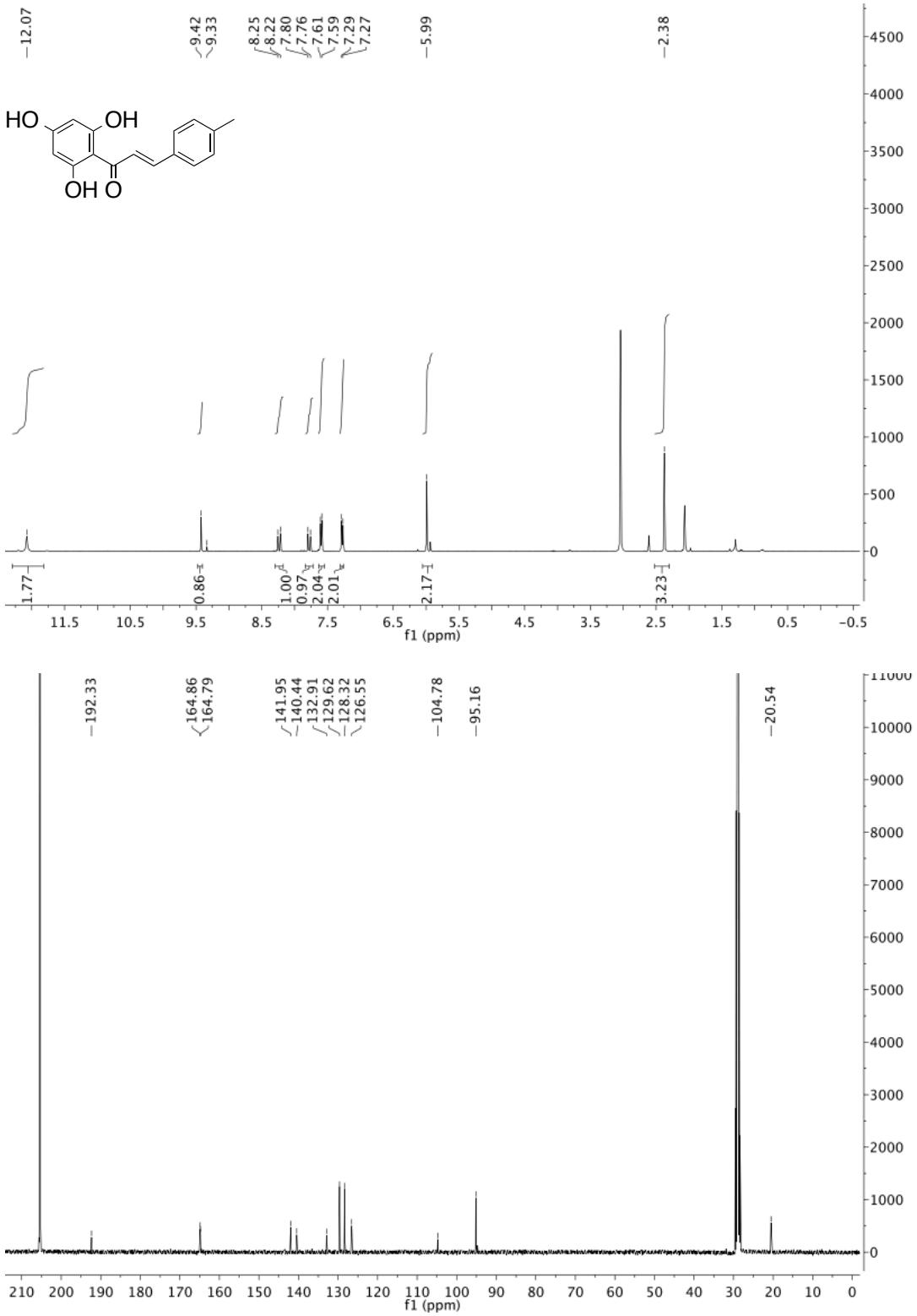

(*E*)-3-(4-methyloxyphenyl)-1-(2,4,6-trihydroxyphenyl)prop-2-en-1-one (22e)

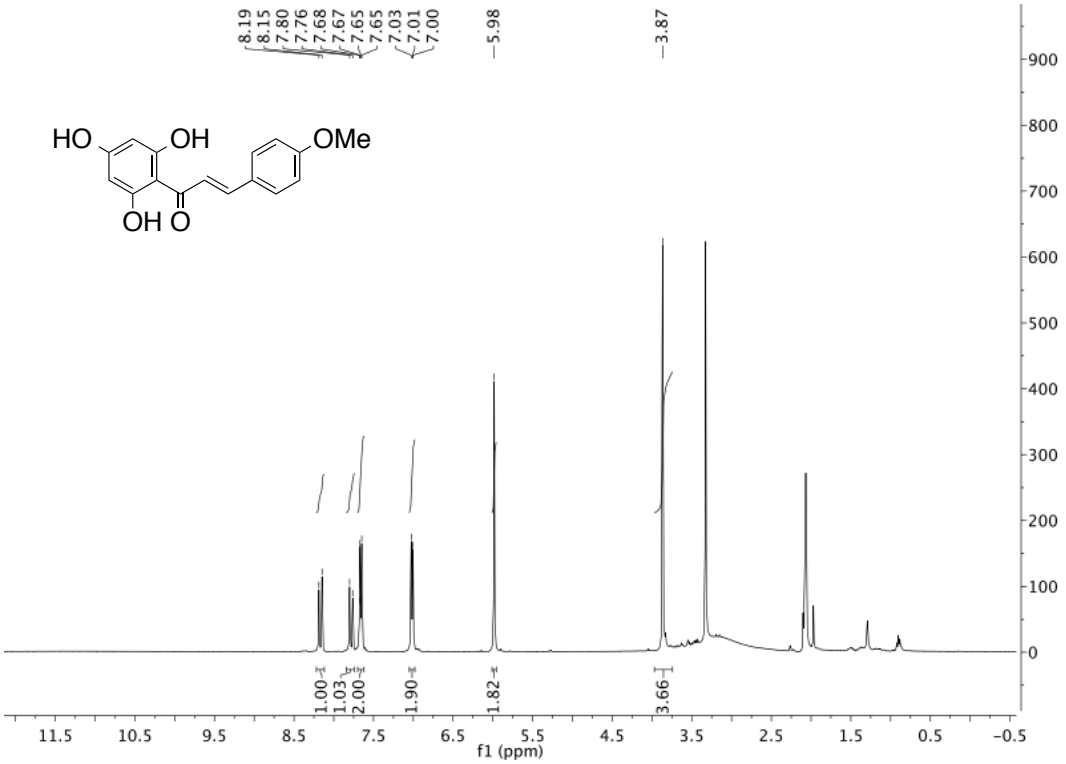

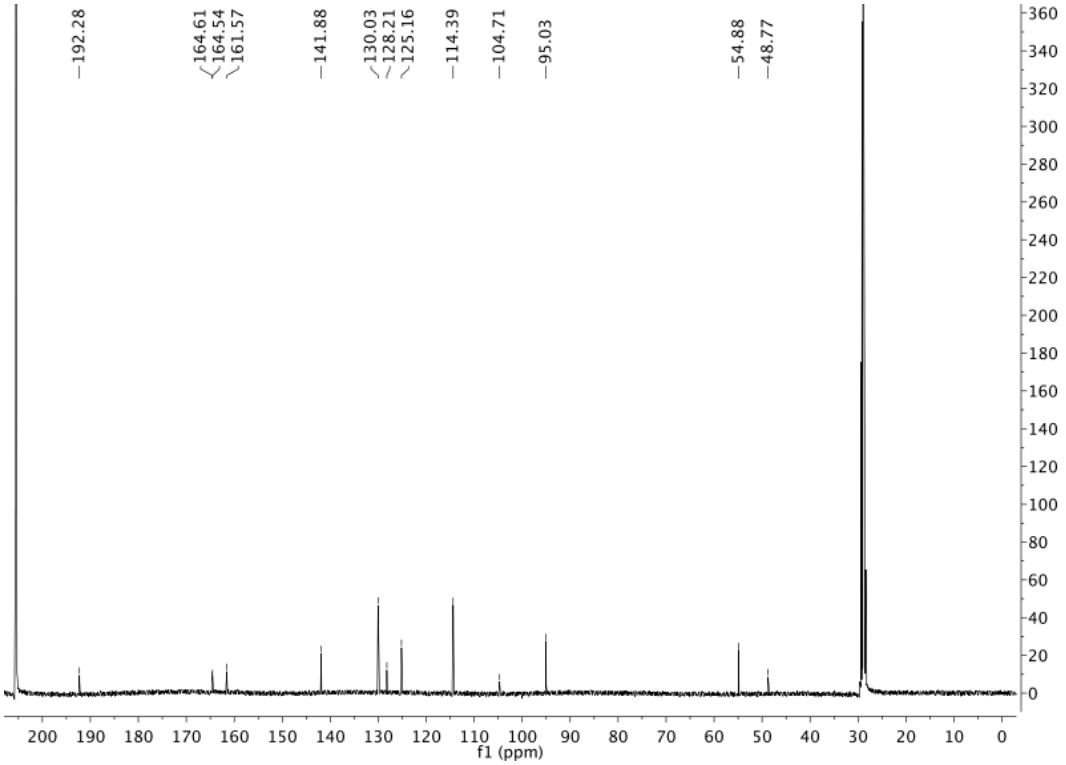

***(E)*-3-(4-ethyloxyphenyl)-1-(2,4,6-trihydroxyphenyl)prop-2-en-1-one (22f)**

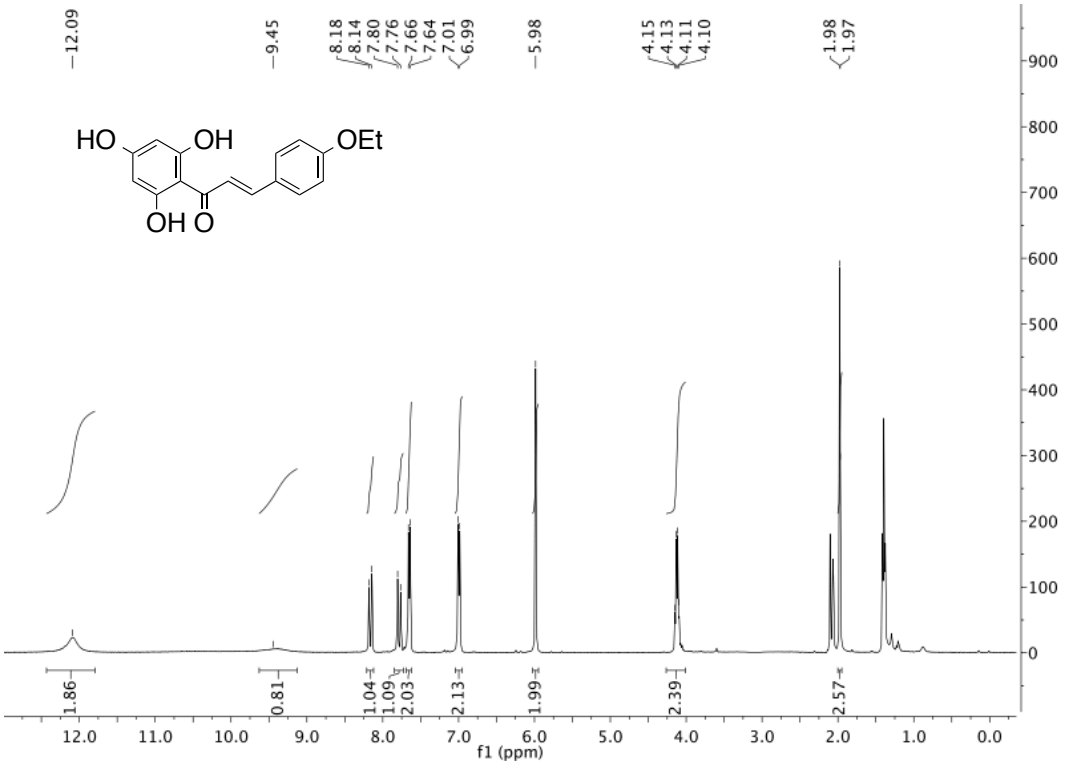

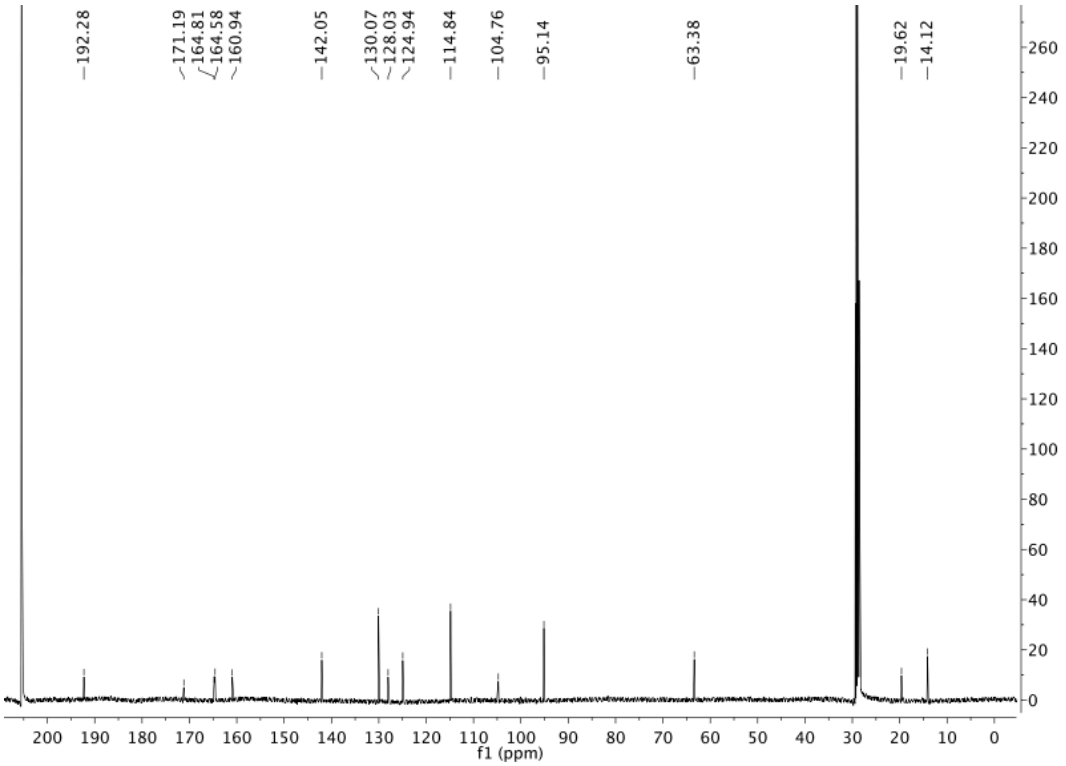

***(E)*-3-(4-allyloxyphenyl)-1-(2,4,6-trihydroxyphenyl)prop-2-en-1-one (22g)**

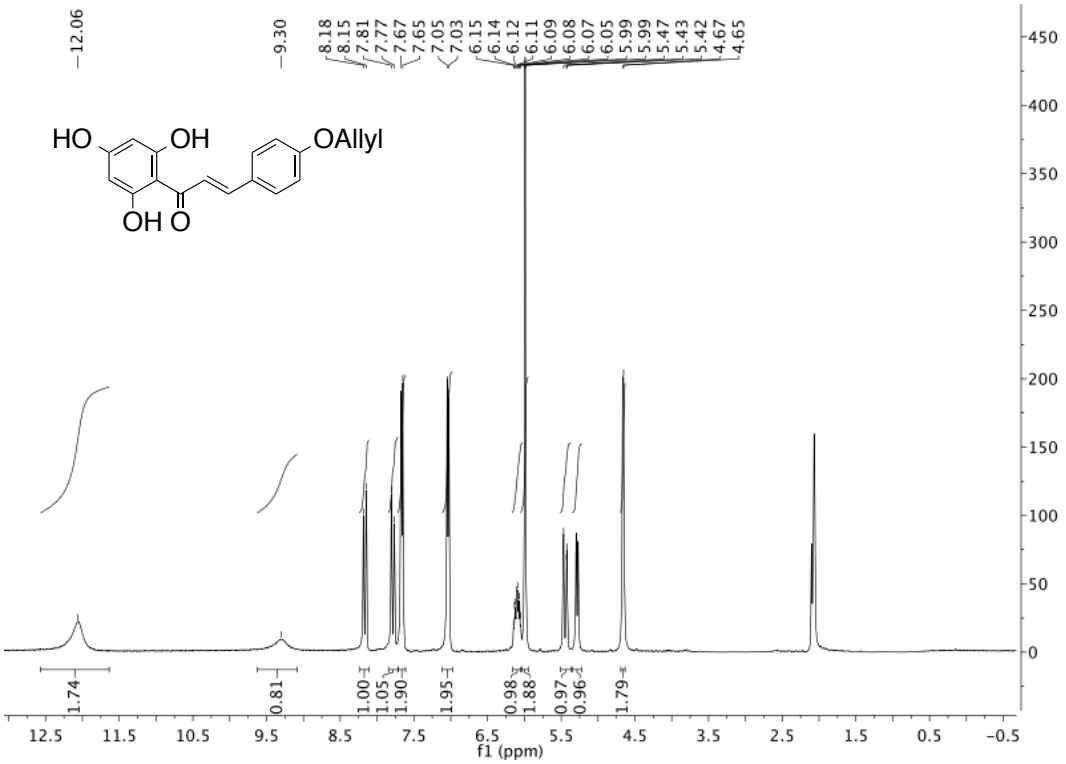

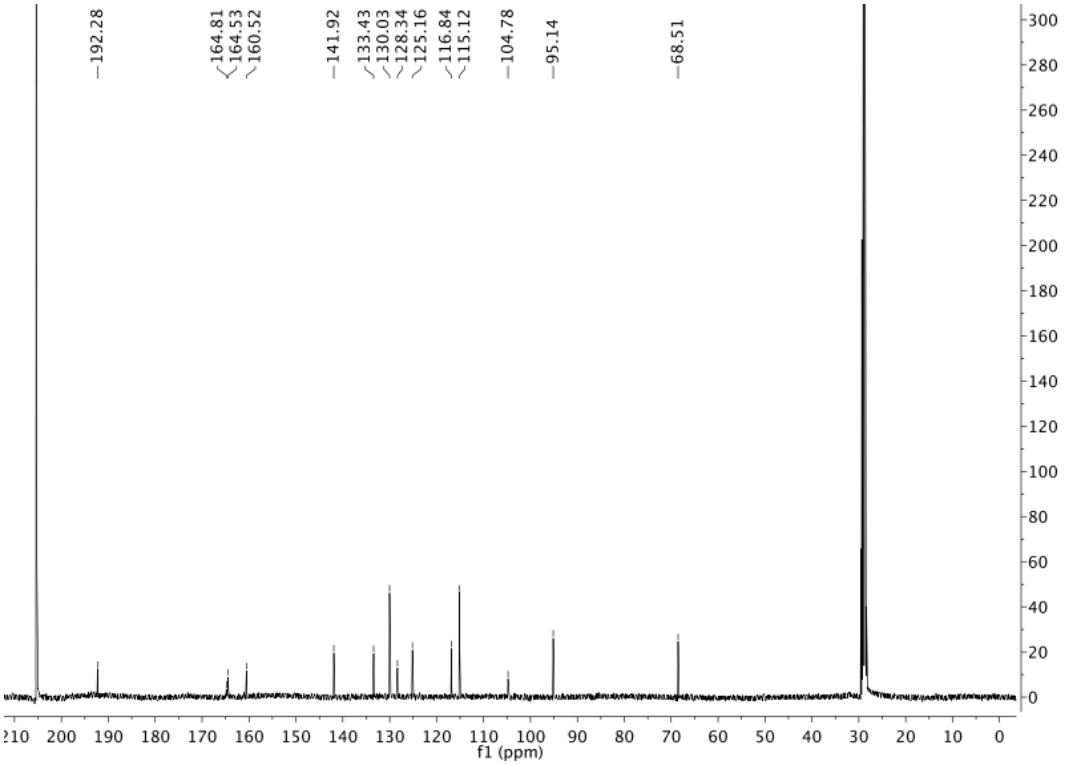

***(E)*-3-(4-(benzyloxy)phenyl)-1-(2,4,6-trihydroxyphenyl)prop-2-en-1-one (22h)**

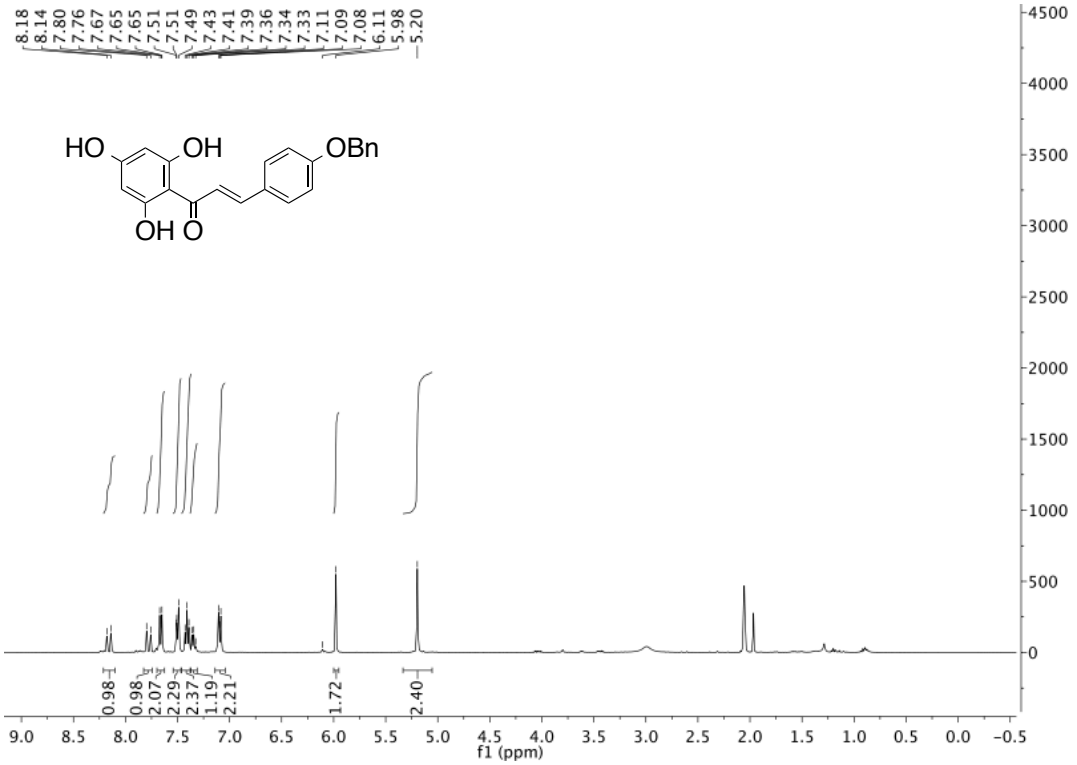

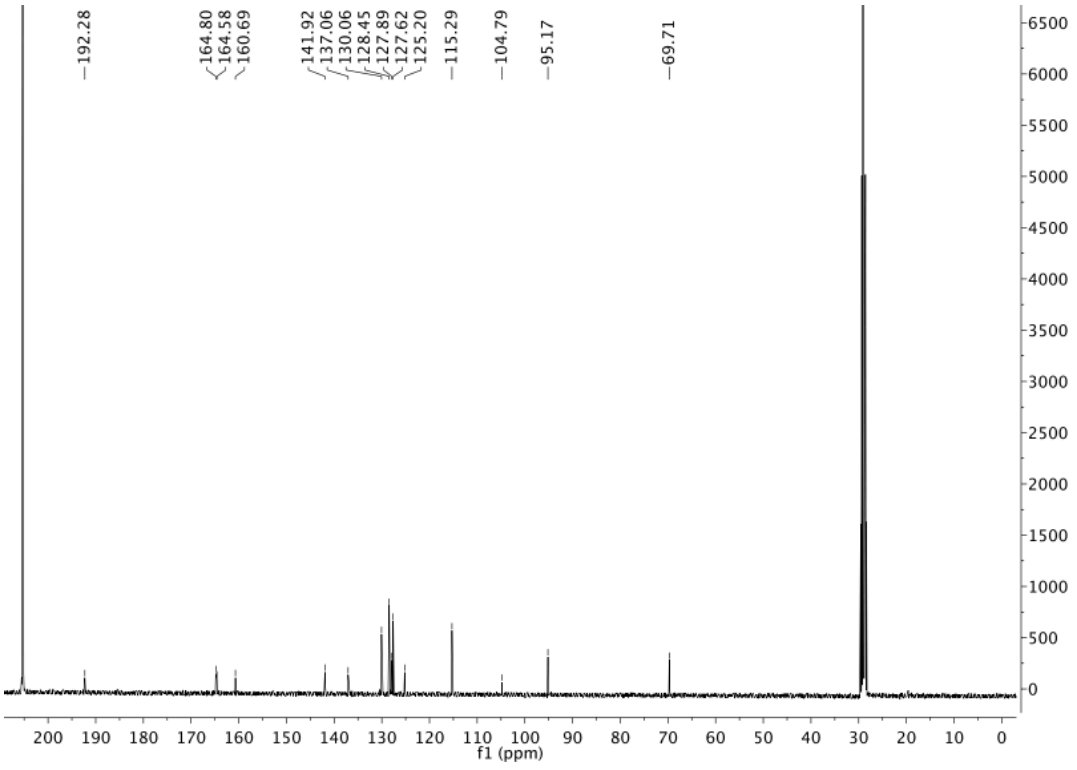

***(E)*-3-(5-methylfuran-2-yl)-1-(2,4,6-trihydroxyphenyl)prop-2-en-1-one (22i)**

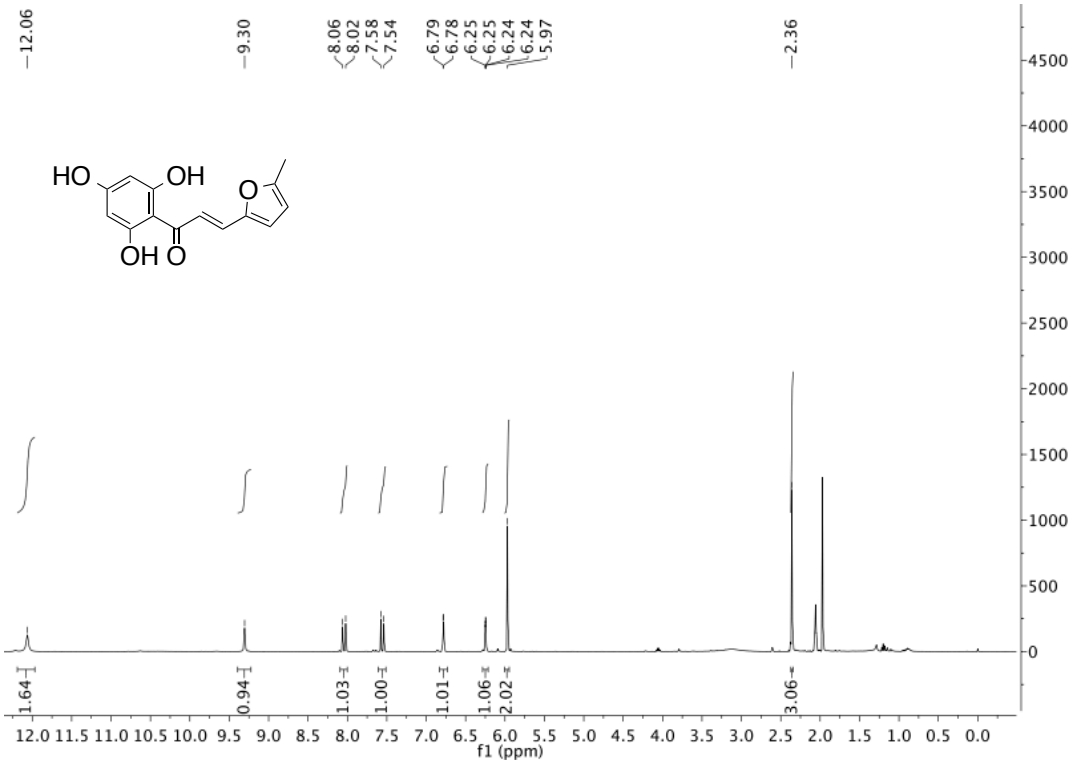

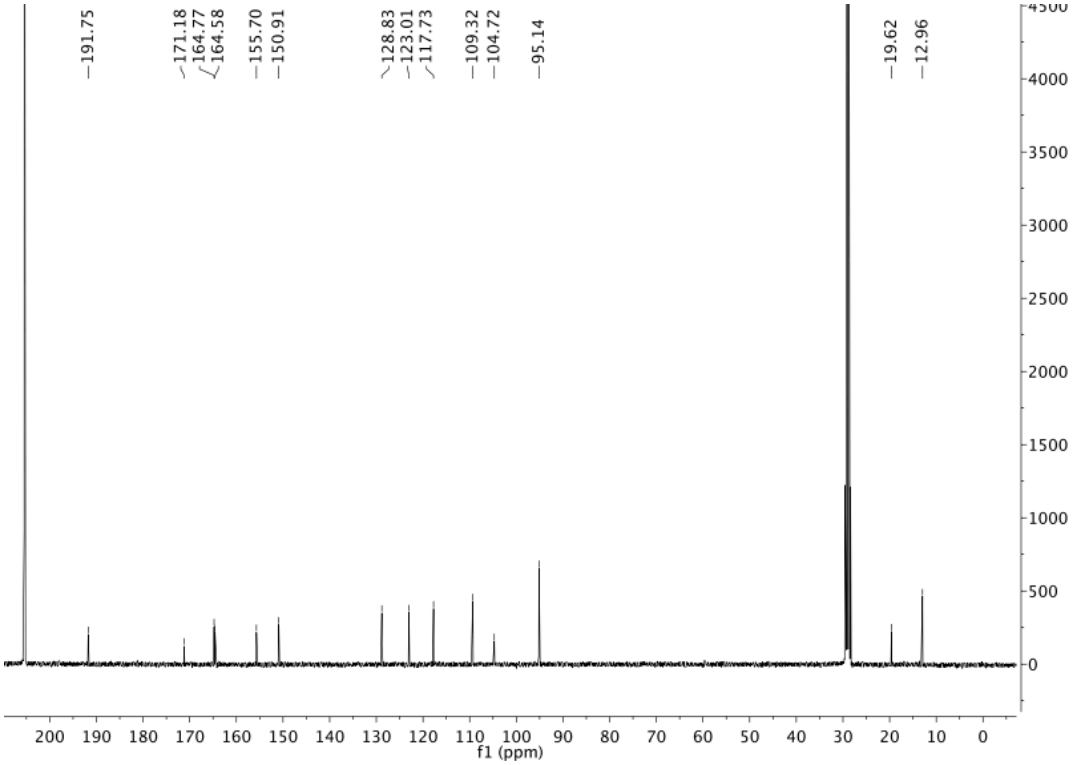

***(E)*-1-(2,4-dihydroxyphenyl)-3-(4-fluorophenyl)prop-2-en-1-one (26a)**

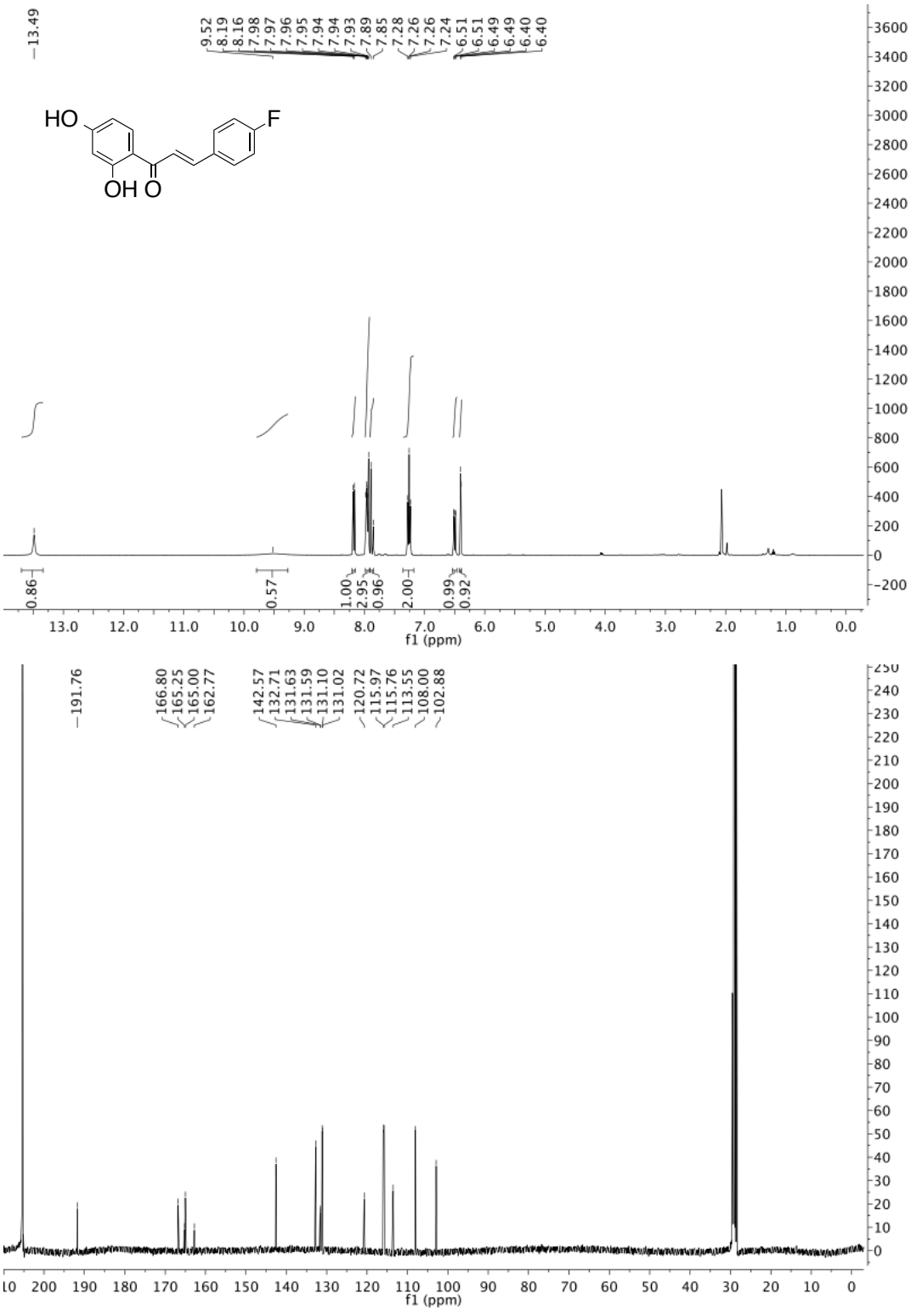

***(E)*-3-(4-bromophenyl)-1-(2,4-dihydroxyphenyl)prop-2-en-1-one (26b)**

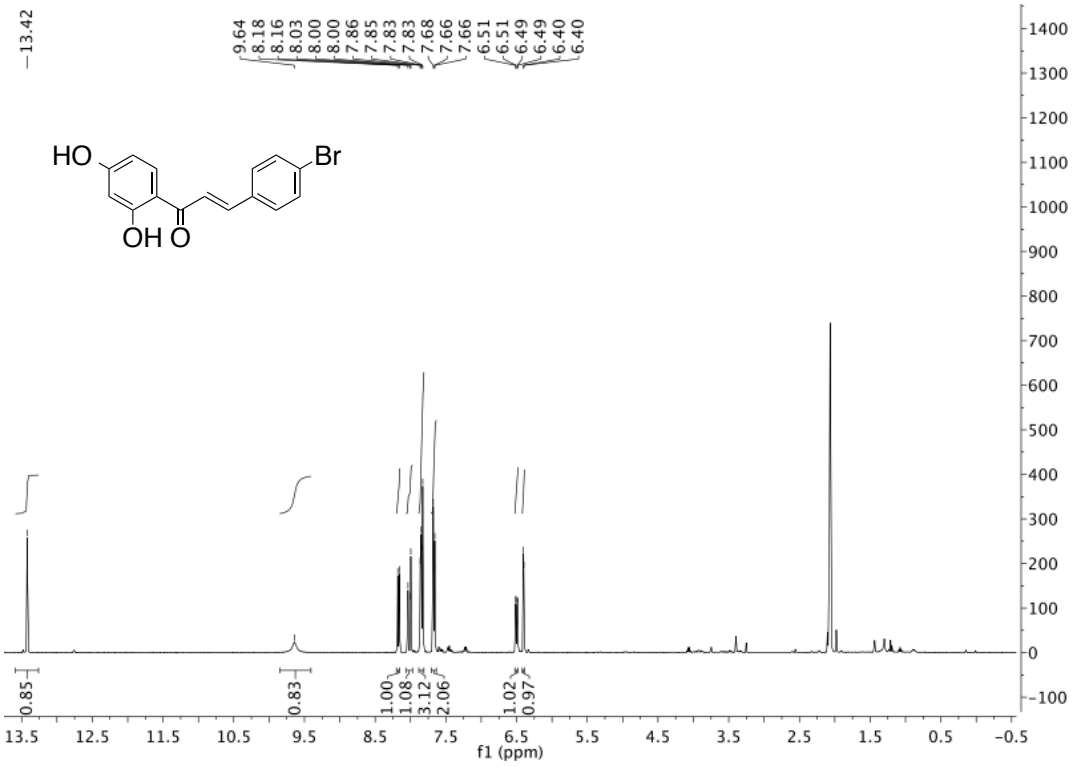

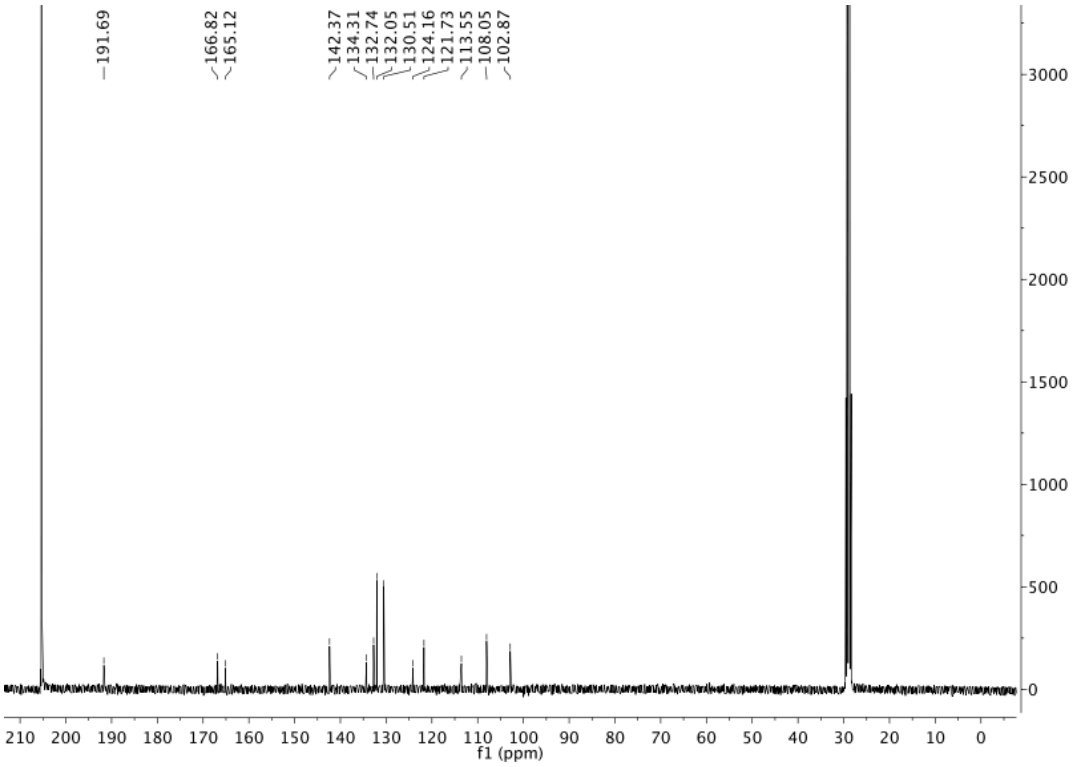

***(E)*-1-(2,4-dihydroxyphenyl)-3-(4-methylphenyl)prop-2-en-1-one (26c)**

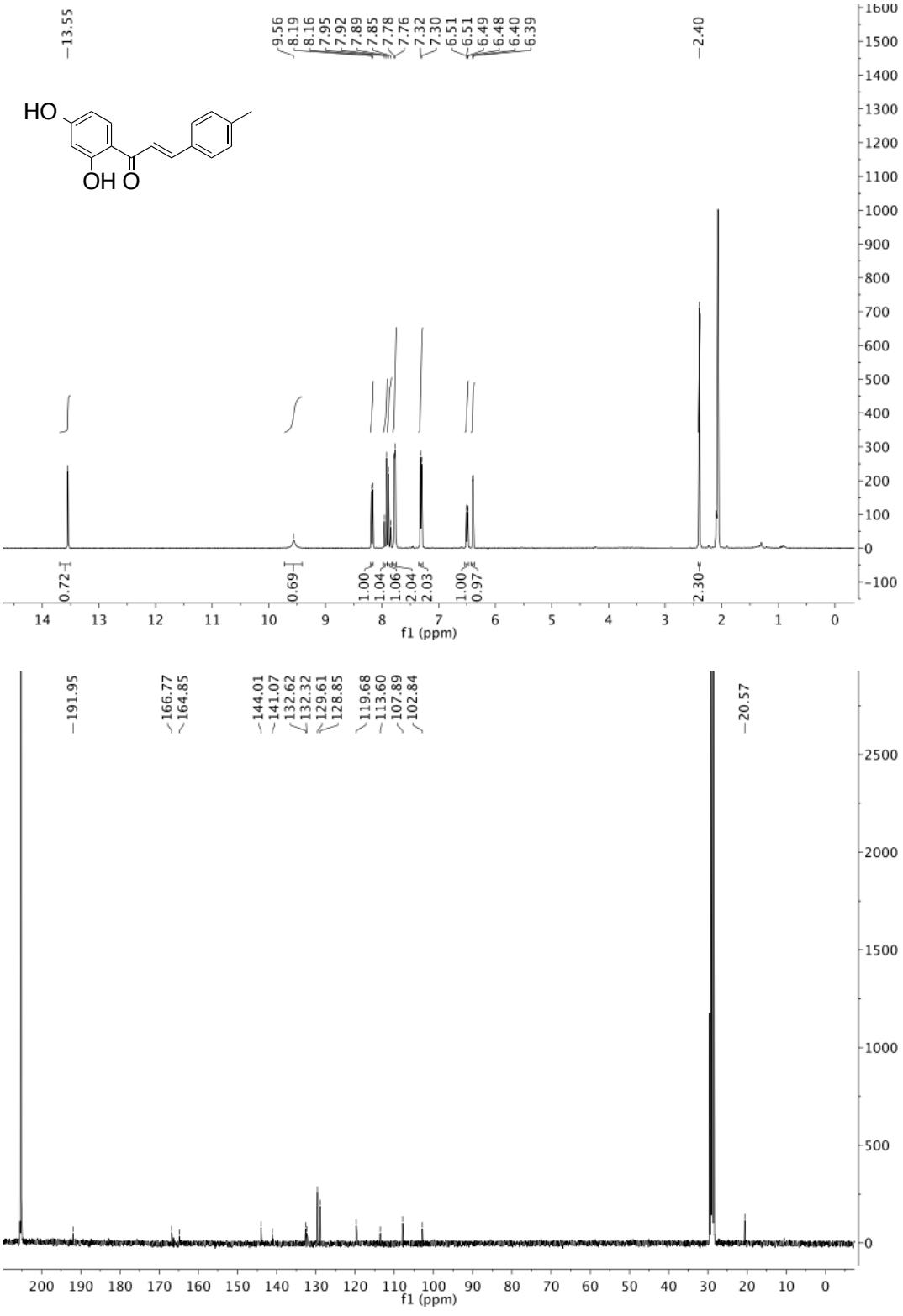

(E)-3-(4-(benzyloxy)phenyl)-1-(2,4-dihydroxyphenyl)prop-2-en-1-one (26h)

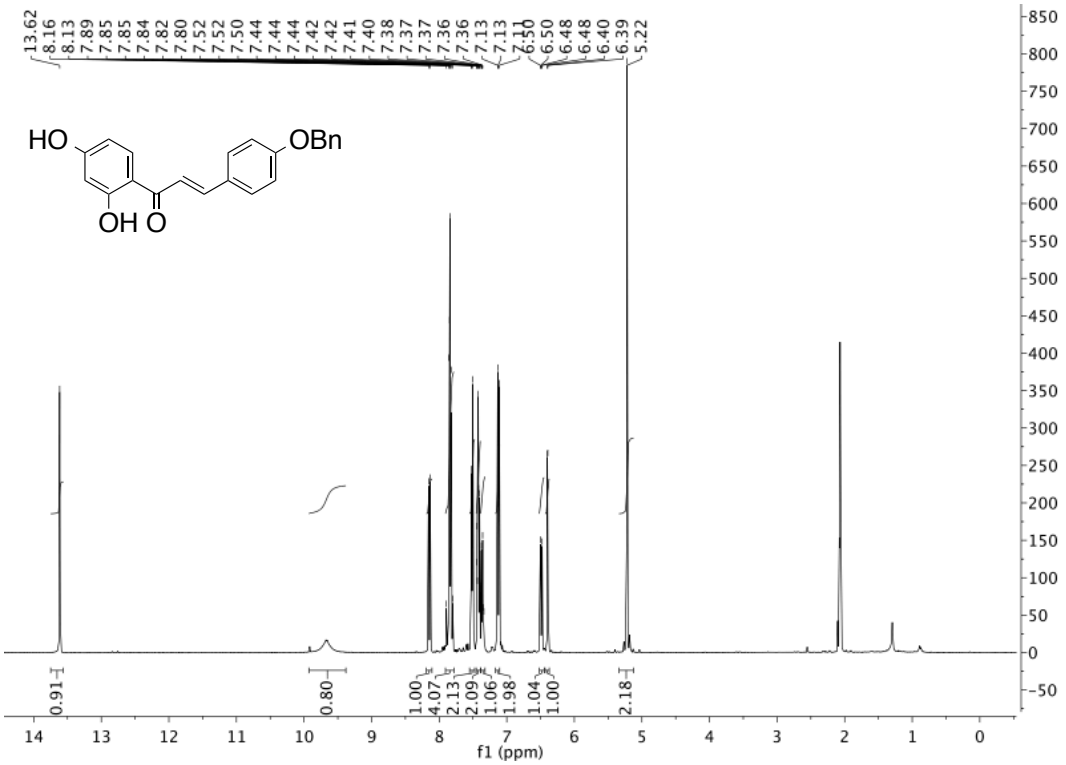

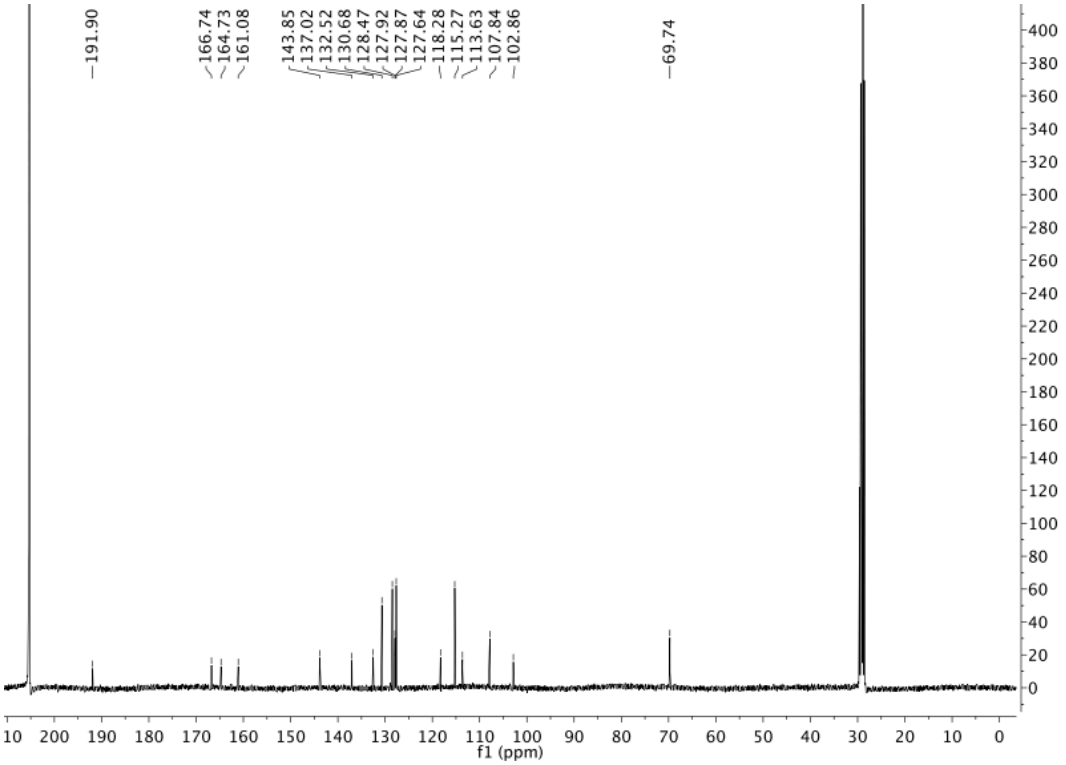

***(E)*-1-(2,4-dihydroxyphenyl)-3-(5-methylfuran-2-yl)prop-2-en-1-one (26i)**

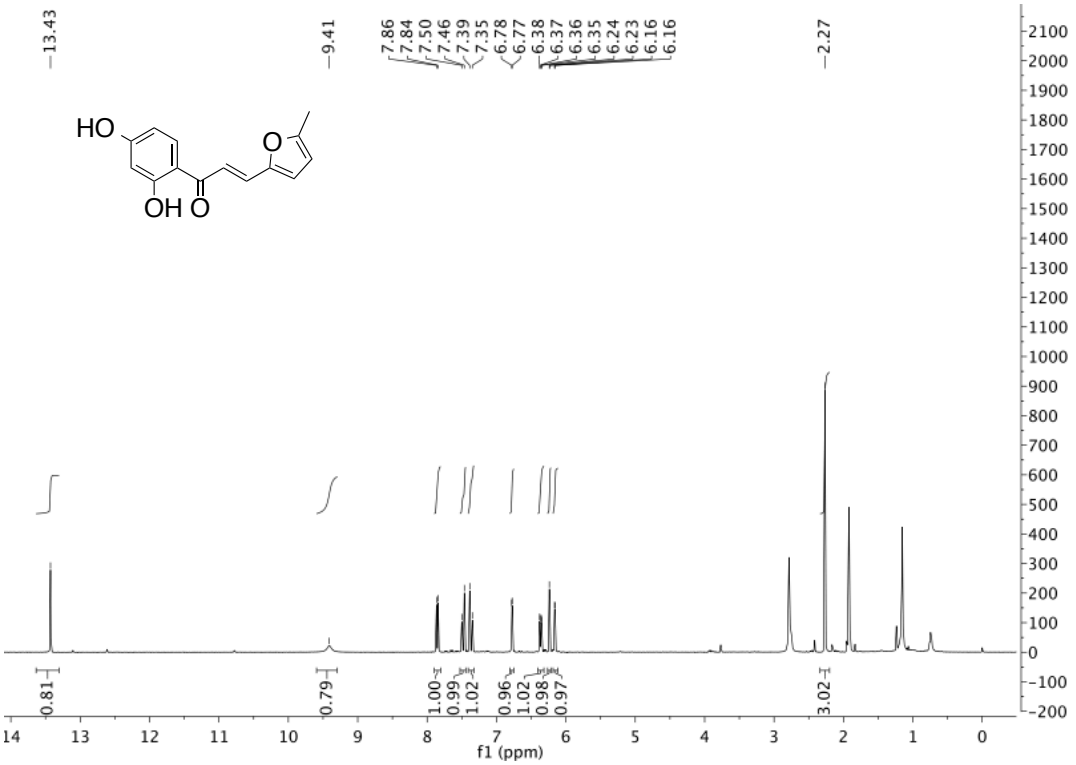

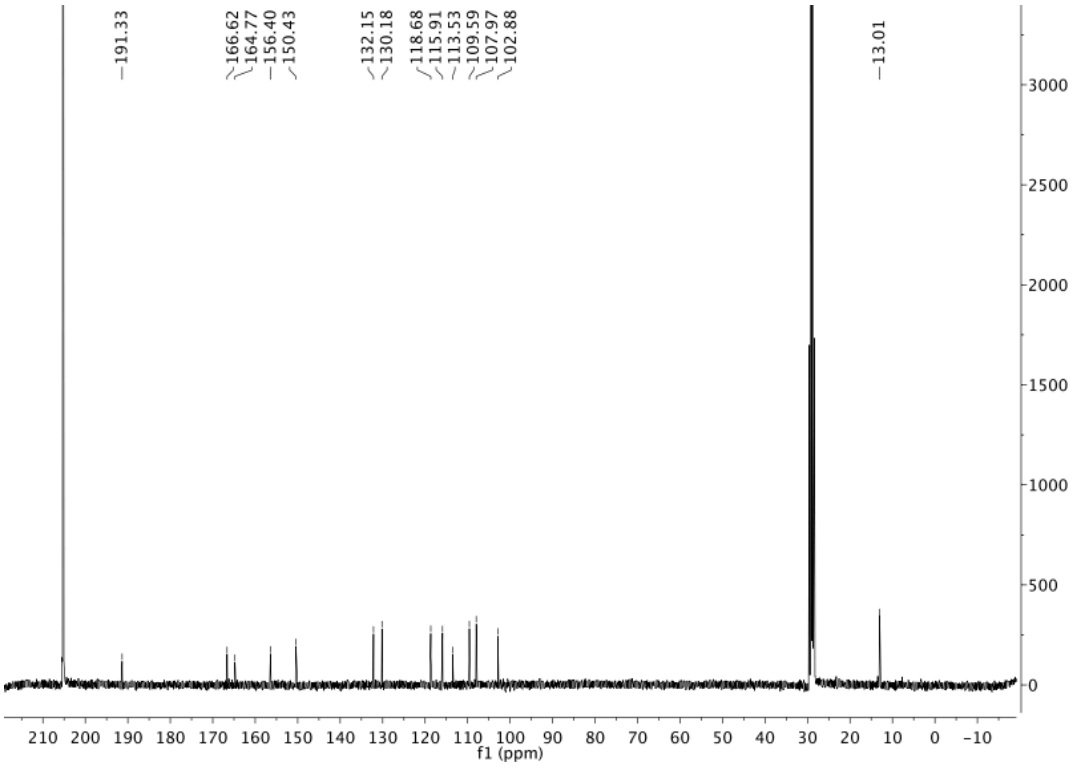

1.6 Dihydrochalcones

3-(4-fluorophenyl)-1-(2,4,6-trihydroxyphenyl)propan-1-one (18a)

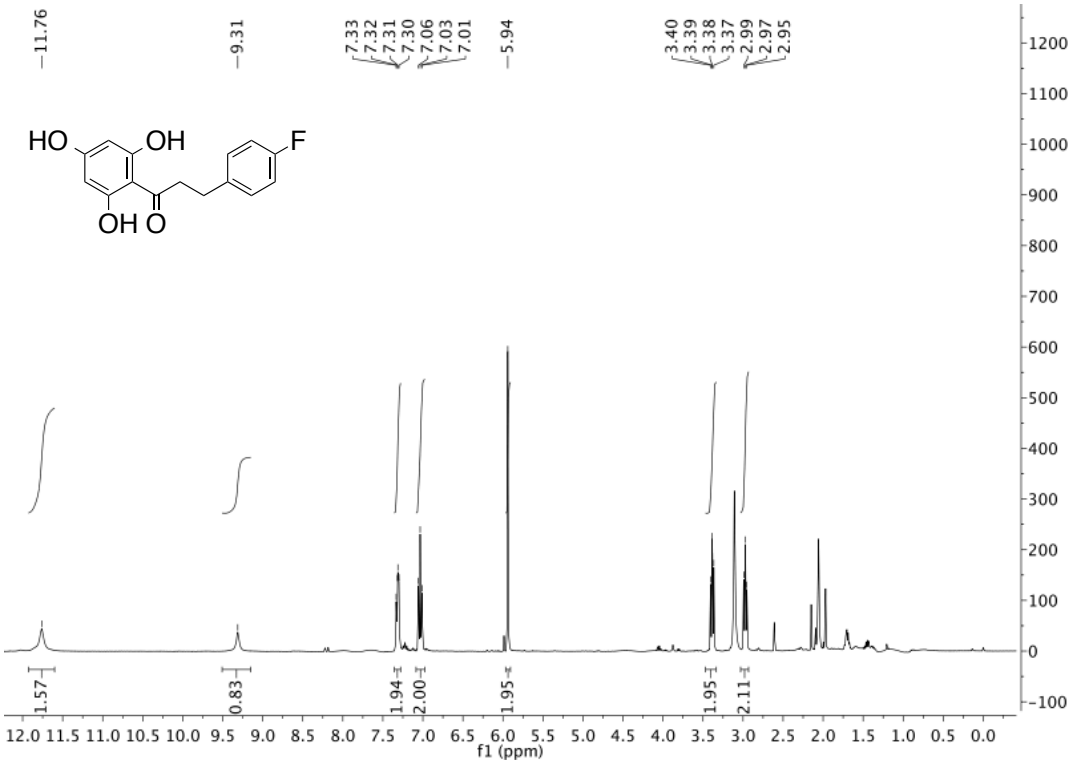

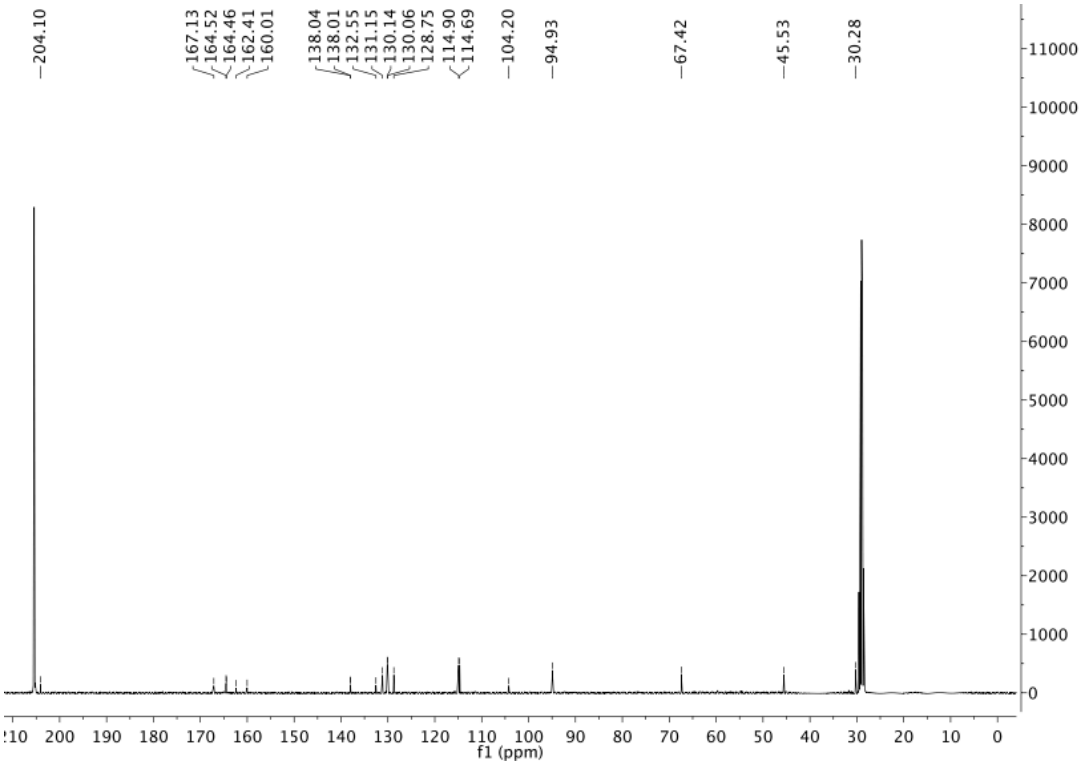

3-(phenyl)-1-(2,4,6-trihydroxyphenyl)propan-1-one (18c)

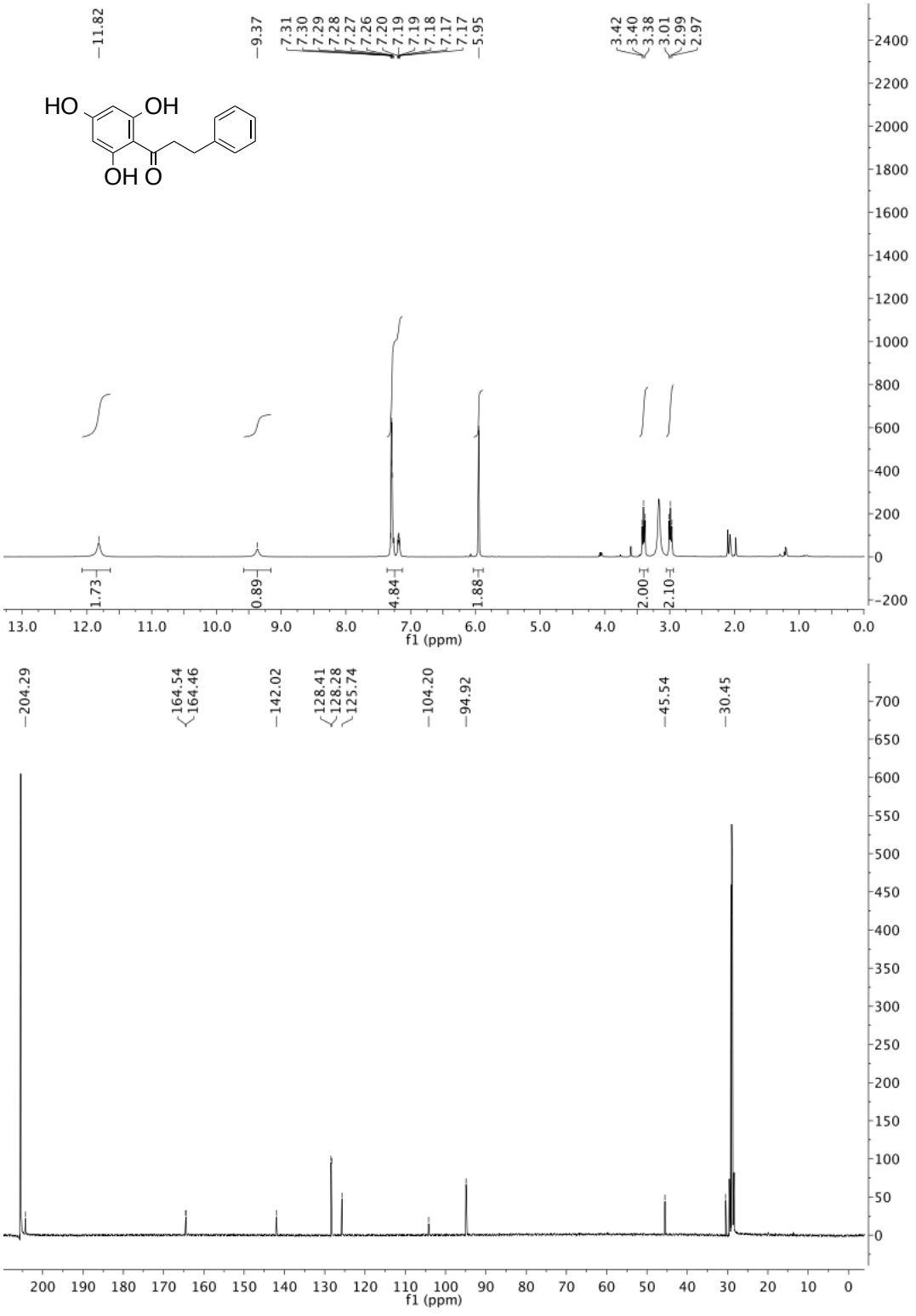

3-(4-methylphenyl)-1-(2,4,6-trihydroxyphenyl)propan-1-one (18d)

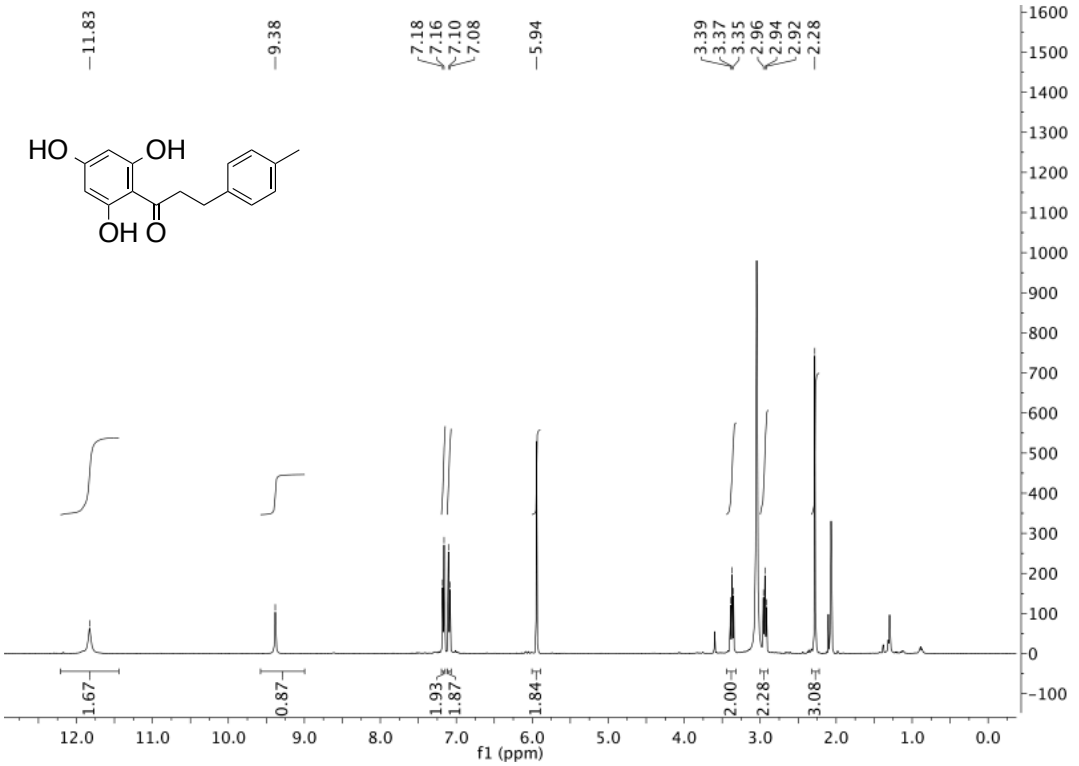

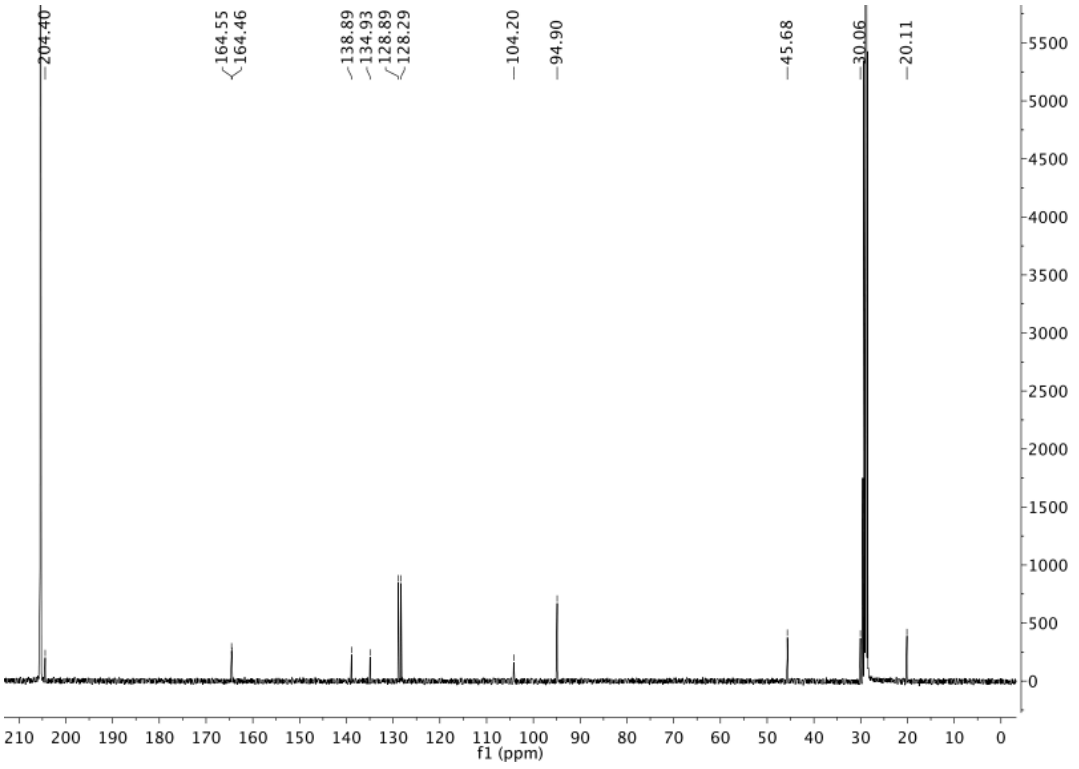

3-(4-methoxyphenyl)-1-(2,4,6-trihydroxyphenyl)propan-1-one (18e)

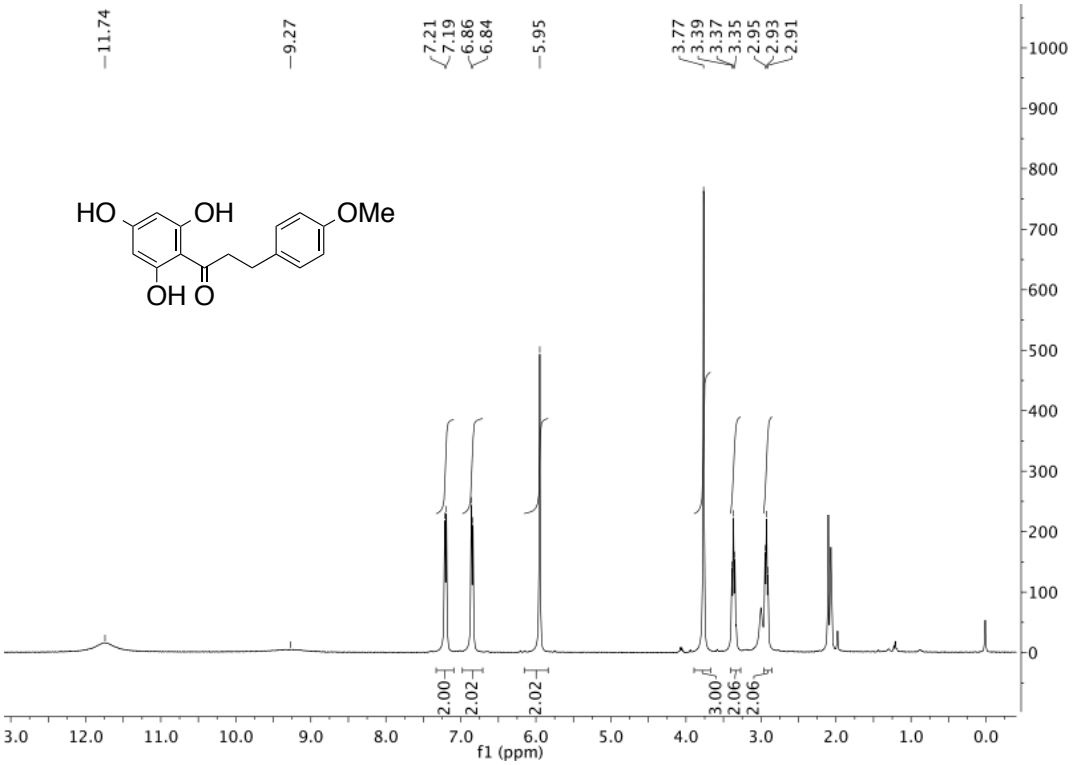

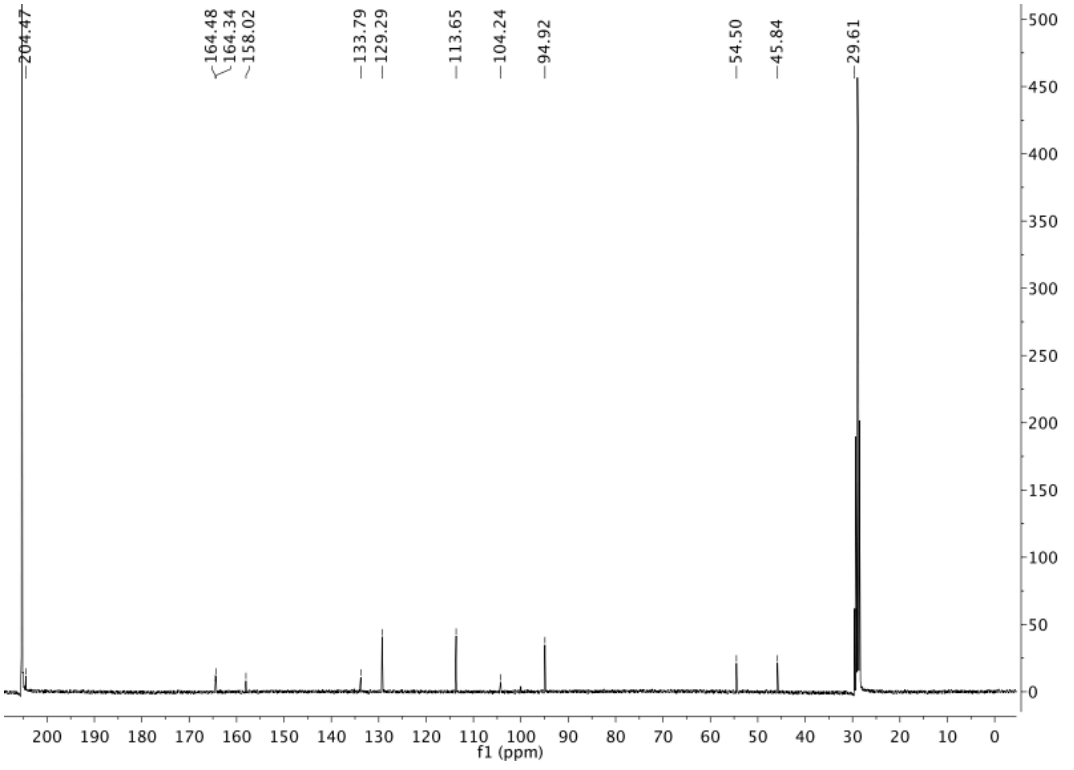

3-(4-ethoxyphenyl)-1-(2,4,6-trihydroxyphenyl)propan-1-one (18f)

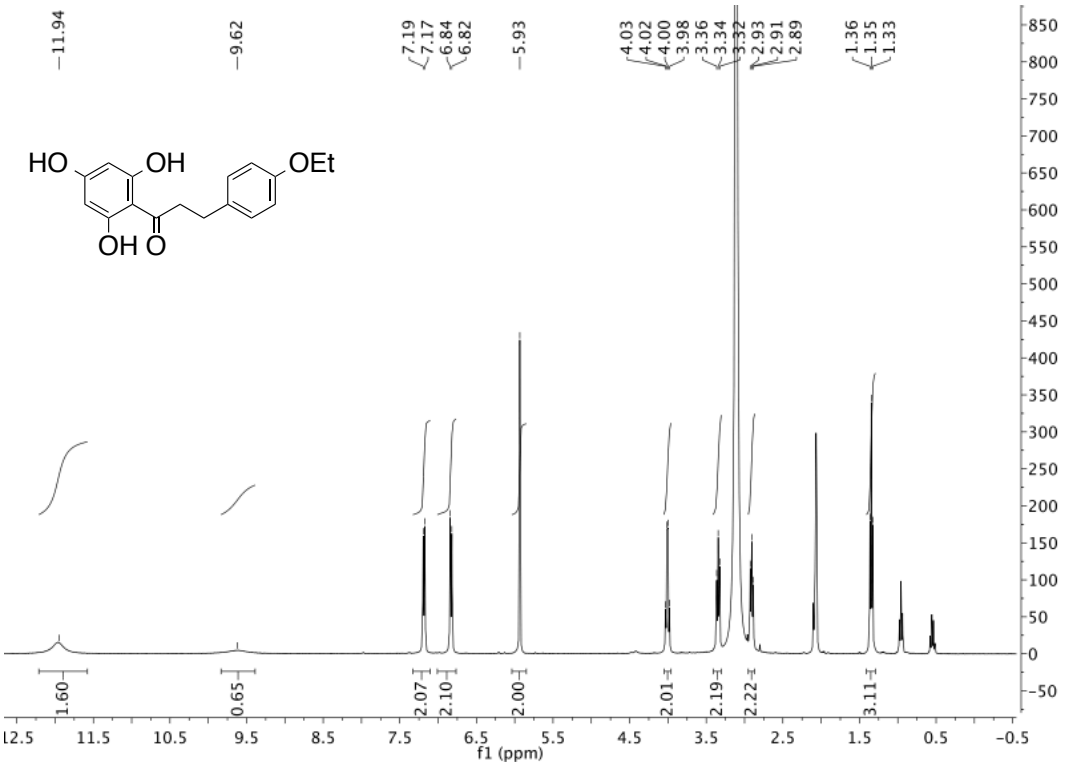

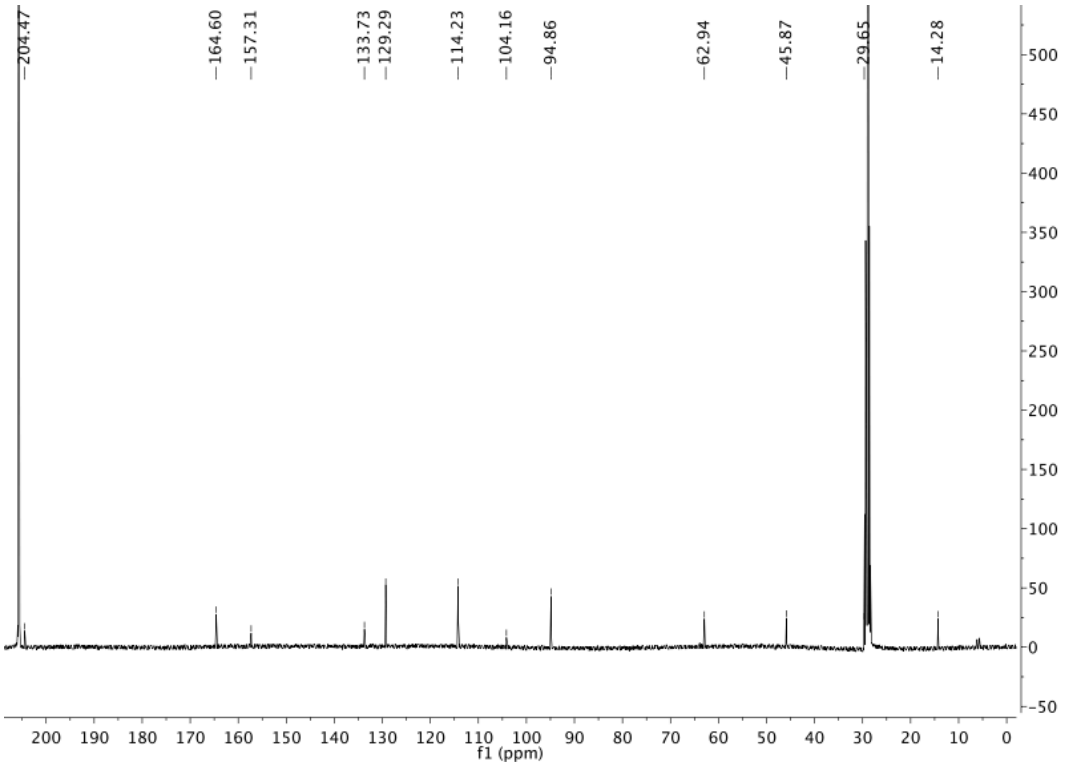

3-(4-propyloxyphenyl)-1-(2,4,6-trihydroxyphenyl)propan-1-one (18g)

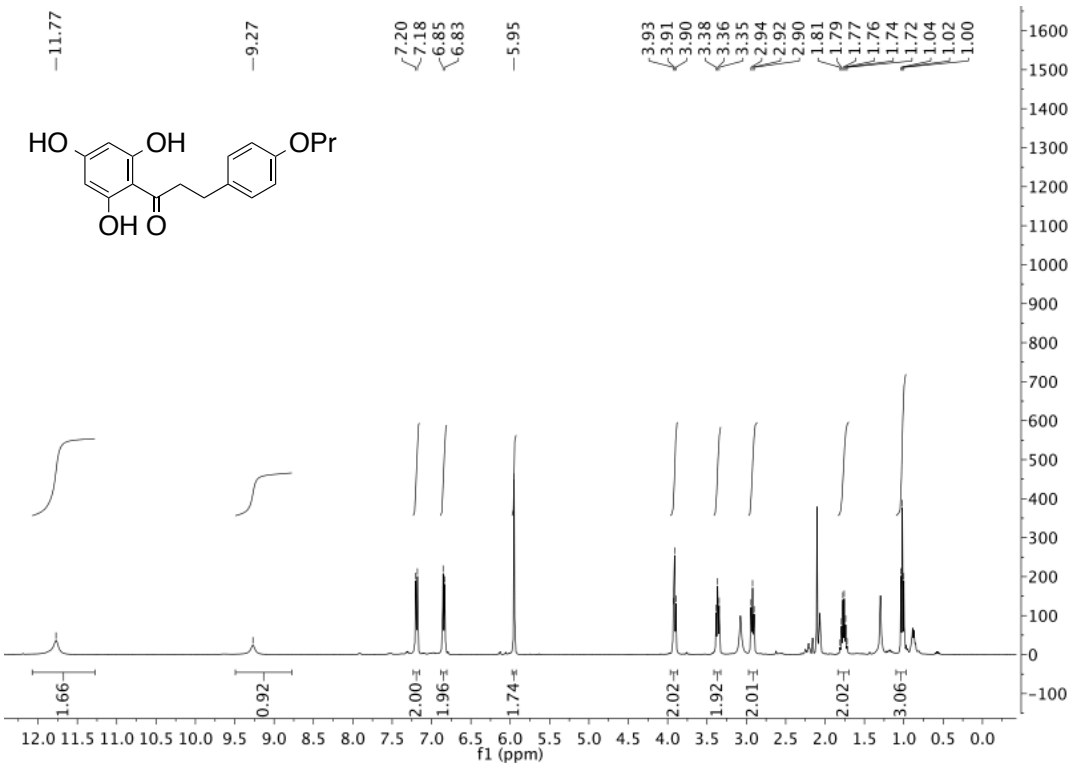

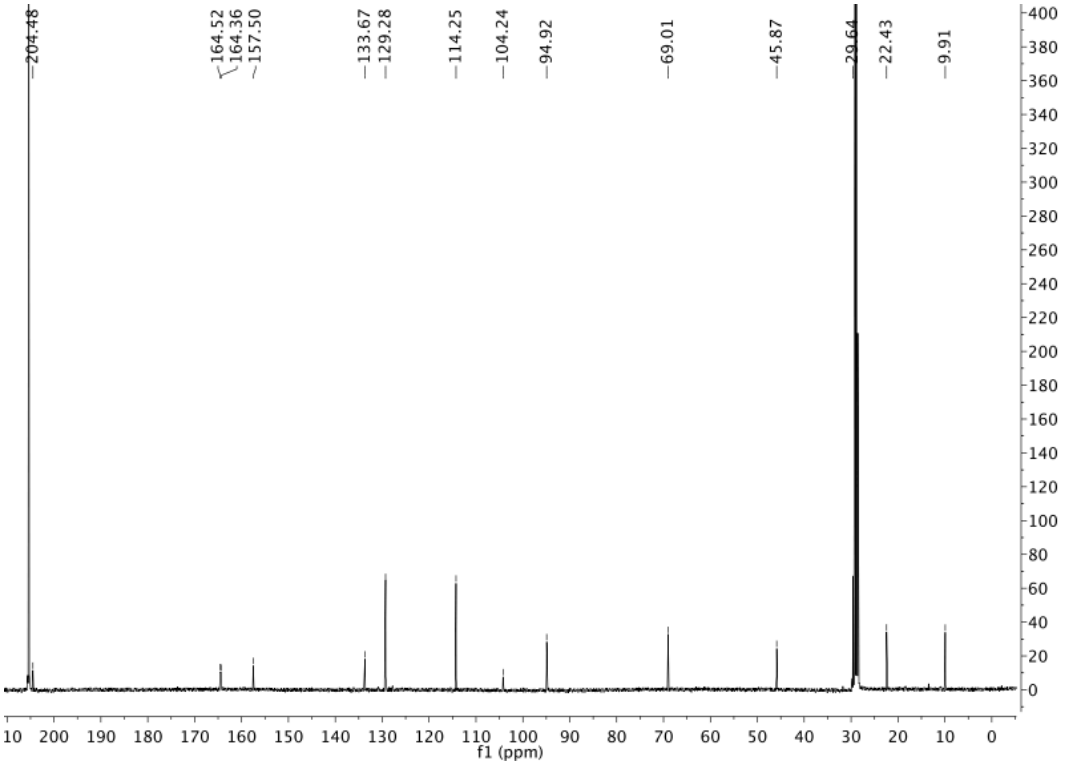

3-(4-hydroxyphenyl)-1-(2,4,6-trihydroxyphenyl)propan-1-one (18h)

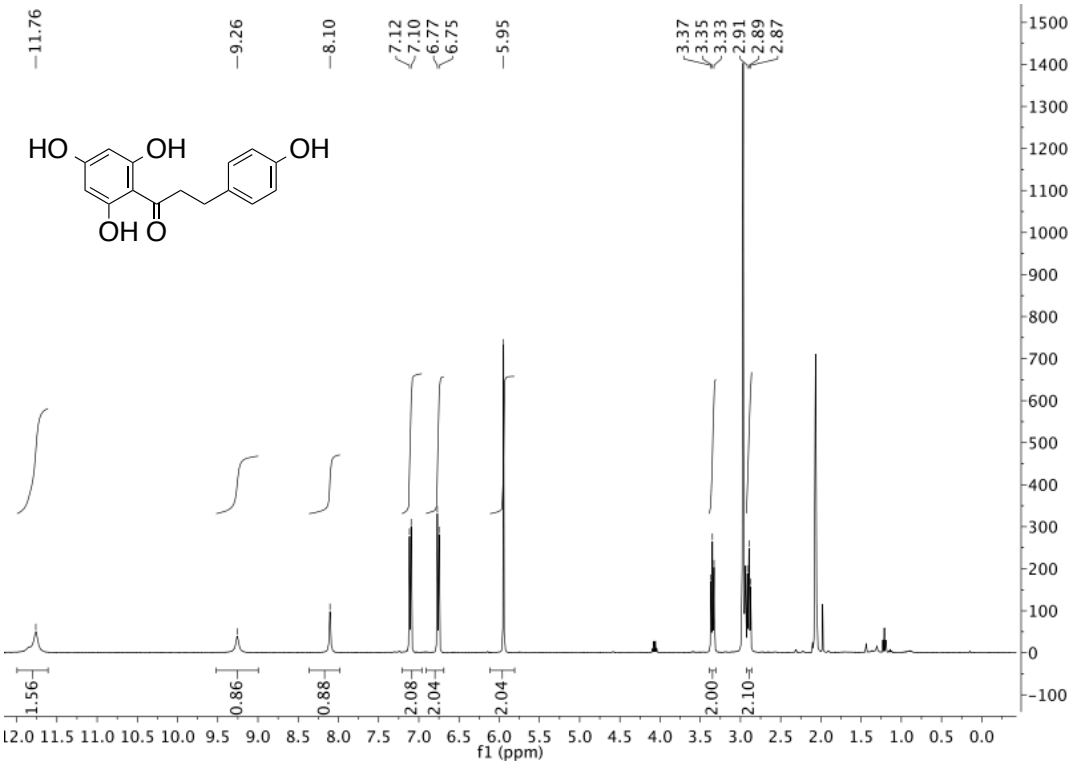

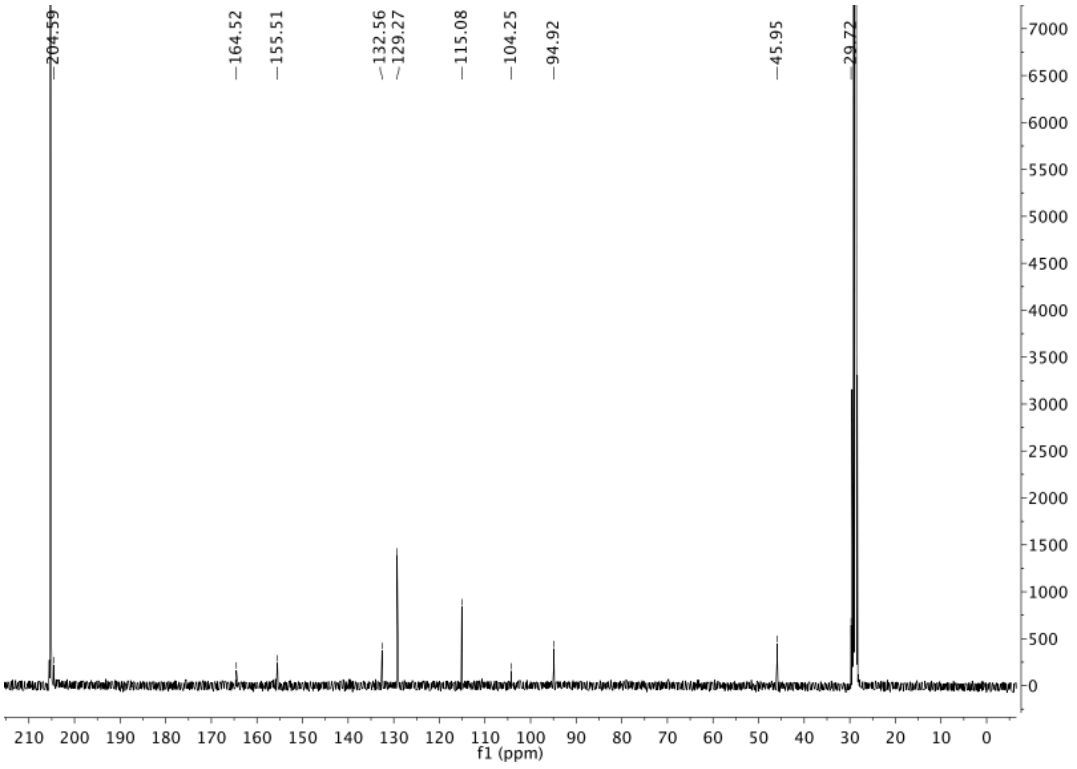

3-(5-methylfuran-2-yl)-1-(2,4,6-trihydroxyphenyl)propan-1-one (18i)

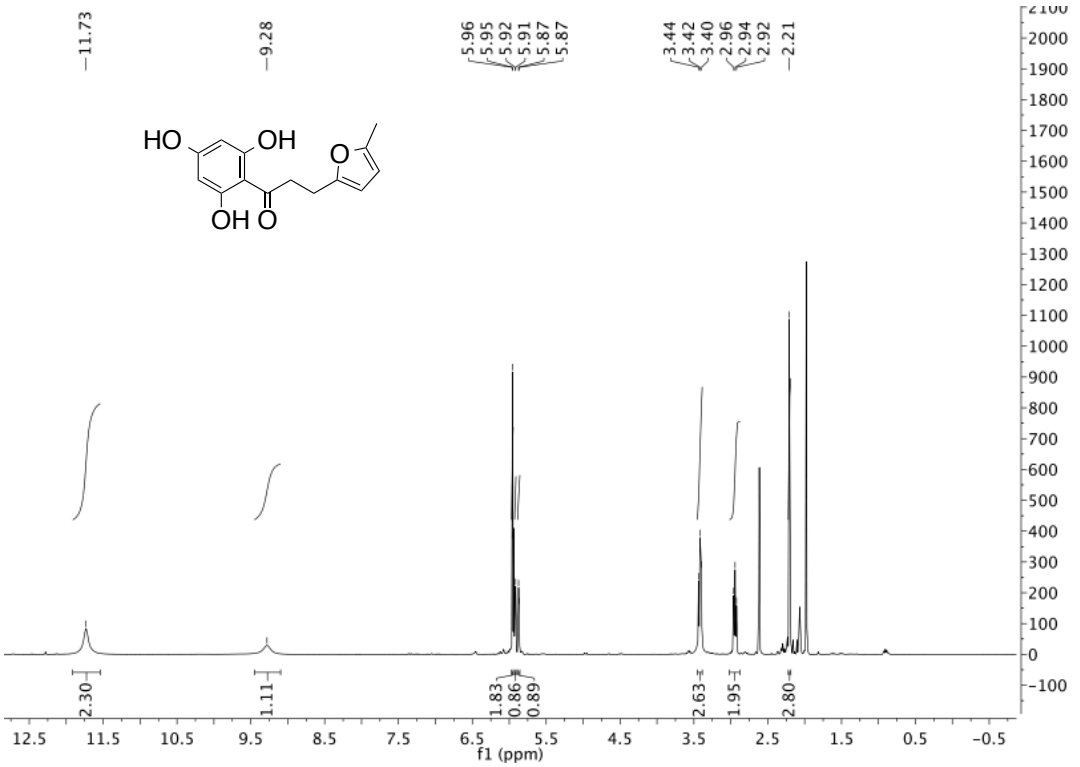

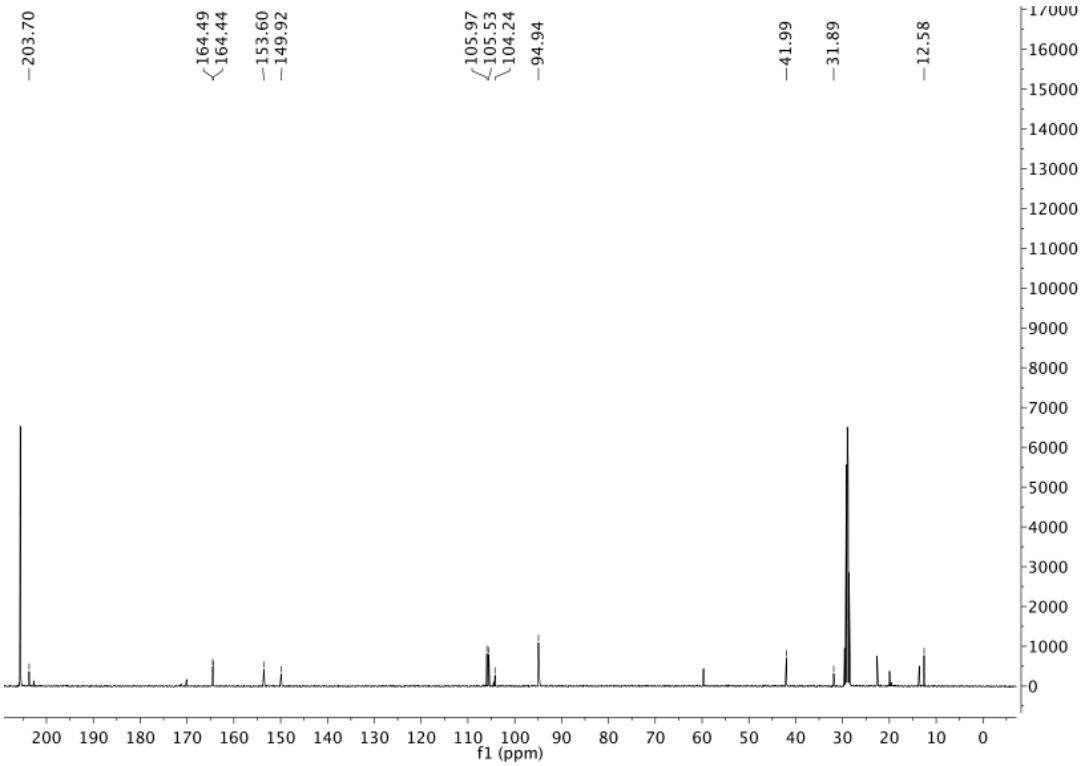

1-(2,4-dihydroxyphenyl)-3-(4-fluorophenyl)propan-1-one (29a)

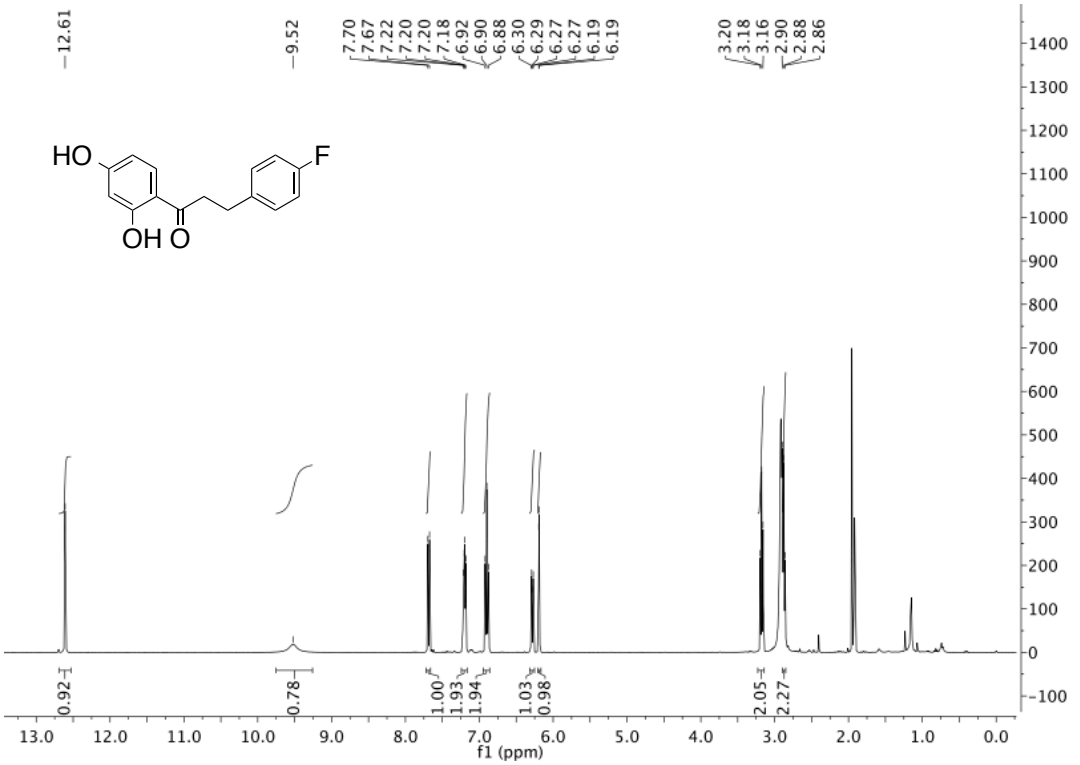

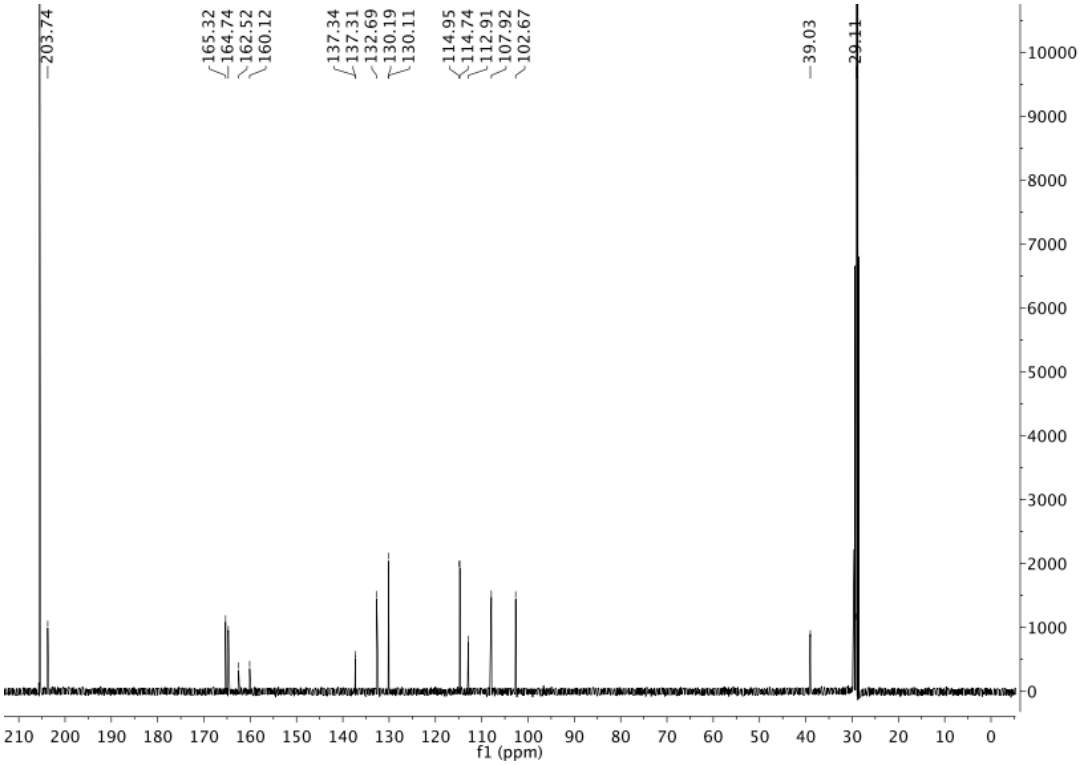

1-(2,4-dihydroxyphenyl)propan-1-one)-3-phenyl-propan-1-one (29c)

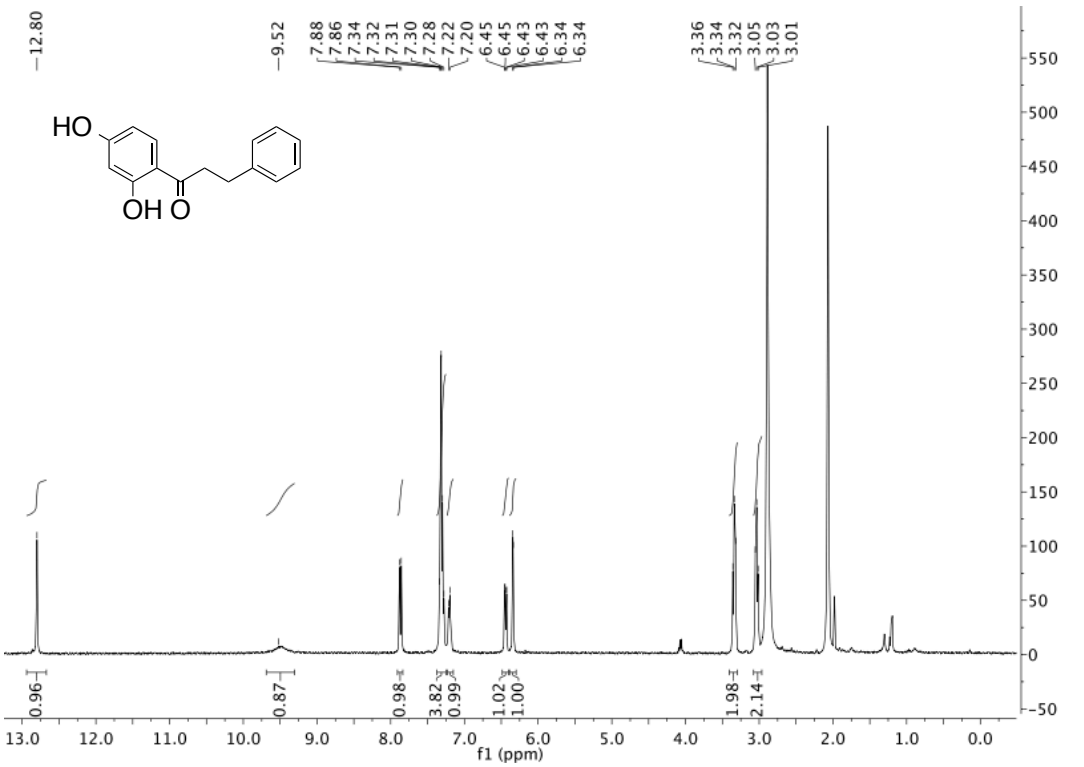

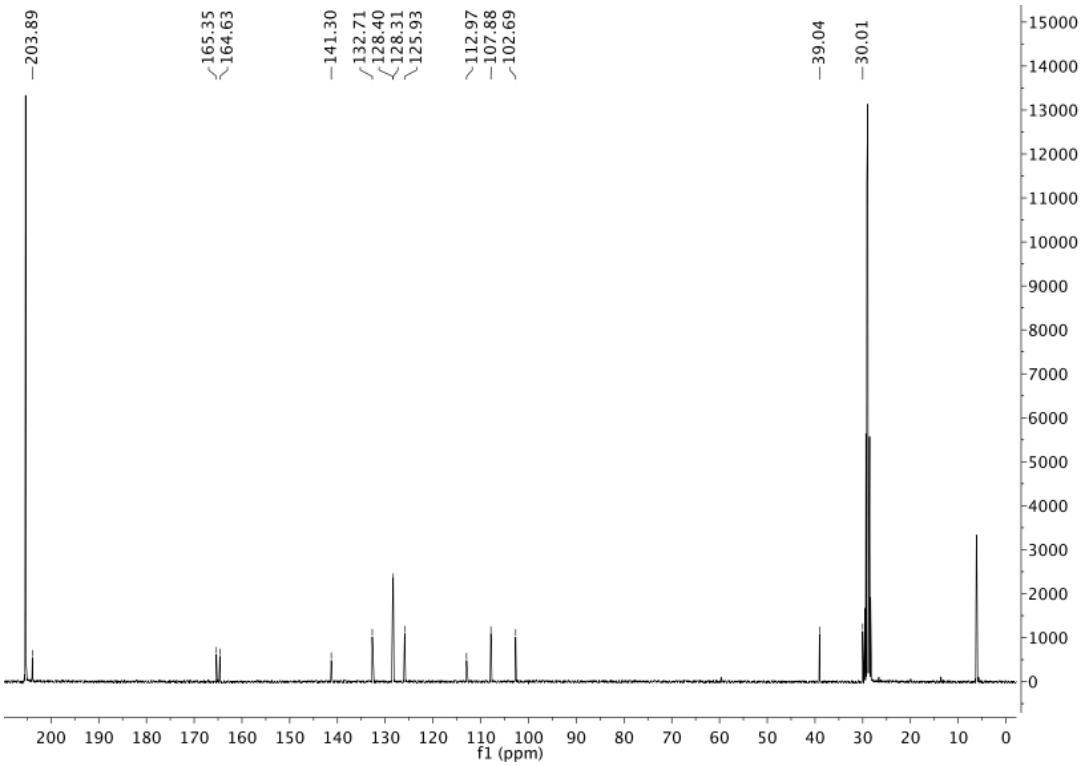

1-(2,4-dihydroxyphenyl)-3-(4-methylphenyl)propan-1-one (29d)

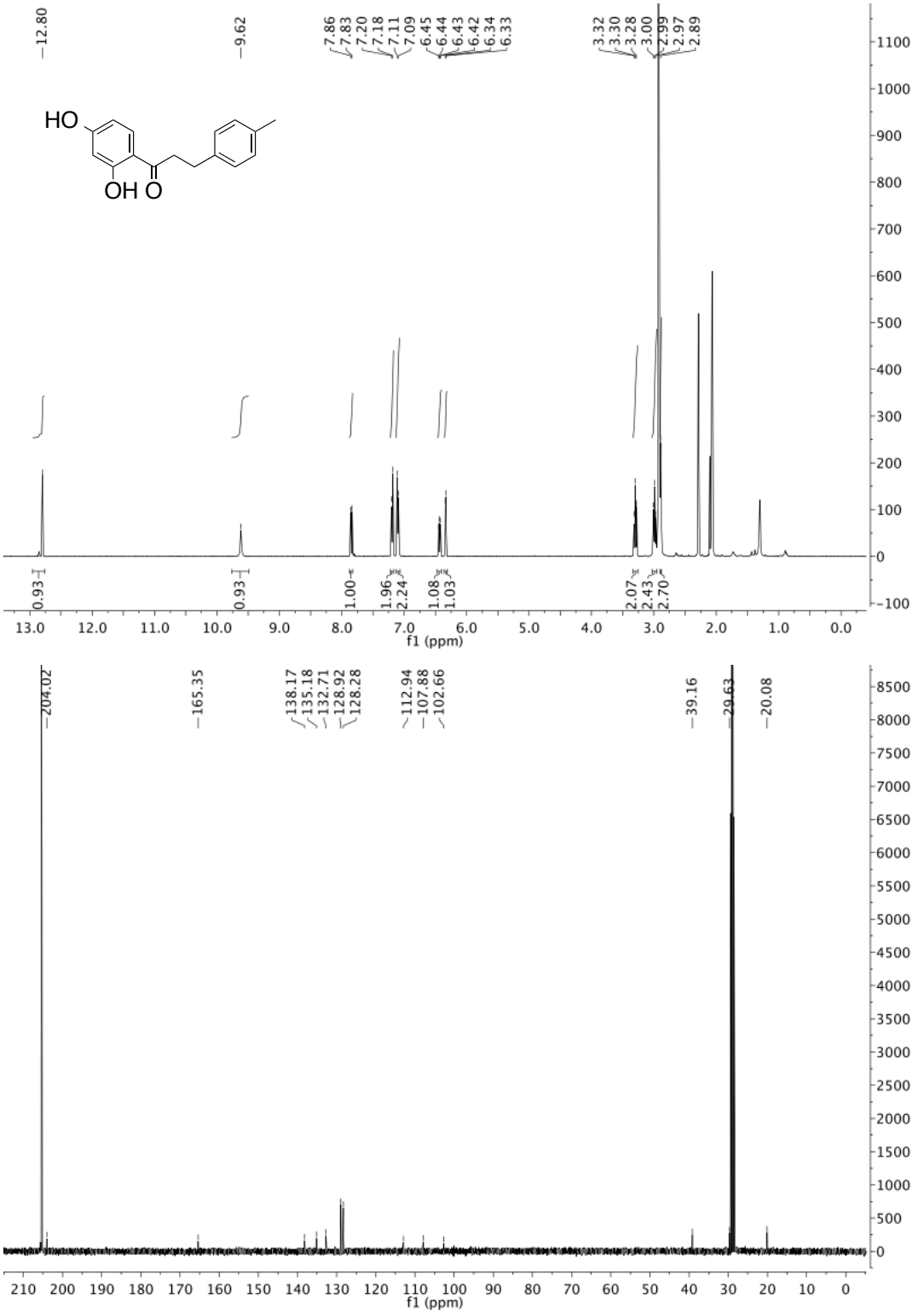

1-(2,4-dihydroxyphenyl)-3-(4-hydroxyphenyl)propan-1-one (29h)

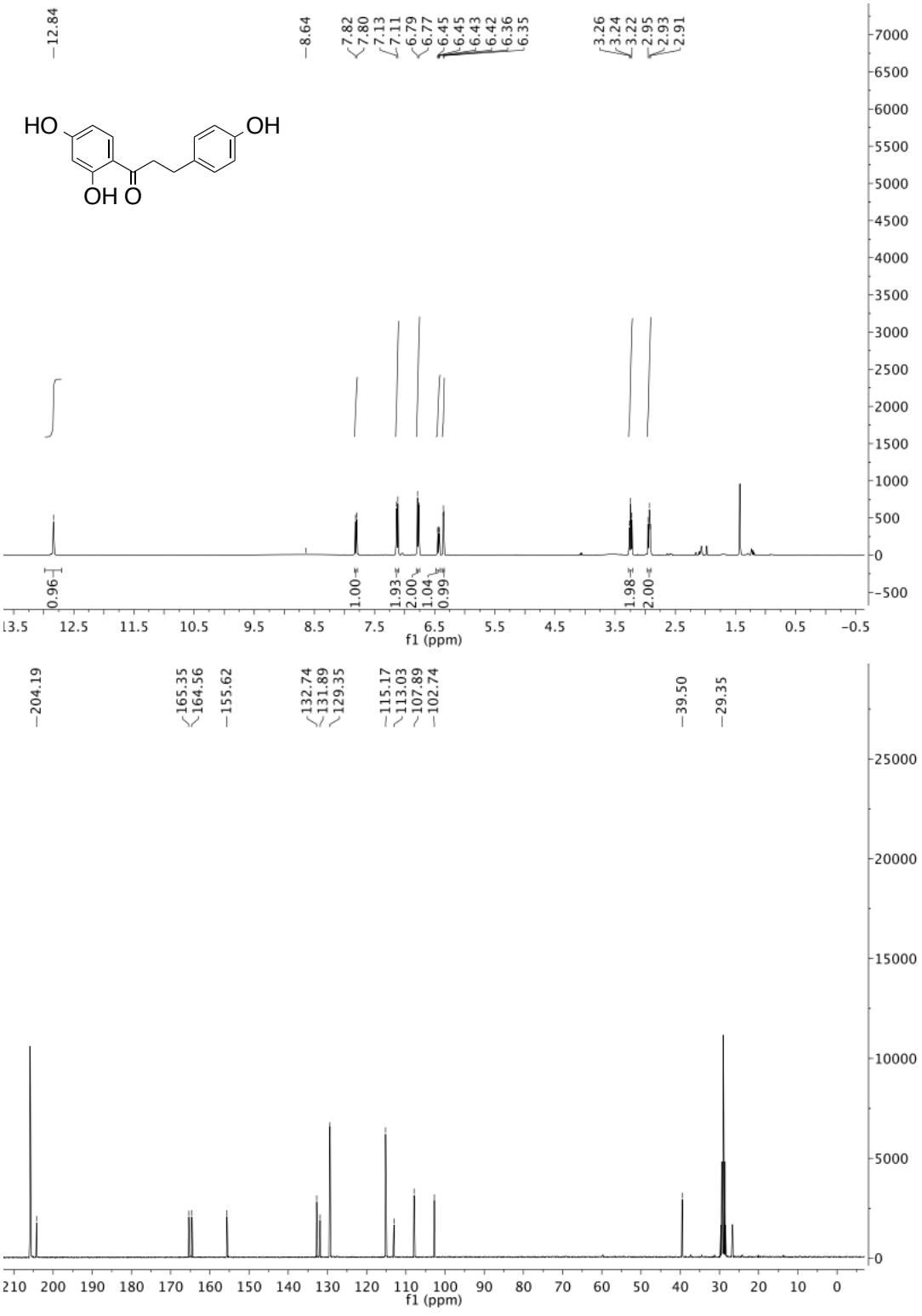

1-(2,4-dihydroxyphenyl)-3-(5-methylfuran-2-yl)propan-1-one (29i)

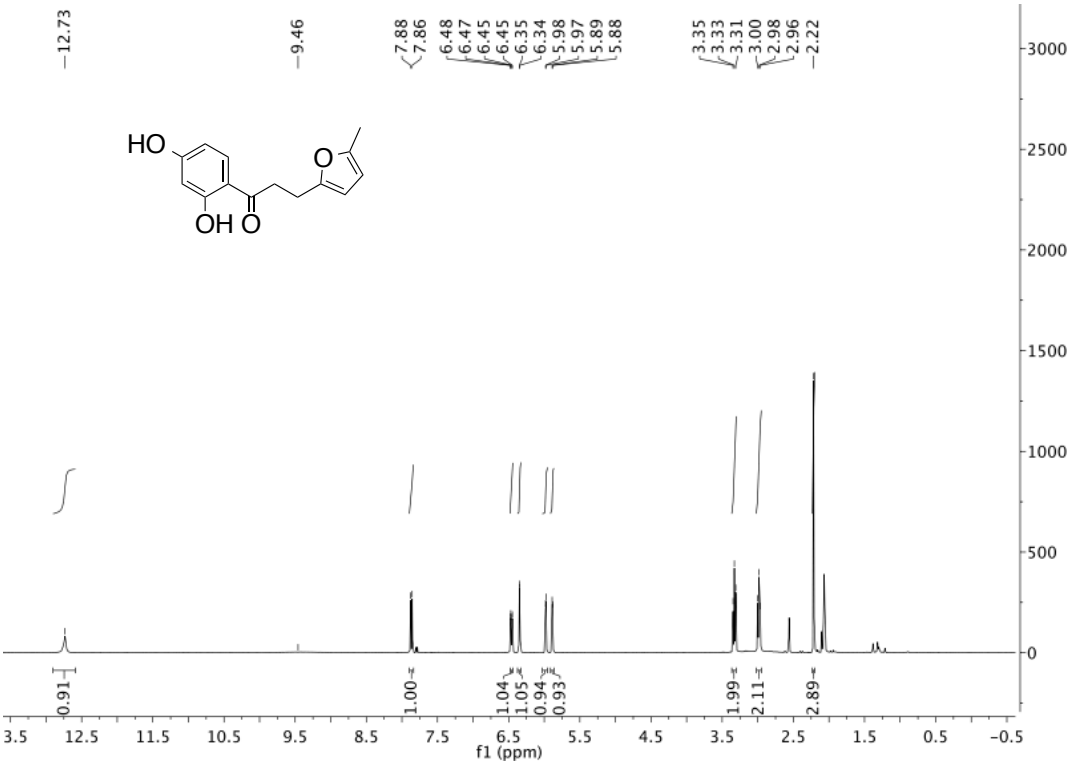

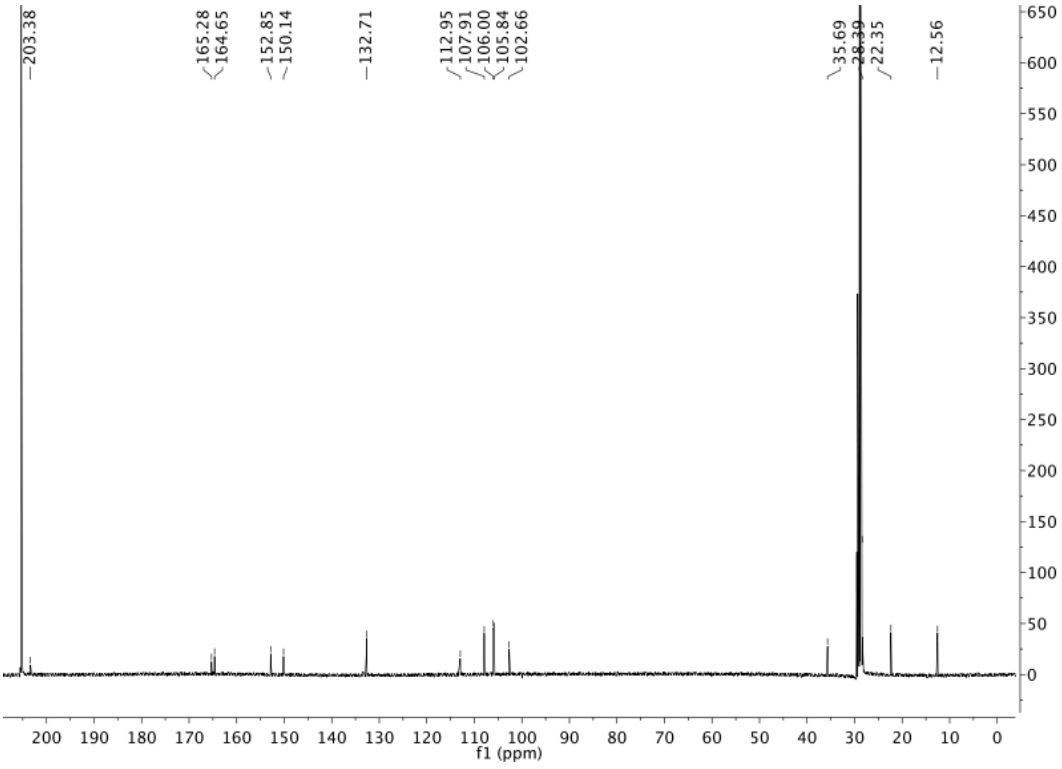

1-(4-fluoro-2-hydroxyphenyl)-3-(4-fluorophenyl)propan-1-one (30a)

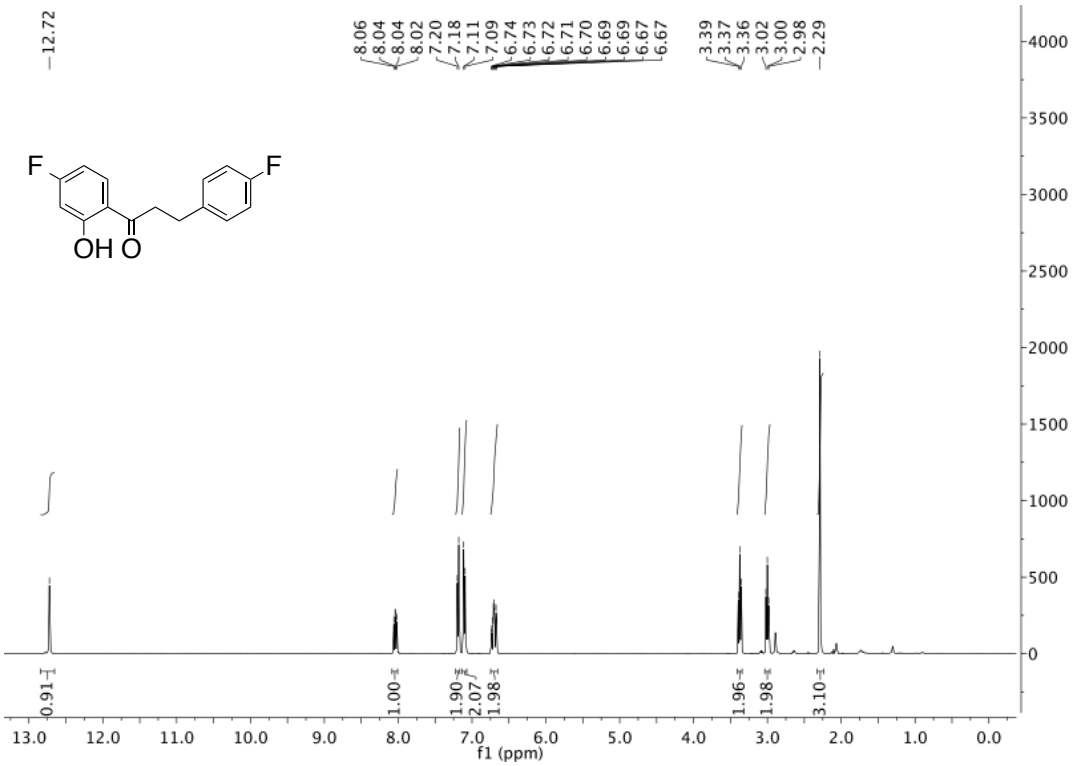

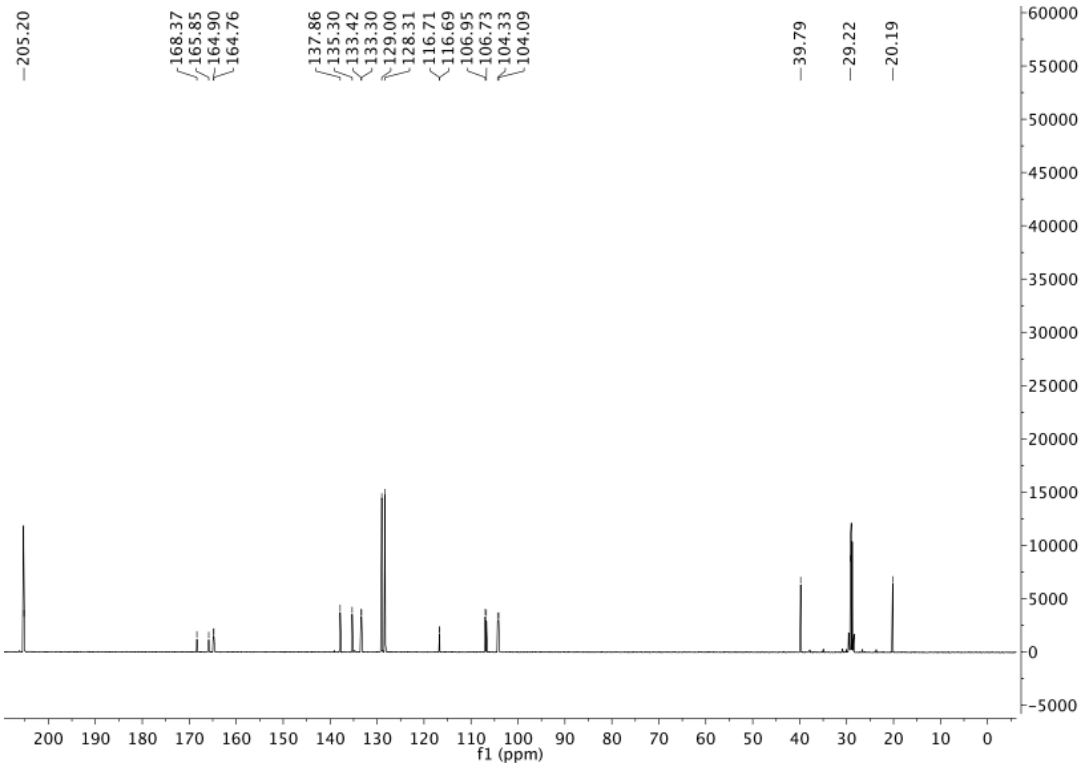

1-(4-fluoro-2-hydroxyphenyl)-3-(phenyl)propan-1-one (30c)

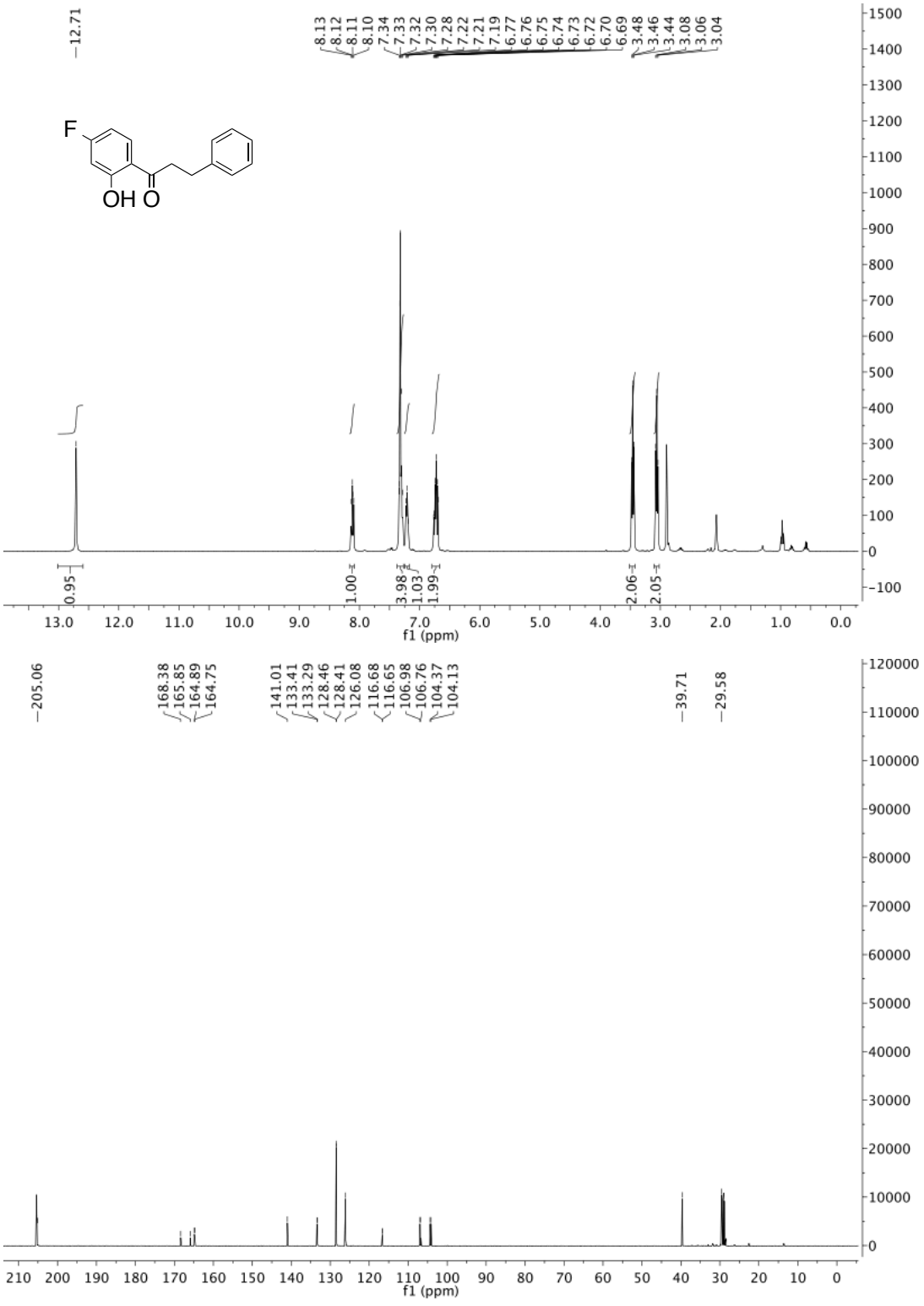

1-(4-fluoro-2-hydroxyphenyl)-3-(4-methylphenyl)propan-1-one (30d)

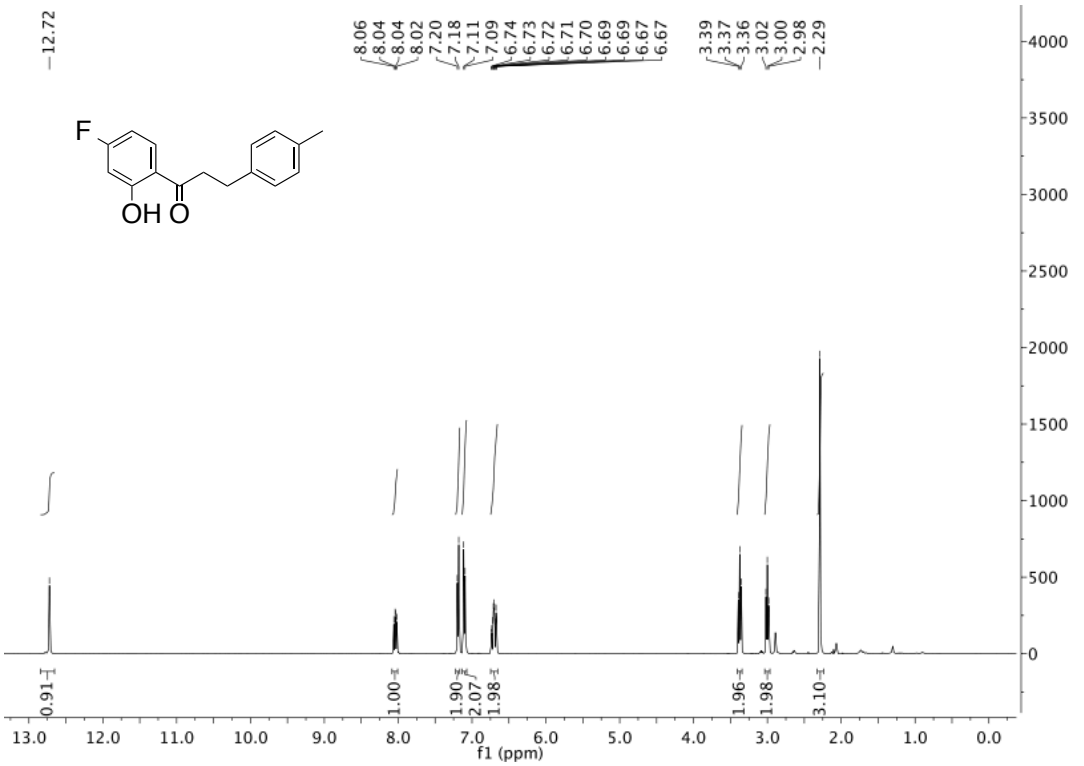

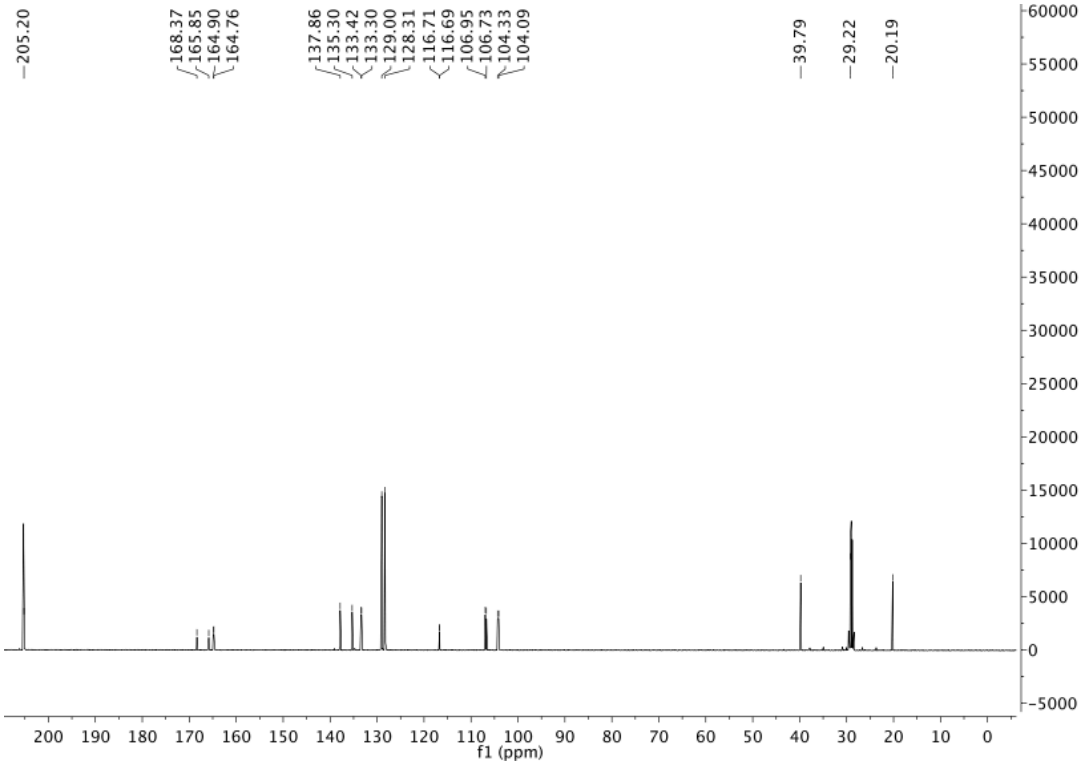

1-(4-fluoro-2-hydroxyphenyl)-3-(4-hydroxyphenyl)propan-1-one (30h)

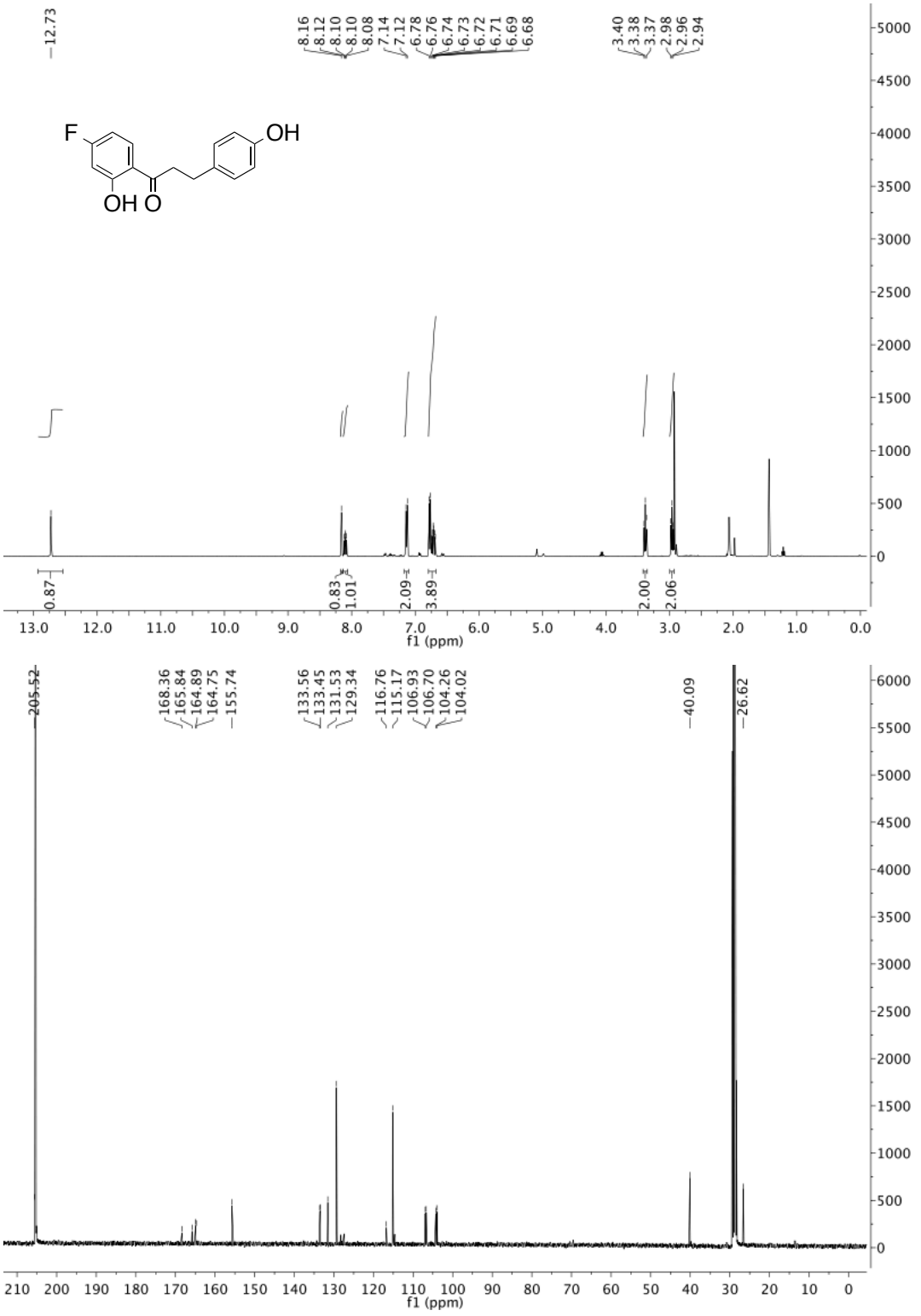

1-(4-fluoro-2-hydroxyphenyl)-3-(5-methylfuran-2-yl)propan-1-one (30i)

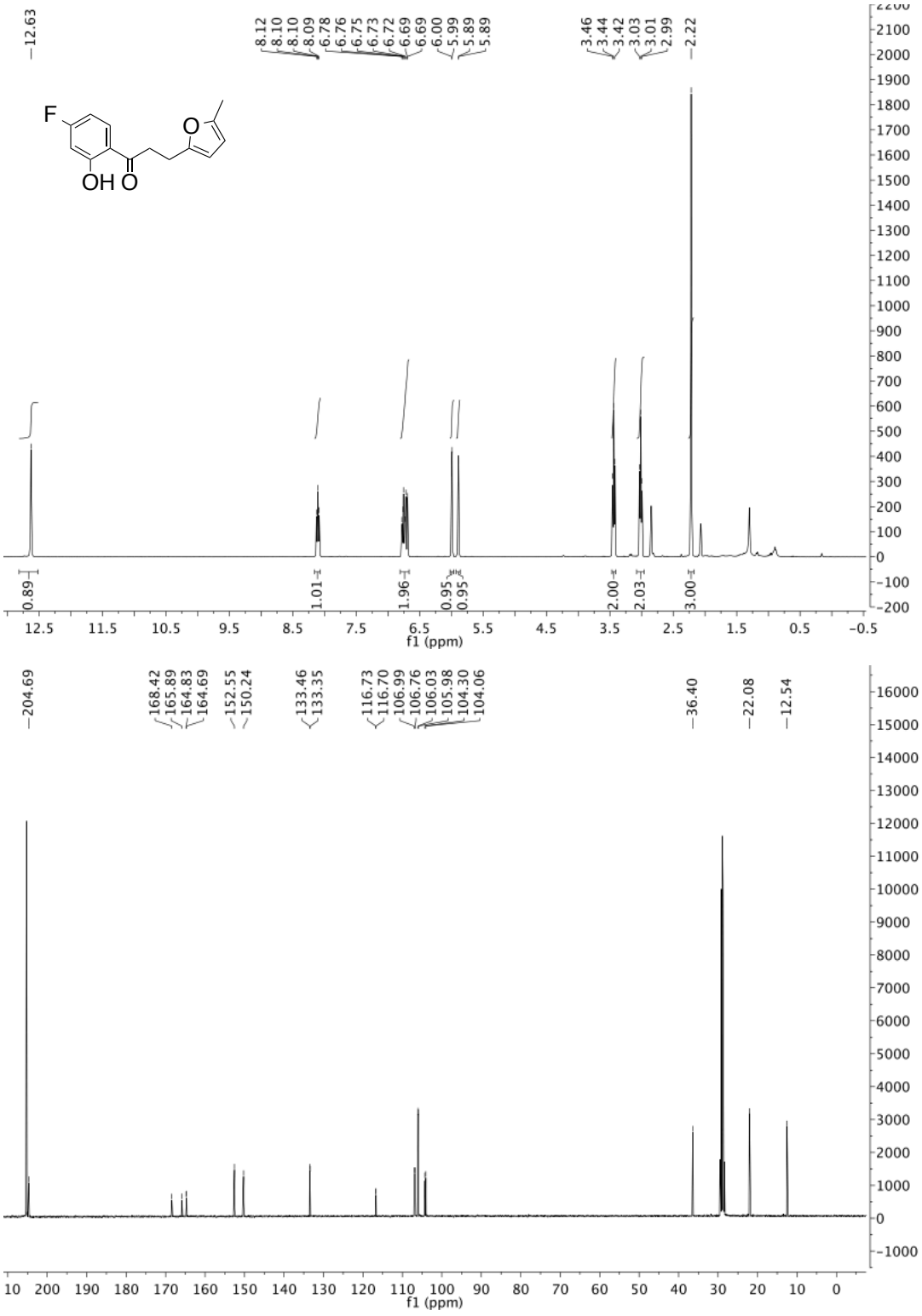

1-(4-fluoro-2-hydroxyphenyl)-3-(5-methyltetrahydrofuran-2-yl)propan-1-one (30j)

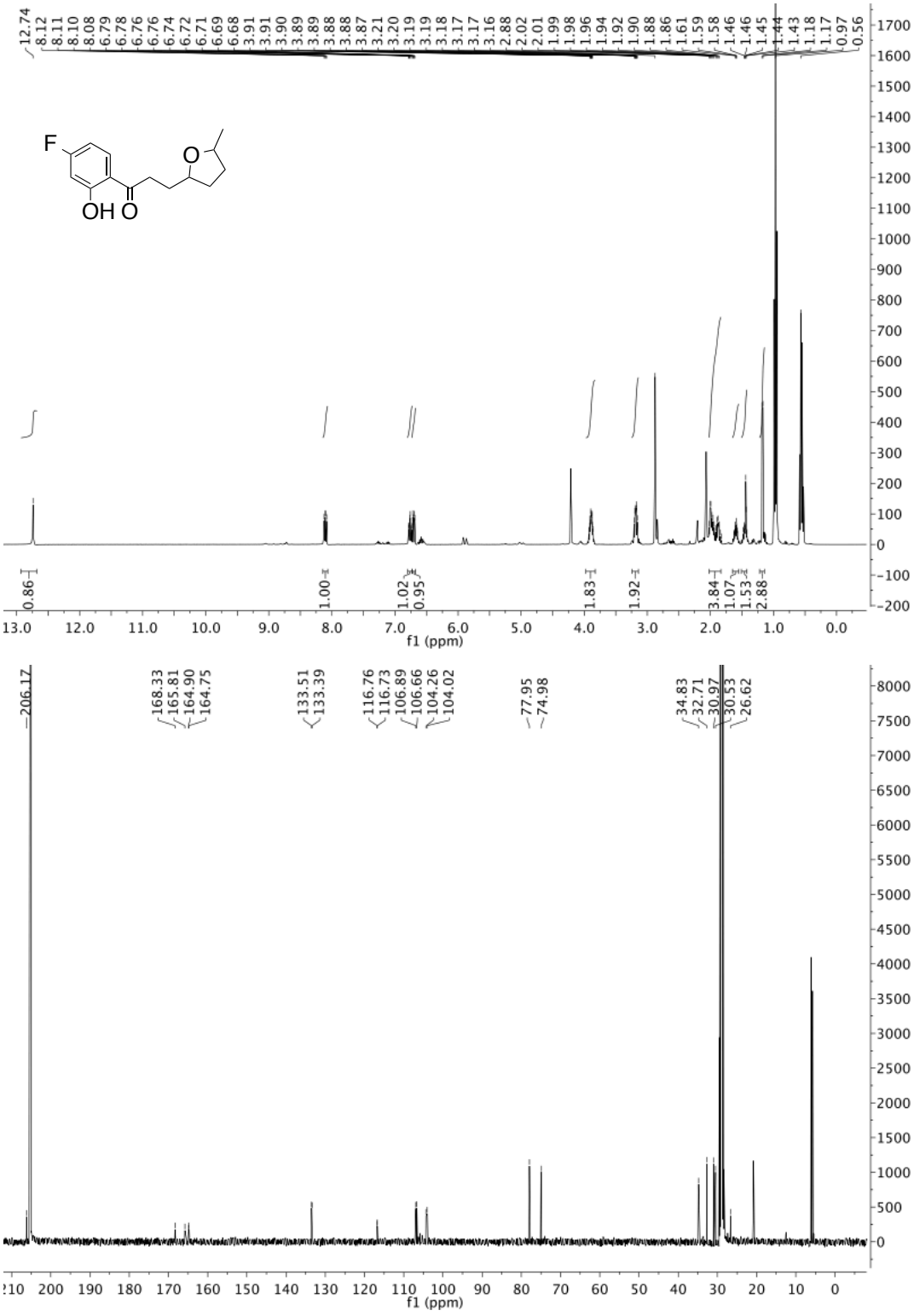

1.7 Protected C-glucosyl dihydrochalcones

3-(4-fluorophenyl)-1-[3-(2,3,4,6-tetra-*O*-benzyl-β-D-glucopyranosyl)-2,4,6-trihydroxyphenyl]propan-1-one (37a)

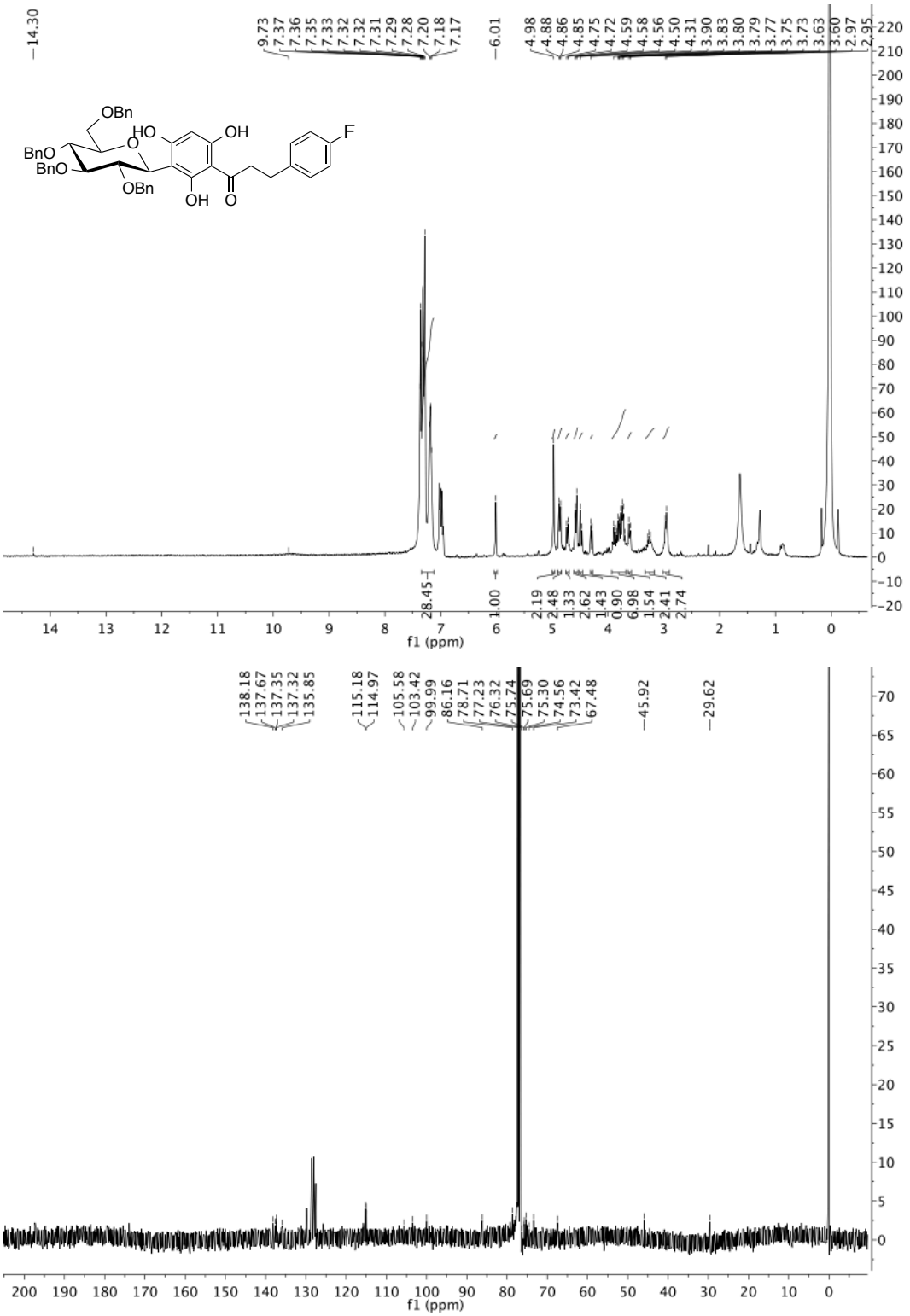

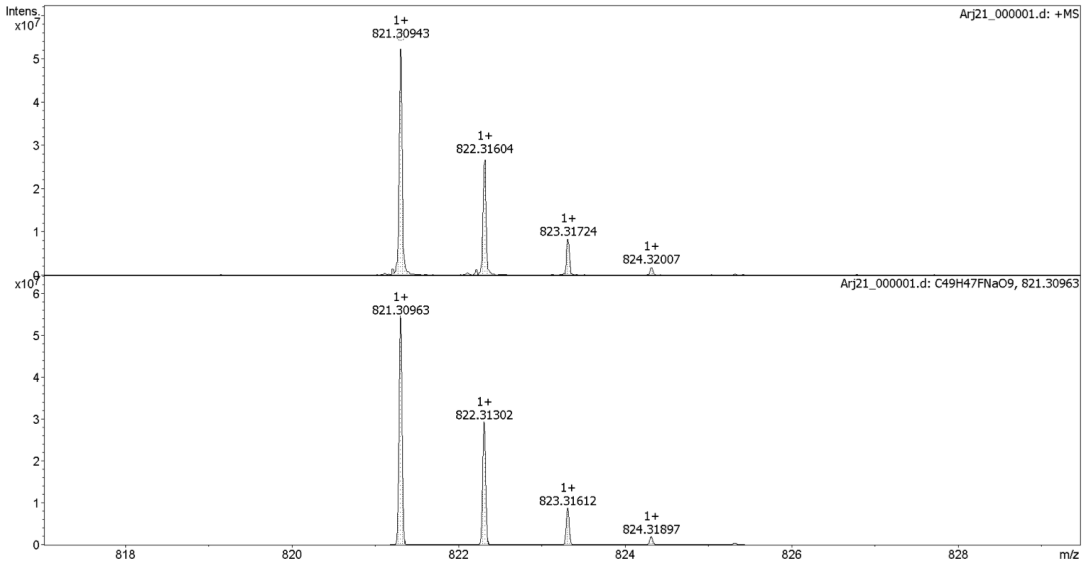
Intens.
x10^7
Arj21_000001.d: +MS
1+
821.30943
1+
822.31604
1+
823.31724
1+
824.32007
x10^7
Arj21_000001.d: C49H47FNaO9, 821.30963
1+
821.30963
1+
822.31302
1+
823.31612
1+
824.31897
818
820
822
824
826
828
m/z

3-phenyl-1-[3-(2,3,4,6-tetra-*O*-benzyl-β-D-glucopyranosyl)-2,4,6-trihydroxyphenyl]-propan-1-one (37c)

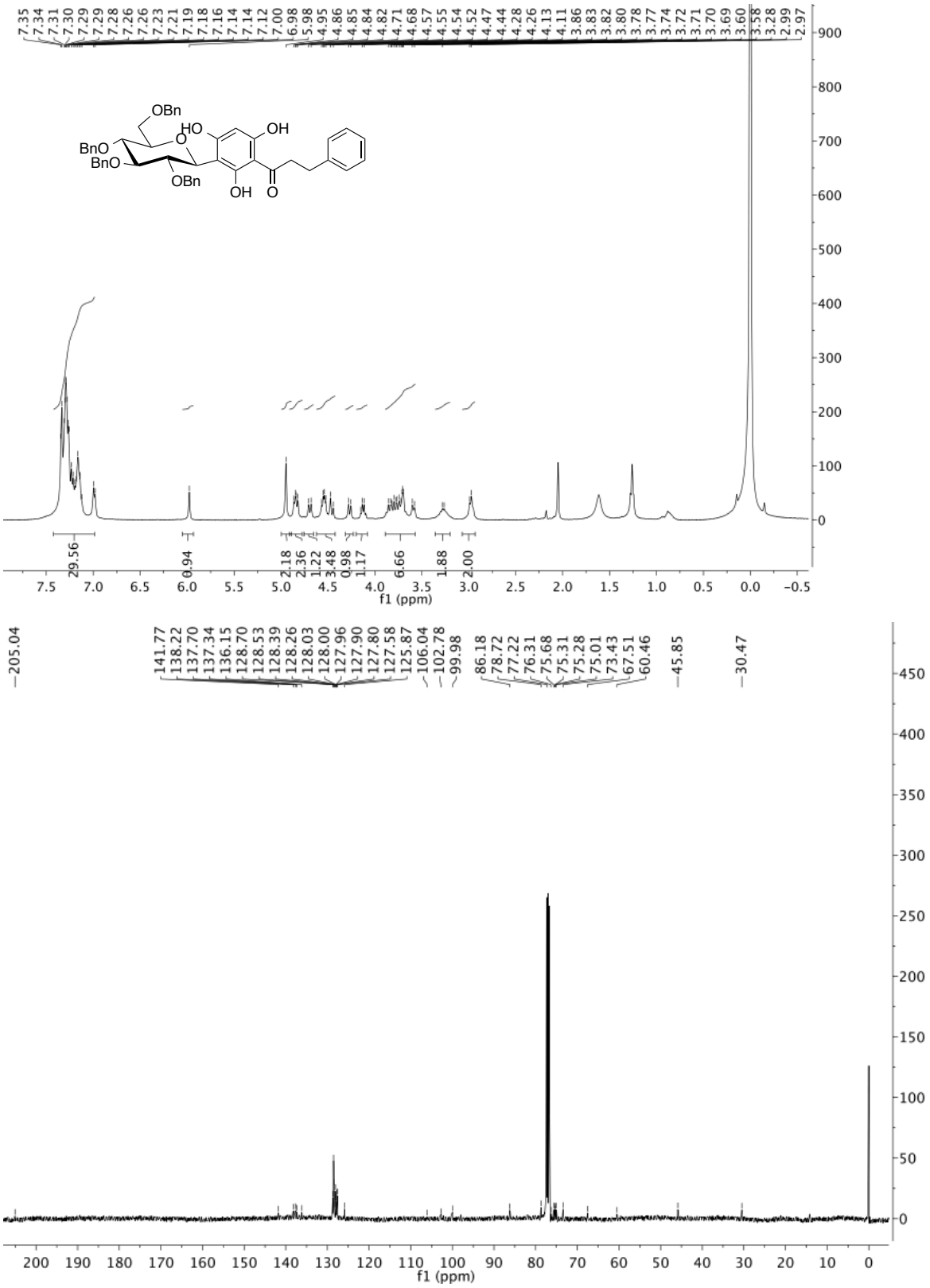

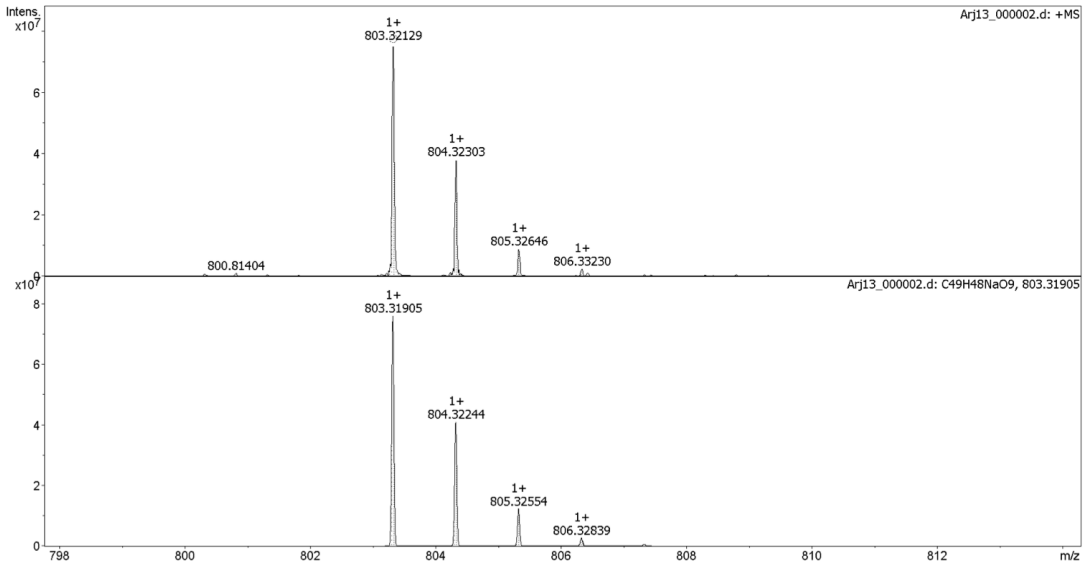
Intens.
x10^7
Arj13_000002.d: +MS
1+
803.32129
1+
804.32303
1+
805.32646
1+
806.33230
800.81404
x10^7
Arj13_000002.d: C49H48NaO9, 803.31905
1+
803.31905
1+
804.32244
1+
805.32554
1+
806.32839
798
800
802
804
806
808
810
812
m/z

3-(4-methylphenyl)-1-[3-(2,3,4,6-tetra-*O*-benzyl-β-D-glucopyranosyl)-2,4,6-tri-hydroxy-phenyl]propan-1-one (37d)

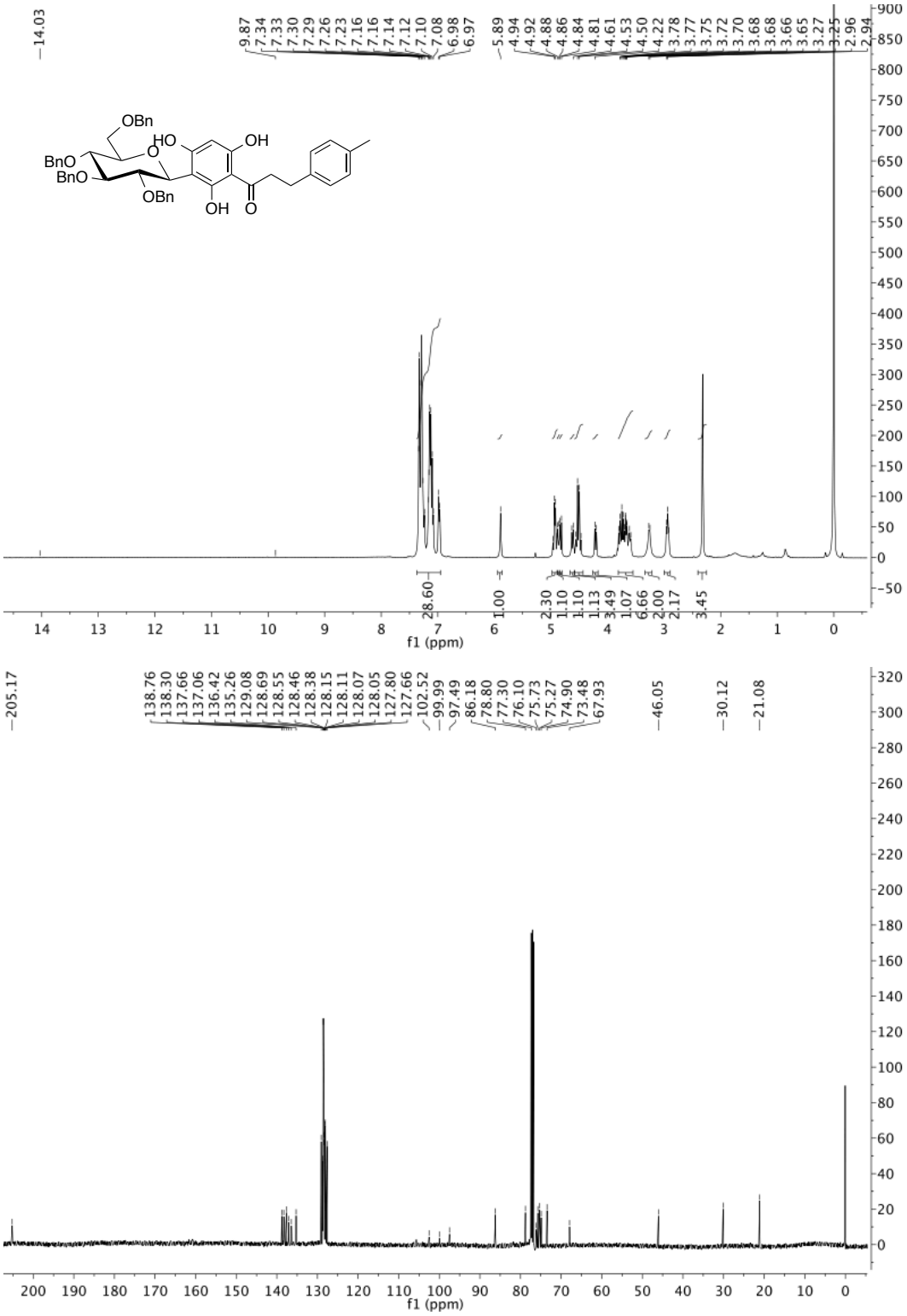

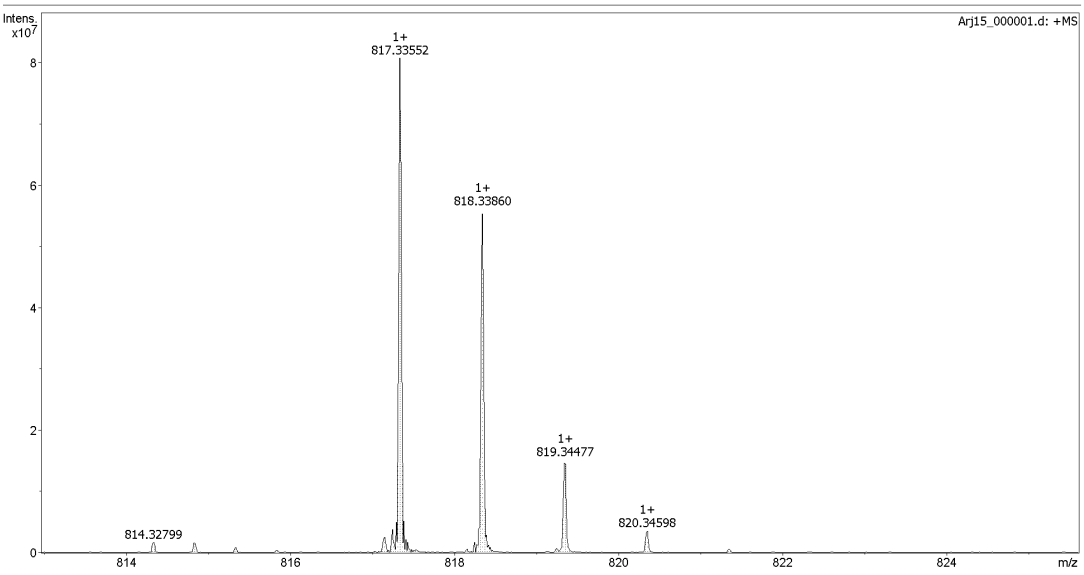
Intens.
x10^7
Arj15_000001.d: +MS
1+
817.33552
1+
818.33860
1+
819.34477
1+
820.34598
814.32799
8
6
4
2
0
814
816
818
820
822
824
m/z

3-(4-methyloxyphenyl)-1-[3-(2,3,4,6-tetra-*O*-benzyl-β-D-glucopyranosyl)-2,4,6-trihydroxyphenyl]propan-1-one (37e)

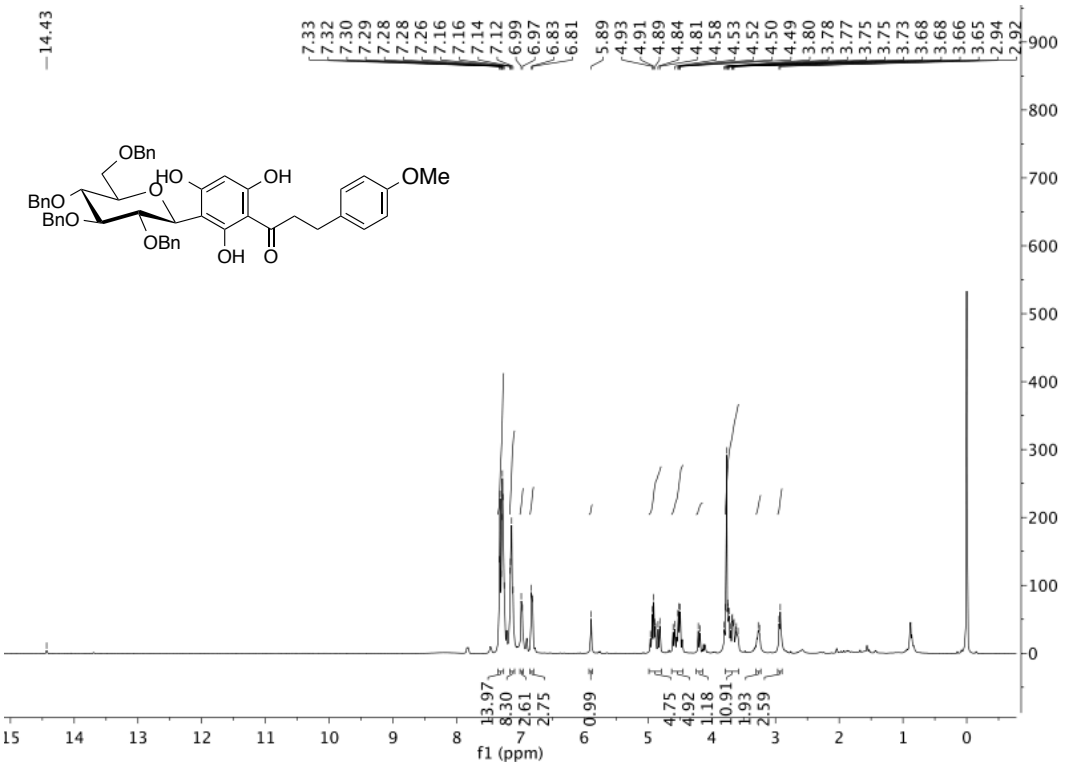

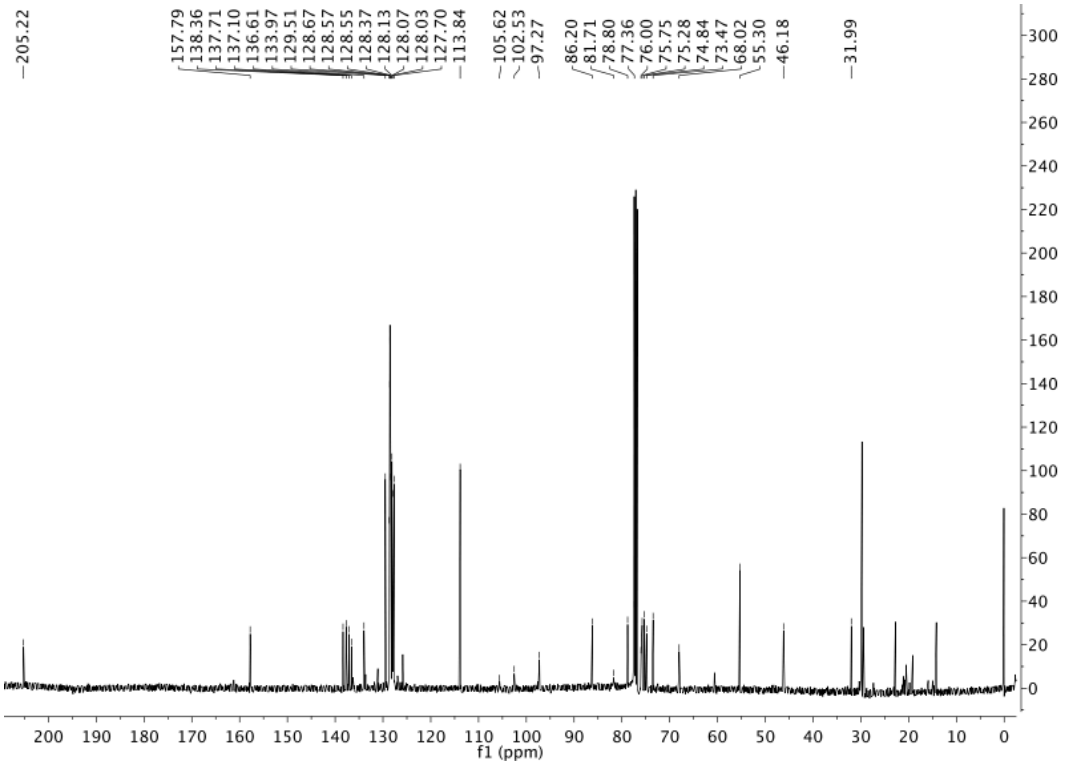

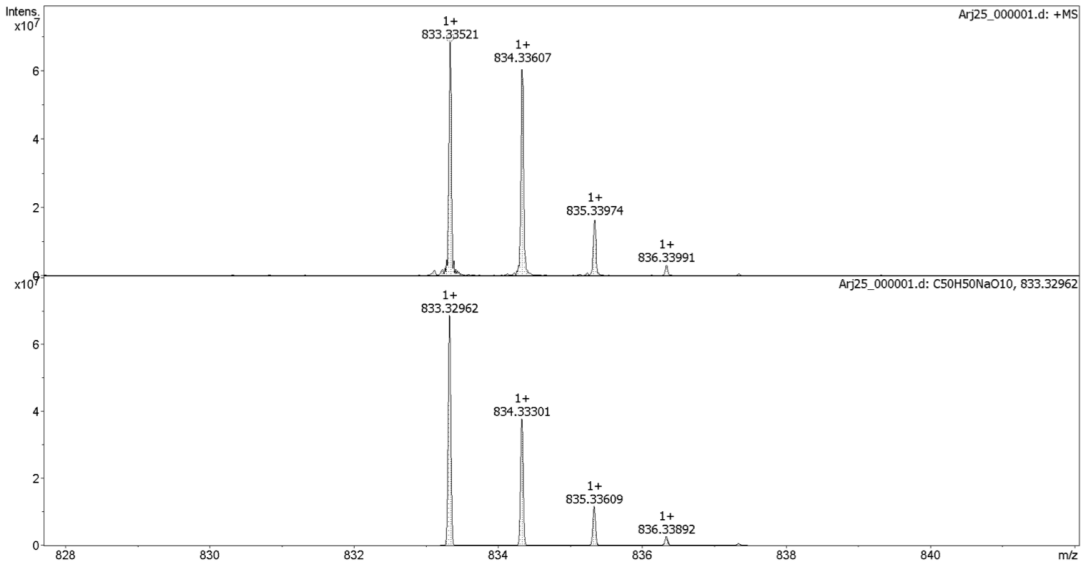
Intens.
x10^7
Arj25_000001.d: +MS
1+
833.33521
1+
834.33607
1+
835.33974
1+
836.33991
x10^7
Arj25_000001.d: C50H50NaO10, 833.32962
1+
833.32962
1+
834.33301
1+
835.33609
1+
836.33892
828
830
832
834
836
838
840
m/z

3-(4-ethyloxyphenyl)-1-[3-(2,3,4,6-tetra-*O*-benzyl-β-D-glucopyranosyl)-2,4,6-trihydroxyphenyl]propan-1-one (37f)

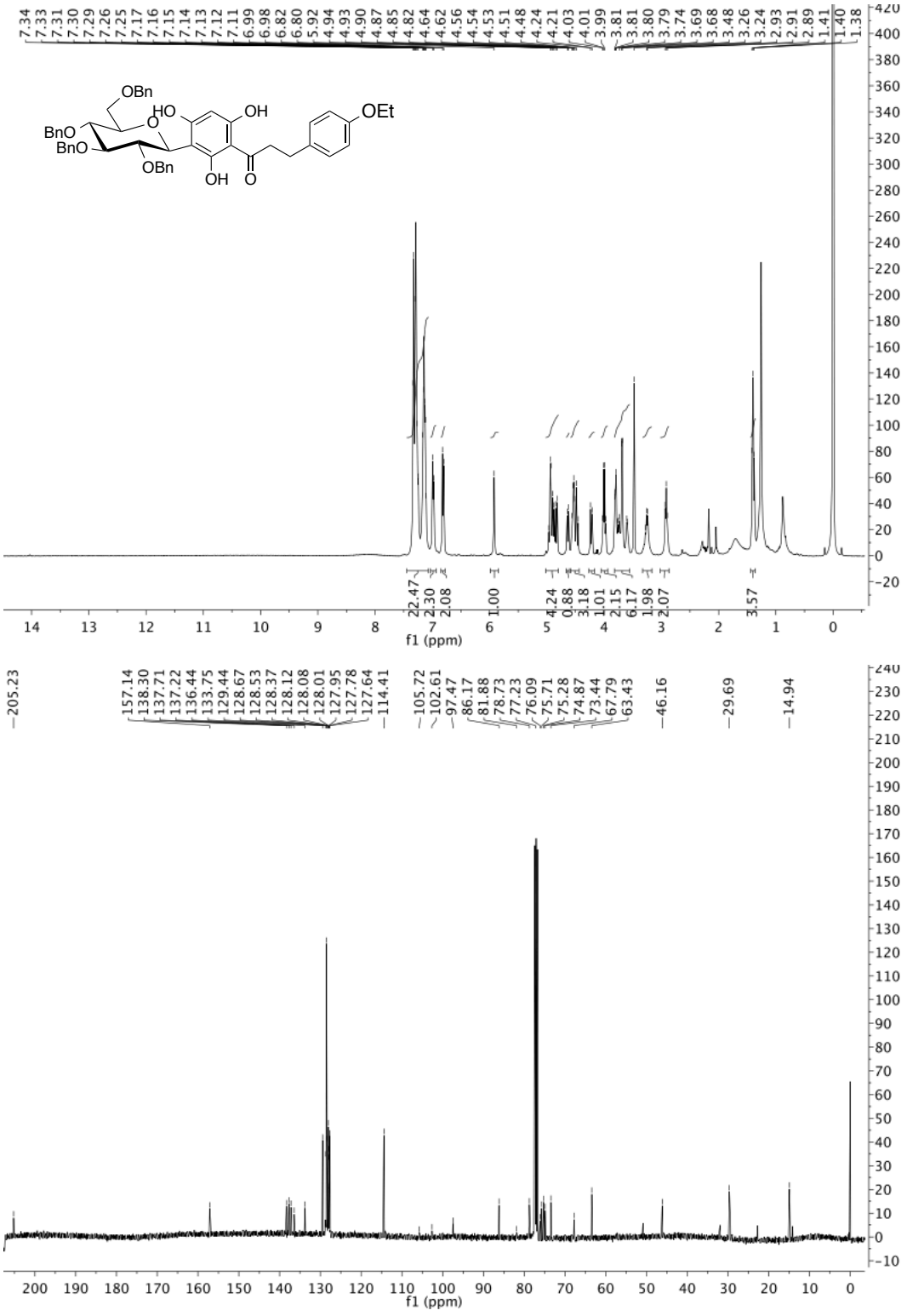

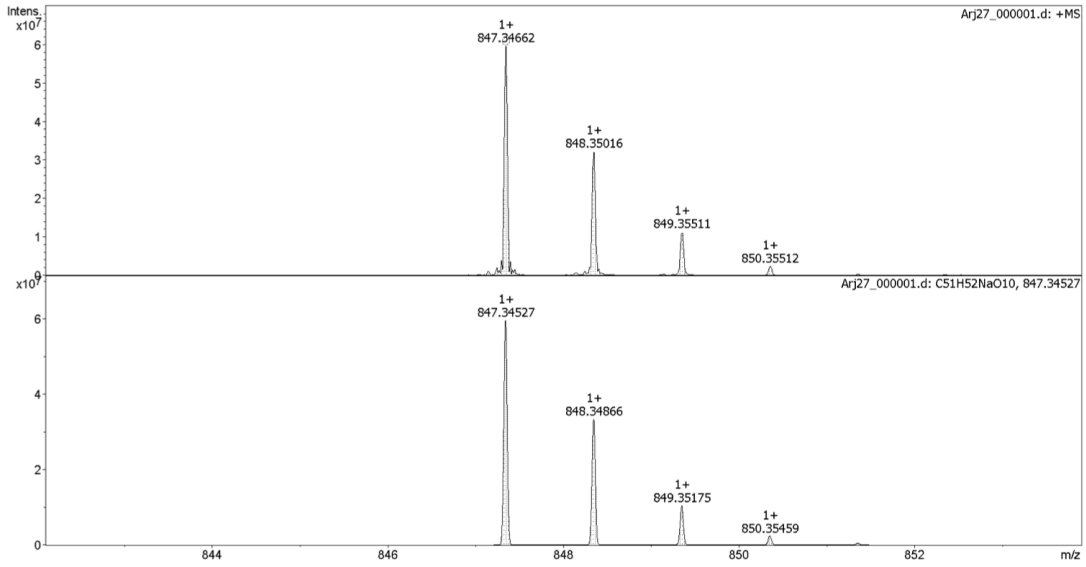
Intens.
x10^7
Arj27_000001.d: +MS
1+
847.34662
1+
848.35016
1+
849.35511
1+
850.35512
x10^7
Arj27_000001.d: C51H52NaO10, 847.34527
1+
847.34527
1+
848.34866
1+
849.35175
1+
850.35459
844
846
848
850
852
m/z

3-(4-propyloxyphenyl)-1-[3-(2,3,4,6-tetra-*O*-benzyl-β-D-glucopyranosyl)-2,4,6-trihydroxyphenyl]propan-1-one (37g)

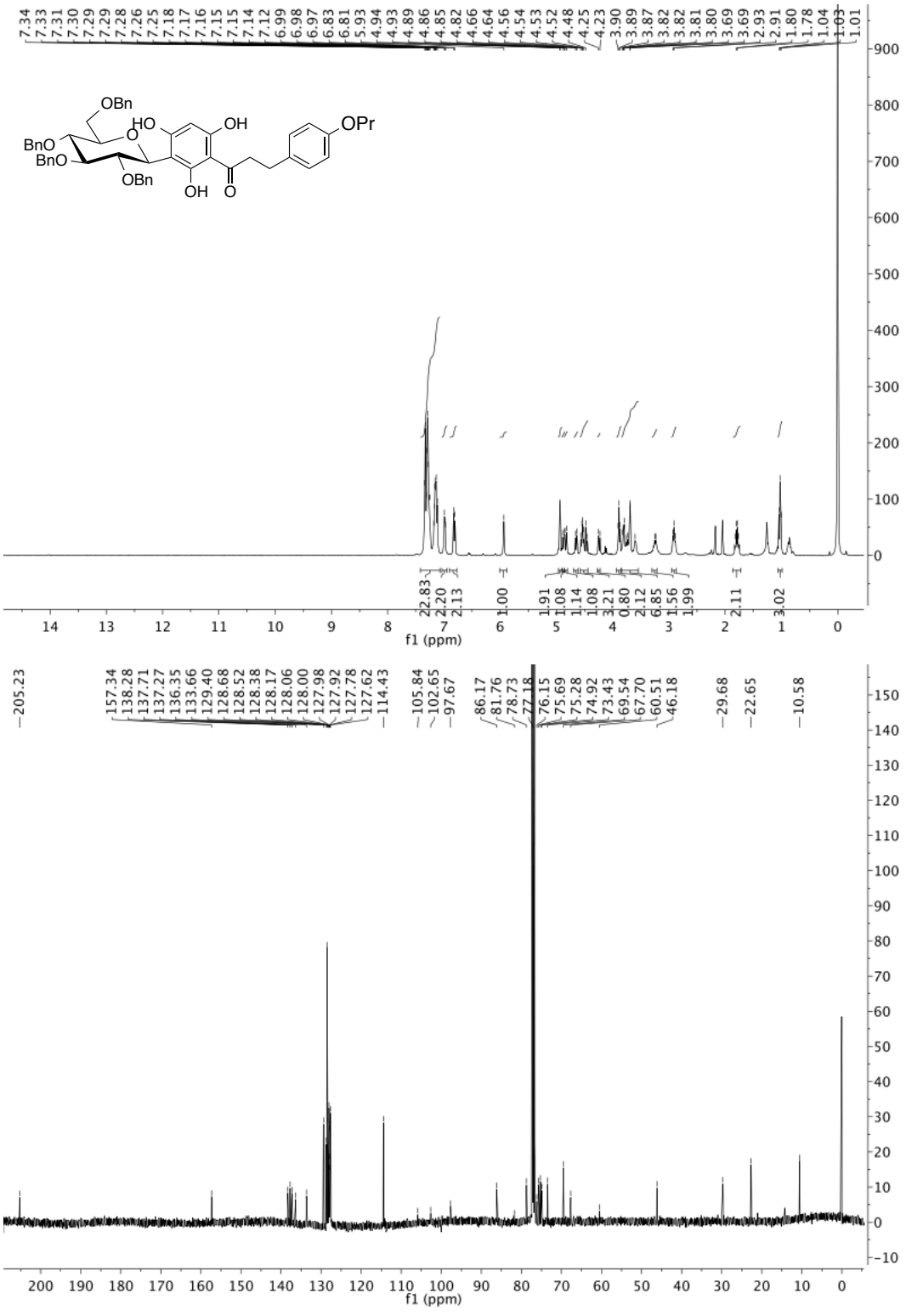

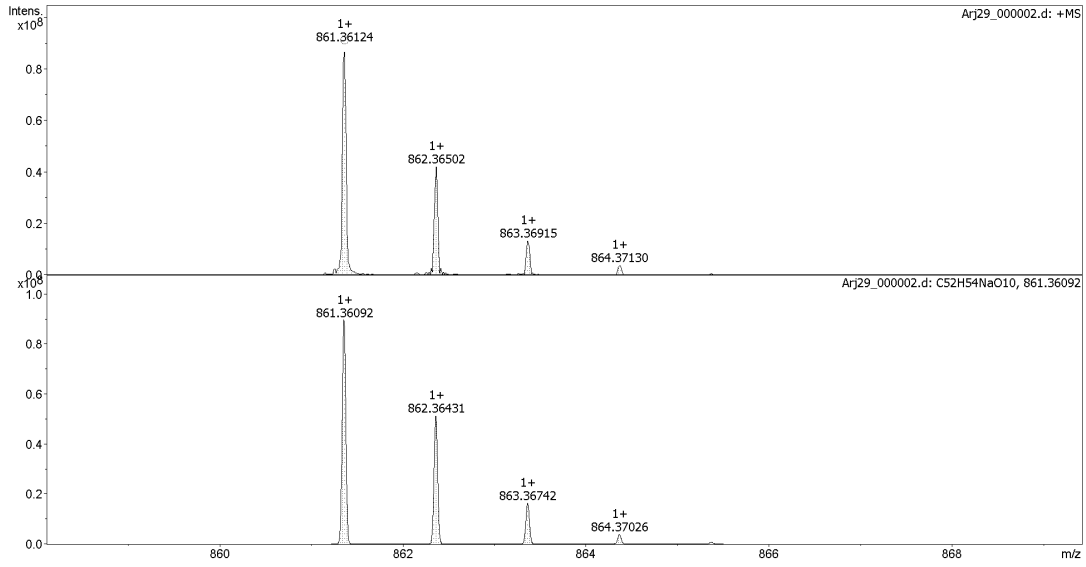
Intens.
x10^8
Arj29_000002.d: +MS
1+
861.36124
1+
862.36502
1+
863.36915
1+
864.37130
x10^8
Arj29_000002.d: C52H54NaO10, 861.36092
1+
861.36092
1+
862.36431
1+
863.36742
1+
864.37026
0.0
0.2
0.4
0.6
0.8
1.0
860
862
864
866
868
m/z

2-[3-(2,3,4,6-tetra-*O*-benzyl-β-D-glucopyranosyl)-2,4,6-trihydroxyphenyl]-ethanone (39)

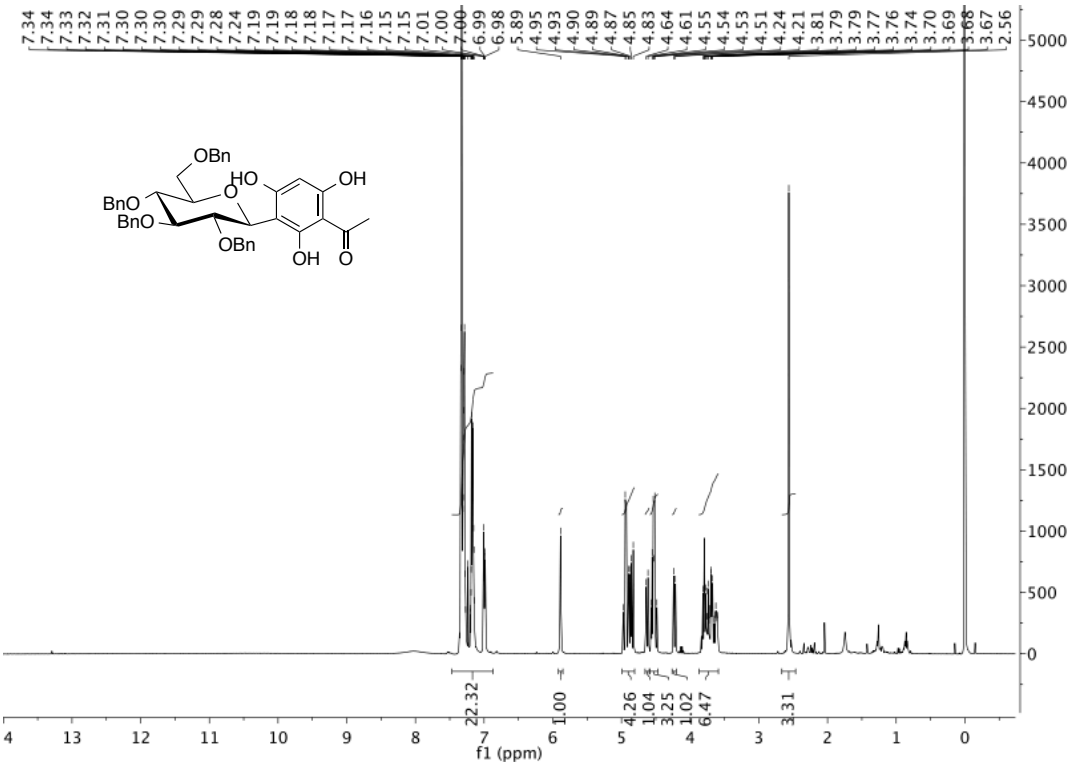

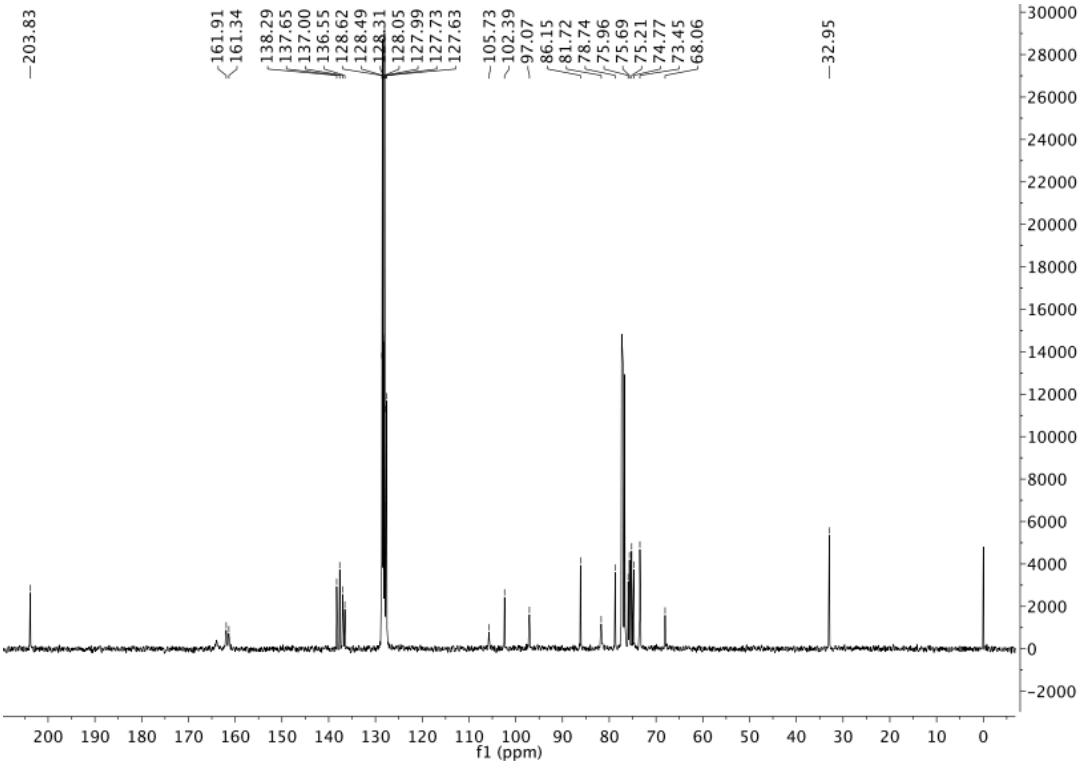

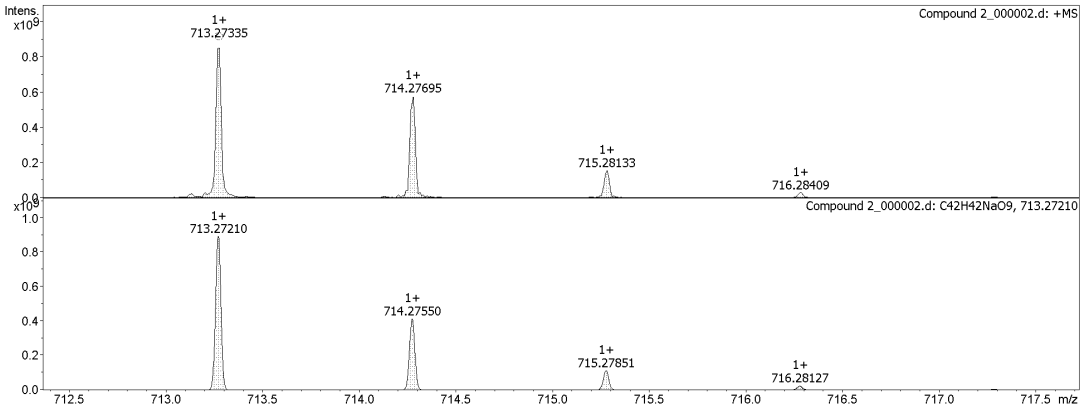
Intens.
x10^9
Compound 2_000002.d: +MS
1+
713.27335
1+
714.27695
1+
715.28133
1+
716.28409
x10^9
Compound 2_000002.d: C42H42NaO9, 713.27210
1+
713.27210
1+
714.27550
1+
715.27851
1+
716.28127
712.5
713.0
713.5
714.0
714.5
715.0
715.5
716.0
716.5
717.0
717.5 m/z

2-[3-(2,3,4,6-tetra-*O*-benzyl-β-D-glucopyranosyl)-2,4-di-*O*-benzyl-6-hydroxyphenyl]-ethanone (31)

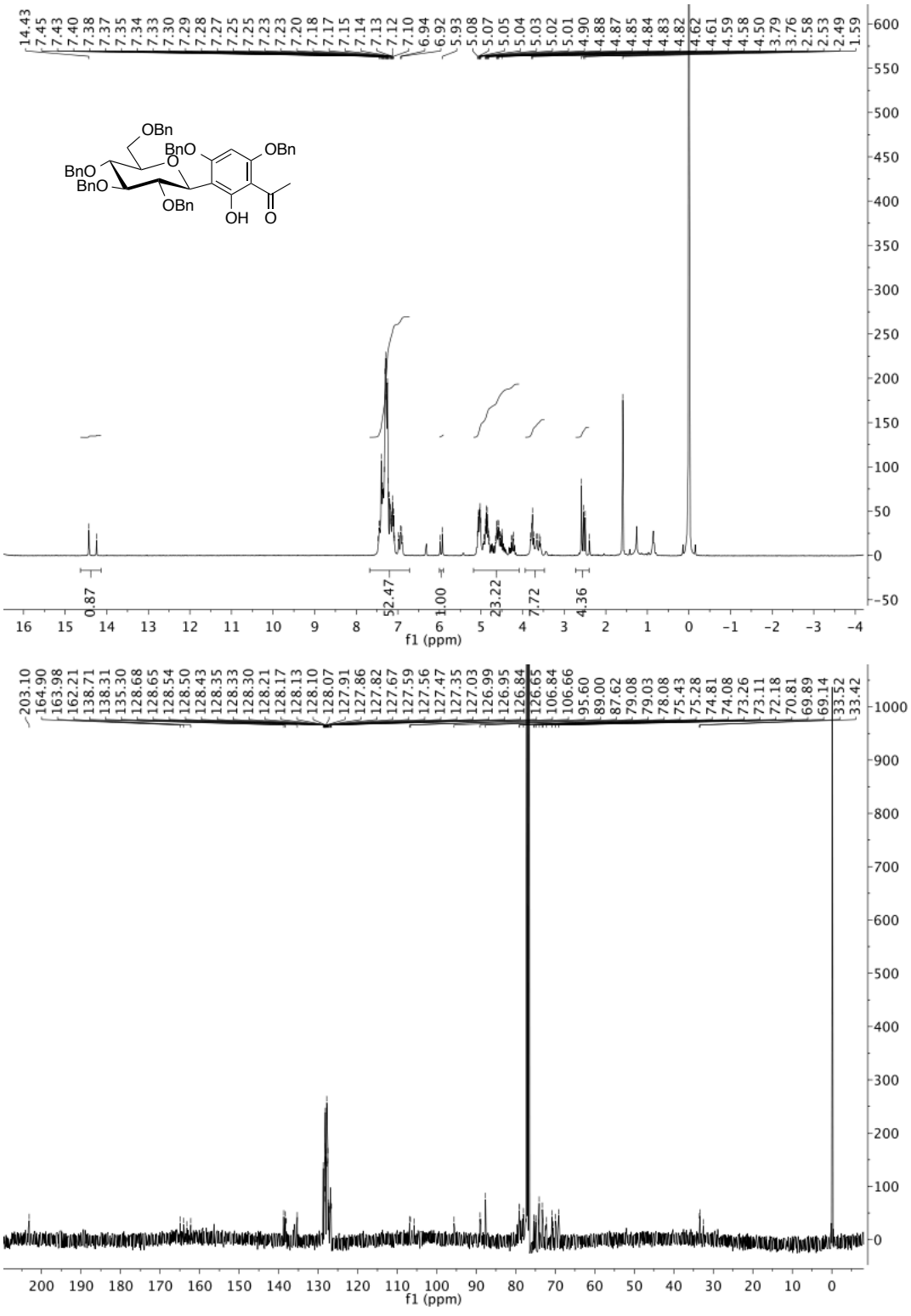

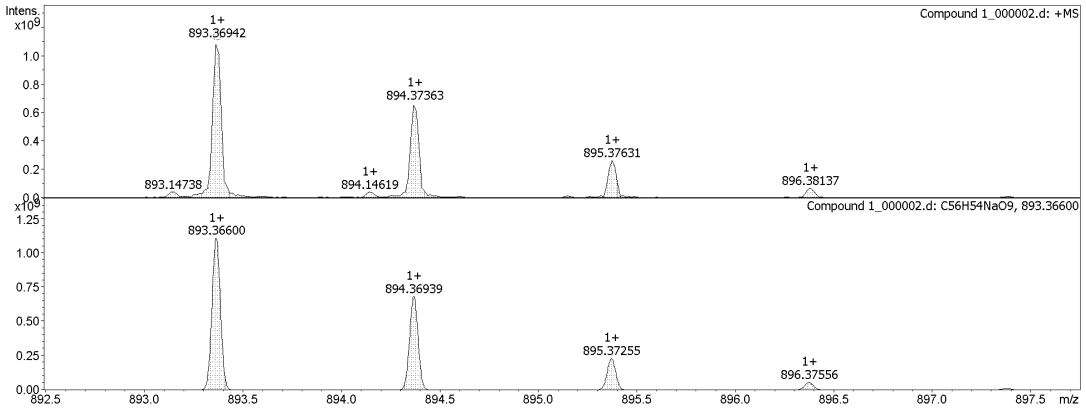
Intens.
x10^9
Compound 1_000002.d: +MS
1+
893.36942
1+
894.37363
1+
895.37631
1+
896.38137
893.14738
1+
894.14619
x10^9
Compound 1_000002.d: C56H54NaO9, 893.36600
1+
893.36600
1+
894.36939
1+
895.37255
1+
896.37556
892.5
893.0
893.5
894.0
894.5
895.0
895.5
896.0
896.5
897.0
897.5
m/z

3-(4-benzyloxyphenyl)-1-[3-(2,3,4,6-tetra-*O*-benzyl-β-D-glucopyranosyl)-2,4-di-*O*-benzyl-6-hydroxyphenyl]propan-1-one (32)

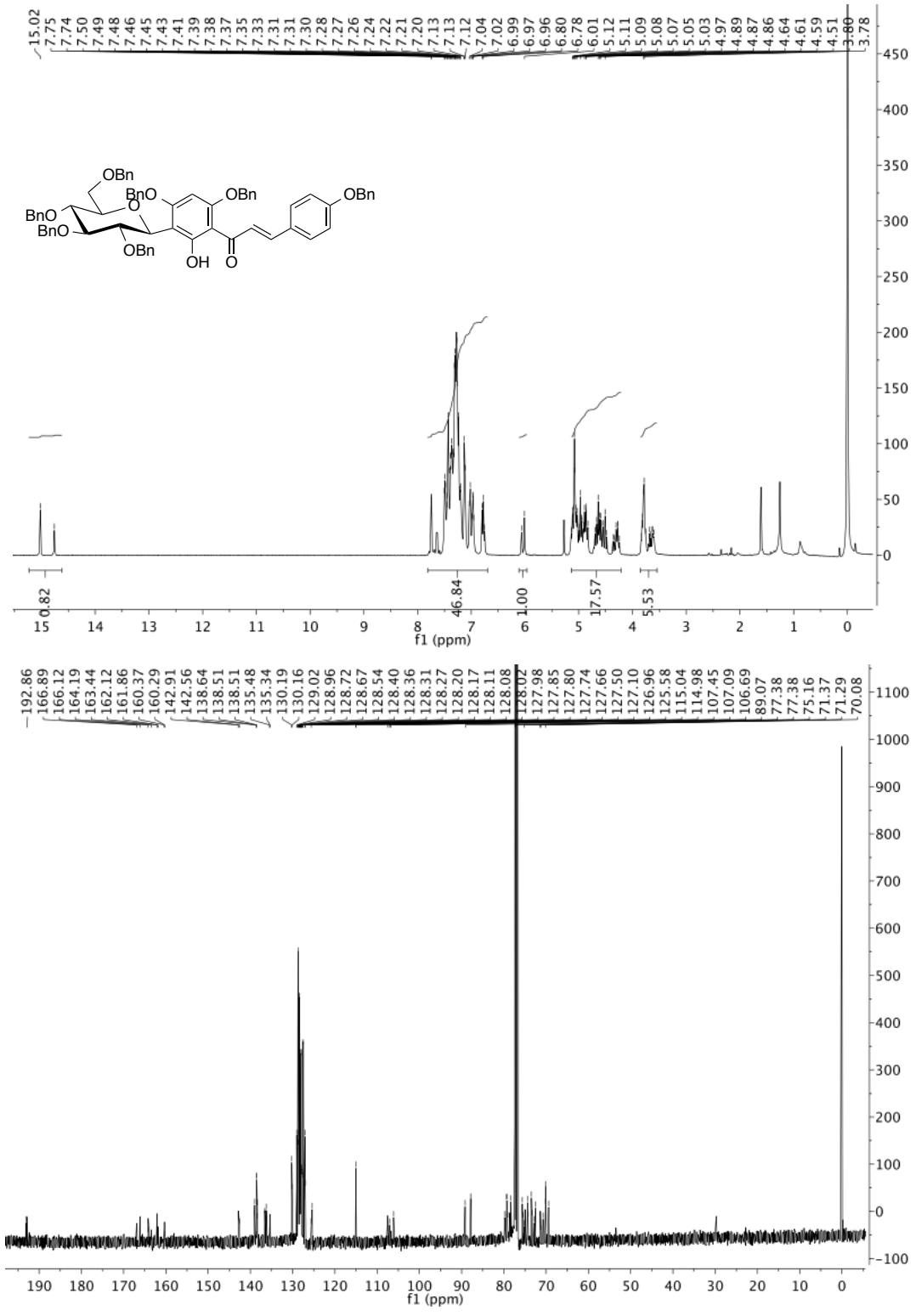

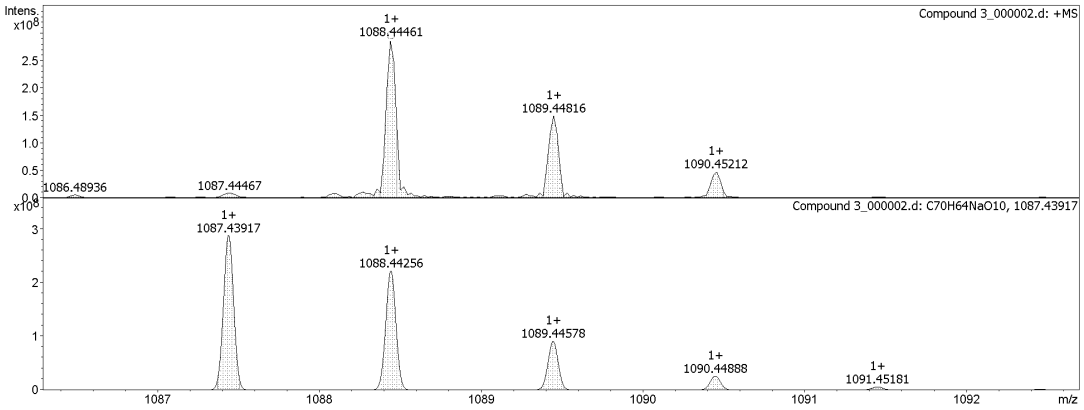
Intens.
x10^8
Compound 3_000002.d: +MS
1+
1088.44461
1+
1089.44816
1+
1090.45212
1086.48936
1087.44467
x10^8
Compound 3_000002.d: C70H64NaO10, 1087.43917
1+
1087.43917
1+
1088.44256
1+
1089.44578
1+
1090.44888
1+
1091.45181
1087
1088
1089
1090
1091
1092
m/z

1.8 C-Glucosyl dihydrochalcones

3-(4-fluorophenyl)-1-[3-β-D-glucopyranosyl)-2,4,6-trihydroxyphenyl]propan-1-one (33a)

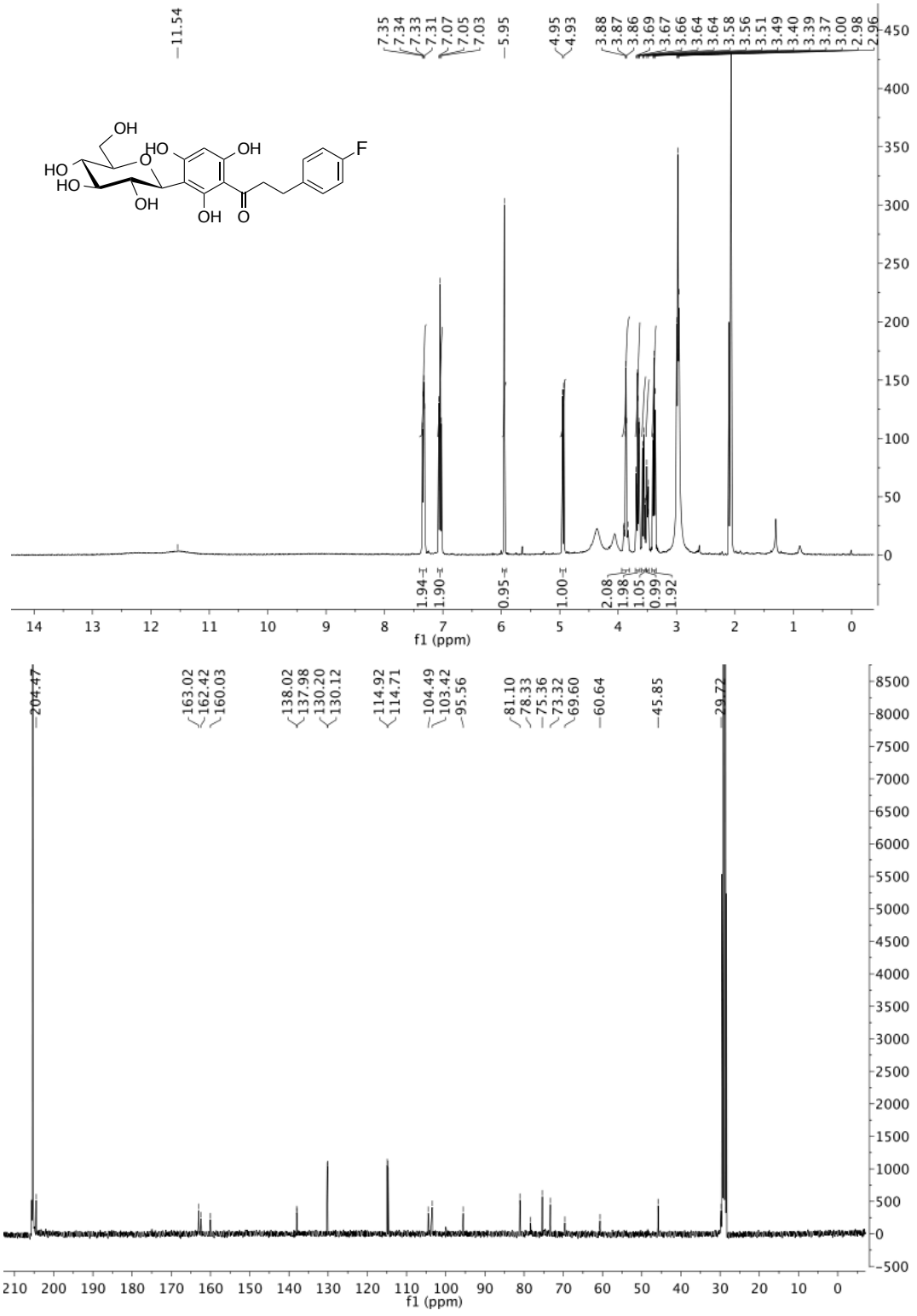

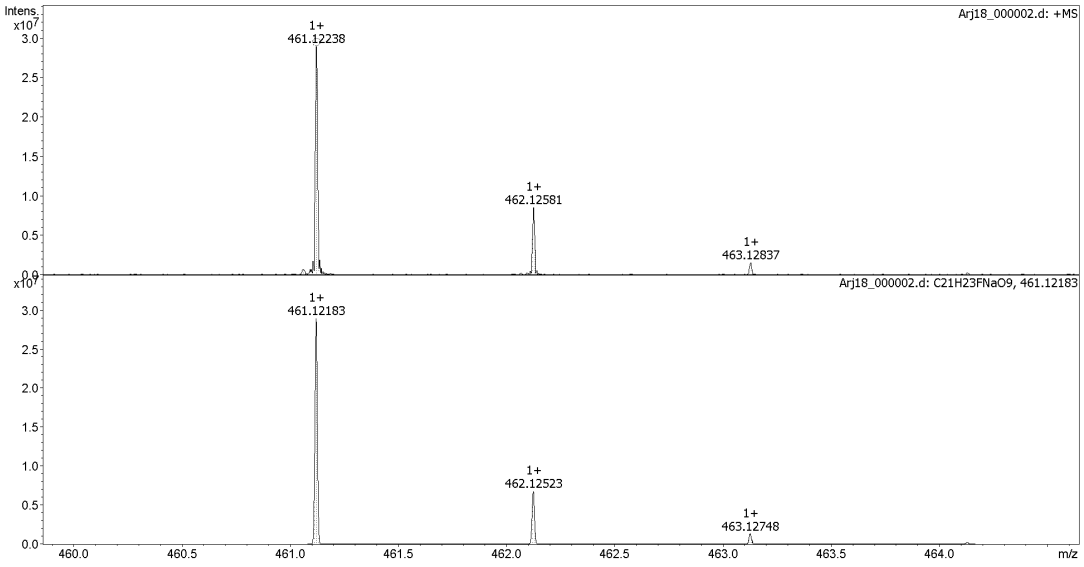
Intens.
x10^7
3.0
2.5
2.0
1.5
1.0
0.5
0.0
Arj18_000002.d: +MS
1+
461.12238
1+
462.12581
1+
463.12837
x10^7
Arj18_000002.d: C21H23FNaO9, 461.12183
1+
461.12183
1+
462.12523
1+
463.12748
460.0
460.5
461.0
461.5
462.0
462.5
463.0
463.5
464.0
m/z

3-phenyl-1-[3-β-D-glucopyranosyl)-2,4,6-trihydroxyphenyl]propan-1-one (33c)

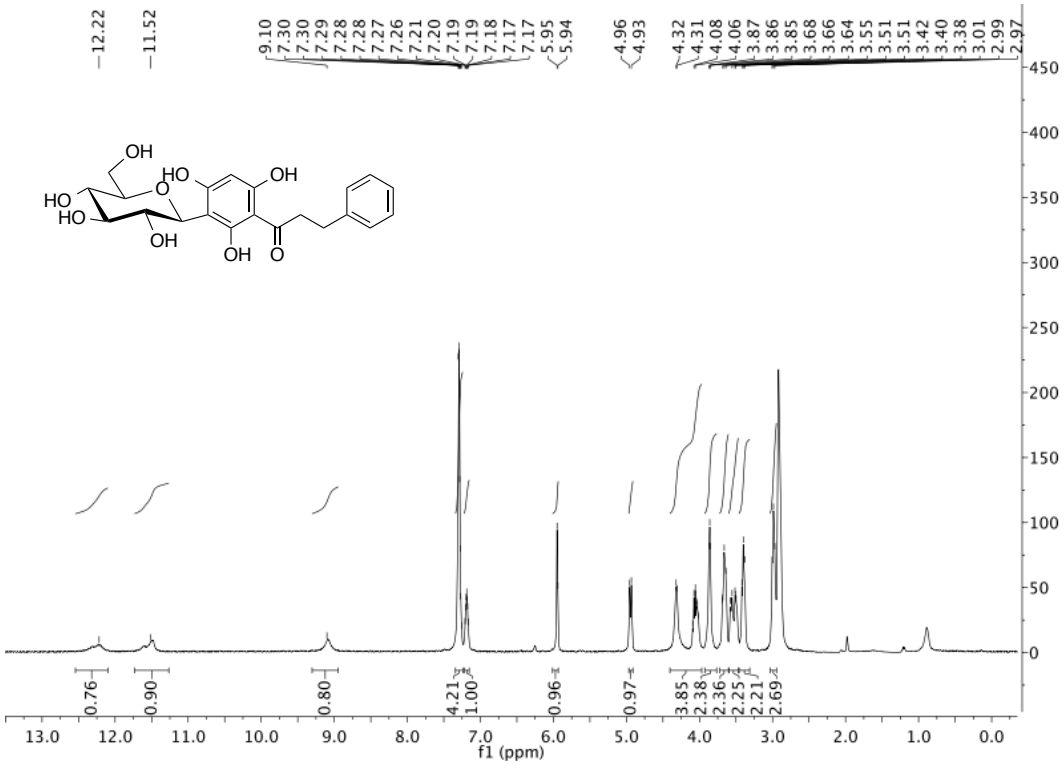

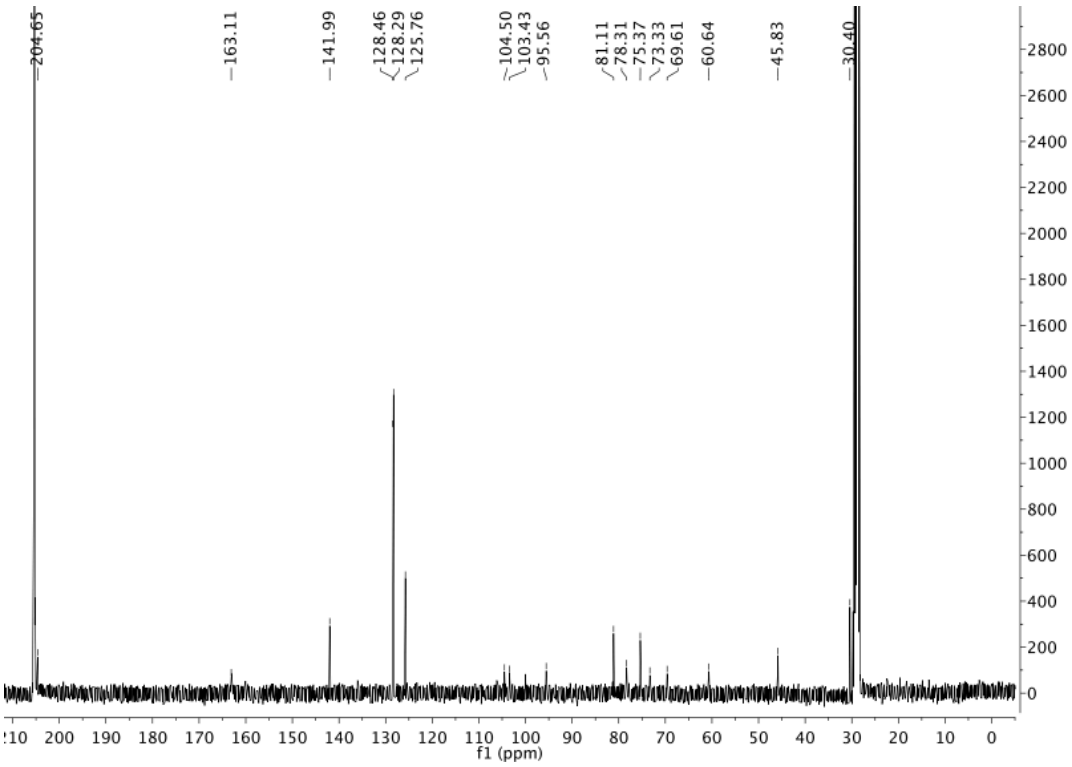

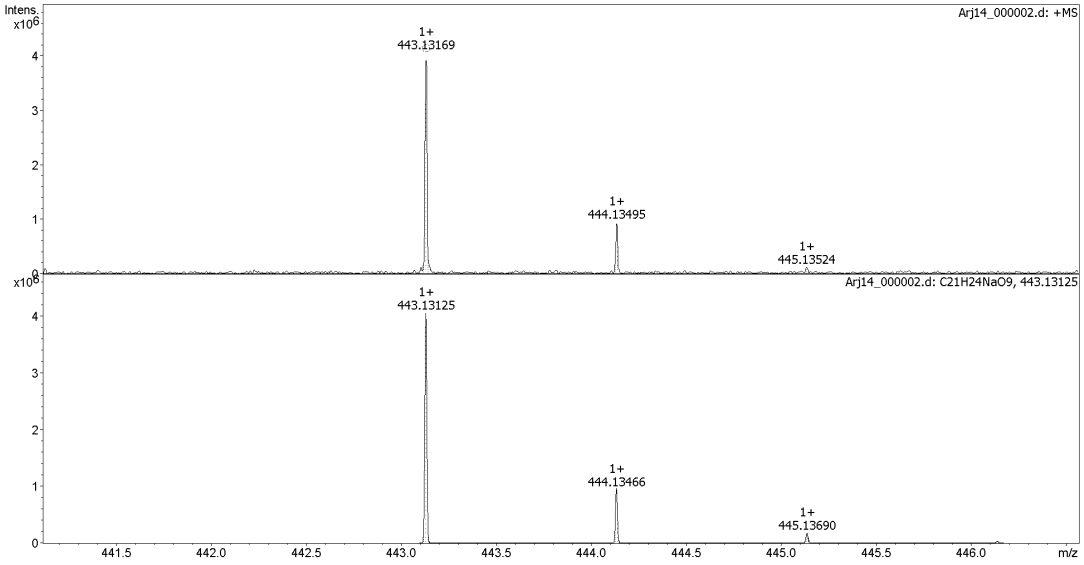
Intens.
x10^6
Arj14_000002.d: +MS
1+
443.13169
1+
444.13495
1+
445.13524
x10^6
Arj14_000002.d: C21H24NaO9, 443.13125
1+
443.13125
1+
444.13466
1+
445.13690
441.5
442.0
442.5
443.0
443.5
444.0
444.5
445.0
445.5
446.0
m/z

3-(4-methylphenyl)-1-[3-β-D-glucopyranosyl)-2,4,6-trihydroxyphenyl]propan-1-one (33d)

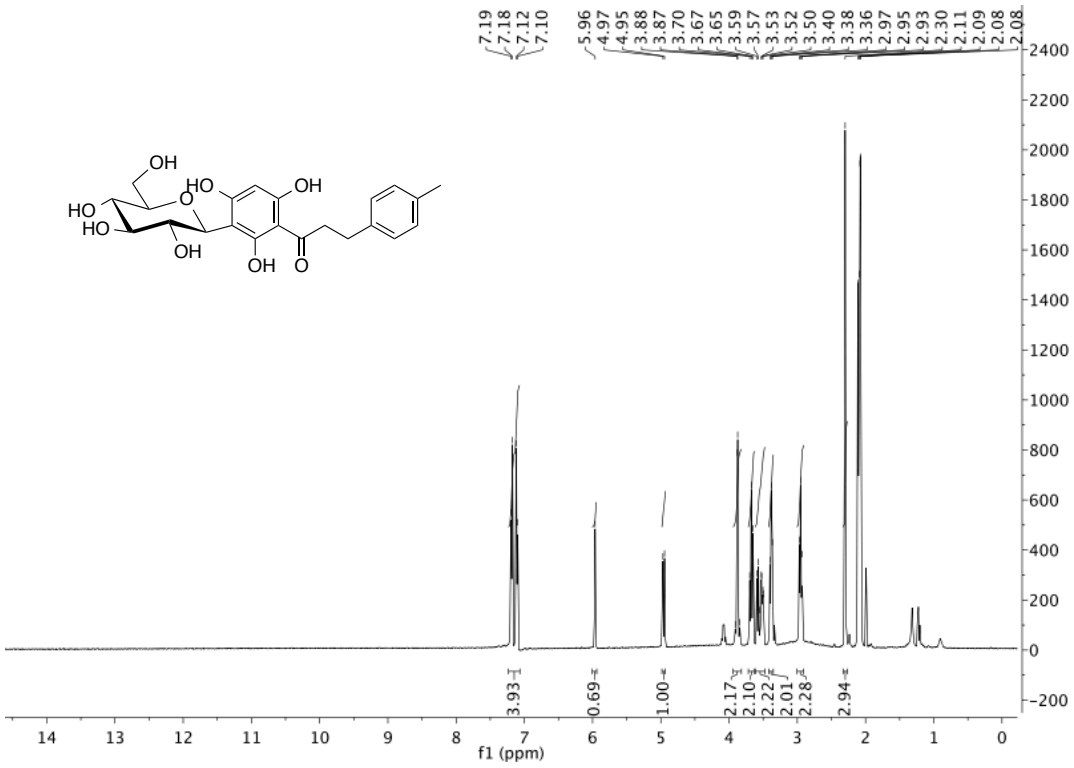

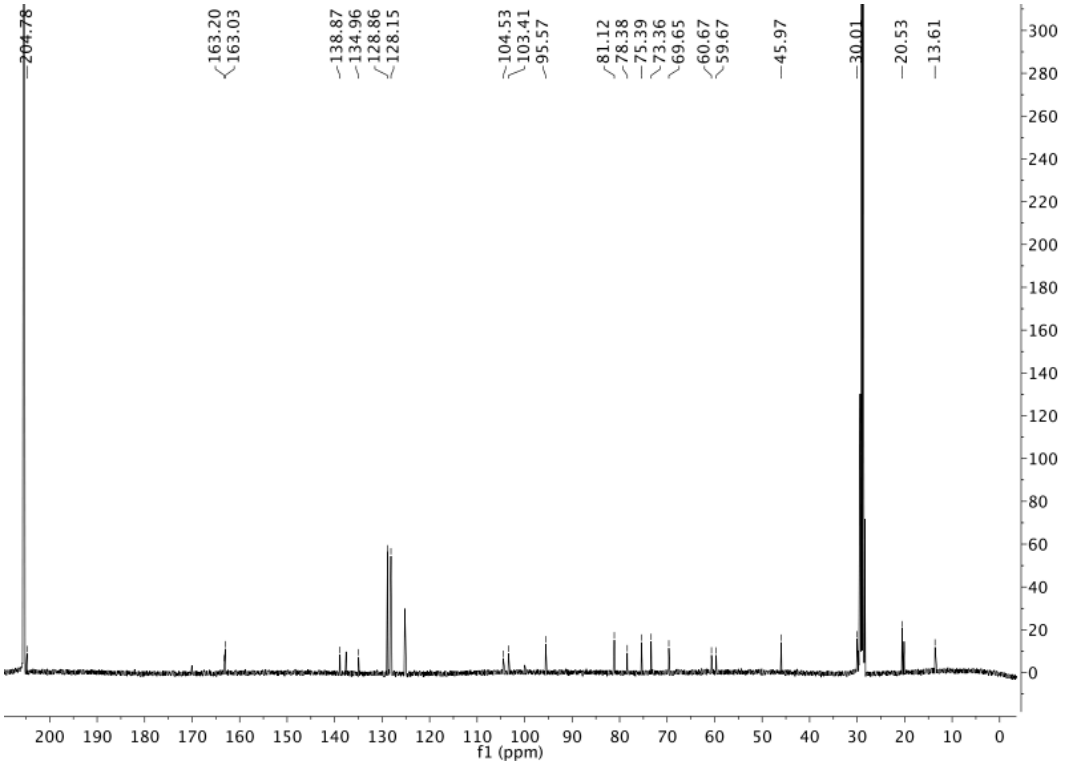

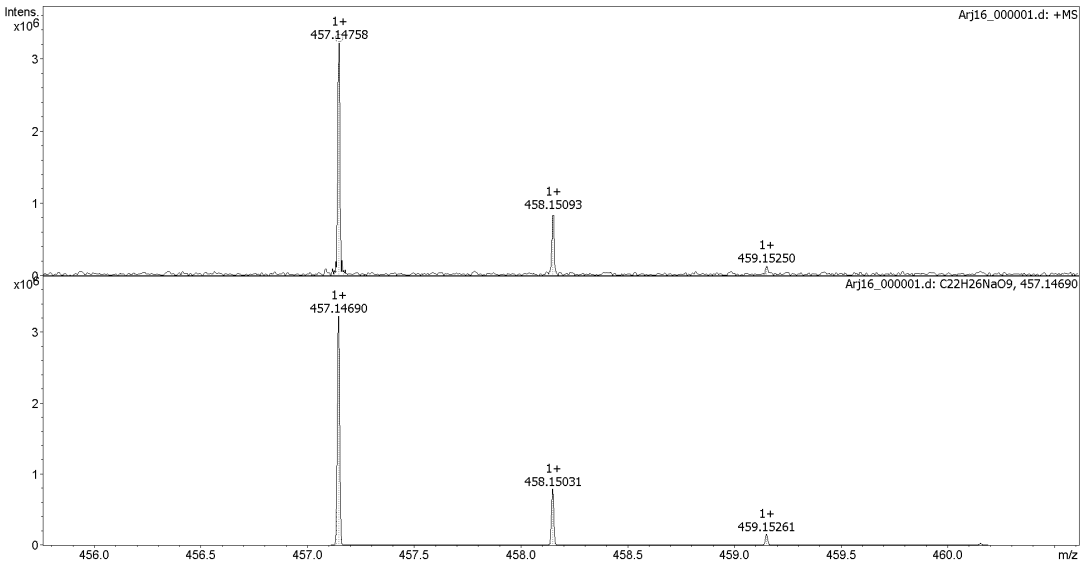
Intens.
x10^6
Arj16_000001.d: +MS
1+
457.14758
1+
458.15093
1+
459.15250
x10^6
Arj16_000001.d: C22H26NaO9, 457.14690
1+
457.14690
1+
458.15031
1+
459.15261
456.0
456.5
457.0
457.5
458.0
458.5
459.0
459.5
460.0
m/z

3-(4-methoxyphenyl)-1-[3-β-D-glucopyranosyl)-2,4,6-trihydroxyphenyl]propan-1-one (33e)

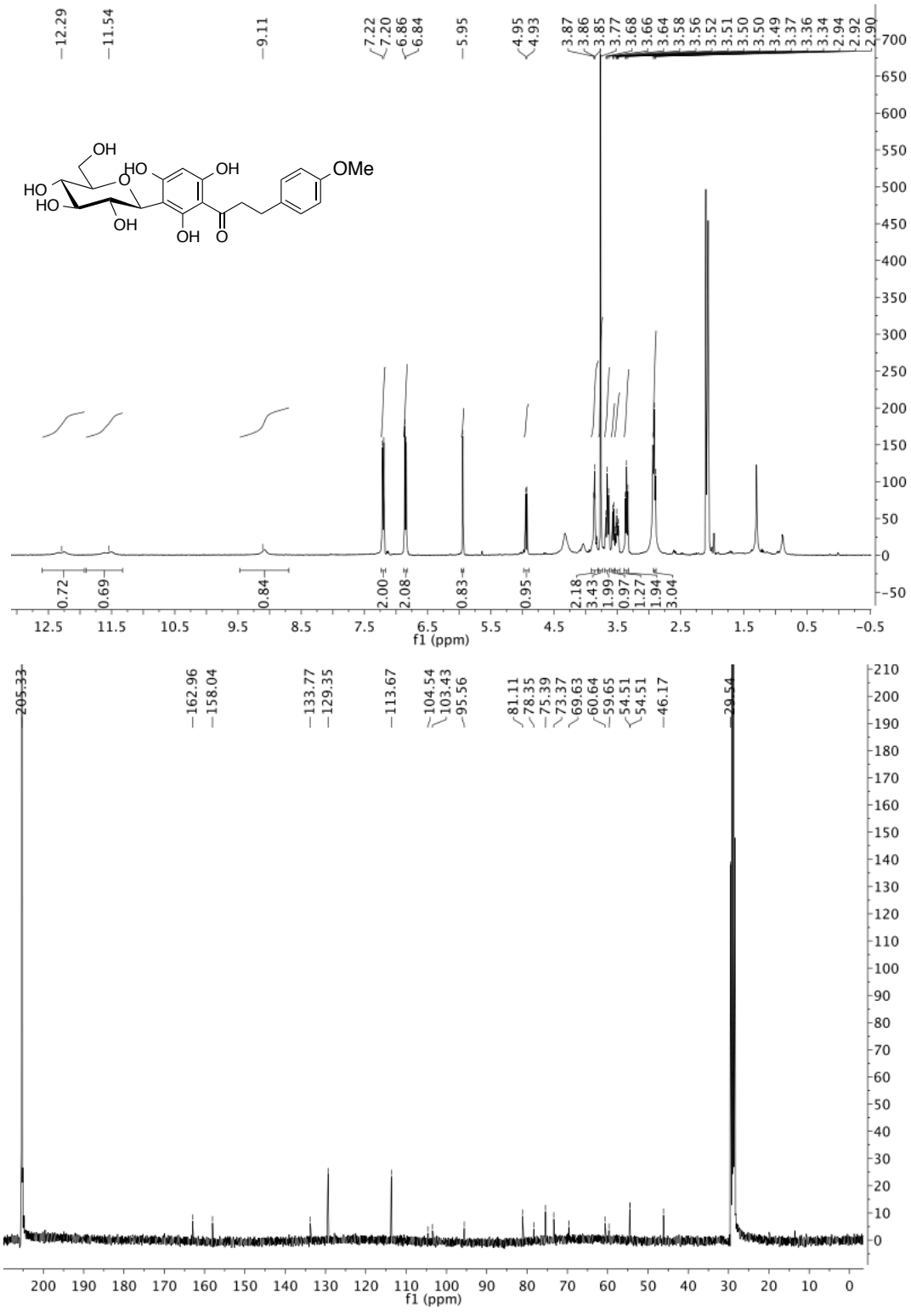

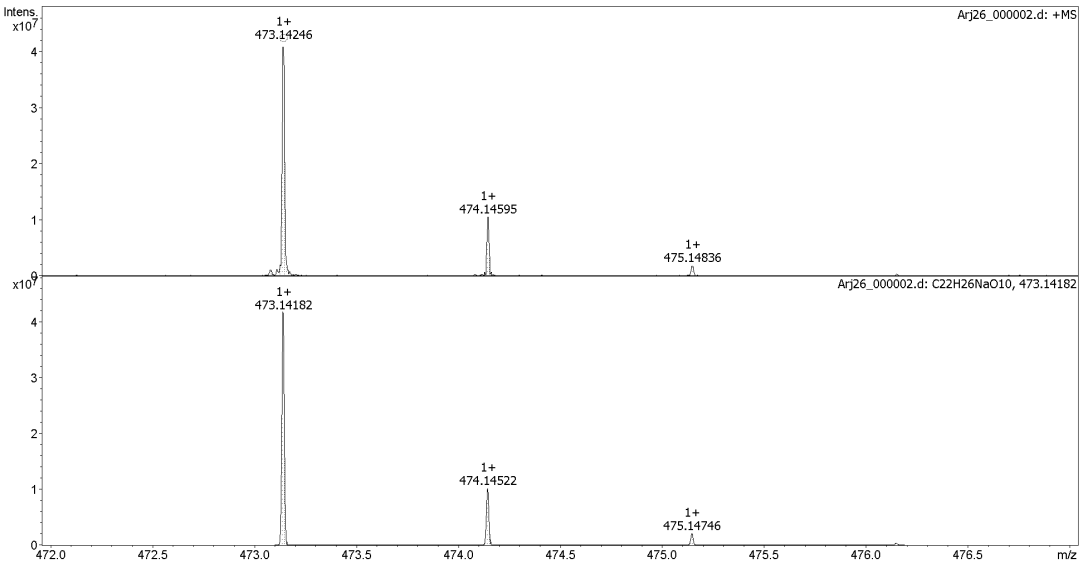
Intens.
x10^7
Arj26_000002.d: +MS
1+
473.14246
1+
474.14595
1+
475.14836
x10^7
Arj26_000002.d: C22H26NaO10, 473.14182
1+
473.14182
1+
474.14522
1+
475.14746
472.0
472.5
473.0
473.5
474.0
474.5
475.0
475.5
476.0
476.5
m/z

3-(4-ethoxyphenyl)-1-[3-β-D-glucopyranosyl)-2,4,6-trihydroxyphenyl]propan-1-one (33f)

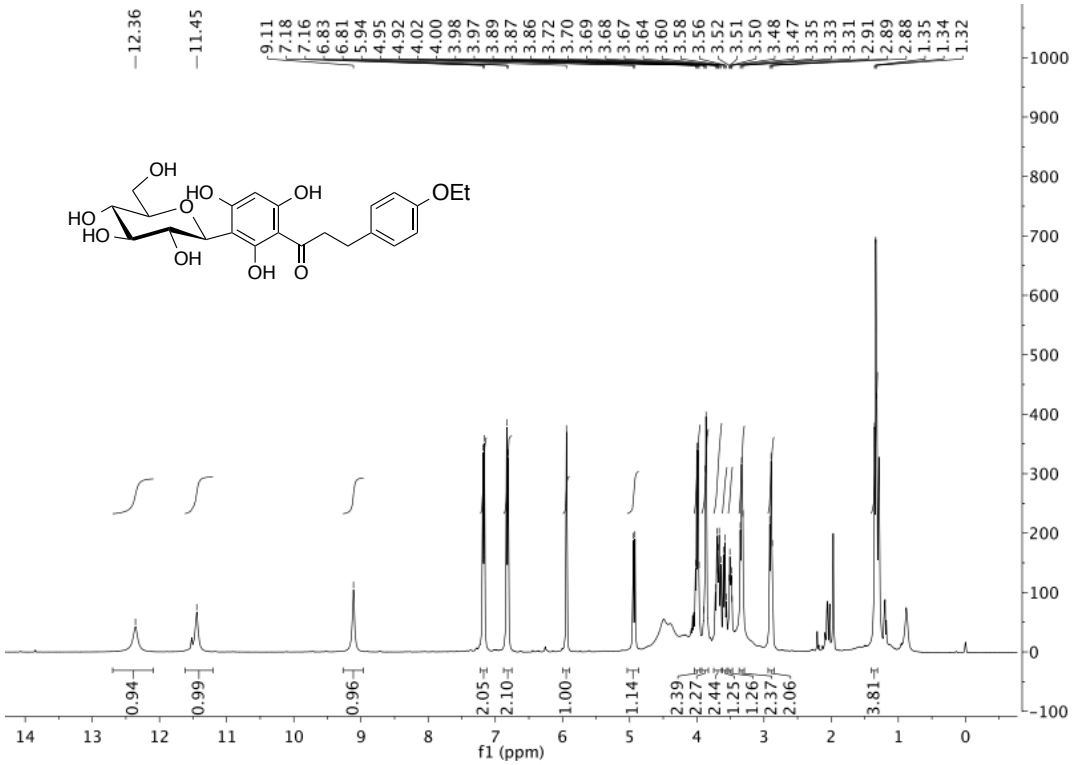

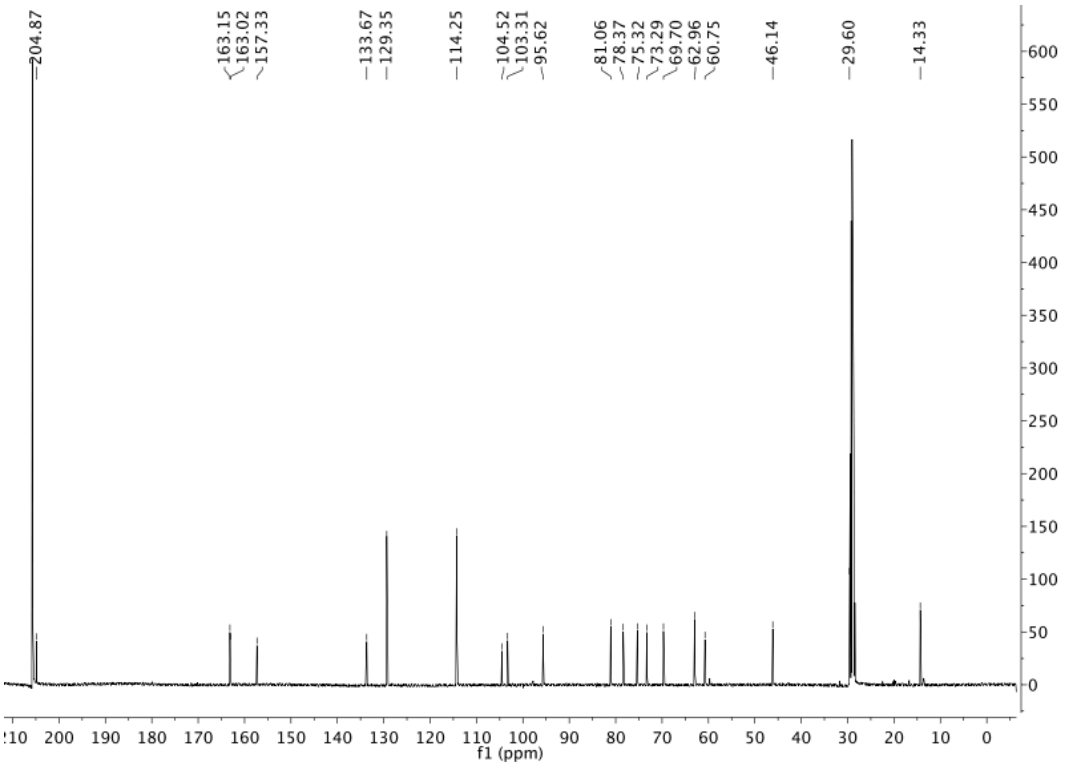

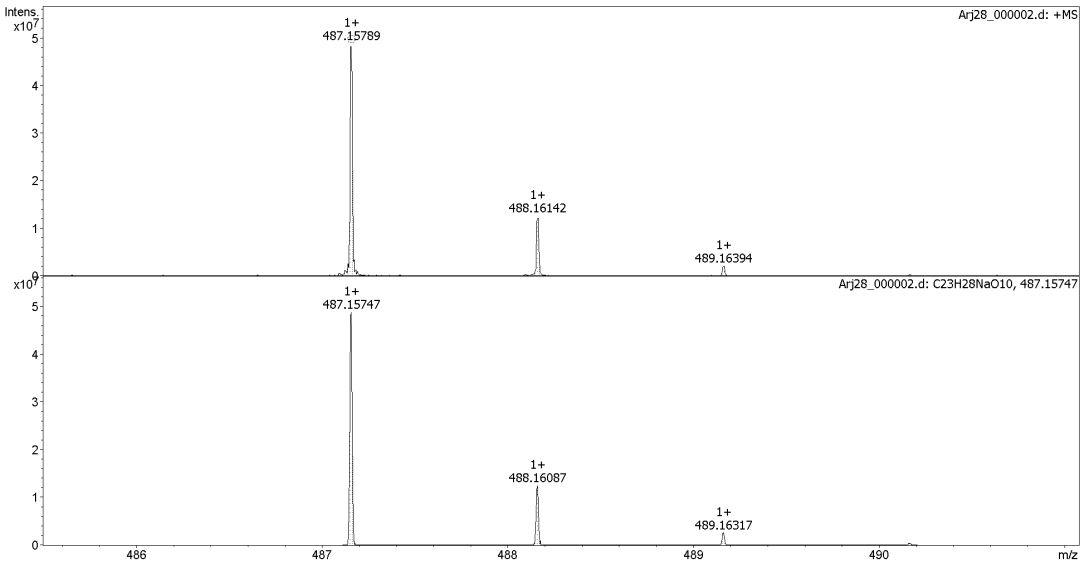
Intens.
x10^7
Arj28_000002.d: +MS
1+
487.15789
1+
488.16142
1+
489.16394
x10^7
Arj28_000002.d: C23H28NaO10, 487.15747
1+
487.15747
1+
488.16087
1+
489.16317
0
1
2
3
4
5
486
487
488
489
490
m/z

3-(4-propyloxyphenyl)-1-[3-β-D-glucopyranosyl)-2,4,6-trihydroxyphenyl]propan-1-one (33g)

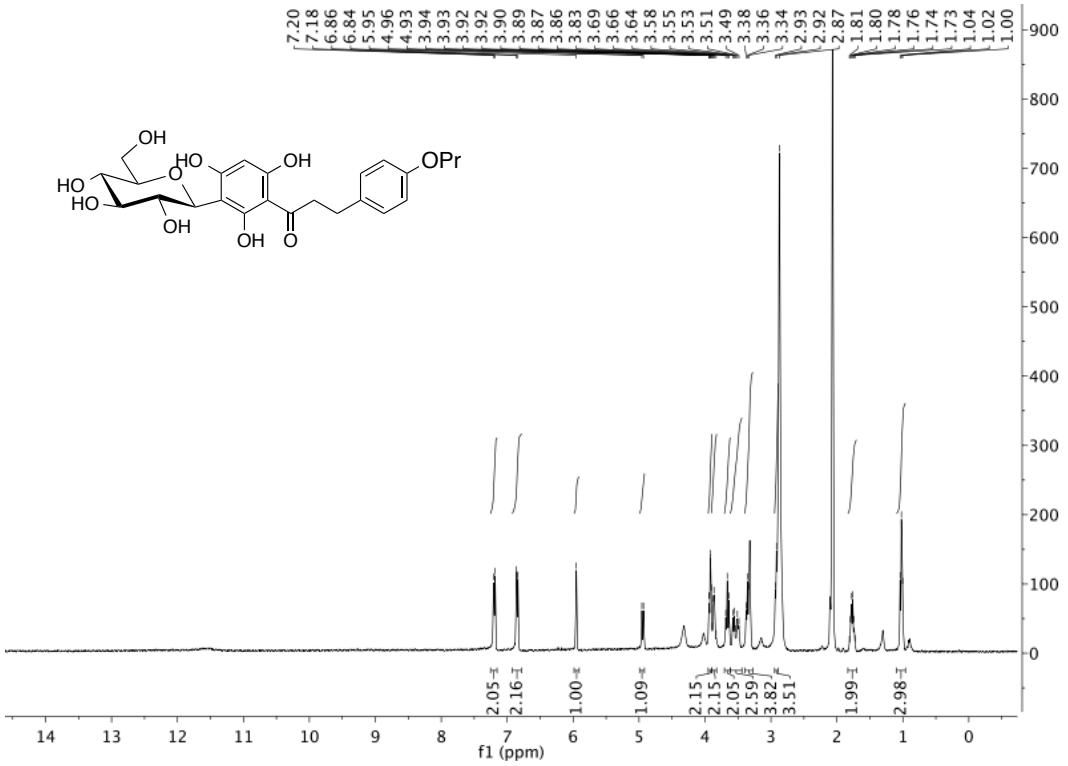

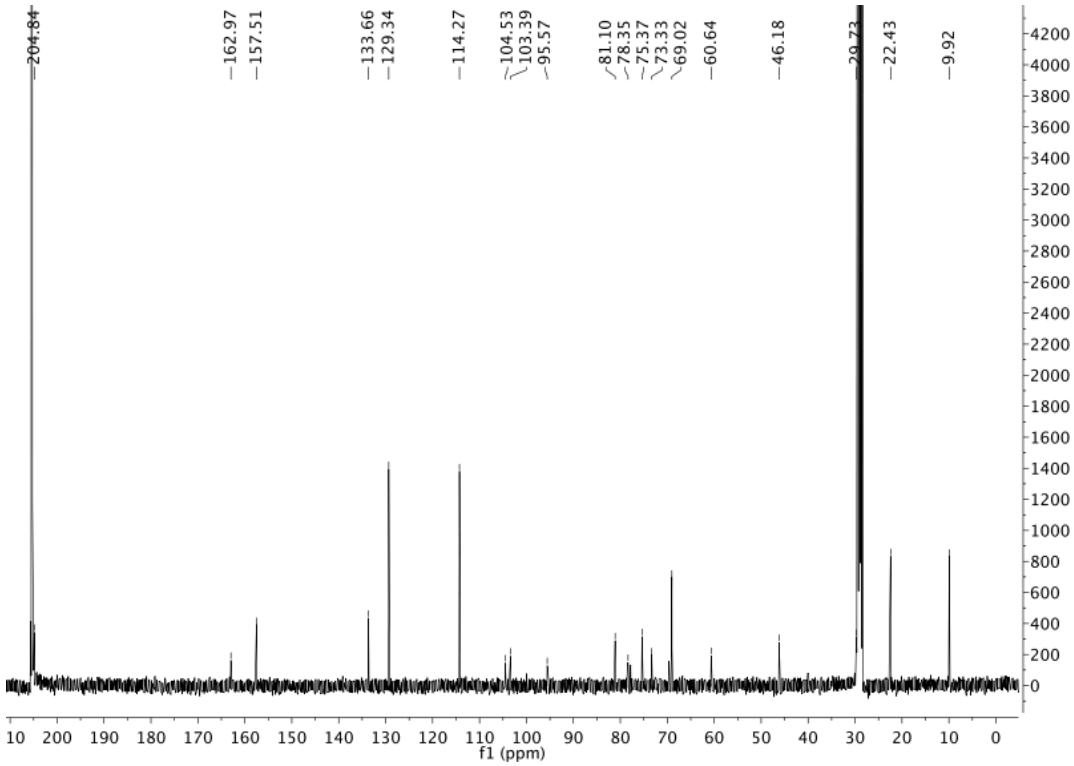

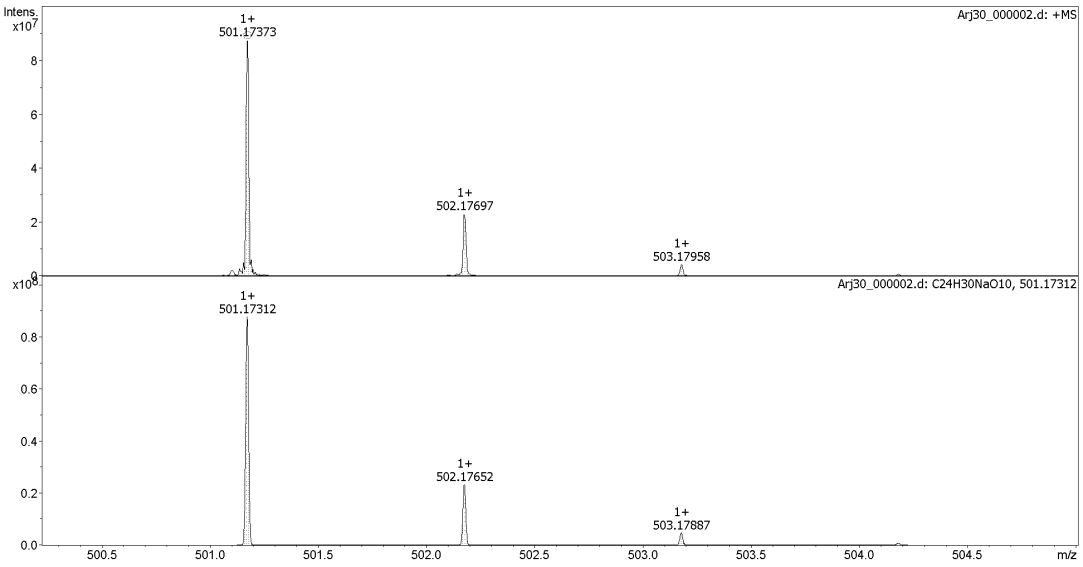
Intens.
x10^7
1+
501.17373
1+
502.17697
1+
503.17958
Arj30_000002.d: +MS
x10^6
1+
501.17312
1+
502.17652
1+
503.17887
Arj30_000002.d: C24H30NaO10, 501.17312
m/z

3-(4-hydroxyphenyl)-1-[3-β-D-glucopyranosyl)-2,4,6-trihydroxyphenyl]propan-1-one (33h)

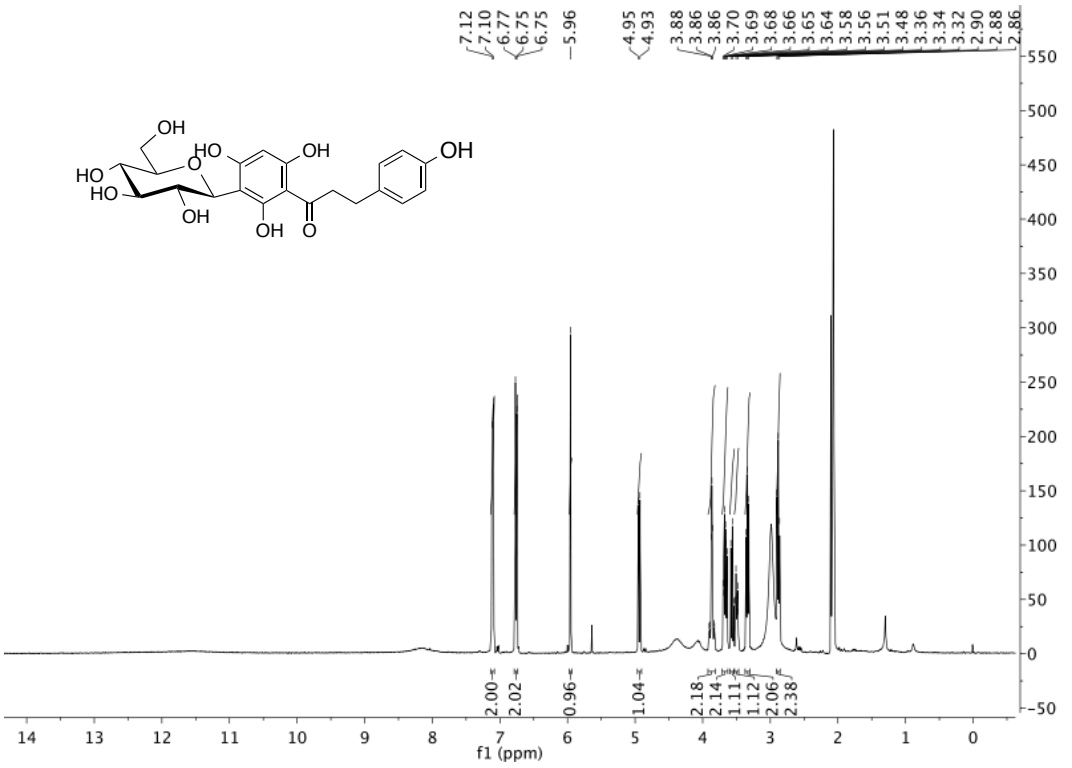

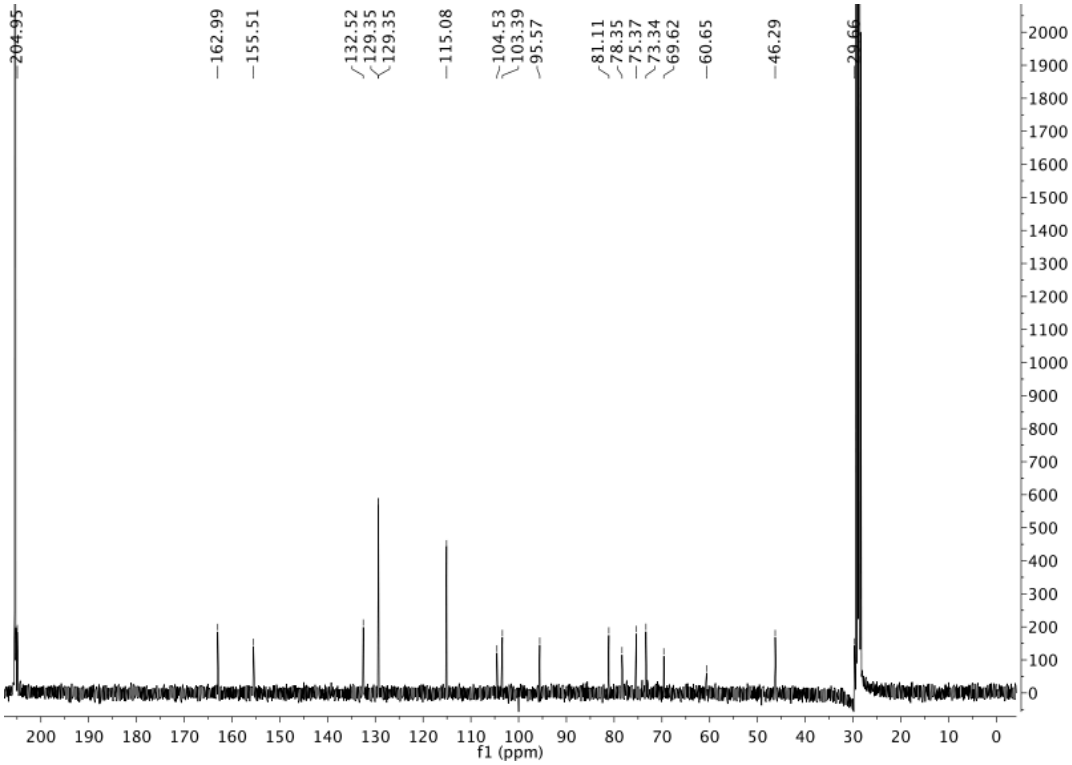

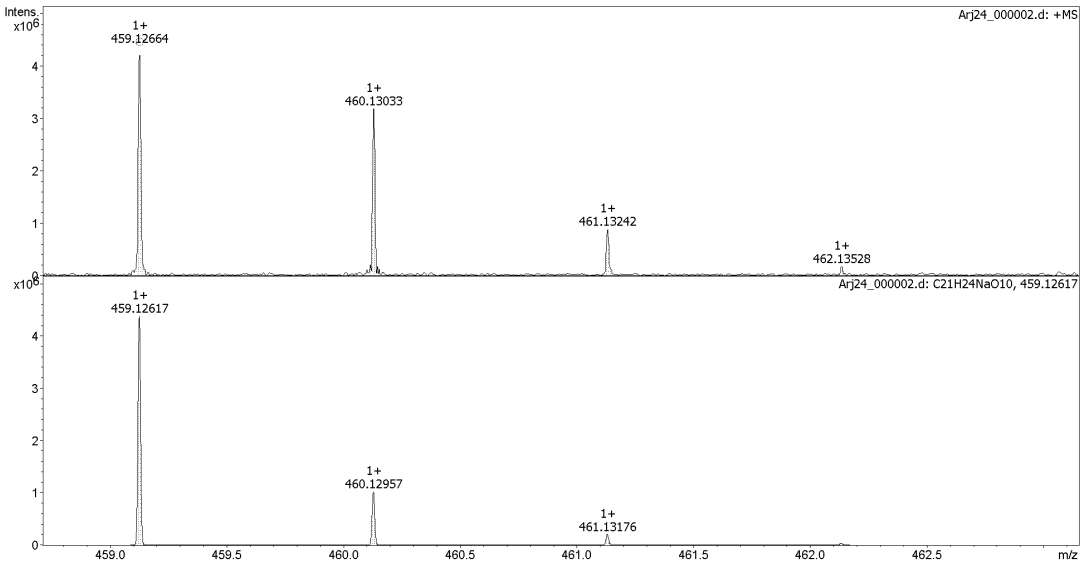
Intens.
x10^6
Arj24_000002.d: +MS
1+
459.12664
1+
460.13033
1+
461.13242
1+
462.13528
x10^6
Arj24_000002.d: C21H24NaO10, 459.12617
1+
459.12617
1+
460.12957
1+
461.13176
459.0
459.5
460.0
460.5
461.0
461.5
462.0
462.5
m/z

1.9 Disaccharides

Disaccharide α-D-GlCNAc-(1→4)-β-D-GlcApnp (45)

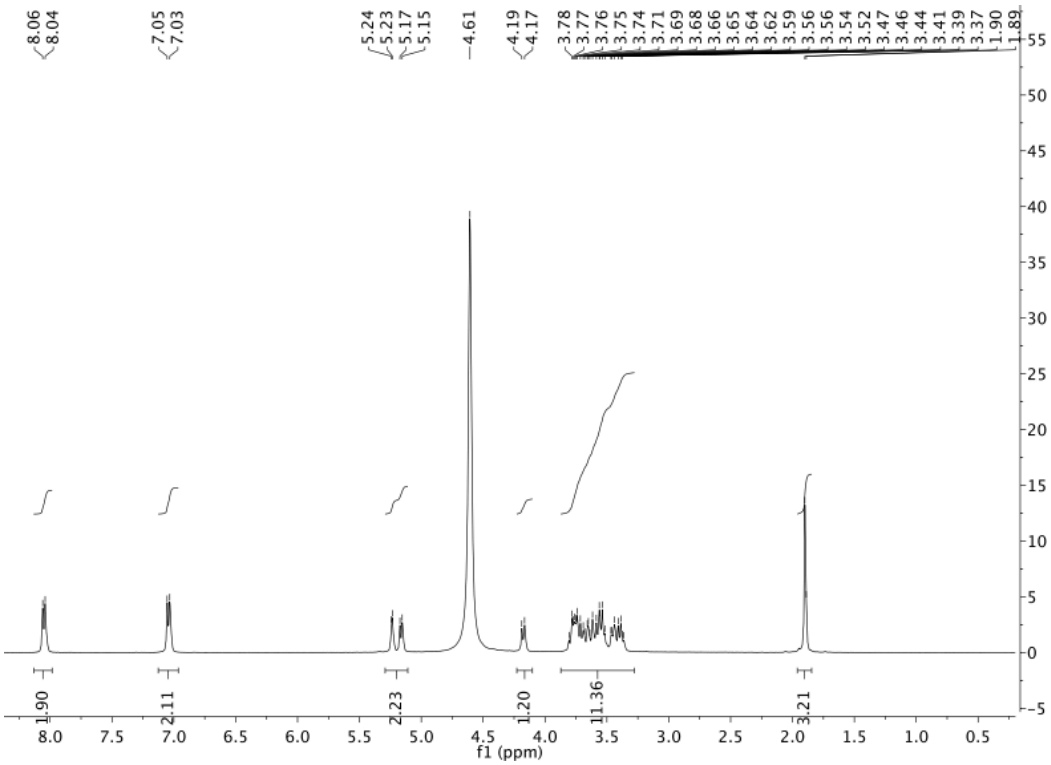

Disaccharide α-D-GlCNTFA-(1→4)-β-D-GlcApnp (50)

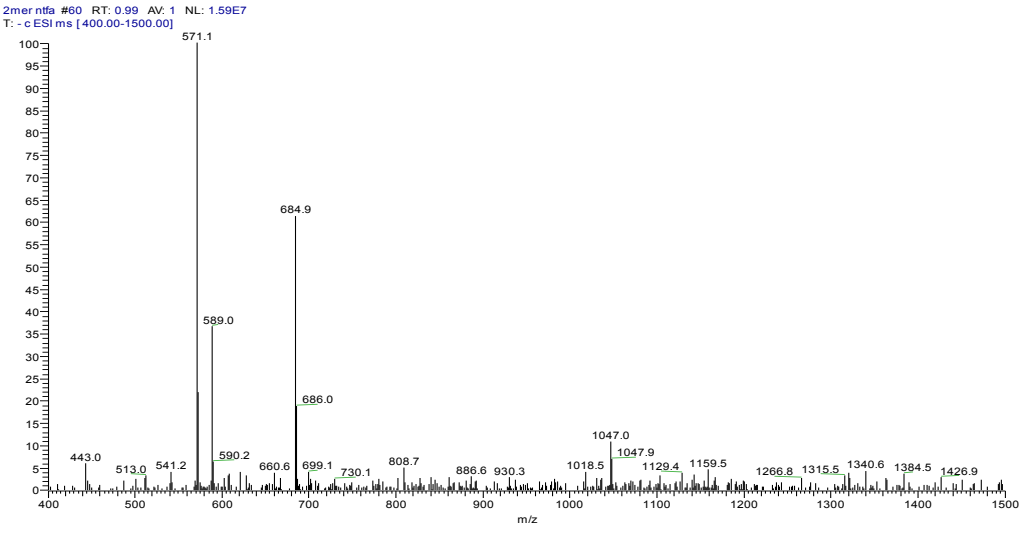

1.10 Trisaccharides

Trisaccharide β-D-GlcA-(1→4)-α-D-GlCNAc-(1→4)-β-D-GlcApnp (46)